

ORTHO-QUINODIMETHANES IN ASYMMETRIC SYNTHESIS OF LIGNANS

4

by

Shawn P. Maddaford

a thesis

submitted to the Faculty of Graduate Studies
of the University of Manitoba in partial fulfillment
of the requirements for the degree of
Doctor of Philosophy

University of Manitoba
Winnipeg, Manitoba, Canada
November 5, 1993



National Library
of Canada

Acquisitions and
Bibliographic Services Branch

395 Wellington Street
Ottawa, Ontario
K1A 0N4

Bibliothèque nationale
du Canada

Direction des acquisitions et
des services bibliographiques

395, rue Wellington
Ottawa (Ontario)
K1A 0N4

Your file *Votre référence*

Our file *Notre référence*

The author has granted an irrevocable non-exclusive licence allowing the National Library of Canada to reproduce, loan, distribute or sell copies of his/her thesis by any means and in any form or format, making this thesis available to interested persons.

L'auteur a accordé une licence irrévocable et non exclusive permettant à la Bibliothèque nationale du Canada de reproduire, prêter, distribuer ou vendre des copies de sa thèse de quelque manière et sous quelque forme que ce soit pour mettre des exemplaires de cette thèse à la disposition des personnes intéressées.

The author retains ownership of the copyright in his/her thesis. Neither the thesis nor substantial extracts from it may be printed or otherwise reproduced without his/her permission.

L'auteur conserve la propriété du droit d'auteur qui protège sa thèse. Ni la thèse ni des extraits substantiels de celle-ci ne doivent être imprimés ou autrement reproduits sans son autorisation.

ISBN 0-612-13332-X

Canada

Name SHAWN PATRICK MADDAFORO

Dissertation Abstracts International is arranged by broad, general subject categories. Please select the one subject which most nearly describes the content of your dissertation. Enter the corresponding four-digit code in the spaces provided.

ORGANIC CHEMISTRY

SUBJECT TERM

0490

U·M·I

SUBJECT CODE

Subject Categories

THE HUMANITIES AND SOCIAL SCIENCES**COMMUNICATIONS AND THE ARTS**

Architecture 0729
 Art History 0377
 Cinema 0900
 Dance 0378
 Fine Arts 0357
 Information Science 0723
 Journalism 0391
 Library Science 0399
 Mass Communications 0708
 Music 0413
 Speech Communication 0459
 Theater 0465

EDUCATION

General 0515
 Administration 0514
 Adult and Continuing 0516
 Agricultural 0517
 Art 0273
 Bilingual and Multicultural 0282
 Business 0688
 Community College 0275
 Curriculum and Instruction 0727
 Early Childhood 0518
 Elementary 0524
 Finance 0277
 Guidance and Counseling 0519
 Health 0680
 Higher 0745
 History of 0520
 Home Economics 0278
 Industrial 0521
 Language and Literature 0279
 Mathematics 0280
 Music 0522
 Philosophy of 0998
 Physical 0523

Psychology 0525
 Reading 0535
 Religious 0527
 Sciences 0714
 Secondary 0533
 Social Sciences 0534
 Sociology of 0340
 Special 0529
 Teacher Training 0530
 Technology 0710
 Tests and Measurements 0288
 Vocational 0747

LANGUAGE, LITERATURE AND LINGUISTICS

Language
 General 0679
 Ancient 0289
 Linguistics 0290
 Modern 0291
 Literature
 General 0401
 Classical 0294
 Comparative 0295
 Medieval 0297
 Modern 0298
 African 0316
 American 0591
 Asian 0305
 Canadian (English) 0352
 Canadian (French) 0355
 English 0593
 Germanic 0311
 Latin American 0312
 Middle Eastern 0315
 Romance 0313
 Slavic and East European 0314

PHILOSOPHY, RELIGION AND THEOLOGY

Philosophy 0422
 Religion
 General 0318
 Biblical Studies 0321
 Clergy 0319
 History of 0320
 Philosophy of 0322
 Theology 0469

SOCIAL SCIENCES

American Studies 0323
 Anthropology
 Archaeology 0324
 Cultural 0326
 Physical 0327
 Business Administration
 General 0310
 Accounting 0272
 Banking 0770
 Management 0454
 Marketing 0338
 Canadian Studies 0385
 Economics
 General 0501
 Agricultural 0503
 Commerce-Business 0505
 Finance 0508
 History 0509
 Labor 0510
 Theory 0511
 Folklore 0358
 Geography 0366
 Gerontology 0351
 History
 General 0578

Ancient 0579
 Medieval 0581
 Modern 0582
 Black 0328
 African 0331
 Asia, Australia and Oceania 0332
 Canadian 0334
 European 0335
 Latin American 0336
 Middle Eastern 0333
 United States 0337
 History of Science 0585
 Law 0398
 Political Science
 General 0615
 International Law and
 Relations 0616
 Public Administration 0617
 Recreation 0814
 Social Work 0452
 Sociology
 General 0626
 Criminology and Penology 0627
 Demography 0938
 Ethnic and Racial Studies 0631
 Individual and Family
 Studies 0628
 Industrial and Labor
 Relations 0629
 Public and Social Welfare 0630
 Social Structure and
 Development 0700
 Theory and Methods 0344
 Transportation 0709
 Urban and Regional Planning 0999
 Women's Studies 0453

THE SCIENCES AND ENGINEERING**BIOLOGICAL SCIENCES**

Agriculture
 General 0473
 Agronomy 0285
 Animal Culture and
 Nutrition 0475
 Animal Pathology 0476
 Food Science and
 Technology 0359
 Forestry and Wildlife 0478
 Plant Culture 0479
 Plant Pathology 0480
 Plant Physiology 0817
 Range Management 0777
 Wood Technology 0746
 Biology
 General 0306
 Anatomy 0287
 Biostatistics 0308
 Botany 0309
 Cell 0379
 Ecology 0329
 Entomology 0353
 Genetics 0369
 Limnology 0793
 Microbiology 0410
 Molecular 0307
 Neuroscience 0317
 Oceanography 0416
 Physiology 0433
 Radiation 0821
 Veterinary Science 0778
 Zoology 0472
 Biophysics
 General 0786
 Medical 0760

EARTH SCIENCES

Biogeochemistry 0425
 Geochemistry 0996

Geodesy 0370
 Geology 0372
 Geophysics 0373
 Hydrology 0388
 Mineralogy 0411
 Paleobotany 0345
 Paleocology 0426
 Paleontology 0418
 Paleozoology 0985
 Palynology 0427
 Physical Geography 0368
 Physical Oceanography 0415

HEALTH AND ENVIRONMENTAL SCIENCES

Environmental Sciences 0768
 Health Sciences
 General 0566
 Audiology 0300
 Chemotherapy 0992
 Dentistry 0567
 Education 0350
 Hospital Management 0769
 Human Development 0758
 Immunology 0982
 Medicine and Surgery 0564
 Mental Health 0347
 Nursing 0569
 Nutrition 0570
 Obstetrics and Gynecology 0380
 Occupational Health and
 Therapy 0354
 Ophthalmology 0381
 Pathology 0571
 Pharmacology 0419
 Pharmacy 0572
 Physical Therapy 0382
 Public Health 0573
 Radiology 0574
 Recreation 0575

Speech Pathology 0460
 Toxicology 0383
 Home Economics 0386

PHYSICAL SCIENCES**Pure Sciences**

Chemistry
 General 0485
 Agricultural 0749
 Analytical 0486
 Biochemistry 0487
 Inorganic 0488
 Nuclear 0738
 Organic 0490
 Pharmaceutical 0491
 Physical 0494
 Polymer 0495
 Radiation 0754
 Mathematics 0405
 Physics
 General 0605
 Acoustics 0986
 Astronomy and
 Astrophysics 0606
 Atmospheric Science 0608
 Atomic 0748
 Electronics and Electricity 0607
 Elementary Particles and
 High Energy 0798
 Fluid and Plasma 0759
 Molecular 0609
 Nuclear 0610
 Optics 0752
 Radiation 0756
 Solid State 0611
 Statistics 0463

Applied Sciences

Applied Mechanics 0346
 Computer Science 0984

Engineering
 General 0537
 Aerospace 0538
 Agricultural 0539
 Automotive 0540
 Biomedical 0541
 Chemical 0542
 Civil 0543
 Electronics and Electrical 0544
 Heat and Thermodynamics 0348
 Hydraulic 0545
 Industrial 0546
 Marine 0547
 Materials Science 0794
 Mechanical 0548
 Metallurgy 0743
 Mining 0551
 Nuclear 0552
 Packaging 0549
 Petroleum 0765
 Sanitary and Municipal 0554
 System Science 0790
 Geotechnology 0428
 Operations Research 0796
 Plastics Technology 0795
 Textile Technology 0994

PSYCHOLOGY

General 0621
 Behavioral 0384
 Clinical 0622
 Developmental 0620
 Experimental 0623
 Industrial 0624
 Personality 0625
 Physiological 0989
 Psychobiology 0349
 Psychometrics 0632
 Social 0451



Nom _____

Dissertation Abstracts International est organisé en catégories de sujets. Veuillez s.v.p. choisir le sujet qui décrit le mieux votre thèse et inscrivez le code numérique approprié dans l'espace réservé ci-dessous.



SUJET

CODE DE SUJET

Catégories par sujets

HUMANITÉS ET SCIENCES SOCIALES

COMMUNICATIONS ET LES ARTS

Architecture	0729
Beaux-arts	0357
Bibliothéconomie	0399
Cinéma	0900
Communication verbale	0459
Communications	0708
Danse	0378
Histoire de l'art	0377
Journalisme	0391
Musique	0413
Sciences de l'information	0723
Théâtre	0465

ÉDUCATION

Généralités	515
Administration	0514
Art	0273
Collèges communautaires	0275
Commerce	0688
Économie domestique	0278
Éducation permanente	0516
Éducation préscolaire	0518
Éducation sanitaire	0680
Enseignement agricole	0517
Enseignement bilingue et multiculturel	0282
Enseignement industriel	0521
Enseignement primaire	0524
Enseignement professionnel	0747
Enseignement religieux	0527
Enseignement secondaire	0533
Enseignement spécial	0529
Enseignement supérieur	0745
Évaluation	0288
Finances	0277
Formation des enseignants	0530
Histoire de l'éducation	0520
Langues et littérature	0279

Lecture	0535
Mathématiques	0280
Musique	0522
Orientalisation et consultation	0519
Philosophie de l'éducation	0998
Physique	0523
Programmes d'études et enseignement	0727
Psychologie	0525
Sciences	0714
Sciences sociales	0534
Sociologie de l'éducation	0340
Technologie	0710

LANGUE, LITTÉRATURE ET LINGUISTIQUE

Langues	
Généralités	0679
Anciennes	0289
Linguistique	0290
Modernes	0291
Littérature	
Généralités	0401
Anciennes	0294
Comparée	0295
Médiévale	0297
Moderne	0298
Africaine	0316
Américaine	0591
Anglaise	0593
Asiatique	0305
Canadienne (Anglaise)	0352
Canadienne (Française)	0355
Germanique	0311
Latino-américaine	0312
Moyen-orientale	0315
Romane	0313
Slave et est-européenne	0314

PHILOSOPHIE, RELIGION ET THÉOLOGIE

Philosophie	0422
Religion	
Généralités	0318
Clergé	0319
Études bibliques	0321
Histoire des religions	0320
Philosophie de la religion	0322
Théologie	0469

SCIENCES SOCIALES

Anthropologie	
Archéologie	0324
Culturelle	0326
Physique	0327
Droit	0398
Économie	
Généralités	0501
Commerce-Affaires	0505
Économie agricole	0503
Économie du travail	0510
Finances	0508
Histoire	0509
Théorie	0511
Études américaines	0323
Études canadiennes	0385
Études féministes	0453
Folklore	0358
Géographie	0366
Gérontologie	0351
Gestion des affaires	
Généralités	0310
Administration	0454
Banques	0770
Comptabilité	0272
Marketing	0338
Histoire	
Histoire générale	0578

Ancienne	0579
Médiévale	0581
Moderne	0582
Histoire des noirs	0328
Africaine	0331
Canadienne	0334
États-Unis	0337
Européenne	0335
Moyen-orientale	0333
Latino-américaine	0336
Asie, Australie et Océanie	0332
Histoire des sciences	0585
Loisirs	0814
Planification urbaine et régionale	0999
Science politique	
Généralités	0615
Administration publique	0617
Droit et relations internationales	0616
Sociologie	
Généralités	0626
Aide et bien-être social	0630
Criminologie et établissements pénitentiaires	0627
Démographie	0938
Études de l'individu et de la famille	0628
Études des relations interethniques et des relations raciales	0631
Structure et développement social	0700
Théorie et méthodes	0344
Travail et relations industrielles	0629
Transports	0709
Travail social	0452

SCIENCES ET INGÉNIERIE

SCIENCES BIOLOGIQUES

Agriculture	
Généralités	0473
Agronomie	0285
Alimentation et technologie alimentaire	0359
Culture	0479
Élevage et alimentation	0475
Exploitation des pâturages	0777
Pathologie animale	0476
Pathologie végétale	0480
Physiologie végétale	0817
Sylviculture et taune	0478
Technologie du bois	0746
Biologie	
Généralités	0306
Anatomie	0287
Biologie (Statistiques)	0308
Biologie moléculaire	0307
Botanique	0309
Cellule	0379
Écologie	0329
Entomologie	0353
Génétique	0369
Limnologie	0793
Microbiologie	0410
Neurologie	0317
Océanographie	0416
Physiologie	0433
Radiation	0821
Science vétérinaire	0778
Zoologie	0472
Biophysique	
Généralités	0786
Médicale	0760

Géologie	0372
Géophysique	0373
Hydrologie	0388
Minéralogie	0411
Océanographie physique	0415
Paléobotanique	0345
Paléocologie	0426
Paléontologie	0418
Paléozoologie	0985
Palynologie	0427

SCIENCES DE LA SANTÉ ET DE L'ENVIRONNEMENT

Économie domestique	0386
Sciences de l'environnement	0768
Sciences de la santé	
Généralités	0566
Administration des hôpitaux	0769
Alimentation et nutrition	0570
Audiologie	0300
Chimiothérapie	0992
Dentisterie	0567
Développement humain	0758
Enseignement	0350
Immunologie	0982
Loisirs	0575
Médecine du travail et thérapie	0354
Médecine et chirurgie	0564
Obstétrique et gynécologie	0380
Ophtalmologie	0381
Orthophonie	0460
Pathologie	0571
Pharmacie	0572
Pharmacologie	0419
Physiothérapie	0382
Radiologie	0574
Santé mentale	0347
Santé publique	0573
Soins infirmiers	0569
Toxicologie	0383

SCIENCES PHYSIQUES

Sciences Pures	
Chimie	
Généralités	0485
Biochimie	487
Chimie agricole	0749
Chimie analytique	0486
Chimie minérale	0488
Chimie nucléaire	0738
Chimie organique	0490
Chimie pharmaceutique	0491
Physique	0494
Polymères	0495
Radiation	0754
Mathématiques	0405
Physique	
Généralités	0605
Acoustique	0986
Astronomie et astrophysique	0606
Électromagnétique et électricité	0607
Fluides et plasma	0759
Météorologie	0608
Optique	0752
Particules (Physique nucléaire)	0798
Physique atomique	0748
Physique de l'état solide	0611
Physique moléculaire	0609
Physique nucléaire	0610
Radiation	0756
Statistiques	0463

Sciences Appliquées Et Technologie

Informatique	0984
Ingénierie	
Généralités	0537
Aéronautique	0539
Automobile	0540

Biomédicale	0541
Chaleur et thermodynamique	0348
Conditionnement (Emballage)	0549
Génie aérospatial	0538
Génie chimique	0542
Génie civil	0543
Génie électronique et électrique	0544
Génie industriel	0546
Génie mécanique	0548
Génie nucléaire	0552
Ingénierie des systèmes	0790
Mécanique navale	0547
Métallurgie	0743
Science des matériaux	0794
Technique du pétrole	0765
Technique minière	0551
Techniques sanitaires et municipales	0554
Technologie hydraulique	0545
Mécanique appliquée	0346
Géotechnologie	0428
Matériaux plastiques (Technologie)	0795
Recherche opérationnelle	0796
Textiles et tissus (Technologie)	0794

PSYCHOLOGIE

Généralités	0621
Personnalité	0625
Psychobiologie	0349
Psychologie clinique	0622
Psychologie du comportement	0384
Psychologie du développement	0620
Psychologie expérimentale	0623
Psychologie industrielle	0624
Psychologie physiologique	0989
Psychologie sociale	0451
Psychométrie	0632



ORTHO-QUINODIMETHANES IN ASYMMETRIC SYNTHESIS OF LIGNANS

BY

SHAWN P. MADDAFORD

A Thesis submitted to the Faculty of Graduate Studies of the University of Manitoba
in partial fulfillment of the requirements of the degree of

DOCTOR OF PHILOSOPHY

© 1994

Permission has been granted to the LIBRARY OF THE UNIVERSITY OF MANITOBA
to lend or sell copies of this thesis, to the NATIONAL LIBRARY OF CANADA to
microfilm this thesis and to lend or sell copies of the film, and LIBRARY
MICROFILMS to publish an abstract of this thesis.

The author reserves other publication rights, and neither the thesis nor extensive
extracts from it may be printed or other-wise reproduced without the author's written
permission.

Acknowledgments

This thesis would not have been possible if it were not for following individuals to whom I express my utmost gratitude: my supervisor, Dr. Jim Charlton for providing me with the opportunity to work in such a pleasurable and stimulating environment and for allowing me to make independent decisions with regards to my thesis work but at the same time offering his invaluable experience and guidance. I would also like to thank my committee members: Dr. Tony Secco, Dr. Norman Hunter, Dr. John Templeton and Dr. Brian Keay for helping me to realize my goals. Many other people deserve thanks as well including my close friends: Leo Spyropoulos, Les Tari, Angela Toms, Ioana Ciric and my family members for their positive support during the last four years of my graduate career. To the many summer students that assisted me I also express my gratitude. Dr.'s K Koh and G. Plourde I thank for helping me develop my technical skills as a researcher. I would also thank those members of the Chemistry department technical staff who are really the hub of much of the research that occurs in this department. Finally, I would like to the University of Manitoba and the Natural Sciences and Engineering Research Council of Canada for the financial support in the form of scholarships.

TABLE OF CONTENTS

Abstract:	1
Chapter 1: Introduction	3
1.1 Discovery of Biologically Important Aryltetralin Lignans	3
1.2 Development of Clinical Derivatives of Podophyllotoxin	7
1.3 Mechanism of Action and Structure-Activity Relationships	11
1.4 Asymmetric Synthesis, Diastereoselectivity and Enantioselectivity in the Diels-Alder Reaction	16
1.5 Stereochemical Control (<i>Endo/Exo</i>) in the Diels-Alder Reaction	25
1.6 Generation of <i>o</i> -Quinodimethanes	25
1.7 Diastereoselectivity in the Reactions of <i>o</i> -QDMs	33
1.8 Diastereofacial Control in the Diels-Alder Reaction	42
1.9 Asymmetric Synthesis of Aryltetralin Lignans	56
Thesis Objectives	65
Chapter 2: Results and Discussion	67
2.1.1 Elucidation of the Mechanism of the Stereoselective Addition of α -Hydroxy- <i>o</i> -QDM to Lactate and Mandelate Substituted Dienophiles	68
2.1.2 Molecular Modeling of the Diastereoselectivity	87
2.1.2.1 Force Field (MMX) Calculations	88

2.1.2.2	Molecular Orbital (AM1) Calculations	94
2.2.1	General Asymmetric Synthesis of Aryltetralin Lignans	102
2.2.2	NMR and Conformational Analysis	118
2.3	Stereoselective Addition of α -Hydroxy- α -phenyl- <i>o</i> -QDM to the Fumarate of Methyl Mandelate	136
Chapter 3: Conclusions		150
Experimental		153
Compound		
18	<i>Benzocyclobutenol</i>	153
30	<i>1-Methoxybenzocyclobutene</i>	153
51	<i>1-Phenyl-benzocyclobutene-1-ol</i>	154
95	<i>(-)-α-Dimethylretrodendrin</i>	155
115	<i>Acrylate of rac-lactonitrile</i>	156
116	<i>Acrylate of rac-3-hydroxy-2-butanone</i>	156
117	<i>Fumarate of methyl (S)-lactate</i>	156
118	<i>Fumarate of methyl (R)-mandelate</i>	157
120	<i>Di-t-butyl fumarate</i>	157
121	<i>Di-(2-hydroxyethyl) fumarate</i>	158
122	<i>Di-(2-chloroethyl) fumarate</i>	158
123	<i>Di-(2-fluoroethyl) fumarate</i>	158
124,5	<i>Cycloadducts 124 and 125</i>	159
126,7	<i>Cycloadducts 126 and 127</i>	160
128,9	<i>Cycloadducts 128 and 129</i>	160
130a-d	<i>Cycloadducts 130a-d</i>	161
131	<i>Cycloadduct 131</i>	162
132	<i>Lactone 132</i>	163
133a-d	<i>Cycloadducts 133a-d ;30% DMSO/toluene</i>	164

134a,d	<i>Exo-si and Exo-re lactones 134a and 134d</i>	165
135	<i>(+)-Exocycloadduct</i>	165
138	<i>1-(3,4-Dimethoxyphenyl)-3-hydroxy-5,6-dimethoxy- 1,3dihydrobenzo[c]-thiophene-2,2-dioxide</i>	166
139	<i>6-(3,4-Dimethoxybenzyl)veratraldehyde</i>	166
141	<i>6-Bromoveratraldehyde</i>	167
142	<i>α-(3,4-Dimethoxyphenyl)-6-bromoveratryl alcohol</i>	168
143	<i>6-Bromo-3,4,9,10-tetramethoxybenzophenone</i>	168
144	<i>3-Hydroxy-(3,4-dimethoxy-6-bromophenyl)-3- (3',4'-dimethoxyphenyl)-propionitrile</i>	169
145	<i>3-(3,4-Dimethoxy-6-bromophenyl)-3'-(3',4'- dimethoxyphenyl)-acrylonitrile</i>	170
146	<i>3-(3,4-Dimethoxy-6-bromophenyl)-3-(3',4'- dimethoxyphenyl)-propionitrile</i>	170
147	<i>Ethyl-3-(3,4-dimethoxy-6-bromophenyl)-3',4'- dimethoxyphenyl)-propionate</i>	171
148	<i>6-Bromoveratraldehyde-(ethylene glycol acetal)</i>	171
150	<i>1-Hydroxy-2(3,4-dimethoxyphenyl)-6,7- dimethoxybenzofuran</i>	172
152	<i>5,6-Dimethoxy-3-(3,4-dimethoxyphenyl)-phthalide</i>	172
153	<i>3,4-Dimethoxy-6-(3,4-dimethoxybenzyl)- benzoic acid</i>	173
154	<i>6-(3,4-Dimethoxybenzyl)-veratryl alcohol</i>	174
155	<i>1-(3,4-Dimethoxybenzyl)-6-bromoveratrole</i>	174
160	<i>Elimination product</i>	175
162	<i>3-Carbomethoxy-(6,7-dimethoxy)-1-(1,2-cis)-(3',4'- dimethoxyphenyl)-1,2,3,4-tetrahydronaphthalene-</i>	

	<i>(2,3-cis)-2-carboxylic acid</i>	175
163	<i>(+)-Picrodimethylretrodendrin</i>	176
164	<i>3-Carbomethoxy-(6,7-dimethoxy)-1-(1,2-cis)-(3',4'-dimethoxyphenyl)-1,2,3,4-tetrahydronaphthalene-(2,3-trans)-2-carboxylic acid</i>	177
165	<i>2,3-Trans-acid-alcohol</i>	178
166	<i>(+)-Isodimethylretrodendrin</i>	178
167	<i>(-)-Isopicrodimethylretrodendrin</i>	179
168	<i>Di-(R-α-methoxycarbonylbenzyl)-1(S)-hydroxy-1(S)-phenyl-1,2,3,4-tetrahydronaphthalene-2(R)-3(S)-dicarboxylate</i>	180
169	<i>Di-(R-α-methoxycarbonylbenzyl)-1(S)-phenyl-1,2,3,4-tetrahydronaphthalene-2(S)-3(S)-dicarboxylate</i>	181
171	<i>Di-(R-α-methoxycarbonylbenzyl)-4(R)-hydroxy-1(S)-phenyl-1,2,3,4-tetrahydronaphthalene-2(S)-3(R)-dicarboxylate</i>	182
172	<i>Alkene 172</i>	183
174	<i>Cycloadduct 174</i>	184
175	<i>1(S)-(3',4'-Dimethoxyphenyl)-6,7-dimethoxy-1,2,3,4-tetrahydronaphthalene-2(S),3(S)-(methyl(R)-mandelate)-dicarboxylate</i>	184
176	<i>2-Methyl-4,5,9,10-tetramethoxybenzophenone</i>	186
178	<i>2-Methyl-3,4-dimethoxy-3',4'-dimethoxybenzhydrol</i>	186
179	<i>1-Hydroxy-1-(3',4'-dimethoxyphenyl)-4,5-dimethoxybenzocyclobutene</i>	187
181	<i>1-Hydroxy-4,5-dimethoxybenzocyclobutene</i>	188
182	<i>4,5-Dimethoxybenzocyclobutenone</i>	188

Abbreviations

AcOH	glacial acetic acid
AM1	Austin Method 1 (semi-empirical molecular orbital)
Ar	aryl
Atm	atmospheres
ax	axial
BO	bond order
br	broad
¹³ C-NMR	carbon-13 nuclear magnetic resonance
C ₆ D ₆	deuterobenzene
calcd.	calculated
CDCl ₃	deuteriochloroform
cf.	compare with/to
CN	cyano
COSY	Correlated Spectroscopy
d	doublet
dd	doublet of doublets
ddd	doublet of doublets of doublets
de	diastereomeric excess
DME	dimethoxyethane
DMF	dimethylformamide
DMSO	dimethylsulfoxide
DNA	Deoxyribonucleic acid
dt	doublet of triplets
ee	enantiomeric excess

eq	equatorial
equiv.	equivalents
EtOAc	ethyl acetate
FMO	Frontier Molecular Orbital
g	grams
¹ H-NMR	proton magnetic resonance
H _f	heat of formation
H [‡]	heat of formation (transition state)
HOMO	Highest Occupied Molecular Orbital
HPLC	High Pressure Liquid Chromatography
hr	hours
HRMS	High Resolution Mass Spectrometry
i.v.	intravenous
ID ₅₀	dose required to produce a 50% cell reduction
IR	Infrared Spectroscopy
ISC	intersystem crossing
J	J or spin-spin coupling
kcal	kilocalories
L-1210	Leukemia L-1210
LDA	lithium diisopropylamide
LiEt ₃ BH	lithium triethylborohydride (Super Hydride)
lit	literature
LUMO	Lowest Unoccupied Molecular Orbital
M	molarity
MeOH	methanol
mg	milligrams
MHz	megaHertz

min	minutes
mL	milliliters
mm	millimeters
MM2	Molecular Mechanics 2
MMX	Molecular Mechanics (PCMODEL)
mol	moles
mp	melting point (°C)
MS	Mass Spectrometry
n-BuLi	normal-butyllithium
NEM	N-ethylmaleimide
nm	nanometers
NOE	Nuclear Overhauser Effect
o-QDM	orthoquinodimethane
ODS-2	octadecylsilyl-2
P	podophyllotoxin
P-815	mouse sarcoma (cancer cells)
p-TsOH	<i>para</i> -toluenesulfonic acid
PCC	pyridinium chlorochromate
PD	podophyllotoxin- β -D-glucopyranoside
PDC	pyridinium dichromate
Ph	phenyl
ppm	parts per million
rel.	relative
rf	retention factor
RMS	root mean square
rt	room temperature
s	singlet

SP-G	benzylidene glucosides of podophyllin
t	triplet
TCNE	tetracyanoethylene
tert	tertiary
TFA	trifluoroacetic acid
THF	tetrahydrofuran
TLC	thin layer chromatography
TMS	tetramethylsilane
tt	triplet of triplets
UV	ultraviolet
VM-26	Teniposide
VP-16	Etoposide
vs	versus
$[\alpha]_D^{20}$	specific rotation measured at 20 ⁰ C (sodium D-line)

List of Schemes

Scheme	Page	Scheme	Page
1.0	5	1.24	34
1.1	8	1.25	35
1.2	10	1.26	35
1.3	11	1.27	36
1.4	15	1.28	36
1.5	17	1.29	37
1.6	18	1.30	38
1.7	19	1.31	39
1.8	20	1.32	40
1.9	21	1.33	41
1.10	21	1.34	42
1.11	22	1.35	42
1.12	23	1.36	43
1.13	24	1.37	44
1.14	24	1.38	45
1.15	26	1.39	46
1.16	26	1.40	47
1.17	27	1.41	48
1.18	28	1.42	48
1.19	29	1.43	49
1.20	31	1.44	50
1.21	31	1.45	50
1.22	33	1.46	51
1.23	33	1.47	52

Scheme	Page	Scheme	Page
1.48	52	2.11	77
1.49	53	2.12	78
1.50	54	2.13	82
1.51	55	2.14	83
1.52	55	2.15	85
1.53	56	2.16	90
1.54	57	2.17	90
1.55	58	2.18	91
1.56	59	2.19	92
1.57	60	2.20	102
1.58	60	2.21	103
1.59	61,62	2.22	104
1.60	62	2.23	104
1.61	63	2.24	106
1.62	63	2.25	107
1.63	64	2.26	108
2.1	68	2.27	110
2.2	69	2.28	111
2.3	70	2.29	112
2.4	70	2.30	113
2.5	71	2.31	114
2.6	71	2.32	115
2.7	72	2.33	117
2.8	73	2.34	118
2.9	74	2.35	136
2.10	75	2.36	138

Scheme	Page	Scheme	Page
2.37	145	2.41	147
2.38	146	2.42	147
2.39	147	2.43	148
2.40	147		

List of Tables

Table	Page	Table	Page
1	6	7	122
2	13	8	127
3	13	9	128
4	30	10	129
5	86	11	130
6a,b	119	12	141

List of Figures

Figure	Page	Figure	Page
1	76	9	97
2	79	10	98
3	80	11	99
4	84	12	100
5	88	13	120
6	93	14	121
7	95	15	123
8	96	16	124

Figure	Page
17	125
18	126
19	127
20	131
21	132

Figure	Page
22	133
23	134
24	139
25	143

Abstract

The fumarates and acrylates of methyl (S)-lactate and methyl (R)-mandelate are known to undergo asymmetric cycloaddition to α -hydroxy-*o*-quinodimethanes (α -hydroxy-*o*-QDMs) with high asymmetric induction. These cycloadducts arise from an unprecedented *exo* transition state. In this work, it is proposed that an intermolecular hydrogen bond between the α -hydroxy-*o*-QDM and the chiral auxiliary of the dienophile controls both the *exo* diastereoselectivity and the addition to one face of the dienophile. Modifications of the chiral auxiliary, solvent effects, and blocking of the hydroxyl group supported the hydrogen bonding theory. In addition, molecular modeling studies (molecular mechanics and molecular orbital calculations) of the transition states for the addition of the acrylate of methyl (S)-lactate to α -hydroxy-*o*-QDM revealed that a hydrogen bond in *exo* transition state is sterically feasible and is responsible for the control of the diastereoselectivity. This hydrogen bond, contained within an entropically unfavorable 9-membered ring, serves as a mediator of molecular recognition, whereby diene and dienophile are directed towards the formation of a single product.

Using the stereoselective addition of an α -hydroxy- α' -aryl-*o*-QDM to the fumarate of methyl (R)-mandelate, a single cycloadduct was synthesized in 44% yield and subsequently converted to the natural product lignan (-)- α -dimethylretrodendrin (optically pure) and three of its non-naturally occurring diastereomers. Conformational analysis of these four lignans (NMR and molecular mechanics methods) reveal that the 2,3-*cis* lignans possess axial pendant aryl groups, suggesting that previous conformational assignments of analogous lignans reported in the literature are incorrect. Potential structure-activity relationships are assessed by conformational comparison with lignans possessing antitumor activity.

The cycloaddition of α -hydroxy- α -phenyl(aryl)-*o*-QDM to the fumarate of methyl

(R)-mandelate is shown to proceed through an *endo* transition state with high diastereoselectivity. The propensity for the addition to the *si* face of the dienophile is not a result of intermolecular hydrogen bonding in the transition state. Helmchen's ground state conformational model for lactate substituted dienophiles is consonant with addition of the *o*-QDM to the *si* face of the fumarate of methyl (R)-mandelate. The absolute stereochemistry of the major *endo* adduct has been deduced using proton NMR and chemical correlation. The adduct was stereoselectively deoxygenated using the method of ionic hydrogenolysis resulting in an unprecedented stereoinversion of the C1-center. Two mechanisms are proposed to explain the stereoinversion of this center. The reduction product has the thermodynamically less stable 1,2-*cis* stereochemistry and is suitable for the synthesis of podophyllotoxin and other potent antitumor analogues.

Chapter 1

Introduction

Asymmetric organic synthesis has received considerable attention in recent years due to the increasing need for methods for preparing optically pure compounds. Contained within the vast body of asymmetric reactions, one finds the asymmetric Diels-Alder reaction. This reaction is deemed one of the most important organic reactions as it allows for the formation of two new bonds with concomitant generation of up to four contiguous chiral centers. The cycloaddition reactions of *o*-quinodimethanes (*o*-QDMs) represent an important class within the hierarchy of the Diels-Alder reaction. This thesis work involves the reactions of *o*-QDMs in the synthesis of an important group of molecules known as aryltetralin lignans. A complete review of all of the asymmetric syntheses of aryltetralin lignans will be made with specific focus on those involving the use of *o*-QDMs. A cursory description of the generation of *o*-QDMs as well as the rules of the Diels-Alder reaction and the factors controlling its diastereoselectivity will be included.

1.1 Discovery of Biologically Important Aryltetralin Lignans

Extracts from natural sources (galenicals) often find widespread medicinal use. The root and rhizome extracts from several herbaceous perennials belonging to the *Podophyllum* class, namely *Podophyllum emodi* Wallach and *P. peltatum* Linnaeus, have been used by North American Indians and the natives of the Himalayas for the treatment of warts.¹ In 1615, Champlain was instructed by the North American Indians on the use of the root extracts as a cathartic, anthelmintic and mortal poison. Dating back to

900-950 AD, a report in the *Leech Book of Bald*, an old English medical text, suggested the use of root extracts from the roots of wild chervil for the treatment of cancer. *P. peltatum* is indigenous to Canada and the United States, where it is called the May Apple or American Mandrake, and it spans the region from Quebec to Florida. A third species, *P. sikkimensis*, from the Himalayan region, was investigated by Chatterjee and Mukerjee.² All of the extracts from these plants contain a complex mixture of compounds that constitutes the biologically active resin known as podophyllin.

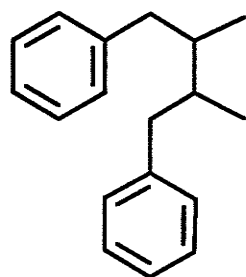
In the 1940's, podophyllin was subjected to extensive pharmacological and clinical testing for a plethora of diseases including skin diseases from infectious agents (condyloma acuminatum (a type of venereal wart), verrucae, granuloma inguinale, molluscum contagiosum, tinea capitis), dermatoses (eczema, psoriasis, neurodermatosis), metabolic diseases (amyloidus cutis, acanthosis nigricans, gout, rheumatoid arthritis), benign and malignant tumor growths.

Naturally, as the clinical effects of podophyllin were elucidated, an investigation of the various chemical constituents of podophyllin ensued. The resin was first extracted from podophyllum (the dried plant roots) by King in 1835.² The extraction process involved slow percolation of alcohol through the dried root material and evaporation. The syrup that was obtained was stirred in a cooled dilute acid solution which eventually resulted in the isolation of about 4 to 15% resin depending on which species of plant was used. Podwysotszki was the first to carry out a chemical separation of the resin in 1880.² From the resin of the American Mandrake, he isolated a crystalline substance which he named "podophyllotoxin" and coloring matter which he coined "quercetin". He also isolated a crystalline compound which he named picropodophyllin which he could also obtain by alkaline treatment of podophyllotoxin. It turns out that this new compound was an artifact produced by the slaked lime he used in the isolation process. Extensive chemical and pharmacological examination of podophyllin was pursued by many groups and is reviewed in detail by Hartwell and Schrecker.² By 1955, some 16 compounds in

total had been isolated from the various podophyllin resins obtained from four podophyllum plant species.

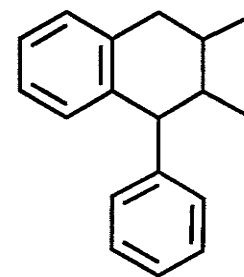
The compounds were classified into two categories; the lignans and the flavonol pigments. The lignans, the name of which was suggested by Haworth, contain the 2,3-dibenzylbutane skeleton **1** (Scheme 1.0). This structural unit is probably formed via dimerization of two phenylpropene units. The lignans isolated from podophyllin fall into another sub-class known as aryltetralin lignans **2** (Scheme 1.0).

Scheme 1.0



1

Lignan Skeleton



2

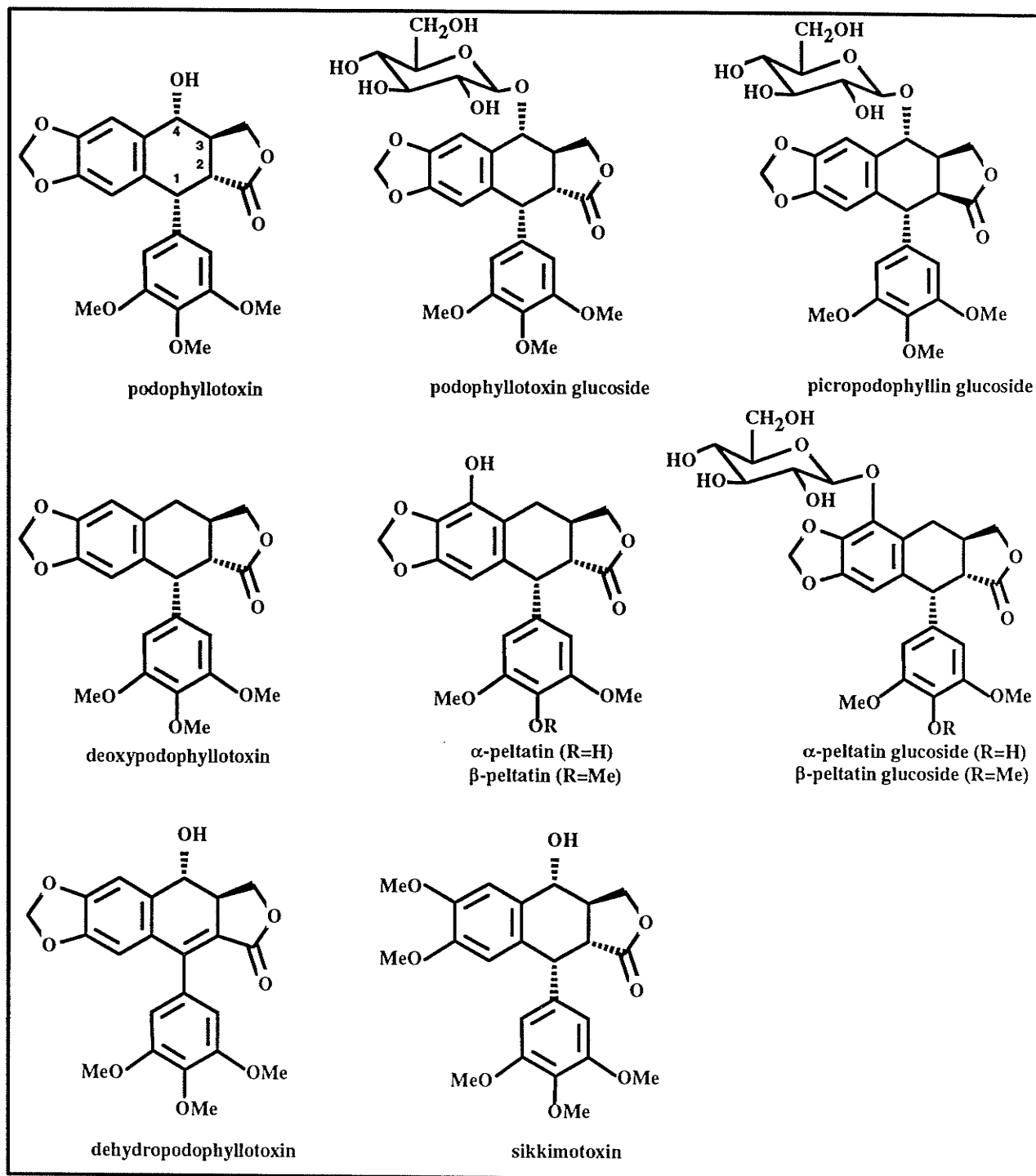
Aryltetralin Lignan Skeleton

Lignan skeleton and aryltetralin lignan skeleton showing the fused ring system for **2**.

The twelve aryltetralin lignans that were originally isolated from podophyllin, as reviewed by Hartwell and Schrecker, are shown in Table 1. All of the aryltetralin lignans isolated from podophyllin feature a pendant aryl ring in the saturated portion of the tetrahydronaphthalene ring (Table 1). Some of these lignans have a hydroxyl group in the 4-position as in podophyllotoxin, sikkimotoxin and picropodophyllotoxin with the peltatins having a phenolic hydroxyl group on the tetralin ring. The aforementioned lignans may also exist in β -glycosilated forms where the 4-hydroxyl group or the phenolic hydroxyl (peltatins) bears a glucose sugar.

All of the lignans shown in Table 1, with the exception of the C2 epimerized picropodophyllotoxin derivatives, have a 1,2-*cis*-2,3-*trans* stereochemistry. It is interesting to note that all of these naturally occurring lignans have the same absolute stereochemistry at the C3 carbon center. Lignans with other possible absolute

Table 1. Aryltetralin Lignans Isolated from Podophyllin Resin.



stereochemistries are also possible. Consider podophyllotoxin which has four chiral centers. There are a total of eight possible diastereomers, each one having a corresponding enantiomer resulting in 16 possible stereoisomers which have the podophyllotoxin skeleton. Because of the large number of possible isomers, the organic chemist is faced with the difficult task of controlling both the relative stereochemistry and the absolute stereochemistry when undertaking an asymmetric synthesis. Many of the stratagems used to control the absolute stereochemistry described in the literature will be reviewed in the section **Asymmetric Syntheses of Aryltetralin Lignans**.

1.2 Development of Clinical Derivatives of Podophyllotoxin

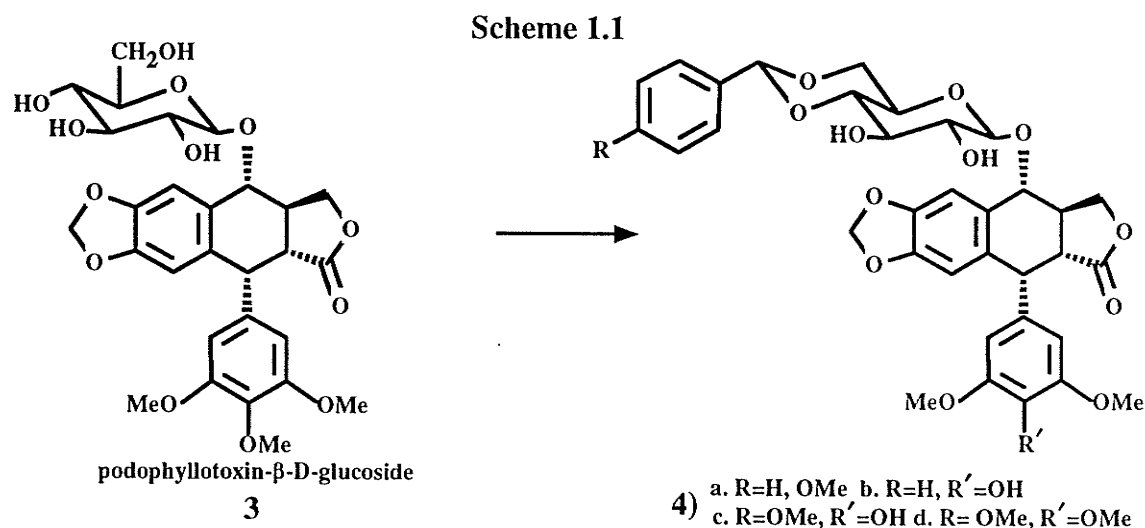
The work performed by Kaplan in the treatment of the condyloma acuminatum by topical application of podophyllin stimulated interest in its use as a potential tumor damaging agent.² In a paper by King and Sullivan, it was shown that topical application of podophyllin on normal human and rabbit skin resulted in significant cytological changes.⁴ Hartwell and Shear had shown that podophyllin had disruptive effects on cancer cell in animals.⁵ Attempts to use podophyllotoxins for the treatment of human cancers were largely unsuccessful since many noxious side effects were observed including nausea, vomiting, diarrhea and damage to normal cells.

Testing of the glucosides of podophyllotoxin, α - and β -peltatin and 4'-demethylpodophyllotoxin revealed an inhibition in the growth of cell cultures and mice tumors by stopping cell division in early metaphase. *In vitro*, the glycosides were much less active than the corresponding aglycones albeit they did not display the same noxious effects. Although these compounds showed the desirable increase in water solubility and reduction in the side effects, they did not mature as clinically useful drugs due to their diminished antimitotic activity.

The first attempts at modification of podophyllotoxin- β -D-glucopyranoside (PD)

were carried out by von Wartburg *et al.* and a recent review of the structural modifications of this compound as well the pharmacology of the analogues has been published.⁶ Initial modification of the 4'-demethyl glucosides involved preparation of 4'-O-alkyl homologues. These compounds showed no therapeutic advantages over the 4'-hydroxyl glucosides. Modification of the sugar moiety by complete esterification of the hydroxyl groups resulted in inferior products having decreased water solubility and antitumor potency.

Continued modification of the sugar moiety was examined in terms of blocking only two of the hydroxyl groups. This was accomplished by condensation of PD with various aldehydes using a Lewis acid to give the P-benzylidene- β -D-glucopyranosides **4** (Scheme 1.1).



These new glucosides (**4a-d**) were found to have higher mitotic inhibiting effects (mitotic index), in comparison to the natural glucosides, as measured by determining the *in vitro* drug concentration (ID-50) necessary to inhibit the proliferation of mouse tumor cells (P-815) by 50%. These compounds also had increased absorption by the intestinal tract and enhanced lifetimes within the body as compared to podophyllotoxin glucoside **3**. The increased lifetimes were probably due to their increased resistance to the action of β -glucosidases. When these compounds were administered by i.v. (intravenous), high

accumulations were found in the bone marrow, liver and kidney with the lowest concentrations found in the brain.

Although the benzylidene glucosides of podophyllotoxin and 4'-demethylpodophyllotoxin showed an increase in the mitotic index, their tumor-inhibiting effects in mouse sarcoma (tumor cells from connective tissue) and Leukemia (L-1210) were poor. Instead of using the pure glucosides, it was eventually found that benzylidene condensation with impure podophyllum extracts containing podophyllotoxin glucoside and many other components resulted in a mixture having increased antitumor potential. Hence, mice that were inoculated with leukemia cells would have a substantial increase in their life span when they were administered the mixture. This new mixture was given the code name SP-G and was eventually marketed under the trade of Proresid[®].

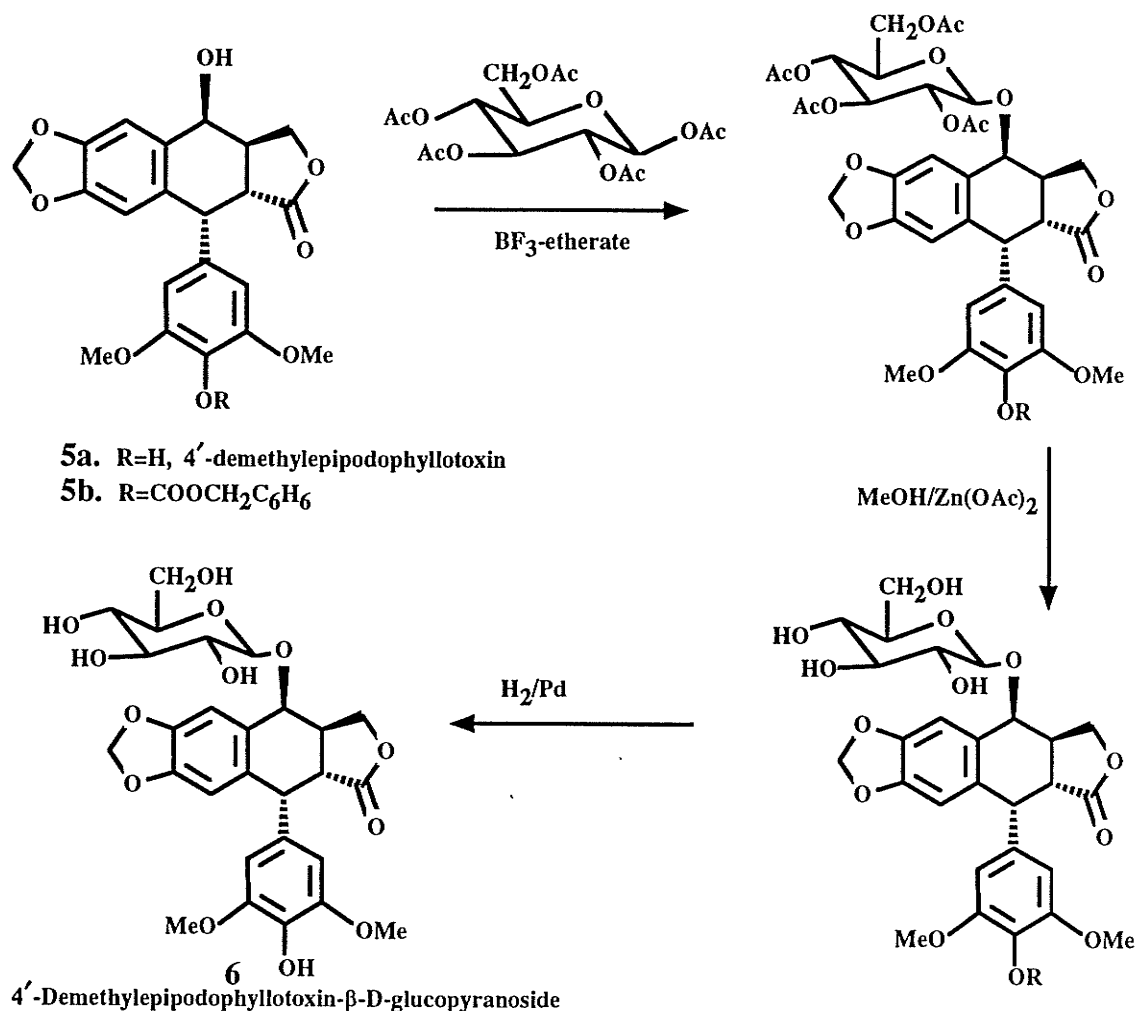
By chromatographic separation of SP-G, the compound that was responsible for the tumor inhibiting effects in mouse leukemia L-1210 was isolated and its structure elucidated.⁶ The compound (4'-demethylepipodophyllotoxin benzylidene glucoside) had an epimerized 4-oxy group (opposite configuration) with respect to podophyllotoxin benzylidene glucoside. This compound produced a large increase in the life span of leukemia infected mice.

As the natural abundance of epi-isomer was quite low, complete pharmacological studies required its synthesis according to Scheme 1.2. A synthetic pathway involving podophyllotoxin as the starting material was chosen due to the scarcity of 4'-demethylpodophyllotoxin. The 4-hydroxyl group was selectively removed by treatment with HBr and the corresponding 4-bromo derivative solvolyzed to give 4'-demethylepipodophyllotoxin (5a).⁷ The phenolic group was protected with a benzyloxy carbonyl group (5b) and the product condensed with 2,3,4,6-tetra-O-acetyl- β -D-glucopyranose at low temperatures to give the 4-epi tetracetyl glucoside. Deblocking of the acetate groups and hydrogenolysis of the benzyloxy

carbonyl group furnished the required

4'-demethyl-epipodophyllotoxin- β -D-glucopyranoside (**6**). This precursor was condensed with over 60 aldehydes and their cytostatic activity assayed.⁸ These 4'-demethyl

Scheme 1.2

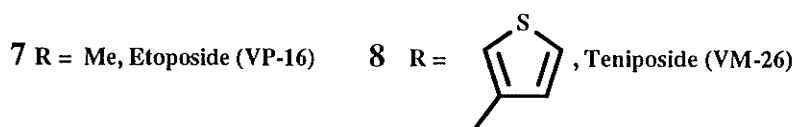
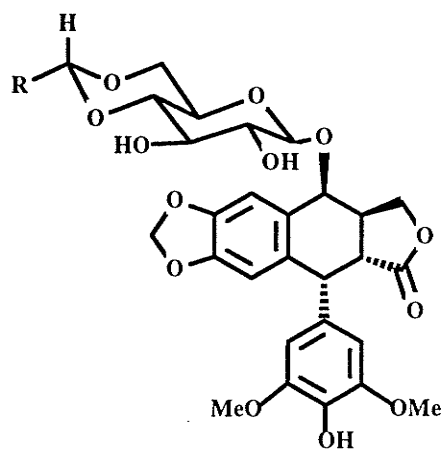


epi-glucoside derivatives generally had much higher cytostatic potencies than the corresponding benzylidene glucosides of podophyllotoxin, peltatin, and epipodophyllotoxin. Two of these compounds, namely etoposide (VP-16) (**7**) and teniposide (VM-26) (**8**), showed promising antitumor effects and were selected for in depth pharmacological studies (Scheme 1.3). Teniposide was first tested in humans in 1967 and etoposide in 1971. Today, etoposide and teniposide are used primarily in the

clinical treatment of testicular and small-cell lung cancers, lymphomas, leukemias and Kaposi's sarcoma.

Research in the modification and derivatization of 4'-demethyl-epipodophyllotoxin is ongoing. Many 4-alkylamino⁹ and 4-arylamino¹⁰ derivatives and synthetic 2-aza-podophyllotoxin¹¹ analogues have been prepared and found to have significant antitumor properties. Recently, 5-methoxypodophyllotoxin, isolated from *Linum flavum* roots, and its β -D-glucoside derivative have been tested against murine Ehrlich ascites and human cervix uteri(HeLa) tumor cell lines and possess about the same activity as podophyllotoxin.¹²

Scheme 1.3



1.3 Mechanism of Action and Structure-Activity Relationships

The mechanism of action of the cytostatic activity of podophyllotoxin was shown by King and Sullivan to arise from an inhibition of cell spindle formation.⁴ The binding of

podophyllotoxin to tubulin prevented tubulin from polymerizing into the microtubules which form the spindle fibers resulting in a cessation of cell division in metaphase and chromosomal clumping. The ability of many of the podophyllotoxin analogues to poison spindle formation does not always correlate with observed antitumor activity.⁶ For instance, 4'-demethyl-podophyllotoxin benzylidene glucoside and 1-O-*p*-chlorophenylcarbamoyl-4'-demethyl-epipodophyllotoxin are poor spindle poisons (i.e. during mitosis) with the latter being a strong inhibitor of the entry of cells into mitosis (i.e. premitotic inhibitor). This suggests a second mechanism (preprophase) of action for cytostatic activity. The nature of the arrest of cell division was first alluded to by Huang *et al.* who showed chromosomal aberrations in VM-treated cells.¹³ It was later shown by Loike *et al.* that DNA fragmentation was occurring in VM and VP treated cancer cells. However, treatment of purified DNA with VP did not result in any strand breakage.¹⁴ The breakage of double strand DNA is not a direct result of VP or VM interaction with the DNA but rather is a result of the stabilization of a cleavable complex between DNA topoisomerase II (DNA gyrase) and DNA.^{15,16} DNA topoisomerases are enzymes that change the topology of DNA. They are responsible for the changes in the degree of supercoiling of DNA via cleavage of the DNA and rejoining as well as catenation/decatenation of circular double stranded DNA.^{17,18} Thus, treatment with the drug results in an interference with the enzyme's rejoining ability, producing fragmented DNA and ultimately stopping the cells from entering mitosis.

The structural, stereochemical, and conformational aspects of the podophyllum derivatives are intimately related to their efficacy as antitumor agents. In terms of structural requirements, it is evident that demethylation of the 4' position of podophyllotoxin is important. The substituent attached to C4 also dramatically affects the mode of action. If the substituent is a glucose molecule with an aldehyde condensed to it then the mode of action changes from spindle poisoning to DNA strand breakage. Replacement of the methylenedioxy group with methoxy groups in podophyllotoxin

(giving sikkimotoxin) results in reduction of cytostatic activity by almost three orders of magnitude.

The relative configuration of the groups on the tetralin ring is also important with regards to the effectiveness of the drug. Comparing the mitotic inhibition for the eight diastereomers of podophyllotoxin, it is apparent that a 1,2-*cis* stereochemistry and the *trans* lactone ring are requirements for activity (Table 3, entries 1, 2, and 6).

Epimerization of the 4-oxy group to the epi isomer (Table 2) for the 4'-demethyl- β -D-glucosides results in a substantial increase in the life span of leukemia infected animals (cf. entries 5 and 6, 8 and 9; Table 2).⁶ However, the antitumor effect is marginal for the epimer of 4'-demethylpodophyllotoxin (entry 3, Table 2), albeit the spindle poisoning mechanism decreased by an order of magnitude.

Table 2. Selected podophyllotoxin derivatives and their cytostatic activities.⁶

Entry	Compound	ID-50 (P-815) μ g/ml	L-1210 %incr. life span
1	podophyllotoxin	0.005	35
2	4'-demethylpodophyllotoxin	0.007	10
3	4'-demethylepipodophyllotoxin	0.06	7
4	podophyllotoxin- β -D-glucoside	6	7
5	4'-demethylpodophyllotoxin- β -D-glucoside	2	0
6	4'-demethylepipodophyllotoxin- β -D-glucoside	4	34
7	benzylidene-podophyllotoxin- β -D-glucoside	3	5
8	benzylidene-4'-demethylpodophyllotoxin- β -D-glucoside	0.8	29
9	benzylidene-4'-demethylepipodophyllotoxin- β -D-glucoside	0.009	65
10	SP-G	0.5	65
11	Etoposide	0.05	167
12	Teniposide	0.005	121

Table 3. Stereochemistry at ring B of podophyllotoxin as related to cytostatic potency.⁶

Entry	Compound	configuration			ID-50 (P-815) μ g/ml
		H1,H2	H2,H3	H3,H4	
1	podophyllotoxin	trans	trans	cis	0.005
2	epipodophyllotoxin	cis	trans	cis	0.03
3	picropodophyllotoxin	trans	cis	trans	0.2
4	epipicropodophyllotoxin	cis	cis	trans	1
5	isopodophyllotoxin	trans	trans	trans	1
6	epiisopodophyllotoxin	cis	trans	trans	0.02
7	isopicropodophyllotoxin	trans	cis	cis	0.5
8	epiisopicropodophyllotoxin	cis	cis	cis	0.6

Another important feature affecting biological activity which is partially determined by configuration is that of conformation.¹⁹ Conformation is not strictly

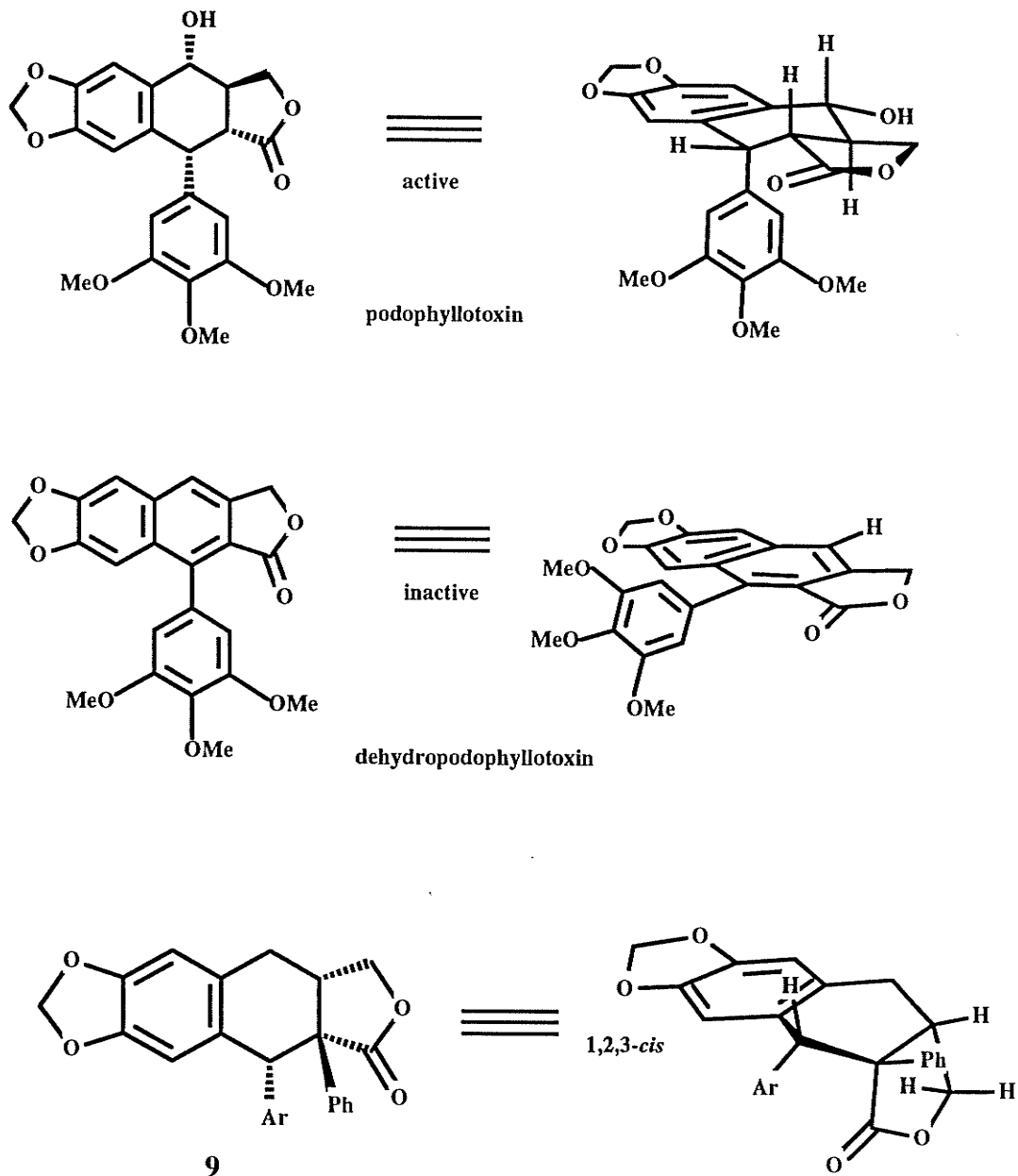
determined by configuration as some molecules that have a particular configuration may be conformationally flexible thus allowing them to adopt an energetically and biologically favorable conformation.

Podophyllotoxin has a rigid conformation imposed upon it by the *trans* lactone ring fusion (Scheme 1.4). NMR studies of various cytostatically active podophyllotoxin derivatives suggest that all of these compounds bearing the 1,2-*cis*-2,3-*trans* geometry have the same solution conformation.¹⁹ Evaluation of the H1 to H2 coupling constants allows calculation of dihedral angles using Karplus-type relationships. It was found that the derivatives of podophyllotoxin, including etoposide (VP-16-213) and epipodophyllotoxin all have H_{1,2} dihedral angles of 50 ± 4° indicating that the pendant aryl group has an axial disposition with respect to C and D rings. It is this conformational feature that has been deemed an important criterion for antitumor activity. Loike *et al.* have shown that dehydropodophyllotoxin is inactive towards inhibition of microtubule activity and they have attributed this to the planar orientation of the E ring with respect to the ABCD ring system (Scheme 1.4).²⁰ Picropodophyllotoxin, which has substantially reduced antimitotic activity, has a calculated average dihedral angle of 130° for H_{1,2} consistent with the molecule having a preferred conformation with an equatorial aryl group. As picropodophyllotoxin is a flexible molecule, the residual antimitotic activity has been attributed to a minor conformation in which the molecule possesses an axial aryl group.¹⁹ In contrast to the belief that the quasiaxial aryl group is a prerequisite for antitumor activity, Beard *et al.* have found that the all-*cis*-2-phenyl substituted deoxyisopicropodophyllotoxin **9** adopts a solution and solid state conformation in which the aryl group is in the equatorial position and still exerts a modest antitumor effect (Scheme 1.4).²¹

Quite often stereospecificity of drug/receptor interactions is an important criterion of drug efficacy. For many drugs, the absolute stereochemistry of the molecule is important since only one enantiomer will have the desired biological activity. This

Scheme 1.4

Active and inactive conformations of podophyllotoxin and dehydropodophyllotoxin.



stereospecificity has been rationalized via the mechanism of three point attachment. In this scheme, three chemically unique groups within the drug interact with a receptor site having a center or plane of asymmetry at the point of attachment.

The importance of this stereospecificity is exemplified in the cytostatic activity of various podophyllotoxin congeners and their corresponding optical antipodes. For

instance, (-)- β -apopicropodophyllotoxin (ID-50 = 0.002 $\mu\text{g/mL}$) is about as potent as podophyllotoxin whereas its optical antipode has essentially no effect (ID-50 = 2 $\mu\text{g/mL}$). Similarly, there is a significant decrease in the cytostatic potency of isodesoxy-podophyllotoxin when the (+)-isomer is changed to the (-)-isomer.

1.4 Asymmetric Synthesis, Diastereoselectivity and Enantioselectivity in the Diels-Alder Reaction.

The importance of producing optically pure compounds for use as drugs can be justified on the basis of the inherent stereospecificity requirements for the action of many drugs (see previous section). One method of preparing optically or enantiomerically pure (homochiral) compounds is by way of an asymmetric synthesis. An asymmetric reaction can be defined as one in which an achiral substrate or a prochiral center within a substrate, is converted to a chiral molecule or a chiral center such that one chiral form of the molecule or chiral center predominates over the other form. In a nonasymmetric synthesis, both optical forms are produced in equal amounts giving rise to a mixture of stereoisomers.

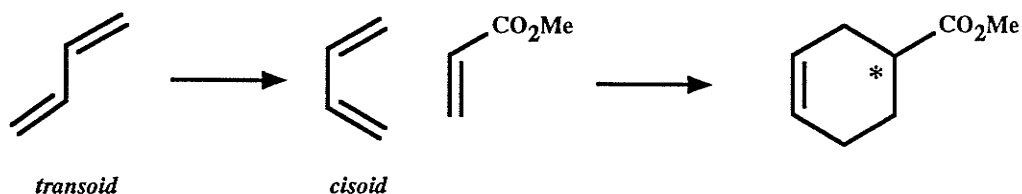
In order to achieve asymmetric induction in a reaction, the reactants must be within a chiral environment. In biological systems, the chiral environment may be the active site of an enzyme in which the substrate is converted to an optically pure product. To achieve the same enantioselectivity as that of the enzyme, the synthetic chemist must similarly impose a chiral environment. This is accomplished by the introduction of a chiral control element which may be incorporated into the final product or removed at later stages in the synthesis. Alternatively, the chiral control element may be part of a catalyst whereby there is no incorporation of the chiral auxiliary into the final product.

In order to fully delineate the concepts of asymmetric synthesis, one must differentiate between the idea of an enantioselective and a diastereoselective synthesis.

This is best done through illustration and the following example of a Diels-Alder cycloaddition reaction between butadiene and methyl acrylate may be edifying.

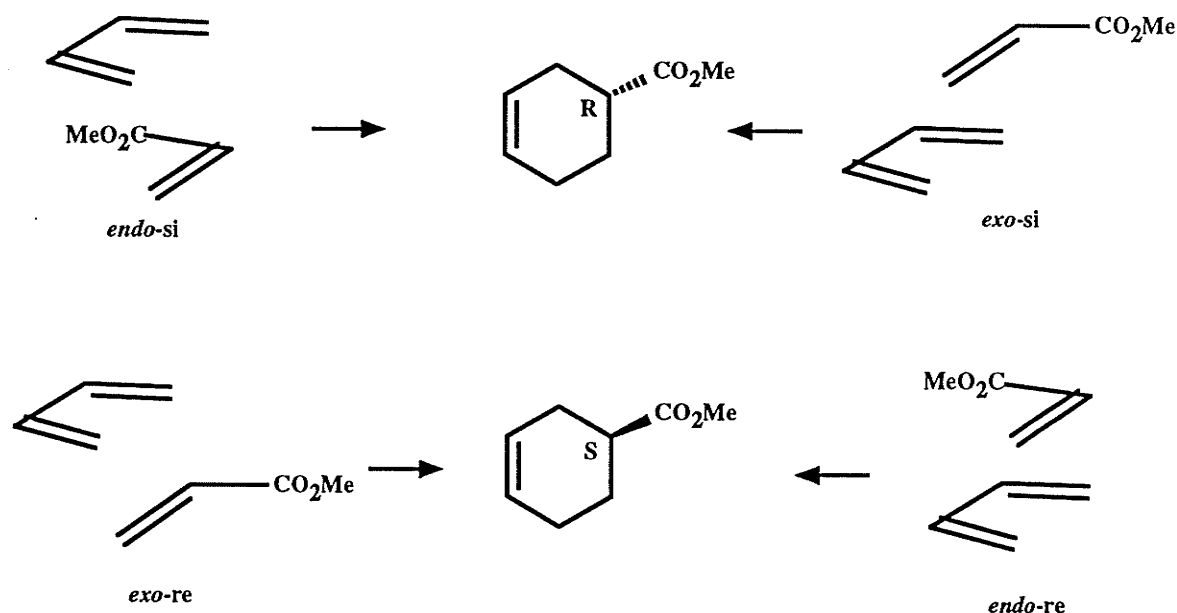
In order for a Diels-Alder reaction to occur, the diene must first undergo rotation about the central bond to generate the *cisoid* conformation (Scheme 1.5). This *cisoid* conformation, although present in only 1% abundance with respect to the *transoid* isomer, can now undergo reaction with a dienophile like methyl acrylate. Although this reaction

Scheme 1.5



creates a new chiral center as indicated by the starred carbon (*), both enantiomers will be produced in equal amounts since both the starting diene and dienophile are achiral. The reason for this becomes evident when we consider the possible transition states leading to the final products. In this reaction, there are four possible transition states; two *endo* and two *exo* (Scheme 1.6). The preferred *endo* transition state is the one in which the carboxymethyl group lies underneath the diene whereas the *exo* transition state has the carboxymethyl group directed away from the underside of the diene. For the *endo* or *exo* transition states, butadiene can add to either face of the acrylate with equal probability. Butadiene is C₂ symmetric and therefore addition to either of its faces are equivalent. Although the two faces of the acrylate are enantiotopic, the transition state energies for addition to either the *re* or *si* face of the acrylate are identical. This results in equal formation of the two enantiomers and hence the reaction is not enantioselective. However, if one is able to preferentially form one enantiomer over the other then the reaction would be enantioselective and would constitute an asymmetric reaction. Asymmetric induction could be accomplished if one face of the acrylate were blocked or

Scheme 1.6

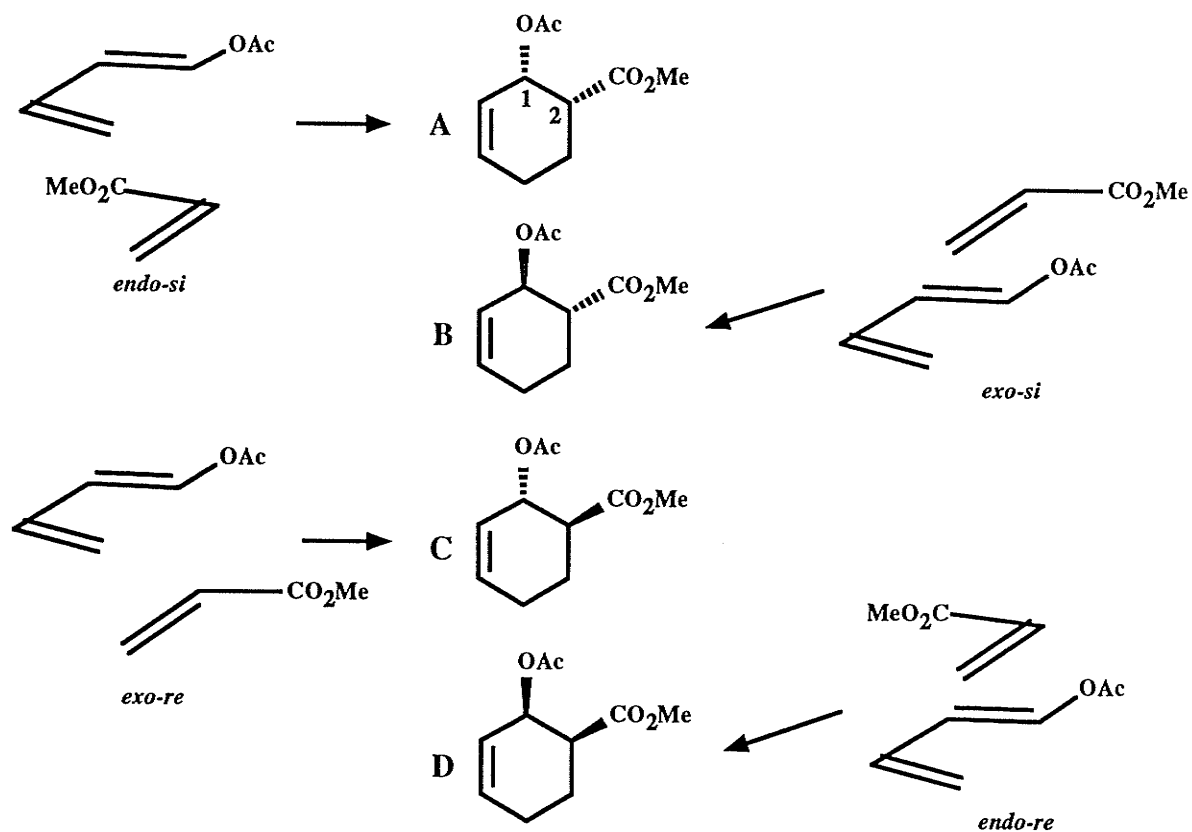


were less reactive for some reason. It should be noted that in this particular example, addition to the *si* face of the acrylate gives rise to the *R* chiral center and addition to the *re* face gives the *S* chiral center irrespective of whether the reaction proceeded through an *endo* or *exo* transition state.

The consequences of diastereoselectivity can be realized if, for example, a substituent is added to the terminal position of the diene. Consider the addition of 1-acetoxy butadiene to methyl acrylate (Scheme 1.7). As shown, this reaction cannot be enantioselective as both enantiomers in each respective pair A/D and B/C would be produced in equal amounts. However, the *endo* and *exo* transition states leading to the two diastereomeric pairs AD and BC respectively are different in energy and thus the reaction is said to be diastereoselective since A and D would be preferentially produced over B and C.

For an unsymmetrical diene bearing a group in either the 1 or 2 position and reacting with an unsymmetrical dienophile, there are two possible regiomic isomers that can form (Scheme 1.8). The 1,2 (*ortho*) or 1,4 (*para*) products for the 1 and 2-substituted

Scheme 1.7

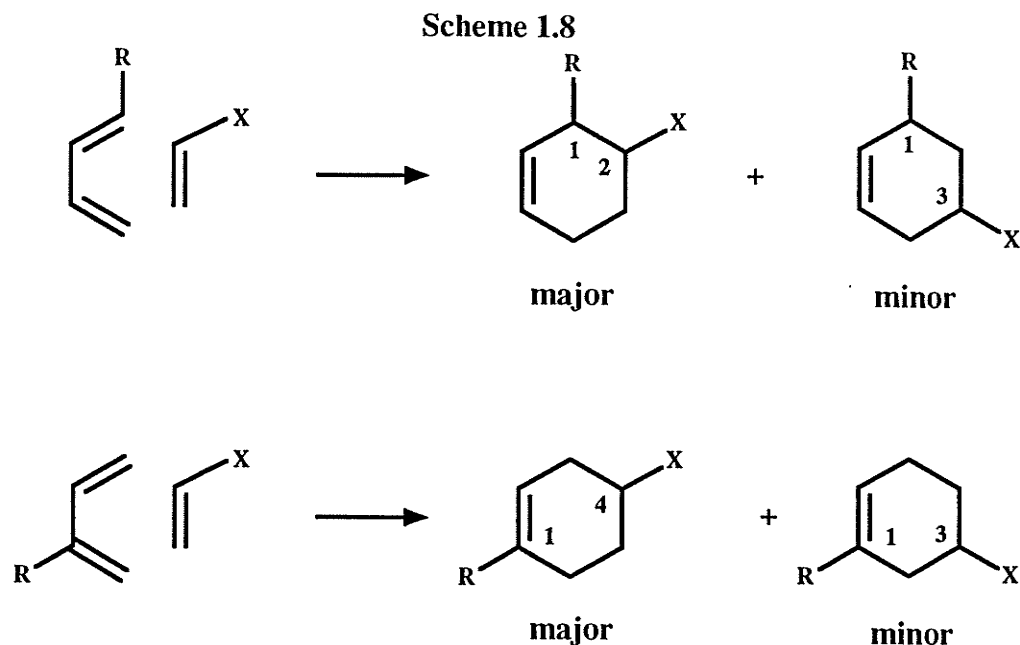


dienes respectively are preferred over the *meta* products. The *ortho* or 1,2-adducts arise from head-to-head addition whereas head-to-tail addition gives rise to the 1,3-adducts.

This regioselectivity can be rationalized on the basis of Frontier molecular orbital (FMO) theory. For Diels-Alder reactions, FMO theory suggests that *reactions are allowed only when all overlaps between the highest-occupied molecular orbital (HOMO) of one reactant and the lowest-unoccupied molecular orbital (LUMO) of the other are such that a positive lobe overlaps only with another positive lobe and a negative lobe only with another negative lobe.*²²

Diels-Alder reactions can be classified into three types:²³

1. **Normal Electron Demand.** The normal electron demand reaction is dominated by interaction of the diene-HOMO and dienophile-LUMO.
2. **Neutral Electron Demand.** In the neutral electron demand reaction both the diene-HOMO/dienophile-LUMO and the diene-LUMO/dienophile-HOMO interactions



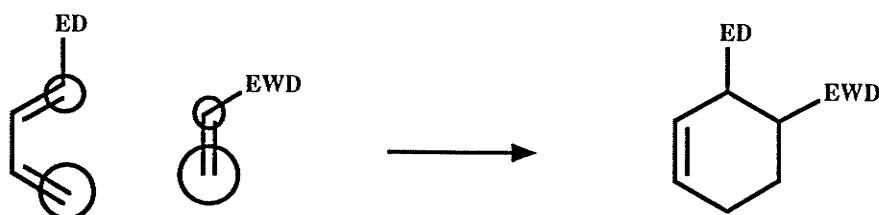
are important in controlling the regioselectivity.

3. Inverse Electron Demand. The dominant orbital interactions involve the diene-LUMO and the dienophile-HOMO overlaps.

The preferred interactions can be determined by comparing the relative differences in energy between the two HOMO/LUMO orbitals. Those orbitals which are closest in energy will be the ones which determine the type of reaction and hence the regiochemistry of the reaction.

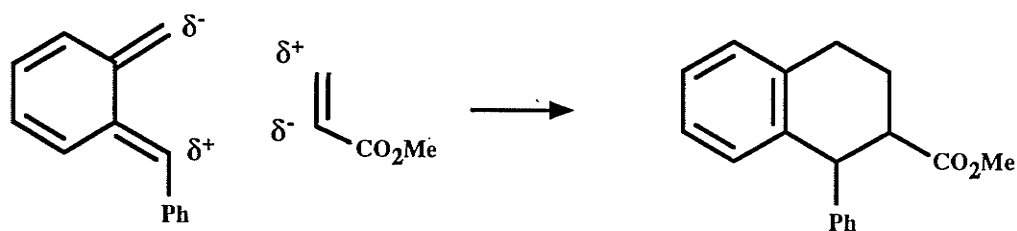
Most Diels-Alder reactions are the normal electron demand type, hence the most favorable interaction is between the HOMO of the diene and the LUMO of the dienophile. The orientation of the substituents in the final product can be predicted on the basis of the preferred interaction of the terminal HOMO orbital of the diene bearing the largest coefficient with the LUMO orbital of the dienophile bearing the largest coefficient (Scheme 1.9). This implies that dienes with electron donating substituents in the 1-position reacting with dienophiles bearing electron withdrawing groups will add to give *ortho* products. Sometimes, the relative magnitudes of the orbital coefficients for terminal positions of the diene are the same and thus the primary orbital effects do not always

Scheme 1.9

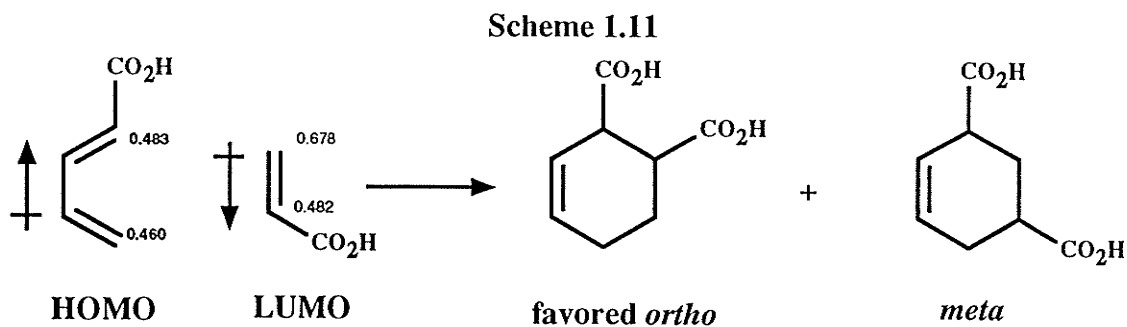


control the regioselectivity. This is the case for the addition of an *E*- α -aryl-*o*-quinodimethane reacting with methyl acrylate (Scheme 1.10).²⁴ Although the reaction proceeded in a head-to-head manner, the regioselectivity cannot be attributed to primary orbital interactions as ab-initio calculations show that the C_1 and C_4 orbital coefficients of *E*- α -phenyl-*o*-quinodimethane are almost equal.²⁵ However, the calculations also show a decrease in the electron density of the carbon atom bearing the phenyl group. This asymmetric charge distribution results in an electric dipole that interacts with the dipole of methyl acrylate resulting in head-to-head addition in the transition state. Other authors have argued against the importance of dipole-dipole

Scheme 1.10



interactions in determining the regiochemistry of the reaction.²⁶ For instance, dipole-dipole interactions for the addition of 1-carboxybutadiene and acrylic acid favor the *meta* isomer yet the *ortho* isomer is preferred (8.8:1, *ortho:meta*) (Scheme 1.11). The preference for the *ortho* isomer in this case cannot be attributed to the primary frontier orbital interactions. Examination of the relative energies of the HOMO and LUMO orbitals for acrylic acid and 1-carboxymethyl-1,3-butadiene suggest that the preferred orbital interaction is between the HOMO of the diene and the LUMO of the dienophile.²⁷ Although Fleming suggests the preference for *ortho* addition is explained by FMO



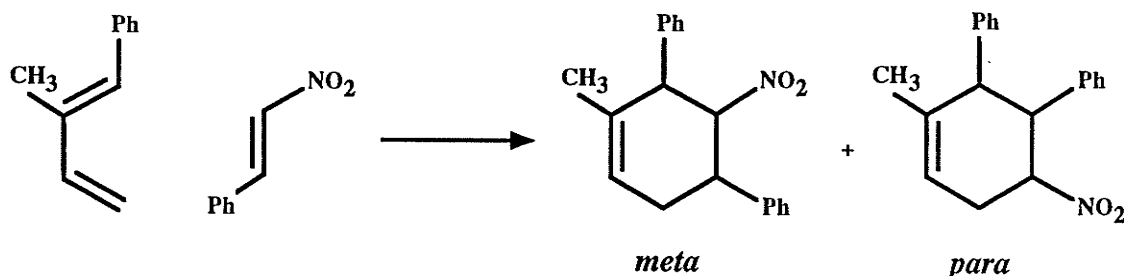
theory,²⁷ overlap of the largest HOMO-diene²⁸ and LUMO-dienophile²⁹ orbital coefficients predicts a preference for *meta* addition. This preference for *ortho* addition must find explanation in another form.

Secondary orbital interactions may also have a role in determining regiochemical preferences in certain cases.^{26,27} For normal electron demand reactions, this secondary interaction involves interaction between the HOMO secondary orbitals of the diene with the LUMO secondary orbitals of the dienophile. This secondary orbital effect is only possible for the *endo* transition state whereby a vacant orbital on the carbonyl carbon can overlap with the C2 carbon of the diene.

Addition of Lewis acids can have significant effects on the rate of the reaction as they substantially lower the frontier orbital energies. Concomitant with the lowering of the orbital energies is an increase in the magnitude of the LUMO coefficient of the carbonyl carbon of the dienophile and an increase in the difference in the magnitudes of the LUMO coefficients of the alkene.²⁶ This suggests an increase in the domination of HOMO-diene/LUMO-dienophile interaction thus promoting an increase in the regioselectivity over the uncatalyzed reaction with the *ortho* isomer being the predominant one. However, the increase in the magnitude of the carbonyl coefficient upon addition of the catalyst results in a greater influence of the secondary orbital interactions which may favor the opposite regioisomer. For the addition of 2-phenyl-1,3-butadiene to methyl acrylate, the primary interactions supersede the secondary interactions resulting in an increased preponderance of the *para* isomer. A very dramatic effect is observed for the

addition of 1-phenyl-2-methyl-1,3-butadiene to β -nitrostyrene (Scheme 1.12). In the uncatalyzed reaction, the primary HOMO-diene/LUMO-dienophile interaction predominates over the weak secondary orbital interaction and leads to exclusive formation

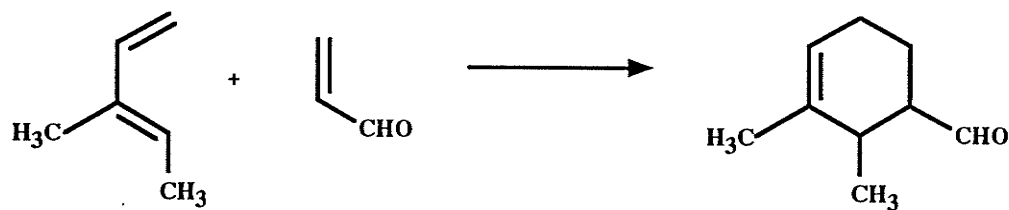
Scheme 1.12



of the *para* isomer. Upon catalysis however, the *meta* isomer becomes the exclusive product as a result of the greatly enhanced secondary orbital interactions. This interaction involves the overlap of the LUMO coefficient on the nitrogen with the C2-HOMO coefficient of the diene.

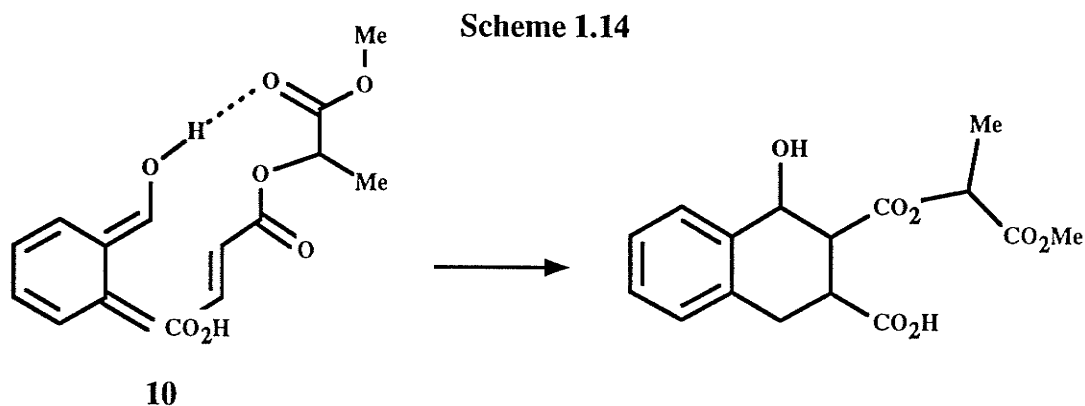
The validity of FMO theory as a predictive model for regiochemical preferences has been met with controversy.³⁰ There are many examples where FMO theory predicts one preference and experiment demonstrates the other. Also, discrepancies exist in the prediction of regioselectivity for competing substituents on dienes using the substituent additivity rules. As an example of the latter, calculation of the terminal coefficients of 1-acylamino-4-methoxybutadiene suggests an equal directing effect of the two groups whereas a strong directing effect of the methoxy group follows from additivity of the corresponding monosubstituted dienes. FMO theory and resonance theory both predict that electron donating groups in the 2-position have a greater regiodirecting ability than donors substituted in the 1-position and would favor *para* products yet experiment shows that the *ortho* products are preferred over the *para* products (Scheme 1.13).

Scheme 1.13



Kahn *et al.* proposed that inclusion of secondary orbital interactions for explaining regioselectivity within the FMO approximation is unfounded.³⁰ They suggest an alternate approach to FMO theory for the ordering of regiochemistry based on the matching of complementary reactivity surfaces for diene and dienophile. For normal demand Diels-Alder reactants, the nucleophilic reactivity surface of the dienophile is assessed by its interaction with a test hydride nucleophile. The corresponding electrophilic reactivity (electrostatic potential) surface of the diene is assessed by its interaction with a test proton electrophile. The points of highest reactivity on the diene and dienophile are then matched in order to determine the regiochemical preferences.

A very interesting example of regiochemical control via intermolecular hydrogen bonding has also been observed.³¹ The addition of α -hydroxy-*o*-quinodimethane **10** to mono-lactyl fumarate gives a single product with the hydroxyl group *ortho* to the lactyl ester group (Scheme 1.14). In this example, a hydrogen bond between the lactyl carbonyl and the hydroxyl group may control the regioselectivity.



1.5 Stereochemical Control (*Endo/Exo*) in the Diels-Alder Reaction

While the primary orbital interactions generally dominate the regiochemistry of the products, secondary orbital interactions can influence the diastereoselectivity or the *exo/endo* ratio. This secondary orbital interaction involves an overlap of a p_z orbital of the diene with the LUMO on the α -substituent of the dienophile. This interaction can provide for a net stabilization in the *endo* transition state. This interaction is not physically possible in the *exo* transition state.

Other factors besides secondary orbital interactions may be important in the control of diastereoselectivity. In the additions of methyl acrylate to various 1-substituted dienes, it was found that highly electron donating substituents on the diene fail to control the *endo* diastereoselectivity.²⁹ Molecular orbital calculation shows that increasing the electron donating ability of the group not only increases the difference in the magnitudes of the C2 and C3 HOMO coefficients but also increases the gross orbital charge or exclusion shell volume at C2. While the secondary orbital interactions favor the *endo* isomer, the increased closed-shell repulsions disfavor it. Thus the *endo/exo* selectivity is controlled by a balance of these two competing interactions.

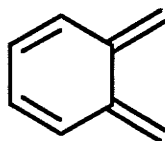
1.6 Generation of *o*-Quinodimethanes

This section will deal with the generation and reactivity of *o*-quinodimethanes of the types which are pertinent to the experimental work in this thesis. An extensive review of orthoquinodimethanes has been published which describes their generation, reactivity, diastereoselectivity, and their use in natural product synthesis.³²

An *o*-quinodimethane, also known as an *o*-xylylene or an *o*-quinodimethide, has the general structure given by **11** (Scheme 1.15). This reactive intermediate has only been isolated in a glassy matrix at -196°C by photolysis of the corresponding

dihydrodiazanaphthalene.³³ In solution at room temperature their lifetimes are generally less than one second.

Scheme 1.15

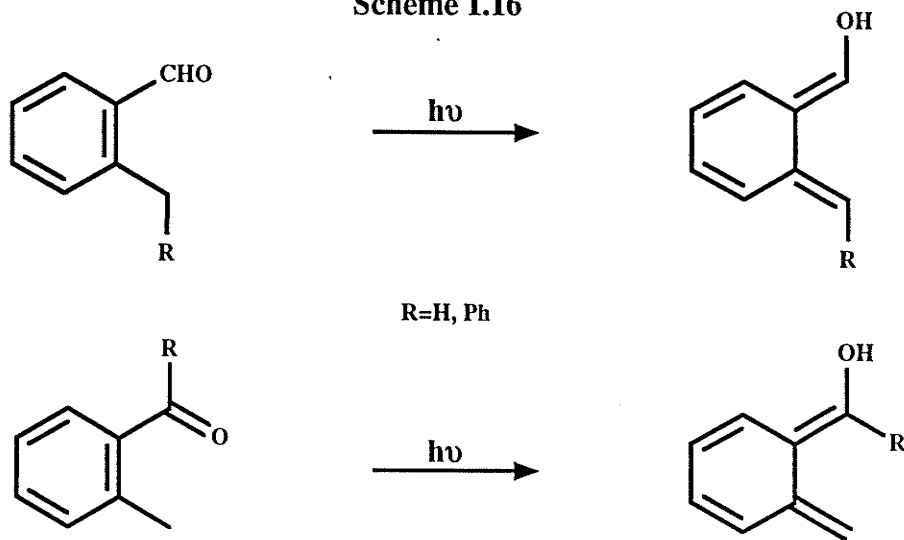


11

o-Quinodimethanes can be generated by a variety of methods including 1,4-elimination processes, Diels-Alder cycloreversions (expulsion of CO₂ and N₂), photochemical expulsion of carbon monoxide, extrusion of SO₂ from sulfones and sultines, thermolysis of benzocyclobutenes, and photoenolization.³² The three methods that will be discussed here are the thermolysis of sulfones and benzocyclobutenols and the photoenolization of *ortho* alkyl substituted benzaldehydes and ketones.

The photolysis of *o*-alkylbenzophenones or *o*-alkylbenzaldehydes provides a convenient method for preparation of α -hydroxy-*o*-quinodimethanes as the corresponding ketones and aldehydes are readily prepared (Scheme 1.16). The mechanism involves an

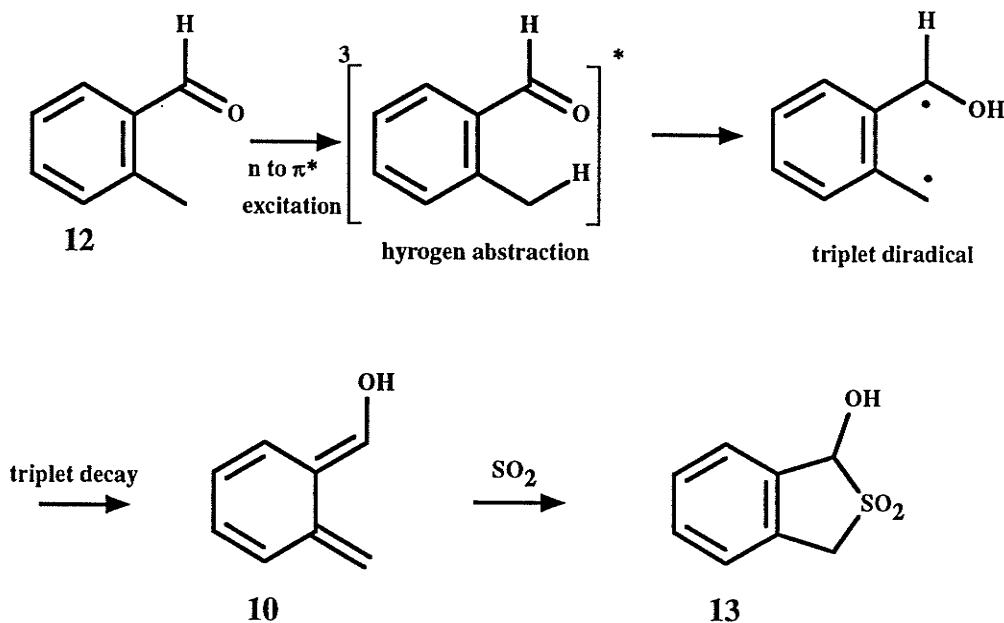
Scheme 1.16



to π^* excitation of the carbonyl group followed by intersystem crossing to the first excited triplet state (Scheme 1.17). The excited carbonyl group must be able to rotate inward to

allow for the subsequent intramolecular hydrogen abstraction step. The triplet diradical then decays to the ground state dienol via internal conversion.³⁴ The α -hydroxy-*o*-QDM

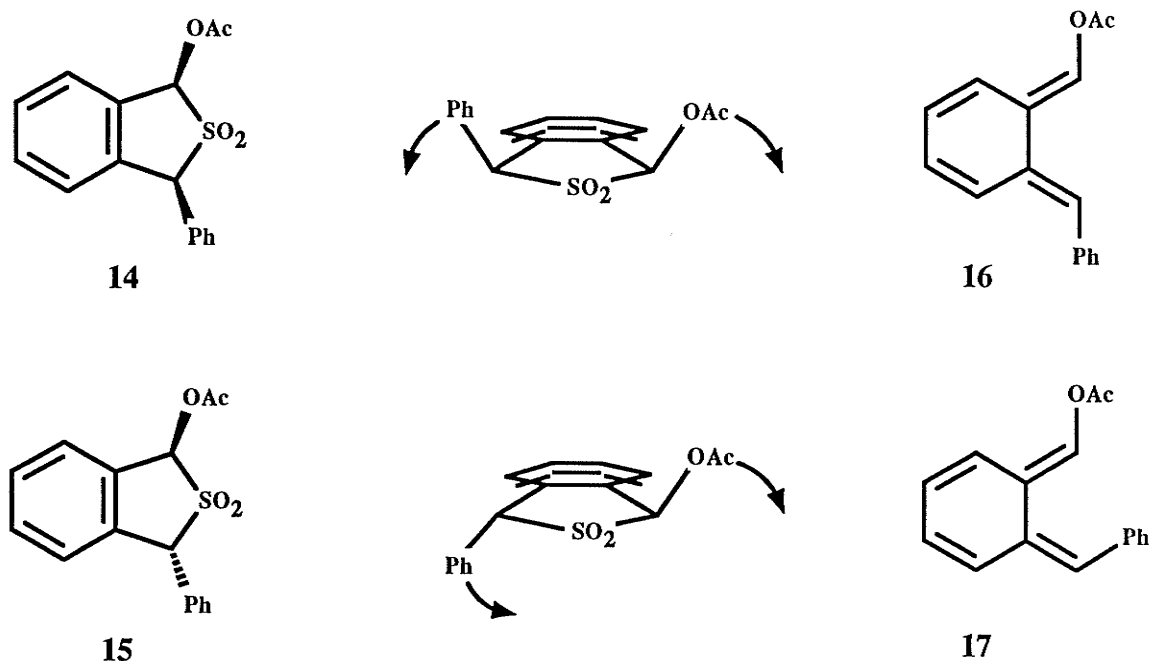
Scheme 1.17



10 can then be trapped with various dienophiles or alternatively with SO_2 giving the corresponding hydroxysulfone **13**.^{35,36} These sulfones can serve as *o*-QDM precursors via thermolysis and extrusion of SO_2 . Hydroxy-sulfones are relatively stable and serve as suitable precursors for the attachment of α -alkoxy groups.³⁵ For 1,3-substituted alkoxy-sulfones, the relative stereochemistry of the sulfone is intimately related to the geometry of the precursor α -alkoxy- α' -subst-*o*-QDM and vice-versa.²⁵ Starting from the *cis*-acetoxy-sulfone **14**, pericyclic extrusion of SO_2 yields the *E,E*- α -acetoxy- α' -phenyl-*o*-QDM **16** (Scheme 1.18). Presumably the *Z,Z* geometry is unfavorable for steric reasons. Thermolysis of the diastereomeric *trans*-acetoxy-sulfone **15** results in formation of the *E,Z*- α -acetoxy- α' -phenyl **17**. It is also conceivable that the *Z,E*-isomer having the acetyloxy group inward and the phenyl group outward could form. However, Sammes has noted the reluctance of α -oxy groups to occupy the *Z*-position.³⁷ Given the observed geometries of the *o*-QDMs derived from the thermolysis of their

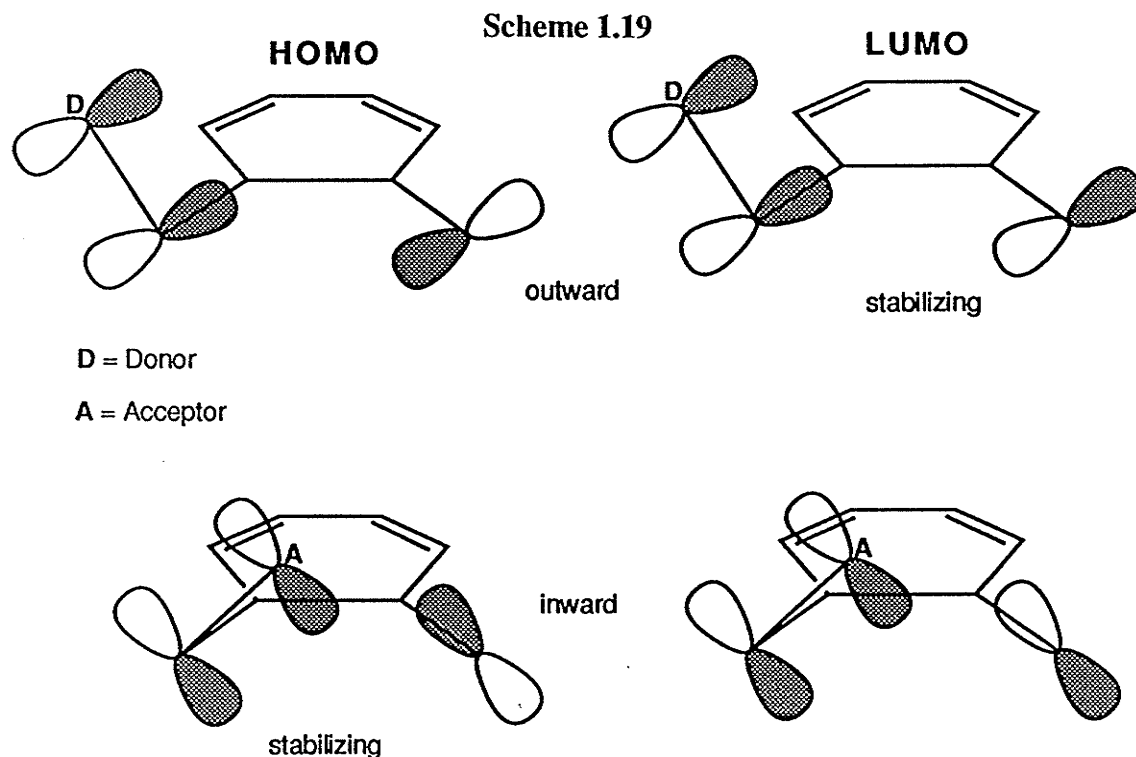
respective sulfones, the electrocyclic ring opening of sulfones must proceed via a disrotatory process.

Scheme 1.18



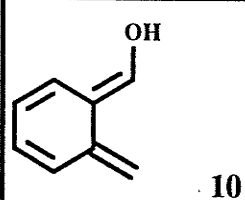
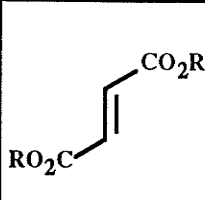
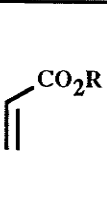
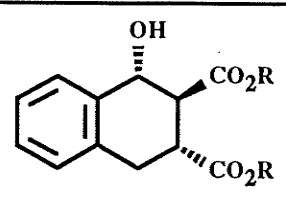
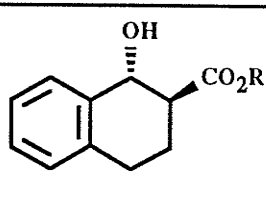
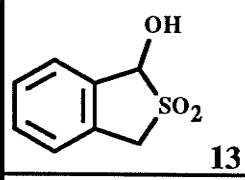
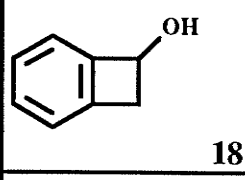
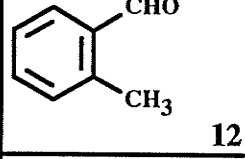
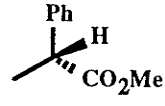
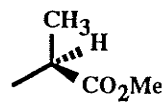
Benzocyclobutene derivatives, like benzocyclobutenol **18** (Table 4), serve as synthetically useful *o*-QDM precursors. Benzocyclobutenes ring open via a thermally allowed conrotatory process to give the reactive *o*-QDM. The direction of the rotation depends on the nature of the substituents attached to the ring. Experimentally, groups such as cyano, alkoxy, amino, ester and alkyl groups all favor strong outward rotation whereas strong acceptor groups such as formyl, ketones, iminium, and dialkylboronyl favor inward rotation.³⁸ Although cyano and ester groups are generally thought of as acceptor groups, they both display a strong preference for outward rotation. It must be remembered that cyano and ester groups are relatively poor acceptor groups as they possess doubly filled orbitals in the form of non-bonding electrons. Recently, Jefford *et al.* have proposed that this twisting preference, known as torquoselectivity, arises from electronic effects between interacting molecular orbitals of the substituent and the breaking C-C bond (Scheme 1.19).³⁸ For donating groups, outward conrotation allows

for a stabilizing overlap with the LUMO of the breaking bond. Conversely, inward conrotation leads to an unfavorable interaction of a doubly occupied donor orbital with the HOMO of the breaking bond. For acceptor groups, rotational preferences are reversed because overlap of the empty acceptor orbital (LUMO) with the HOMO of the breaking bond is more favorable. It is also interesting to note that inward rotation of an acceptor group engenders a Hückel array of molecular orbitals.



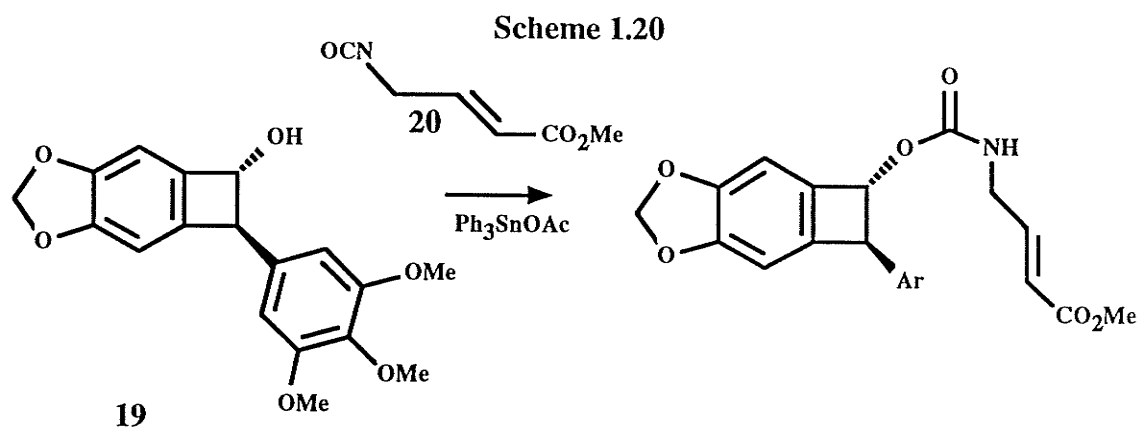
As *o*-QDM precursors, benzocyclobutenes and benzocyclobutenols have distinct advantages over the use of sulfones and *o*-alkylbenzaldehydes. Table 4 shows the reactions of α -hydroxy-*o*-QDM, generated from three sources, with methyl lactate and methyl mandelate substituted fumarates and acrylates. For comparison, benzocyclobutenol **18** efficiently reacts with the acrylate and fumarate of methyl *S*-lactate, whereas the corresponding hydroxysulfone **13** reacts only with the fumarate. The photolysis of *o*-methylbenzaldehyde **12** in the presence of the fumarate of methyl *S*-lactate leads to isomerization of fumarate to maleate in addition to cycloadduct formation. The production of maleate presents the possibility for the production of other

Table 4. Reaction of α -hydroxy-*o*-QDM with mandyl and lactyl dienophiles.

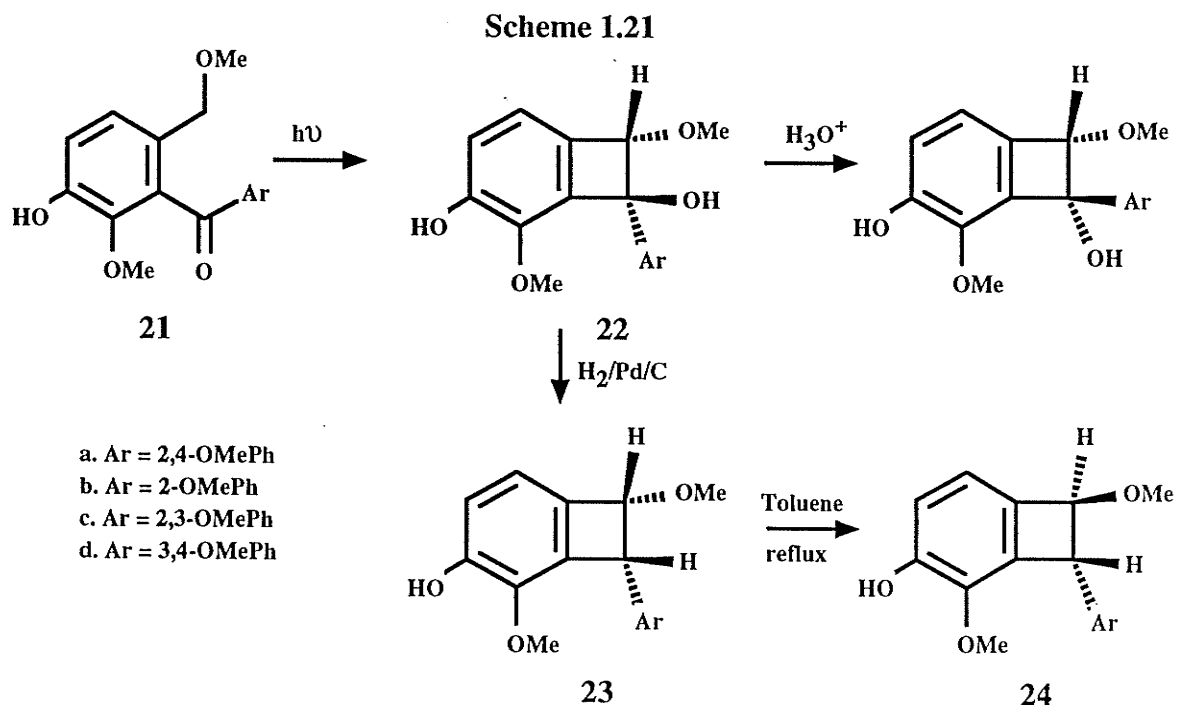
<i>o</i> -QDM precursor	fumarate	acrylate	fumarate product	acrylate product
 10				
 13	Toluene 110° C	Toluene 110° C	R=mandelate 55 % R=lactate 58%	R=mandelate 0 % R=lactate 0%
 18	Toluene 110° C	Toluene 110° C	R=mandelate 96 % R=lactate 58%	R=mandelate 56 % R=lactate 73%
 12	Benzene h ν /rt	Benzene h ν /rt	R=mandelate 52 % R=lactate 55%	R=mandelate 51 % R=lactate 55%
 R=mandelate		 R=lactate		

cycloadducts.^{39,40} This isomerization presumably arises from triplet energy transfer from *o*-methylbenzaldehyde to fumarate.

Benzocyclobutenols, although efficient sources of *o*-QDMs, are sometimes difficult to synthesize because of their instability. In Durst's synthesis of podophyllotoxin, the requisite benzocyclobutenol **19** was found to be extremely labile at temperatures above 0°C (Scheme 1.20). In addition, the synthesis suffered from the large number of steps and difficulties in tethering the dienophile **20** to the inherently unstable benzocyclobutenol.⁴¹ Jung also failed at many attempts in the synthesis of **19**⁴² but eventually succeeded in its synthesis via a method similar to the benzyne route used by Durst.⁴³ More recently, Saá has synthesized a benzocyclobutenol analogue of **19** by photolysis of the phenolic



benzophenone **21a** in THF to give 1-aryl-2-methoxybenzocyclobutenol **22a** which was subsequently stereoselectively converted to the *cis* 1-methoxy-2-aryl-benzocyclobutene **23a** by hydrogenolysis (Scheme 1.21).⁴⁴ However, the observed diastereomeric ratios of **23** to **24** was found to be highly dependent on the substituent pattern found on the aryl ring. It is interesting to note that the mixture could be converted to the more thermodynamically stable isomer **24** by refluxing in toluene. It is unlikely that isomerization occurred via a disrotatory ring closure reaction as this is a forbidden transition state which violates the Woodward-Hoffmann rules.⁴⁵

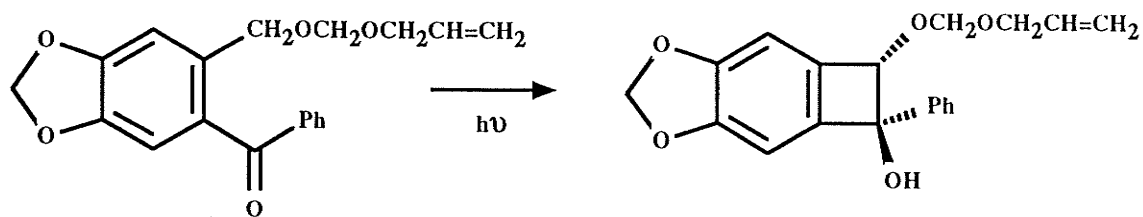


The mechanism of photochemical cyclization of *o*-alkylbenzaldehydes and *o*-alkylbenzophenones to benzocyclobutenols ostensibly precludes the existence of an intermediate dienol which would have to subsequently cyclize to give the benzocyclobutenol. Evidence for the absence of an intermediate dienol was substantiated through irradiation experiments which revealed that benzocyclobutenols are formed in the presence of deuterated acids with no observable deuterium incorporation in the benzylic position of the starting benzophenone **21** or the product benzocyclobutenol **22**. Deuterium incorporation would result from protonation of the dienol regenerating a deuterated benzophenone which could then undergo photolysis leading to a deuterated benzocyclobutenol. Molecular orbital calculations (AM1) revealed that, in general, 1,2-dioxygenated benzocyclobutenes (**22a-d**) are less stable than the corresponding *o*-quinodimethanes by 5-7 kcal/mol. Thus AM1 calculations also disfavour a dienol intermediate.⁴⁶ It has been proposed that benzocyclobutenol formation from irradiation of congested benzophenones may proceed via a reaction-induced intersystem crossing (ISC) mechanism.⁴⁶ The triplet biradical, produced from hydrogen atom abstraction by the excited carbonyl group, must undergo ISC to a singlet state before bond formation can occur.⁴⁷ As bonds bearing the terminal biradical ends rotate along the reaction coordinate, the triplet and singlet energies rise until the singlet becomes stabilized by partial bond formation. At this point, the singlet and triplet energy manifolds cross and results in ISC to the singlet. Why the irradiation of non-sterically congested benzophenones and aldehydes does not produce benzocyclobutenols is unclear.

Photochemical formation of benzocyclobutenols such as **22** (Scheme 1.21) appears to require the presence of a methoxy group *ortho* to the ketone which forces the aryl group to become perpendicular, thus impeding the electronic influence of the methoxy groups.

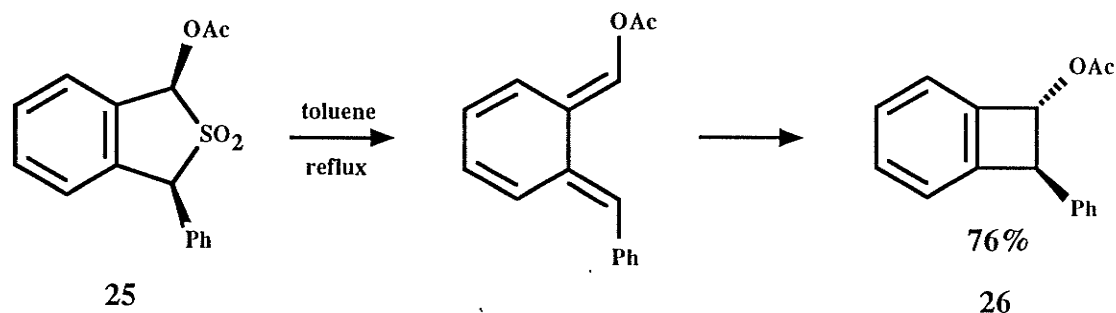
Kraus has reported a similar photochemical cyclization albeit the precursor benzophenone did not have the 2-methoxy group which Saá deemed necessary for benzocyclobutenol formation (Scheme 1.22).⁴⁸

Scheme 1.22



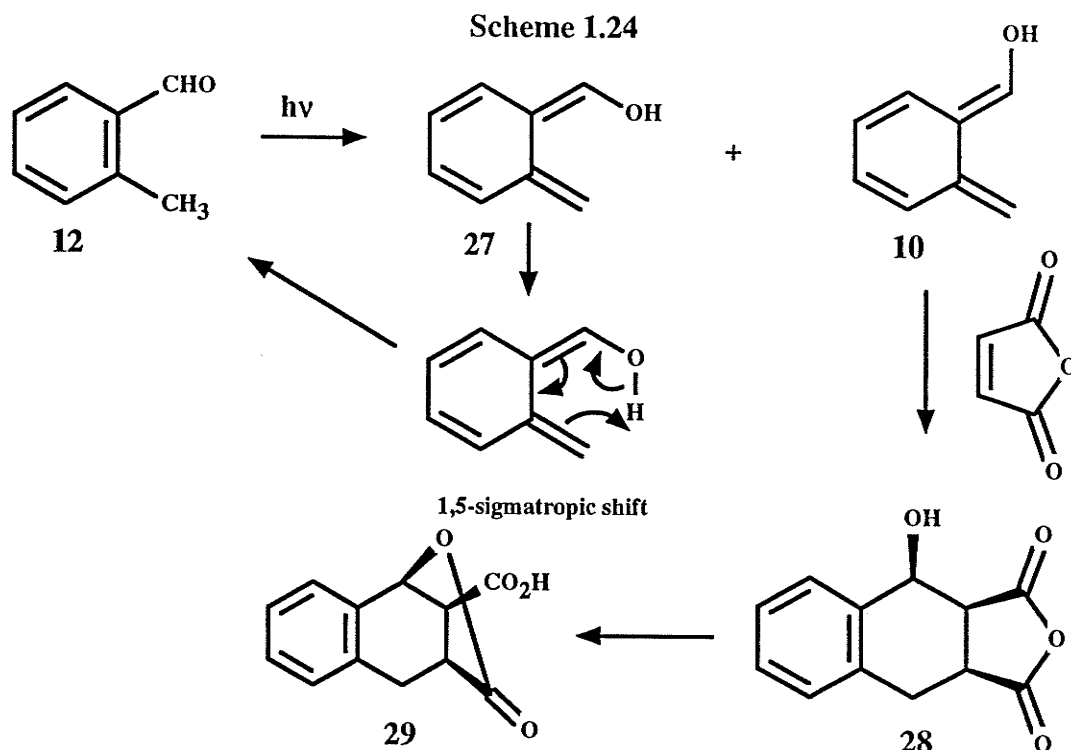
An interesting example of benzocyclobutene formation arising from an *o*-QDM precursor was reported by Charlton *et al.*²⁵ In this case, thermolysis of the *cis*-1-acetoxy-3-phenyl sulfone **25** led to the formation of *trans*-1-acetoxy-2-phenylbenzocyclobutene **26** presumably through the intermediate *E,E*-*o*-QDM (Scheme 1.23). One must therefore conclude in this case that benzocyclobutene **26** is more stable than the intermediate *E,E*-*o*-QDM.

Scheme 1.23



1.7 Diastereoselectivity in the Reactions of *o*-QDMs.

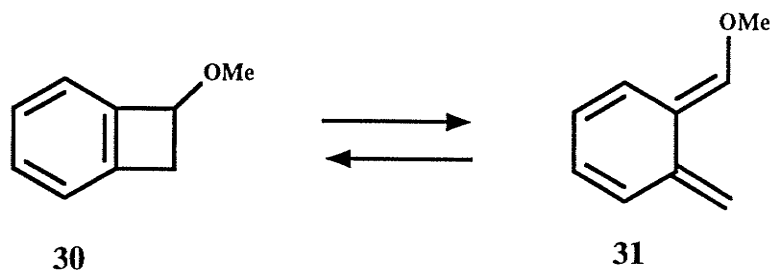
This section will be devoted to the reactions of various substituted *o*-quinodimethanes with dienophiles with reference to the diastereochemical preferences. The stereochemical outcome of the reaction of *o*-QDMs with dienophiles depends significantly on the substitution and geometry of the *o*-QDM and dienophile. α -Hydroxy-*o*-QDM was first generated by Sammes *et al.* by photolysis of *o*-methylbenzaldehyde⁴⁹ and was trapped with maleic anhydride giving a single adduct **28** having the all-*cis* geometry (Scheme 1.24). The stereochemistry was confirmed by



thermally induced cyclization to give the 1,3-lactone **29**. The same adduct was also formed from the thermolysis of benzocyclobutenol in the presence of maleic anhydride.⁵⁰ Although it has been shown that both the *E* **10** and *Z*-*o*-QDM **27** are produced upon photolysis,⁵¹ the lifetime of the *Z*-dienol **27**, as measured by flash photolysis, is much shorter than the *E*-dienol **10**. The *Z*-dienol likely undergoes rapid return to the starting aldehyde by a 1,5-sigmatropic hydrogen shift thus precluding its reaction with maleic anhydride. Given the short lifetime of the *Z*-dienol **27**, the cycloadduct **28** probably arises exclusively from **10**.

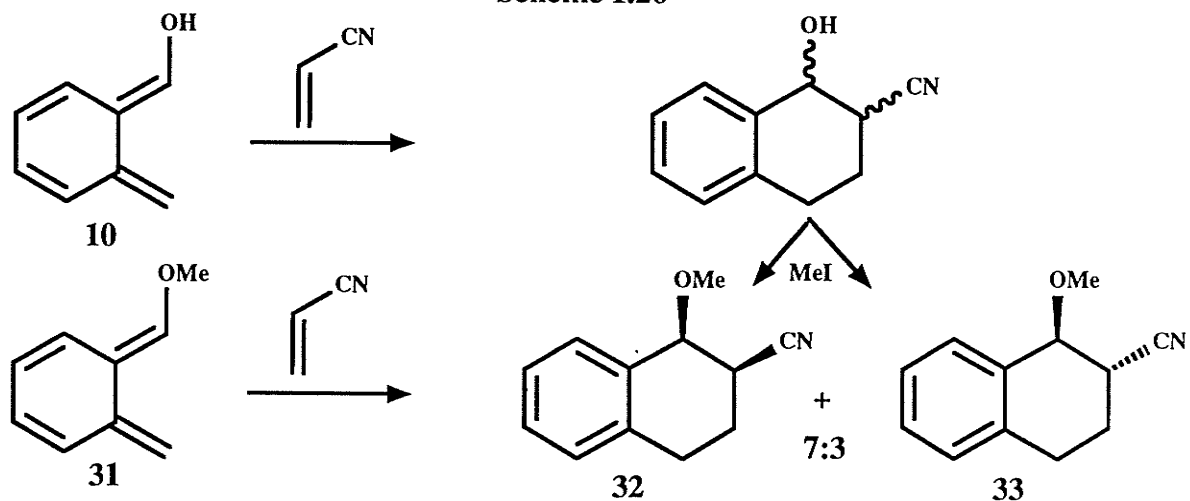
The cycloadduct formation does not appear to involve a preassociation with the benzocyclobutenol before reaction. The reaction of (+)-1-methoxybenzocyclobutene **30** with maleic anhydride gave rise to racemic products establishing the trapping of a planar, achiral intermediate **31** (Scheme 1.25).⁵⁰ Similar results were obtained for the chiral benzocyclobutenol **18** reacting with maleic anhydride in which racemic adducts were obtained. This indicates that hydrogen bonding between the benzocyclobutenol and

Scheme 1.25

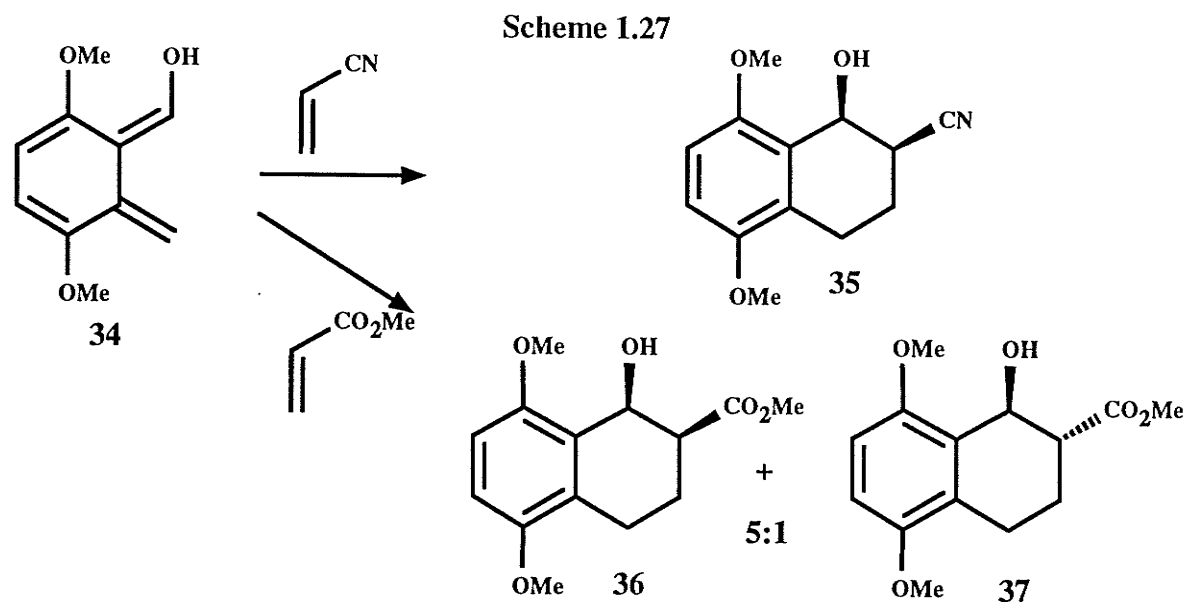


dienophile is not important before ring opening. However, both reactions diastereoselectively formed *endo* products (1,2-*cis*). Reaction of dienol **10** with acrylonitrile was non-stereoselective and characterization of the mixture of adducts by methylation revealed a 7:3 mixture of *endo* **32** and *exo* **33** isomers respectively (Scheme

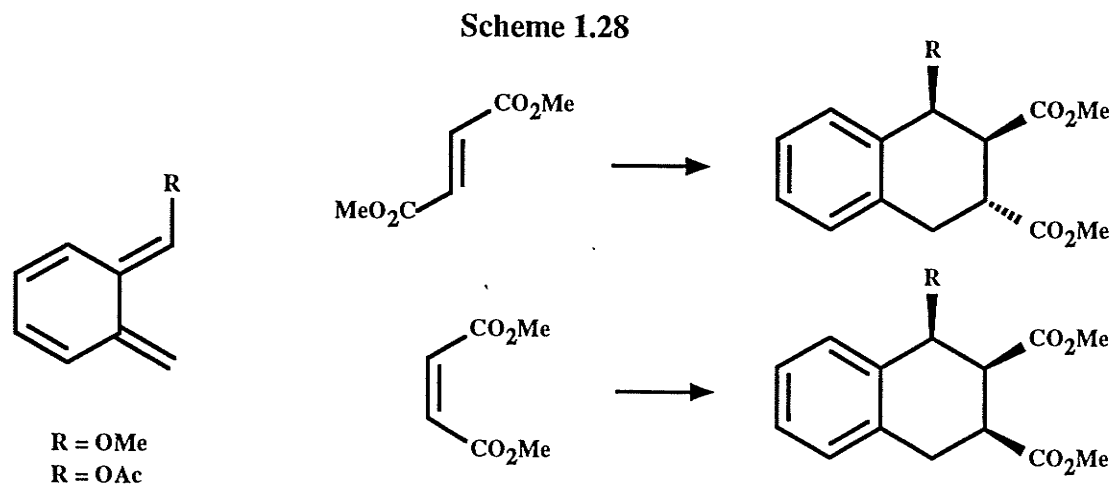
Scheme 1.26



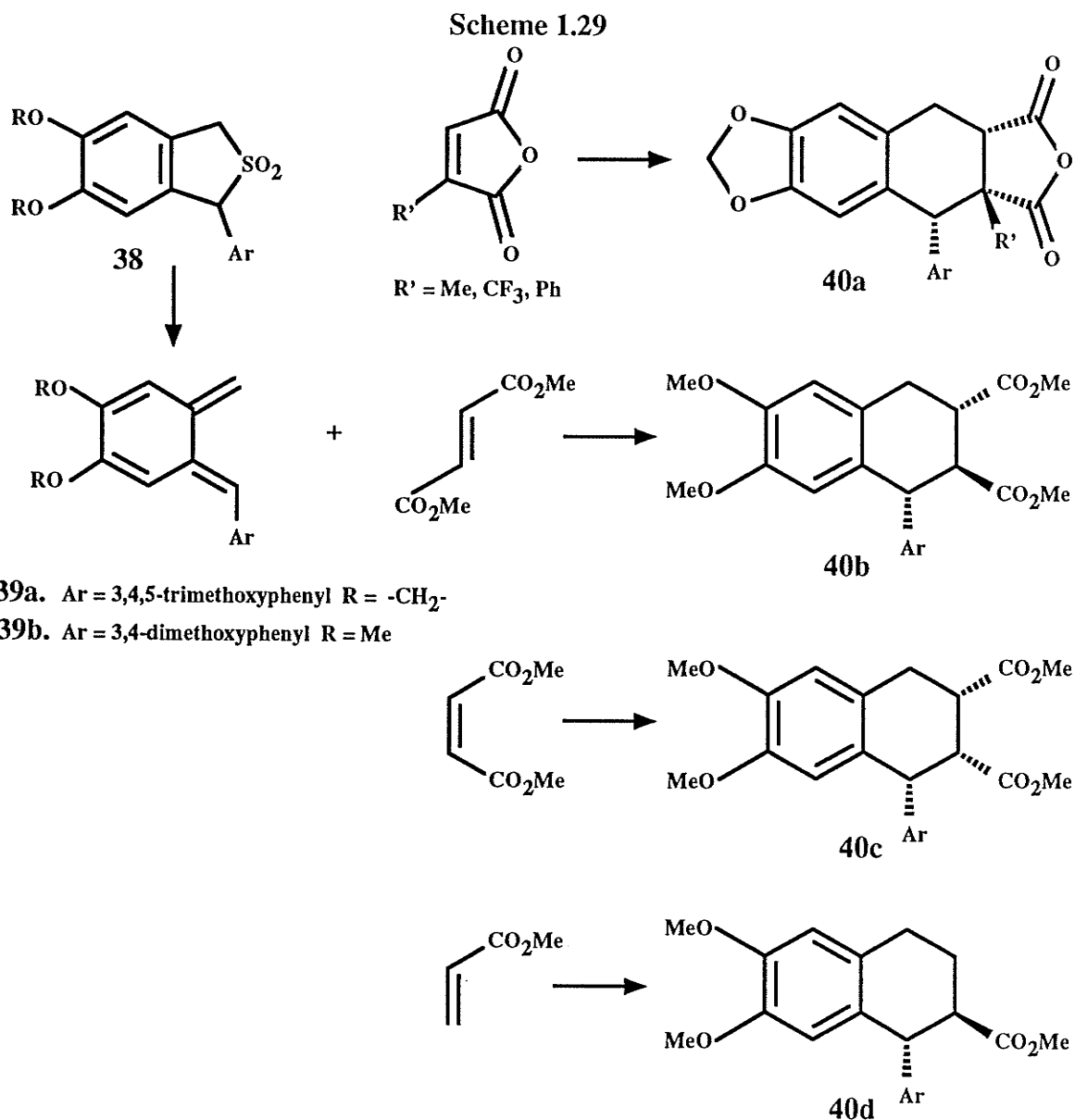
1.26). Cycloaddition of the methoxy derivative **31** with acrylonitrile gave the same mixture. The lower selectivity was attributed to the reduced propensity for secondary orbital interactions with acrylonitrile. Wallace *et al.* reported the reaction of the dimethoxy substituted benzocyclobutenol **34** with acrylonitrile and methyl acrylate (Scheme 1.27).⁵² Cycloaddition with acrylonitrile gave exclusively *endo* adduct **35** in 80% yield whereas methyl acrylate gave a mixture of *endo* **36** and *exo* **37** isomers in a 5:1 ratio respectively. The α -oxy-*o*-QDMs have also been added to other dienophiles such as dimethyl fumarate and dimethyl maleate (Scheme 1.28).^{25,35,52} In each case, the



cycloaddition occurs to give adducts having a 1,2-*cis* stereochemistry arising from *endo* addition. The addition of α -aryl and phenyl *o*-QDMs to dienophiles reveals some



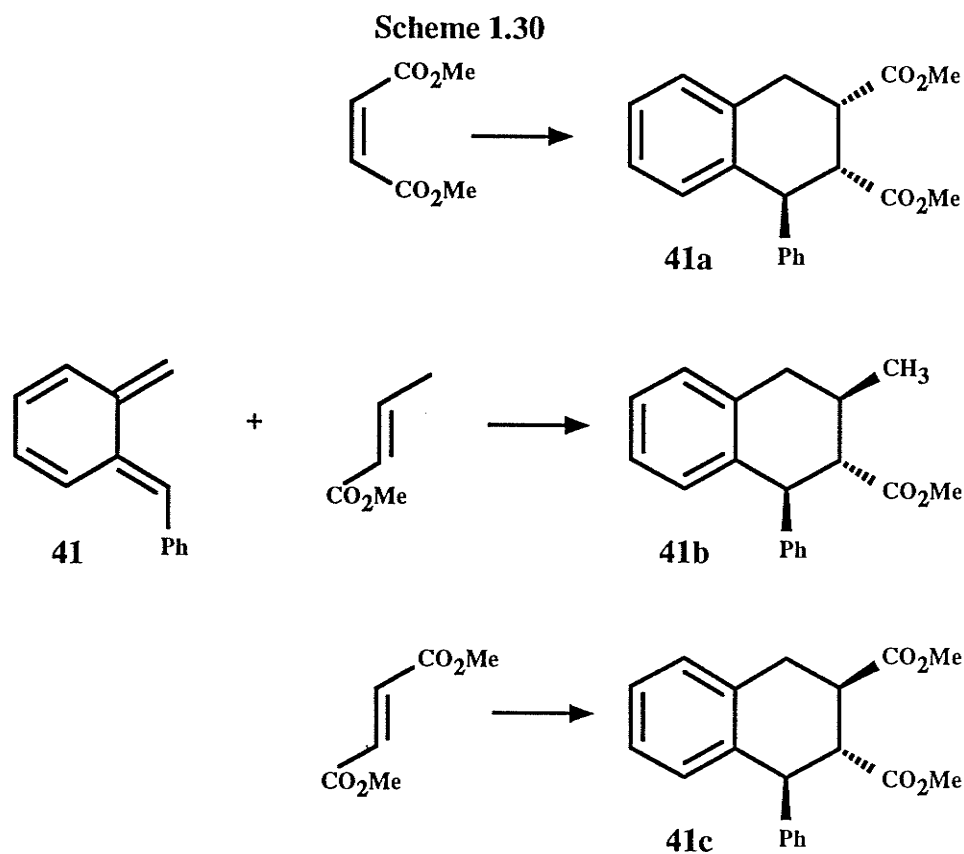
interesting steric factors which control the diastereoselectivity. In the synthesis of some podophyllotoxin analogues, Mann *et al.* thermolyzed sulfone **38** to generate *E*- α -aryl-*o*-QDM **39a** (Scheme 1.29). Various 1-substituted maleic anhydrides were allowed to react with **39a** to give *endo* adducts **40a**.²¹ The cycloaddition was regioselective with the adducts having the 1-substituent *ortho* to the aryl group. Mann and Piper reported that cycloaddition of methyl acrylate with the *E*-aryl-*o*-QDM **39b** at 200°C



gave the 1,2-*trans* adduct as the major product (Scheme 1.29).²⁴ Shorter reaction times resulted in an increase in the amount of *endo* product which is the product predicted by FMO theory. They concluded that the reaction was reversible such that the thermodynamically favored *exo* product was formed preferentially. Upon reaction of **39b** with dimethyl fumarate, the major product formed was again the *exo* product with the 1-aryl group and 2-carboxymethyl group in a *trans* disposition. In contrast to the previous examples, cycloaddition of **39b** with dimethyl maleate or maleic anhydride gave

exclusively *endo* adducts indicating the dominance of secondary orbital interactions and lack of reversibility with these two dienophiles.

Dissonant with Mann's results, Durst *et al.* found that the addition of dimethyl maleate to *E*- α -phenyl-*o*-QDM **41** resulted in the formation of *exo* product **41a** (Scheme 1.30).³⁵ Methyl crotonate also added regioselectively giving *exo* products **41b** as did the

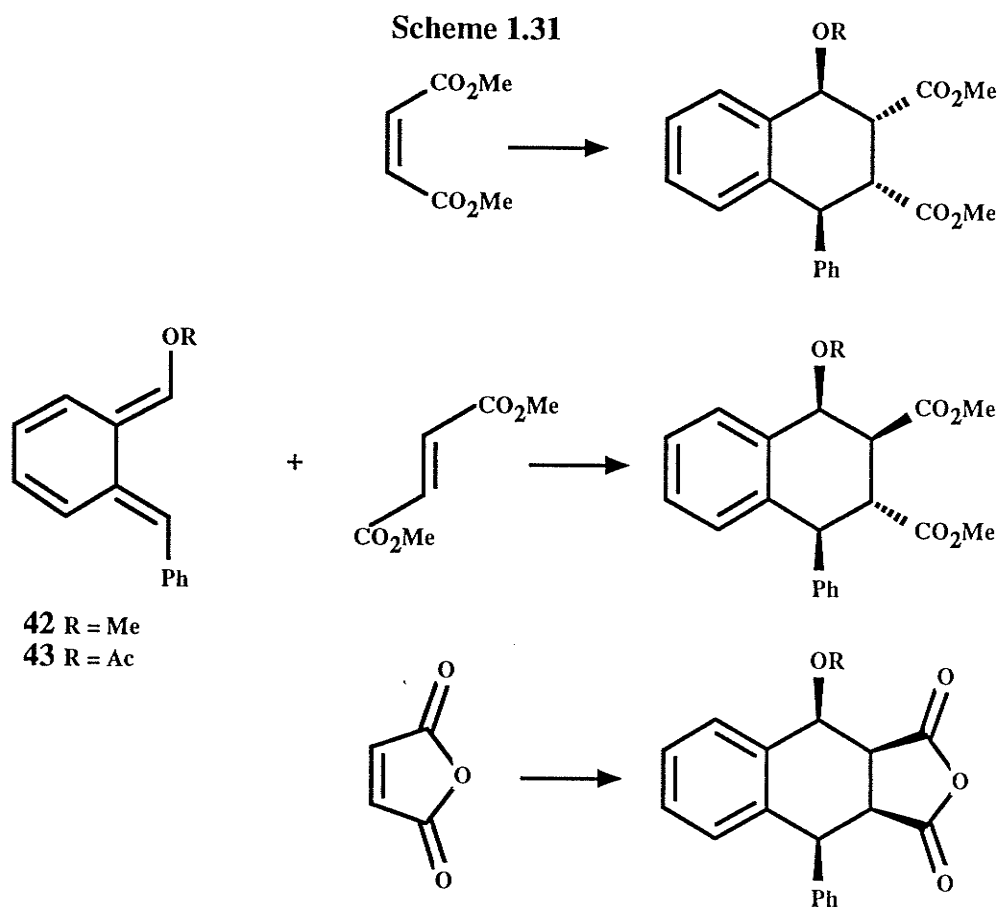


addition of dimethyl fumarate giving **41c**. From these latter examples, it is evident that the phenyl group has a directing effect in the transition state which is likely steric in nature. Since the cycloadditions were performed at 80°C, it is unlikely that these latter reactions were reversible. Thus, the major product must arise from an interaction in the transition state and not from a thermodynamic equilibrium.

Reiterating, *o*-QDMs bearing α -oxy groups prefer to add *endo* whereas those bearing α -aryl groups prefer to add *exo*.

To ascertain the efficacy of the phenyl group as a directing group notwithstanding

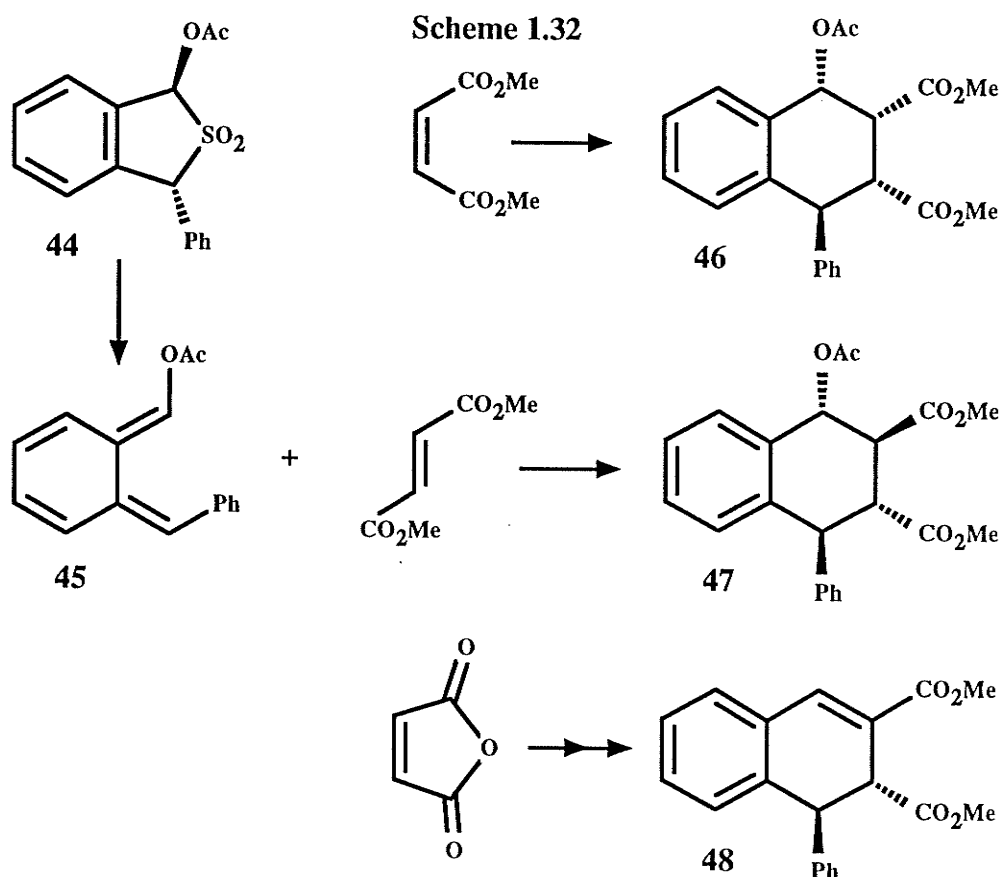
the directing effect of the oxy group, dimethyl fumarate and dimethyl maleate were reacted with *E,E*- α -methoxy- α' -phenyl-*o*-QDM **42** and *E,E*- α -acetoxy- α' -phenyl-*o*-QDM **43** (Scheme 1.31).^{25,35} In the case of dimethyl maleate, addition to **42** was found to be at least 90% diastereoselective with the *exo* isomer predominating. Addition of the maleate to **43** resulted in a somewhat lower yield giving two products in a 3:1 *exo* to *endo* ratio. When dimethyl fumarate was added to **42** and **43**, products having a



trans-1-aryl-2-carbomethoxy disposition were formed preferentially. This result is expected as both directing effects work in concert. Maleic anhydride addition to **43** resulted in the formation of *endo* adducts.

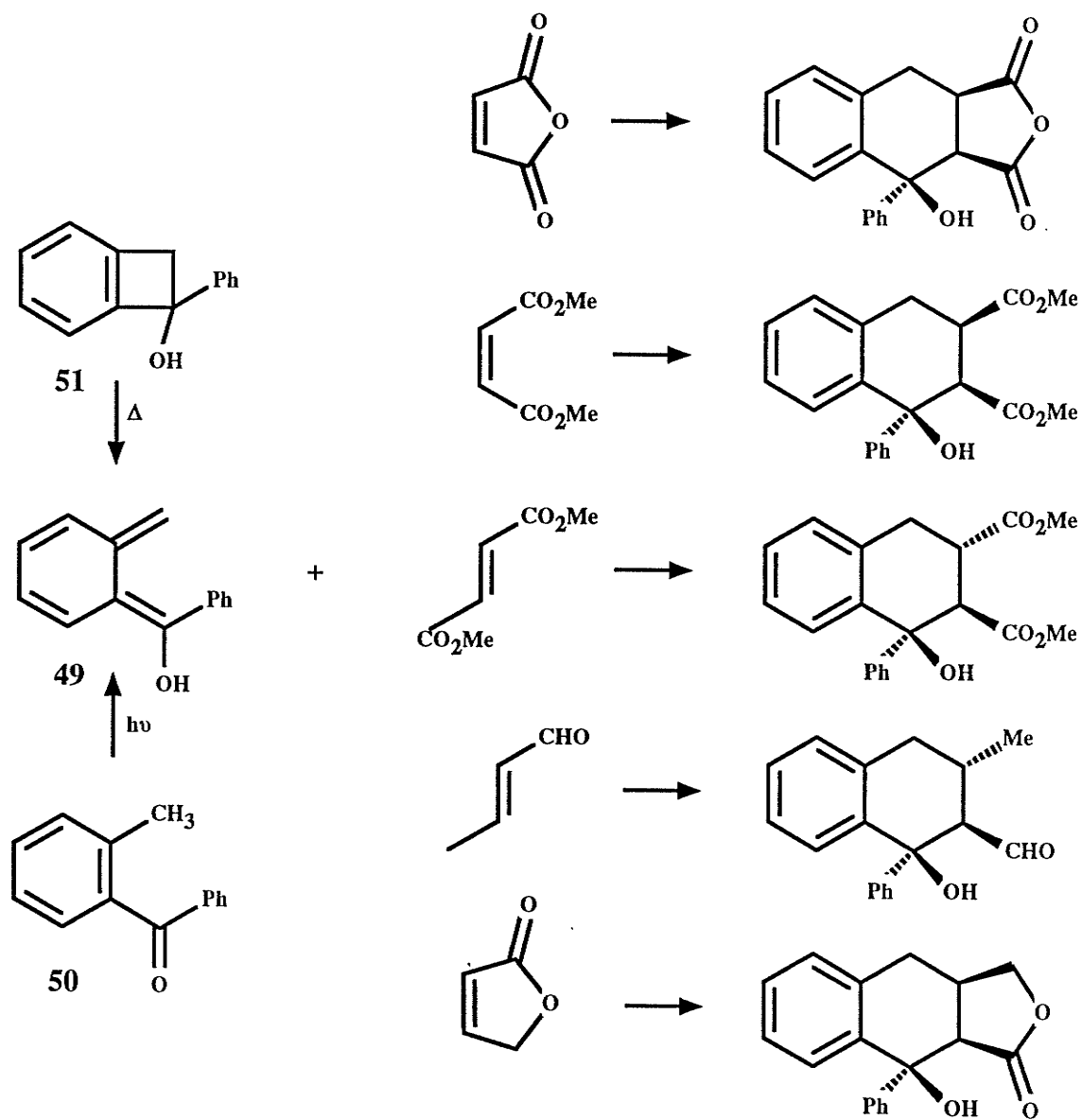
The stereochemistry of cycloaddition of the *E,Z*- α -acetoxy- α' -phenyl-*o*-QDM to various dienophiles has also been studied.²⁵ The *E,Z*-*o*-QDM **45** was generated via thermal extrusion of SO₂ from the *trans*-1-acetoxy-3-phenyl sulfone **44** and was reacted

with the usual dienophiles (Scheme 1.32). As expected, addition of **45** to dimethyl fumarate gave the all *trans* cycloadduct **47** in 94% yield. Addition occurred *exo* with respect to the acetoxy group thus revealing the overwhelming influence of steric repulsion over secondary orbital interactions. Dimethyl maleate followed the expected pattern to give a cycloadduct **46** having the 1,2-*trans* stereochemistry arising from an *endo* transition state with respect to the acetoxy group (*exo* with respect to the phenyl group). The addition of maleic anhydride initially gave a mixture of products that was converted primarily to the *trans*-alkene **48** indicating *endo* addition.



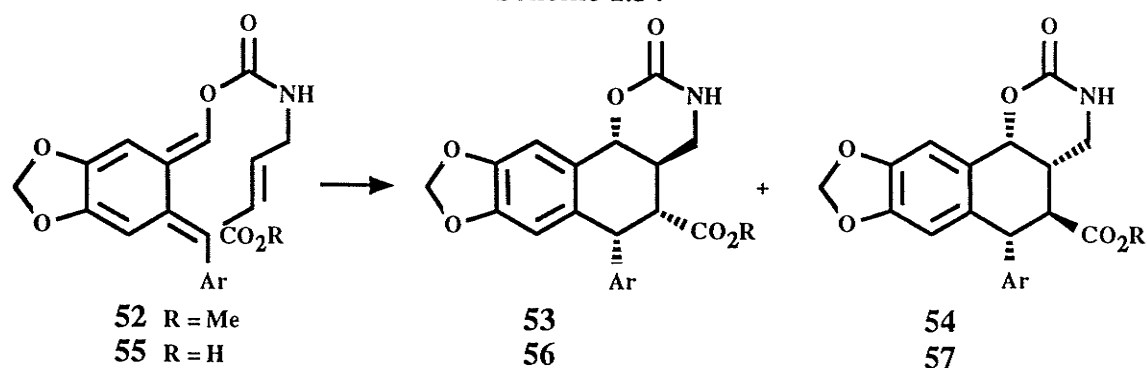
Of importance to the work in this thesis is the addition of *E*- α -hydroxy- α -phenyl-*o*-QDM **49** to various dienophiles (Scheme 1.33). Intermediate **49** can be generated either photochemically by irradiation of 2-methylbenzophenone⁵³⁻⁵⁶ **50** or by thermolysis of 1-hydroxy-1-phenylbenzocyclobutene⁵⁷ **51**. In each case, previous studies have shown that *endo* addition occurs with respect to the hydroxyl group.

Scheme 1.33



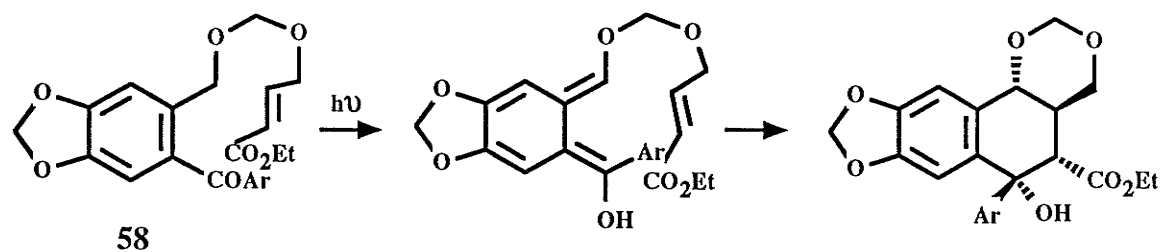
Intramolecular Diels-Alder reactions have also been used to control the product stereochemistry. Durst *et al.* used this strategy in their synthesis of podophyllotoxin (Scheme 1.34).⁴¹ Thermolysis of urethane **52** in nitromethane at 90°C gave a 3:1 ratio of the *exo* **53** and *endo* **54** products. An effect was also observed when the methyl ester of **52** was replaced with a carboxylic acid group. Under the same conditions, thermolysis of the acid **55** gave a 5:1 (**56** to **57**) mixture of *exo* and *endo* products. The ratio of *exo* to *endo* products was also found to be sensitive to solvent polarity.

Scheme 1.34



A similar strategy was used by Kraus *et al.* in their synthesis of podophyllotoxin (Scheme 1.35).⁴⁸ The intermediate *o*-QDM was generated photochemically by irradiation of benzophenone 58. Cycloaddition proceeded efficiently through an *exo* transition state (relative to C₄) without any benzocyclobutene by-products.

Scheme 1.35

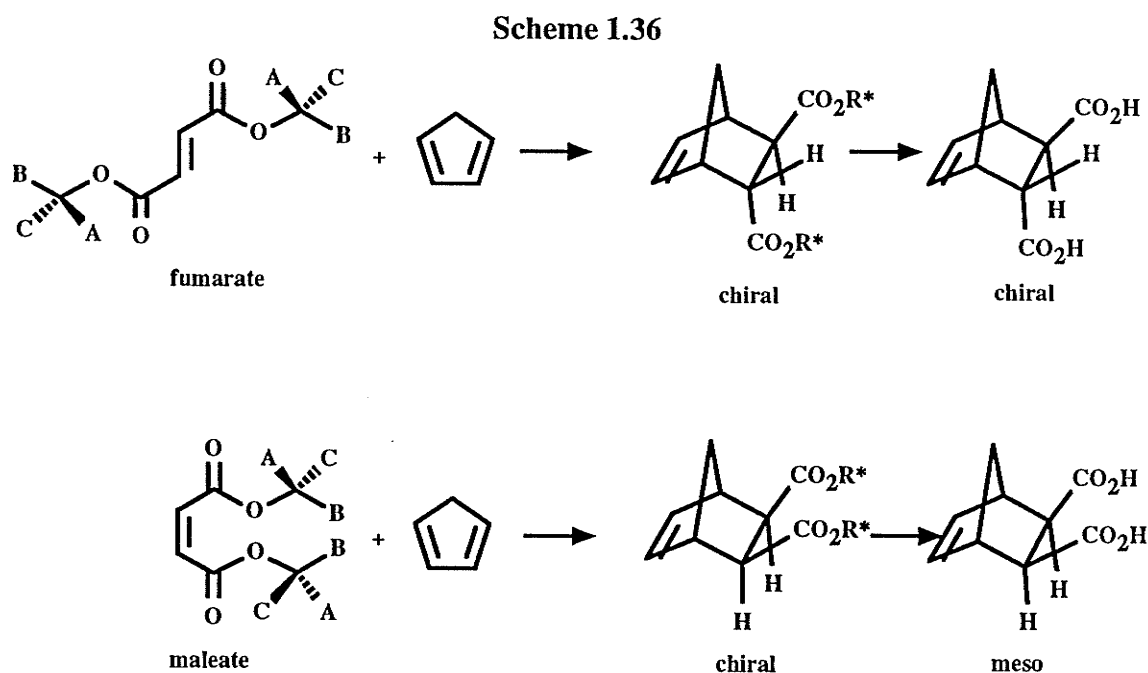


1.8 Diastereofacial Control in the Diels-Alder Reaction.

The previous section dealt with the diastereoselective control of the relative stereochemistry introduced during the Diels-Alder reaction of *o*-QDMs with dienophiles. However, since the interacting diene and dienophile were both achiral, both enantiomers were produced giving a racemic mixture. In order to make the reaction enantioselective, discrimination between the two reacting faces of either the diene or dienophile must be achieved. This may be accomplished by attachment of a chiral control element to either the diene or dienophile or by the use of a chiral catalyst. The judicious choice of method

will of course be specific to individual situations and is therefore without generalization.

Some consideration of symmetry is required in order to gain insight into the understanding of asymmetric induction. Consider the addition of the C_2 -symmetric,

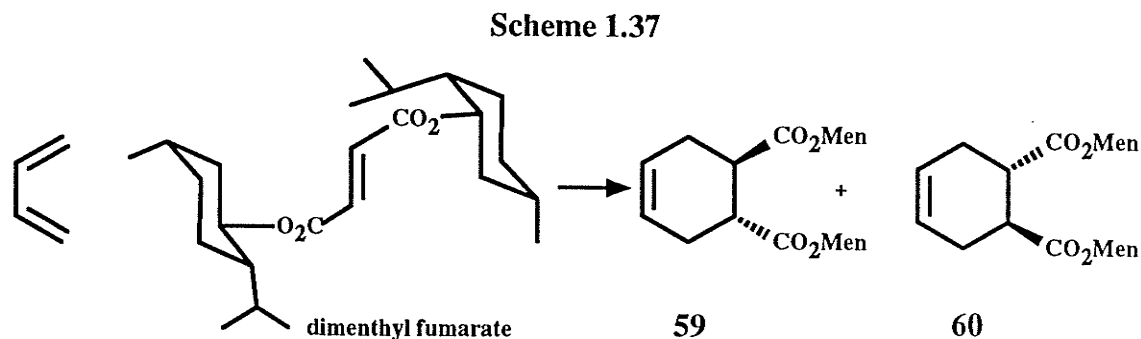


achiral 1,3-cyclopentadiene with a C_2 -symmetric fumarate bearing identical chiral groups (Scheme 1.36). Addition of one face of the fumarate to either face of diene are equivalent as the two faces are related by symmetry. However, addition of the diene to one face of the fumarate is not equivalent to addition to the other. This will become apparent in the first example. The preferred addition to one face of the fumarate followed by removal of the chiral ester groups will then constitute an enantioselective synthesis. It is important to note that *endo* and *exo* addition have no meaning in this example. The addition of the corresponding maleate bearing the same chiral groups to 1,3-cyclopentadiene is however superfluous. Although the initial adduct contains chiral groups, the product with the chiral auxiliaries removed is achiral (commonly referred to as a meso compound). Therefore, this step does not correspond to an asymmetric synthesis although it may be diastereoselective for *endo* or *exo* products.

An early example of an asymmetric cycloaddition reaction involved the addition of

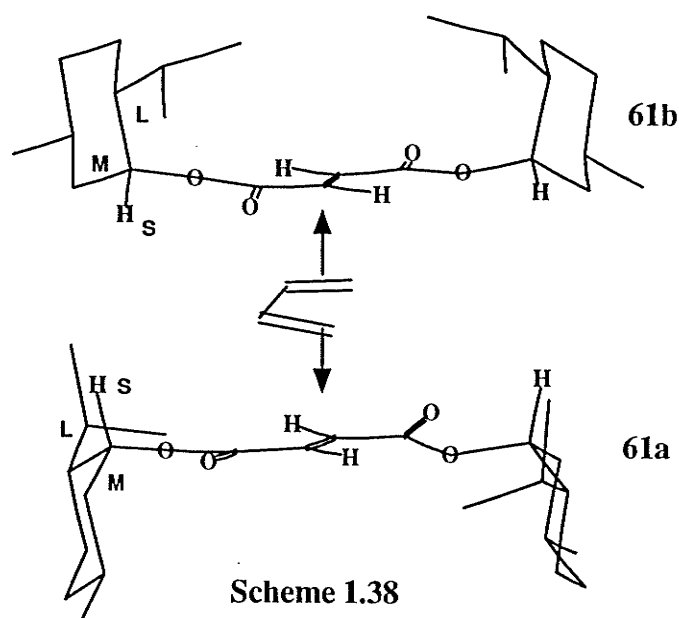
(-)-dimenthyl fumarate with butadiene to give cycloadducts **59** and **60** (Scheme 1.37).⁵⁸

In order to ascertain the steric course of the reaction, the absolute configuration was determined by chemical correlation. By reduction of the adducts to the known *trans*-4-cyclohexene-1,2-dimethanol, it was possible to show that the product was 1.2% optically pure. To explain the mechanism of facial addition based on a kinetic model, it



was necessary to show that the reaction was not thermodynamically controlled. The reaction was shown to be under kinetic control by demonstrating that the optical purity of the reaction did not vary with time although the yield of the reaction did. Similarly, experiments run six times longer than required to assure completion changed neither the yield nor the optical purity. After demonstrating that the addition was kinetically controlled, a *transoid* conformation was assumed for the fumarate moiety in accord with Prelog's postulate.⁵⁹ It was then assumed that the addition to the fumarate occurred such that the diene approached the least sterically hindered face. To determine which face was least sterically hindered, a modified Cram-Prelog model was used. In this model, a preferred conformation was adopted such that the large (L) group occupied a position contained in the fumarate plane as shown in **61a** (Scheme 1.38). Approach would then occur from the side of the small (S) group away from the medium (M) group giving rise to the R(-) isomer. Two other possible reactive conformations about the ester oxygen bond might also exist. Placement of the (M) group in the plane, as shown in **61b**, with approach toward the (S) group gives rise to the S(+) isomer. Placement of the (S) group

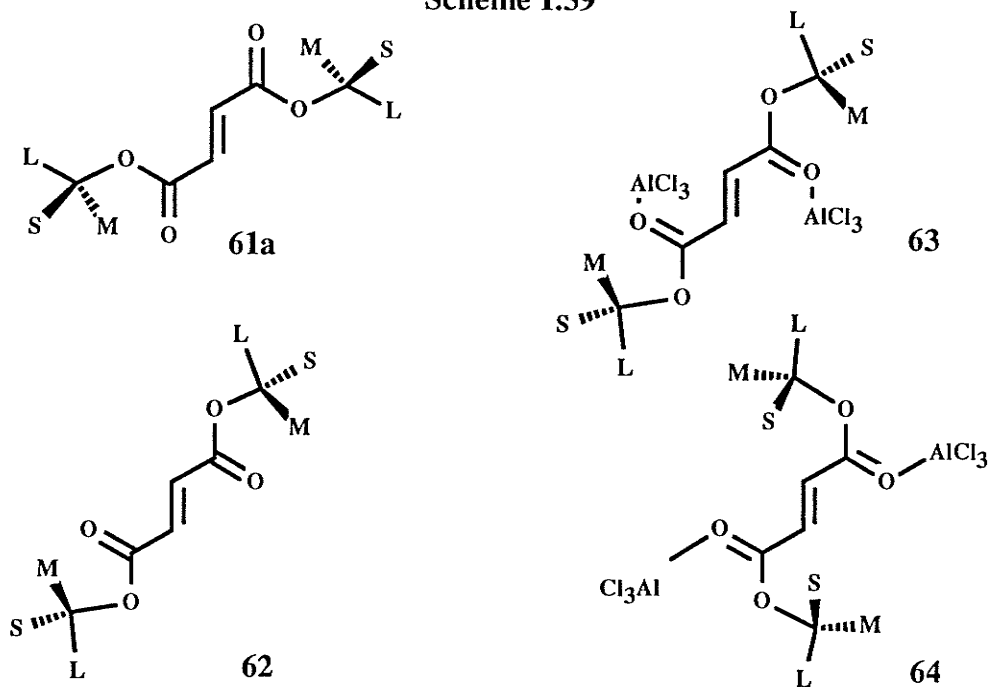
in the plane would give rise to the R(-) isomer. Assuming that **61a** is the major conformation, one predicts a preponderance of the R isomer. However, the authors suggest that this conformation is predisposed to an increased steric interaction resulting from the displacement of the equatorial isopropyl group toward the (S) side of the fumarate. This implies that addition should occur from the side of the medium group ultimately leading to formation of the S-(+) isomer. If both of the carbonyls in the dienophile were to adopt a *s-cis* conformation as in **62** (Scheme 1.39), then the model predicts a preponderance of the S-(+) isomer.



A small temperature dependence was found whereby the facial selectivity increased with increasing temperature. This unusual temperature effect was explained by the increasing importance of other conformations resulting from rotation about the O-acyl bond. At room temperature the optical yield was 0%. It was postulated that if the reaction were carried out at lower temperatures, the S-(+) isomer would predominate and would arise from addition to the (M) face of **61a** or the (S) face of **61b** (Scheme 1.38). This preponderance of the S-(+) isomer was observed upon the addition of a Lewis acid to the reaction mixture at low temperatures (-70°C). An increase in the optical purity from 2%

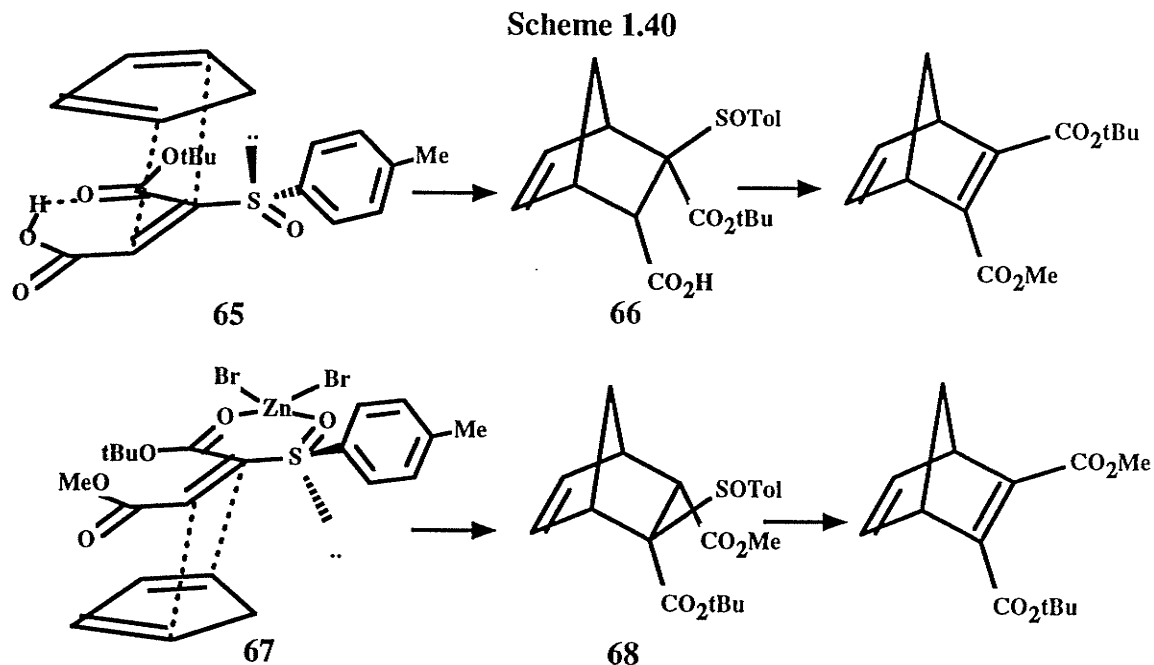
for the R(-) isomer to 78% for the S(+) isomer was observed. It was assumed that the complexation to the carbonyl oxygen produced a resonance effect with the ethereal oxygen which prohibited rotation about the O-acyl bond. It is also possible that complexation of the catalyst with the dienophile might have changed the conformation of the dienophile from *s-trans* **61a** to *s-cis* **63** or **64** (Scheme 1.39).

Scheme 1.39



Chiral sulfoxides can be used to control the facial selectivity of Diels-Alder reactions.⁶⁰ The sulfur atom in the sulfoxide is tetrahedral due to the lone pair of electrons on sulfur and hence imposes the chiral environment in the cycloaddition reaction. In the non-Lewis-acid catalyzed cycloaddition of 1,3-cyclopentadiene to the sulfinyl maleate **65** at -20°C, reaction occurred from the *s-cis* dienophile with approach from the side exposing the sterically small lone pair to give cycloadduct **66** (Scheme 1.40). The methyl-ester-maleate **67** in the presence of ZnBr₂ catalyst reacted from the *s-trans* form to give cycloadduct **68** of opposite configuration with respect to **66**. The *s-trans* conformation is stabilized by chelation of the sulfoxide and ester oxygens with the Lewis-acid. The non-catalyzed addition gave lower selectivity presumably due to the fact

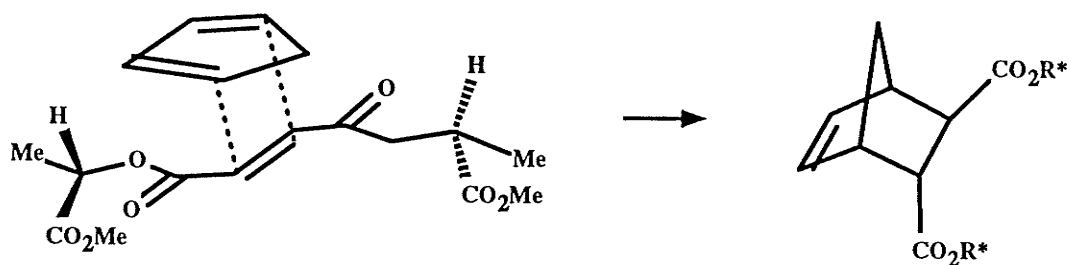
that both the *s-cis* and *s-trans* conformations are present. In the first reaction, the preference for the *s-cis* conformation of the dienophile is likely determined by an intramolecular hydrogen bond. This example is particularly interesting in that complete inversion of the facial selectivity can be achieved by the addition of a Lewis-acid.



Helmchen has reported the stereoselective catalyzed and uncatalyzed addition of the acrylate **69** or fumarate **70** of (*S*)-ethyl lactate to cyclopentadiene (Scheme 1.41).⁶¹ In the former case, a diastereomeric ratio of 80:20 was obtained as *endo* adducts. The fumarate had a higher ratio of 95.5:4.5 at 0°C and 98:2 at -54°C for the uncatalyzed reaction. To explain the observed facial selectivity, it was assumed that **70** reacted from the *s-trans* conformation with the methyl group lying in the plane of the fumarate. Facial discrimination would then arise via the preferred addition to the *re* face which exposed the sterically smaller hydrogen.

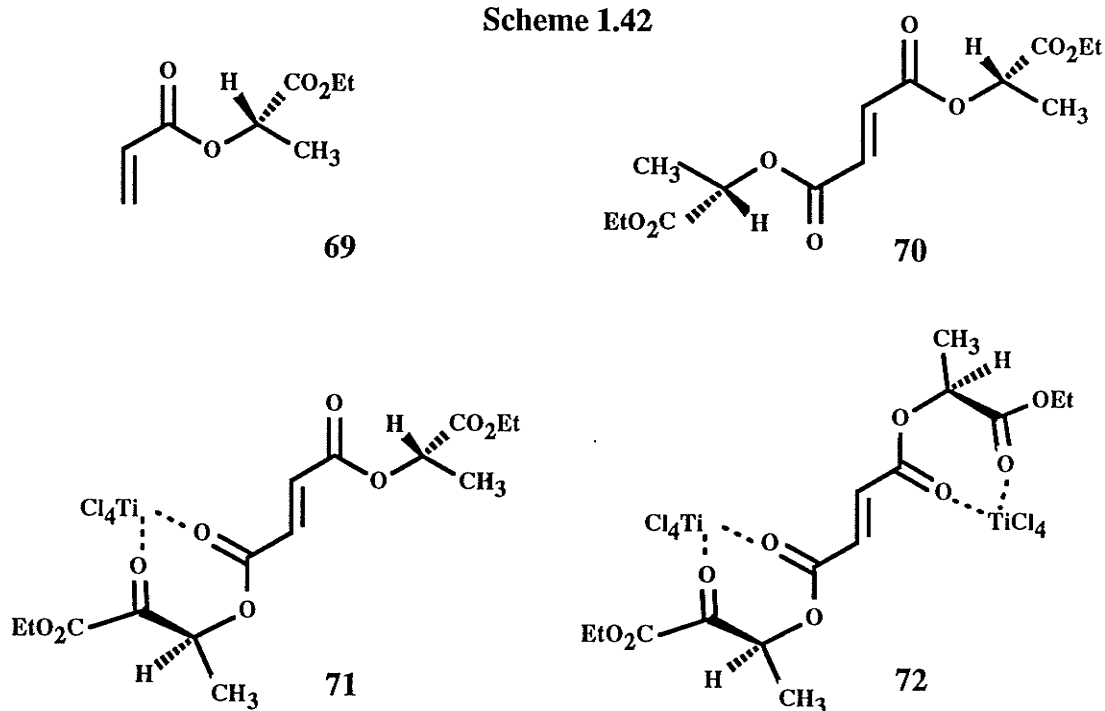
Addition of TiCl_4 catalyst resulted in a concentration dependent inversion of the facial selectivity. The coordination of the catalyst to the lactyl and fumarate carbonyls changed the conformation to *s-cis* thus rendering the *si* face the reactive surface. A 1:1 mixture of catalyst and **70**, according to theory, should produce an antagonistic action of

Scheme 1.41



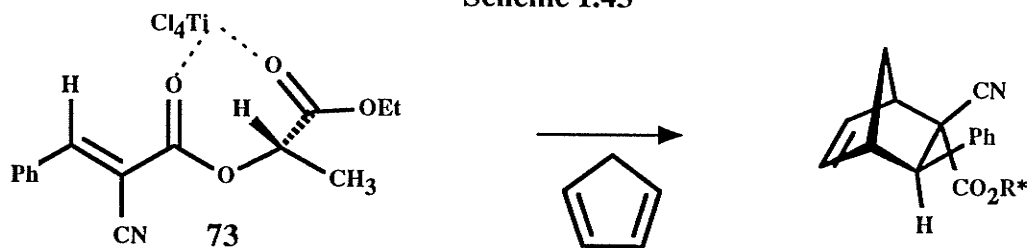
the two chiral auxiliary groups as shown by **71** (Scheme 1.42). Indeed as the catalyst concentration was increased, resulting in the formation of **72**, a synergistic action was observed until an ultimate 95:5 (*si:re*) selectivity was obtained. A similar system which

Scheme 1.42



implemented the lactate chiral auxiliary was used by Cativiela in the reaction of cyclopentadiene with the *E*-2-cyanocinnamate-lactate ester **73** (Scheme 1.43).⁶² Again, a reversal of the facial selectivity was observed together with an increase in the *endo* selectivity when TiCl_4 was employed as a catalyst. This reversal was attributed to a change in the preferred conformation of the diene from *s-trans* to *s-cis*. The use of AlCl_2Et as a catalyst resulted in poor diastereoselectivity.

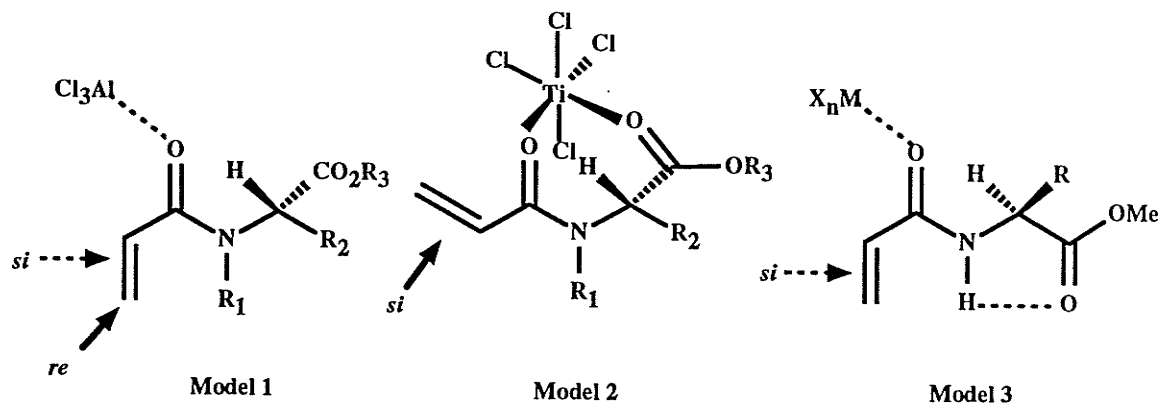
Scheme 1.43



In light of the fact that α -hydroxy esters such as ethyl lactate can be used as efficient chiral auxiliaries when attached to acrylates or fumarates, Cativiela *et al.* studied the ability of α -amino acids to serve as chiral auxiliaries in similar cycloaddition reactions (Scheme 1.44).⁶³ Various *N*-acryloyl-L-amino acid esters **74a-e** were reacted with cyclopentadiene in the presence of TiCl_4 , AlCl_3 , or EtAlCl_2 . Three conformational models were proposed in order to explain the observed facial addition. In model 1, a four coordinate catalyst like aluminum coordinates at only one site and elicits an anti-periplanar (*s-trans*) conformation for the dienophile. Addition occurs to the *re* face of the dienophile opposite the bulky ester group. This model suggests that an increase in the size of the ester from methyl to benzyl will result in an increase in the diastereoselectivity. Model 2 incites a conceptual similarity with Helmchen's model and can be used to explain the results obtained for the *N*-acryloyl-L-proline esters **74a,b** in the presence of TiCl_4 . Chelation of the catalyst with the two carbonyl groups imposes a *syn-periplanar* (*s-cis*) conformation on the dienophile. A chlorine atom from the catalyst shields the *re* face of the acrylate so that attack occurs preferentially on the *si* face. The third model becomes active for acyclic amino acids where the amide alkyl group is replaced by a hydrogen atom which then forms a hydrogen bond with the ester carbonyl. This promotes a change in the conformation in which the amide backbone atoms are in plane and facial discrimination involves the selective addition opposite the side of the bulky R group of the amino acid. Thus a greater facial discrimination is observed when the R group is changed from methyl in alanine **74d** to benzyl in phenylalanine **74c**. In this model, whether AlCl_3 or TiCl_4 is used, the dienophile adopts an *s-cis* (*syn*) conformation as bivalent

coordination to titanium is now encumbered by the presence of the intramolecular hydrogen bond.

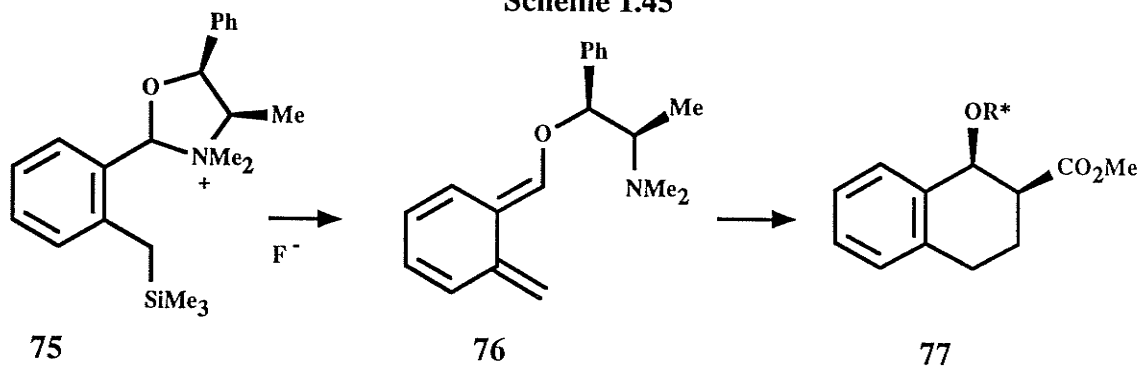
Scheme 1.44



	R ₁	R ₂	R ₃	Model (catalyst)
74 a	-CH ₂ -CH ₂ -CH ₂ -		CH ₃ -	1 (AlCl ₃), 2 (TiCl ₄)
b	-CH ₂ -CH ₂ -CH ₂ -		PhCH ₂ -	1 (AlCl ₃), 2 (TiCl ₄)
c	H	PhCH ₂ -	CH ₃ -	3 (AlCl ₃ , TiCl ₄)
d	H	CH ₃ -	CH ₃ -	3 (AlCl ₃ , TiCl ₄)
e	CH ₃	CH ₃ -	CH ₃ -	2 (TiCl ₄)

It has been proposed that π -stacking may play an important role in the control of the reactive conformation of dienes bearing chiral auxiliaries incorporating phenyl groups.⁶⁴ Ito *et al.* have reacted the oxazolidinium derivative **75** with fluoride ion to generate the intermediate *o*-QDM **76** which was trapped *in situ* with methyl acrylate to give *endo* adducts with a preponderance of the R,R-isomer **77** (Scheme 1.45).⁶⁵

Scheme 1.45



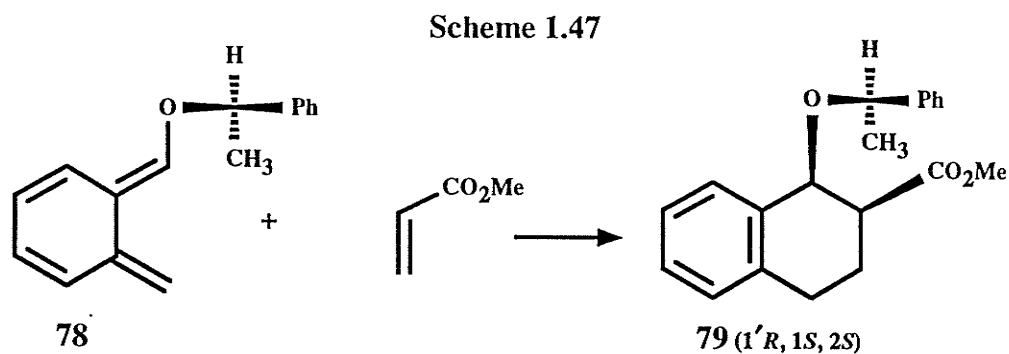
Following the model of Trost,⁶⁴ they proposed that the phenyl substituent in the chiral auxiliary π -stacked with the *re* face of the *o*-QDM thus preventing addition to that face. In this model, the phenyl groups fold over the diene face which results in the smallest non-bonded interactions (Scheme 1.46). In **A**, the large group projecting towards the diene face encounters a marked steric repulsion whereas these non-bonded interactions are minimized in conformation **B** which presents the small group to the diene face. Addition of the dienophile is directed towards the face of **B** which is not blocked by the π -stacked phenyl group. However, their conclusions based on this model seem rather dubious. An

Scheme 1.46

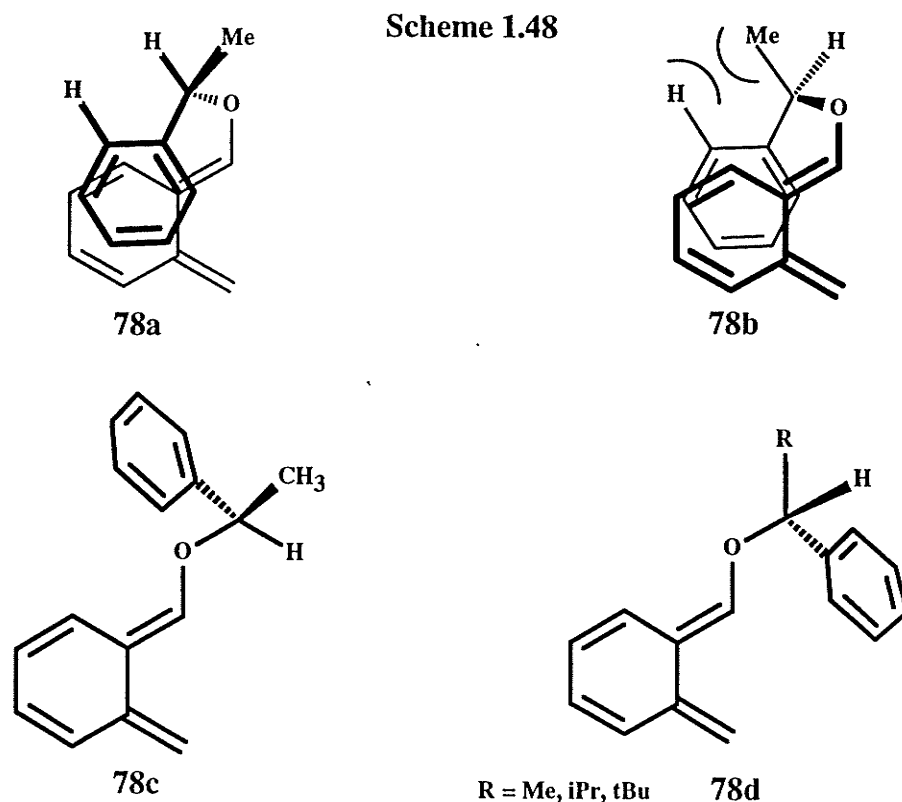


analysis of the proposed conformation reveals that π -stacking with the *re* face imposes greater non-bonding interactions than does π -stacking with the *si* face. Thus a π -stacking mechanism should favor addition of the dienophile to the *re* face of the *o*-QDM.

Charlton has studied the addition of α -alkoxy-*o*-QDM **78** bearing the 1-*R*-phenylethyl substituent (Scheme 1.47).⁶⁶ Application of the π -stacking model⁶⁵ suggested that reaction should occur from the *re* face of **78a** (Scheme 1.48). However, determination of the absolute configuration of cycloadduct **79**, obtained from reaction of **78** with methyl acrylate, revealed that preferential addition to the *si* face of **78b** had occurred. This led to the abandonment of the π -stacking mechanism and the proposal of a new reactive conformation for **78**. Facial selectivity based on the new conformation **78c** arises from the preferred addition to the side exposing the sterically smaller methyl group. Later studies by Posner and Wettlaufer on a similar system seemed to be inconsistent with



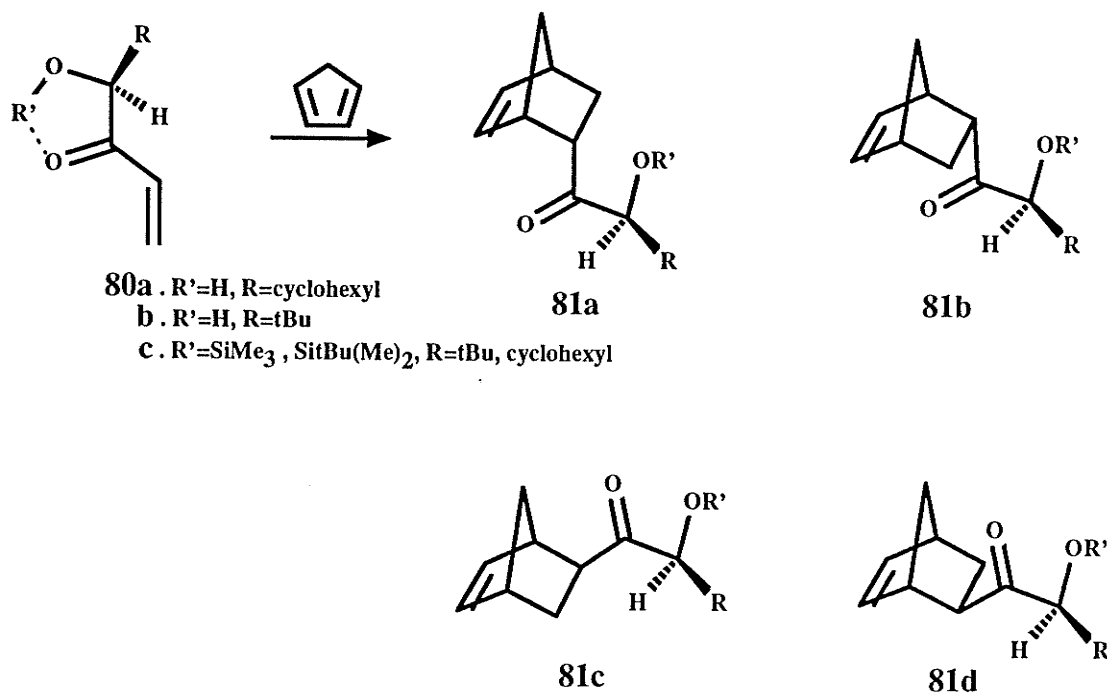
this new model and prompted a reinvestigation of the mechanism.^{67,68} It was found that changing the methyl group in the chiral auxiliary of **78** to isopropyl and t-butyl groups led to a progressive increase in the de. Again the model was inconsistent with experiment and required the adoption of a new model in which the bulky alkyl group lay in the plane of the *o*-QDM. Thus, an increase in the size of the alkyl group results in a predominance of



78d. This increase in the diastereoselectivity is attributable to a "freezing out" of conformation **78d** due to hindered rotation about the ether bond. Thus the bulky t-butyl group helps to lock the conformation thus excluding other rotamers which would allow addition to the *re* face of the diene.

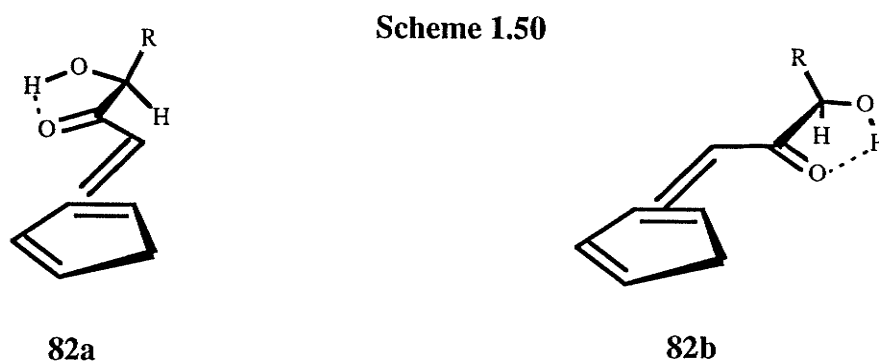
The concept of locking the conformation of the chiral auxiliary is indeed an attractive approach for increasing the facial selectivity. Intramolecular hydrogen bonding has been used by Masamune to lock the conformation of the chiral auxiliary attached to the dienophile (Scheme 1.49).⁶⁹ In addition, Masamune suggested that bringing the chiral auxiliary one atom closer to the reacting centers would result in an increase in the selectivity over the acrylic acid esters bearing remote chiral centers. Masamune reacted vinyl lithium with (S)-hexahydromandelic acid in the preparation of dienophile **80a**. Formation of a strong intramolecular hydrogen bonded 5-membered chelate was evidenced by the presence of a single OH peak in the infrared spectrum under varying concentrations. Reaction of **80a** with cyclopentadiene at temperatures of 25°C and -55°C

Scheme 1.49



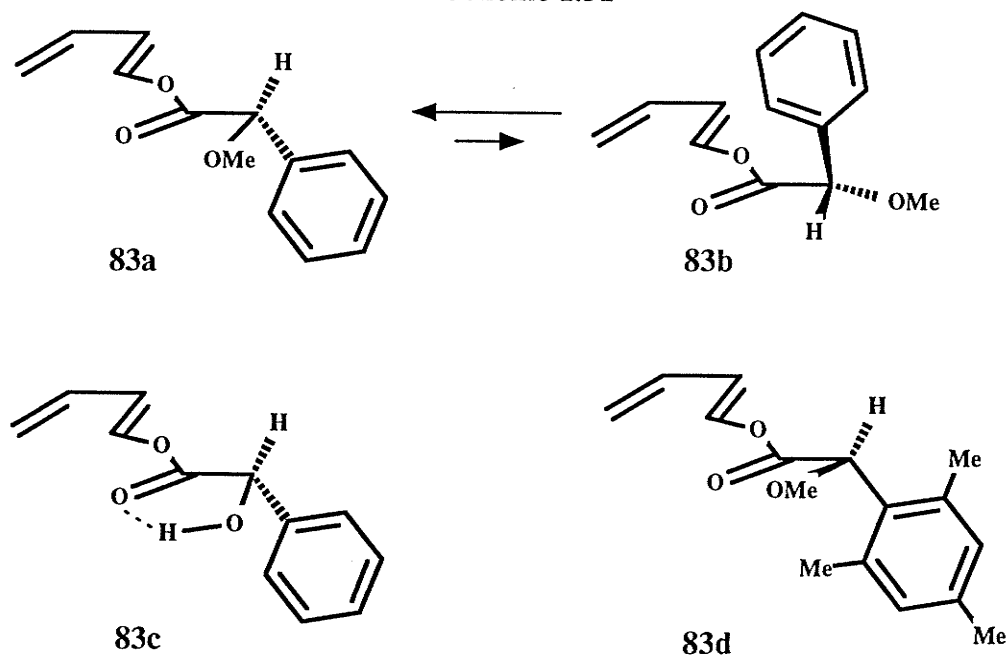
resulted in de's of 13:1 and 28:1 respectively. *Endo* products **81a** and **81b** were favored over the *exo* products **81c** and **81d** by a 7:1 ratio. Replacement of the cyclohexyl group in **80a** with a bulkier t-butyl group resulted in diastereoselectivities as high as 100:1 (**81a**:**81b**). Protection of the hydroxyl group with a silyl group in either **80a** or **80b** completely destroyed the facial selectivity thereby indicating the importance of the

intramolecular hydrogen bond. Finally, an analysis of the major *endo* and *exo* products revealed that they arose from transition states **82a** and **82b** respectively (Scheme 1.50).



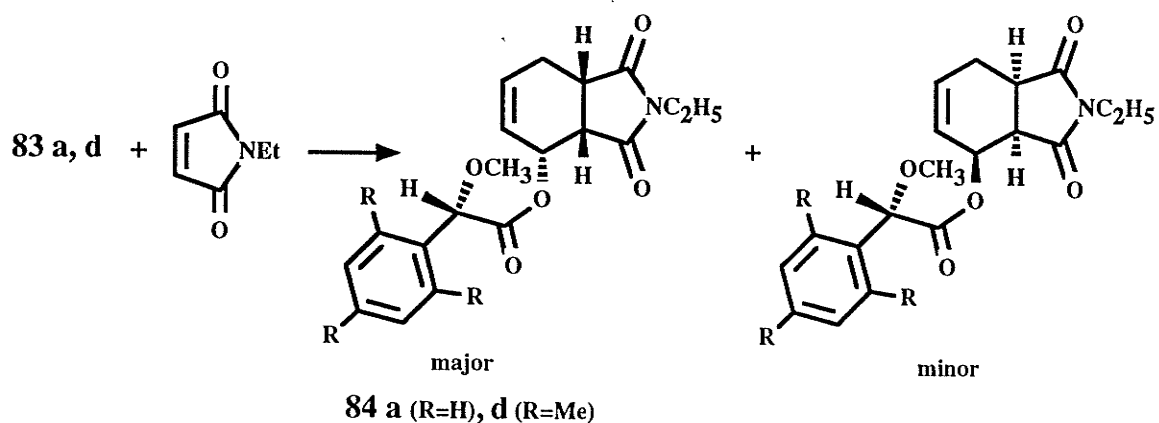
Intramolecular hydrogen bonding, in the previous example, was used to lock the conformation of the dienophile to improve the selectivity. One could also envisage that an intermolecular hydrogen bond between the diene and dienophile might be used to bring the two reacting species together and serve as a tether to reduce the conformational flexibility in the transition state. In this case an attractive interaction (the hydrogen bond) would serve as a mediator of molecular recognition. Thorton *et al.* studied the ability of intermolecular hydrogen bonding to control the diastereoselectivity in the cycloaddition of *N*-ethylmaleimide (NEM) with a modified version of Trost's diene **83a** bearing a remote chiral auxiliary (Scheme 1.51).^{70,71} Tucker *et al.* proposed that the preferred conformation of **83a** had the methoxy group eclipsed with the carbonyl group together with a conformation slightly higher in energy, **83b** (Scheme 1.51).⁷² An assumption was made that the reactive transition state conformation of the diene was the same as the ground state conformation proposed by Houk which had a perpendicular phenyl group.⁷² Enhancement of the perpendicular conformation was anticipated by deblocking the oxy group so that intramolecular hydrogen bonding could occur thus locking it in conformation **83c**. Modeling also showed that incorporation of *ortho* methyl groups on the phenyl ring in **83d** froze the auxiliary in a conformation similar to **83a**. Predictably, reaction of **83a** and **83d** with NEM gave *endo* cycloadducts **84a,d** (Scheme 1.52) arising

Scheme 1.51



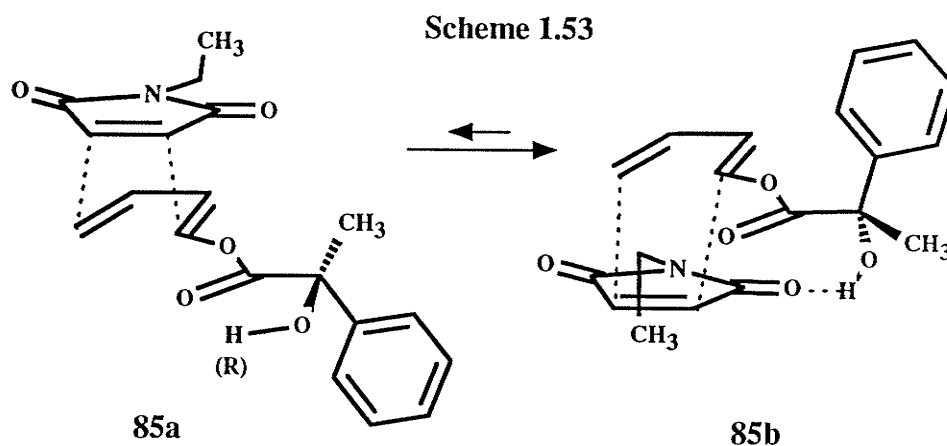
from the stereoelectronically favored conformers. The minor adducts probably arose from conformations similar to **83b**. In spite of the predicted outcome based on the preferred conformation of **83c**, an overwhelming reversal of facial selectivity was observed for the free hydroxyl dienes like **83c**. Thornton rationalized that this effective control by the

Scheme 1.52



remote chiral center was possible if hydrogen bonding occurred in the transition state. Thus he proposed two *endo* transition states **85a** and **85b** (Scheme 1.53). The diene conformation in **85a** was thought to be similar to **83d** so that the dienophile approaches

from the top away from the aryl group. In transition state **85b**, the diene was believed to host a conformation similar to **83b**. Although this conformation is stereoelectronically less favorable, it permits the stabilization of the transition state via intermolecular hydrogen bonding and thus leads to products with the opposite relative stereochemistry. If the hydroxyl group is replaced by a methoxy or siloxy group then transition state **85a** is favored leading to the products **84a,d**

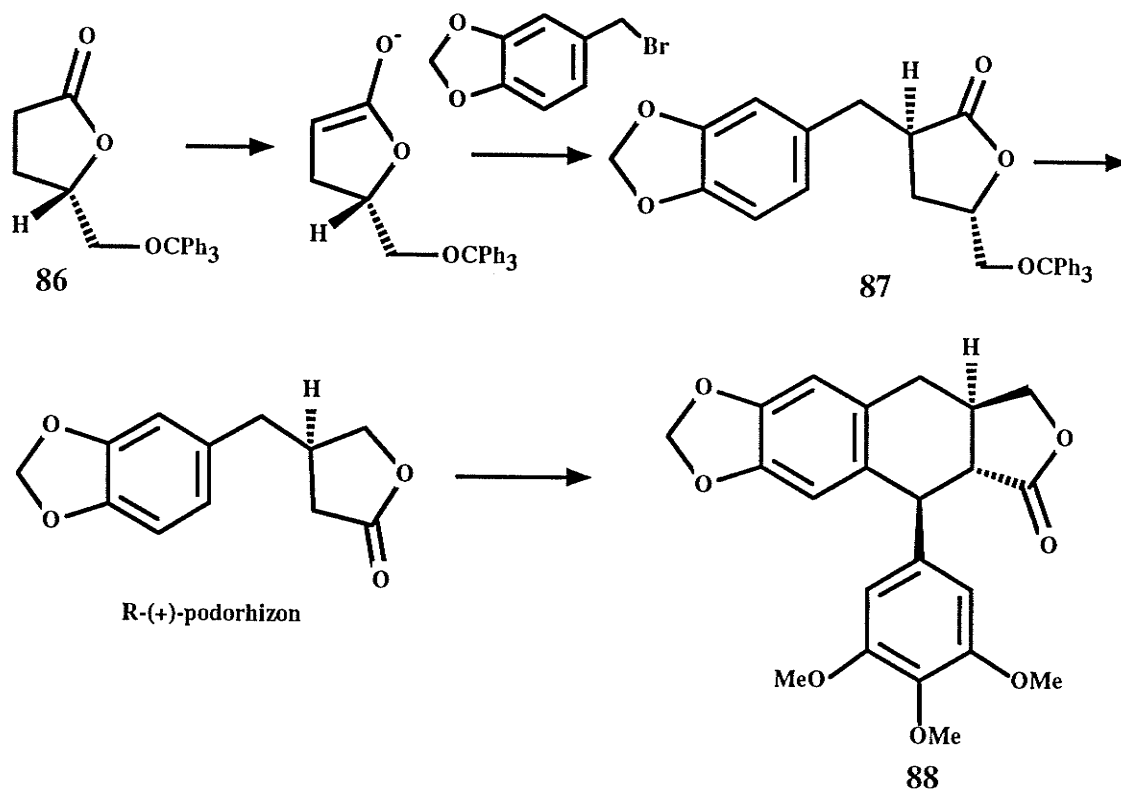


1.9 Asymmetric Synthesis of Aryltetralin Lignans

As part of this thesis work includes the asymmetric synthesis of some aryltetralin lignans, a brief review of the asymmetric syntheses present in the literature is appropriate. Many non-asymmetric syntheses of the aforementioned are present in the literature.^{21,24,41,48,73-84} Fewer asymmetric syntheses have been described. A review paper by Ward discusses many of the asymmetric and non-asymmetric syntheses of lignans.⁷⁴

One of the first asymmetric syntheses of an aryltetralin lignan was described by Koga *et al.* in 1979.⁸⁵ Synthesis of the optically pure (-)-isodeoxypodophyllotoxin **88** started with the alkylation of the readily available chiral γ -butyrolactone **86** with piperonyl bromide (Scheme 1.54). In this key asymmetric step, addition of the bromide to the enolate of **86** occurred from the least sterically hindered face of the enolate. When a bulky

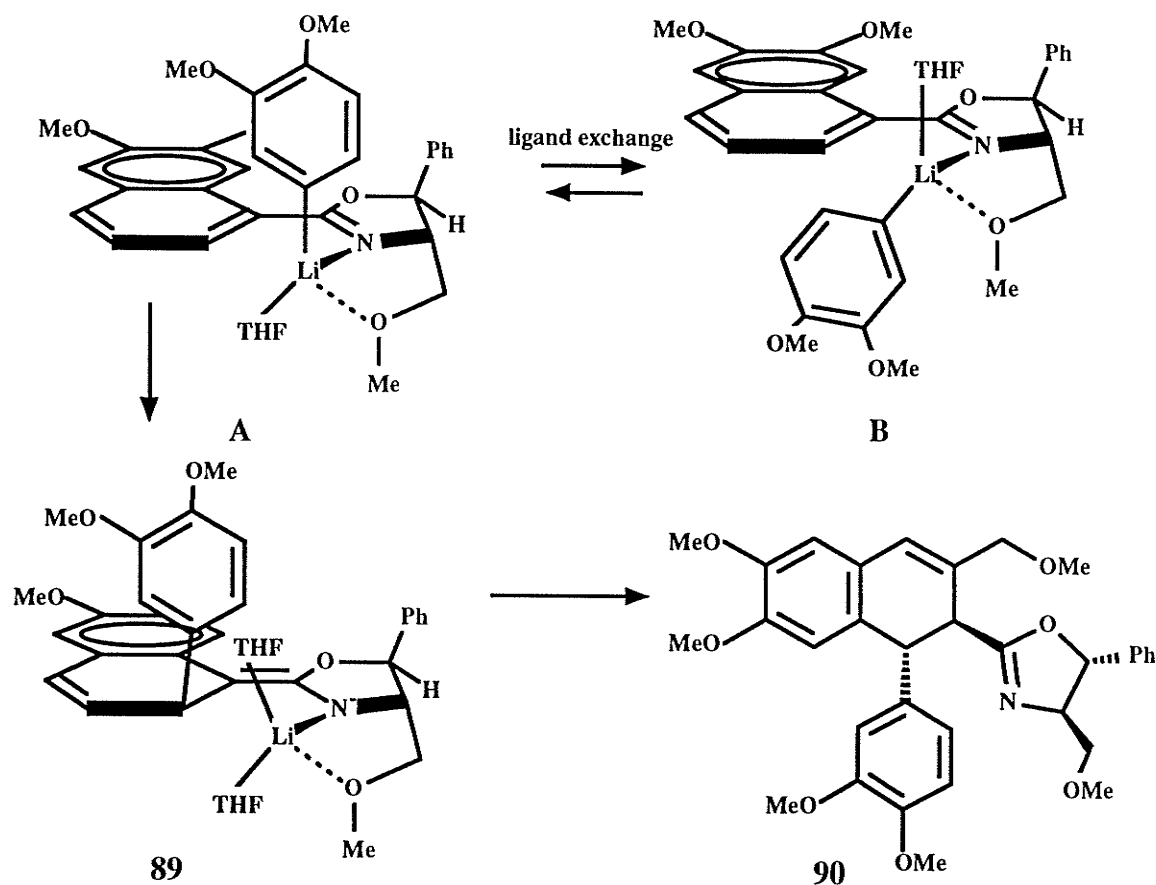
Scheme 1.54



trityl group was used, a 79:21 ratio of diastereomers was obtained. The alkylation product **87** was converted to the known R-(+)-podorhizon. The anion of podorhizon was condensed with trimethoxybenzaldehyde and the alcohol subsequently cyclized to optically pure **88**.

Meyers *et al.* have applied an asymmetric conjugate addition of an aryllithium species to a chiral naphthoyloxazoline intermediate in their synthesis of (+)-phyltetralin (Scheme 1.55).⁸⁶ The stereoselectivity of the addition step was attributed to a coordination effect rather than a steric interaction. The tetra-coordinate lithium species was believed to exist in two equilibrium forms A and B. The rate of ligand exchange between the two forms was believed to be dependent on the ligand coordination ability. The use of a better coordinating solvent like THF (cf. ether), which resulted in higher diastereoselectivity, was believed to result in a more well defined chelate. When ether was used as a solvent, the diastereoselectivity dropped from 95:5 to 70:30 suggesting that

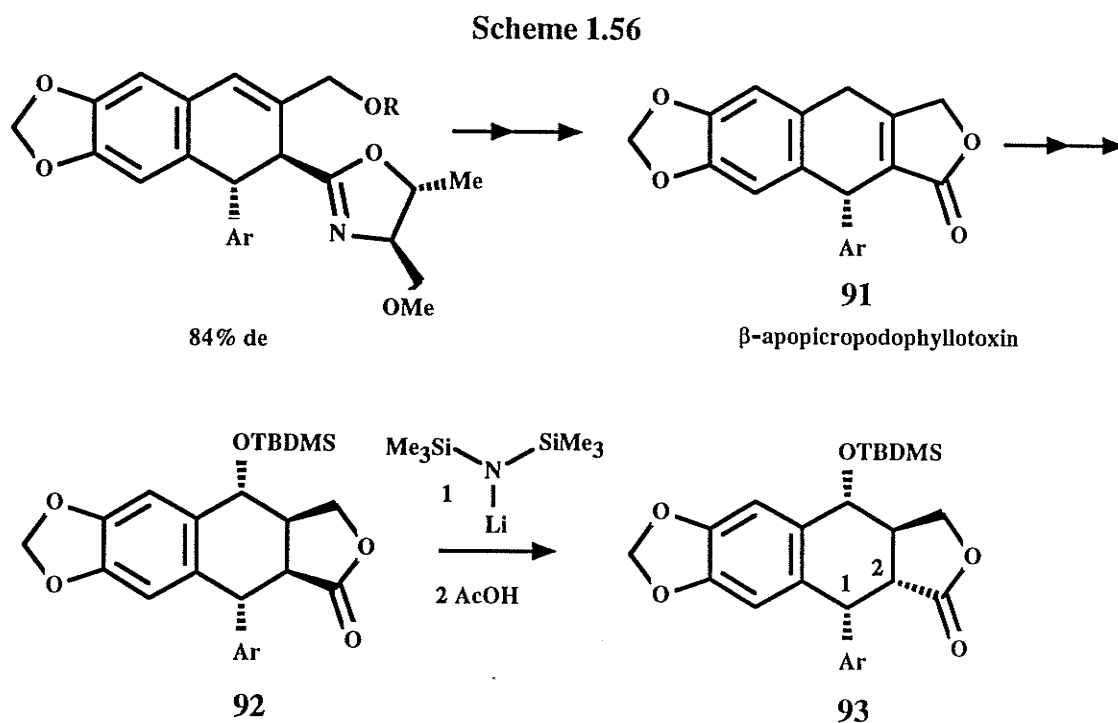
Scheme 1.55



a more random addition was occurring to a poorly defined chelate. Between the two chelate forms A and B, only chelate A has the correct aryllithium disposition for the 1,5 suprafacial sigmatropic rearrangement to occur. Once the azaenolate **89** had formed, protonation occurred from the more accessible face opposite the aryl group giving the 1,2-*trans* oxazoline derivative **90**. The synthesis of (+)-phlytetralin was completed in 44% yield with a 68% optical purity.

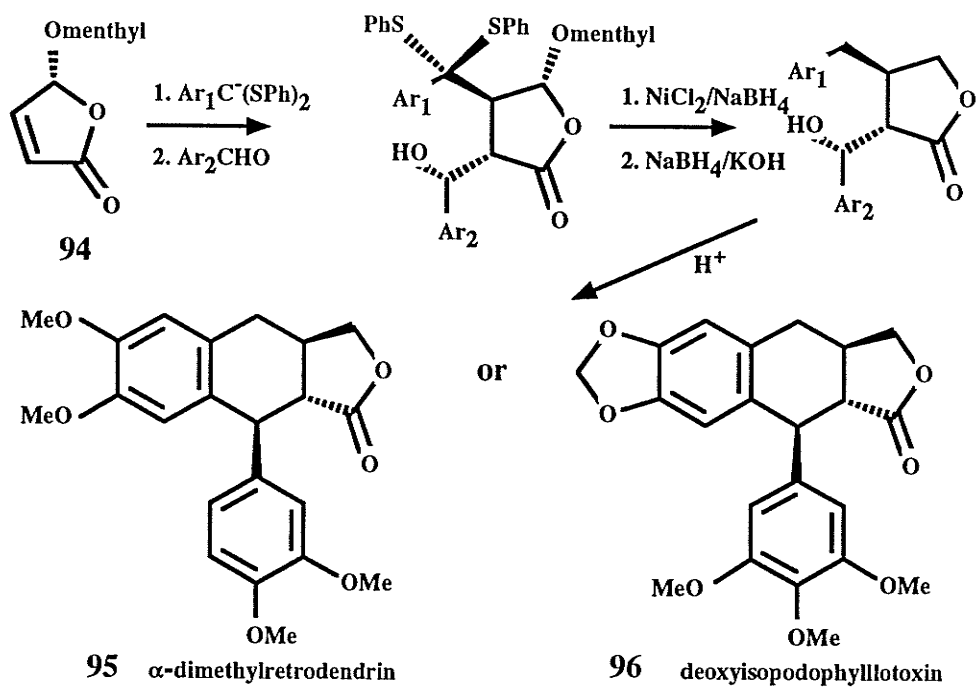
Meyers *et al.* used a similar strategy in the first published asymmetric synthesis of podophyllotoxin (Scheme 1.56).⁸⁷ Again, the synthesis involved the asymmetric conjugate addition of an aryllithium species to the appropriately substituted naphthoyloxazoline derivative in 84% de. The synthesis was exceedingly long (24 steps) and had a relatively low overall yield of 5%. When the intermediate

β -apopicropodophyllotoxin **91** was ring opened, the next species **92** had an undesirable 1,2-*trans* stereochemistry which ultimately had to be epimerized to the 1,2-*cis* stereochemistry via kinetic protonation of the C₂ enolate of **92**. Unfortunately this step was inefficient and resulted in a 1:1 mixture of the desirable podophyllotoxin and the C₂ epimeric picropodophyllotoxin.



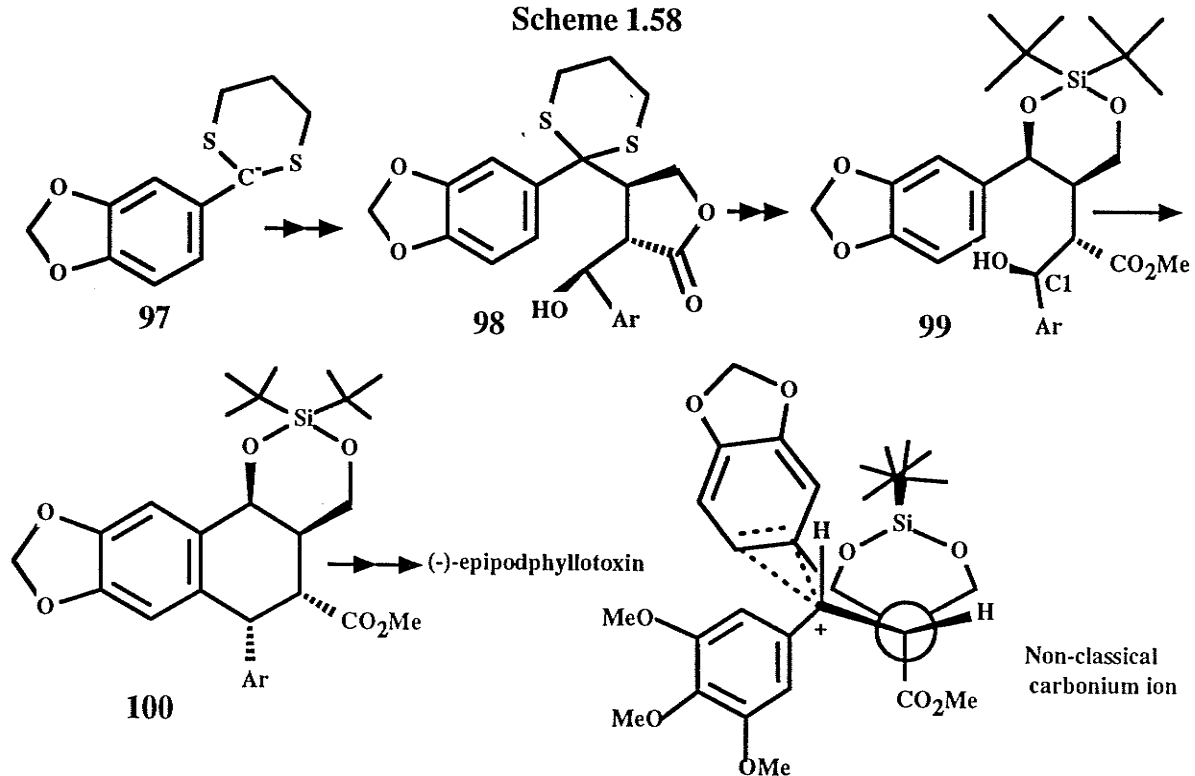
The relative thermodynamic stability of the 1,2-*trans* geometry is a thermodynamic trap which plagues many of these syntheses. For instance, while Pelter *et al.* successfully introduced the correct stereochemistry at the two and three positions of the tetralin fragment via tandem Michael addition to the chiral butenolide **94**, final acid mediated ring closure produced **95** α -dimethylretrodendrin or (-)-4-deoxyisopodophyllotoxin **96** which had the all *trans* stereochemistry (Scheme 1.57).⁸⁸

Scheme 1.57



The elusive 1,2-*cis* stereochemical control has been bested by Van Speybroeck *et al.*⁸⁹ Using a method similar to Pelter's conjugate addition, they carried out the conjugate addition of dithiolane anion **97** to butenolide **94** to effect chirality transfer (Scheme 1.58).

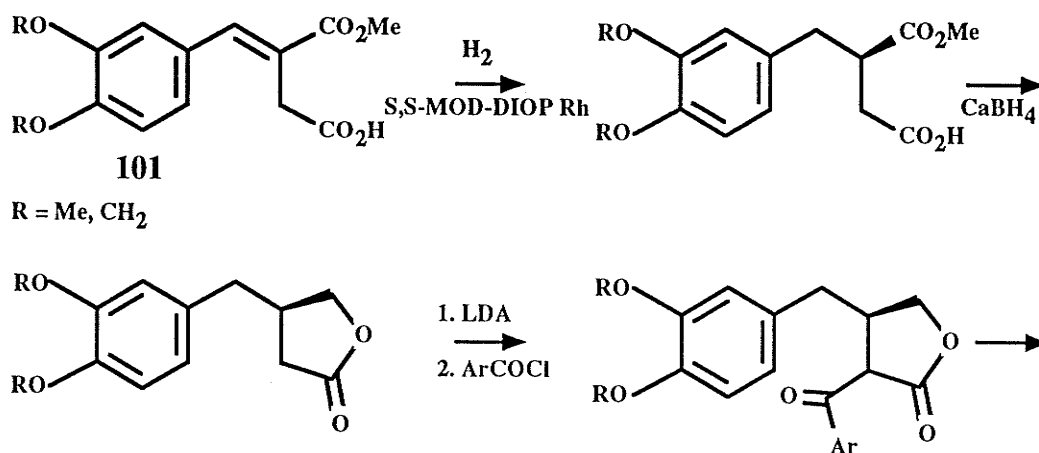
Scheme 1.58

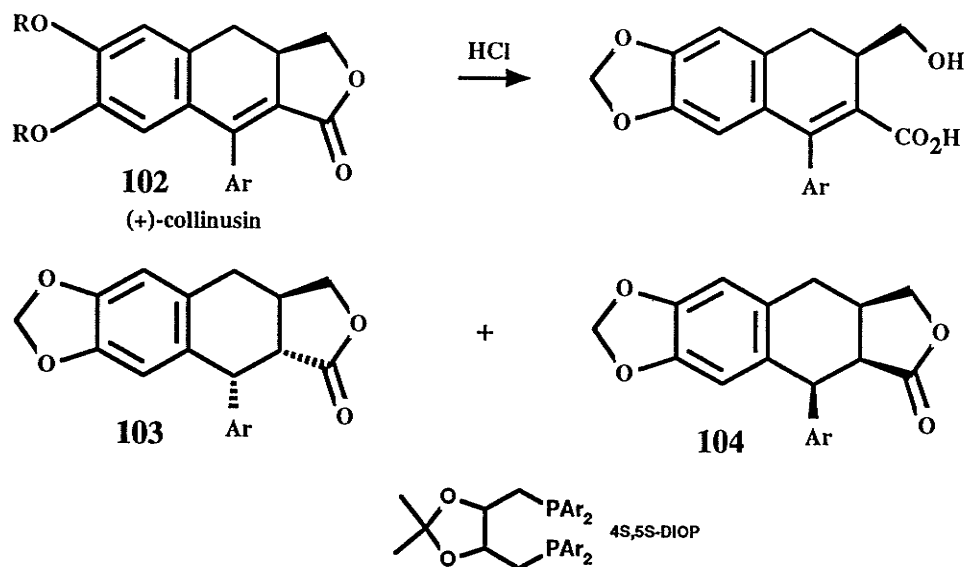


The de of the reaction was estimated at 95%. After removal of the chiral auxiliary and condensation of the anion with trimethoxybenzaldehyde, the stage was set for the stereoselective ring closure reaction. In the event of an acid catalyzed ring closure of the intermediate alcohol **98**, the incorrect 1,2-*trans* stereochemistry resulted. However, incorporation of a *cis*-substituted siladioxane ring as shown in **99** and subsequent cyclization resulted in the exclusive formation of the 1,2-*cis*-2,3-*trans* tetralin **100** which was eventually converted to (-)-epipodophyllotoxin in 20% overall yield. If the C₁ epimer of **99** is cyclized under identical conditions the resultant product is the 1,2-*trans*-2,3-*cis* tetralin. Consideration of steric requirements ruled out an S_N2 mechanism. Thus it was postulated that the incipient carbonium ion at C₁, which formed a non-classical intermediate, was intercepted by the aromatic ring before rotation could occur.

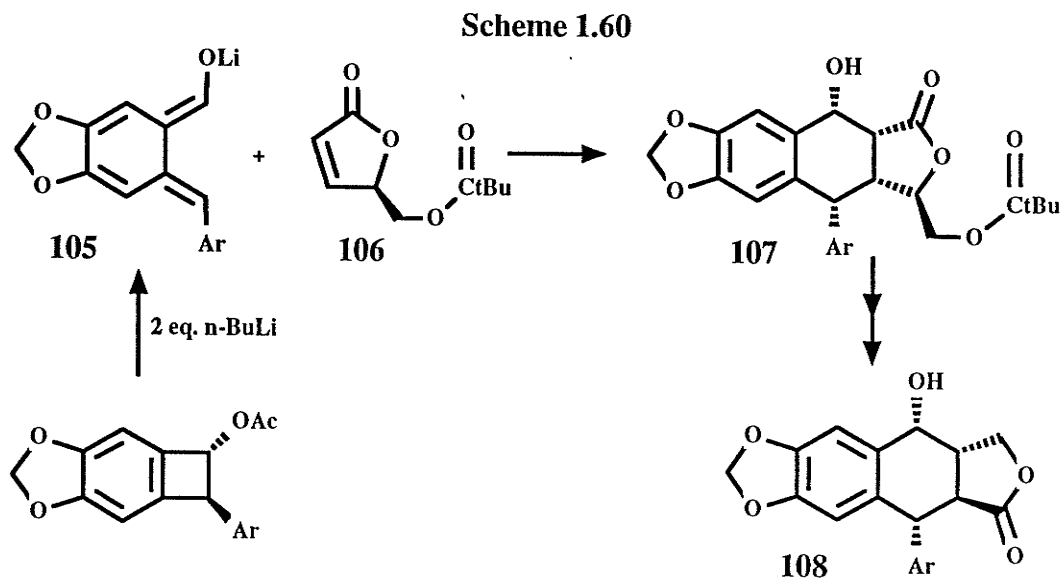
Achiwa *et al.* have carried out total syntheses of (+)-collinusin **102**⁹⁰ and (-)-deoxypodophyllotoxin **103** (Scheme 1.59).⁹¹ The chirality was introduced by asymmetric catalytic hydrogenation of the half-ester alkene **101** using a chiral rhodium bis-phosphine catalyst. However, in the synthesis of deopodophyllotoxin a 1.5:1 mixture of (-)-deoxypodophyllotoxin **103** (1,2-*cis*-2,3-*trans*) and (+)-isodeoxypodophyllotoxin (1,2,3-*cis*) **104** was obtained in the final steps.

Scheme 1.59





Choy has carried out a synthesis of (-)-epiisopodophyllotoxin **108** by an anionic Diels-Alder addition of the lithio- α -oxy- α' -aryl-*o*-QDM **105** to the chiral butenolide **106** (Scheme 1.60).⁹² *o*-QDM **105**, generated by treatment of the 1-acetoxy-2-aryl-benzocyclobutene with methyllithium, reacted with **106** through *endo* addition giving the all-*cis* lactone **107**. Unfortunately, the 1,2-*cis* stereochemistry was lost completely by epimerization of the C₂ center in the remaining steps of the synthesis.

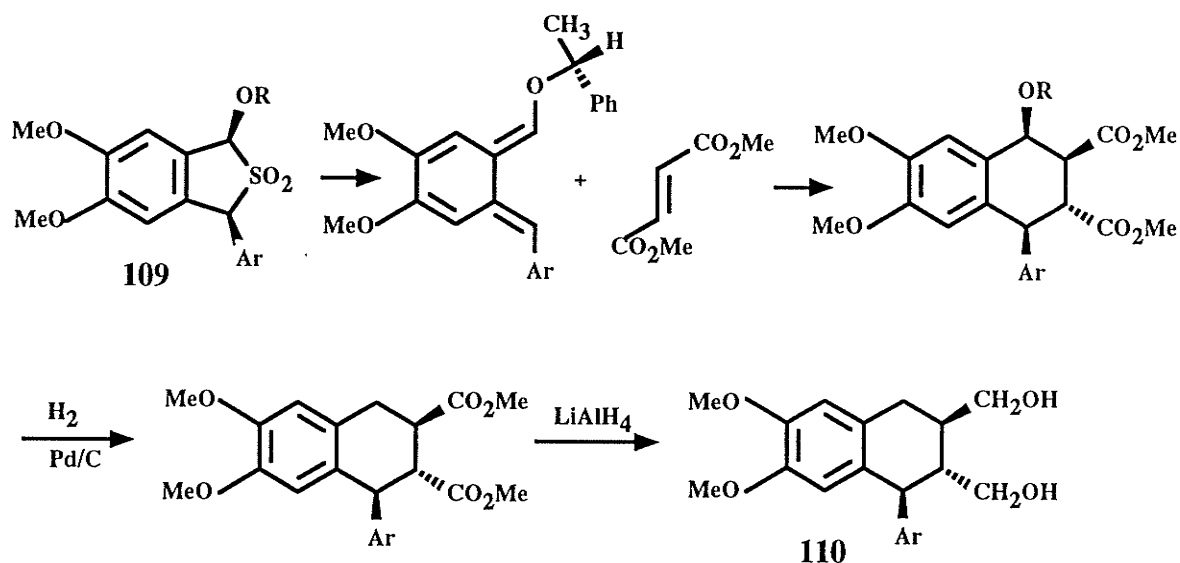


Charlton *et al.* have carried out the syntheses of a variety of aryltetralin lignans including (+)-isolariciresinol dimethyl ether (Scheme 1.61),⁹³ two podophyllotoxin

analogues (Scheme 1.62),⁹⁴ and (-)-neopodophyllotoxin⁹⁵ (Scheme 1.63) using *o*-QDMs.

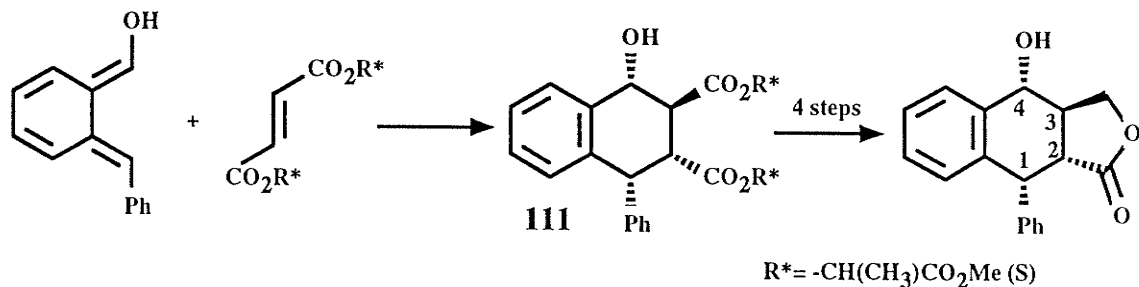
In the synthesis of isolariciresinol dimethyl ether, a *cis*-sulfone **109** bearing the (R)-phenylethyl chiral auxiliary was cycloaddled to dimethyl fumarate yielding *endo* adducts in a 70:30 mixture (de = 40%). Hydrogenolysis and reduction gave (+)-isolariciresinol dimethyl ether **110** in 83% optical purity. In their analogue and

Scheme 1.61

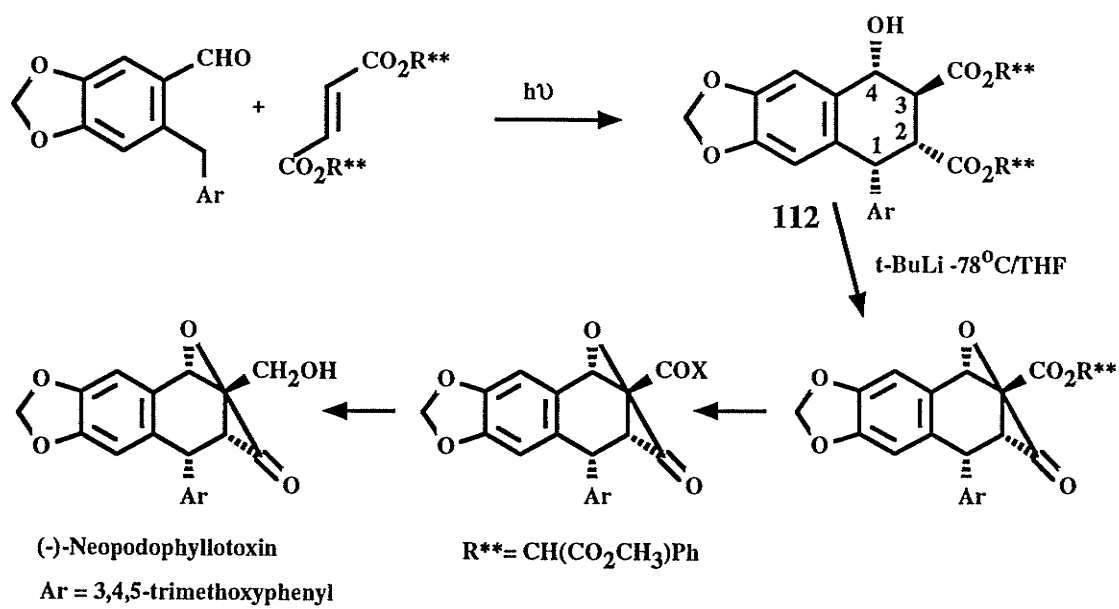


neopodophyllotoxin syntheses, achiral *o*-QDMs bearing α -hydroxy groups were cycloaddled to the fumarates of methyl (S)-lactate and methyl (S)-mandelate respectively. The cycloadducts **111** and **112** arose from unprecedented *exo* transition states which furnished the desired 1,2-*cis* stereochemistry. The origin of this unusual diastereoselectivity shall be discussed in full in the results and discussion section of this thesis.

Scheme 1.62



Scheme 1.63



Thesis Objectives

At the outset of this thesis work, several objectives were established based on previous work in the area of orthoquinodimethane chemistry. The main goals of this thesis are outlined as follows:

1) To determine the mechanism of the stereoselective addition of α -hydroxy-orthoquinodimethane to the acrylate of methyl lactate.

It had been observed by previous researchers that the addition of an α -hydroxy-orthoquinodimethane to the fumarate or acrylate of methyl (S)-lactate proceeded to selectively give products possessing an unprecedented stereochemistry. These products arose from an unexpected *exo* transition state. All other previous accounts of intermolecular cycloadditions reactions for similar types of systems were known to proceed through *endo* transition states. It was thought that hydrogen bonding in the transition state might somehow be controlling the reaction. Two questions were therefore posed: 1) does a hydrogen bond in the transition state lead the reaction towards the formation of *exo* cycloadducts and 2) what controls the preference for the addition to one face of the dienophile?

2) To develop a general method for the asymmetric synthesis of aryltetralin lignans such that all possible stereochemistries could be achieved starting from a single cycloadduct.

Since the reactions of α -hydroxy- α' -*o*-QDMs with the fumarates of either methyl lactate or methyl mandelate were known to proceed with high asymmetric induction, it was very desirable to use these reactions in organic synthesis. Specifically, these reactions are particularly suited towards the synthesis of aryltetralin lignans, many of which show notable antitumor activity (see Chapter 1). Plourde had used the addition of

α -hydroxy- α' -phenyl-*o*-QDM to the fumarate of methyl (S)-lactate in the synthesis of a podophyllotoxin analogue. Koh used a similar strategy to synthesize podophyllotoxin. Both of these strategies were limited to the synthesis of a single lignan of a single relative stereochemistry. A question was therefore posed. Could the same cycloaddition reaction be used for the synthesis of lignans possessing a variety of stereochemistries?

3) To determine the stereochemistry of the addition of α -hydroxy- α -phenyl-*o*-QDM to the fumarate of methyl (R)-mandelate and its possible application to lignan synthesis.

Many syntheses of aryltetralin lignans employ α -hydroxy- α' -*o*-QDMs intermediates. However, difficulties in the photochemical or thermal generation of the *o*-QDM have been encountered. The photochemical preparation of *o*-QDMs in the presence fumarate dienophiles has led to triplet quenching by the dienophile. Similarly, the corresponding 1-hydroxy-2-arylbenzocyclobutenes needed to generate the appropriate orthoquinodimethanes are difficult to synthesize due to their thermal instability. However, 1-hydroxy-1-arylbenzocyclobutenes are easy to prepare and thermally stable relative to their 2-aryl counterparts. With this in mind, Koh carried out the cycloaddition of the fumarate of methyl mandelate with 1-hydroxy-1-phenylbenzocyclobutene and found that only one product was formed. However, the stereochemistry of this cycloadduct was unknown and needed to be determined. Two questions were posed: 1) what was the relative and absolute stereochemistry of the adduct and 2) could this adduct be converted to an intermediate that was potentially suitable to the synthesis of aryltetralin lignans?

Chapter 2

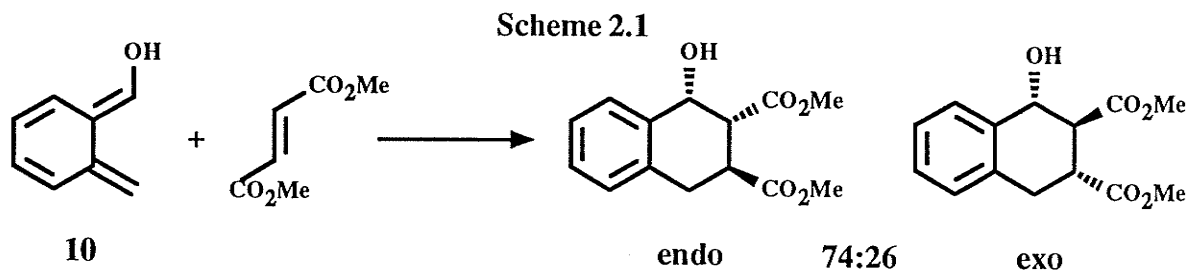
Results and Discussion

The results and discussion section of this thesis is divided into three main sections:

- (1) Section 2.1.1. This section is a discussion of the mechanism of the cycloaddition of methyl lactate and methyl mandelate substituted fumarates and acrylates to α -hydroxy-*o*-QDMs. A hydrogen bonding model is proposed to explain the observed diastereoselectivity of the aforementioned reactions. This first section (2.1.1) describes the effects of solvent polarity, replacement of the lactate chiral auxiliary with alternative groups, and replacement of the hydroxyl group on the *o*-QDM with methoxyl. In section 2.1.2, the validity of a hydrogen bond in the transition state of the cycloaddition reaction is examined in terms of a molecular model. Force field calculations (MMX) on the transition state (section 2.1.2.1) probe the stabilizing effects of a hydrogen bond in the transition state. Calculations using a semi-empirical molecular orbital method (AM1) are used to corroborate the findings of the MMX calculations (section 2.1.2.2).
- (2) The application of the aforementioned reactions in organic synthesis is explored in section 2.2.1. A general asymmetric synthesis of aryltetralin lignans, including (-)- α -dimethylretrodendrin, using the addition of (R)-mandeloxo fumarate to α -hydroxy- α' -aryl-*o*-QDM, is described. To assess the possible antitumor ability of these compounds, the preferred conformations of the four lignans are elucidated and compared to the conformations of structurally similar lignans possessing known antitumor activity (section 2.2.2).
- (3) As an alternative route to aryl tetralin lignans, the additions of (R)-mandeloxo fumarate to the isomeric α -hydroxy- α -aryl-*o*-QDMs are examined. The determination of the absolute stereochemistry of the cycloadducts is discussed and a method for the conversion of the adducts to potential lignan precursors is developed (section 2.3).

2.1.1 Elucidation of the Mechanism of the Stereoselective Addition of α -Hydroxy-*o*-QDM to Lactate and Mandelate Substituted Dienophiles.

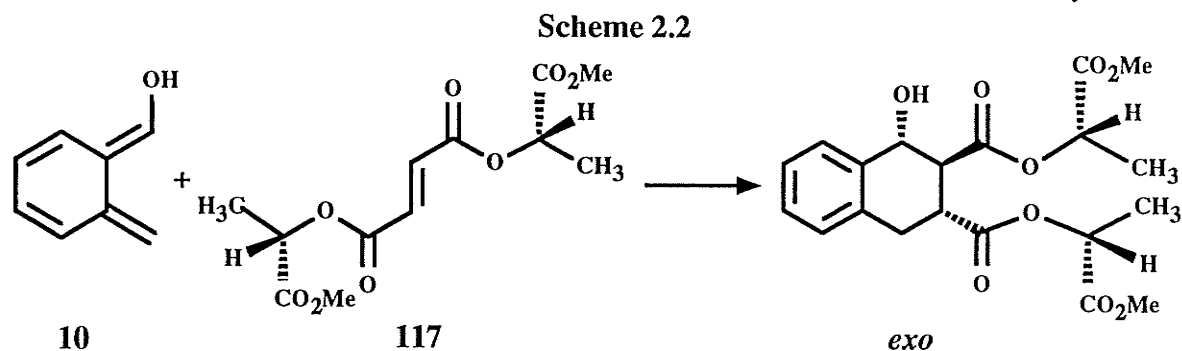
In the introduction, the addition of α -hydroxy-orthoquinodimethanes to dienophiles bearing the lactate or mandelate chiral auxiliaries were shown to add diastereoselectively via an *exo* transition state. This was in contrast to the addition of dimethyl fumarate or methyl acrylate which added predominately in an *endo* fashion. Specifically, cycloaddition of α -hydroxy-*o*-QDM **10** with dimethyl fumarate at room temperature resulted in a 74:26 *endo* to *exo* ratio (Scheme 2.1).⁹⁶ Since the reaction was under kinetic control, the product ratios directly reflected the difference in the free energies of the transition states and at room temperature this corresponds to an energy difference of about 0.6 kcal. At the outset of this research, it was proposed that the



unusual propensity for *exo* addition to lactyl or mandyl substituted dienophiles may be due to an intermolecular hydrogen bond. This hydrogen bond was believed to occur between the hydroxyl group of the orthoquinodimethane and the carbonyl group of the chiral auxiliary. The strength of a hydrogen bond varies from 1 to 10 kcal.⁹⁷ If we assume that hydrogen bonding can only occur in the *exo* transition state and not in the *endo* transition state, then the premise of a hydrogen bond is quite reasonable in that it could overcome the normal 0.6 kcal preference for *endo* isomer formation when addition occurs to dimethyl fumarate.

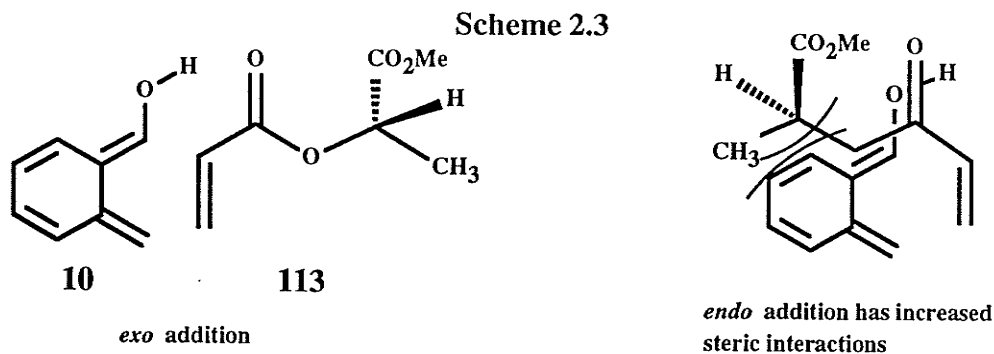
The cycloadduct from the reaction of the fumarate of methyl (*S*)-lactate and α -hydroxy-*o*-QDM was predominantly *exo* and also of a single absolute stereochemistry

(Scheme 2.2). A suitable mechanistic model should be able to explain both the *exo* diastereoselectivity and the absolute stereoselectivity, which arises due to selective reaction at only one face of the dienophile. The fumarate of ethyl (*S*)-lactate is known to react with other dienes with moderate facial selectivity⁶¹ and it is possible that intermolecular hydrogen bonding in the transition state can increase this selectivity.

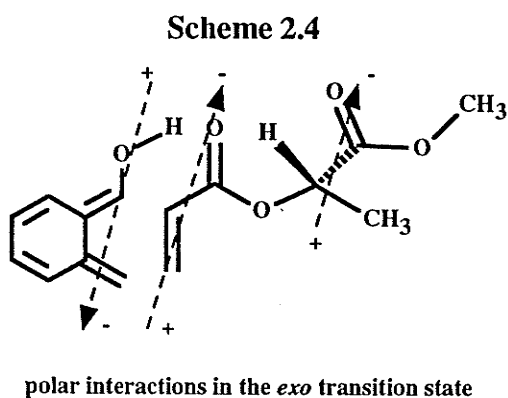


It should be possible to test the hypothesis of stereochemical control mediated by intermolecular hydrogen bonding by observing the effects of modifications that specifically disrupt this hydrogen bonding. Perturbation of the hydrogen bonding interaction should result in a decrease in *exo* selectivity. It is possible to disrupt the intermolecular hydrogen bond in several ways: (1) addition of a solvent to the reaction mixture which can accept a hydrogen bond from the hydroxyl group of the *o*-QDM, or donate a hydrogen bond to the carbonyl of the lactate group, (2) replacement of the hydrogen of the hydroxyl group with a methyl group, or (3) alteration of the chiral auxiliary to reduce its hydrogen bonding ability.

In addition to the hydrogen bonding theory, two other theories could explain the observed *exo* diastereoselectivity. One might imagine that a steric interaction between the lactyl group and the *o*-quinodimethane favors an *exo* transition state. This seems to be quite plausible for the addition of α -hydroxy-*o*-QDM **10** to lactyl acrylate **113** (Scheme 2.3). However, given the highly symmetrical nature of dilactyl fumarate **117** which also adds *exo* (Scheme 2.2), it seems unlikely that major steric differences exist between the *endo* and *exo* transition states for this dienophile.



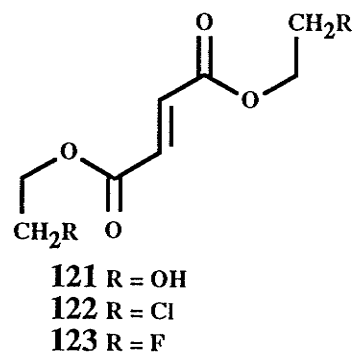
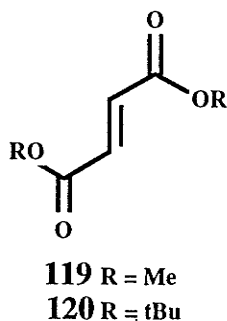
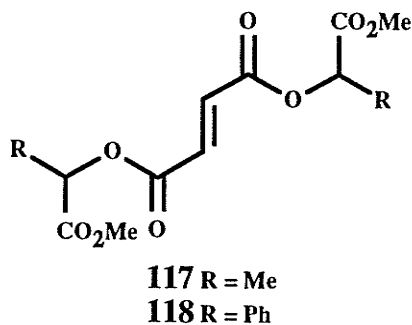
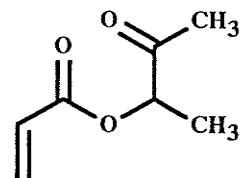
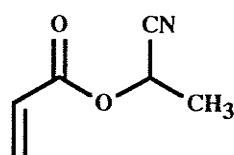
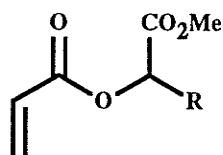
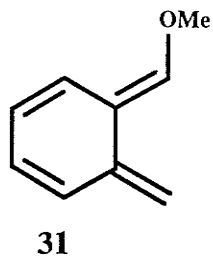
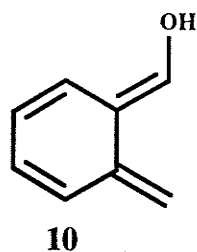
An explanation based on polar interactions might also be possible. Perhaps the dipoles of the two reactants interact more favorably in the *exo* transition state than in the *endo* transition state (Scheme 2.4). It would be difficult to distinguish between a hydrogen bonding interaction and a polar interaction based on polar solvent effects, as both would be masked by the addition of a polar, hydrogen bonding solvent. However one might be able to distinguish them by exchanging the polar carbonyl group in the chiral auxiliary with an equally polar group incapable of hydrogen bonding.



In order to investigate the possible factors which control the *exo/endo* selectivity, and in some cases the diastereofacial selectivity, a series of test dienophiles were synthesized and reacted with *o*-QDM **10** (Scheme 2.5). In addition, the hydroxyl group of the *o*-QDM was converted to a methoxyl group as in **31** and its effects on the *exo/endo* and facial selectivity examined. The effect of the addition of dimethyl sulfoxide (DMSO), a strong hydrogen bond acceptor solvent, on the diastereoselectivity was also examined.

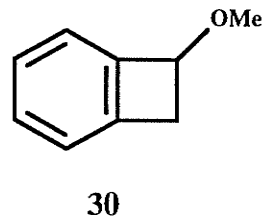
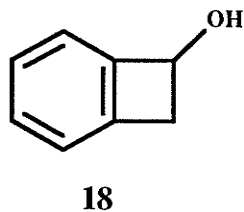
Benzocyclobutenes **18** and **30** were chosen as orthoquinodimethane precursors to

Scheme 2.5



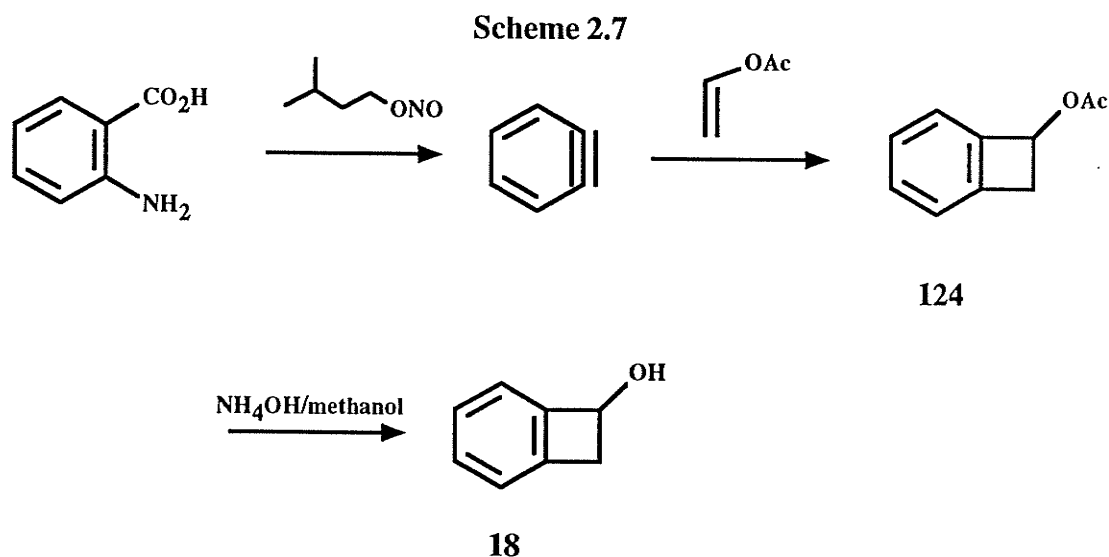
10 and **31** (Scheme 2.6), as they were known to react efficiently with both acrylates and fumarates and were also readily available. Benzocyclobutenol **18** was prepared according

Scheme 2.6



to the known benzyne method.⁹⁸ Diazotization of anthranilic acid (2-aminobenzoic acid) with isoamyl nitrite in refluxing vinyl acetate gave 1-acetoxybenzocyclobutene **124** in 46% yield (Scheme 2.7). Deacetylation of the acetate was accomplished by stirring in a 30% NH₄OH/methanol solution giving benzocyclobutenol **18**.

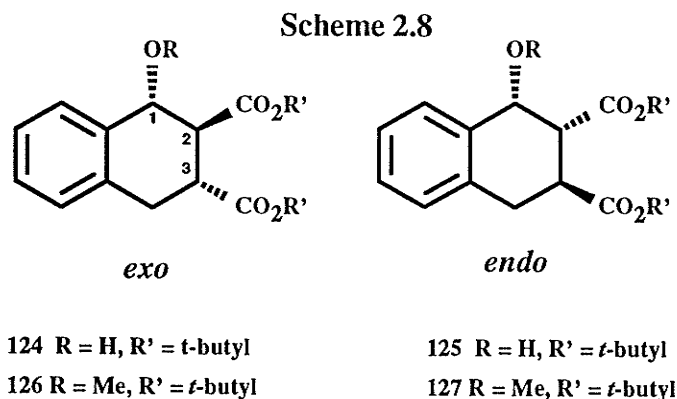
1-Methoxybenzocyclobutene **30** was synthesized in quantitative yield by treatment of **18** with excess methyl iodide and silver oxide.⁹⁸



In the following discussion of the cycloaddition of **18** and **30** with the various dienophiles mentioned above, the analysis of the product ratios was performed using either ¹H-NMR (300 or 500 MHz) or HPLC (ODS-2, methanol, water, acetonitrile combinations). The assignment of the relative stereochemistries (*endo* vs *exo*) of the cycloadducts was made using ¹H-NMR. For all of the cycloadducts, H₁ appears between 4.6 and 5.2 ppm (in CDCl₃). The coupling constants J_{1,2} are indicative of the relative stereochemistry on the tetralin ring. Couplings constants for the *endo* adducts (1,2-*cis*) are on the order of 2-5 Hz while *exo* adducts (1,2-*trans*) are in the range of 7-12 Hz.^{35,39,94}

To determine if the steric bulk of the lactyl group was responsible for the *exo* diastereoselectivity, a steric mimic of the lactyl chiral auxiliary, namely di-*tert*-butyl fumarate **120** was prepared. Initial attempts at generating the fumarate by heating neat *t*-butyl alcohol and fumaryl chloride led to substantial amounts of fumaric acid. It is likely that hydrochloric acid produced by the reaction caused the elimination of water from *t*-butyl alcohol. This adventitious water could then go on to react with the fumaryl chloride to give the observed product. Alternatively, the hydrochloric acid may have cleaved the *t*-butyl fumarate to produce fumaric acid and isobutylene. When fumaryl

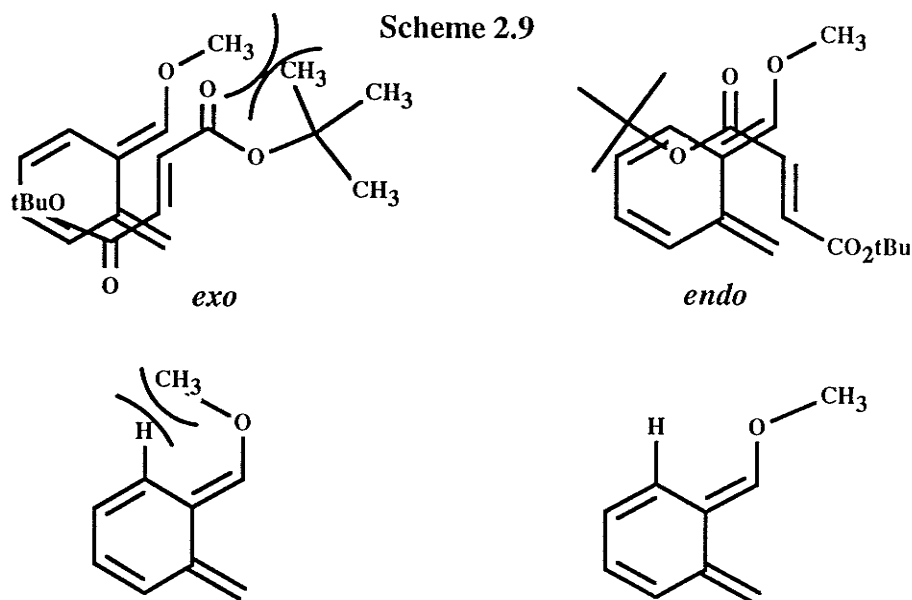
chloride and *t*-butyl alcohol were refluxed in benzene in the presence of molecular sieves under a Dean-Stark head to remove the water, a 24% yield of di-*tert*-butyl fumarate **120** was obtained. Thermolysis of benzocyclobutenol **18** in the presence of di-*tert*-butyl fumarate **120** led to the formation of two adducts (Scheme 2.8). Examination of the crude $^1\text{H-NMR}$ revealed doublets at 4.88 ppm ($J = 8.88$) and 5.03 ppm ($J = 3.57$) corresponding to the *exo* and *endo* adducts **124** and **125**. Integration of these signals gave a 1.5:1 ratio of *endo* to *exo*: cf 2.85:1 (*endo/exo*) ratio for dimethyl fumarate **119**. Although this



corresponds to a slight increase in the amount of *exo* product, relative to the reaction of α -hydroxy-*o*-QDM **10** with dimethyl fumarate, *endo* still predominates. The increase is not significant enough to conclude that the *exo* preference, observed when the lactyl substituted dienophile **117** is reacted with **10**, is a result of the steric bulk of the lactyl group.

To assess the effects of the hydroxyl group on the cycloaddition reaction, 1-methoxybenzocyclobutene **30** was thermolysed in the presence of di-*tert*-butyl fumarate **120**. Analysis of the crude reaction mixture by $^1\text{H-NMR}$ indicated that the reaction proceeded very cleanly with the formation of primarily *endo* adduct **127** (Scheme 2.8). The $^1\text{H-NMR}$ also revealed a doublet at 4.74 ppm ($J=8.1$) indicating an *exo* cycloadduct **126**. Integration of this peak relative to the H_1 of the *endo* cycloadduct **127** (4.53 ppm, $J=3.39$) gave an *endo/exo* ratio of 88:12. It is evident from this result that the presence of the α -methoxy group on the *o*-QDM results in an enhancement of the *endo* selectivity

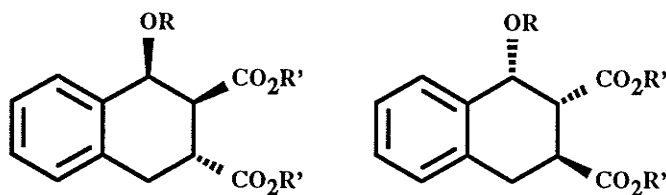
relative to the α -hydroxy-*o*-QDM. This may be attributable to an increase in the absolute difference in the magnitudes of the C_2 and C_3 orbital coefficients. A more plausible explanation is that an increased steric interaction of the methoxy group with the bulky ester group in the *exo* transition state favors *endo* addition (Scheme 2.9). In this model, it must be assumed that the methoxy group is turned away from the *o*-QDM for steric reasons.



The reaction of dilactyl fumarate **117** with α -methoxy-*o*-QDM **31** serves as an effective probe for the effects of the α -hydroxyl group on the *exo/endo* selectivity. In addition, the role of the proposed hydrogen bond in the control of the facial selectivity with respect to the chiral dienophile can be studied. The reaction of α -methoxy-*o*-QDM **31** with di-*tert*-butyl fumarate **120** resulted in a preferred *endo* addition and the same stereoselectivity might be expected for dilactyl fumarate **117**. If the hydrogen bond **only** controls the *endolexo* selectivity, then one would expect that the reaction with **117** would produce a preferred *endo* adduct with high absolute stereoselectivity. If the hydrogen bonding also enhanced the facial selectivity with respect to the dienophile then reaction with α -methoxy-*o*-QDM **31** might give reduced facial selectivity (a mixture of *endo* diastereomers).

Reaction of dilactyl fumarate **117**, prepared by heating methyl (S)-lactate with fumaryl chloride,⁹⁴ with **30** in refluxing toluene gave predominately *endo* adducts in a 62% combined yield. The ¹H-NMR of the crude product in CDCl₃ showed two overlapping doublets at 4.68 (J=3.00) and 4.66 (J=3.31). Integration of the two peaks was possible by rerunning the NMR in C₆D₆. Integration of the doublets at 4.75 ppm (J=2.96) and 4.56 ppm (J=3.33) gave a 1.57:1 ratio for the two *endo* adducts **128** and **129** (Scheme 2.10). For the sake of comparison the HPLC ratio was also obtained (Figure 1).

Scheme 2.10



128 R = Me, R' = methyl (S)-lactate

129 R = Me, R' = methyl (S)-lactate

Separation of the *endo* isomers was possible on a reverse phase column (ODS-2; octadecylsilyl) using a ternary solvent mixture (57% methanol, 37% water, 6% acetonitrile; isocratic). *Endo* adducts **129** (retention time = 16.4 min) and **128** (retention time = 19 min) were sufficiently resolved to allow integration of the peaks and isolation for characterization purposes. Thus a ratio of 1.56:1 (**128** to **129**) was found, in agreement with the NMR ratio. Although it was possible to determine the relative stereochemistry within the tetralin ring via ¹H-NMR, it was impossible to relate the relative stereochemistry of the ring to the chiral auxiliary. No information regarding the slight facial selectivity (slight preference for one *endo* diastereomer) could be obtained. The dramatic decrease in the facial selectivity (absolute selectivity rather than *endo/exo* selectivity) for this reaction relative to the reaction of α -hydroxy-*o*-QDM with dilactyl fumarate reflects upon the apparent importance of the hydroxyl group to facial selectivity in the latter reaction.

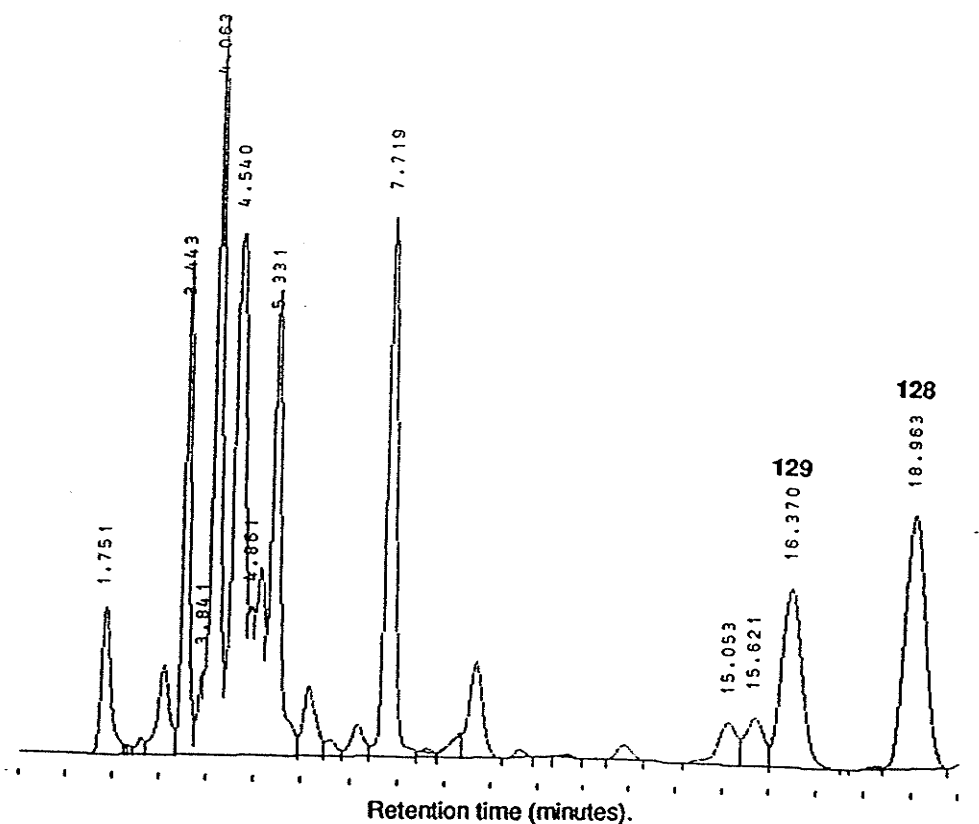
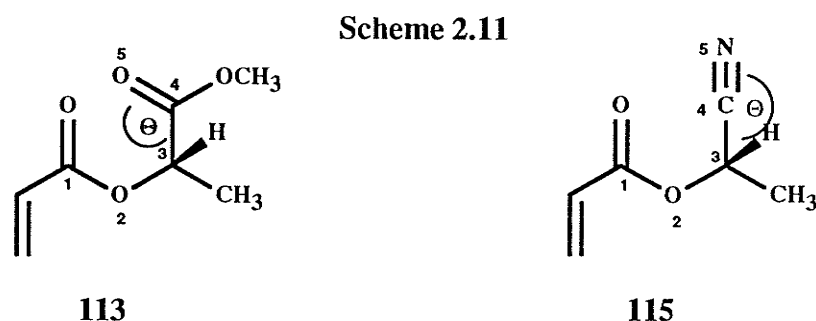


Figure 1. HPLC trace of the crude reaction mixture of endo adducts 128 and 129.

At this point there is still little evidence bearing directly on why dilactyl fumarate reacts with α -hydroxy-*o*-QDM to give *exo* products. It is only known that the effect can be blocked by replacing the hydroxyl group with a methoxyl group on the *o*-QDM, or by replacing the lactyl groups on the dienophile with *tert*-butyl or methyl groups. While it is tempting to attribute the effect of methoxyl group replacement to a disruption of hydrogen bonding, it is also possible that the methoxyl group simply sterically disfavors the *exo* transition state. The argument for an increased steric effect in the *exo* transition state may be reasonable in light of the fact that α -hydroxy-*o*-QDM **10** adds to di-*tert*-butyl fumarate **120** giving a mixture of *exo* and *endo* adducts while α -methoxy-*o*-QDM **31** adds to **120** to give almost exclusively *endo* adduct.

To determine whether a polar effect or a hydrogen bond is favoring the *exo* transition state in the reaction of dilactyl fumarate with α -hydroxy-*o*-QDM, dienophiles

115, **121**, **122**, and **123** were investigated (Scheme 2.5). Dienophile **115** was chosen because of its structural similarity with lactyl acrylate **113**, the electronegative element being separated from C₁ by the same number of atoms. The cyano group, which mimics the polarity of the ester group, has a bond angle of 180° whereas the carbonyl group has a bond angle of 120° (Scheme 2.11). The linearity of the cyano group should make hydrogen bonding in the transition state sterically impossible as the nitrogen atom will be further removed from the hydroxyl group of the *o*-QDM resulting in an increase in the hydrogen bond length.

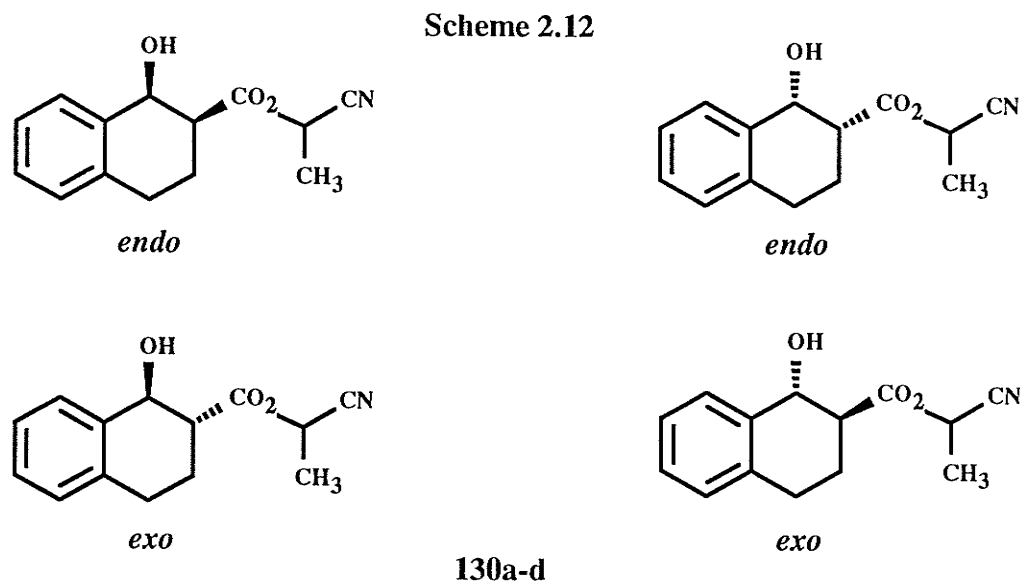


Acrylate **115** was synthesized using a method similar to that reported previously.⁴⁰ Thus **115** was prepared in 30% overall yield by heating excess acryloyl chloride and racemic lactonitrile in refluxing methylene chloride for 68 hours. It is not necessary to use optically pure lactonitrile as optical purity should have little or no effect on diastereomer ratios.

The acrylate was found to be extremely difficult to purify due to its high vapor pressure. Initial attempts to purify the acrylate by traditional chromatography techniques resulted in substantial losses during the evaporation of the eluent. In addition, the product was difficult to visualize on TLC at 254 nm. The acrylate was best purified by fractional distillation to remove CH₂Cl₂ and the majority of the unreacted acryloyl chloride. The distillate (bp = 160°C, 1 Atm) was further purified by chromatography on silica (10% EtOAc/hexanes). The purity of the individual fractions was best determined using ¹H-NMR (80 MHz) and the solvent removed by fractional distillation. The IR of **115** did

not show a characteristic CN absorption although the CN functionality could be observed in the ^{13}C -NMR (117.46 ppm).

Cycloaddition of **115** with benzocyclobutenol **18** gave a complex mixture of diastereomers **130a-d** (Scheme 2.12). Examination of the ^1H -NMR at 300 MHz (CDCl_3)



revealed the presence of at least three isomers as shown by the overlapping H_1 doublets at 5.1 ppm. The ^1H -NMR of the isomers in benzene- D_6 did not allow complete separation of the signals for integration. The crude product of the reaction was run in mixtures of $\text{CDCl}_3/\text{C}_6\text{D}_6$ in hopes of finding conditions which would allow determination of the product ratios based on the integration of the H_1 signals (Figure 2). The field strength at 300 MHz was insufficient to allow identification of all of the H_1 signals even for the best solvent combination (20% CDCl_3 in deuterobenzene). At higher field (500 MHz), the mixture that gave the best separation of peaks clearly showed four doublets ($J=9.1, 8.9, 3.25, \text{ and } 3.45$ Hz) in a ratio of 14:25:36:25 respectively (assigned *exo-a*, *exo-b*, *endo-c*, *endo-d*)(Figure 3).

Chromatography of the crude product (20% ethyl acetate/hexanes) gave a mixture of cycloadducts **130a-d** in 58% combined yield. Attempts to separate the isomers by chromatography on silica failed although isolation of three of the diastereomers was possible using HPLC on a reverse phase (ODS-2) column using a methanol/water eluent

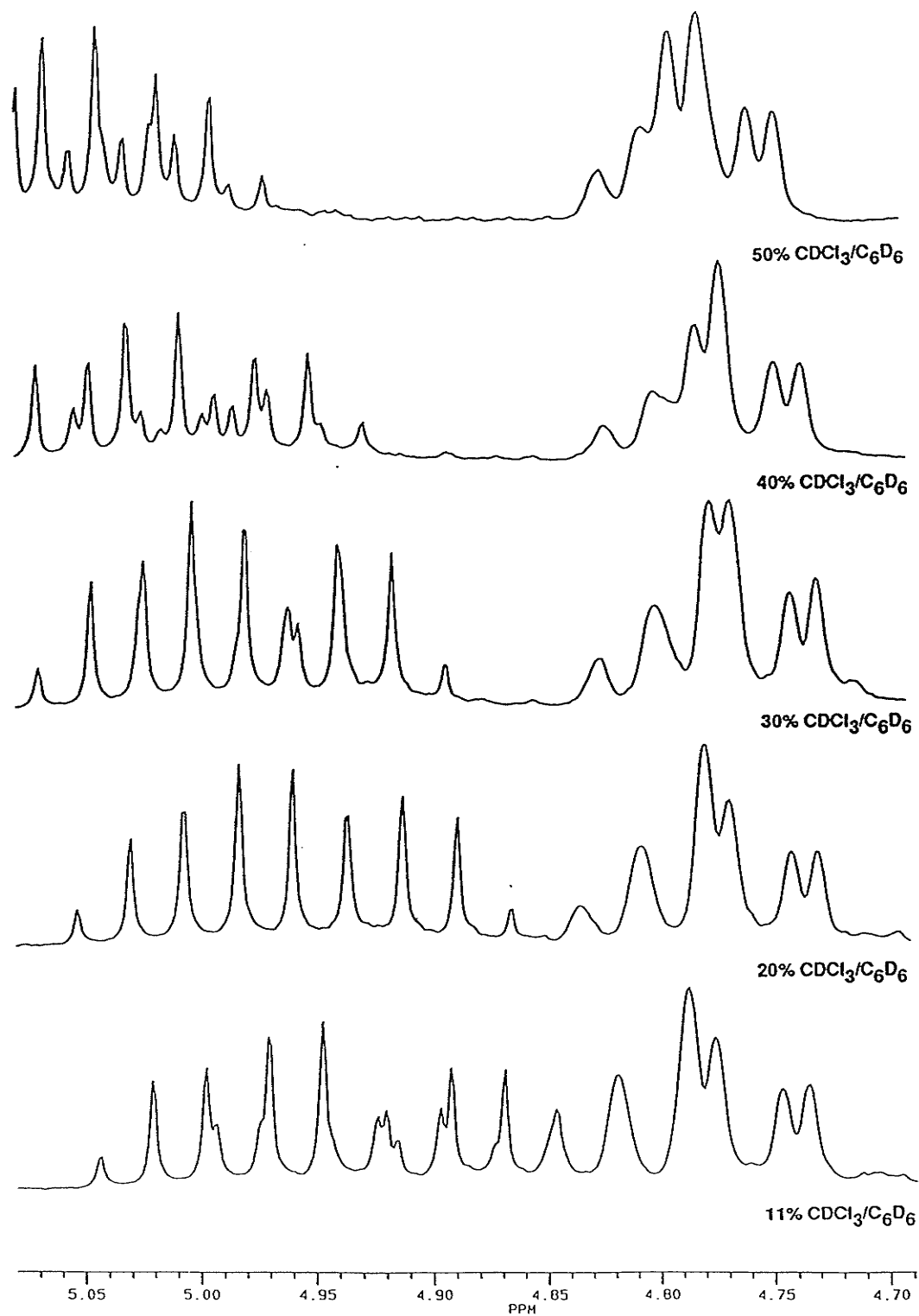


Figure 2. 300 MHz $^1\text{H-NMR}$ spectra of the crude reaction product (10 with acrylate 115) in mixtures of $\text{CDCl}_3/\text{C}_6\text{D}_6$.

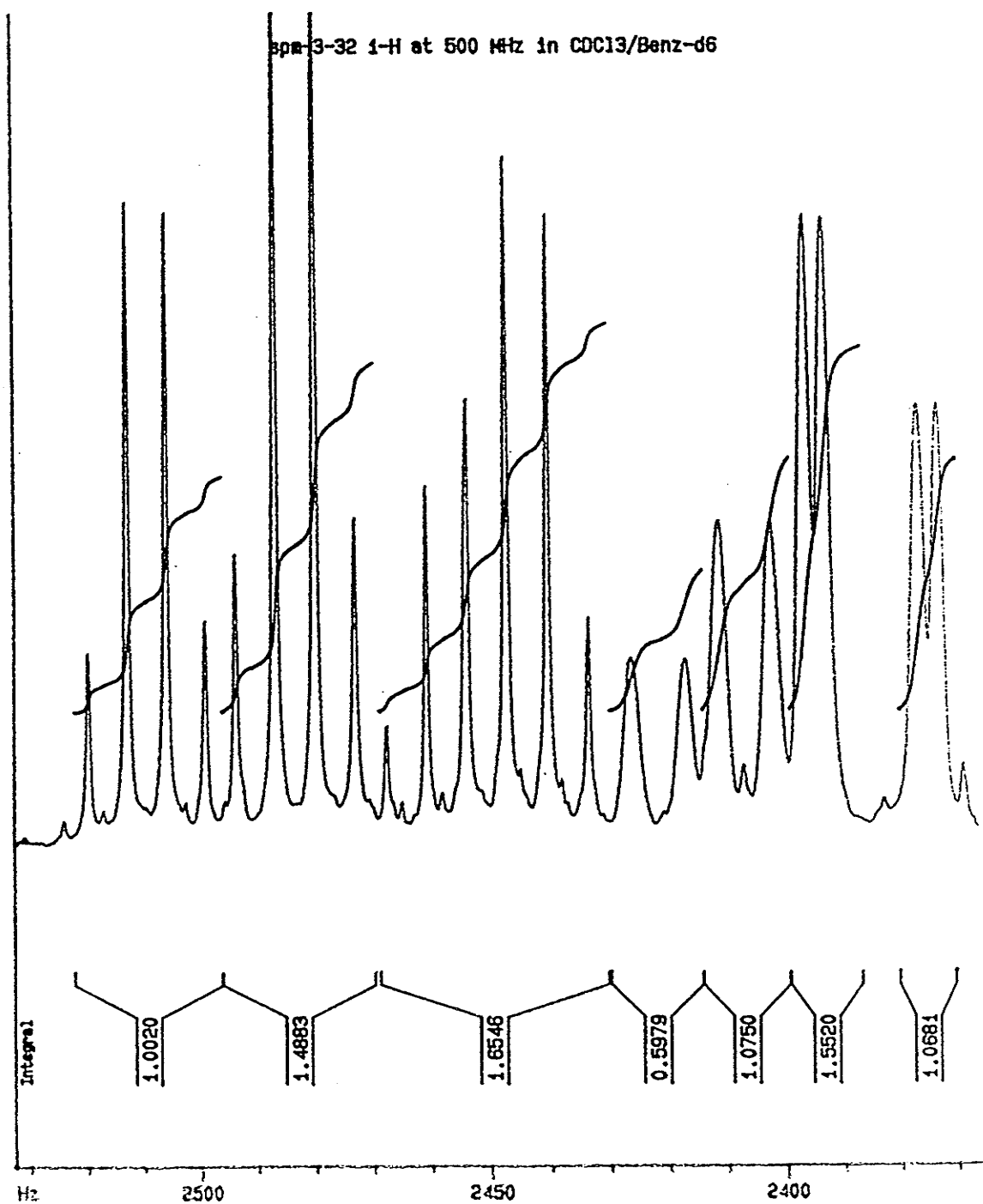


Figure 3. 500 MHz ¹H-NMR spectrum (20% CDCl₃/C₆D₆) of crude product for the reaction of 10 with acrylate 115.

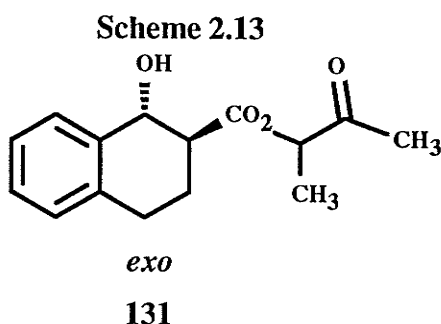
with elution gradient (35:65 to 54:46 over 38 minutes). The peaks at 31.22 (*exo*-2), 32.11 (*endo*-1), and 35.38 (*endo*-2) minutes were collected and characterized by ¹H-NMR and low resolution mass spectrometry. The parent ions in the mass spectra had molecular masses of 227 corresponding to a loss of water. Unfortunately, exact mass analysis of these ions was not possible. However, the purified mixture of diastereomers gave the correct elemental composition as determined by combustion analysis.

The results of this experiment demonstrate the inability of the cyano group to control the *exo/endo* selectivity as well as the facial selectivity. Comparing the structures of the methyl lactate and lactonitrile chiral auxiliaries, it seems reasonable that they would have the same lowest energy conformations with similar steric contributions in the transition state. Given the fact that the cyano group favors *endo* addition (61:39 *endo:exo*) and fails control the diastereofacial selectivity even with the hydroxyl group on the *o*-QDM, it would seem that the selectivity is intimately related to the presence of an intermolecular hydrogen bond. Based on the arguments above, it would appear that the lactyl group can participate in hydrogen bonding whereas the lactonitrile group cannot, due to the linearity of the cyano group. A similar effect was observed by Thornton who noted that the reaction of the modified Trost's diene **83c** (Scheme 1.51) with tetracyanoethylene (TCNE) was not facially selective whereas the reaction of **83c** with NEM was facially selective.^{70,71} The lack of facial discrimination in the case of TCNE was attributed to the inability of the linear cyano group to hydrogen bond with the chiral auxiliary of the diene.

A finer analysis of the important structural features of the chiral auxiliary was necessary. If the carbonyl group was necessary to allow hydrogen bonding, then replacement of the ester group in the lactate with a ketone group should result in the same selectivity. Dienophile **116** was chosen to determine if the carbonyl group alone was sufficient for hydrogen bonding (Scheme 2.5). Acrylate **116** was prepared from acryloyl chloride and racemic 3-hydroxy-2-butanone in refluxing methylene chloride in 66% yield.

The product was found to be extremely sensitive to light. Exposure of the acrylate to sunlight at room temperature for eight hours resulted in its complete polymerization. Storage of the product in the dark at 0°C for a year resulted in no decomposition or polymerization.

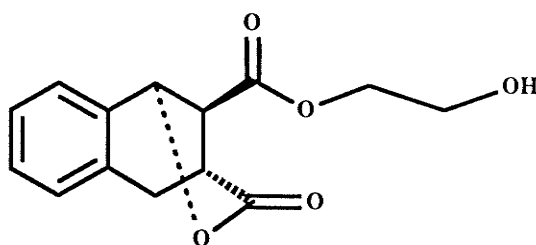
Cycloaddition of benzocyclobutenol and **116** afforded a single *exo* cycloadduct **131** as evidenced from the ¹H-NMR of the crude product (4.98 ppm, H1, J=9.32) (Scheme 2.13). Purification of the product on silica followed by recrystallization afforded **131** in 45% yield (mp 65-69°C). It was assumed that acrylate **116** reacted from the same face as did **113**. This example confirms the importance of the carbonyl group in the control of the stereochemistry.



It was still unknown whether or not the hydrogen bond acceptor oxygen had to be sp² (carbonyl group). An sp³ oxygen should also serve as an adequate hydrogen bond acceptor providing the oxygen atom could adopt a favorable orientation in the transition state. To test this hypothesis, the fumarate of ethylene glycol **121** was prepared from fumaryl chloride and a large excess of ethylene glycol (prevents polymerization). Similarly, the 2-chloro and 2-fluoroethanol fumarates **122** and **123** were prepared for comparison. Reaction of **121** with benzocyclobutenol gave a mixture of products. ¹H-NMR analysis of the crude product showed doublets at 5.43 (J=5.17), 5.12 (J=3.65) and 4.86 (J=9.53) ppm (CDCl₃). Chromatography of the mixture on silica gel resulted in the isolation of only one of the three products in 22% yield (mp 114-115°C). The IR spectrum of the major product showed two carbonyl stretches at 1788 and 1745 cm⁻¹. The

stretch at 1745 cm^{-1} was indicative of an ester carbonyl while that at 1788 cm^{-1} was consistent with a lactone carbonyl.⁴⁰ In addition, the H1 signal in the NMR was shifted to lower field (5.43 vs 5.2 to 4.6 ppm range for *endo* and *exo* cycloadducts). The major product was assigned the lactone structure **132** by comparison to a similar structure in the literature (Scheme 2.14).⁴⁰ The compounds giving rise to the doublets at 5.12 and 4.86

Scheme 2.14

**132**

ppm were tentatively assigned as *endo* and *exo* products respectively on the basis of the coupling constants. Presumably the *exo* cycloadduct readily closes to the lactone **132** as has been noted for similar cycloadducts.⁴⁰ The total *exo/endo* ratio from NMR integration was 80:20. Reaction of the chloro or fluoro dienophiles **122** and **123** with **18** gave a mixture of *endo* and *exo* cycloadducts in equal amounts. No attempt was made to isolate the products. An $^1\text{H-NMR}$ analysis of the crude products for these two reactions showed a parallel peak pattern with the H1 region of the products of the reaction of **121** with benzocyclobutenol. In the case of **122**, integration of the peaks at 5.42 (lactone), 5.11 (*endo*) and 4.90 ($J=8.38$, *exo*) revealed an *endo/exo* ratio of 1.12:1. The corresponding fluoro derivative **123** gave identical results upon integration of the peaks at 5.4, 5.11, and 4.91 (*endo/exo* 1.17:1).

Examination of the results with these three dienophiles reveals that there is no correlation between the electronegativity of the sp^3 heteroatom and the diastereoselectivity. If the reaction were controlled by a simple polar effect then one would expect fumarate **123** to give the greatest amount of *exo* product. However, both chlorine and fluorine are much weaker hydrogen bond lone pair donors than oxygen. It is

therefore reasonable to conclude that hydrogen bonding is responsible for the control of the observed *exo* selectivity in the transition state for the reaction of the fumarate of ethylene glycol and α -hydroxy-*o*-QDM.

If the proposed hydrogen bond theory is correct, then polar solvents should disrupt hydrogen bonding and in addition, the diastereoselectivity should be affected. A profound solvent effect was observed for the reaction of α -hydroxy-*o*-QDM **10** with the fumarate of methyl (*S*)-lactate **117**. When **10** (from thermolysis of **18** at 100°C) was reacted with **117** in toluene containing 30% dimethyl sulfoxide (DMSO) by volume, a mixture of four products **133a-d** was obtained. The reaction performed in 50% DMSO/toluene resulted in almost no cycloadduct formation and gave mostly the starting fumarate and *o*-methyl benzaldehyde. The products obtained from the reaction in 30% DMSO could not be separated by column chromatography on silica. Once again it was necessary to use HPLC to isolate the products and determine their ratios (Figure 4). The isomers could be

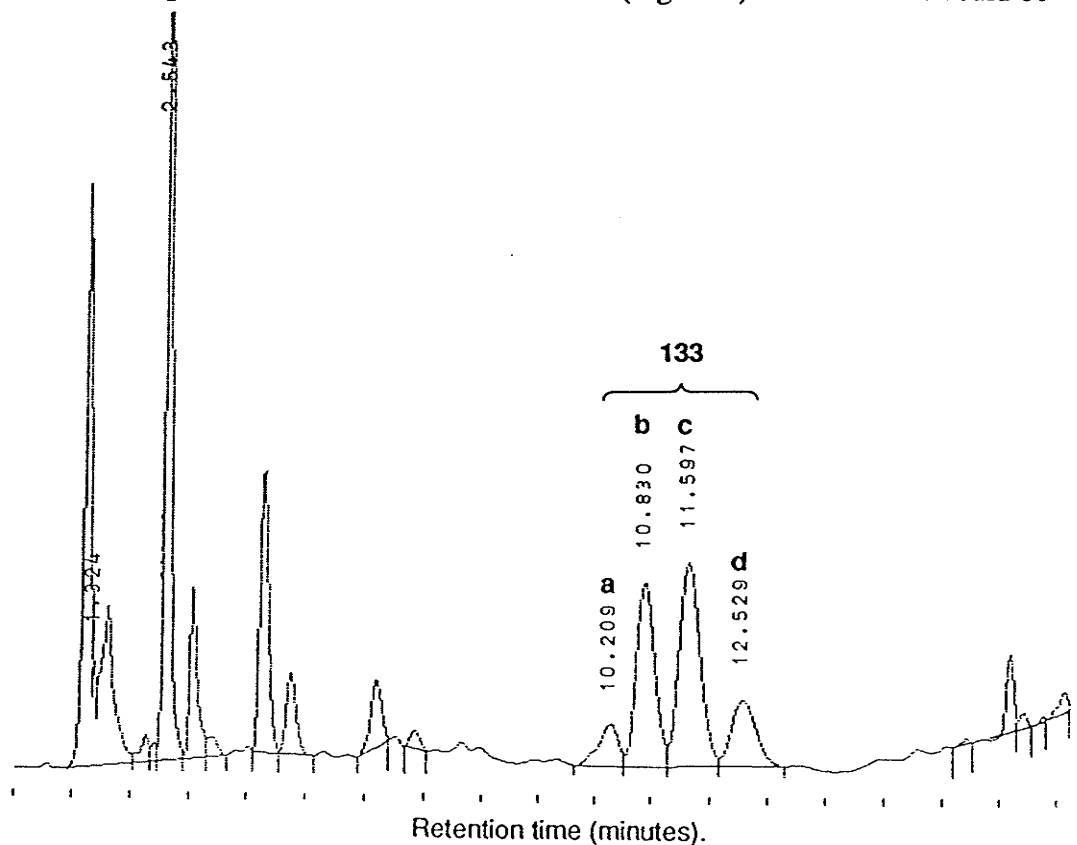


Figure 4. HPLC trace of the crude reaction products from the addition of **10** and **117** in 30% DMSO/toluene.

separated using a ternary solvent mixture of 5% acetonitrile, 42% water, and 53% methanol ($\lambda=254$ nm, 2 mL/min) on a reverse phase column. The isomers appeared at retention times of 10.21, 10.83, 11.60, and 12.53 minutes. The ratios of these peaks were 9:34:42:15 respectively and presumed to be *exo-si*, *endo-1*, *endo-2*, and *exo-re*. An authentic sample of the *exo-re* product was prepared^{39,40} and injected using the same solvent parameters. Chromatographic overlay confirmed that the peak at 12.53 minutes was the *exo-re* isomer **133d**. The two major *endo* adducts were collected and characterized by ¹H-NMR and mass spectrometry, although it was not possible to determine which was the *endo-si* and which was the *endo-re* isomer. The remaining minor *exo-si* isomer could not be isolated in sufficient quantities for characterization. However, it was possible to verify its existence by conversion of both *exo* isomers to their corresponding lactones **134a,d** (Scheme 2.15). Thus treatment of the crude product in a 30% tetrahydrofuran/water solution made basic (pH=11, 5% NaHCO₃) with aqueous sodium bicarbonate resulted in the complete conversion of the *exo* products to the corresponding 1,3-lactones. HPLC analysis of the crude reaction mixture showed that two *exo* cycloadduct peaks had disappeared and that two new peaks in the chromatogram had

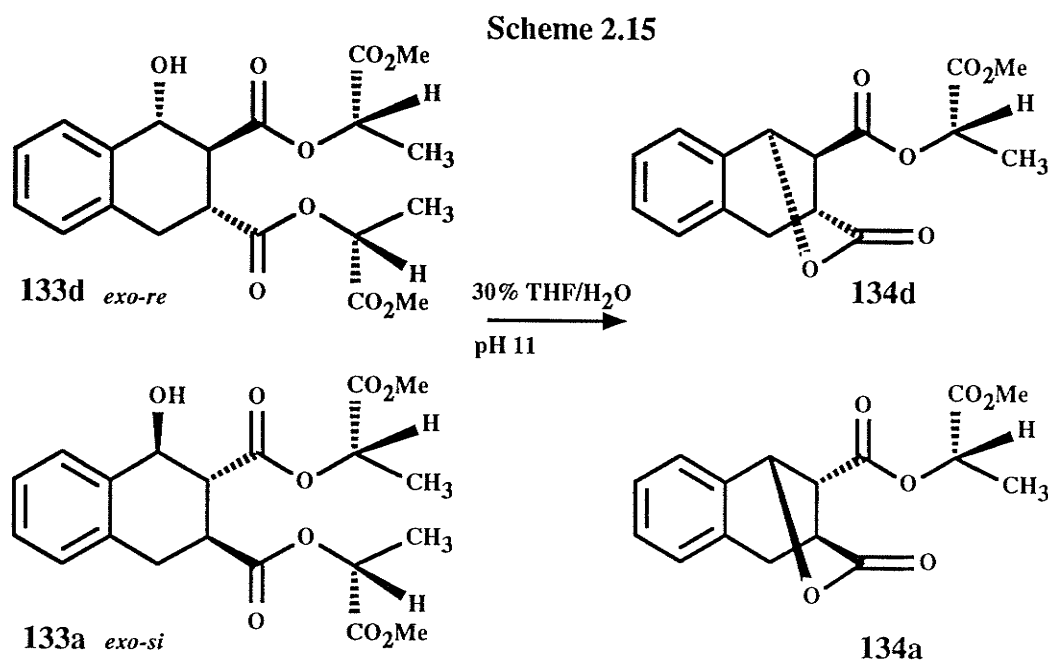
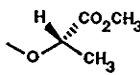
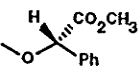
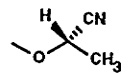
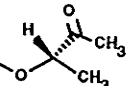
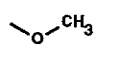
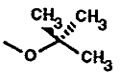
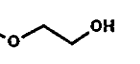
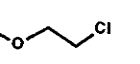
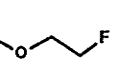
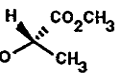
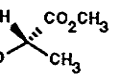
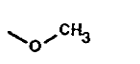
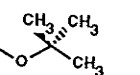


Table 5. Effects of chiral auxiliary on diastereoselectivity

a ¹ , f ²	Dienophile	o-QDM	Yield%	Facial Selectivity	Endo:Exo	Ref.
a		13	77	95:5	exo only	37
a		13	56	95:5	exo only	96
a		13	58	36:25 endo, 25:14exo	61:39	
a		13	45	> 90:10	exo	
f		13	87	-	74:26	93
f		13	43	-	60:40	
f		13	22	-	20:80	
f		13	-	-	53:47	
f		13	-	-	54:46	
f	 30% DMSO/toluene	13	-	42:34 endo, 15:9 exo	76:24	
f		38	62	61:39	endo only	
f		38	38	-	endo major	33
f		38	98	-	88:12	

1. a = acrylate 2. f = fumarate

appeared at 5.8 and 6.4 minutes. A pure sample of the lactone⁴⁰ corresponding to the *exo-re* cycloadduct was injected and exhibited a retention time of 5.8 minutes. The ratio of the lactone peaks (*exo-re:exo-si*) was 1.6:1 and the ratio of *endo1* to *endo-2* was 1.2:1. This compares well with the results from Figure 4 (1.7:1 *exo*, 1.2:1 *endo*). The overall *endo:exo* ratio was 3.2:1 indicating a substantial increase in the amount of *endo* product. As expected, DMSO appears to interfere with the normal diastereoselectivity by hydrogen bonding to the hydroxyl group of the *o*-QDM thereby preventing the formation of the hydrogen bond to the dienophile in the transition state. This results in the formation of more *endo* products and a loss in the asymmetric induction for both the *endo* and *exo* products.

The complete set of results for the studies discussed above is given in Table 5. In summary, we can see a pattern of reactivity. Only *o*-QDM **10**, which bears an α -hydroxy group, adds to give *exo* products with high diastereoselectivity. *o*-QDM **31**, which bears an α -methoxy group, adds to give mostly *endo* adducts. The steric bulk of the dienophile makes little difference to the *exo/endo* ratio as evidenced by the reaction of dimethyl and di-*tert*-butyl fumarate **119** and **120**. Finally, only dienophiles which have a strong hydrogen bonding acceptor group, with the exception of **115**, give *exo* adducts.

2.1.2 Molecular Modeling of the Diastereoselectivity

With the overwhelming evidence suggesting the presence of an intermolecular hydrogen bond in the transition state, a molecular model of the transition state for the stereoselective addition of the fumarates and acrylates of methyl (S)-lactate to α -hydroxy-*o*-QDM was sought. The preference for *exo* addition extends even to *o*-QDM's bearing α' -aryl groups which would normally add *endo* with respect to the hydroxyl group (*exo* with respect to the aryl group).^{94,95} The stabilizing effects of the hydrogen bond in the transition state appears to be enough to overcome even the steric

effects of the aryl group in the transition state. Since lactyl acrylate **113** adds to *o*-QDM **10** with the same selectivity as does the fumarate **117** with α -hydroxy- α' -aryl-*o*-QDM, it was deemed that it was only necessary to model the addition of **10** to **113**. Hopefully the model can explain both the *exo* selectivity and the high facial selectivity with respect to the diene.

2.1.2.1 Force Field (MMX) Calculations

The initial model for the addition of **10** to **113** was based on Helmchen's model for the addition of the acrylate of ethyl (*S*)-lactate **69** to cyclopentadiene. In Helmchen's model for the non-Lewis-acid catalyzed reaction, it was assumed that the acrylate adopted the *s-trans* conformation and only the addition of a Lewis-acid forced the dienophile to adopt the *s-cis* conformation. In this work, an *s-trans* conformation was assumed for the dienophile. Using the molecular modeling program PCMODEL,¹⁰⁰ a transition state was constructed by docking the α -hydroxy-orthoquinodimethane to the acrylate **113** in the *s-trans* conformation according to Figure 5. The distances of the primary carbon atoms in

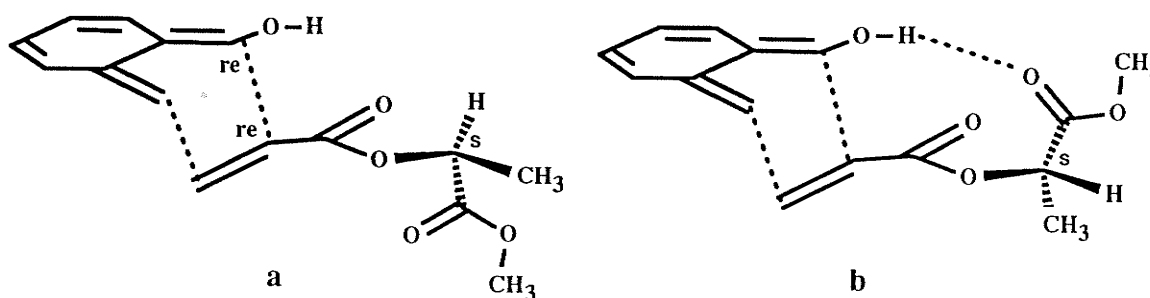


Fig 5. Possible transition state structures for the Diels-Alder reaction of α -hydroxy-*o*-QDM with acrylate **113**.

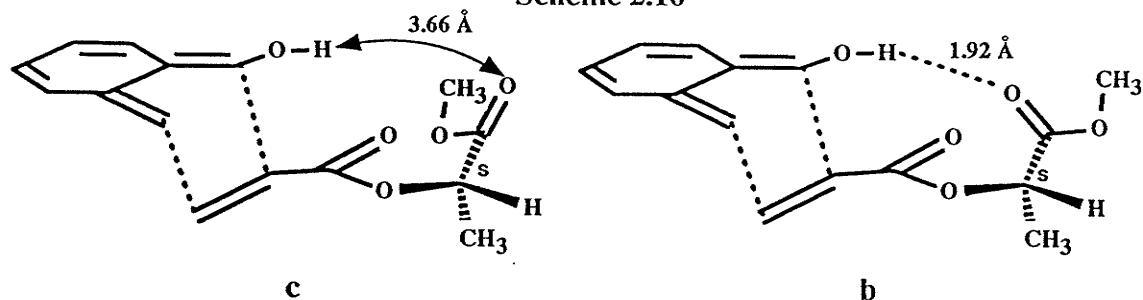
the transition state were fixed at 3.00 Å by incorporation of appropriate force constants (5 mDyne/Å) with the minimum energy distances set to 3.00 Å. Molecular mechanics minimization led to transition state a. Conformations a and b (Figure 5) correspond to the

addition to the *re* face of the acrylate having the (S) chiral auxiliary. The conformation of the acrylate in **a** represents the lowest ground state conformation determined from previous force field calculations carried out on the free acrylate (Helmchen's model).⁶¹ In this case addition from the *exo* transition state would occur from the side of the sterically smaller hydrogen. However, this model did not facilitate the formation of the controlling hydrogen bond. Through a slight conformational change via rotation about the ester bonds, it was possible to bring the lactyl carbonyl group to an acceptable hydrogen bonding distance as shown in **b**. This model is different from Helmchen's model in that the hydrogen lies in the plane of dienophile and addition occurs from the side of the ester group. In Helmchen's model, addition occurred opposite the ester group. Minimization of both transition states **a** and **b** revealed that **b** was lower in energy by 1.5 kcal. Although an intermolecular distance of 3 Å is too early for a transition state (the transition state distances calculated for the reaction of ethylene and cyclopentadiene are 2.205 (3-21G))¹⁰¹ it was shown that the carbonyl group in **b** was close enough for hydrogen bonding (1.92 Å). It would seem at least that the formation of an intermolecular hydrogen bond is possible and has a stabilizing effect on the transition state.

Having shown that an intermolecular hydrogen bond was sterically feasible, calculations were carried out on the additions to the *re* and *si* faces of **10** for both configurations and various conformations of the lactyl group with the dienophile in the *s-trans* form. For simplicity, calculations were performed on the *exo-re* transition state for the acrylate of both methyl (S)-lactate and methyl (R)-lactate. Such a calculation is equivalent to comparing the *exo-re*-(S) transition state to the *exo-si*-(S) transition state because the *exo-re*-(R) transition state is the mirror image of the *exo-si*-(S) transition state.

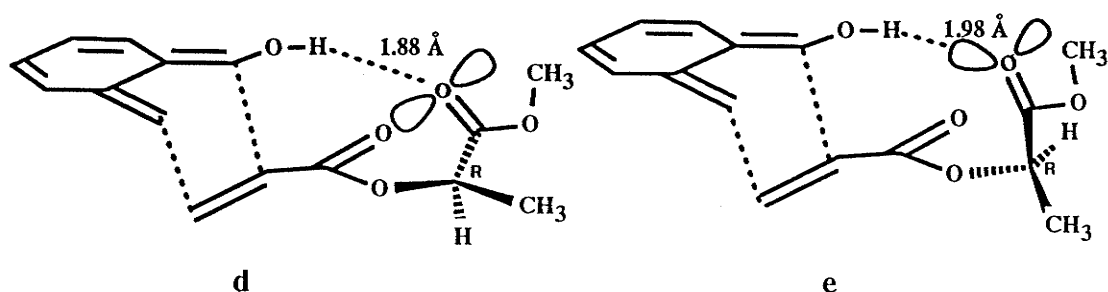
The calculations show that there are several low energy conformations for the lactyl group. Although it was shown that *exo-re*-(S) transition state **b** was lower in energy than transition state **a**, an even more stable conformation **c** was found (Scheme 2.16). It is interesting to note that conformation **c** is similar to **b** except that the carbonyl group has

Scheme 2.16



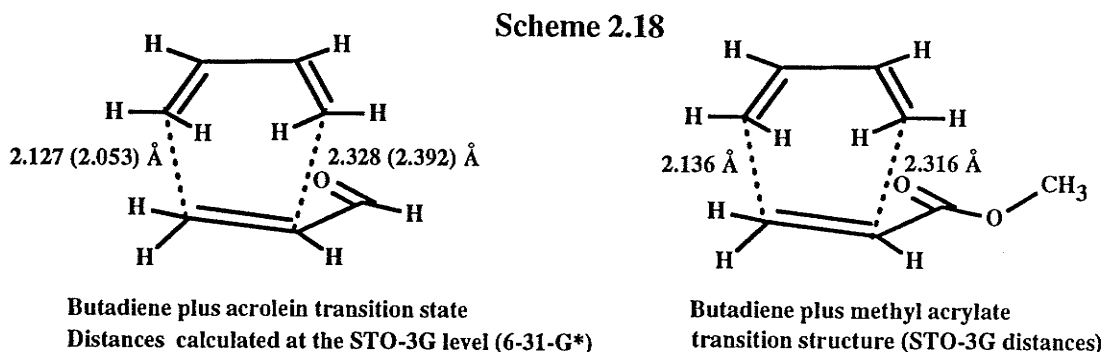
twisted out of a hydrogen bonding position. It is likely that a slight unfavorable torsional distortion is necessary in order to maintain the hydrogen bond in **b**. To examine the *exo-si*-(S) transition state, the chiral center in **b** was epimerized giving transition state **d** (Scheme 2.17). Surprisingly this transition state was lowest in energy while still maintaining the hydrogen bond (1.88 Å). Another slightly less stable hydrogen bonded conformer (R-lactate) was found and is depicted by **e**. In **e**, the hydrogen is essentially eclipsed with the acrylate carbonyl and the lactate carbonyl lone pair axis is directed along the hydrogen bond. Normally, a hydrogen bond has directionality which is determined by a competition between the electron donor dipole-proton donor dipole interaction and the favorable interaction achieved when the donor hydrogen lies along the lone pair axis of the acceptor.^{9A7}

Scheme 2.17



The failure of the *s-trans* model to predict the preference for addition to the *re* face of the *o*-QDM (S-lactate) prompted the examination of the *s-cis* geometry of the dienophile as a model. In addition, it may be that a 3.0 Å separation between the diene and dienophile is too large (early transition state) to give accurate transition state energies.

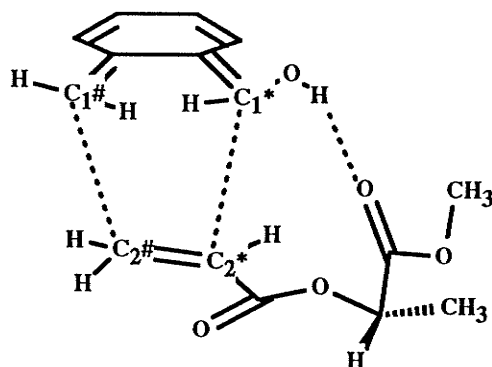
To better approximate the true geometry of the transition state, transition state atoms were used and the bond orders (BO) of the primary bonds adjusted to reproduce the distances observed in the addition of butadiene with acrolein (Scheme 2.18).¹⁰² The distances are



calculated from Badgers rule.¹⁰⁰ Thus the new bond length (l) in the transition state is calculated from the length of a fully formed sp^3 bond ($l_0 \equiv 1.5 \text{ \AA}$) and is given by the equation: $l = l_0 - 0.6 \ln(\text{BO})$. The stretching force constants of the newly forming bonds in the transition state are the force constants for fully formed sp^3 carbon bonds multiplied by the bond order BO (Scheme 2.19). In a similar way, the angle bending force constants are modified. A bond approaching zero will force bond angles of 90° between the transition state atoms $C1^*$ and $C2^*$ and any other atom connected to $C1^*$ or $C2^*$. As the bond order approaches 1.0 (fully formed sp^3 carbon bonds), the bond angles will spread to the ideal tetrahedral value of 109° . In this work, bond orders of 0.24 ($C1^*$ atom bearing the hydroxyl group to $C2^*$) and 0.42 for $C1^\#$ and $C2^\#$ gave distances similar to the butadiene plus acrolein transition state. The acrylate was rotated into the cisoid conformation and the transition states for both the *exo-re-(S)-s-cis* and the *exo-re-(R)-s-cis* examined. Only those transition states for which a hydrogen bond could be formed were considered. For comparison, the lowest energy *s-trans* conformers for both the (*R*) and (*S*)-lactate were investigated. The ORTEP diagrams for the transition states are shown in Figure 6.

The results of these calculations reveal that the *exo-re-(S)-s-cis* transition state is lowest in energy by 0.8 kcal/mol (Figure 6, $E=0$). It is noteworthy that the *s-cis* dienophile exists in the lowest energy conformation proposed by Helmchen for the

Scheme 2.19



Lewis-acid catalyzed Diels-Alder cycloaddition (cf. cyclopentadiene with the acrylate of ethyl (*S*)-lactate) with addition occurring from the side of the lactate ester group. Also, the hydrogen bond persists in its most favorable orientation, along the lone pair axis of the carbonyl group. Another hydrogen bonded conformer was found for *exo-re-(S)-s-cis* transition state (Figure 6, $E=2.6$). This conformer was 2.6 kcal/mol higher in energy. The hydrogen bond in this case was not directed along the lone pair axis and the hydrogen attached to the chiral auxiliary was eclipsed with the acrylate carbonyl. If the chiral auxiliary is epimerized to give the *R*-lactate, a large torsional interaction between the methyl group and the carbonyl group forces a rotation such that the hydrogen again becomes eclipsed (Figure 6, $E=3.7$). When this happens, the carbonyl group is rotated to a position too distant for hydrogen bonding to occur. Presumably the methyl group, in the case of the *R* chiral auxiliary, is too bulky to accommodate a geometry which permits hydrogen bonding. There is however, another conformer of the *R*-isomer which does permit hydrogen bonding (Figure 6, $E=0.8$). The conformation of this isomer is identical to the lowest energy transition state conformation found for the *S*-isomer, the only difference between them is the juxtaposed methyl and hydrogen groups.

The more sophisticated calculations performed on the cisoid dienophile conformations were also performed on the transoid conformations. As found previously, the *exo-si-(S)-s-trans* (same as *exo-re-(R)-s-trans*) was also lowest in energy by 0.7 kcal.

Comparing the lowest energy conformations of the *s-cis* and *s-trans* dienophiles

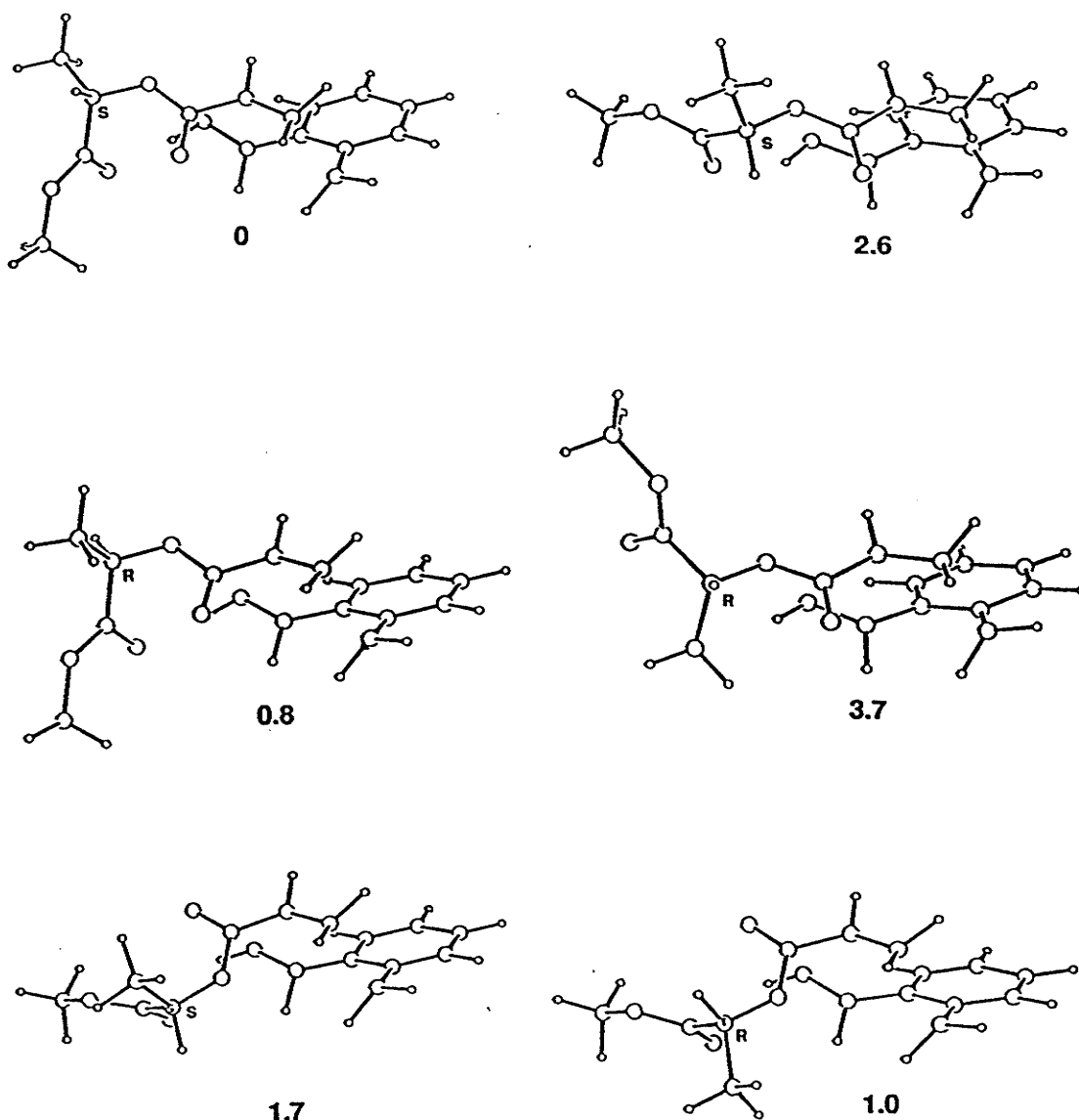


Figure 6. ORTEP diagrams for the transition states modeled with bond orders adjusted to 0.42 and 0.24. Energies are relative to the *exo-re-(S)-s-cis* transition state (0 kcal/mol)

calculated for the (*S*)-lactate group, one observes an elongation of the hydrogen bond in the *s-trans* isomer (2.29 Å vs 1.99 Å). The energy of interaction for the hydrogen bond within the force field equation is proportional to $1/r^2$ (this is in addition to the normal Coulomb and van der Waals interaction). This elongation of the hydrogen bond in the *s-trans* transition state may be responsible for the preference of the *s-cis* conformation.

In conclusion, it is acceptable to say that the molecular mechanics calculations are

consistent with the experimental results within the context of the proposed hydrogen bonding interaction in the transition state. Although the *exo-re*-(S)-*s-cis* transition state is lowest in energy, the small energy differences between this and the other transition states and the "uncharted" confines of parametrized transition state modeling limits the interpretation to affirmance rather than prediction.

2.1.2.2 Molecular Orbital (AM1) Calculations

The empirical force field calculations performed on the *s-cis* transition states using transition state atoms were consistent with the preferred addition of α -hydroxy-*o*-QDM to the *re* face of the acrylate of methyl (S)-lactate. It also indicated that a hydrogen bond in the *exo* transition state was sterically feasible. However, no attempt to model the corresponding *endo* transition state was made as the effects of secondary orbital interactions are not included within the force field (MMX) parametrization. Only the relative steric energies of the *exo* and *endo* transition states can be compared and it was felt that this comparison would be fruitless.

In addition to the molecular mechanics calculations, semi-empirical molecular orbital (AM1) calculations were carried out on the *exo-s-cis* and *exo-s-trans* transition states using the molecular orbital program SPARTAN.¹⁰³ Calculations were also performed on the *endo-si*-(S)-*s-cis* transition state for comparison with the *exo-re*-(S)-*s-cis* transition state. An approximate transition state geometry for the addition of lactyl acrylate to α -hydroxy-*o*-QDM was generated by locating the *exo* transition state for the addition of acrolein in the *s-cis* conformation to butadiene (Figure 7). The presence of one imaginary eigenvalue (corresponding to a negative vibrational frequency) after diagonalization of the force constant matrix confirmed that the stationary point located was a true transition structure.³⁸ Analysis of this vibration revealed that the motion was along the direction of the transition vector. Movement along this vector corresponds to a

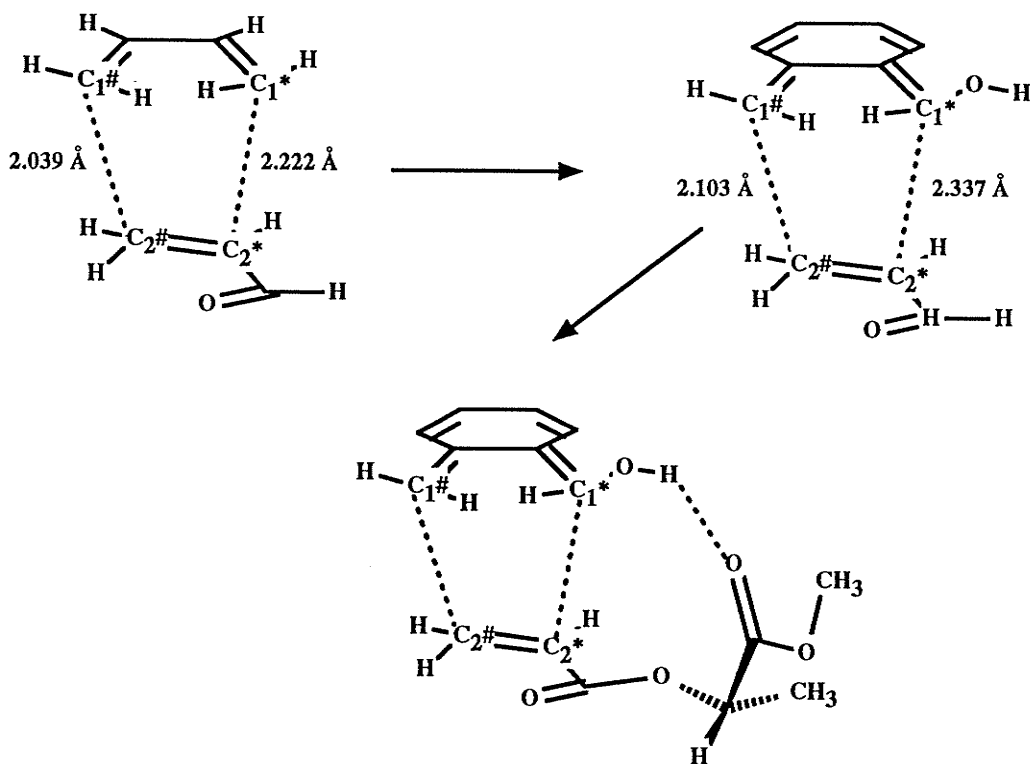


Figure 7. AM1 transition structures of butadiene plus acrolein, α -hydroxy-*o*-QDM and acrolein, and finally α -hydroxy-*o*-QDM and the acrylate of methyl (*S*)-lactate.

decrease in the potential energy of the molecule and represents a finite segment of the reaction path towards the formation of products (or reactants). Those atoms necessary to complete the remaining *o*-QDM skeleton were added and the geometry reoptimized to the transition state (Figure 7). Next, the aldehyde hydrogen in acrolein was replaced by the (*S*)-lactyl chiral auxiliary and the lactyl group rotated to a hydrogen bonding position. The geometry of this structure was then optimized (Figure 7).

The *exo-re*-(*S*)-*s-cis* transition structure approached convergence to the extent of a evanescent gradient (rms gradient was 0.0000 kcal/Å) with a heat of formation of -131.80 kcal/mol. In this transition structure, the hydrogen attached to the chiral center eclipses the acrylate ester carbonyl structure and is essentially identical to the preferred conformation found from the MMX calculations (Figure 8). The conformation of the lactyl group deviates from the lowest energy *s-cis* conformation calculated by Helmchen through a slight torsion about the carbon-oxygen bond of the chiral auxiliary. The enolic

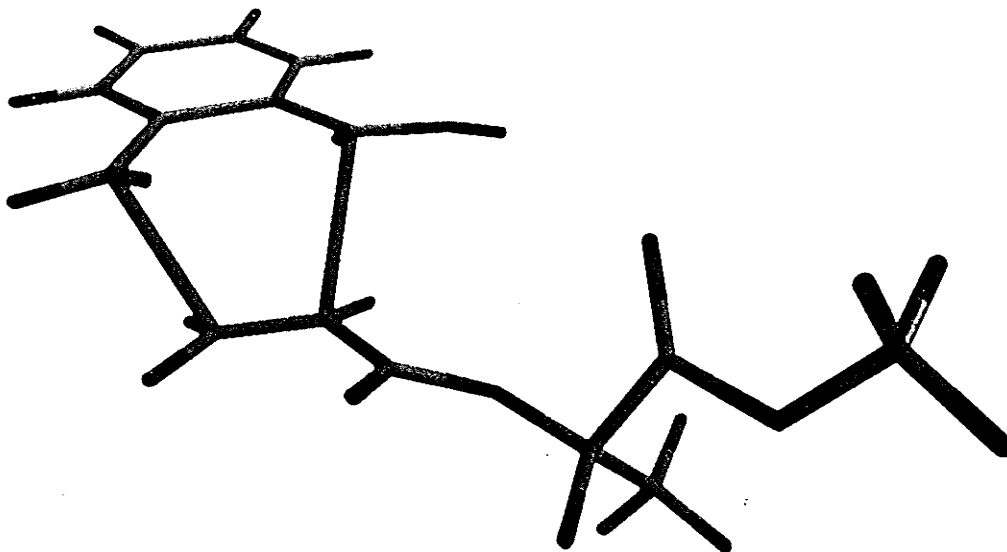


Figure 8. AM1 *exo-re-(S)-s-cis* transition structure for the addition of α -hydroxy-*o*-QDM and lactyl acrylate.

hydrogen of the *o*-QDM lies along the lone pair axis of the carbonyl group and forms an O-H-O angle of 149° . Although this value deviates from the ideal 180° angle, it still lies within the typical angular range of a hydrogen bond. The length of the hydrogen bond is 2.10 \AA , typical of O-H-O hydrogen bonds (cf. 2.11 \AA from MMX calculation).

It is interesting to compare the geometries of the *exo* transition states found for the three reactions shown in Figure 7. An analysis of the dihedral angles between the primary forming bonds for the three transition states reveals that *exo-re-(S)-s-cis* transition state has a torsion angle of 13.7° whereas the acrolein/butadiene and acrolein/ α -hydroxy-*o*-QDM transition states have dihedral angles of 2.3° and 3° respectively (to be denoted as the twist angle; see Figure 9). This twist is known as "twist mode asynchronicity" and corresponds to a twisting motion about the $C1^*-C2^*$ forming bond.¹⁰² It has been shown that for the transition state of butadiene plus ethylene, this

type of twisting motion corresponds to the lowest energy vibrational motion of the transition state. The small increase in energy imparted by the twist in the *exo-re-(S)-s-cis* transition state is likely alleviated by energy gains due to an improvement of the hydrogen bond geometry.

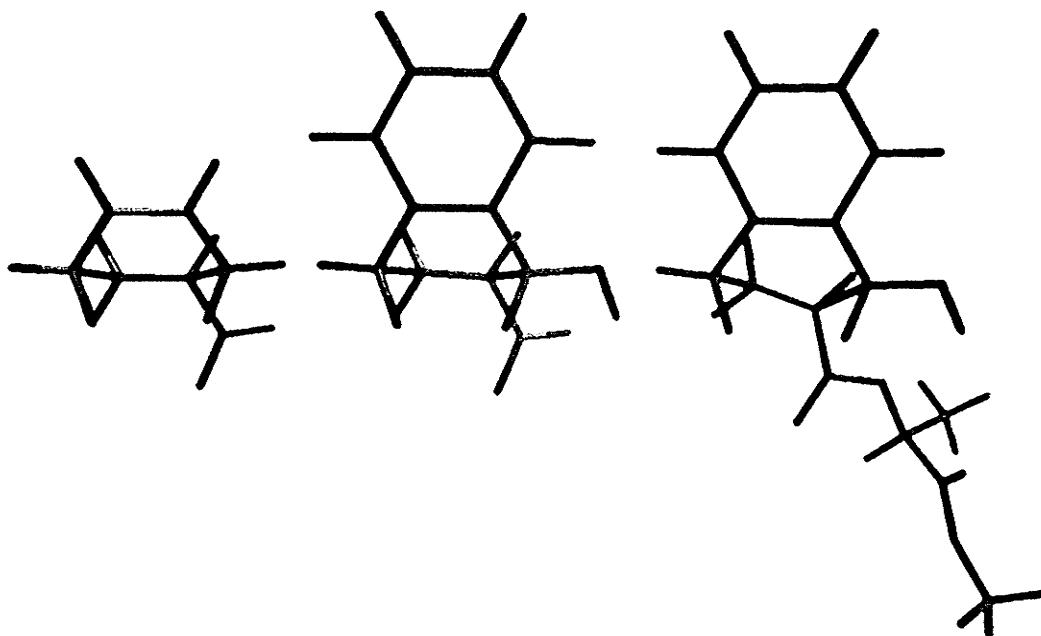


Figure 9. Comparison of the twist mode asynchronicity in the *exo-re-(S)-s-cis* transition state to that of the butadiene and α -hydroxy-*o*-QDM plus acrolein transition states.

The *exo-re-(R)-s-cis* transition state, corresponding to addition of the *o*-QDM to the *si* face of the acrylate, was higher in energy than the *exo-re-(S)-s-cis* transition state by 2.02 kcal ($H_f = -129.77$ kcal, see Figure 10). Analysis of the calculated vibrational frequencies revealed one negative frequency (-662 cm^{-1}) indicating that the transition state had been located. The lowest real frequency stretch (21 cm^{-1}) corresponds to a twisting motion of the *o*-QDM with respect to the acrylate. The second real lowest energy stretch (25 cm^{-1}) corresponds to a pivoting motion about the internal $C1^*-C2^*$ bond (twist mode asynchronicity). The third lowest frequency (40 cm^{-1}) corresponds to a side to side

rocking motion of the hydrogen bonded lactate carbonyl. All of these three motions can help facilitate the formation of a more suitable geometry for hydrogen bonding.

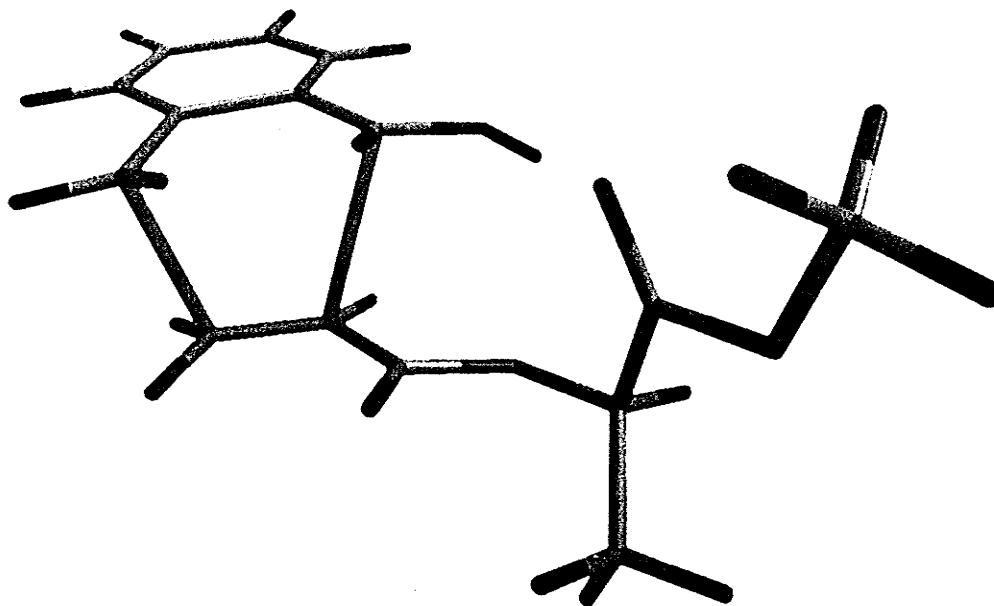


Figure 10. AM1 *exo-re-(R)-s-cis* transition structure for the addition of α -hydroxy-o-QDM and lactyl acrylate.

The increase in the energy of this transition state would seem to stem from a steric interaction between the acrylate carbonyl group and the eclipsing methyl group of the chiral auxiliary. This steric interaction is manifested as a rotation about the bond between the ester oxygen and the chiral carbon which ultimately leads to a planar conformation similar to Helmchen's conformation. Despite the slight conformational change of the lactyl group, the hydrogen bond angle has been maintained at 149° with a hydrogen bond length of 2.11 \AA . An analysis of the geometry indicates that the twist angle is slightly smaller than the twist angle for the *exo-re-(S)-s-cis* transition state (9.6° vs 13.7°).

The *exo-re-(R)-s-trans* transition state was slightly higher in energy than the *exo-re-(S)-s-cis* transition state by 0.85 kcal (cf. 1.0 kcal from the MMX calculation). In this transition state, the hydrogen bond length has increased to 2.28 \AA (cf. 2.29 \AA from the

MMX calculation). It would appear that the *s-trans* conformation is not as conducive to hydrogen bonding as is the *s-cis* conformation. The twist angle of 3.4° is similar to that found for the addition of α -hydroxy-*o*-QDM **10** to acrolein (3°) and may reflect the inefficacy of the *s-trans* acrylate to adopt a geometry amenable to the formation of a strong hydrogen bond. Similarly, the relatively high hydrogen bond angle of 132° also shows that the *s-trans* acrylate is relatively indisposed towards strong hydrogen bonding.

The two computational methods (AM1 versus MM2/MMX) predict very different geometries with respect to the preferred conformation of the lactyl group in the *exo-re-(R)-s-trans* transition state. The AM1 calculations predict that one of the lone pair electrons should lie along the hydrogen bond axis whereas the MMX calculations predict that the hydrogen bond axis should bisect the two lone pair electrons. The *exo-re-(R)-s-trans* transition states found from molecular mechanics (MMX) and molecular orbital theory (AM1) are shown for comparison (Figure 11).

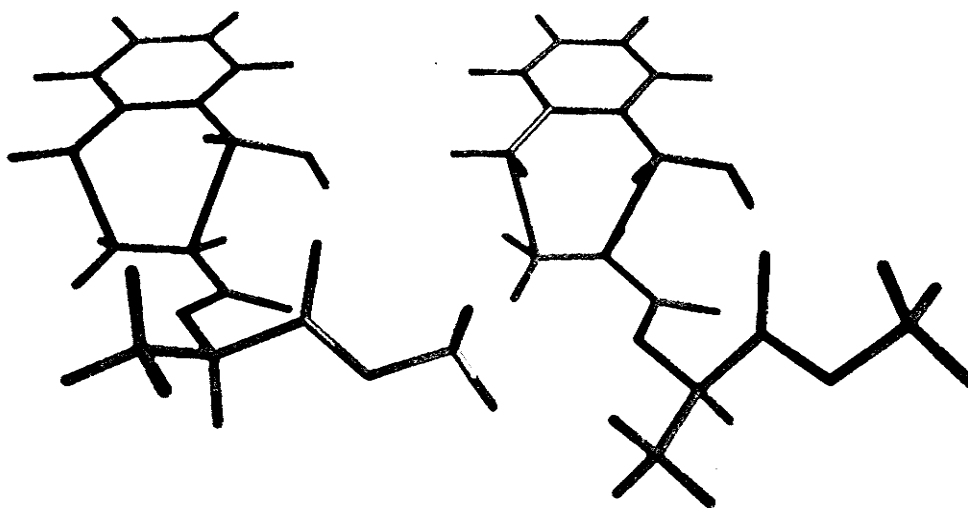


Figure 11. Comparison of the *exo-re-(R)-s-trans* transition states calculated from MMX (left) and AM1 (right). Note the difference in the conformation of the lactyl group.

The *endo-si-(S)-s-cis* transition state, which was believed to be the lowest energy *endo* transition state in accord with Helmchen's model for the Lewis-acid catalyzed addition of acrylate **69** (see Scheme 1.42) to cyclopentadiene, was examined at the AM1 level of theory (Figure 12). The energy of this transition state ($H_f = -123.94$ kcal) was substantially higher in energy than any of the *exo* transition states (Figure 12).

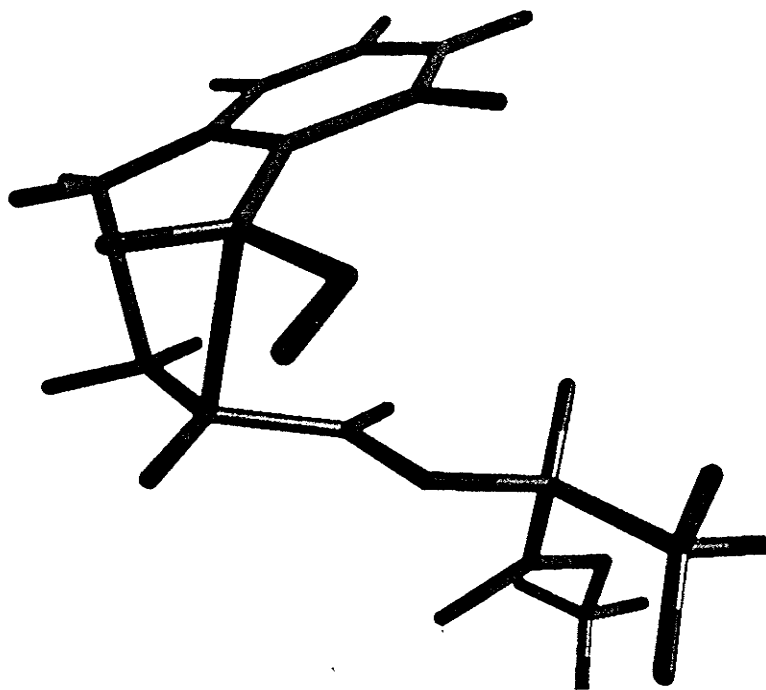


Figure 12. AM1 *endo-si-(S)-s-cis* transition structure for the addition of α -hydroxy-o-QDM to lactyl acrylate.

In summary, very high stereochemical control by a remote chiral auxiliary has been observed leading to an unprecedented *exo* transition state. This stereochemical control is mediated by the formation of a hydrogen bond in the *exo* transition state. The hydrogen bond is contained within a 9-membered ring similar to the hydrogen bonded *endo* transition state found by Thorton.^{70,71} Although the formation of a 9-membered ring is entropically unfavorable as it restricts the degrees of freedom of motion, a substantial rate enhancement is observed for *exo* addition. Large rate enhancements have also been observed for other Diels-Alder reactions involving dienolic substrates such as

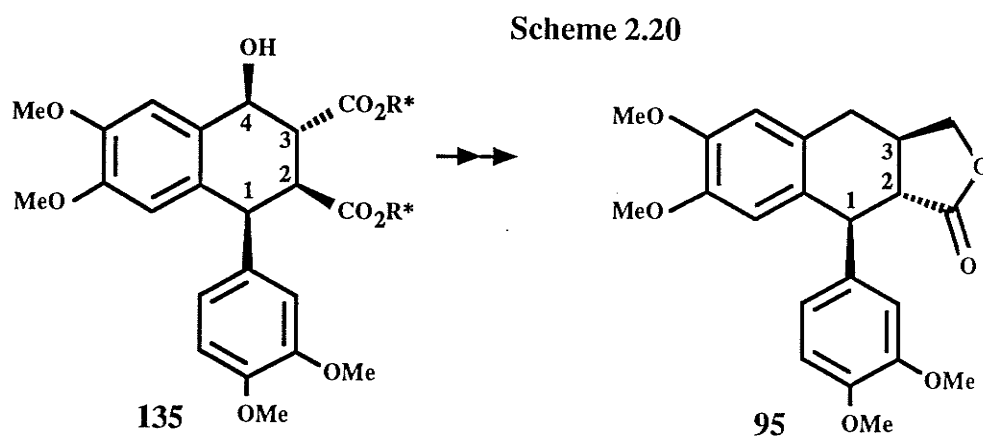
9-hydroxyanthracene, which are hydrogen bonded not to the dienophile, but to a hydrogen bond acceptor such as triethylamine.¹⁰⁴

The formation of the hydrogen bond to the *o*-QDM likely results in considerable charge transfer from the donor carbonyl of the lactate group to the acceptor oxygen of the *o*-QDM. This would effectively increase the electron density of the *o*-QDM π -system thereby raising the energy of the HOMO orbitals with respect to the LUMO of the dienophile resulting in a rate enhancement. As an alternative point of view, this hydrogen bond can be considered as a *modus operandi* whereby diene and dienophile are "directed" towards a fruitful encounter leading to the formation of products.

2.2.1 General Asymmetric Synthesis of Aryltetralin Lignans

Although Rodrigo *et al.*⁷⁵ have reported a general nonasymmetric route leading to eight diastereomers of podophyllotoxin, a general asymmetric synthesis of lignans, applicable to the synthesis of a wide variety of lignans, has not been described.

As discussed previously, the fumarates of methyl lactate or methyl mandelate readily undergo Diels-Alder cycloaddition to α -hydroxy- α' -phenyl-*o*-QDMs with high diastereoselectivity. These reactions furnished cycloadducts with the necessary absolute stereochemistry for the synthesis of two podophyllotoxin analogues⁹⁴ and (-)-neopodophyllotoxin.⁹⁵ It was hoped that these same types of cycloadducts (cf. **135**, **112**) could be used in the synthesis of lignans with other relative stereochemistries. One lignan that posed an interesting synthetic challenge was α -dimethylretrodendrin **95** (Scheme 2.20).⁸⁸ This deoxygenated lignan has the 1,2-*trans*-2,3-*trans* geometry whereas

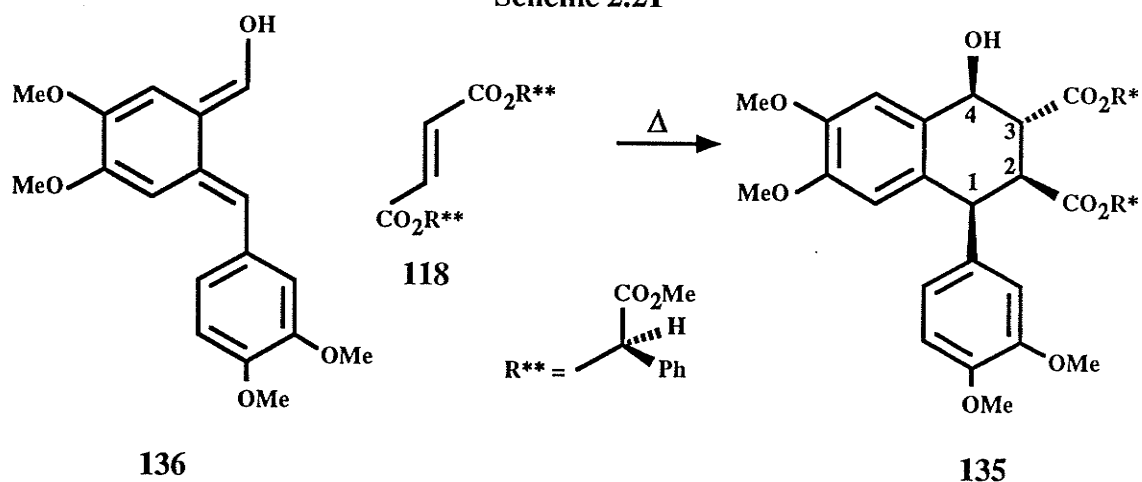


the aforementioned cycloadducts have the 1,2-*cis*-2,3-*trans* geometry. Thus a synthesis of **95** from **135** would require the eventual epimerization at C₂ and C₃.

A synthesis of cycloadduct **135** requires the generation of *o*-QDM **136** and its subsequent addition to the appropriately substituted chiral fumarate **118** (Scheme 2.21). The absolute configuration of the fumarate will depend on the synthetic approach to **95**.

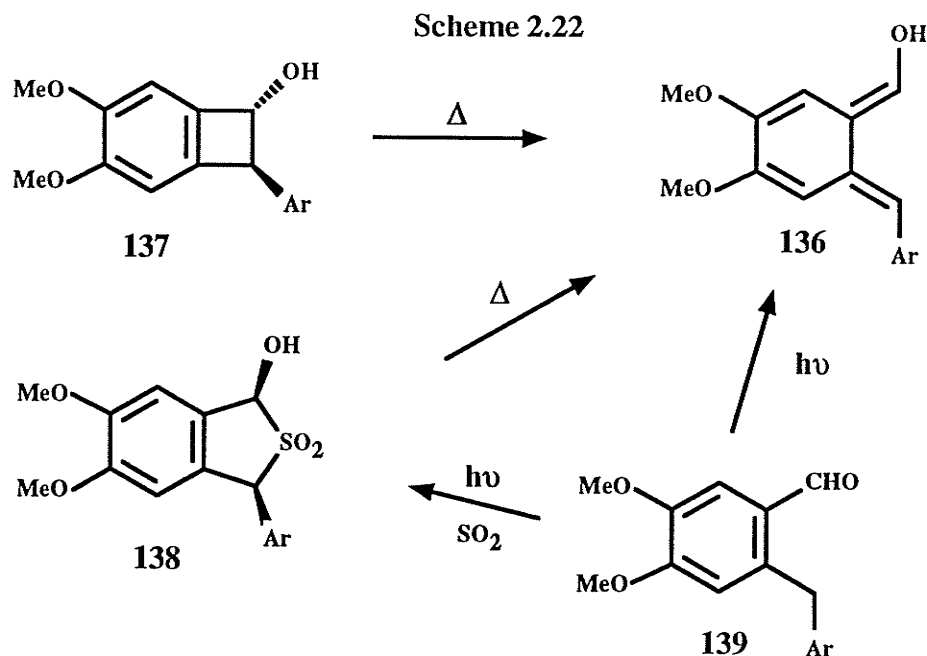
The most non-labile center in the requisite cycloadduct **135** is C₁. The remaining centers are susceptible to epimerization and it is therefore judicious to choose C₁ as the

Scheme 2.21

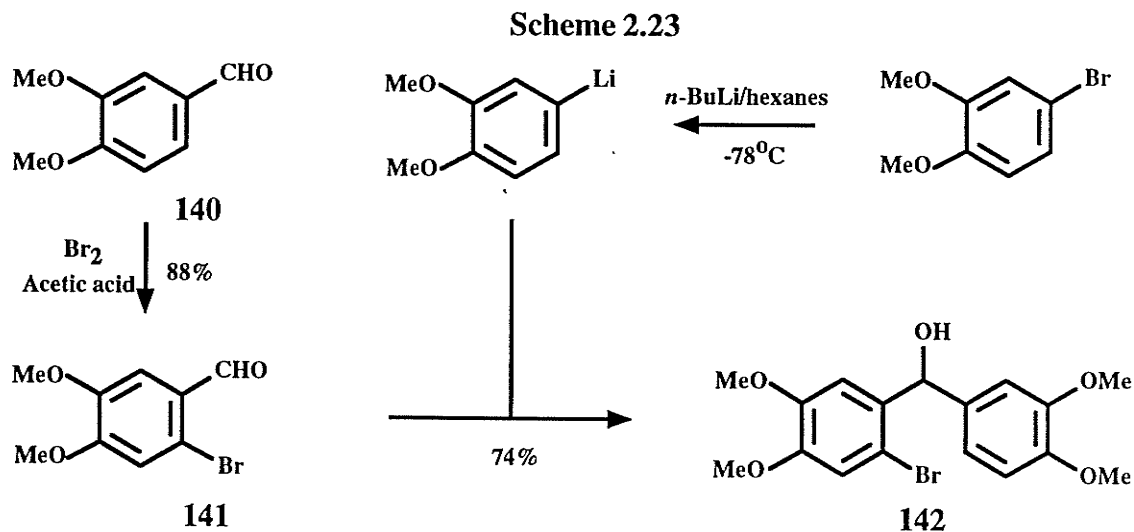


center of fixed stereochemistry. The remaining centers could then be inverted relative to C_1 . Given the absolute stereochemistry of this fixed center, it was necessary to synthesize **135** from either the fumarate bearing the R-lactate or R-mandelate chiral auxiliary. Since R-lactate is not readily available,⁹⁹ the fumarate of methyl (R)-mandelate was chosen. Methyl (R)-mandelate was prepared by esterification of (R)-mandelic acid in refluxing methanol/sulfuric acid (88% yield)⁹⁹. The fumarate of methyl (R)-mandelate was available by simply heating methyl (R)-mandelate with fumaryl chloride at 110°C for 18 hours (66% yield).⁹⁹

In principle one could generate *o*-QDM **136** either by thermolysis of benzocyclobutenol **137** or hydroxy-sulfone **138** or by photolysis of aldehyde **139** (Scheme 2.22). Both the sulfone and the aldehyde have been previously prepared in 39% and 58% yields respectively.⁹³ However the preparation of the aldehyde using the literature method was plagued with variable yields. The synthesis of benzocyclobutenol **19**, an analogue of **137**, was described by Macdonald and Durst⁴¹ as well as Jung.⁴³ Although **19** was reported to be thermally unstable above 0°C,⁴¹ this route to **137** was investigated on the premise that benzocyclobutenols were known to efficiently react with dienophiles under mild conditions. The proposed synthesis of **137** started with the bromination of veratraldehyde **140** (88% yield) in acetic acid using two equivalents of bromine (Scheme



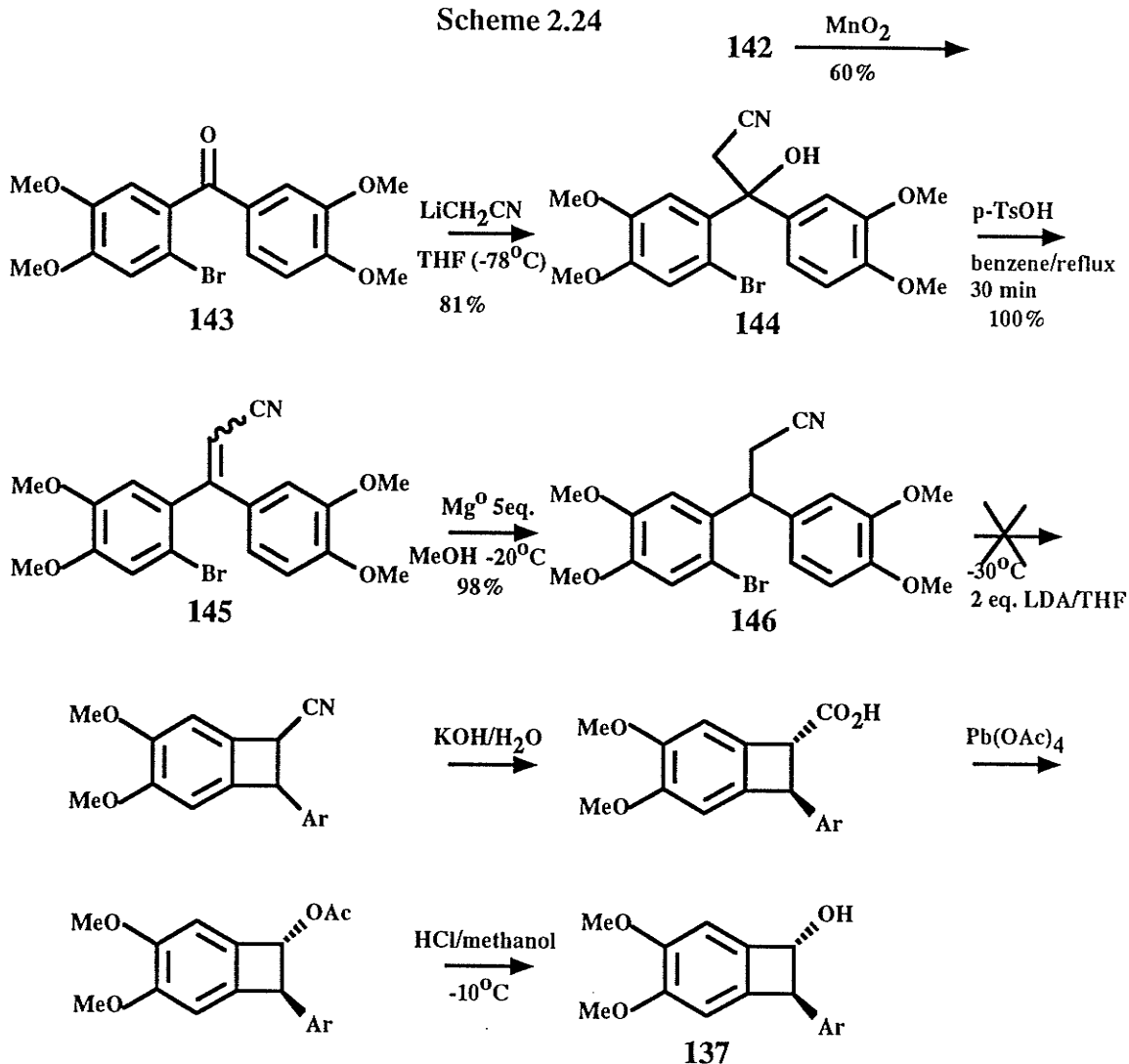
2.23).⁹³ The 4-lithio aryl anion, generated by treatment of 4-bromoveratrole with a slight excess of *n*-BuLi (1.1 molar equivalents) at -78°C (dry ice/acetone), was added to **141** to give the diarylmethanol **142** in 74% yield after chromatography. Oxidation of the



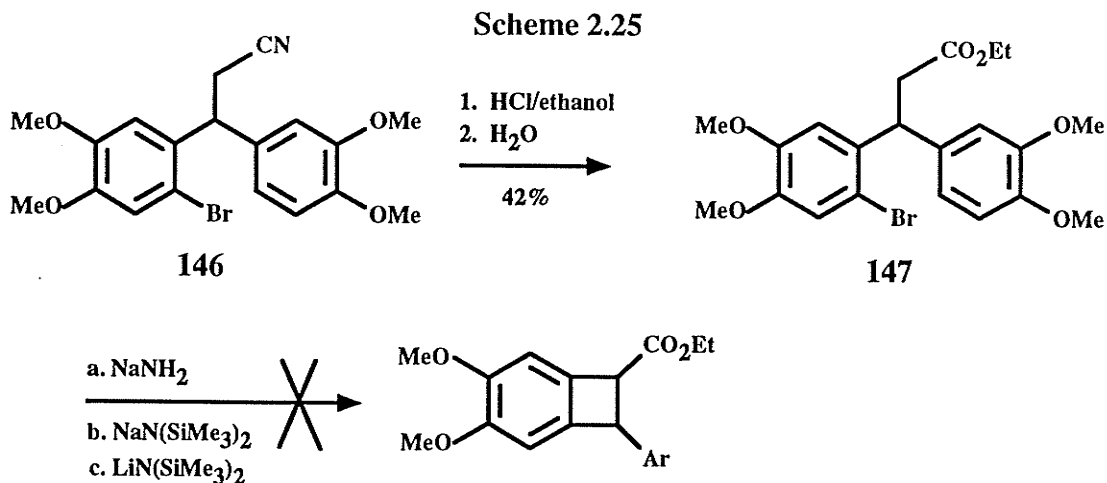
benzylic alcohol **142** was accomplished by refluxing in benzene in the presence of five equivalents of freshly prepared MnO_2 ¹⁰⁵ giving the crystalline ketone **143** in 60% yield (mp 126°C , IR 1661 cm^{-1}) (Scheme 2.24). The anion of acetonitrile was prepared by treatment with LDA at -78°C followed by its addition to the ketone **143** to give **144** in 81% yield (mp 144°C). The resultant alcohol **144** was easily dehydrated in quantitative

yield by refluxing in benzene in the presence of *p*-toluenesulfonic acid. The 1:1 mixture of alkenes **145** was subsequently reduced (magnesium in methanol/-20°C) to the saturated cyano compound **146** in 98% yield. Yields for this reaction were initially variable and often it was found that no reduction would occur even at room temperature. To circumvent this problem, it was necessary to prepare the surface of the magnesium by a series of washings: 10% HCl followed by water, acetone, and finally diethyl ether. The reaction could also be initiated by prior treatment of the magnesium/methanol mixture with a small crystal of iodine. Normal catalytic hydrogenation of the alkene would not have been appropriate as it would likely have removed the aromatic bromide. Unfortunately, the subsequent cyclization step could not be effected using Jung's method. Treatment of **146** with 2.1 molar equivalents of LDA at -78°C resulted only in the recovery of the starting material. The first equivalent of LDA is added to deprotonate the carbon alpha to the cyano group while the second equivalent is added to form the benzyne. Recovery of the starting bromide suggests that the benzyne had not formed. Given the failure of Jung's approach, Durst's approach to benzocyclobutenol was attempted. This procedure involves the use of the ethyl ester derivative instead of the cyano group to activate the alpha position towards deprotonation. The cyano derivative **146** was converted to the ethyl ester **147** by treatment with dry HCl/ethanol at room temperature for 17 hours (Scheme 2.25). The intermediate imino ethyl ester was hydrolysed to the ethyl ester by the addition of water followed by refluxing for 24 hours. Purification of the product on silica gave the desired product as a colourless oil in 42% yield (IR 1733 cm⁻¹) which crystallized on standing (mp 64-66°C). Treatment of the ester **147** with 2.2 molar equivalents of LDA at -78°C followed by warming to room temperature again resulted in recovery of the starting material with no trace of any other products in the ¹H-NMR of the crude product. Several attempts were made without success. It was thought that the inability of LDA to form the benzyne may be due to the steric bulk of the base and therefore Durst's original procedure using sodamide (NaNH₂) in liquid ammonia was

Scheme 2.24



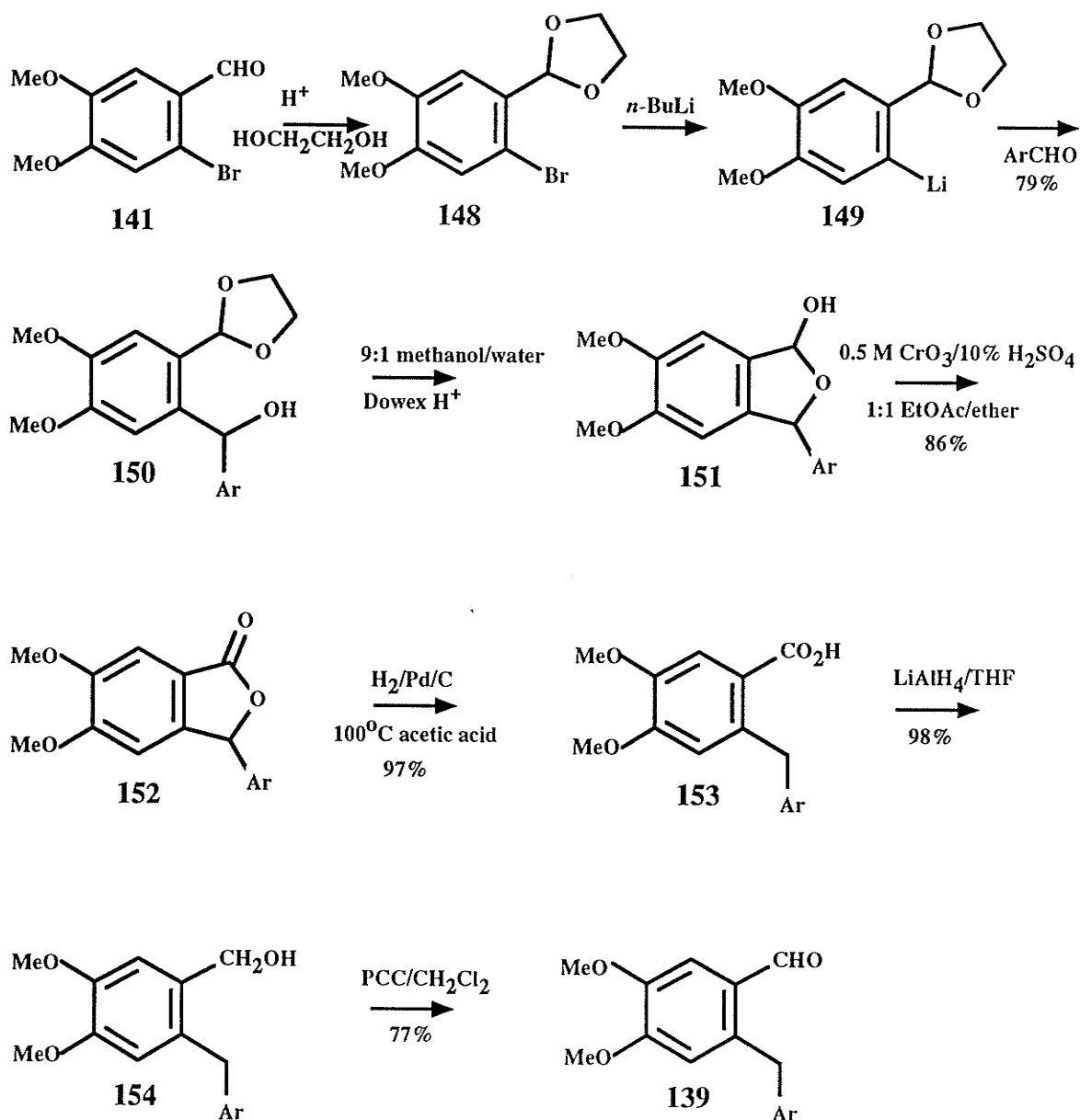
attempted. The sodamide was prepared by the addition of 4 molar equivalents of sodium to liquid ammonia at -78°C . In order to prevent the possibility of Birch reduction, it was necessary to allow the complete reaction of metallic sodium as indicated by the disappearance of the blue color. Unfortunately, no cyclization product could be detected after treating **147** with sodamide and only the starting material was recovered. Again, attention was turned towards the selection of another base. Attempts at cyclization using sodium bis(trimethylsilyl)-amide in THF at -20°C failed as did the more soluble lithium bis(trimethylsilyl)-amide. In view of the problems encountered, the synthesis of benzocyclobutenol **137** was abandoned.



Generation of *o*-QDM **136** from the irradiation of aldehyde⁹³ **139** was also pursued. A relatively long but simple synthesis of the corresponding 3,4-methylenedioxy aldehyde has been described by Arnold *et al.*¹⁰⁶ A slightly modified version of their synthesis was used (Scheme 2.26). The ethylene glycol acetal **148** was prepared from the bromo-aldehyde **141** and ethylene glycol. The acetal was then treated with a slight excess of *n*-butyllithium (1.05 molar equivalents) at -78°C in THF which generated the intermediate aryllithium species **149**. The aryl anion was then treated with veratraldehyde to furnish the alcohol **150** in 79% yield after chromatography (mp $138\text{--}139^\circ\text{C}$). The $^1\text{H-NMR}$ spectrum of **150** was identical to that previously reported by Alauddin.¹⁰⁷ Hydrolysis of the acetal in EtOAc/THF/1% H_2SO_4 (5:1:4) mixture was inefficient. Even after 17 hours at room temperature, substantial amounts of starting acetal **150** was present. A one phase system consisting of 50:50 acetone/1% H_2SO_4 was also examined. However, after 2.5 hours at room temperature, the TLC of the mixture (70% EtOAc/hexanes) revealed two new products which had a smaller *rf* value than **150**. In addition, some starting material was still present. Optimum hydrolysis conditions were obtained using a 9:1 mixture of methanol and water in the presence of a strongly acidic cation exchange resin (Dowex 50W-X8). The reaction was complete after 1.5 hours (room temperature) with the exclusive formation of the lactol **151** (not isolated, larger *rf* value; 70% EtOAc/hexanes). The majority of the solvent was evaporated and the resultant red tar was

immediately oxidized with chromium trioxide (two phase mixture of 0.5 M CrO_3 in 10% aqueous sulfuric and 1:1 solution of ether and EtOAc) to give lactone **152** in 86% yield (starting from acetal **150**, mp 184-185°C, IR 1762 cm^{-1}). Hydrogenolysis of the lactone in acetic acid (5% Pd/C, 1 Atm H_2) at 115°C furnished the carboxylic acid **153** in 97% yield (mp 152-157°C, IR 1735). Before the hydrogenolysis step, it was imperative to remove all

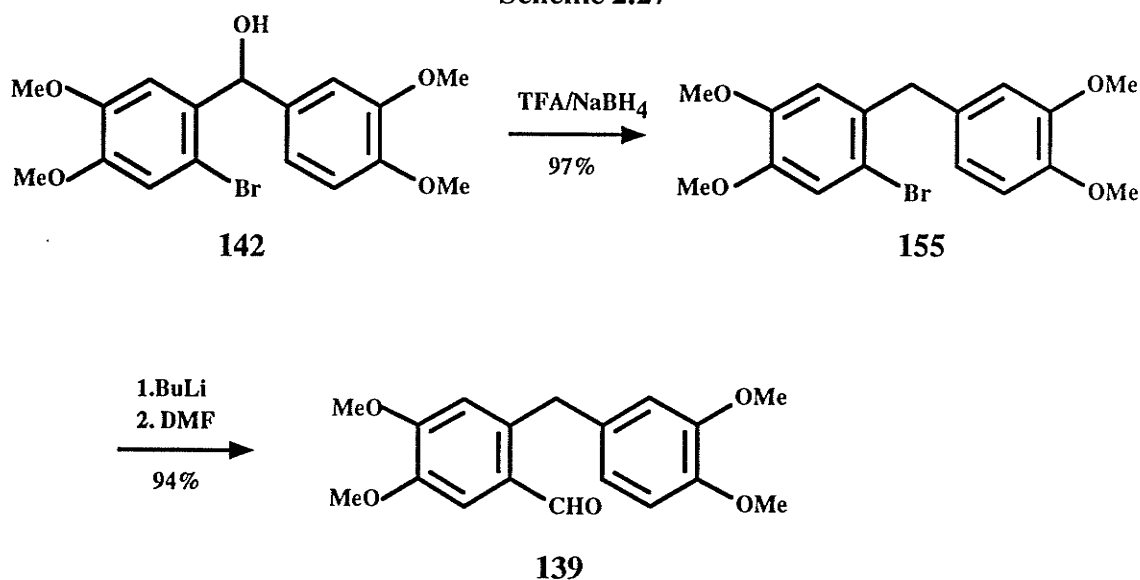
Scheme 2.26



of the chromium salts via filtration through silica gel. Neglect of this step resulted in the poisoning of the palladium catalyst. The acid was easily reduced with lithium aluminum hydride in THF (room temperature) to the corresponding alcohol **154** in high yield (98%, mp 103-105°C, lit¹⁰⁷. mp 103-105°C). Oxidation of alcohol **154** was carried out using three different oxidizing agents. Manganese dioxide oxidation of **154** in refluxing benzene (4 hours) gave the desired aldehyde **139** in 58% yield after chromatography. The major impurity, although not characterized, appeared to be a product resulting from oxidation of the benzylic position to the corresponding ketone. Oxidation of **154** with chromium trioxide (0.5 M in 10% H₂SO₄/water) using a two phase ether system gave **139** in 62% yield. Pyridinium chlorochromate (PCC; also known as Corey's reagent¹⁰⁸) was found to be a relatively good oxidant. Oxidation of **154** using two molar equivalents of PCC gave the aldehyde in 77%. In summary, the aldehyde was available from veratraldehyde in eight steps in 44% overall yield.

Given the overall length of the above synthesis of **139**, a shorter route was developed. This synthesis started with the addition of lithio-3,4-dimethoxybenzene to 6-bromoveratraldehyde **141** (-78°C) giving **142** as described in the attempted synthesis of benzocyclobutenol **137** (Scheme 2.24). The diarylmethanol **142** could be cleanly deoxygenated by the method of ionic reduction of diarylmethanols using a mixture of sodium borohydride and trifluoroacetic acid (TFA) (Scheme 2.27).¹⁰⁹ In this case, addition of a methylene chloride solution of **142** to a mixture of TFA and NaBH₄ at 0°C produced a deep purple coloured solution which rapidly decolourized to give **155** in 97% yield after chromatography. It was also possible to use a 1:1 mixture of glacial acetic acid and TFA to give **155** in 95% yield. The use of acetic acid in this case reduces the volume of TFA and thus the cost of the synthesis. It was found that purification of the starting alcohol **142** was necessary before the TFA/NaBH₄ reduction step as use of the crude addition product gave an intractable mixture of products. Treatment of the bromide **155** with one molar equivalent of *n*-butyllithium at -78°C followed by the addition of three

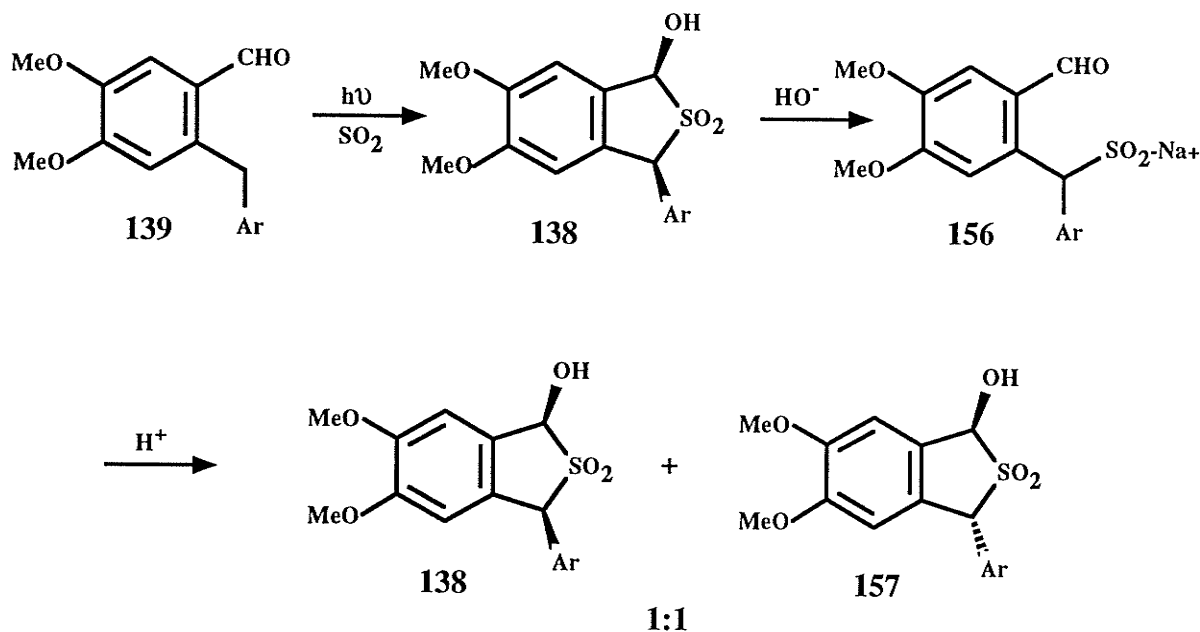
Scheme 2.27



equivalents of dimethylformamide gave the aldehyde **139** in 94% yield. The aldehyde was deemed >95% pure from the ^1H -nmr spectrum of the crude product and was used without purification in the next step. Thus, aldehyde **139** was available from veratraldehyde in four steps and 59% overall yield.

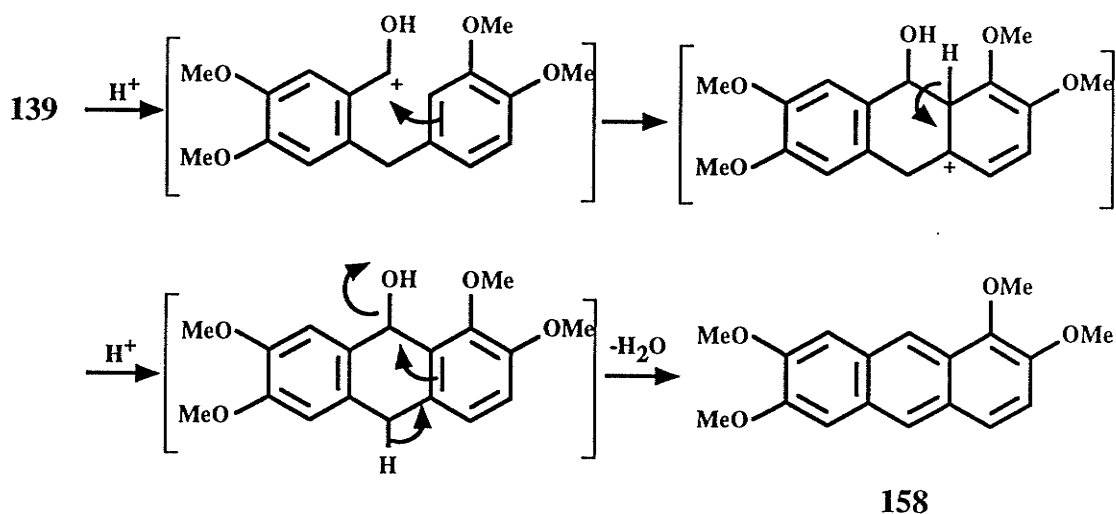
Irradiation of the aldehyde **139** in benzene in the presence of fumarate **118** using a mercury lamp (Hanovia 450 Watt, medium pressure) gave the desired *exo* cycloadduct **135** ($J_{4,3} = 9.4$ Hz, $[\alpha]_{\text{D}}^{20} +51.3^\circ$, IR 3495 (br, OH), 1745 (ester) cm^{-1}) in 30% yield after chromatography. This method was unfortunately plagued with the problem of isomerization of the fumarate **118** to the corresponding maleate. This isomerization is likely a result of triplet energy transfer from the excited aldehyde to the fumarate. The same effect was also observed by Koh when the enantiomer of **118** was irradiated in the presence of the corresponding 3,4-methylenedioxy aldehyde.⁹⁵ This inherently inefficient step could be obviated by the use of the hydroxy sulfone **138**. Alauddin had previously synthesized **138** by irradiation of **139** in the presence of sulfur dioxide (Scheme 2.28).⁹³ However purification of the sulfone involved base extraction to form the water soluble sulfinate anion followed by acidification giving a mixture of the *cis* and *trans* sulfones **138** and **157** respectively (Scheme 2.28). Unfortunately, thermolysis of the *trans*-sulfone

Scheme 2.28



results in the undesirable *E,Z*-*o*-QDM.⁹³ In this work, initial attempts to prepare **138** by irradiation of **139** in anhydrous benzene containing SO_2 resulted in substantial anthracene formation. This anthracene formation could be prevented by the addition of a small amount of pyridine. Presumably, adventitious water reacts with SO_2 to form sulfurous acid which catalyzes the cyclization of **139** to 1,2,6,7-tetramethoxyanthracene (Scheme 2.29). The presence of anthracene **158** could be detected by its characteristic blue fluorescent colour on TLC. Irradiation of the aldehyde under a continuous stream of SO_2 (saturated solution) resulted in only 50% conversion to a mixture of the *cis* and *trans* sulfones (δ : *trans* 5.67, 5.63; *cis* 5.46, 5.32; 1.2:1, *trans*:*cis*) even after 24 hours. This suggested that an equilibrium existed between **139**, **138**, and **157**. The slow formation of the sulfone was probably due to the high UV absorption of SO_2 in benzene between 265 and 360 nm. Slow thermal decomposition of **138** and **157** completed the equilibrium process. It was found that if the SO_2 concentration was decreased to about 4-5 g/100 mL, the reaction went to completion in 6 hours with the *cis* sulfone being the major component as indicated by TLC. At higher concentrations of SO_2 the solution becomes more polar. This increase in polarity may be responsible for the increase in the amount of the *trans*

Scheme 2.29

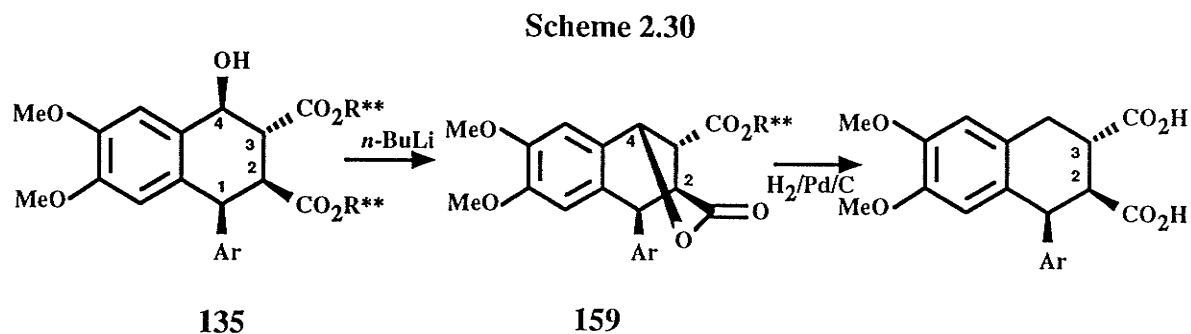


sulfone as it has been observed previously that the *cis* sulfone isomerizes to the *trans* sulfone in polar solvents.¹⁰⁷ Previous experience with the photolysis of *o*-benzyl benzaldehydes suggests that only the *cis* sulfone is formed initially.⁹⁴ No attempt was made to purify the crude sulfone mixture given the facile epimerization of the *cis* to the *trans* sulfone.

Using a method similar to that used in the synthesis of the podophyllotoxin analogues,⁹⁴ *exo*-cycloadduct **135** was synthesized in 44% yield (based on aldehyde **139**; 90:10 ratio of **135** to other diastereomers) by slow addition of a methylene chloride solution of **138** to a refluxing solution of the dimandeloxymumarate **118** in toluene (Scheme 2.21, 2.22). The major cycloadduct (identical with the major product from the reaction of **139** with **118**) exhibited a large $J_{3,4}$ coupling of 9.4 Hz indicating a *trans* disposition of the 4-hydroxyl and the 3-carboxy groups consonant with previous findings.⁹⁵ The minor cycloadducts (ca. 5%) were isolated as a mixture and were not characterized. They exhibited $^1\text{H-NMR}$ doublets at 5.47 and 5.18 ppm with couplings of about 3 Hz typical of the H1 signals of endo cycloadducts.³⁵

The synthesis of the permethylene lignan lactones like podophyllotoxin or α -dimethylretrodendrin requires regiodifferentiation of the 2 and 3-ester groups on the tetralin ring. This could have been achieved using the previously reported lactonization

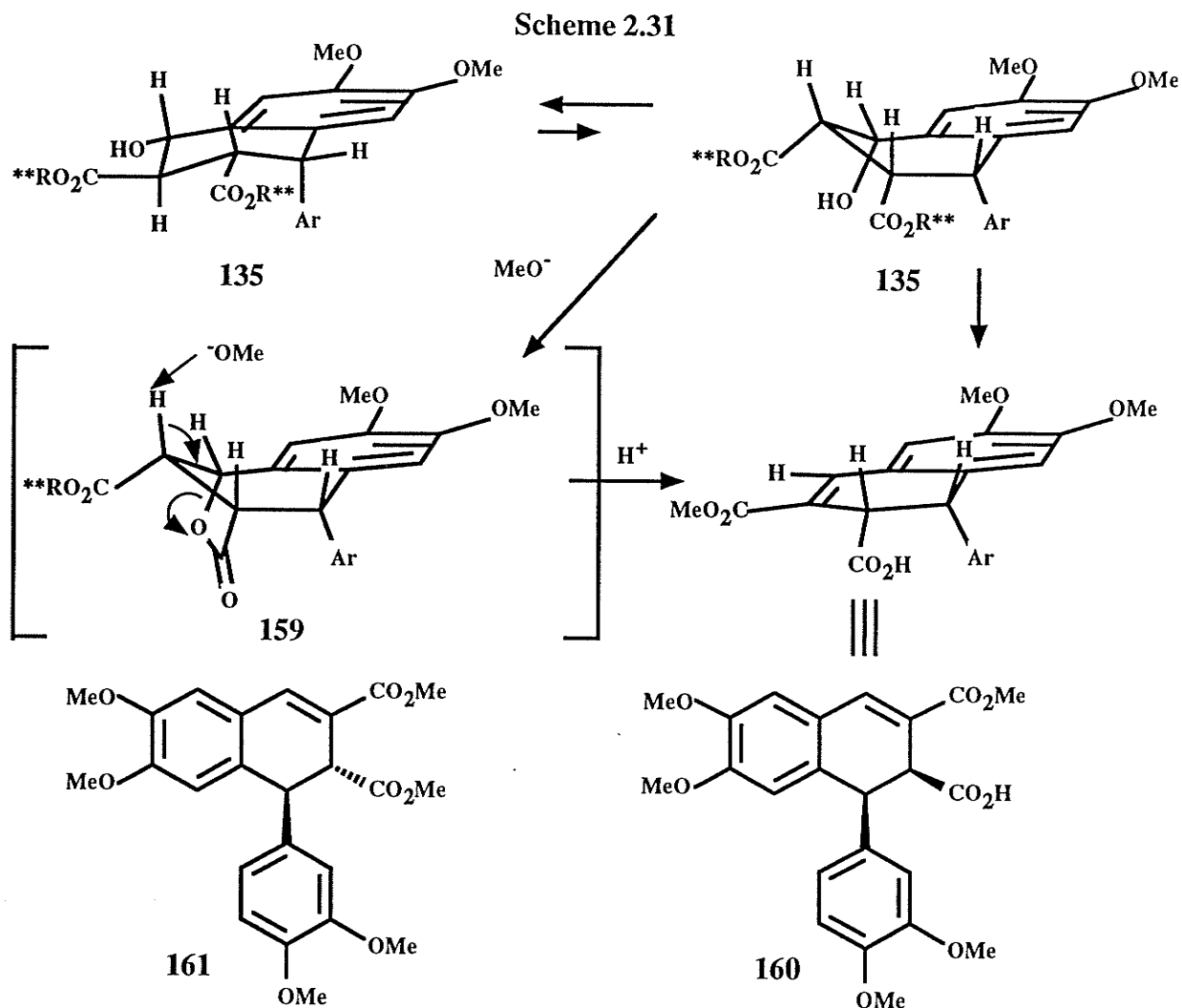
method which involves treatment of the cycloadduct with one molar equivalent of *n*-butyllithium.^{94,95} However, disconnection of the C4-oxy group in the lactone via catalytic hydrogenolysis, a requirement for the synthesis of the 4-deoxy lignans, would also cleave the remaining C3 mandelate group resulting in an undifferentiated 2,3-diacid (Scheme 2.30). As an alternative to the lactone method, it was felt that it might be



possible to carry out a tandem lactonization/base induced 3,4-elimination. This might be accomplished by treatment of the cycloadduct with two equivalents of strong base. The use of *n*-butyllithium would not be judicious as in addition to being a very strong base, it is also a good nucleophile. The bulkier *t*-butyllithium was tried. However, treatment of **135** with two equivalents of *t*-butyllithium at -78°C resulted in a complicated mixture. A gratifying result was obtained when the base was changed to sodium methoxide.

Treatment of **135** with anhydrous methanol/sodium methoxide (0.1 M) at room temperature gave the elimination product **160** in 97% yield (IR 1743, 1711 cm⁻¹; [α]_D²⁰-321°) (Scheme 2.31). The relative stereochemistry of the aryl and the 2-carboxylic acid group was assigned as *cis* on the basis of the H_{1,2} coupling constant of 7.7 Hz. The analogous 1,2-*trans* dimethyl ester **161** has a smaller coupling constants of 2.5 Hz.⁹³ A plausible mechanism for the formation of **160** may involve initial formation of the 2,4-lactone **159** followed by elimination and transesterification of the 3-mandelate group (Scheme 2.31). In order for the lactone to form, the cycloadduct must be able to adopt a half-chair conformation. The H₃ proton is now *trans*-diaxial with respect to oxygen at the 4-position and can readily undergo elimination. It is also conceivable that lactone **159** is

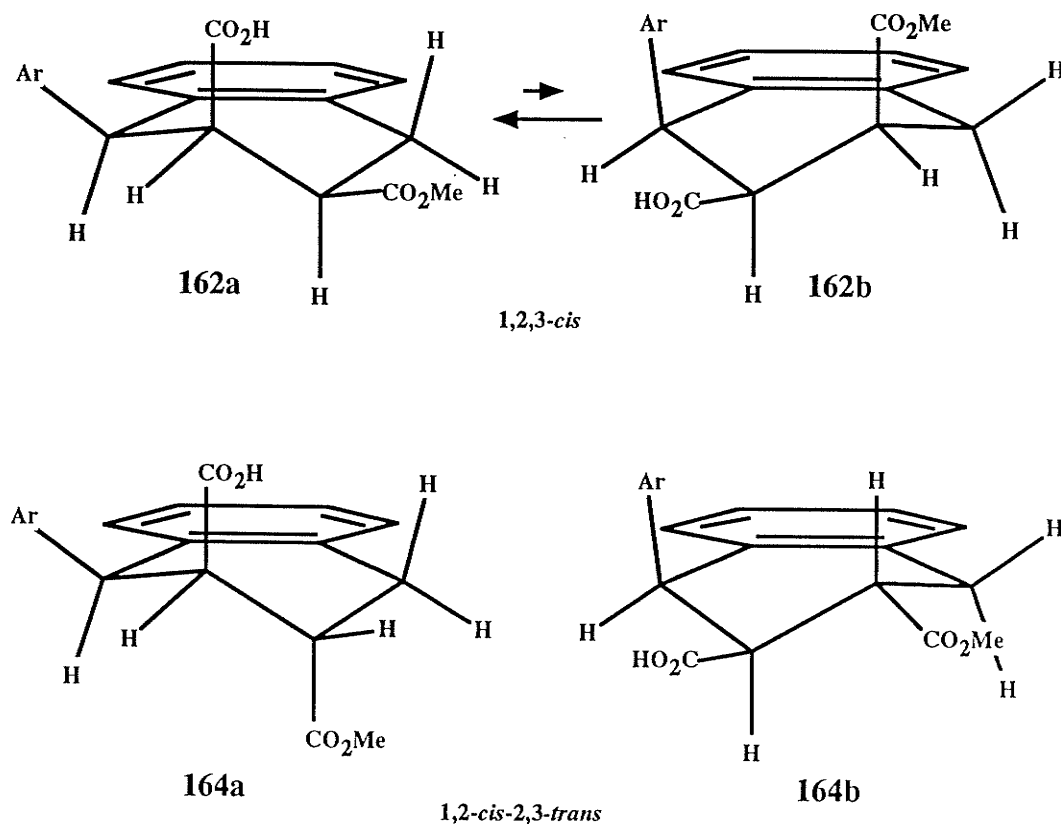
not an intermediate but that abstraction of the H2 proton and hydroxide transfer are concurrent (one step mechanism). About 3% of compound **161** was formed during the conversion of **135** to **160** (Scheme 2.31). Compound **161** had spectroscopic properties identical to those previously reported.⁹³



One should note the significant fourfold success of conversion of **135** to **160**. Firstly, differentiation of the 2 and 3-ester groups has been accomplished with retention of the thermodynamically unfavorable 1,2-*cis* stereochemistry. Secondly, the formation of the carboxylate anion under basic conditions precludes epimerization at the 2-position due to the decreased acidity at the α -carbon. Thirdly, elimination resulted in deoxygenation and double bond formation which allows for manipulation of the stereochemistry at C3.

Fourthly, transesterification of the 3-mandelate group enables one to catalytically hydrogenate the double bond without the hydrogenolysis of the ester to the acid which would have occurred if the mandelate group were still present. Catalytic hydrogenation of **160** in ethyl acetate/acetic acid over 5% Pd/C gave the all-*cis* compound **162** in 87% yield (mp 195-196°C; $[\alpha]_D^{20}$ -88°; IR 3057 (CO₂H), 1734, 1712 cm⁻¹) (Scheme 2.32,2.33). As expected, the H_{1,2} coupling of 5 Hz confirmed that the 1,2-*cis* stereochemistry was retained in the hydrogenation step. The stereochemistry at C3 which resulted from the hydrogenation step was determined from an analysis of the H_{2,3}, H_{3,4axial} and H_{3,4equatorial} coupling constants (Scheme 2.32). There are two possible conformations for the all-*cis* geometry as depicted by **162a** and **162b**. In **162a**, the aryl group occupies an equatorial position and in **162b**, an axial position. The other possible product of hydrogenation (1,2-*cis*-2,3-*trans*) can also exist in two conformations **164a** and **164b**. One cannot unequivocally distinguish between **162a** and **162b** based on the H_{1,2} or H_{2,3} couplings as

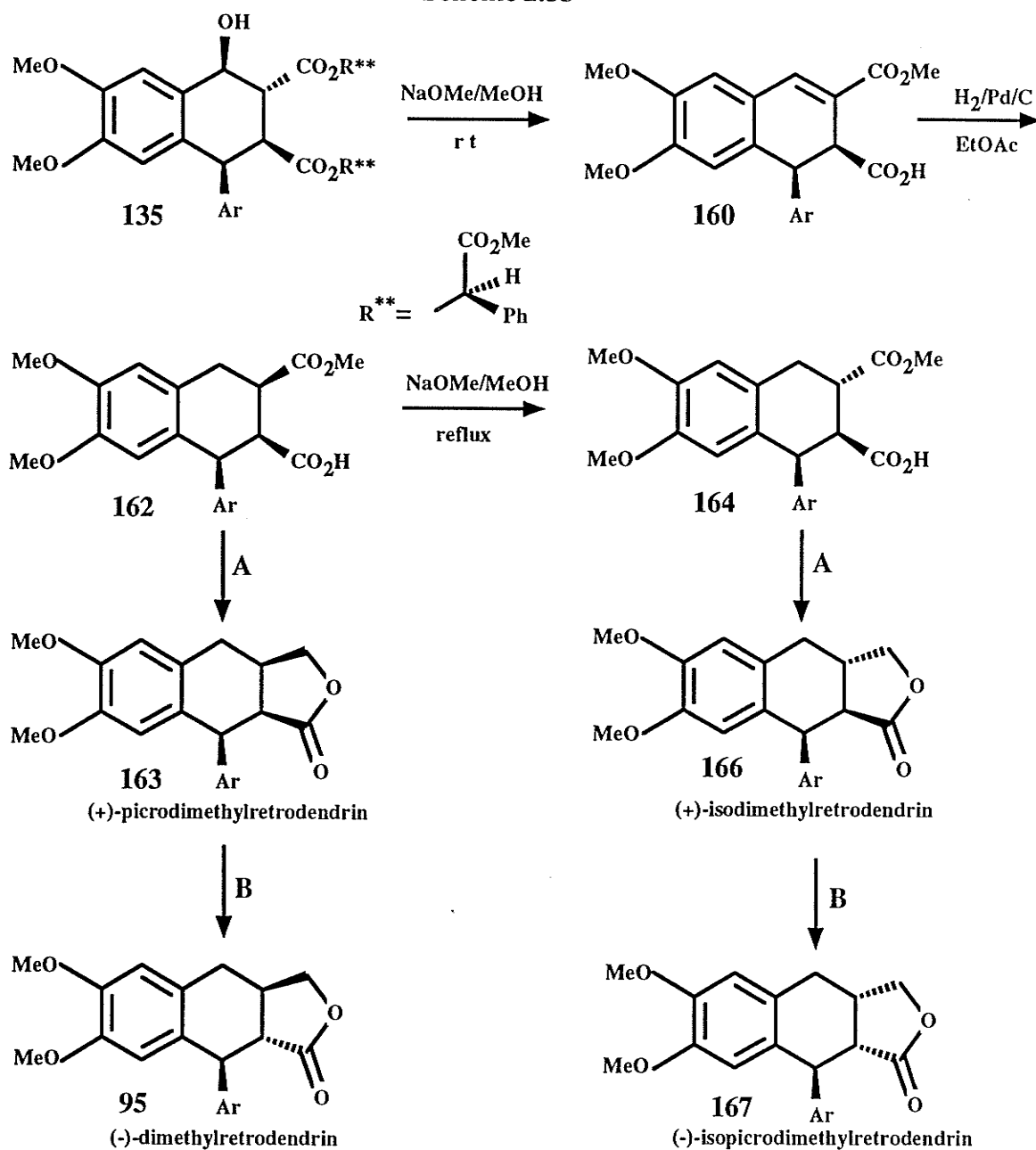
Scheme 2.32



one expects them to be similar in both conformers. The observed $H_{2,3}$ coupling of 3.7 Hz, typical of axial-equatorial coupled protons, immediately excludes **164b**. The $H_{3,4}$ couplings of 5.5 and 12.2 Hz implies that H3 is axially disposed. The large coupling of 12.2 Hz arises from the coupling of the axial H3 and H4 protons while the 5.5 Hz coupling is to H_{4eq} . Based on the $H_{2,3}$ and $H_{3,4}$ coupling constants, it was concluded that the structure was **162a**. The reported hydrogenation of the 1,2-*trans* alkene **161** gives the all-*trans* saturated lignan suggesting that hydrogen addition occurs preferentially to the face opposite the sterically large aryl group.⁹³ Similarly then, stereoselective hydrogenation of **160** to give **162** (all-*cis*) can be explained by the preference for addition to the sterically least hindered face of the alkene.

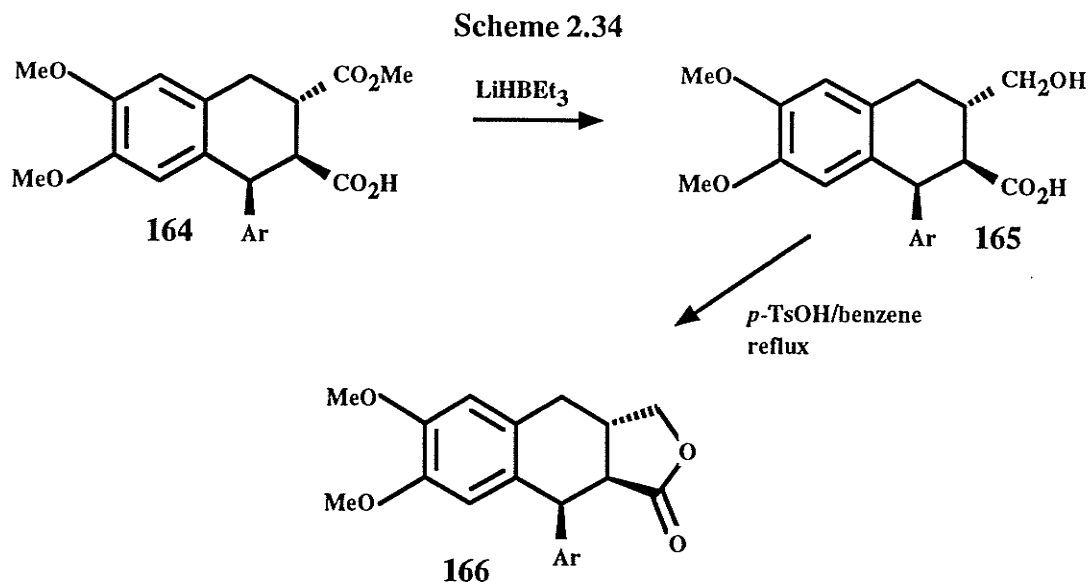
Intermediate **162** was the thermodynamic summit from which all of the diastereomers of dimethylretrodendrin were synthesized (Scheme 2.33). Entry into the all-*cis* configuration was possible by reduction of the 3-ester group using lithium triethylborohydride ($LiEt_3BH$) in THF. Upon aqueous acid workup of the reduction product, incomplete cyclization to lactone **163** was observed as evident from 1H -NMR of the crude product. It was found that the yield of the reaction could be increased from 78% to 84% by refluxing the crude product in benzene in the presence of a trace of *p*-toluenesulfonic acid ($[\alpha]_D^{20} +143^\circ$; IR 1768 (lactone CO) cm^{-1}). Base catalyzed epimerization of **163** was possible by refluxing in 0.1 M sodium *t*-butoxide/*t*-butanol to give optically pure (-)- α -dimethylretrodendrin **95** in 94% yield (mp 182-183°C, lit¹¹⁰ 188-189°C; $[\alpha]_D^{20} -58^\circ$, lit¹¹⁰ $[\alpha]_D^{20} -58^\circ$). Access to the podophyllotoxin geometry was possible using a method similar to that reported by Takano.⁸² Compound **162** (1,2,3-*cis*) was converted to compound **164** (1,2-*cis*-2,3-*trans*) in 83% yield by refluxing in sodium methoxide/methanol solution followed by aqueous workup. The large $H_{2,3}$ coupling constant ($J_{2,3} = 11.7$ Hz) confirmed the equatorial nature of the 2,3-ester groups as depicted by **164b**. Reduction of **164** with $LiEt_3BH$ in THF and dilute acid workup gave the open hydroxy-acid **165** in 76% yield ($[\alpha]_D^{20} +177^\circ$; IR 1701 cm^{-1} (CO, acid) (Scheme 2.34).

Scheme 2.33



A. $\text{LiHBEt}_3/\text{THF}$ B. 0.1 M NaOtBu/tBuOH reflux

Treatment of **165** with *p*-toluenesulfonic acid in refluxing benzene afforded lactone **166** (1,2-*cis*-2,3-*trans*) in 53% yield. Alternatively, this intervening step could be omitted by slow evaporation of the aqueous acidic workup solution at room temperature to give **166** directly in 79% yield ($[\alpha]_{\text{D}}^{20} +115^\circ$; IR 1779 cm^{-1}). As mentioned in the introduction, it is well known that C2 of podophyllotoxin undergoes facile base catalyzed epimerization to

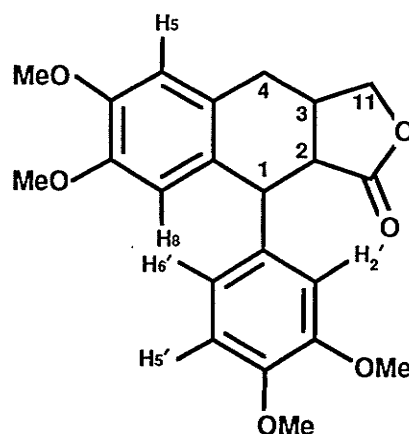


give picropodophyllotoxin. In this case, **166** could be cleanly converted to the C2 epimer **167** in 87% by refluxing in sodium *t*-butoxide/*t*-butanol ($[\alpha]_{\text{D}}^{20} -17.2^\circ$; IR 1769 cm^{-1}).

The three diastereomers of dimethylretrodendrin are named using the nomenclature convention developed for podophyllotoxin. Thus compounds **163**, **166**, and **167** are named with respect to **95**. The relative stereochemistries at centers 1 and 2 are designated as iso and picro respectively.

2.2.2 NMR and Conformational Analysis

The $^1\text{H-NMR}$ chemical shifts and coupling constants for the four lignans are shown in Table 6a and Table 6b respectively. The NMR spectra of the lignans are shown in Figure 13. A wealth of information regarding stereochemistry and conformation can be gained by examination of the coupling constants and chemical shifts. In addition to chemical shifts and couplings, NOE difference spectroscopy and molecular mechanics calculations were performed in order to help resolve the conformational preferences for the four lignans. The protons are designated with respect to the numbering scheme shown below. The geometry of the *trans* lactones in dimethylretrodendrin **95** and



Lignan numbering scheme.

Table 6a. Chemical Shifts for Lignans **95**, **163**, **166**, and **167** in CDCl_3 (δ)

Compound	H1	H2	H3	H4	H4 β	H5	H6'	H2'	H8	H5'	H11	H11 β
163	4.52	3.07	3.15	2.71	2.99	6.77	6.51	6.87	6.71	6.72	3.35	4.38
95	4.12	2.50	2.63	2.93	3.00	6.61	6.79	6.71	6.33	6.83	3.99	4.53
166	4.64	2.77	3.09	2.77	2.77	6.68	6.36	6.95	6.52	6.67	3.92	4.44
167	4.44	3.32	3.03	2.51	2.89	6.68	6.57	6.69	6.62	6.77	3.96	4.44

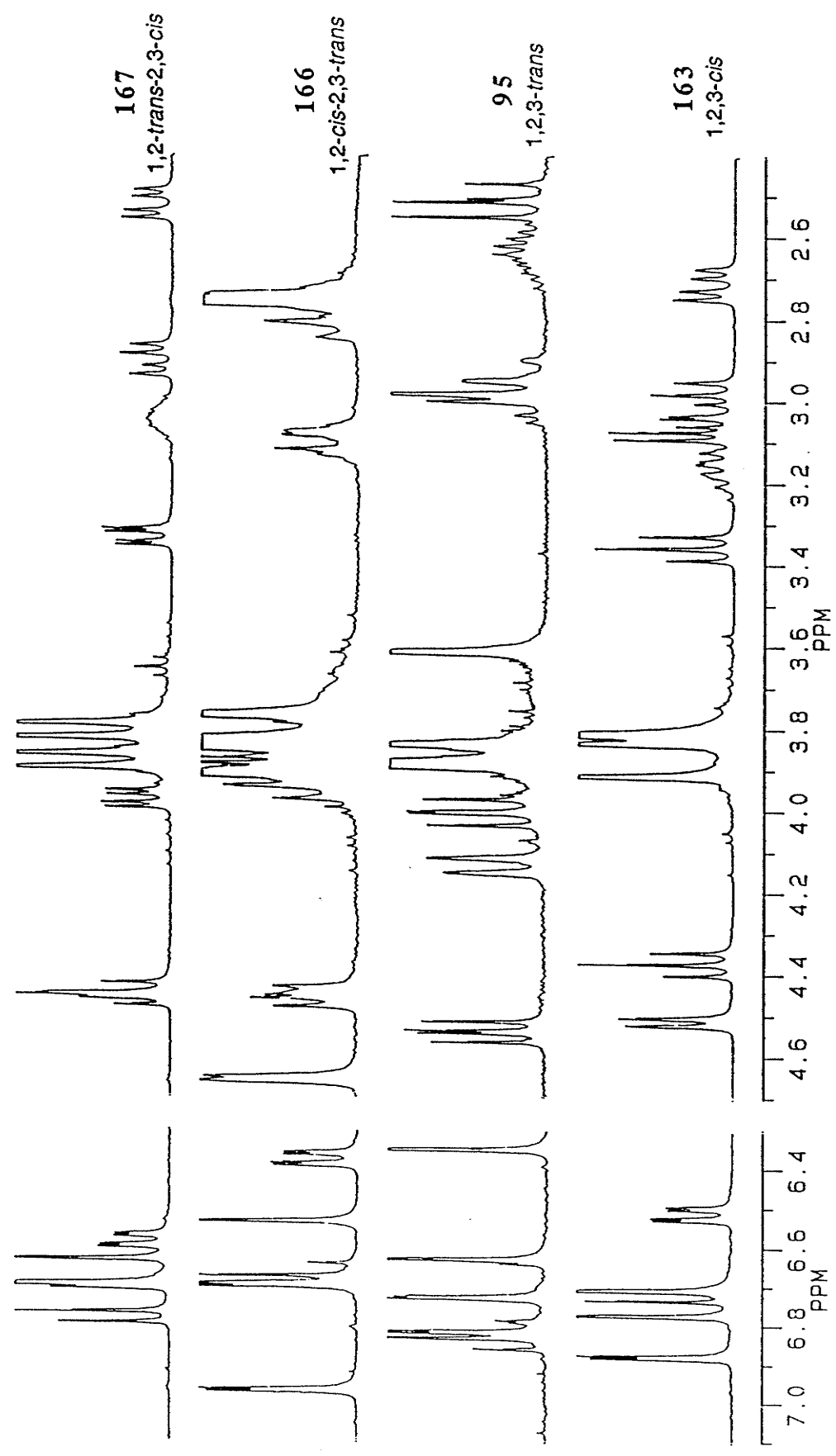
Table 6b. Observed Coupling Constants for Lignans **95**, **163**, **166**, and **167** in CDCl_3

Compound	J _{1,2}	J _{2,3}	J _{3,4α}	J _{3,4β}	J _{11α11β}	J _{11α,3}	J _{11β,3}	J _{4α,4β}
163	5.5	10.1	6.1	9.0	8.5	8.5	8.5	15.8
95	10.9	13.5	14	5.3	8.6	10.4	6.4	14
166	3.4	-	-	-	8.6	9.9	6.2	-
167	2.5	9.6	5.1	6.5	9.1	7.4	3.4	15.4

isodimethylretrodendrin **166** renders the molecules conformationally inflexible so that the assignment of coupling constants to a particular conformation becomes unambiguous.

The H1 proton for the all-*trans* lignan **95** is shifted to substantially higher field than the H1 protons of the remaining lignans (Figure 13). This suggests that H1 has an axial orientation and therefore lies above the deshielding plane of the tetralin ring. The equatorial nature of the pendant aryl ring is evident from the relative upfield shift of the H8 proton, which lies in the shielding plane of this ring (Figure 14). The equatorial nature of the pendant aryl group also manifests itself in the upfield shift of the C7 methoxy group to 3.6 ppm (*ortho* to H8; 12.6% NOE to OMe when H8 is irradiated). The large coupling

Figure 13. ¹H-NMR spectra of lactones 167, 166, 95, and 163 in CDCl₃ at 300 MHz.



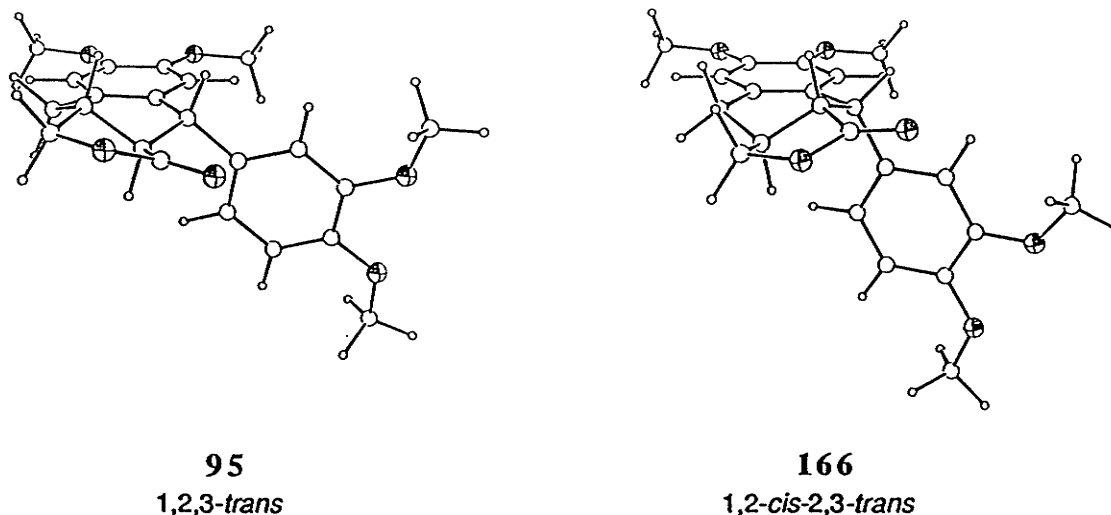


Figure 14. Ortep diagrams for lactones **95** and **166** (MM2 structures) between H1 and H2 (10.9 Hz) as well as H2 and H3 (13.5 Hz) suggests that these protons all lie in a *trans*-diaxial arrangement (Figure 14). NOE difference spectroscopy was applied to confirm the conformation of the tetralin ring. Irradiation of H1 gave NOE's to H3 (5.9%), H8 (4.8%), H2' (6.3%), and H6' (7.6%). The NOE to H3 indicates that they are on the same side of the tetralin ring. The NOE values to the ortho protons H2' and H6' are about the same value (1.2:1) indicating a slight population difference for the two rotamers of the pendant aryl. Irradiation of the H2' and H6' *ortho* protons both give rise to NOE's of 8.8 and 10.5% to H1 (1.2:1). The equatorial nature of the aryl ring is evident from the enhancement of the H8 proton (2.0, 2.8) when H2' and H6' are irradiated. The H1_β and H4_β methylene protons (the β proton lies on the side opposite the aryl group) were identified on the basis of their observed NOE enhancements when H3 was irradiated (5.9 and 3.4% respectively).

The rotational barrier of the aryl group was estimated from force field calculations (MMX). The C6'C1'C1H1 dihedral was driven from 0° to 180° in 5° increments producing a barrier of 8.5 kcal (Figure 15). The full rotation was completed by driving the H1C1C1'C2' dihedral from 185 to 360° (5° steps). The majority of the barrier arises

Table 7. NOE enhancements for (-)-dimethylretrodendrin (**95**)

		Observed NOE %enhancements										
		H ₁	H ₂	H ₃	H _{4α}	H _{4β}	H ₅	H ₈	H _{2'}	H _{6'}	H _{11α}	H _{11β}
Irrad.	H ₁		3.3	5.9				4.8	6.3	7.6		
	H ₂				4.8				4.6	4.1	4.3	
	H ₃	9.7				3.4						5.9
	H _{4α,4β}		6.2				7.1				3.7	
	H ₅					5.6						
	H ₈	4.7							0.9			
	H _{2'}	8.8	4.7					2.0				
	H _{6'}	10.5	4.3					2.8				
	H _{11α}		4.3		2.3							27.6
	H _{11β}			7.7							31.3	

from a large closed shell repulsion between the *ortho* protons of the aryl ring and the lone pair on the carbonyl oxygen. The ORTEP of **95** after geometry optimization is shown in Figure 14. Examination of the ORTEP of **95** reveals that the normal to the plane of the ester carbonyl points towards the H1 proton. The upfield shift of this proton likely arises from the shielding effects of the carbonyl group and the shielding effects of the equatorial aryl ring.

Two interesting features are present in the NMR spectrum of the 1,2-*cis*-2,3-*trans* lactone **166**. The first feature is the downfield shift of the H1 proton to 4.64 ppm. This downfield shift of H1 may be due to its axial orientation. Additionally, the H1 proton of **166** lies in the deshielding plane of the carbonyl group (see Figure 14). The second notable feature is the large chemical shift anisotropy of the H_{2'} and H_{6'} protons as compared to lactones **95** and **167**. H_{6'} is shifted upfield to 6.36 ppm while H_{2'} is shifted downfield to 6.95 ppm ($\Delta_{2',6'} = 0.59$ ppm; cf. $\Delta_{2',6'} = -0.08$ ppm for **95**). This shift anisotropy is likely due to a conformational preference for the aryl group. Energy

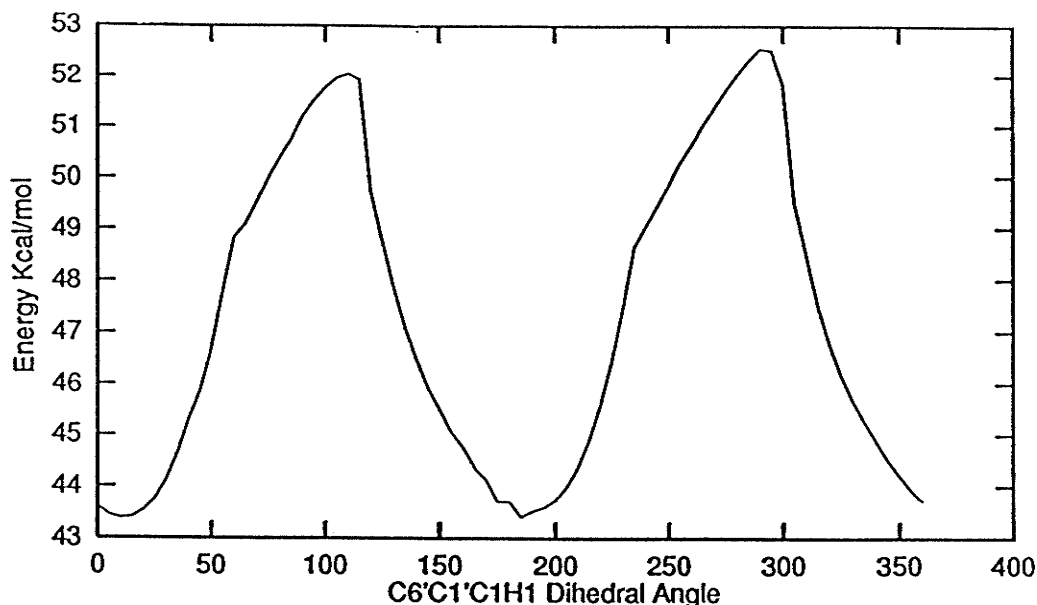


Figure 15. C1-aryl rotational barrier for dimethylretrodendrin (**95**)

calculations (MMX) on **95** (1,2,3-*trans*) and **166** (1,2-*cis*-2,3-*trans*) reveal that the preferred rotamer in both molecules are ones in which the C3' methoxy group lies under the tetralin ring system ($\Delta E = 0.170, 0.06$ kcal respectively). For the preferred conformation, the H6' lies in the deshielding plane while the H2' proton lies in the shielding region of the tetralin ring system. The calculations therefore do not support the observed chemical shift changes of these two *ortho* protons. Based on the calculations, one would expect H6' to move to lower field and H2' to move to higher field. Experimentally, the H6' proton of **166** moves to higher field while the H2' proton moves to lower field relative to the H2' and H6' protons of **95**. The two-fold barrier for the rotation of the aryl group in **166** was estimated to be about 5.3 kcal suggesting rapid rotation at room temperature (Figure 16). The small energy difference between the two conformers (0.06 kcal) would seem to indicate a lack of conformational bias.

Although the calculations suggested an opposite shift sense, it was felt that the shift difference between H2' and H6' would be more pronounced when the aryl group was axially disposed. This axial disposition would allow for the placement of one proton in

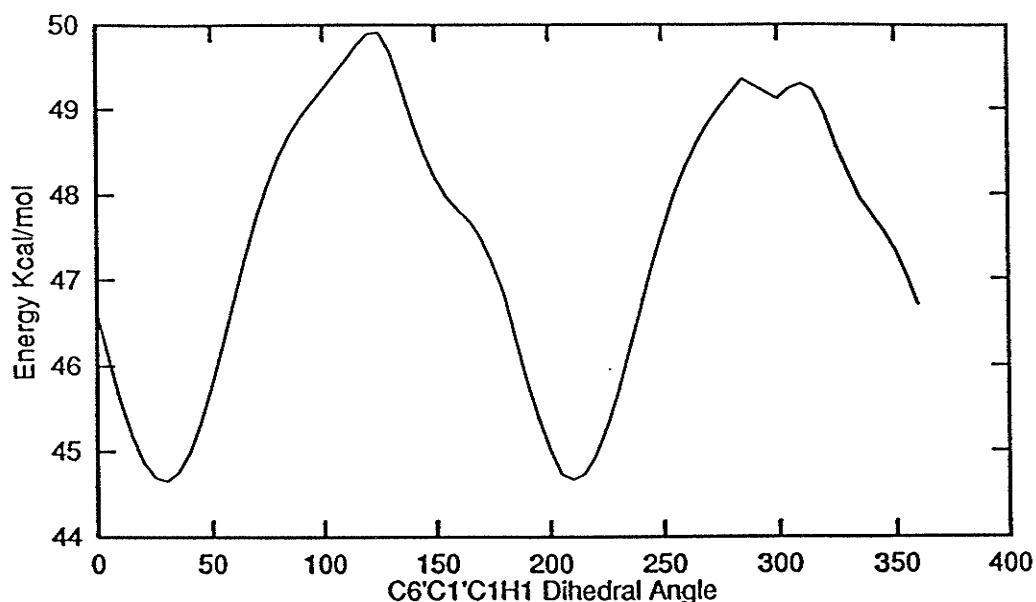


Figure 16. C1-aryl rotational barrier for isodimethylretrodendrin (166)

the shielding region under the aryltetralin ring and the other in the deshielding plane of the aryltetralin ring. When the aryl group is equatorial, the *ortho* protons would have intermediate shielding and deshielding contributions to their chemical shifts. The chemical shift of the H1 protons in general will also depend on its orientation with respect to the plane of the tetralin ring. Thus, when the aryl group is axial, H1 is equatorial and therefore deshielded. A plot of the chemical shift difference between H2' and H6' ($\Delta\delta_{2'6'}$) and the chemical shift of the H1 proton for the four lactones shows a correlation exists between the shift difference of the *ortho* protons and the orientation of the aryl group (Figure 17). It is assumed that the major influence on the chemical shift of H1 is the diamagnetic effect produced by the tetralin aromatic ring.

The two lignans **167** and **163** have the *cis*-2,3-lactone ring fusion. It has been proposed that the 1,2-*cis* fusion gives rise to conformationally flexible molecules which exist in the boat forms A/B and C/D (Figure 18).^{19,75} Ayres *et al.*¹¹¹ have reported a $H_{1,2}$ coupling constant for the 4-hydroxy analogue picropodophyllotoxin (Table 1) of 6.75 Hz suggesting that the preferred conformation is similar to C. This is a reasonable conclusion

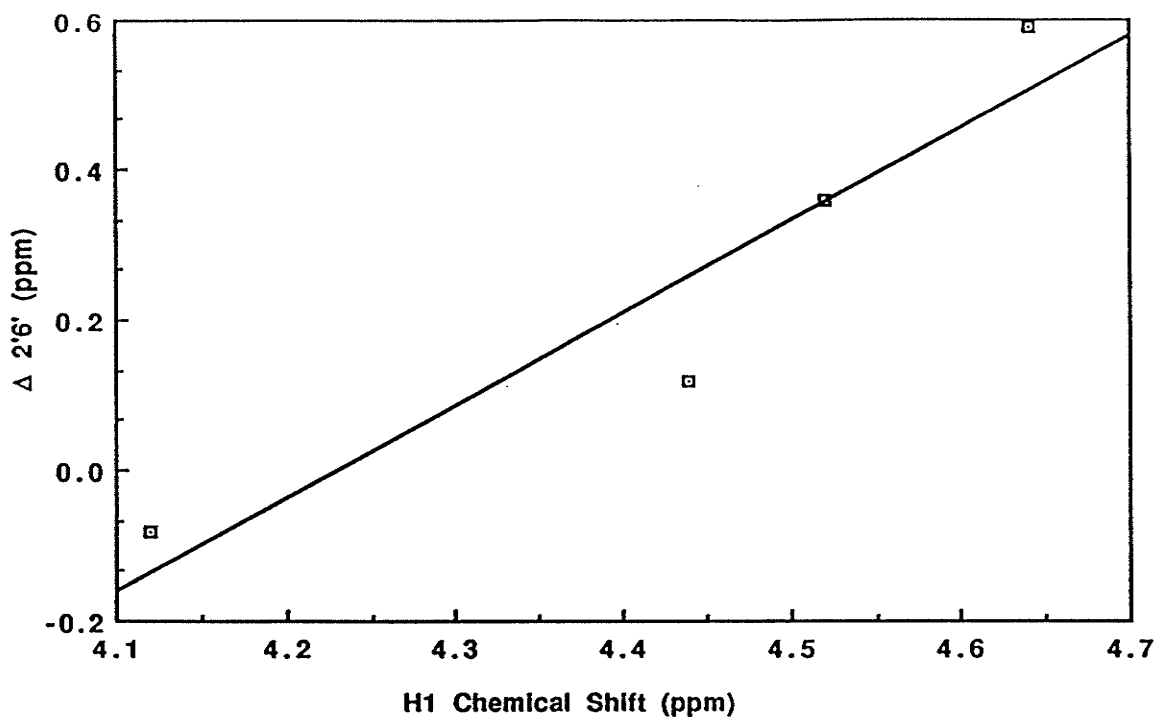


Figure 17. Correlation between the H1 chemical shift and the H2'H6' shift difference.

given the unfavorable 1,4-diaxial interaction of the aryl and hydroxyl groups present in conformation **D**. In deoxypicropodophyllotoxin, the $H_{1,2}$ coupling is 3.0 Hz.⁷⁵ However, the authors imprudently suggested that the preferred conformation was similar to **C**. Given the *trans*-diaxial arrangement of H1 and H2 in **C**, one would expect a large coupling constant. Using a Karplus relationship modified to include group electronegativity effects,¹⁹ the observed $J_{1,2}$ of 2.8 Hz for **167** gives a conformationally averaged dihedral angle of 118°. This compares well with the reported $J_{1,2}$ value of 3.0 Hz (119°) for deoxypicropodophyllotoxin.⁷⁵ Molecular mechanics calculations were performed on lactone **167**. In addition to the two boat conformations **C** and **D** (Figure 18), an intermediate chair conformation **E** was located (Figure 19). The relative energies are 0/0.60/1.01 kcal for conformations **C**, **E**, and **D** respectively. Fractional populations calculated from the Boltzmann distribution suggested that the major conformer should be **C** (65%). The minor conformers **E** and **D** had fractional populations of 23% and 12% respectively. The conformationally averaged coupling constants were calculated by

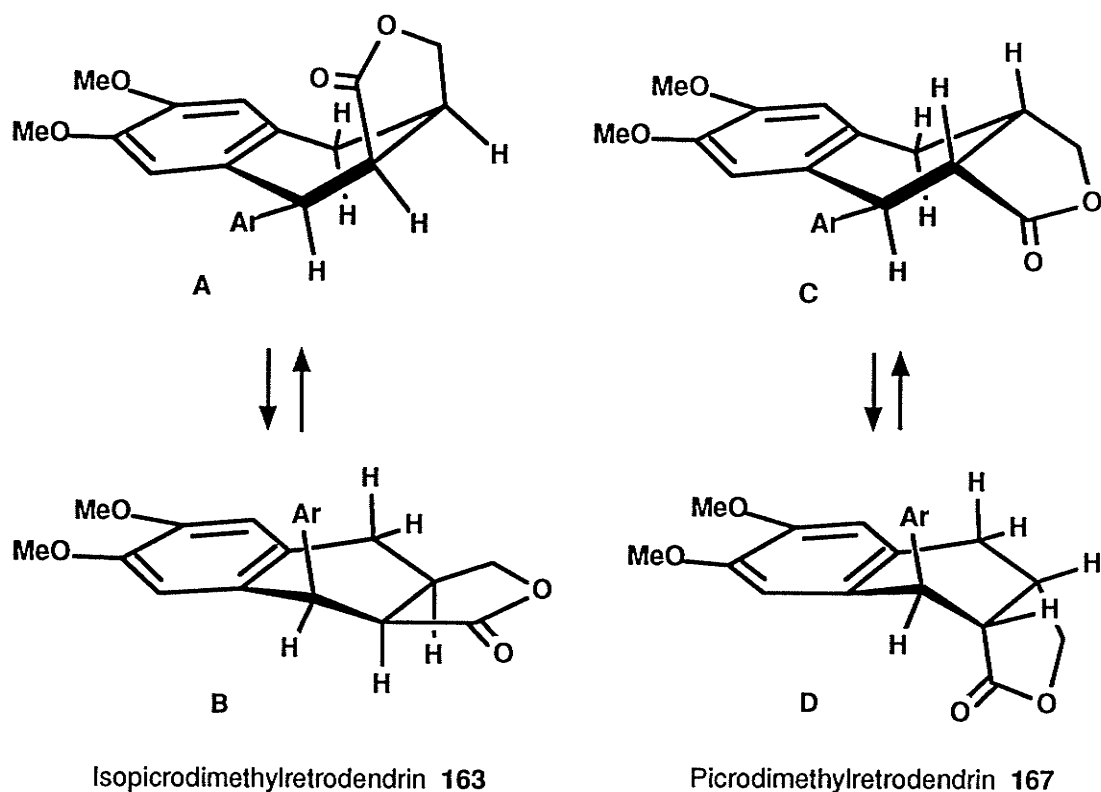


Figure 18. Proposed conformations of the 2,3-*cis* lactones.

weighting the coupling constants calculated for each individual conformation (modified Karplus).¹⁰⁰ The coupling constants and dihedral angles calculated for each conformation are given in Table 8. A comparison of the weight averaged couplings with the observed couplings show large discrepancies for $J_{1,2}$ (2.8 vs 6.2) and $J_{3,4\beta}$ (6.5 vs 10.9). It is expected that these coupling constants will most accurately reflect the conformation of the six-membered ring. The $H_{2,3}$ is expected to be relatively insensitive to conformation as the *cis*-fusion in the lactone ring keeps these protons eclipsed in both **C** and **D**. A slight decrease of the coupling would be observed if conformation **E** becomes moderately populated. The $J_{3,11\alpha}$ and $J_{3,11\beta}$ values do not faithfully reflect the conformation of the tetralin ring as torsional changes within the lactone ring alone will affect their values.

Given the inability of the force field calculations to predict the relative conformational energies, the population of each conformer was determined by appropriately weighting the calculated coupling constants of each low energy

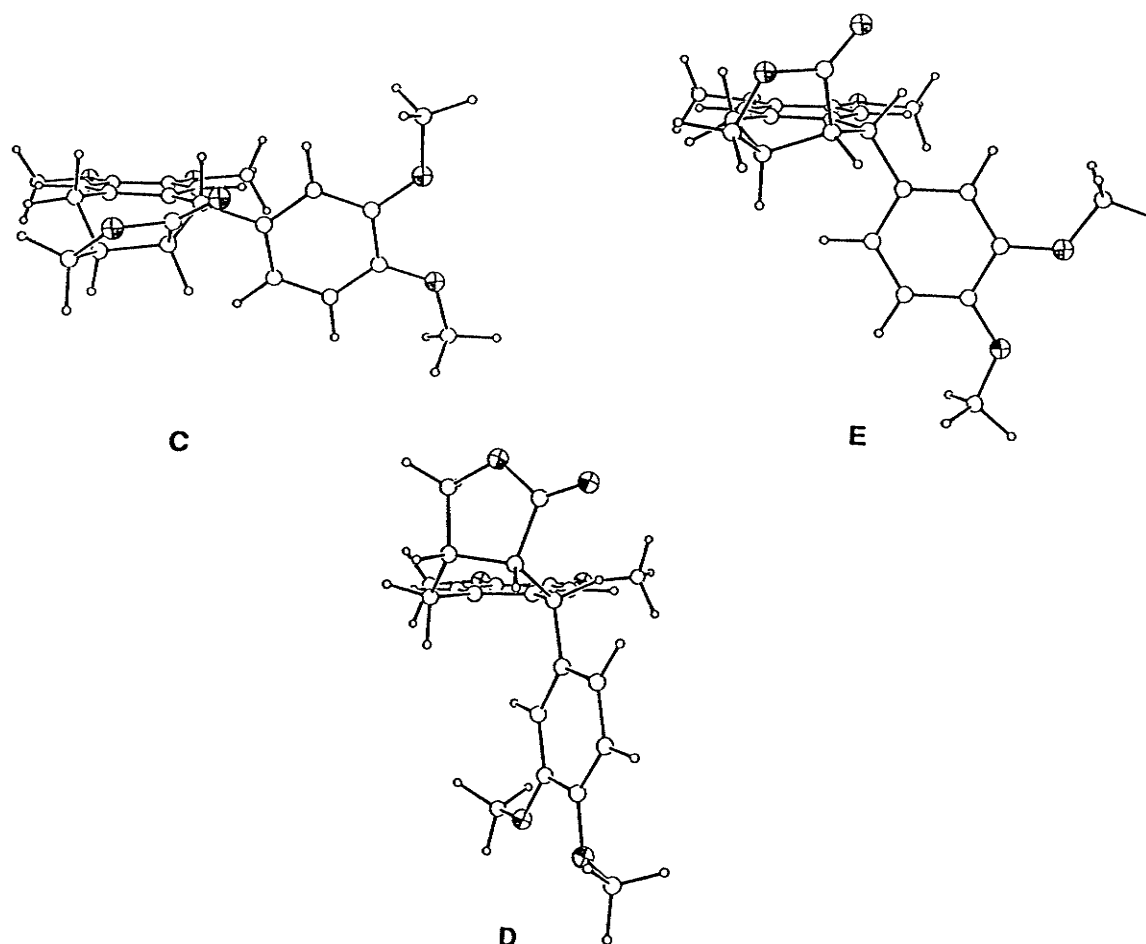


Figure 19. Calculated conformations of the flexible 1,2-trans-2,3-cis lactone (167)

Table 8. Calculated coupling constants for conformers C, E, D (167)

(J)	Obs.	Calc (θ)			Weighted Average
		C	E	D	
1,2	2.8	9.35(146)	0.32(88)	0.38(91)	6.19
2,3	9.6	8.59(28)	5.19(46)	10.37(15)	8.02
3,4 α	5.1	3.45(58)	5.66(44)	3.79(54)	4.00
3,4 β	6.5	12.35(177)	11.36(161)	2.52(63)	10.94
3,11 α	7.4	6.58(27)	4.67(40)	9.01(24)	6.43
3,11 β	3.4	1.91(98)	1.02(86)	10.2(130)	2.70

conformation obtained from the force field calculations. A series of linear equations (coefficients *c*, *e*, and *d* represent fractional populations of conformations *C*, *E*, and *D*) were constructed using the observed couplings and the weighted couplings determined using a Karplus equation. Only those couplings which faithfully represented the

$$1. J_{1,2}(\text{obs}) = 9.35c + 0.32e + 0.38d$$

$$2. J_{2,3}(\text{obs}) = 8.95c + 5.19e + 10.4d$$

$$3. J_{3,4\alpha}(\text{obs}) = 3.45c + 5.66e + 3.79d$$

$$4. J_{3,4\beta}(\text{obs}) = 12.4c + 11.4e + 2.52d$$

conformation of the tetralin ring were chosen (see above). Using the method of least squares, the best fit parameters of equations 1 to 4 were determined by minimizing the function given by equation 5.¹¹² The normalized best values of the coefficients in

$$5. \sum (J_{\text{obs}} - J_{\text{calc}})^2$$

equations 1-4 are given in Table 9. The calculated and observed couplings (Table 9) are in good agreement (rms deviation = 0.33 Hz). For comparison, equations 1, 3, and 4 were

	$\Sigma(J_{\text{obs}} - J_{\text{calc}})^2$	Exact soln. (eqns. 1,3,4)	Boltzmann (MM2 energies)
$J_{1,2}$	2.33	2.10	6.19
$J_{2,3}$	9.05	9.75	8.02
$J_{3,4}$	4.05	3.82	4.00
$J_{3,4\beta}$	6.24	4.61	10.9
<i>c</i>	0.22	0.19	0.65
<i>e</i>	0.18	0.05	0.23
<i>d</i>	0.60	0.76	0.12
rms deviation (Hz)	0.33	0.60	1.47

Table 9. A comparison of the calculated coupling constants for 167.

solved exactly and the coefficients normalized to unity. The agreement between the calculated and observed couplings by the latter method is not as good (rms deviation =

0.60 Hz). The populations of **C**, **D**, and **E** calculated from the exact solution of equations 1, 3, and 4 were 19%, 76%, and 5% respectively.

The preponderance of conformers **D** (60%) and **E** (18%), which have the aryl group axially disposed, over conformation **C** (22%) which has an equatorial aryl group, is in accord with the chemical shift correlation shown in Figure 17. The preference for the axial aryl group was also verified from NOE difference experiments (Table 10).

Irradiation of $H_{6'}$ gave an NOE of 1.4% to $H_{4\alpha}$. Similarly, the fact that irradiation of $H_{4\beta}$ and $H_{4\alpha}$ gave NOE's of 7.2 and 4% to H_5 respectively suggests that $H_{4\beta}$ (conformer **D**) occupies the equatorial position to a greater extent than $H_{4\alpha}$ (conformer **C**). The presence of conformer **C** was verified by the small observable NOE (0.9%) to H_1 when $H_{4\beta}$ was irradiated. In **C**, the H_1 and H_4 protons are diaxial. It is interesting to note that while irradiation of H_1 gave an NOE to $H_{6'}$ (3.7), no NOE was observed to $H_{2'}$.

Table 10. NOE enhancements for (-)-isopicrodimethylretrodendrin (**167**).

		Observed NOE %enhancements										
		H_1	H_2	H_3	$H_{4\alpha}$	$H_{4\beta}$	H_5	H_8	$H_{2'}$	$H_{6'}$	$H_{11\alpha}$	$H_{11\beta}$
Irrad.	$H_{1,11\alpha}$		8.1*	6.7				11.0		3.7		31.2
	H_2	9.5		7.9					5.8	2.9		
	H_3											
	$H_{4\alpha}$					27.9	4			1.6		
	$H_{4\beta}$	0.9		2.8	25.6		7.2					5.9
	$H_{2'}$											
	$H_{6'}$	5.5	3.5		1.4							
	$H_{11\beta}$					3.2	1.4				26.8	

Picrodimethylretrodendrin **163**, which has the 1,2,3-*cis* relative stereochemistry, has some very unusual features in the 1H -NMR spectrum. The first is the large $\Delta 2'6'$ shift difference of 0.36 ppm (Table 6a) which suggests that the preferred conformation is one in which the aryl group has an axial orientation (Figure 17; conformer **163B**, Figure 18). In

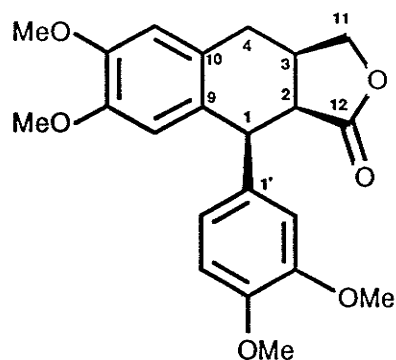
contrast, Rodrigo has proposed that the all-*cis* 4-oxy/deoxygenated lactones preferentially adopt conformations similar to **163A** on the basis of the conformation observed for 4-methoxyisopropodophyllin determined by X-ray analysis.⁷⁵ There is however, strong evidence supporting **163B** as the preferred conformation. Irradiation of the H_{4 α} proton resulted in observable NOE's of 3.6% and 7.7% to the *ortho* protons of the C4 aromatic ring (H_{2'} and H_{6'} respectively). NOE's of this magnitude could only arise if **163B** (Figure 18) is the dominant conformation in solution.

Table 11. NOE enhancements for (+)-picrodimethylretrodendrin (**163**).

		Observed NOE %enhancements										
		H ₁	H ₂	H ₃	H _{4α}	H _{4β}	H ₅	H ₈	H _{2'}	H _{6'}	H _{11α}	H _{11β}
Irrad.	H ₂	12.5										
	H _{4α}					27.5			3.6	7.7	8.5	
	H _{2'}	6.8										
	H _{6'}	4.7										
	H _{11β}			10.8							28.3	

The second unusual feature in the ¹H-NMR spectrum of **163** is the high field shift of the H_{11 α} (3.35 ppm) as compared with the H_{11 α} shifts of the other three lactones (3.92-3.99 ppm). The H_{11 β} proton at 4.38 ppm resides near the shift region of the other H_{11 β} protons (4.44-4.53). The chemical shifts of these two protons can be compared to the 2-methyl derivative of deoxyisopropodophyllotoxin (3.27 and 4.25 ppm) which was shown from X-ray analysis to adopt a conformation similar to **163B** (to be discussed later).²¹

Molecular mechanics calculations were carried out on **163** with the starting conformation given by **163A** (Figure 18, E = 47.5 kcal). By driving the C9C1C2C12 dihedral (ω_A) in steps, with geometry optimization at each step, it was possible to generate an intermediate conformer **F** (E = 46.8 kcal) which was conformationally



Torsional angle numbering scheme.

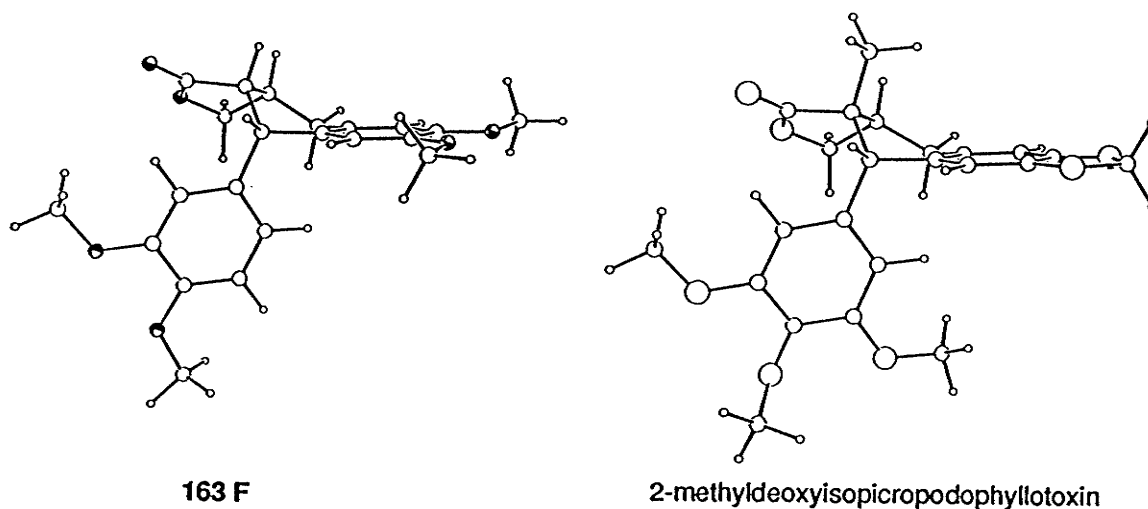


Figure 20. Comparison of the preferred conformations of 2-methyldeoxyisopicropodophyllotoxin (right)[†] and **163F** (left). [†]Facsimile generated using PCMODEL.^{21,100} identical to 2-methyldeoxyisopicropodophyllotoxin (Figure 20).²¹ Continued driving of this torsion angle yielded conformation **B** ($E = 47.2$ kcal). By starting at **A** and driving the C10C4C3C11 torsion angle (ω_B), it was possible to generate the half-chair conformation **G** ($E = 46.9$ kcal). Thus a total of four conformations were located (Figure 21). It was impossible to interconvert conformations **G** and **B** by driving either of these torsion angles. This interconversion could be achieved by driving the torsion angle in the lactone ring which interconnects it with the tetralin ring (C12C2C3C11 or ω_C). The conformational potential energy surface of **163** could be generated by alternately driving (5° increments) the ω_A and ω_C torsion angles over the ranges of -50° to -180° and -30° to 40° respectively. All four conformations were located on the contour map and are

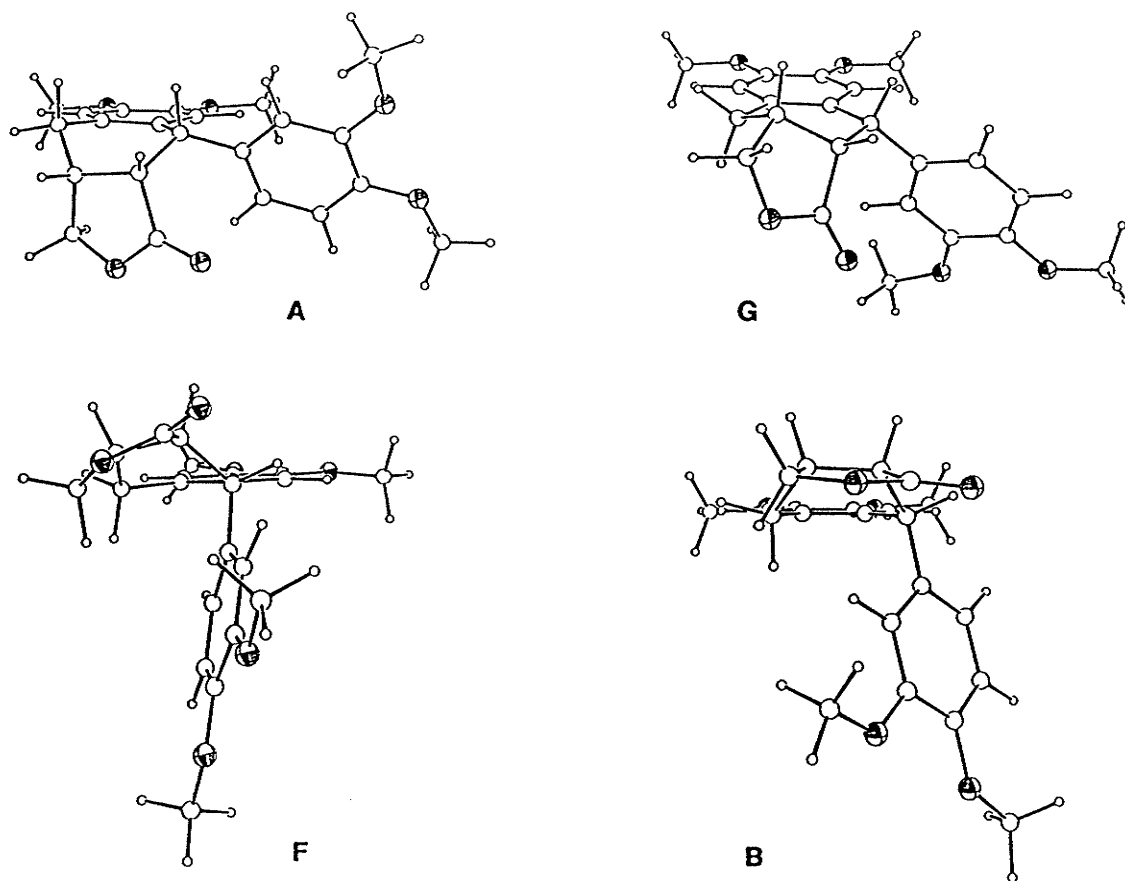


Figure 21. ORTEP diagrams representing the four lowest energy conformations of 163. displayed in Figure 22. Examination of the energy surface reveals a large hill in the central portion of the map. The presence of this potential summit accounts for the inability of driving a single torsion angle to achieve the remaining three conformations when starting from any single conformation. For example, to achieve **G** from **B** by driving the ω_A angle would require the concomitant change of the ω_C torsion angle along a path other than the lowest energy path. In theory, conformational interconversion will always follow the lowest energy pathway in accord with the principle of microscopic reversibility. If we start at **A** and drive along the ω_A torsion angle, the path taken to **B** follows along the front of the hill. Driving the ω_B torsion from **A** must therefore follow along the back of the hill arriving at **G** since **F** and **B** are not intermediates along the path to **G**.

Based on the calculated energies, conformation **F** is predicted to be the dominant

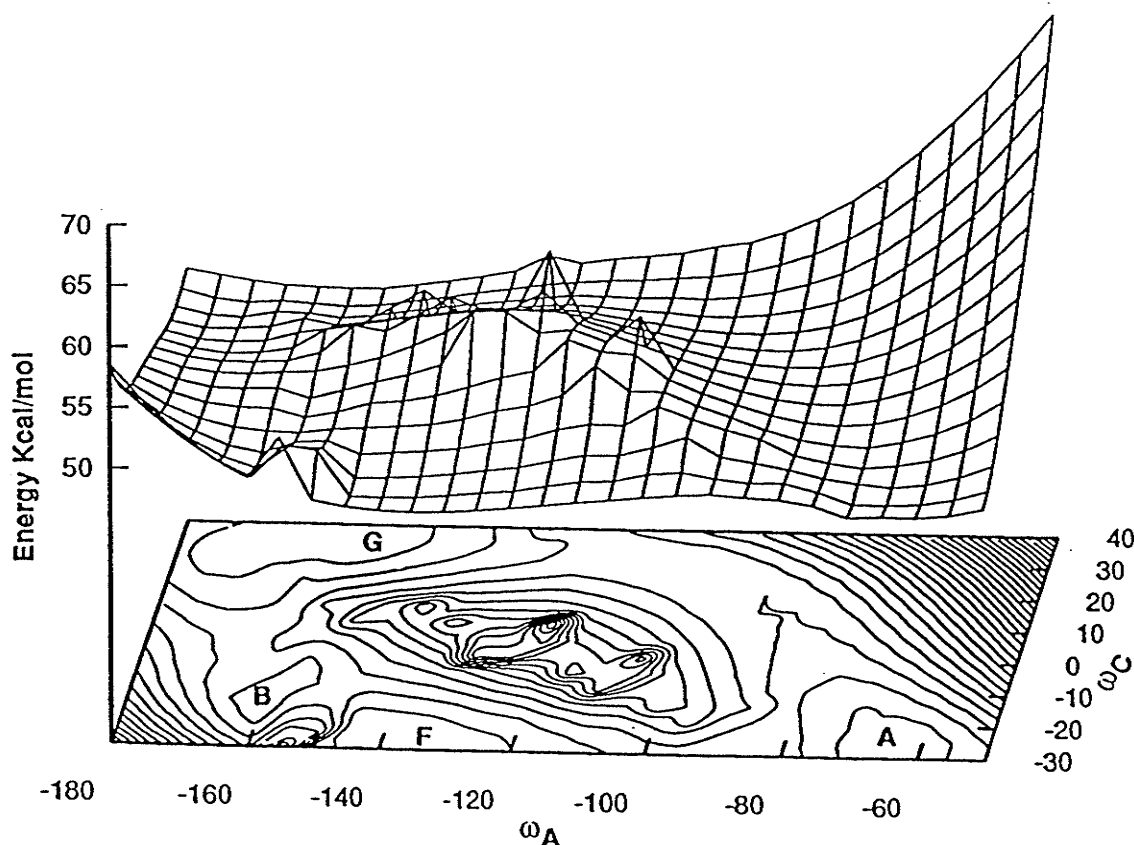


Figure 22. Potential energy surface for **163** showing the four lowest energy conformations.

one and is consonant with that found from NOE experiments. The high field shift of $H11_{\alpha}$ can be explained on the basis of a preponderance of this conformation. Examination of the geometry of **F** reveals that the $H11_{\alpha}$ proton lies in the shielding plane of the pendant aromatic ring (Figure 20, 21).

The rotational motion of the aryl group in **163** was found to be correlated with the interconversion of the four conformations. For instance, rotation of the aryl group in **A** with concomitant geometry optimization of the rest of the molecule resulted in its conversion to conformer **B**. Rotation by 360° degrees did not reconvert **B** back to **A** but instead converted it to **F**. It was found that both **B** and **F** were interconvertible by rotation of the aryl group. In conformer **B**, the *ortho* proton of the aryl group lies under the lactone ring and forces it to adopt a planar conformation. The four-fold rotational barrier of the aryl group in **163** is shown in Figure 23.

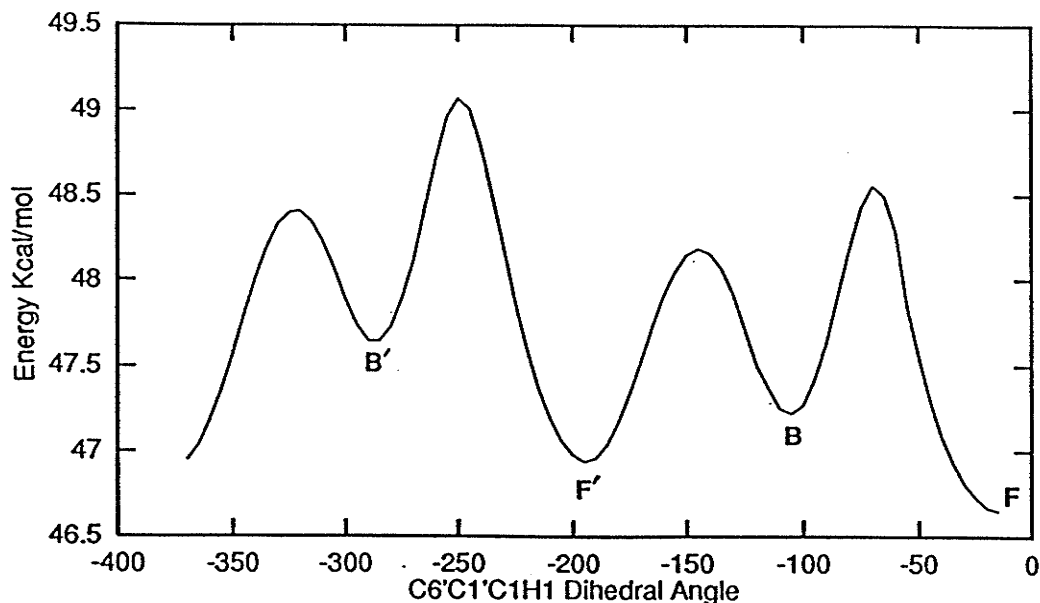


Figure 23. Rotation of the C1-aryl group showing the interconversion of **163B** and **163F**

Some discussion of biological activity with respect to conformation is warranted. Beard *et al.*²¹ have shown that the *trans* lactone ring is not an absolute requirement for antitumor activity as evidenced by the modest activity of the 1,2,3-*cis* derivatives 2-methylisopicropodophyllotoxin and 2-phenyldeoxyisopicropodophyllotoxin **9**. The activity of the former compound is likely attributable to its conformational similarity with podophyllotoxin in that the aryl ring has an axial disposition (Figure 20). One might expect that **163** would also show a similar level of activity given its conformational similarity with 2-methyldeoxyisopicropodophyllotoxin.

A structure-activity disparity exists for **9** in that it is known to adopt a conformation similar to **163A** (as shown in Scheme 1.4) in both solution and the solid state.²¹ Picropodophyllotoxin, the C2 epimer of podophyllotoxin has a preferred conformation similar to **167C**. The residual antitumor activity possessed by picropodophyllotoxin is believed to arise from the minor conformation which has an axial aryl group. Deoxypicropodophyllotoxin is about an order of magnitude more cytotoxic than picropodophyllotoxin.⁶ This is reasonable given that **167**, and thus

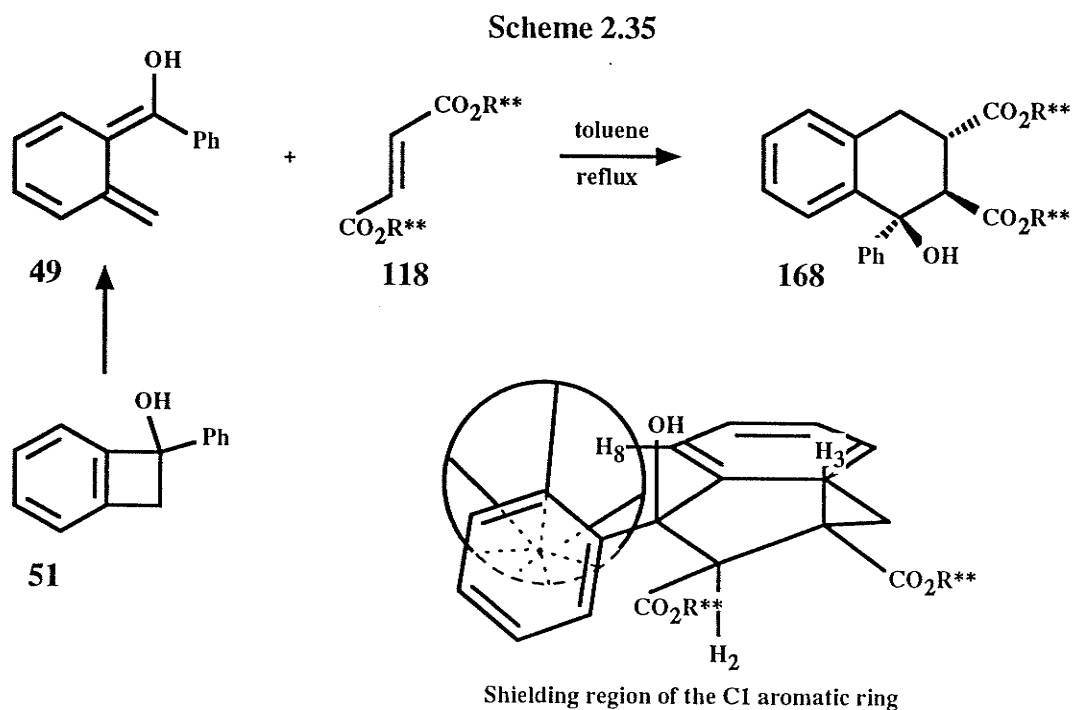
deoxypicropodophyllotoxin, possess an axial aryl group in the preferred conformation.

In conclusion, a general asymmetric method for the synthesis of deoxygenated lignans of all possible stereochemistries has been carried out. The conversion of deoxypodophyllotoxin to podophyllotoxin has been previously accomplished by bromination of the benzylic position (NBS) and hydrolysis in the presence of silica gel.¹⁰⁸ Thus it should be possible to hydroxylate the deoxypodophyllotoxin analogue **166** using the same method and therefore enable comparison of its antitumor activity with podophyllotoxin. By changing the chiral auxiliary from methyl (R)-mandelate to methyl (S)-mandelate, it would also be possible to synthesize all of the corresponding enantiomers. If desired, this would allow one to explore the effects of the absolute chirality on the global biological activity; including toxic side effects.

2.3 Stereoselective Addition of α -Hydroxy- α -phenyl-*o*-QDM to the Fumarate of Methyl Mandelate.

The previous section dealt with the addition of the fumarate of methyl (R)-mandelate **118** to α -hydroxy- α' -aryl-*o*-QDM **136** and the application of this reaction to the synthesis of aryltetralin lignans. In this section, the addition of the same fumarate to the isomeric α -hydroxy- α -aryl-*o*-QDM shall be discussed in terms of its diastereoselectivity and its potential application in the synthesis of aryltetralin lignans.

It was initially shown by Koh¹¹⁴ that the addition of orthoquinodimethane **49**, generated from the thermolysis of benzocyclobutenol **51**, to fumarate **118** gave a single cycloadduct (Scheme 2.35). Thus, cycloadduct **168** was made in 50% isolated yield by heating dimandylfumarate **118** and benzocyclobutenol **51** at 110°C in toluene. No signals consistent with the presence of other cycloadducts could be detected in the ¹H-NMR of the crude product.¹¹⁴



In this work, benzocyclobutenol **51** was made by the addition of phenyllithium to benzocyclobutenone in 75% yield after chromatography (mp 61-62°C).

Benzocyclobutenone was readily available by oxidation of benzocyclobutenol **18** (pyridinium dichromate) in 92% yield. Refluxing a solution of 1-phenylbenzocyclobuten-1-ol **51** and the fumarate of methyl (R)-mandelate **118** afforded the crystalline cycloadduct **168** in 57% yield after recrystallization (ethyl acetate/hexanes).

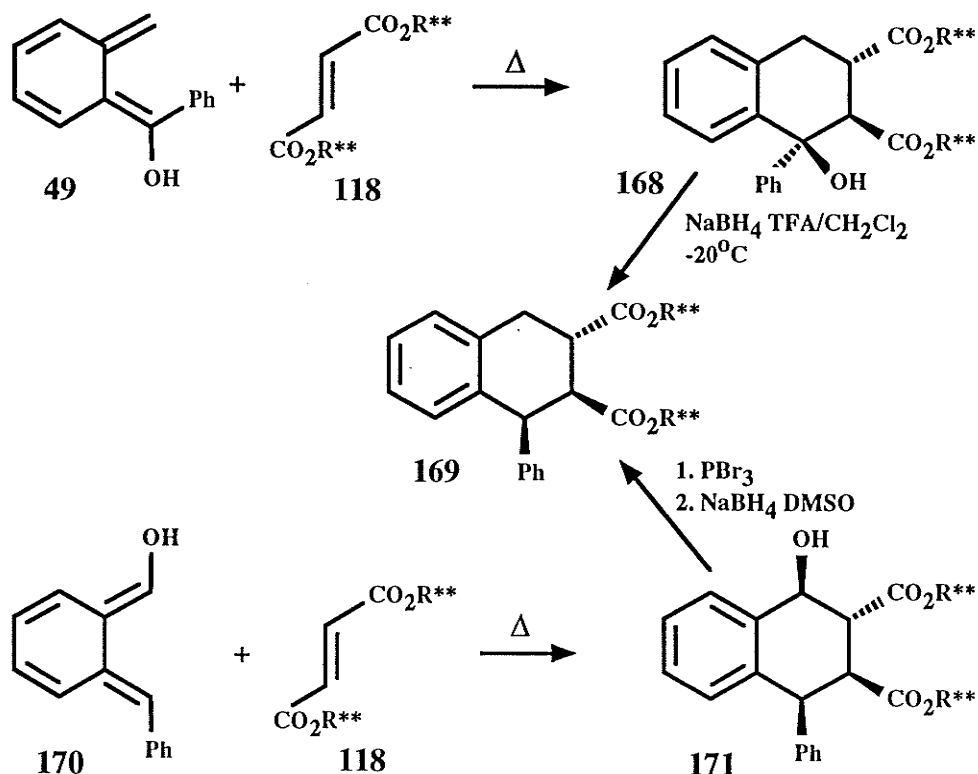
An aim of this work was to determine the absolute stereochemistry of the cycloadduct **168**. The relative stereochemistry of **168** was deduced from the $^1\text{H-NMR}$ spectrum. The H8 proton exhibited an upfield shift to 6.97 ppm which is indicative of an equatorial phenyl group.³⁵ The relative stereochemistry of the remaining ester groups at C2 and C3 were assigned based on the large diaxial $\text{H}_{2,3}$ and $\text{H}_{3,4a}$ coupling constants ($J_{2,3} = 9.32$, $J_{3,4a} = 12.7$).

The absolute stereochemistry of **168** was elucidated by chemical correlation. Removal of the C1-hydroxyl group was accomplished using a reducing mixture of NaBH_4 and TFA to give **169** (35% yield) in addition to a minor reduction product having the all-*trans* stereochemistry (Scheme 2.32). Although this latter product was not isolated and characterized, its presence was detected as a doublet (4.35 ppm, $J_{1,2} = 10$ Hz) in the $^1\text{H-NMR}$ spectrum of the crude reduction mixture.

The stereoinversion of the C1 center observed in the reduction of **168** to **169** is unprecedented. In the reduction of diarylmethanols using this method, it is believed that an intermediate cation is formed after the protonation of the hydroxyl group. Although the cation could not be detected via the formation of a coloured species typical of diaryl cations,¹¹⁵ its presence cannot be excluded. Perhaps the neighboring ester group directs the reducing agent preferentially to one face of the cation either by coordination to the reducing agent or the cation. Alternatively, the mechanism may involve a tightly ion-paired species that undergoes stereoinversion by virtue of stereoelectronic requirements of an $\text{S}_{\text{N}}2$ displacement mechanism.

To correlate the structure of **169** to a compound of known absolute stereochemistry, the cycloadduct from the reaction of α -hydroxy- α' -phenyl-*o*-QDM⁹⁴ **170** and fumarate⁹⁹ **118** (R-mandelate) was prepared. The absolute and relative stereochemistry of this cycloadduct **171** was assigned by analogy to previous examples.^{40,94,95,99} Cycloadduct **171** was converted to the bromide by treatment with PBr₃ followed by reduction with NaBH₄ in DMSO to give **169**. The H_{1,2} coupling of 5.53 Hz was indicative of a 1,2-*cis* geometry with the 1-phenyl group occupying an axial position. The equatorial nature of the 3-ester group was evident from the large diaxial coupling of the H₃ and H_{4a} protons (11.56 Hz). The conformation of **169** is virtually identical to the conformation of **164b** (see Scheme 2.32)).

Scheme 2.36



In determining the mode of addition (*endo* vs *exo*), one must know the geometry of the intermediate *o*-QDM **49**. The hydroxyl group was assigned to the *Z*-position on the basis of Houk's torquoselectivity rules.³⁸ The preference for outward movement of the

hydroxyl group upon thermolysis of **51** was corroborated by AM1 molecular orbital calculations¹⁰³ performed on the transition state (Figure 24). The ΔH^\ddagger for the outward rotation of the hydroxyl group had a calculated value of 32 kcal/mol while the inward rotation had a ΔH^\ddagger of 36 kcal.

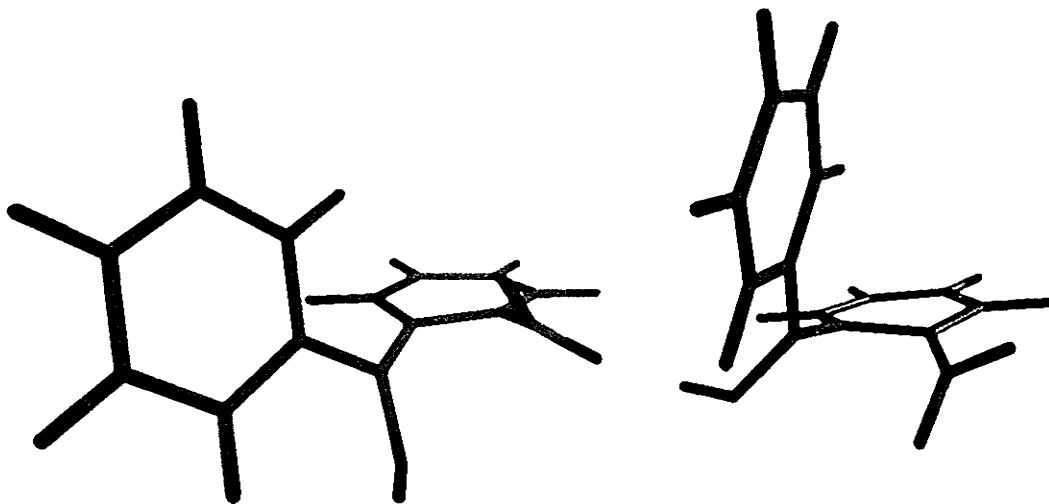
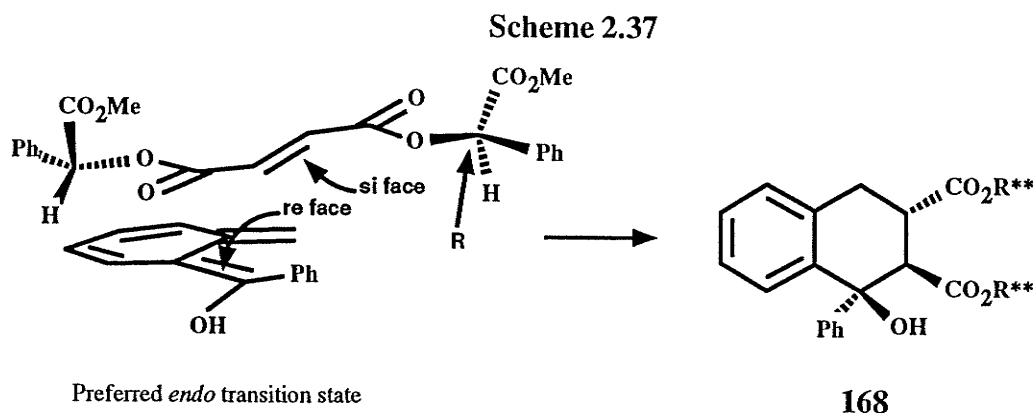


Figure 24. AM1 transition structures for the inward (left) and outward (right) ring opening of 1-hydroxy-1-phenylbenzocyclobutene

Assuming that the assignment of the absolute stereochemistry of the molecule was correct, the cycloadduct must have arisen from an *endo* transition state with addition of the *si* face of the dienophile to the *re* face of the *o*-QDM (Scheme 2.37). In section 2.1, it was noted that hydrogen bonding in the *endo* transition state was sterically impossible. For the addition of *o*-QDM **49** to fumarate **118**, hydrogen bonding cannot be controlling the diastereoselectivity. Discrimination against the *exo* transition state might arise from a large steric interaction between the inwardly turned phenyl group of the *o*-QDM and the dienophile. Given the absence of a hydrogen bond in the transition state, the dienophile would likely adopt the *transoid* conformation shown above. Assuming a *s-trans*



conformation for **118**, the addition of **49** to the *si* of **118** may then be explained by Helmchen's model.⁶¹

The NaBH₄/TFA mixture used for the removal of the hydroxyl group in the cycloadduct arising from the stereoselective addition of α -hydroxy- α -phenyl-*o*-QDM to dimandyl fumarate was initially used as an expedient in the elucidation of the absolute stereochemistry. Intermediates like **169**, generated using this reduction method, may also serve as useful precursors for the synthesis of aryltetralin lignans.

The reduction of diarylmethanols with NaBH₄ in acidic media (TFA or glacial AcOH) employs one of three methodologies:¹¹⁶

1. Addition of NaBH₄ to a solution of the substrate in neat carboxylic acid.
2. Dropwise addition of the acid to a mixture of the substrate and NaBH₄ in a suitable solvent like THF.
3. Addition of the substrate, neat or in the presence of a cosolvent, to a mixture of NaBH₄ and the acid.

Initial attempts at the reduction of **168** to **169** using method 3 gave non-reproducible results with mixtures of the desired and elimination products (Table 12).

The use of polar cosolvents such as THF, DME, isopropanol or ethanol resulted in the exclusive elimination of water from **168** to give **172** (Scheme 2.38). When TFA was replaced by AcOH or if a mixture of TFA and AcOH were used only starting material was recovered. It has been reported that the reduction of diarylmethanols and triarylmethanols

Table 12. Sodium Borohydride/Trifluoroacetic acid reduction of 168.

Temp °C	Catalyst	Reaction solvent	Addition solvent	Red.	Elim.	S.M	Time min
-20	BF ₃	1:1 BF ₃ /CH ₂ Cl ₂	CH ₂ Cl ₂	10	80	10	20
-10	AcOH	AcOH	CH ₂ Cl ₂			100	40
-78	TFA	1:1 TFA/CH ₂ Cl ₂	CH ₂ Cl ₂	18	82		120
-20	TFA	1:1 TFA/DME	4:1 DME/CH ₂ Cl ₂		71	29	5
-10	TFA	TFA	CH ₂ Cl ₂	31	69		60
25	TFA	TFA	CH ₂ Cl ₂	3	97		180
-20	TFA	TFA 1.61 H ⁺ :H ⁻ ; 860 H ⁻ eq.	CH ₂ Cl ₂	68 [*]	32		100
-10	TFA	TFA	CH ₂ Cl ₂	45 [†]	55		23
-10	TFA	isopropanol	isopropanol		100 [‡]		44
-10	TFA	ethanol	ethanol		100 [‡]		42
-20	TFA	TFA 1.12 H ⁺ :H ⁻ ; 2500 H ⁻ eq.	CH ₂ Cl ₂	88 [#]	12		19
-20	TFA	THF	THF		100		20
0	TFA	TFA	CH ₂ Cl ₂	45 [°]	55		10
0	TFA	AcOH	1:1 AcOH/CH ₂ Cl ₂			100	30
-78	TFA	TFA/AcOH/CH ₂ Cl ₂ 0.96 H ⁺ :H ⁻ ; 2660 H ⁻ eq.	CH ₂ Cl ₂			100	30

Red. (reduction), Elim (elimination), S.M. (starting material), AcOH (acetic acid)

THF (tetrahydrofuran), TFA (trifluoroacetic acid), DME (1,2-dimethoxyethane)

* 4.7:1 cis/trans ratio

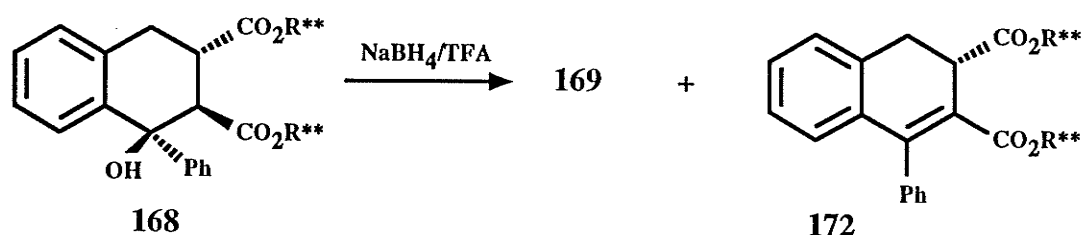
† 5.3:1 cis/trans ratio

‡ inverse addition of TFA to NaBH₄/alcohol/isopropanol over four minutes

° 4.2:1 cis/trans ratio

5.2:1 cis/trans ratio

Scheme 2.38



with NaBH_4 in AcOH is slow or fails completely.^{109,115} When BF_3 -etherate was employed as a catalyst, only 10% reduction was observed, the remaining material being the starting alcohol and the alkene **172**. It is evident that temperatures around -20°C are necessary to prevent elimination. At -78°C the solution freezes out and may impede the mixing of the reducing mixture and the alcohol solution. When 860 hydride equivalents were used ($1.61\text{H}^+:\text{H}^-$) 68% reduction (32% elimination) was observed. The amount of reduction increased to 88% when 2500 hydride equivalents were used although the H^+ to H^- ratio was slightly lower ($1.12\text{H}^+:\text{H}^-$). In order to determine the best conditions for the reduction, a series of reactions were performed in which the total amount of alcohol (4.2 mmol in CH_2Cl_2) and NaBH_4 (2450 H^- mole equivalents) were held constant and the ratio of TFA and NaBH_4 (H^+/H^-) varied from 10 mole % H^+ to 75 mole% H^- . A typical experiment involved the addition of powdered NaBH_4 to a cooled solution of TFA (-23°C ; $\text{CCl}_4/\text{dry ice}$). It was necessary to keep the system under a stream of nitrogen in order to prevent the buildup of hydrogen gas. After precisely 10 seconds, when the effervescing had subsided, a solution of **168** in CH_2Cl_2 was added to the vigorously stirred mixture of TFA and NaBH_4 . The total reaction time was kept constant for each experiment (37 minutes). A plot of the mole fraction of reduction product as a percentage of the total material against the mole fraction of NaBH_4 (in terms of H^-) is shown in Figure 25. The optimum yield for reduction occurs in the range of 25-35 mole% hydride. When the hydride mole fraction is increased beyond about 50%, substantial amounts of starting material begin to appear. The intersection of the two curves reveals that only starting material is recovered beyond 80 mole % hydride.

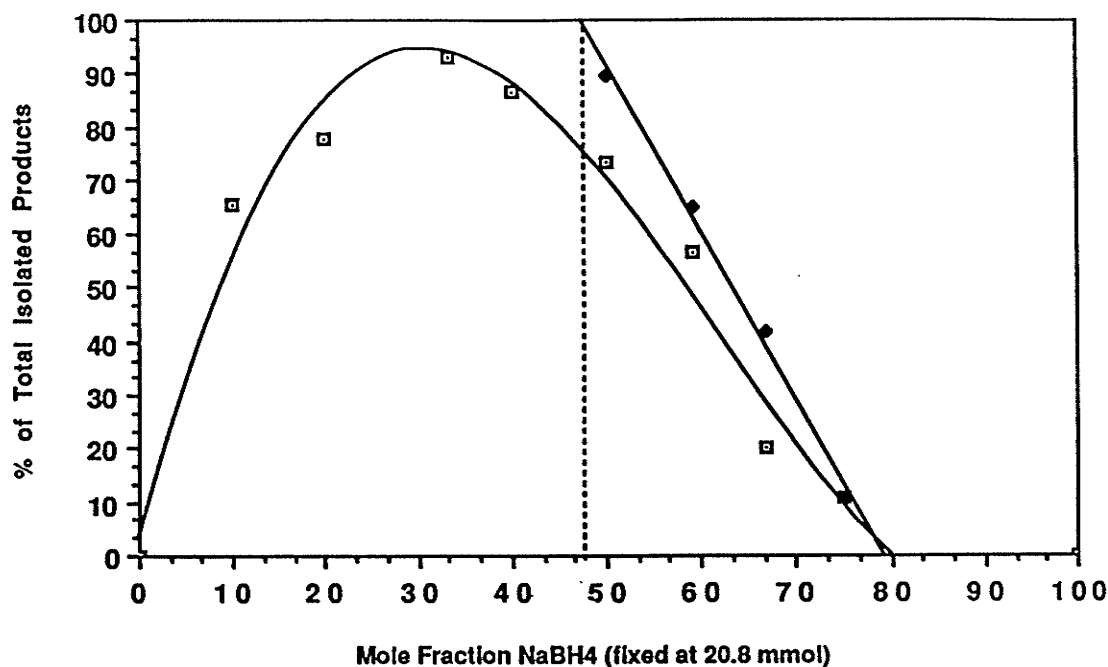
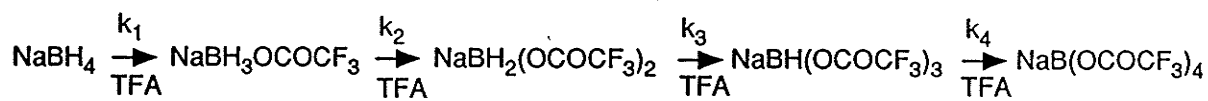


Figure 25. Optimization of the reduction of **181** in NaBH₄/TFA. The area under the curve represents the total amount of reduction product while that between the curves represents the % elimination. The area to the right of the straight line represents starting material.

The addition of TFA to NaBH₄ results in the rapid replacement of a hydride by a trifluoroacetoxy group giving a monotrifluoroacetoxyborohydride species.¹¹⁵ Continued addition of TFA results in the sequential replacement of the hydride groups by acetoxy



groups with each subsequent species being a weaker reducing reagent due to electron withdrawing effects of the trifluoroacetate group as well as the increased steric demand.

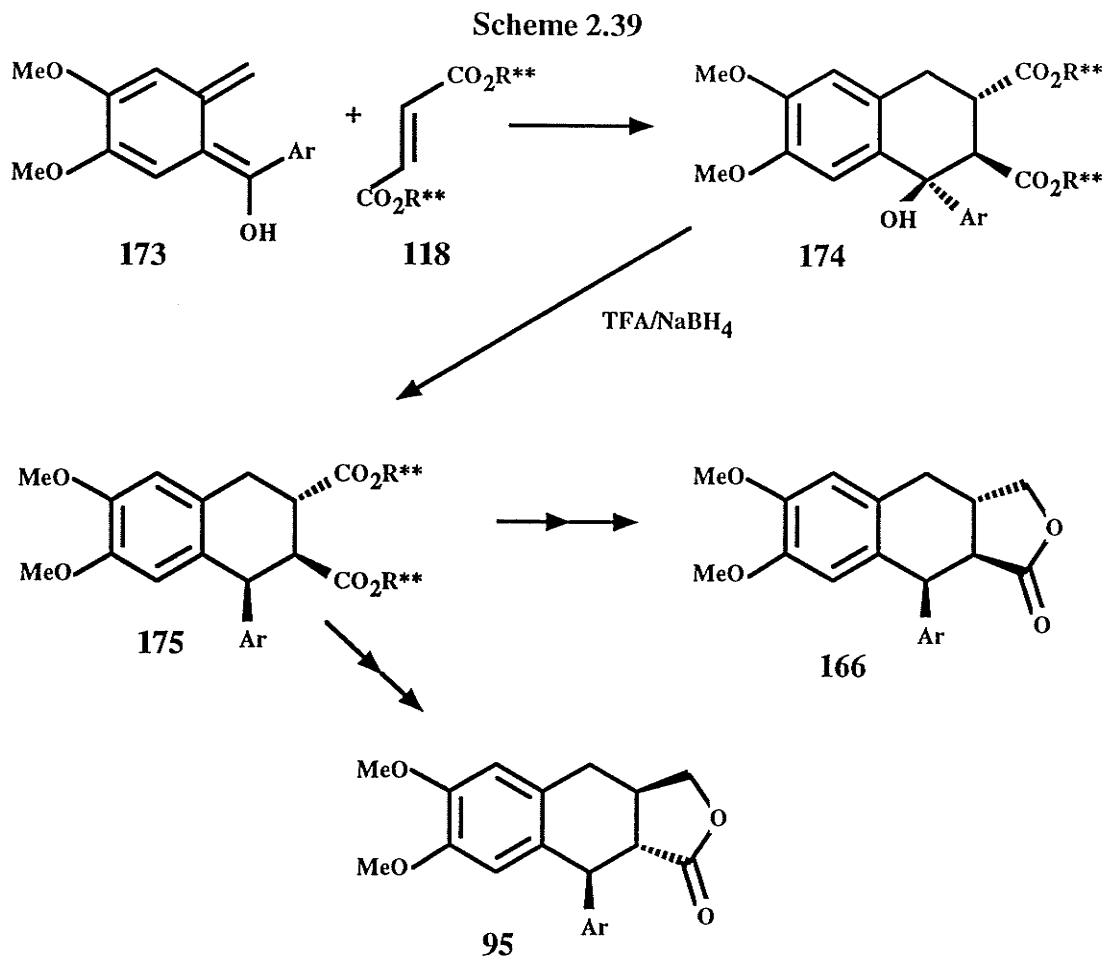
At the optimum ratio for reduction (25-35 mole% H⁻) one would expect all of the hydrides to be consumed so that NaB(OCOCF₃)₄ would be the dominant species in solution. Even at 10 mole%, 65% reduction was observed. The value of k₄ at -23°C is obviously much smaller than the rate constant for reduction of **168** by NaBH(OCOCF₃)₃. The increase in the amount of elimination product at high TFA concentrations may be due simple dilution effects or to an increase in rate of formation of NaB(OCOCF₃)₄. It is of

great interest to note that at concentrations of about 50 mole% H^- one begins to see the appearance of starting material even though an enormous excess of reducing agent is present (2450 H^- equivalents). At about the same concentration of NaBH_4 , the solution becomes solid. The main reducing agent between 50 and 56 mole% is $\text{NaBH}(\text{OCOCF}_3)_3$, and given the fact that k_4 must be relatively slow, there will always be adventitious TFA to catalyze the cation formation. Perhaps, when the solution becomes solid, only the trifluoroacetyloxyborohydride derivative is soluble in methylene chloride so that it is the only reducing species in solution. As the mole fraction of NaBH_4 is increased, the amount of $\text{NaBH}(\text{OCOCF}_3)_3$ decreases continually until finally all of the reducing agent is either $\text{NaBH}_3(\text{OCOCF}_3)$ or NaBH_4 .

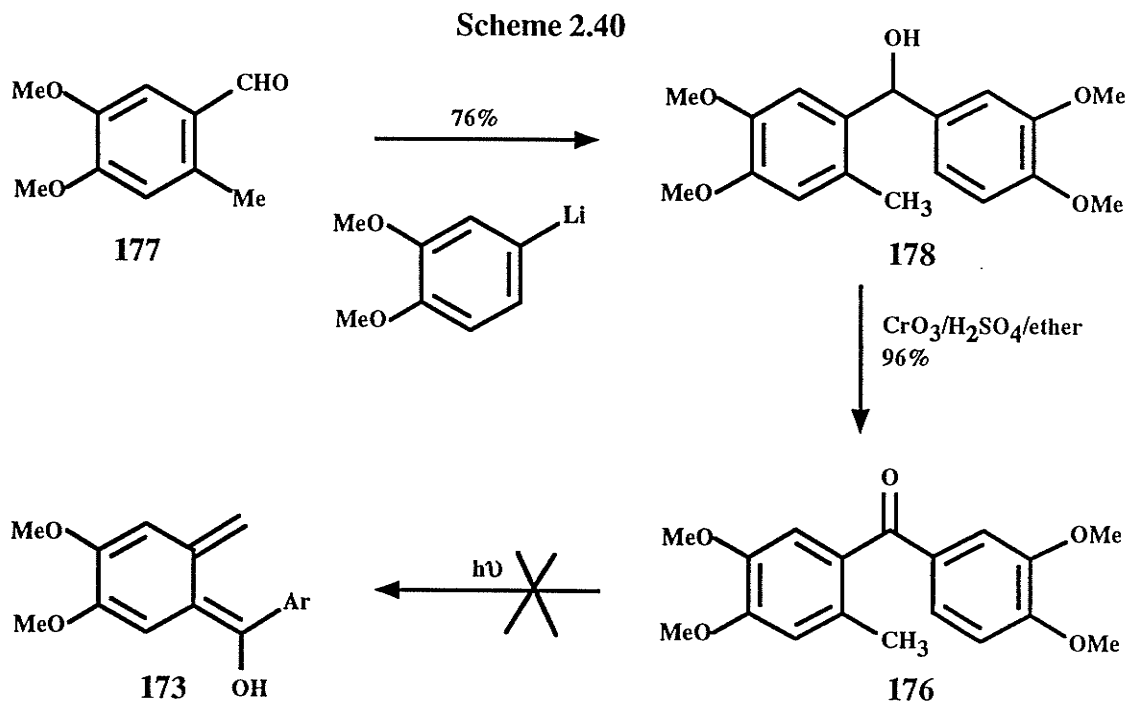
Alkenes that can form resonance-stabilized cations upon protonation by acid have also been reduced using the NaBH_4/TFA mixture. For instance 1,1-diphenylethene can be reduced to 1,1-diphenylethane in high yield¹⁰⁹ yet the alkene **172** is a side product in reduction of **168** to **169**. It is conceivable that elimination of the alcohol to the alkene actually preceded the reduction of the cation and its presence in the product mixture was simply a result of incomplete reduction. To test if the alkene was an intermediate in the reduction, the alcohol **168** was treated with neat TFA to give the alkene **172** in quantitative yield. Treatment of **172** with NaBH_4/TFA at 0°C in CH_2Cl_2 produced no trace of the reduction product. Apparently TFA is not a strong enough acid to protonate the alkene which is inherently electrophilic due to conjugation with the ester group.

With the optimized conditions for the reduction cycloadduct **168** in hand, it was hoped that these same conditions could be used to reduce 1-hydroxy-1-aryl cycloadducts bearing oxygenation in the aromatic rings. Thus the addition of α -hydroxy- α -aryl-*o*-QDM **173** to the fumarate of methyl (R)-mandelate **118** should generate the cycloadduct **174** with the correct absolute stereochemistry for the synthesis of lignans like (-)- α -dimethylretrodendrin **95** and (+)-isodimethylretrodendrin **166** (Scheme 2.39).

It was hoped that *o*-QDM **173** would be available via the photolysis of



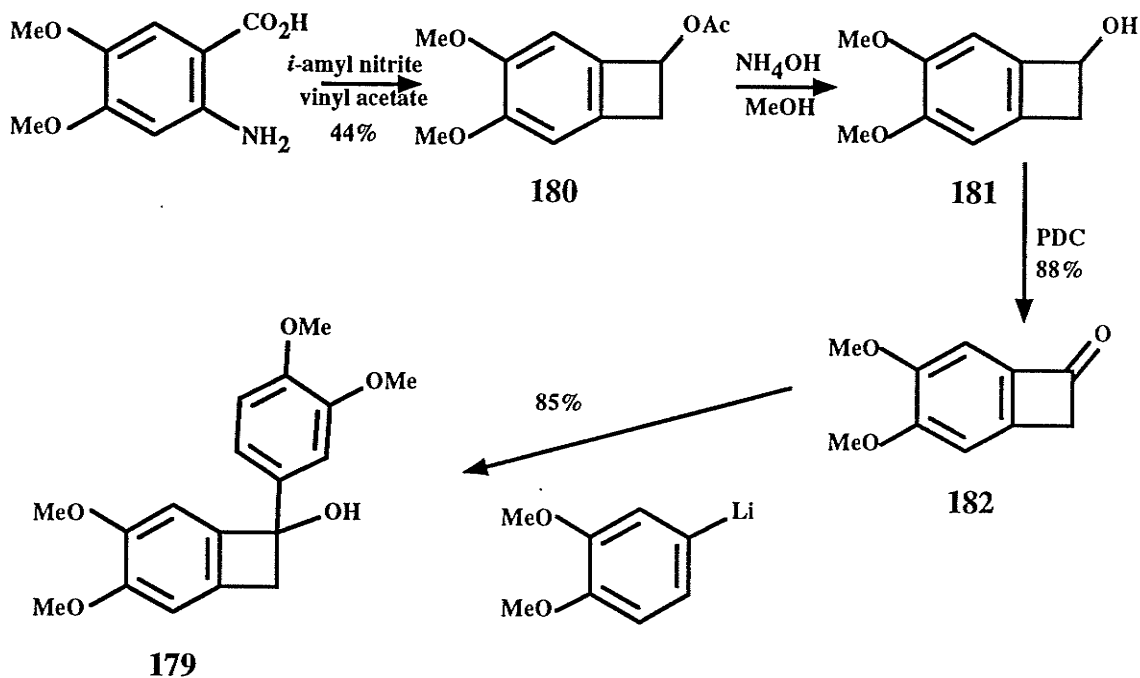
benzophenone **176** analogous to photolysis of benzophenone **58** carried out by Kraus (Scheme 2.40).⁴⁸ The synthesis of **176** started from 2-methyl-4,5-dimethoxybenzaldehyde **177**.¹¹⁷ Addition of a slight excess of *n*-BuLi (1.1 molar equiv.) to a solution of 4-bromoveratrole in THF at -78°C generated the intermediate aryllithium which was subsequently treated with a solution of **177** in THF to give alcohol **178** in 76% yield (IR: 3598, 3513 cm⁻¹) after chromatography on silica (20-30% ethyl acetate/hexanes). The alcohol was oxidized with chromium trioxide (0.5 M CrO₃ in 10% H₂SO₄/H₂O) in ether to give benzophenone **176** in 96% yield after chromatography (IR (CH₂Cl₂): 1653 cm⁻¹; mp 121-122°C). Irradiation of **176** in a benzene solution of fumarate **118** produced no trace of cycloadduct **174** even after 2 hours nor could the presence of any benzocyclobutenol be detected in the ¹H-NMR of the crude product. It was noted by Saá that irradiation of



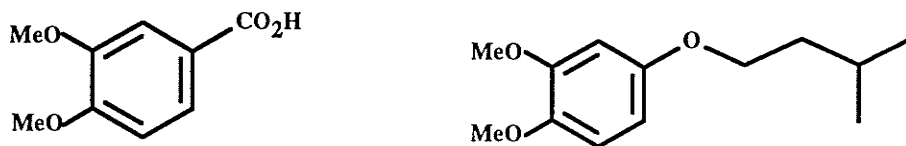
benzene solutions of various substituted benzophenones had slower reaction times and lower yields of benzocyclobutenols than did THF solutions of the same benzophenones.^{44,46} However, irradiation of **176** in THF for 2.5 hours gave none of the desired benzocyclobutenol **179**.

Generation of the requisite *o*-QDM **173** via thermolysis of benzocyclobutenol **179** was next considered (Scheme 2.41). Benzocyclobutenol **181** has been synthesized from acetate **180** which was in turn prepared by trapping the benzyne produced from diazotization of 2-amino-4,5-dimethoxybenzoic acid with isoamyl nitrite with vinyl acetate.¹¹⁷ Thus, refluxing a solution of 2-amino-4,5-dimethoxybenzoic acid in vinyl acetate/THF with 2 mole equivalents of isoamyl nitrite produced **180** in 44% yield. It was necessary to use either THF or 1,2-dimethoxyethane (DME) as a cosolvent as the anthranilic acid was insoluble in vinyl acetate alone. One of the minor products isolated from the reaction was 3,4-dimethoxybenzoic acid and another compound, which appeared from the ¹H-NMR to be the product resulting from the addition of isoamyl alcohol (by-product of the diazotization reaction) to the benzyne (Scheme 2.42). Alcohols are

Scheme 2.41

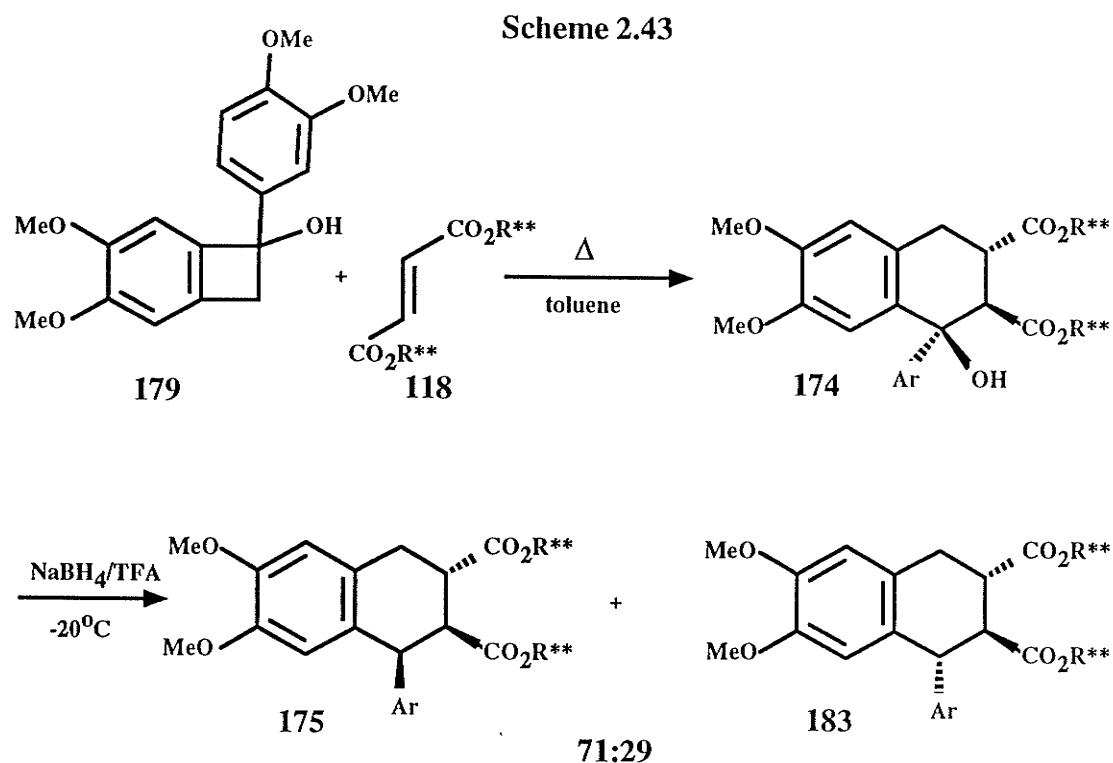


Scheme 2.42



known to readily undergo addition to benzyne.¹¹⁸ In an attempt to prevent this problem, *tert*-butyl nitrite was used to diazotize the anthranilic acid. It was hoped that the sterically bulkier *tert*-butyl alcohol would not add to the benzyne. Unfortunately, the use of *tert*-butyl nitrite made no improvement to the yield of acetate **180**. Acetate **180** was deacetylated by stirring in a 30% aqueous NH_4OH /methanol solution at room temperature to give alcohol **181**.¹¹⁷ Oxidation of **181** using PCC in methylene chloride gave low yields of the known ketone **182**¹²⁰ (55%) (Scheme 2.41). When pyridinium dichromate (PDC) was used, a reagent suitable for oxidation of acid sensitive compounds,¹¹⁹ alcohol **181** underwent clean oxidation to the ketone **182** in 88% yield. Addition of

3,4-dimethoxyphenyllithium to **182** at -78° gave benzocyclobutenol **179** in 85% yield. Thermolysis of **179** in refluxing toluene in the presence of (R)-dimandyl fumarate **118** gave cycloadduct **174** in 31% yield after chromatography on silica (Scheme 2.43). The $^1\text{H-NMR}$ spectrum of **174**, and therefore its absolute stereochemistry, was assigned on the basis of its similarity to cycloadduct **168**. The major cycloadduct was reduced at -23°C



using a mixture of NaBH_4 and TFA (33 mol% H^- , 220 H^- mole equivalents). Addition of a solution of the alcohol in methylene chloride to the NaBH_4/TFA mixture at -20°C resulted in the formation of a dark blue mixture. This blue colour, indicative of the formation of the dibenzylic cation, decolorized upon the addition of more NaBH_4 . $^1\text{H-NMR}$ analysis of the crude product showed the presence of two reduction products as indicated by the doublets at 4.56 ppm ($J = 5.48$; **175**) and 4.22 ppm ($J = 9.9$; **183**) in the ratio of 71:29 respectively. The major product was characterized completely and the minor product characterized by $^1\text{H-NMR}$ only.

The 71:29 (**175**:**183**) ratio obtained upon reduction of **174** represents a significant

decrease in the stereoselectivity (cf 83:17 1,2-*cis*:1,2-*trans* ratio for the reduction of **168**) for this reaction. Such a dramatic effect of the presence of the aromatic methoxyl groups on the stereoselectivity of reduction was unexpected. Perhaps there are two competing mechanisms whereby the reduction of the cationic species results in the formation of the thermodynamically more stable product (1,2-*trans*) and reduction of the ion-paired species results in the stereoinverted product (1,2-*cis*). The increase in the 1,2-*trans* product **183** may then be explained by an increase in the stability of the cation formed from **174**. The cation stability should increase with an increase in the electron donating ability of the aromatic rings.

It has been shown that the asymmetric cycloaddition of the fumarate of methyl (R)-mandelate to α -hydroxy- α -aryl-*o*-QDMs (**49** and **173**) resulted in the formation of essentially a single *endo* adduct arising from the addition of the *o*-QDM to one face (*si*) of the dienophile. It was possible to stereoselectively remove the hydroxyl group from the cycloadducts to give products having the thermodynamically less stable 1,2-*cis* stereochemistry (products **169** and **175**). These compounds have the same relative stereochemistry as podophyllotoxin. Although these compounds were not converted to lignan products like podophyllotoxin or α -dimethylretrodendrin, it is foreseeable that they could be converted to a variety of lignans with different relative stereochemistries. The remaining synthetic challenge embodies the manipulation of the stereochemistry at the two chiral centers bearing the ester groups together with the regiodifferentiation of the two ester groups to allow the formation of a lactone ring. Synthetic methodologies in the latter area are currently being pursued by others.¹²¹

Chapter 3

Conclusions

All of the research goals proposed at the outset of this thesis work have been achieved.

The mechanism of the stereoselective addition of α -hydroxy-substituted-*o*-quinodimethanes to methyl lactate and methyl mandelate substituted fumarates was elucidated. Overwhelming evidence suggests an intermolecular hydrogen bond in the transition state is responsible for the observed diastereoselectivity. The hydrogen bond controlled not only the *endo/exo* selectivity, but also the addition of the *o*-QDM to one face of the chiral dienophile. A similar intermolecular 9-membered ring hydrogen bonded Diels-Alder transition state has been observed by one other group. However, in Thorton's work on the addition of N-methylmaleimide to a diene bearing a hydroxyl group in the chiral auxiliary, only *endo* addition was observed, suggesting that secondary orbital interactions controlled the diastereoselectivity.^{70,71} In this work, the hydrogen bond was able to counteract the effects of secondary orbital interactions which normally facilitate *endo* addition. This has significant importance and is manifested in the relative stereochemistry of the cycloadducts.

A general asymmetric method for the synthesis of aryl-tetralin lignans having a variety of stereochemistries was developed on the basis of the following conclusions. For *o*-QDMs bearing an α' -aryl group, cycloaddition to lactate or mandelate substituted fumarates results in the thermodynamically less stable 1,2-*cis* stereochemistry. This relative stereochemistry is important when considering a synthesis of lignans bearing a 1,2-*cis* stereochemistry. In addition to the accessibility to lignans bearing a 1,2-*cis* geometry, these *exo* cycloadducts readily undergo facile base induced 2,4-lactone formation thus enabling differentiation of the 2 and 3-ester groups. Thus, the addition of

α -hydroxy- α' -aryl-*o*-QDM **136** to the fumarate of methyl (R)-mandelate led to the formation of an *exo* cycloadduct **135** (90:10 ratio of diastereomers) in 44% yield. By treatment of the adduct with anhydrous sodium methoxide, it was possible to affect a tandem, base induced 2,4-lactonization/3,4-elimination/transesterification. After catalytic hydrogenation of the double bond, this led to an intermediate having the 1,2,3-*cis* stereochemistry that was converted to the natural product lignan α -dimethylretrodendrin and its three diastereomers. This constitutes the first general asymmetric method applicable to the synthesis of aryltetralin lignans with a variety of stereochemistries. The preferred conformations of these molecules were determined using a combination of molecular mechanics calculations and $^1\text{H-NMR}$ studies. The two flexible 2,3-*cis* lactones were shown to possess unexpected conformations bearing axial pendant aryl groups. This was in contrast to that proposed by Rodrigo⁷⁵ who suggested that these types of molecules possessed equatorial aryl groups. This is significant in that it offers an explanation into the possible origin of the unusual antitumor activities displayed by compounds like deoxypicropodophyllotoxin and 2-methyldeoxyisopicropodophyllotoxin.

The additions of α -hydroxy- α -phenyl(aryl)-*o*-QDMs to the fumarate of methyl (R)-mandelate were investigated. These reactions stereoselectively gave *endo* products resulting from addition to the *si* face of the fumarate in accord with Helmchen's model. It is interesting to note that the cycloaddition did not proceed by the hydrogen bonding mechanism discussed above as hydrogen bonding in the *endo* transition state is sterically impossible. It is unclear why the *exo* transition state is not favored in these cases. Similarly, in light of the importance of hydrogen bonding to facial selectivity in the reaction of α -hydroxy-*o*-QDM to the fumarates of methyl lactate or mandelate, the preference for the addition to the *si* face of the fumarate is unprecedented. In the elucidation of the facial selectivity, the cycloadducts were reduced with a mixture of NaBH_4 and TFA. This step resulted in the inversion of the C1 center giving rise to the thermodynamically less stable 1,2-*cis* stereochemistry. Two possible mechanisms were

suggested for this reduction: 1) reduction of an ion paired species and/or 2) reduction of an intermediate cation. The observation that the reduction products have the same relative stereochemistry as deoxypodophyllotoxin and podophyllotoxin, suggests that these intermediates could serve as useful precursors to these compounds.

Experimental

^1H -NMR and ^{13}C -NMR spectra were recorded on a Bruker AM-300 or AMX-500 instrument using tetramethylsilane as internal standard. IR spectra were recorded on a Perkin Elmer 881 spectrometer. Aldrich silica gel (28,859-4) was used for all chromatography. Elemental analyses were performed by Guelph Chemical Laboratories Ltd., Guelph, Ontario, Canada. HRMS/mass spectra were obtained on an Analytical VG 7070E-HF instrument. Melting points were measured on a hot stage instrument and are uncorrected. Optical rotations were recorded on a Rudolf Research Autopol III instrument. Tetrahydrofuran (THF) was distilled from sodium and benzophenone.

Benzocyclobutenol 18

To a refluxing solution of vinyl acetate (200 mL) and isoamyl nitrite (10 g, 85 mmol, 1.2 mole equiv.), in the presence of flame dried molecular sieves, was added solid anthranilic acid (10 g, 73 mmol) over a period of 1/2 h. The solution was refluxed 1 h further and the solution filtered and the solvent evaporated. The brown oil was distilled at reduced pressure (0.5 mm Hg) to give a yellow oil (8.46 g, 72%). The acetate was then dissolved in 60 mL of 30% aqueous NH_4OH /methanol and stirred 5 h at rt. The solution was acidified (10% HCl), saturated (NaCl), extracted with CH_2Cl_2 , and dried (MgSO_4). Evaporation of the solvent and recrystallization from hexane gave a white solid (2.27 g, 36%, 26% overall yield from anthranilic acid); mp 53°C , spectroscopic properties identical to that previously reported.⁹⁸

1-Methoxybenzocyclobutene 30

Benzocyclobutenol (267 mg, 2.23 mmol), silver oxide (0.882 g), and methyl iodide (0.87 mL, 1.98 g, 14 mmol, 6.3 mol equiv.) were stirred in chloroform (17 mL) at room

temperature in a sealed vessel (CH_3I is volatile) for 18 h. The solution was filtered and the solvent evaporated leaving a yellow oil (0.315 g, 100%). $^1\text{H-NMR}$ indicated that the sample was pure. $^1\text{H-NMR}$ (CDCl_3) δ : 7.25-7.13 (m, 4H), 4.99 (dd, 1H, $J=1.83,4.27$), 3.45 (s, 3H, OMe), 3.45 (dd, 1H, $J=4.27, 14.12$), 3.12 (dd, 1H, $J=1.83, 14.12$), identical to that previously reported.⁹⁸

1-Phenyl-benzocyclobuten-1-ol 51

(*Benzocyclobutenone from benzocyclobutenol 18*) Chromium trioxide (2.1 g, 5 mole equiv.) was added to a stirred solution of CH_2Cl_2 (25 mL) and pyridine (1.70 g, 5 mole equiv.) at rt to give a dark red coloured solution after 1 minute. After 5 minutes, benzocyclobutenol **18** (0.515 g, 4.29 mmol) was added and stirred for 12.5 h. The solution was filtered through alumina and the black precipitate washed with CH_2Cl_2 . The solvent was evaporated and the crude product azeotroped with diethyl ether (2 x 25 mL) and dried under a stream of N_2 to give a yellow oil (0.466 g, 92%). The $^1\text{H-NMR}$ spectrum of the crude product indicated that it was greater than 95% pure. The ketone was used in the next step.

n-Butyllithium (7.2 mmol, 2.2 M, 3.3 mL) was added to a cooled solution (-78°C ; dry ice/acetone; under N_2) of THF (15 mL) and bromobenzene (1.16 g, 7.41 mmol) and stirred for 5 min. Dropwise addition of benzocyclobutenone (4.36 g, 3.69 mmol) in diethyl ether (10 mL) to the aryllithium solution resulted in a wine coloured solution. An additional 3 mL of ether was used to rinse the remaining ketone into the reaction mixture. After 10 min at -78°C , the solution was quenched with saturated aqueous NH_4Cl (25 mL) and then removed from the cold bath for 15 min. Water (3 mL) was added to dissolve the precipitate and the organic layer separated. The aqueous fraction was extracted with CH_2Cl_2 (2 x 25 mL) and the combined organic extracts were dried (MgSO_4) and the solvent evaporated to give a solid. The crude product was purified on silica (10% ethyl acetate/hexanes) giving **51**⁵⁷ as a colourless solid (0.540 g, 75%); mp $61\text{-}62^\circ\text{C}$; IR

(CH₂Cl₂): 3588 (OH), 1188, 1048 cm⁻¹; ¹H-NMR (CDCl₃) δ: 7.47 (dd, 2H, J = 1.65, 8.4), 7.34-7.21 (m, 6H), 3.65 (d, 1H, J = 14), 3.56 (d, 1H, J = 14), 2.67 (s, 1H, OH); ¹³C-NMR (CDCl₃) δ: 149.07 (C), 143.48 (C), 142.11 (C), 129.65 (CH), 128.26 (2 x CH), 127.65 (CH), 127.41 (CH), 125.59 (2 x CH), 124.11 (CH), 121.63 (CH), 81.47 (C), 49.90 (CH₂); MS *m/e* (rel. %): 196 (M⁺, 27), 195 (100), 194 (9), 181 (5), 179 (8), 178 (14), 177 (9), 167 (3), 166 (3), 165 (14), 152 (7), 119 (18), 105 (35), matches library spectrum of *o*-methylbenzophenone (see general experimental section).

(-)- α -Dimethylretrodendrin 95

Picroretrodendrin **163** (3.5 mg, 0.009 mmol) was refluxed in sodium *t*-butoxide/*t*-butyl alcohol solution (0.1 M, 5 mL) under N₂ for 24 h. The clear solution was diluted with 20% HCl (10 mL) and extracted with CH₂Cl₂ (3 x 10 mL), dried (MgSO₄), and evaporated. The product was purified on silica (30-50% EtOAc/hexanes) and recrystallized (EtOAc/hexanes) giving a colourless solid (3.3 mg, 94%): mp 182-183 °C (lit¹¹⁰ 188-189 °C); [α]_D²⁰ -58° (lit¹¹⁰ -58°); IR (CH₂Cl₂): 1780 cm⁻¹; ¹H NMR (CDCl₃) δ: 6.83 (d, 1H, J = 8.2, H5'), 6.79 (dd, 1H, J = 1.7, 8.3, H6'), 6.71 (d, 1H, J = 1.6, H2'), 6.61 (s, 1H, H5), 6.33 (s, 1H, H8), 4.53 (dd, 1H, J_{11 β ,3} = 6.4, J_{11 β ,11 α} = 8.6, H11 β), 4.12 (d, 1H, J₁₂ = 10.9, H1), 3.99 (dd, 1H, J_{11 α ,11 β} = 8.6, J_{11 α ,3} = 10.4, H11 α), 3.88 (s, 3H), 3.87 (s, 3H), 3.82 (s, 3H), 3.60 (s, 3H), 3.00 (dd, J_{4 β ,3} = 5.3, J_{4 β ,4 α} = 14.8, H4 β), 2.93 (t, 1H, J_{4 α ,4 β} = 14.8, J_{4 α ,3} = 14), 2.63 (m, 1H, H3), 2.50 (dd, 1H, J_{2,1} = 10.9, J_{2,3} = 13.5, H2); ¹³C-NMR (CDCl₃) δ: 175.51 (CO), 148.77 (C), 147.89 (C), 147.77 (C), 147.67 (C), 135.56 (C), 131.35 (C), 126.77 (C), 121.82 (CH), 112.95 (CH), 112.45 (CH), 111.38 (CH), 110.97 (CH), 70.98 (CH₂), 55.96 (CH₃), 55.87 (CH₃), 55.80 (2 x CH₃), 48.91 (CH), 45.77 (CH), 40.15 (CH), 32.61 (CH₂); MS *m/e* (rel. %); HRMS calcd. for C₂₂H₂₄O₆: 384.1573, found 384.1577.

Acrylate of rac-lactonitrile, 115

Acryloyl chloride (5.9 g, 5.3 mL, 65 mmol) and lactonitrile (2.95 g, 3 mL, 37.8 mmol) were refluxed in methylene chloride (50 mL) over dry molecular sieves (6.7 g, 4 Å) for 68 h. The solution was filtered and the solvent evaporated leaving a light yellow liquid. The liquid was fractionally distilled (bp 160°C, 1 Atm) to remove the lower boiling acryloyl chloride and methylene chloride. The distillate was chromatographed on silica gel (5% ethyl acetate/hexanes) to give a colourless liquid (1.4 g, 11.3 mmol, 30%); IR (CH₂Cl₂): 1739 cm⁻¹; ¹H-NMR (CDCl₃) δ: 6.52 (dd, 1H, J = 1.29, 17.21), 6.15 (dd, 1H, J = 10.44, 17.14), 5.98 (dd, 1H, J = 1.29, 10.5), 5.47 (q, 1H, J = 6.9), 1.69 (d, 3H, J = 6.97); ¹³C-NMR (CDCl₃) δ: 164.06, 133.29, 126.64, 117.46, 57.39, 18.79; MS, ammonia ionization *m/e* (rel. %): 143 (M+NH₄⁺, 11), 126 (M+H⁺, 1.1), 99 (2.2), 72 (12), 70 (5), 55 (100), 46 (4); HRMS (EI) calcd. for C₆H₇O₂N: 125.0477, found 125.0484.

Acrylate of rac-3-hydroxy-2-butanone, 116

Acryloyl chloride (5 mL, 61.5 mmol) and 3-hydroxy-2-butanone (5.46 g, 61.9 mmol) were refluxed in CH₂Cl₂ (5 mL) over dry molecular sieves (4Å, 8 g) for four days. The solution was filtered and the solvent evaporated to leave an oil. The crude oil was chromatographed on silica (10% ethyl acetate/hexanes) to give a colourless oil (5.7 g, 66%); IR (CH₂Cl₂): 1730 cm⁻¹; ¹H-NMR (CDCl₃) δ: 6.41 (dd, 1H, J = 1.35, 17.34), 6.13 (dd, 1H, J = 10.40, 17.33), 5.85 (dd, 1H, J = 1.36, 10.40), 5.09 (q, 1H, J = 7.05), 2.12 (s, 3H), 1.38 (d, 3H, J = 7.06); ¹³C-NMR (CDCl₃) δ: 205.61, 165.37, 131.90, 127.67, 75.07, 25.58, 16.02; MS *m/e* (rel. %): 142 (M⁺, 0.4), 100 (1.8), 99 (7.7), 98 (13), 87 (2.4), 55 (100), 43 (36); HRMS calcd. for C₇H₁₀O₃: 142.0630, found 142.0646.

Fumarate of methyl (S)-lactate 117

Fumarate **117** was synthesized according to the literature procedure.³⁹ Fumaryl chloride (2.44 g, 16 mmol) and methyl (S)-lactate (3.32 g, 32 mmol) were heated at 110°C

for 18.5 h. The mixture was diluted with ethyl acetate (30 mL) and washed with 5% aqueous NaHCO₃ (30 mL). The organic layer was dried (MgSO₄) and the solvent evaporated to give a yellow oil (4.47 g). Chromatography of the oil on silica (20% ethyl acetate/hexanes) afforded **117** as a colourless oil (2.51 g, 55%); ¹H-NMR (CDCl₃) δ: 6.97 (s, 2H), 5.22 (q, 2H, J = 7.06), 3.77 (s, 6H), 1.55 (d, 2H, J = 7.06). The ¹H-NMR of **117** was identical to that reported previously.⁴⁰

Fumarate of methyl (R)-mandelate 118

Fumarate **118** was synthesized according to the literature procedure.⁹⁹ Fumaryl chloride (1.37 g, 8.93 mmol, 0.5 mole equiv.) and methyl (R)-mandelate⁹⁹ (2.97 g, 17.9 mmol) were heated at 100°C for 21 h under a dry atmosphere. The yellow oil was crystallized from ethyl acetate/hexanes to give a white crystalline material (2.072 g, 56%); ¹H-NMR (CDCl₃) δ: 7.39-7.48 (m, 10H), 7.06 (s, 2H), 6.04 (s, 2H), 3.74 (s, 6H). The ¹H-NMR of **118** was identical to that reported previously.⁹⁹

Di-t-butyl fumarate, 120

Fumaryl chloride (5.1 g, 0.033 mol) was dissolved in benzene (50 mL) and t-butyl alcohol (15 mL, 4.8 mole equiv.) was added at room temperature. Molecular sieves (5.0 g, 4Å, flame dried under nitrogen) were added and the solution refluxed for 38 h. The resulting solution was filtered through a short column of silica (EtOAc) and the filtrate washed with aqueous NaHCO₃ solution (5%, 3 x 20 mL). The solution was dried (MgSO₄) and evaporated giving a yellow oil (2.99 g, 42%) which crystallized on standing. Flash chromatography on silica (eluent 20% ethyl acetate/hexanes) yielded a colourless solid (1.74 g, 24%), a sample of which was crystallized from ethyl acetate/hexanes; mp 62-63°C; IR (CH₂Cl₂): 1709 cm⁻¹; ¹H-NMR (60 MHz, CDCl₃) δ: 6.73 (s, 2H), 1.53 (s, 18H); ¹³C-NMR (75.47 MHz, CDCl₃) δ: 164.38, 134.53, 81.64, 27.99; MS *m/e* (rel. %): 155 (15), 99 (53), 57 (100), 56 (30); Analysis calcd. for C₁₂H₂₀O₄: C 63.14, H 8.83, found: C 63.41, H 8.91.

Di-(2-hydroxyethyl) fumarate, 121

Fumaryl chloride (1 mL, 1.40 g, 9.16 mmol) and ethylene glycol (5.2 mL, 10 mole equiv.) were stirred at 27°C for 24 h. The solution was diluted with water (25 mL) and extracted with ethyl acetate (3 x 25 mL). The organic phase was dried (Na₂SO₄) and the solvent evaporated leaving a viscous oil (1.51 g). The oil was chromatographed on silica (80% ethyl acetate/hexanes) to give a semicrystalline product (1.01 g, 54%); mp 52-53°C; IR (CH₂Cl₂): 1728 cm⁻¹; ¹H-NMR (CDCl₃) δ: 6.92 (s, 2H), 4.33 (m, 4H), 3.87 (m, 4H), 2.79 (bs, 2H); ¹³C-NMR (75.47 MHz, CDCl₃) δ: 165.06, 133.64, 66.87, 60.67; MS *m/e* (rel. %): 144 (15), 143 (100), 117 (12.5), 99 (65.9), 85 (23), 82 (26), 57 (29); Analysis calcd. for C₈H₁₂O₆: C 47.06, H 5.92, found: C 46.99, H 5.77.

Di-(2-chloroethyl) fumarate 122

2-Chloroethanol (2 mole equiv, 3.72 mL) was slowly added to fumaryl chloride (3 mL, 4.24 g, 27.8 mmol) containing molecular sieves. The mixture was stirred at rt for 2 h at which time the mixture completely solidified. Ethyl acetate and CH₂Cl₂ were added to dissolve the solid. The solution was extracted with 5% aqueous NaHCO₃ and the organic layer dried (Na₂SO₄). Evaporation of the solvent gave a white crystalline solid which was recrystallized from ethyl acetate/hexanes to afford **122** as colourless plates (3.95 g, 59%); mp 60-61°C; IR (CH₂Cl₂): 1733 (s), 1155 (m), 1082 (w), 1030 (w), 980 (w) cm⁻¹; ¹H-NMR (CDCl₃) δ: 6.93 (s, 2H), 4.47 (t, 4H, J = 6.6), 3.74 (t, 4H, J = 6.6). ¹³C-NMR (CDCl₃) δ: 164.29 (CO), 133.59 (CH), 64.87 (CH₂), 41.28 (CH₂); MS *m/e* (rel. %): 163 (34), 161 (100), 133 (9), 99 (12), 64 (13), 63 (30), 62 (41).

Di-(2-fluoroethyl) fumarate 123

Fumaryl chloride (1 mL, 1.40 g, 9.16 mmol) and 2-fluoroethanol (2 mole equiv. 1.08 mL) were stirred over 4 Å molecular sieves at rt for 1 h. The solution was diluted

with ethyl acetate and extracted with 5% aqueous NaHCO₃. The organic layer was dried (Na₂SO₄) and the solvent removed in vacuo to give colourless oil (0.790 g) which crystallized on standing. The solid was recrystallized from EtOAc/hexanes to give white needles (0.526 g, 28%); mp 55-56°C; IR (CH₂Cl₂): 1730 (s), 1300, 1180 (m), 1160 (m), 1071 (w), 1047 (w), 980 (w) cm⁻¹; ¹H-NMR (CDCl₃) δ: 6.95 (s, 2H), 4.66 (dt, 2H, J_{HFgem} = 69, J_{H,Hvic} = 5, J_{HFvic} = 28); ¹³C-NMR (CDCl₃) δ: 164.42 (CO), 133.56 (CH), 82.07, 79.94 (CH₂F), 64.28, 64.02 (CH₂O); MS *m/e* (rel. %): 163 (9), 146 (16), 145 (100), 117 (33), 99 (46), 81 (17), 71 (22), 57 (12).

Cycloadducts **124** and **125**

Benzocyclobutenol **18** (63.5 mg, 0.529 mmol) and di-*t*-butyl fumarate **120** (242 mg, 1.12 mmol, 2.12 mole equiv.) were heated in toluene (5 mL) at 110°C in the presence of molecular sieves (1.0 g, 4Å, dried under vacuum) for 19 h. The solution was filtered through a short silica gel column using ethyl acetate as eluent and the solvent evaporated to leave a yellow oil. A ¹H-NMR spectrum (300 MHz) of this crude product exhibited two doublets at δ 4.88 (J = 8.88, *exo*) and 5.03 (J = 3.57, *endo*) in a ratio of 1.5:1 (*endo/exo*). The two isomers were separated by chromatography on silica (15% ethyl acetate/hexanes) in a combined yield of 45%.

Exo adduct **124**: mp 91-92°C; IR (CH₂Cl₂): 1731 cm⁻¹; ¹H-NMR (CDCl₃) δ: 7.65 (d, 1H, J = 7.2), 7.27-7.18(m, 2H), 7.08(d, 1H, J = 7.03), 4.88 (dd, 1H, J = 8.88, 5.6), 2.8-3.1 (m, 4H), 2.81 (d, 1H, J = 5.6), 1.50 (s, 9H), 1.46 (s, 9H); ¹³C-NMR (CDCl₃) δ: 172.90 (CO), 172.58 (CO), 137.20 (C), 133.57 (C), 128.00 (CH), 127.58 (CH), 126.78 (2 x CH), 81.85 (C), 81.05 (C), 70.35 (CH), 51.58 (CH), 42.07 (CH), 31.74 (CH₂), 28.07 (3 x CH₃), 28.01 (3 x CH₃); MS *m/e* (rel. %): 257 (4.3), 218 (5.4), 189 (9.8), 172 (10), 129 (15), 97 (28), 83 (36), 69 (57), 57 (100); Analysis calcd. for C₂₀H₂₈O₅: C 68.94, H 8.10; found: C 68.62, H 8.10.

Endo adduct **125**: mp 99-102°C; IR (CH₂Cl₂): 1733 cm⁻¹; ¹H-NMR (CDCl₃) δ: 7.39-7.35 (m, 1H), 7.27-7.20 (m, 2H), 7.15-7.11 (m, 1H), 5.03 (dd, 1H, J = 4.63, 3.57),

3.23-3.12 (m, 2H), 2.99 (dd, 1H, $J = 11.05, 3.57$), 2.82 (dd, 1H, $J = 18.10, 12.99$), 2.17 (bd, 1H), 1.50 (s, 9H), 1.48 (s, 9H); $^{13}\text{C-NMR}$ (CDCl_3) δ : 173.83 (CO), 171.78 (CO), 136.44 (C), 134.19 (C), 129.33 (CH), 128.60 (CH), 128.47 (CH), 126.74 (CH), 81.39 (C), 80.68 (C), 68.52 (CH), 48.87 (CH), 38.30 (CH), 31.99 (CH_2), 28.08 (3 x CH_3), 28.01 (3 x CH_3); MS *m/e* (rel. %): 236 (3.8) 235 (11), 217 (13), 189 (27), 173 (18), 172 (19), 145 (19), 129 (26), 69 (14), 57 (100); Analysis calcd. for $\text{C}_{20}\text{H}_{28}\text{O}_5$: C 68.94, H 8.10; found: C 68.98, H 8.23.

Cycloadducts **126** and **127**

Di-*t*-butylfumarate **120** (108 mg, 0.474 mmol) and 1-methoxybenzocyclobutene **30** (111 mg, 0.825 mmol, 1.74 mole equiv.) were heated in toluene (5 mL) at reflux for 16 h in the presence of molecular sieves (4Å, 0.19 g). The solution was filtered through a short silica gel column (eluent EtOAc) and the solvent evaporated at reduced pressure to leave a yellow oil. Further evaporation at 0.5 mm Hg for 4 h (20°C) left an oil (168 mg, 98%). The $^1\text{H-NMR}$ spectrum of this crude product exhibited two doublets at δ 4.53 ($J = 3.39$, **127**) and 4.74 ($J = 8.1$, **126**) in the ratio of 7.7:1. Only the major cycloadduct **127** could be characterized; IR (CH_2Cl_2) 1734 cm^{-1} ; $^1\text{H-NMR}$ (CDCl_3) δ : 7.28-7.13 (m, 4H), 4.53 (d, 1H, $J = 3.39$), 3.36-3.19 (m, 2H), 3.31 (s, 3H), 2.95 (dd, 1H, $J = 11.29, 3.39$), 2.28 (dd, 1H, $J = 16.16, 10.4$), 1.50 (s, 9H), 1.47 (s, 9H); $^{13}\text{C-NMR}$ (CDCl_3) δ : 174.52 (CO), 171.17 (CO), 135.05 (C), 133.69 (C), 129.59 (CH), 128.92 (CH), 128.60 (CH), 125.58 (CH), 80.69 (C), 80.24 (C), 78.29 (CH), 56.99 (CH_3), 48.37 (CH), 38.01 (CH), 31.80 (CH_2), 28.11 (3 x CH_3), 27.99 (3 x CH_3); MS *m/e* (rel. %): 200(62), 172 (35), 156 (24), 155 (32), 129 (80), 128 (100), 127 (58), 126 (20); Analysis calcd. for $\text{C}_{21}\text{H}_{30}\text{O}_5$: C 69.58, H 8.34; found: C 69.46, H 8.37.

Cycloadducts **128** and **129**

The fumarate of methyl (*S*)-lactate, **117** (115 mg, 0.397 mmol), and 1-methoxybenzocyclobutene **30** (66.6 mg, 0.496 mmol) were refluxed together in toluene (10 mL) for 3 days. The solution was filtered through a short column of silica gel (eluent EtOAc)

and evaporated to leave a yellow oil (185 mg). The $^1\text{H-NMR}$ spectrum exhibited two doublets at δ 4.75 ($J = 2.96$) and 4.56 ($J = 3.33$) in a ratio of 1.57:1. HPLC (ODS-2, acetonitrile/water/methanol) exhibited two peaks in a ratio of 1.56:1. Chromatography of the crude oil on silica gel (eluent 5% EtOAc/benzene) gave adduct **128** (62.6 mg) and adduct **129** (27.1 mg)(combined yield 62%).

128: IR (CH_2Cl_2) 1746 cm^{-1} ; $^1\text{H-NMR}$ (CDCl_3) δ : 7.18-7.32 (m, 4H), 5.24 (q, 1H, $J = 7.04$), 5.16 (q, 1H, $J = 7.10$), 4.68 (d, 1H, $J = 3.00$), 3.77 (s, 3H), 3.75 (s, 3H), 3.65 (m, 1H), 3.44 (dd, 1H, $J = 7.04, 17.16$), 3.34 (s, 3H), 3.17 (dd, 1H, $J = 11.62, 3.00$), 2.94 (dd, 1H, $J = 10.94, 17.16$), 1.54 (d, 3H, $J = 7.11$), 1.53 (d, 3H, $J = 7.04$); $^{13}\text{C-NMR}$ (CDCl_3) δ : 174.85 (CO), 171.34 (CO), 171.24 (CO), 170.99 (CO), 134.49 (C), 133.13 (C), 129.63 (CH), 129.14 (CH), 128.87 (CH), 125.66 (CH), 77.19 (CH), 68.65 (2 x CH), 56.67 (CH_3), 52.24 (2 x CH_3), 47.12 (CH), 36.24 (CH), 31.17 (CH_2), 17.20 (CH_3), 16.87 (CH_3); MS *m/e* (rel. %): 422 (M^+ , 1.1), 359 (21), 258 (25), 187 (42), 186 (33), 185 (34), 159 (86), 155 (100), 128 (46); HRMS calcd. for $\text{C}_{21}\text{H}_{26}\text{O}_9$: 422.1577; found 422.1582.

129: IR (CH_2Cl_2) 1745 cm^{-1} ; $^1\text{H-NMR}$ (CDCl_3) δ : 7.19-7.35 (m, 4H), 5.26 (q, 1H, $J = 7.02$), 5.13 (q, 1H, $J = 7.08$), 4.66 (d, 1H, $J = 3.31$), 3.75 (s, 3H), 3.74 (s, 3H), 3.63-3.54 (m, 1H), 3.36-3.26 (m, 2H), 3.28 (s, 3H), 3.01 (dd, 1H, $J = 10.49, 16.92$), 1.55 (d, 3H, $J = 7.04$), 1.48 (d, 1H, $J = 7.05$); $^{13}\text{C-NMR}$ (CDCl_3) δ : 173.52 (CO), 171.12 (CO), 170.96 (CO), 170.87 (CO), 134.60 (C), 132.91 (C), 129.63 (CH), 129.03 (CH), 128.89 (CH), 125.75 (CH), 77.43 (CH), 68.86 (CH), 68.64 (CH), 56.73 (CH_3), 52.26 (CH_3), 47.04 (CH), 37.26 (CH), 37.10 (CH), 31.11 (CH_2), 17.05 (CH_3), 16.72 (CH_3); MS *m/e* (rel. %): 422 (M^+ , 0.5), 359 (1.0), 258 (25), 187 (45), 186 (31), 185 (9), 155 (100), 128 (39); HRMS calcd. for $\text{C}_{21}\text{H}_{26}\text{O}_9$: 422.1577; found 422.1559.

Cycloadducts **130a-d**

Benzocyclobutenol **18** (0.125 g, 1.04 mmol) and acrylate **115** (0.439 g, 3.51 mmol, 3.36 mole equiv.) were refluxed in toluene (anhydrous, 5 mL) in the presence of 4 \AA

molecular sieves (0.92 g) under nitrogen for 11 h. The solution was filtered and the solvent removed in vacuo to leave a yellow oil (0.260 g). The oil was chromatographed on silica (20% ethyl acetate/hexanes) to give a colourless oil (148 mg, 58%) which on examination by $^1\text{H-NMR}$ appeared to be a mixture of four diastereomers; IR (CH_2Cl_2): 3604, 2309, 1748, 1734 cm^{-1} ; Analysis calcd. for $\text{C}_{14}\text{H}_{15}\text{NO}_3$: C 68.56, H 6.16, N 5.71; found: C 68.52, H 6.57, N 5.45. Three of the four isomers were isolated by HPLC on ODS-2 using a methanol-water eluent (44:56 to 70:30 over 36 min) and their $^1\text{H-NMR}$ and mass spectral data are given below in order of their elution.

exo-2: $^1\text{H-NMR}$ (CDCl_3) δ : 7.59 (d, 1H, $J = 9.4$), 7.14-7.3 (m), 7.10 (m, 1H), 5.49 (q, 1H, $J = 6.94$), 5.09 (dd, 1H, $J = 8.7, 6.6$), 2.68-3.0 (m 3H), 2.49 (d, 1H, $J = 6.6$), 2.89-2.2 (m, 1H), 2.03-1.88 (m, 1H, $J = 6.0$), 1.68 (d, 3H, $J = 6.92$); MS *m/e* (rel. %): 227 ($\text{M}^+ - \text{H}_2\text{O}$, 19), 191 (7), 173 (24), 145 (16), 129 (100), 81 (12), 69 (54).

endo-1: $^1\text{H-NMR}$ (CDCl_3) δ : 7.41-7.38 (m, 1H), 7.26-7.10 (m, 3H), 5.51 (q, 1H, $J = 6.90$), 5.10 (bs, 1H), 3.00-2.75 (m, 3H), 2.46 (d, 1H, $J = 5.9$), 2.31-2.03 (m, 2H), 1.69 (d, 3H, $J = 6.93$); MS *m/e* (rel. %): 227 ($\text{M}^+ - \text{H}_2\text{O}$, 14), 191 (3.2), 173 (12), 145 (11), 130 (27), 129 (100), 128 (26.4), 119 (20), 115 (16), 91 (15).

endo-2: $^1\text{H-NMR}$ (CDCl_3) δ : 7.41-7.38 (m, 1H), 7.27-7.22 (m, 2H), 7.17-7.14 (m, 1H), 5.52 (q, 1H, $J = 6.97$), 5.07 (d, 1H, $J = 3.18$), 3.12-2.75 (m, 3H), 2.29-2.10 (m, 2H), 1.71 (d, 3H, $J = 6.98$); MS *m/e* (rel. %): 227 ($\text{M}^+ - \text{H}_2\text{O}$, 21), 173 (8), 155 (2.9), 145 (8), 130 (39), 129 (100), 128 (34), 119 (20), 115 (16), 91 (13).

Cycloadduct 131

Benzocyclobutenol **18** (0.219 g, 1.82 mmol) and acrylate **116** (0.268 g, 1.89 mmol, 1.04 mole equiv.) were refluxed in toluene (10 mL) in the presence of molecular sieves (4Å, 0.5 g) for 19 h. The solution was filtered through silica gel (EtOAc) and the solvent evaporated under reduced pressure to leave a yellow oil (0.471 g). The oil was chromatographed on silica (40% ethyl acetate/hexanes) and recrystallized from ethyl

acetate/hexanes to give long, colourless crystals (0.215 g, 45%); mp 65-69°C; IR (CH₂Cl₂) 1721 cm⁻¹; ¹H-NMR (300 MHz, CDCl₃) δ: 7.65 (d, 1H, J_{8,7} = 7.19), 7.22 (m, 2H), 7.08 (d, 1H, J_{5,6} = 7.06), 5.26 (q, 1H, J = 7.19), 4.98 (d, 1H, J_{1,2} = 9.315), 3.68 (d, 1H, J = 2.82), 2.88-2.776 (m, 3H), 2.21 (s, 3H), 2.20-2.12 (m, 1H), 2.07-1.92 (m, 1H), 1.48 (d, 3H, J = 7.19); ¹³C-NMR (75.47 MHz, CDCl₃) δ: 205.88 (CO), 174.35 (CO), 137.44 (C), 135.32 (C), 128.22 (CH), 127.28 (CH), 126.93 (CH), 126.38 (CH), 75.23 (CH), 70.52 (CH), 48.77 (CH), 28.13 (CH₂), 25.68 (CH₂), 23.69 (CH₃), 15.80 (CH₃); MS *m/e* (rel. %): 244 (2.2), 191 (17), 173 (25), 157 (30), 146 (27), 129 (100), 105 (43), 91 (27); HRMS calcd. for C₁₅H₁₈O₄: 262.1205; found 262.1203.

Lactone 132

The fumarate of ethylene glycol **121** (330 mg, 1.62 mmol) and benzocyclobutenol **18** (214 mg, 1.78 mmol, 1.1 mole equiv.) were refluxed in toluene (10 mL) in the presence of molecular sieves (4Å) for 18 h. The solution was filtered through a short column of silica (eluent, ethyl acetate) and the solvent evaporated in vacuo. The ¹H-NMR spectrum of the crude product revealed the presence of three doublets at δ 5.43 (J = 5.18), 5.12 (J = 3.65) and 4.86 (J = 9.53). The crude oil was chromatographed on silica (eluent 70% ethyl acetate/hexanes) to give only one pure fraction (93 mg, 22%); mp 114-115°C; IR (CH₂Cl₂) 3600, 1788, 1745 cm⁻¹; ¹H-NMR (CDCl₃) δ: 7.35 (dd, 1H, J = 1.71, 7.3), 7.29-7.16 (m, 3H), 5.46 (d, 1H, J = 5.18), 4.18 (ddd, 1H, J = 3.08, 6.04, 9.13), 3.94 (m, 1H), 3.84 (t, 1H, J = 5.19), 3.51 (dd, 1H, J = 17.9, 5.28), 3.46 (bm, 2H), 3.35 (m, 1H, J = 1.14, 5.34), 3.09 (d, 1H, J = 17.9); ¹³C-NMR (CDCl₃) δ: 176.52 (CO), 167.37 (CO), 133.84 (C), 132.83 (C) 130.28 (CH), 129.75 (CH), 128.24 (CH), 126.80 (CH), 78.06 (CH), 66.38 (CH₂), 60.72 (CH₂), 47.64 (CH), 39.04 (CH), 27.32 (CH₂); MS *m/e* (rel. %): 262 (M⁺ 7.0), 200 (12), 173 (5.7), 172 (8.2), 156 (5.9), 129 (100), 128 (77), 127 (16); HRMS calcd. for C₁₄H₁₄O₅: 262.0841; found 262.0845.

Reaction of benzocyclobutenol 18 with the fumarate of methyl (S)-lactate 117 in DMSO/toluene (133a-d)

Benzocyclobutenol **18** (42 mg, 0.35 mmol) and fumarate **117** (83 mg, 0.29 mmol) were heated at 100°C in 30% DMSO/toluene (by volume, 10 mL) over molecular sieves (4 Å, 300 mg) for 21 h. The solution was filtered through a short silica gel column (ethyl acetate eluent), diluted with benzene and extracted with water. The organic fraction was dried (MgSO₄) and the solvent evaporated. Residual solvent was removed at high vacuum (0.5 mm, 30°C) to leave an oil (109 mg, 72%). The major isomers were separated using reverse phase HPLC (ODS-2, 53% water: 41% methanol:6% acetonitrile increasing to 100% methanol). The identity of the fourth eluted peak was established as the *exo-re* adduct by comparison to an authentic sample.^{39,40} The two major adducts, eluting second and third, were isolated and characterized.

Endo adduct 133b: ¹H-NMR (CDCl₃) δ: 7.13-7.42 (m, 4H), 5.22 (q, 1H, J = 7.15), ca. 5.14 (m, 1H), 5.13 (q, 1H, J = 7.01), 3.78 (s, 3H), 3.75 (s, 3H), 3.63 (dt, 1H, J = 5.82, 11.6), 3.43 (d, 1H, J = 4.03), 3.19 (dd, 1H, J = 3.06, 11.54), 3.30 (dd, 1H, J = 11.7, 16.8), 2.96 (dd, 1H, J = 5.82, 16.82), 1.56 (d, 3H, J = 7.2), 1.52 (d, 3H, J = 7.1); MS *m/e* (rel. %): 408 (M⁺, 0.34), 172 (19), 155 (50), 145 (38), 129 (100), 128 (64); HRMS calcd. for C₂₀H₁₈O₉: 408.1432; found 408.1440.

Endo adduct 133c: ¹H-NMR (CDCl₃) δ: 7.45-7.40 (m, 1H), 7.27-7.24 (m, 2H), 7.14-7.20 (m, 1H), 5.35 (d, 1H, J = 3.49), 5.28 (q, 1H, J = 7.17), 5.17 (q, 1H, J = 7.1), 3.93 (bs, 1H), 3.80 (s, 3H), 3.77 (s, 3H), 3.48 (dt, 1H, J = 6.0, 12.3), 3.36 (dd, 1H, J = 6.0, 16.6), 3.22 (dd, 1H, J = 3.49, 11.7), 2.89 (dd, 1H, J = 12.3, 16.6), 1.57 (d, 3H, J = 7.2), 1.55 (d, 3H, J = 7.1); MS *m/e* (rel. %): 408 (M⁺, 0.31), 287 (2.5), 276 (6), 258 (7), 173 (9), 172 (15), 155 (34), 129 (100), 128 (60), 127 (14); HRMS calcd. for C₂₀H₁₈O₉: 408.1432; found 408.1434.

Exo-si and Exo-re lactones 134a and 134d.

The crude mixture of cycloadducts **133a-d** (0.145 g) was stirred in a solution of 30% THF/water (25 mL), which had been adjusted to pH 11 with 5% aqueous NaHCO₃, for 24 h (final pH=8.4). The solution was made basic (pH=11) with 5% NaHCO₃ and then extracted with CH₂Cl₂, dried (MgSO₄) and the solvent evaporated to give an oil (0.107 g). The ¹H-NMR of the crude product indicated that the *exo* isomers **133a,d** had disappeared and new signals consistent with the formation of 1,3-lactones had appeared. The *endo* isomers **133b,c** signals were still present in the spectrum. The mixture of lactones **134a,d** and *endo* adducts **133b,c** were dissolved in methanol and separated by HPLC on an ODS-2 (octadecylsilyl; reverse phase) column (53% water, 41% methanol, 6% acetonitrile; isocratic elution). The lactones **134a** and **134d** had retention times of 6.4 and 5.8 minutes respectively. The two *endo* isomers **133b** and **133c** had retention times of 10.8 and 11.6 minutes.

(+)-Exocycloadduct 135

A solution of the fumarate of methyl (R)-mandelate⁹⁹ (5.87 g, 14.2 mmol) and ZnO (2.0 g) were brought to reflux in toluene (35 mL) under a slight vacuum (210 mm). A solution of the hydroxy sulfone **138** in CH₂Cl₂/toluene (25 mL/10 mL) was added over a period of 50 minutes with concomitant evaporation of SO₂ and CH₂Cl₂. After complete addition, the solution was refluxed 10 minutes longer. Filtration and evaporation afforded a brown oil which was chromatographed on silica (40-60% EtOAc/hexanes) giving **135** as the major adduct (1.93 g, 44%, based on starting aldehyde) as an oil; IR (CH₂Cl₂): 3495 (br, OH), 1745 (CO) cm⁻¹; [α]_D²⁰ +51.3° (c 1.69, CH₂Cl₂); ¹H-NMR (CDCl₃) δ: 7.48-7.45 (m, 2H), 7.40-7.37 (m, 3H), 7.30 (s, 1H), 7.19 (t, 1H, J = 7.3), 6.98 (t, 2H, J = 7.7), 6.89 (d, 2H, J = 7.2), 6.51 (d, 1H, J = 1.6), 6.42-6.36 (m, 3H), 6.24 (s, 1H), 5.54 (s, 1H), 4.99 (dd, 1H, J_{4,3} = 9.4, J_{4,OH} = 2.8, H₄), 4.83 (d, 1H, J = 2.8, OH), 4.54 (d, 1H, J_{1,2} = 5.74, H₁), 3.93 (s, 3H), 3.79 (s, 3H), 3.71 (s, 3H), 3.69 (s, 3H), 3.66 (s, 3H), 3.61 (s, 3H),

3.61 (m, H₂), 3.40 (dd, 1H, $J_{3,4} = 9.4$, $J_{3,2} = 12.5$, H₃); ¹³C NMR (CDCl₃) δ: 174.10 (CO), 171.63 (CO), 170.23 (CO), 168.52 (CO), 148.78 (C), 148.46 (C), 148.09 (C), 147.81 (C), 133.33 (C), 133.07 (C), 132.82 (C), 129.40 (C), 120.01 (C), 128.81 (2 x CH), 128.68 (CH), 128.30 (C), 128.19 (2 x CH), 128.03 (2 x CH), 126.95 (2 x CH), 121.95 (CH), 112.61 (CH), 111.44 (CH), 110.41 (CH), 108.63 (CH), 74.97 (CH), 74.08 (CH), 71.21 (CH), 55.86 (CH₃), 55.80 (2 x CH₃), 55.38 (CH₃), 53.35 (CH₃), 52.45 (CH₃), 46.91 (CH), 46.27 (CH), 45.61 (CH); MS *m/e* (rel. %) 728 (M⁺, 1), 563 (2), 562 (2), 518 (2), 517 (3), 516 (8), 394 (49), 351 (24), 325 (20), 107 (100), 79 (59), 77 (57); HRMS calcd. for C₄₀H₄₀O₁₃ 728.2469; found 728.2426.

1-(3,4-Dimethoxyphenyl)-3-hydroxy-5,6-dimethoxy-1,3-dihydrobenzo[c]-thiophene-2,2-dioxide **138**

This compound was prepared by modified literature procedure.⁹³ The aldehyde **139** (1.93 g, 6.11 mmol) was dissolved in dry benzene (distilled from CaH₂, 50 mL) and pyridine added (10 μL). Benzene (150 mL) containing dissolved SO₂ (13.9 g) was added to the aldehyde solution and irradiated with a water-cooled 450-W Hanovia medium-pressure mercury lamp immersed in the solution for 6 h under a N₂ atmosphere. The solvent was evaporated at room temperature and traces of solvent and SO₂ removed by evaporation at high vacuum (0.5 mm, 25°C). The crude glassy yellow product was used immediately in the cycloaddition step without purification (see synthesis of compound **135**).

6-(3,4-Dimethoxybenzyl)veratraldehyde **139**

Method 1. The alcohol **154** (0.316 g, 1.00 mmol) and MnO₂ (5 mole equiv. 5.00 g) were refluxed in benzene for 4 h. The solution was filtered through silica gel and the solvent removed in vacuo. Chromatography on silica gel (30-50% ethyl acetate/hexanes) afforded the aldehyde as a light yellow solid (0.578 g, 58%).

Method 2. The alcohol **154** (0.230 g, 0.728 mmol) was dissolved in a solution of diethyl ether (20 mL) and THF (10 mL) and cooled in an ice bath. Chromium trioxide (0.5 M in 10% H₂SO₄, 3 mL, 1.5 mmol) was added and the solution stirred vigorously for 1 h. The layers were separated and the aqueous layer extracted with ethyl acetate. The combined organic extracts were washed with 5% aqueous NaHCO₃. The organic layer was dried (Na₂SO₄), filtered, and evaporated to give a yellow oil. Chromatography on silica (50% ethyl acetate/hexanes) afforded the aldehyde as a light yellow solid (0.143 g, 62%).

Method 3. The alcohol **154** (0.528 g, 1.66 mmol) and pyridinium chlorochromate (2 mole equiv., 0.715 g, 3.32 mmol) were stirred at rt in CH₂Cl₂ (20 mL) for 2 h. The solution was decanted and the black precipitate was washed with diethyl ether. The organic fractions were filtered through silica and the solvent evaporated. The crude product was chromatographed on silica (50% ethyl acetate/hexanes) to give a light yellow solid (77%). The spectroscopic properties were identical to those previously reported.⁹³

Method 4. The bromide **155** (2.18 g, 5.93 mmol) was dissolved in THF (50 mL) and cooled to -78°C under N₂. *n*-BuLi (2.5 M/hexanes, 1.2 eq, 7.12 mmol, 2.85 mL) was added and the solution stirred 1 minute followed by addition of DMF (3 eq, 1.38 mL). The solution was stirred 1 h at -78°C and then at room temperature for 50 minutes. The solution was quenched with aqueous 15% ammonium chloride, saturated with NaCl, extracted with CH₂Cl₂, dried (MgSO₄), and evaporated to give a yellow oil (1.81 g). The product was purified by silica gel chromatography (50% ethyl acetate/hexanes) giving a light yellow oil which crystallized on standing (1.76 g, 94%). The spectroscopic properties were identical to those reported in the literature.⁹³

*6-Bromoveratraldehyde*⁹³ **141**

Bromine (12.5 mL, 2 mole equiv.) was added to a solution of veratraldehyde (20 g, 120.4 mmol) in glacial acetic acid (100 mL). A precipitate began forming immediately

and the solution became completely solid after 1 h. The mixture was diluted with water (100 mL), cooled in an ice bath and filtered. The crude product was washed with 100 mL of cold water and recrystallized from 80:20 methanol/water (240 mL), filtered and washed with cold 80:20 methanol/water. The product was air dried at 50°C overnight to give a white crystalline solid (25.8 g, 88%).

α -(3,4-Dimethoxyphenyl)-6-bromoveratryl alcohol 142

4-Bromoveratrole (1.73 g, 7.97 mmol, 1.11 eq) was dissolved in THF (10 mL). The solution was cooled to -78 °C under N₂ and to this was added *n*-BuLi (1.86 M/hexanes, 4.25 mL, 7.91 mmol) dropwise. After 5 minutes, 6-bromoveratraldehyde **141** (1.76 g, 7.19 mmol) in THF (35 mL) was added and the solution warmed to room temperature. The orange solution was stirred 17 h and then quenched with 5% aqueous sodium bicarbonate (20 mL), saturated with NaCl, and finally extracted with ethyl acetate and the solvent evaporated. The yellow oil (3.35 g) was chromatographed on silica to give the pure product as a yellow oil (2.05 g, 74%). ¹H NMR (CDCl₃) δ : 7.08 (s, 1H), 7.00 (s, 1H), 6.97 (d, 1H, J = 1.9), 6.88 (dd, 1H, J = 1.9, 8.3), 6.81 (d, 1H, J = 8.3), 6.08 (s, 1H) 3.86 (s, 6H), 3.85 (s, 3H), 3.84 (s, 3H), 2.35 (bs, OH); ¹³C NMR (CDCl₃) δ : 148.91 (2 x C), 148.69 (C), 148.48 (C), 135.09 (C), 134.75 (C), 118.99 (CH), 115.33 (CH), 112.58(C), 110.94 (CH), 110.78 (CH), 110.09 (CH), 74.29 (CH), 56.18 (CH₃), 56.06 (CH₃), 55.88 (2 x CH₃); MS *m/e* (rel. %) 385 (10), 384 (M⁺, 52), 383 (12), 382 (53), 271 (16), 245 (31), 243 (28), 165 (43), 139 (100), 138 (46); HRMS calcd. for C₁₇H₁₉O₅Br: 382.0415, 384.0395; found: 382.0395, 384.0429.

6-Bromo-3,4,9,10-tetramethoxybenzophenone 143

The alcohol **142** (8.37 g, 21.8 mmol) and MnO₂ (5 mole equiv. 15 g) were refluxed in benzene for 2 days. The product was filtered and the solvent evaporated. The product was chromatographed on silica (30-50% ethyl acetate/hexanes) to give a yellow solid

(4.54 g, 60%). A sample was recrystallized from ethyl acetate/hexanes; mp 125-126°C; IR (CH₂Cl₂): 1661, 1593, 1510, 1270 cm⁻¹; ¹H-NMR (CDCl₃) δ: 7.54 (d, 1H, J = 1.9), 7.27 (dd, 1H, J = 1.9, 8.4), 7.09 (s, 1H), 6.89 (s, 1H), 6.86 (d, 1H, J = 8.4), 3.94 (s, 3H), 3.93 (s, 6H), 3.85 (s, 3H); ¹³C-NMR (CDCl₃) δ: 194.28 (CO), 153.85 (C), 150.60 (C), 149.24 (C), 148.19 (C), 132.78 (C), 129.53 (C), 126.28 (CH), 115.75 (CH), 112.02 (CH), 111.27 (CH), 110.64 (C-Br), 109.99 (CH), 56.36 (CH₃), 56.22 (CH₃), 56.15 (CH₃), 56.08 (CH₃); MS *m/e* (rel. %): 382 (M⁺, 58), 380 (M⁺, 58), 301 (100), 286 (15), 270 (59), 245 (20), 243 (24), 165 (94); HRMS calcd. for C₁₇H₁₇O₅Br: 380.0258, 382.0238; found: 380.0272, 382.0230.

3-Hydroxy-(3,4-dimethoxy-6-bromophenyl)-3-(3',4'-dimethoxyphenyl)propionitrile 144

n-Butyllithium (1.2 mole equiv. 1.86 M, 1.0 mL) was added dropwise to a cooled solution (-78°; dry ice/acetone) of diisopropylamine (1.41 mole equiv. 0.30 mL) and THF (8 mL) under N₂. The solution was then stirred 0.5 h with the subsequent addition of acetonitrile (0.1 mL, 1.91 mmol, 1.25 mole equiv.). After stirring for 10 min, the ketone **143** (0.584 g, 1.53 mmol) in THF (8 mL) was added over a period of 30 seconds. After 1 h, the solution was quenched with 5% aqueous NH₄Cl and then saturated with NaCl. The organic layer was removed and the aqueous phase extracted with ethyl acetate. The organic fractions were combined, dried (MgSO₄), and the solvent evaporated leaving a light yellow oil. The oil was crystallized from hexanes/CH₂Cl₂ to give a colourless product (0.522 g, 81%); mp 143-144°C; IR (CH₂Cl₂): 3589 (OH), 1514 (s) cm⁻¹; ¹H-NMR (CDCl₃) δ: 7.46 (s, 1H), 7.02 (s, 1H), 6.85 (s, 1H), 6.80 (s, 2H), 3.96 (s, 3H), 3.88 (s, 3H), 3.87 (s, 3H), 3.87 (s, 3H), 3.81 (s, 3H), 3.47 (s, 3H), 3.31 (br s, 1H, OH); ¹³C-NMR (CDCl₃) δ: 149.16 (C), 149.03 (2 x C), 147.99 (C), 135.80 (C), 133.80 (C), 118.73 (CH), 117.73 (CH), 117.10 (CN), 111.83 (CH), 111.60 (C-Br), 110.71 (CH), 109.70 (CH), 76.69 (C, benzylic), 56.28 (CH₃), 56.21 (CH₃), 56.02 (CH₃), 55.88 (CH₃), 30.91 (CH₂); MS *m/e* (rel. %): 423 (M⁺, 18), 421 (17), 405 (10), 403 (10), 383 (85), 381

(83), 324 (23), 301 (47), 293 (51), 270 (27), 245 (75), 243 (79), 165 (100), 149 (55);
 HRMS calcd. for $C_{19}H_{20}O_5NBr$: 423.0504, 421.0524; found 423.0502, 421.0506.

3-(3,4-Dimethoxy-6-bromophenyl)-3'-(3',4'-dimethoxyphenyl)acrylonitrile 145

The alcohol **144** (0.518 g, 1.23 mmol) as refluxed in benzene (30 mL) in the presence of *p*-toluenesulfonic acid (39 mg) for 30 min. The solution was cooled and extracted with 5% aqueous $NaHCO_3$ (2 x 10 mL). The organic layer was dried ($MgSO_4$) and the solvent evaporated to give a brown oil which solidified on standing. The sample was carried over for the synthesis of **146**. 1H -NMR ($CDCl_3$) of the mixture of alkenes; δ : 7.26 (s), 7.12 (s, 1H), 7.06 (s, 0.46H), 6.93 (dd, 0.42H, $J = 2.1, 8.4$), 6.85 (s, 1.41H), 6.81 (s, 1H), 5.42 (s, 0.42H), 3.965 (s), 3.946 (s), 3.928 (s), 3.907 (s), 3.897 (s), 3.888 (s), 3.872 (s), 3.848 (s); MS *m/e* (rel. %): 405 (M^+ , 10), 403 (M^+ , 10), 324 (-Br, 37), 309 (8), 293 (100), 278 (22), 266 (9), 250 (8); HRMS calcd. for $C_{19}H_{18}O_4NBr$: 403.0419, 405.0399; found 403.0748, 405.0455.

3-(3,4-Dimethoxy-6-bromophenyl)-3-(3'4'-dimethoxyphenyl)-propionitrile 146

Magnesium turnings (0.35 g, 14.4 mmol) and a small crystal of iodine were gently warmed in methanol (5 mL) until the evolution of hydrogen gas became quite vigorous. At this point, the solution was cooled in a dry ice/ CCl_4 bath ($-23^\circ C$) and the alkene (0.496 g, 1.23 mmol) in dry THF (9 mL) was added to the methanol solution. The mixture was stirred 3.5 h at which point the TLC (30% ethyl acetate/hexanes) indicated that the reaction was completed. The excess magnesium was destroyed by the addition of 10% aqueous HCl (under N_2). The mixture was extracted (CH_2Cl_2), dried ($MgSO_4$) and the solvent evaporated leaving a brown oil. The product was purified on silica gel using 20-40% ethyl acetate/hexanes (0.489 g, 98%); IR (CH_2Cl_2): 1599 (w), 1513 (s), 1464 (m), 1278 (m), 1028 (m), 789 (m) cm^{-1} ; 1H -NMR ($CDCl_3$) δ : 7.13 (s, 1H), 6.86 (s, 2H), 6.74 (s, 1H), 6.64 (s, 1H), 4.78 (t, 1H, $J=7.1$), 3.88 (s, 3H), 3.87 (s, 3H), 3.84 (s, 3H), 3.76 (s,

3H), 3.08-2.93 (m, ABX, 2H). $^{13}\text{C-NMR}$ (CDCl_3) δ : 149.16 (C), 148.83 (C), 148.71 (C), 148.35 (C), 132.53 (C), 132.39 (C), 119.18 (CH), 118.15 (C), 115.81 (CH), 114.37 (C), 111.48 (3 x CH), 111.20 (CH), 56.15 (2 x CH_3), 55.95 (CH_3), 55.86 (CH_3), 44.86 (CH), 23.24 (CH_2). MS *m/e* (rel. %): 407 (35), 405 (37), 367 (97), 365 (100), 286 (73), 285 (79), 271 (51), 255 (13), 212 (21). HRMS calcd. for $\text{C}_{19}\text{H}_{20}\text{O}_4\text{NBr}$ 405.0575, 407.0555; found 405.0556, 407.0556.

Ethyl-3-(3,4-dimethoxy-6-bromophenyl)-3-(3',4'-dimethoxyphenyl)-propionate 147

The nitrile **146** (0.199 g, 0.490 mmol) was dissolved in absolute ethanol (7 mL) and the solution saturated with HCl gas. Methylene chloride (2 mL) was added and the solution refluxed for 1 h and then stirred at 25°C for 24 h. Ethanol (8 mL) and water (0.8 mL) were added and the solution refluxed 4 h, cooled, and diluted with water. The mixture was extracted with CH_2Cl_2 , dried (MgSO_4), and the solvent evaporated to give a dark oil (0.166 g). The product was chromatographed on silica (30% ethyl acetate/hexanes) to give a colorless oil which crystallized on standing (0.1041 g, 47%). mp 64-66°C. IR (CH_2Cl_2): 1733 (s), 1599, 1512 (s), 1247 (s), 1029 (s) cm^{-1} ; $^1\text{H-NMR}$ (CDCl_3) δ : 6.98 (s, 1H), 6.75 (br s, 3H), 6.70 (s, 1H), 4.89 (t, 1H, $J = 8.1$), 4.05 (q, 2H $J = 7.1$), 3.83 (s, 6H), 3.83 (s, 3H), 3.79 (s, 3H), 2.98 (d, 2H, $J = 8.1$), 1.14 (t, 3H, $J = 7.1$); $^{13}\text{C-NMR}$ (CDCl_3) δ : 171.29 (CO), 148.85 (C), 148.46 (C), 148.12 (C), 147.70 (C), 134.83 (C), 134.54 (C), 119.18 (CH), 115.80 (CH), 114.50 (C), 111.55 (CH), 111.27 (CH), 111.08 (CH), 60.51 (CH_2), 56.09 (CH_3), 56.07 (CH_3), 55.84 (CH_3), 55.81 (CH_3), 44.97 (CH), 40.53 (CH_2), 14.12 (CH_3); MS *m/e* (rel. %): 454 (M^+ , 22), 452 (M^+ , 22), 373 (100), 367 (21), 365 (21), 286 (33), 285 (36), 271 (16), 255 (8); HRMS calcd. for $\text{C}_{21}\text{H}_{25}\text{O}_6\text{Br}$ 452.0834, 454.0814; found 452.0840, 454.0789.

6-Bromoveratraldehyde-(ethylene glycol acetal) 148⁹³

6-bromoveratraldehyde (6.277 g, 25.60 mmol) and ethylene glycol (3.20 g, 2.02

mole equiv.) were refluxed in benzene (60 mL) for 2 h in the presence of *p*-toluenesulfonic acid (0.09 g) using a Dean-Stark trap to remove water. The solution was filtered through 4 inches of silica using 50% ethyl acetate/hexanes. The solvent was evaporated and the solid crystallized from methylene chloride/hexanes to give 6.129 g (83%) of colourless crystals (mp 109-110°C). The product had spectroscopic properties identical to those previously reported.⁹³

1-Hydroxy-2-(3,4-dimethoxyphenyl)-6,7-dimethoxybenzofuran 150

n-BuLi (2.03 M, 1.05 mole equiv. 3.55 mL) was added to a solution of dry THF (20 mL) at -78°C (under N₂). A solution of **148** (2.03 g, 7.02 mmol) in THF (20 mL) was then added dropwise over a period of 6.5 minutes. After 1 minute, veratraldehyde (1.07 mole equiv. 1.22 g, 7.35 mmol) in THF (5 mL) was subsequently added over a period of 10 minutes. After a further 19 minutes at -78°C, the solution was warmed to room temperature, sealed, and stirred at room temperature for 16.5 hours. The solution was quenched with 5% aqueous NH₄Cl (40 mL) and extracted with CH₂Cl₂, dried (MgSO₄) and evaporated to give a yellow oil. The oil was chromatographed on silica (60% ethyl acetate/hexanes) to give an oil (2.029 g; 79%) which crystallized on standing (mp 138-139°C). ¹H-NMR (CDCl₃/TMS) δ: 7.14 (s, 1H), 6.99 (d, 1H, J = 1.72), 6.89 (dd, 1H, J = 8.28, 1.72), 6.84 (d, 1H, J = 8.28), 6.77 (s, 1H), 6.14 (d, 1H, J = 3.93), 5.92 (s, 1H), 4.16, 4.04 (4H, m, CH₂), 3.91 (s, 3H), 3.88 (s, 3H), 3.76 (s, 3H), 3.57 (s, 3H), 3.18 (d, 1H, J = 3.93, OH). The ¹H-NMR was identical to that previously reported.¹⁰⁷

5,6-Dimethoxy-3-(3,4-dimethoxyphenyl)phthalide 152

The acetal **150** (0.540 g, 1.44 mmol) was dissolved in 30 mL of a 9:1 methanol/water solution. This solution was stirred in the presence of Dowex cation exchange resin (50W-X8, 2.0 g, prewashed with methanol) for 2 h. The solution was filtered and the solvent concentrated in vacuo leaving a gummy red oil. This oil was

dissolved in ethyl acetate (10 mL) and diethyl ether (20 mL). A solution of CrO_3 (0.5 M in 10% aqueous H_2SO_4 , 8.7 mL, 3 mole equiv.) was added to the lactol (**151**) solution at 0°C which produced a cream coloured precipitate. After stirring 2 h, the solution was separated and the aqueous layer extracted with ethyl acetate and the combined organic extracts washed with 5% aqueous NaHCO_3 solution. The organic fraction was dried (MgSO_4) and filtered through silica to remove any remaining chromium salts. The solvent was evaporated and the resulting oil chromatographed on silica (70% ethyl acetate/hexanes) to give a cream coloured solid (0.412 g, 86%); mp $184\text{-}185^\circ\text{C}$; IR (CH_2Cl_2) cm^{-1} : 1762; $^1\text{H-NMR}$ (CDCl_3) δ : 7.34 (s, 1H), 6.87 (s, 2H), 6.68 (s, 1H), 6.66 (s, 1H), 6.24 (s, 1H), 3.97 (s, 3H), 3.89 (s, 6H), 3.81 (s, 3H); $^{13}\text{C-NMR}$ (CDCl_3) δ : 170.69 (CO), 155.0 (C), 150.67 (C), 149.96 (C), 149.45 (C), 144.13 (C), 128.83 (C), 120.29 (CH), 117.86 (C), 111.17 (CH), 110.06 (CH), 105.86 (CH), 104.08 (CH), 82.42 (CH), 56.40 (2 x CH_3), 56.34 (CH_3), 55.99 (CH_3); MS *m/e* (rel. %): 330 (M^+ , 99), 299 (33), 271 (16), 207 (36), 182 (48), 165 (100), 149 (64), 135 (60); HRMS calcd. for $\text{C}_{18}\text{H}_{18}\text{O}_6$ 330.1103; found 330.1111.

3,4-Dimethoxy-6-(3,4-dimethoxybenzyl)benzoic acid 153.

The phthalide **152** (1.917 g, 5.80 mmol) was dissolved in glacial acetic acid (65 mL) and hydrogenolysed over 5% palladium/carbon (140 mg) at 110°C for three days (1 Atm H_2). The product was filtered through silica using ethyl acetate as eluent and the solvent evaporated to give a white solid. The solid was air dried overnight (1.866 g, 97%). mp $152\text{-}157^\circ\text{C}$; IR (CH_2Cl_2): 1735 cm^{-1} ; $^1\text{H-NMR}$ (CDCl_3) δ : 7.60 (s, 1H), 6.75 (m, 2H), 6.66 (m, 2H), 4.37 (s, 2H), 3.92 (s, 3H), 3.84 (s, 3H), 3.83 (s, 3H), 3.82 (s, 3H); $^{13}\text{C-NMR}$ (CDCl_3) δ : 171.33 (CO), 152.71 (C), 148.80 (C), 147.28 (C), 146.80 (C), 138.74 (C), 133.52 (C), 120.74 (CH), 119.62 (C), 114.11 (CH), 113.93 (CH), 112.40 (CH), 111.14 (CH), 56.03 (CH_3), 55.90 (CH_3), 55.88 (CH_3), 55.80 (CH_3), 38.97 (CH_2); MS *m/e* (rel. %): 332 (M^+ , 54), 314 (27), 299 (9), 283 (18), 271 (12), 193 (15), 165 (14), 149 (69), 69 (39),

57 (100); HRMS calcd. for $C_{18}H_{20}O_6$ 332.1260; found 332.1250.

6-(3,4-Dimethoxybenzyl)-veratryl alcohol 154.

The acid **153** (2.555 g, 7.687 mmol) was dissolved in dry THF (75 mL). Powdered $LiAlH_4$ (0.584 g, 2.0 mole equiv.) was added to the solution (effervescence) with vigorous stirring in an ice bath. The solution was stirred two days at room temperature. The reaction was worked up by the addition of water (0.6 mL), then 15% NaOH solution (0.06 mL), and finally water (1.8 mL). The resultant grey suspension was stirred 15 minutes and then filtered using ethyl acetate as eluent. The solvent was evaporated and the crude oil chromatographed on silica (70% ethyl acetate/hexanes) to give a beige solid (2.389 g, 98%); mp 103-105°C, lit mp 103-105°C¹⁰⁷. The 1H -NMR of **154** was identical to that reported previously.¹⁰⁷ MS *m/e* (rel. %): 319 (8), 318 (M^+ , 39), 300 (30), 299 (13), 285 (13), 270 (20), 269 (100), 254 (10), 238 (16), 180 (25), 179 (10), 139 (17); HRMS calcd. for $C_{18}H_{22}O_5$: 318.1467; found 318.1461.

1-(3,4-Dimethoxybenzyl)-6-bromoveratrole 155

To a solution of glacial acetic acid (15 mL) and trifluoroacetic acid (15 mL) at 0°C was added $NaBH_4$ (10 eq, 1.36 g). The alcohol **142** (1.38 g, 3.60 mmol) in CH_2Cl_2 (20 mL) was immediately added giving a dark purple solution which was stirred 1 minute followed by the rapid addition of 5 more equivalents of $NaBH_4$. The solution turned yellow immediately and stirring was continued for another 5 minutes. The sample was diluted with H_2O (40 mL) and extracted with CH_2Cl_2 , dried ($MgSO_4$), and evaporated to give a brown oil. The oil was chromatographed on silica (25 % ethyl acetate/hexanes) giving an oil (1.25 g, 95%). The sample could be crystallized from 2-propanol (0.960 g, 73%) to give a colourless solid; mp 72-73°C; IR (CH_2Cl_2) 1509 (vs), 1029 (s) cm^{-1} ; 1H -NMR ($CDCl_3$) δ : 7.04 (s, 1H), 6.80 (d, 1H, $J = 8.1$), 6.74 (d, 1H, $J = 1.44$), 6.69 (1H, dd, $J = 1.44, 8.1$), 6.64 (s, 1H), 3.99 (s, 2H), 3.86 (s, 6H), 3.84 (s, 3H), 3.76 (s, 3H);

^{13}C -NMR (CDCl_3) δ : 148.91 (C), 148.42 (C), 148.05 (C), 147.46 (C), 132.48 (C), 132.41 (C), 120.66 (CH), 115.52 (CH), 113.54 (CH), 112.11 (CH), 111.20 (CH), 114.42 (C), 56.17 (CH_3), 56.00 (CH_3), 55.88 (CH_3), 55.83 (CH_3), 40.84 (CH_2); MS *m/e* (rel. %) 369 (16), 368 (M^+ , 85), 367 (17), 366 (84), 288 (8), 287 (38), 257 (31), 256 (100), 241 (36), 229 (24), 225 (11); HRMS calcd. for $\text{C}_{17}\text{H}_{19}\text{O}_4\text{Br}$ 366.0466, 368.0446; found 366.0459, 368.0456.

Elimination product 160

The cycloadduct **135** (0.362 g, 0.496 mmol) was stirred in anhydrous NaOMe/methanol (0.1 M, 40 mL, 8 eq) at rt for 1 day. The solution was acidified with 20% HCl (pH ca. 1-2) and extracted with CH_2Cl_2 , dried (MgSO_4), and the solvent evaporated to leave a yellow oil. The oil was chromatographed on silica (45% ethyl acetate/5% glacial acetic acid/hexanes) to give a yellow oil (0.207 g, 97%); $[\alpha]_{\text{D}}^{20}$ -321° (c 0.67, CHCl_3); IR: 1743 (w), 1711 (s) cm^{-1} ; ^1H -NMR δ : 7.64 (s, 1H, alkene), 6.87-6.84 (m, 4H), 6.59 (s, 1H), 4.51 (d, 1H, $J_{1,2} = 7.7$, H1), 3.93 (d, 1H, $J_{2,1} = 7.7$, H2), 3.89 (s, 3H), 3.88 (s, 3H), 3.81 (s, 3H), 3.77 (s, 3H), 3.70 (s, 3H); ^{13}C -NMR (CDCl_3) δ : 174.54 (CO), 167.15 (CO), 150.66 (C), 148.85 (C), 148.47 (C), 147.73 (C), 139.27 (CH), 139.03 (CH), 124.49 (C), 123.64 (C), 122.02 (CH), 112.59 (CH), 112.45 (CH), 111.25 (CH), 111.14 (CH), 56.06 (CH_3), 55.95 (CH_3), 55.83 (CH_3), 55.79 (CH_3), 52.05 (CH_3), 47.55 (CH, C), 46.83 (CH); MS *m/e* (rel. %) 429 (1.5), 428 (6.3, M^+), 396 (36.5), 395 (25.7), 394 (100), 382 (42.8), 351 (27.4), 138 (17.6), 60 (9.7); HRMS calcd. for $\text{C}_{23}\text{H}_{24}\text{O}_8$ 428.1471; found 428.1475.

3-Carbomethoxy-(6,7-dimethoxy)-1-(1,2-cis)-(3',4'-dimethoxyphenyl)-1,2,3,4-tetrahydronaphthalene-(2,3-cis)-2-carboxylic acid 162

The alkene **160** (0.280 g, 0.654 mmol) was dissolved in a mixture of ethyl acetate (30 mL) and acetic acid (10 mL) and Pd/C (5% Pd, dry, 129 mg) was catalyst added. The

mixture was stirred under H₂ (1 Atm, rt) for 24 h followed by filtration through silica (ethyl acetate eluent) and evaporation to give a beige solid (0.288 g). The solid was recrystallized from CH₂Cl₂/hexane to give a colourless solid (242 mg, 86%); mp 195-196°; IR (CH₂Cl₂): 3057 (COOH), 1734 (vs, CO), 1712 (m, CO) cm⁻¹; [α]_D²⁰ -88° (c 0.284, CHCl₃); ¹H-NMR (CDCl₃) δ : 6.81 (s, 2H), 6.73 (s, 1H), 6.66 (s, 1H), 6.43 (s, 1H), 4.40 (d, 1H, J_{1,2} = 6.0, H1), 3.87 (s, 6H), 3.74 (s, 3H), 3.70 (s, 3H), 3.61 (s, 3H), 3.51 (m, 2H, H2, H4a), 3.18 (ddd, 1H, J_{2,3} = 3.68, J_{3,4e} = 5.47, J_{3,4a} = 12.17, H3), 3.00 (dd, J_{4e,4a} = 16.35, J_{4e,3} = 5.45, H4e); ¹³C-NMR δ : 175.69 (CO), 173.25 (CO), 148.61 (C), 148.09 (C), 147.61 (C), 147.12 (C), 133.46 (C), 127.58 (2 x C), 122.18 (CH), 112.79 (CH), 111.88 (CH), 111.14 (CH), 110.92 (CH), 55.92 (CH₃), 55.85 (CH₃), 55.79 (CH₃), 55.74 (CH₃), 52.12 (CH₃), 47.90 (CH), 47.83 (CH), 42.50 (CH), 28.15 (CH₂); MS *m/e* (rel. %): 399 (18), 398 (-CH₃OH, 71), 370 (9), 339 (7), 325 (23), 299 (8), 285 (10), 270 (21), 269 (100), 238 (15), 151 (12); HRMS calcd. for C₂₃H₂₆O₈ 430.1628; found 430.1589, HRMS calcd. for C₂₂H₂₂O₇ (- CH₃OH) 398.1365; found 398.1346.

(+)-Picrodimethylretrodendrin 163

Acid-ester **162** (64.0 mg, 0.149 mmol) was dissolved in THF (15 mL). A solution of LiEt₃BH (1 M, 5.7 eq, 0.84 mL) in THF was added at room temperature under a N₂ atmosphere. Upon initial addition, the solution effervesced and a slight cloudiness persisted for about 2 minutes. Stirring at room temperature was continued for 19 h. Amberlite resin (Aldrich, IRC 718, ion-exchange, 1.0 g) was added and the solution diluted with 20% HCl (5 mL). After 2 h the solution was filtered through silica (70-270 mesh, THF eluent), extracted (ethyl acetate), dried (MgSO₄) and the solvent evaporated to give a yellow oil (0.0848 g). The crude mixture was dissolved in benzene (dry, 25 mL) and refluxed with a trace of *p*-TsOH (1 mg) for 14 h. The solvent was evaporated and the brownish oil chromatographed on silica (40-50% ethyl acetate/hexanes) giving a clear oil (48.2 mg 84%); [α]_D²⁰ +143° (c 0.93, CHCl₃); IR (CH₂Cl₂): 1768 (lactone CO) cm⁻¹;

$^1\text{H-NMR}$ (CDCl_3) δ : 6.87 (d, 1H, $J = 2.1$, $\text{H}2'$), 6.77 (s, 1H, $\text{H}5$), 6.72 (d, 1H, $J = 8.3$, $\text{H}5'$), 6.71 (s, 1H, $\text{H}8$), 6.51 (dd, 1H, $J = 2.2, 8.3$, $\text{H}6'$), 4.52 (d, 1H, $J_{1,2} = 5.53$, $\text{H}1$), 4.38 (t, 1H, $J = 8.5$, $\text{H}11_\beta$), 3.91 (s, 3H), 3.84 (s, 3H), 3.81 (s, 6H), 3.35 (t, 1H, $J = 8.5$, $\text{H}11_\alpha$), 3.15 (m, 1H, $\text{H}3$), 3.07 (dd, 1H, $J_{2,1} = 5.53$, $J_{2,3} = 10.1$, $\text{H}2$), 2.99 (dd, 1H, $J_{4\beta,3} = 8.96$, $J_{4\beta,4\alpha} = 15.7$, $\text{H}4_\beta$), 2.71 (dd, 1H, $J_{4\alpha,3} = 6.12$, $J_{4\alpha,4\beta} = 15.7$, $\text{H}4_\alpha$); $^{13}\text{C-NMR}$ (CDCl_3) δ : 178.04 (CO), 148.77 (C), 148.17 (C), 148.01 (2 x C), 131.00 (C), 130.64 (C), 127.74 (C), 120.78 (CH), 112.64 (CH), 111.77 (CH), 111.53 (CH), 110.90 (CH), 74.23 (CH_2), 56.06 (CH_3), 55.96 (CH_3), 55.86 (CH_3), 55.79 (CH_3), 46.65 (CH), 44.60 (CH), 34.71 (CH), 29.86 (CH_2); MS *m/e* (rel. %): 386 (5), 385 (23), 384 (M^+ , 100), 353 (19), 325 (18), 312 (15), 299 (16), 270 (15), 269 (74), 151 (13), 84 (13); HRMS calcd. for $\text{C}_{22}\text{H}_{24}\text{O}_6$ 384.1573; found 384.1570.

3-Carbomethoxy-(6,7-dimethoxy)-1-(1,2-cis)-(3',4'-dimethoxyphenyl)-1,2,3,4-tetrahydro naphthalene-(2,3-trans)-2-carboxylic acid 164

The micro-half-ester **162** (0.247 g, 0.574 mmol) was dissolved in anhydrous NaOMe/methanol (0.1 M, 40 mL, 7 eq) and refluxed under N_2 for 20 h. The solution was acidified (20% HCl) and extracted with CH_2Cl_2 (3 x 15 mL). The organic layer was dried (MgSO_4) and the solvent evaporated giving a yellow oil (0.25 g). The oil was chromatographed on silica (35% ethyl acetate/5% glacial acetic acid/hexanes) giving a light yellow oil (0.205 g, 83%); IR (CH_2Cl_2): 1734 (CO), 1711 (CO) cm^{-1} ; $[\alpha]_D^{20} +163^\circ$ (c 0.278, CHCl_3); $^1\text{H-NMR}$ (CDCl_3) δ : 6.69 (d, 1H, $J = 8.34$, $\text{H}5'$), 6.66 (s, 1H, $\text{H}5$), 6.58 (d, 1H, $J = 1.91$, $\text{H}2'$), 6.41 (s, 1H, $\text{H}8$), 6.40 (dd, $J = 8.34, 1.91$, $\text{H}6'$), 4.56 (d, 1H, $J_{1,2} = 5.4$, $\text{H}1$), 3.87 (s, 3H), 3.81 (s, 3H), 3.74 (s, 3H), 3.72 (s, 3H), 3.67 (s, 3H), 3.37 (dd, 1H, $J_{2,1} = 5.4$, $J_{2,3} = 11.7$, $\text{H}2$), 3.23 (dd, 1H, $J_{4e,3} = 5.7$, $J_{4e,4a} = 15.8$, $\text{H}4e$), 3.11 (dt, 1H, $J_{3,2} = 11.8$, $J_{3,4e} = 5.7$, $\text{H}3$), 2.88 (dd, 1H, $J_{4a,3} = 11.7$, $J_{4a,4e} = 15.7$, $\text{H}4a$); $^{13}\text{C-NMR}$ (CDCl_3) δ : 178.08 (CO), 175.46 (CO), 148.44 (C), 148.11 (C), 147.98 (2 x C), 133.92 (C), 128.68 (C), 125.57 (C), 121.67 (CH), 112.62 (CH), 112.24 (CH), 110.90 (CH), 110.34 (CH), 55.94

(CH₃), 55.85 (CH₃), 55.80 (CH₃), 55.70 (CH₃), 52.02 (CH₃), 47.79 (CH), 45.51 (CH), 36.94 (CH), 31.99 (CH₂); MS *m/e* (rel. %): 399 (26), 398 (- CH₃OH, 100), 370 (10), 339 (10), 325 (36), 270 (20), 269 (93), 238 (15), 151 (21); HRMS calcd. for C₂₃H₂₆O₈ 398.1365 (-CH₃OH); found 398.1364.

2,3-Trans-acid-alcohol **165**

The half-ester **162** (80 mg, 0.187 mmol) was dissolved in dry THF (20 mL) and the system placed under N₂. LiEt₃BH (10 eq, 2 mL, 1.0 M, in THF) was added dropwise to the solution with concomitant evolution of gas (orange to yellow colour change). The reaction was stirred at rt for 23 h, acidified with dilute HCl (20%, pH 1) followed by the addition of Amberlite resin (Aldrich, IRC 718, 3.2 g). After stirring 3 h, the suspension was filtered (ethyl acetate eluent) and dried (MgSO₄). Evaporation of the solvent gave a yellow oil which was chromatographed on silica (4% glacial acetic acid/66% ethyl acetate/hexanes) to give a colourless oil (57.1 mg, 76%); [α]_D²⁰ +177 (c 0.487, CHCl₃); IR (CH₂Cl₂): 1701 (br, CO acid), 1142 (1° OH) cm⁻¹; ¹H-NMR (CDCl₃) δ: 6.69 (d, 1H, J = 8.3, H5'), 6.65 (s, 1H, H5), 6.59 (bs, 1H, H2'), 6.47 (dd, 1H, J = 8.2, ca 1, H6'), 6.41 (s, 1H, H8), 4.46 (d, 1H, J_{1,2} = 5.3, H1), 4.5 (bs, OH), 3.87 (s, 3H), 3.79 (s, 3H), 3.74 (s, 3H), 3.71 (s, 3H), 3.7 (m, 2H, CH₂OH; from COSY 45), 3.02 (m, 2H, H_{4eq}, H2), 2.75 (dd, 1H, J = 11.0, 16.8, H_{4ax}, 2.34 (br m, 1H, H3); ¹³C-NMR (CDCl₃) δ: 178.15 (CO), 148.15 (C), 147.91 (C), 147.78 (C), 147.58 (C), 134.66 (C), 129.10 (C), 127.30 (C), 121.82 (CH), 113.02 (CH), 112.07 (CH), 110.77 (2 x CH), 65.34 (CH₂), 55.86 (CH₃), 55.83 (CH₃), 55.81 (CH₃), 55.70 (CH₃), 46.79 (2 x CH), 32.38 (CH), 31.60 (CH₂); MS *m/e* (rel. %): 403 (2), 402 (M⁺, 4), 386 (4), 385 (25), 384 (-H₂O, 100), 353 (8), 339 (11), 325 (10), 269 (17), 246 (15), 201 (13), 151 (22); HRMS calcd. for C₂₂H₂₆O₇: 402.1679, found 402.1687, HRMS calcd. -H₂O 384.1573; found 384.1576.

(+)-Isodimethylretrodendrin **166**

Method A. The acid-alcohol **165** (11.9 mg, 0.0296 mmol) was refluxed in dry

benzene (4 mL) over molecular sieves (0.33 g, 4 Å) in the presence of *p*-TsOH (1.3 mg) for 2.5 h. The solution was filtered through silica (ethyl acetate eluent) and the solvent evaporated to give a clear oil (6.0 mg, 53%).

Method B. The half-ester **164** (69.6 mg, 0.162 mmol) was dissolved in dry THF (10 mL) and LiEt₃BH (1.0 M/THF, 5 eq, 0.81 mL) was added under an N₂ atmosphere. The solution was stirred at room temperature for 15 h followed by addition of Amberlite resin (Aldrich, IRC-718) (evolution of gas). Dilute HCl (20%, 10 mL) was added and the mixture stirred for 7 h. Filtration and evaporation under a slight vacuum (ca. 200 mm) gave a crystalline residue (280 mg) which was dissolved in a mixture of CH₂Cl₂ (10 mL), H₂O (10 mL) and methanol (2 mL). The organic fraction was separated and the aqueous layer extracted with CH₂Cl₂ (2 x 10 mL). The combined organic extracts were dried (MgSO₄) and the solvent evaporated. The yellow oil was placed under high vacuum (1 mm, 50 °C, 1 hr) to give a viscous oil (63.4 mg). Chromatography on silica (30-50% ethyl acetate/hexanes) afforded the pure product (49.3 mg, 79%); [α]_D²⁰ +115° (c 0.32, CHCl₃); IR (CH₂Cl₂) 1779 cm⁻¹; ¹H-NMR (CDCl₃) δ: 6.95 (d, 1H, J = 2.0, H2'), 6.68 (s, 1H, H5), 6.67 (d, 1H, J = 8.3, H5'), 6.52 (s, 1H, H8), 6.36 (dd, 1H, J = 2.0, 8.3, H6'), 4.64 (d, 1H, J_{1,2} = 3.4, H1), 4.44 (dd, 1H, J_{11β,3} = 6.2, J_{11β,11α} = 8.6, H11β), 3.92 (t, 1H, J = 9.9, H11α), 3.90 (s, 3H), 3.84 (s, 3H), 3.81 (s, 3H), 3.75 (s, 3H), 3.12-3.06 (m, 1H, H3), 2.83-2.70 (m, 3H, H2, H4_α, H4_β); ¹³C-NMR (CDCl₃) δ: 175.10 (CO), 148.23 (C), 148.03 (2 x C), 147.87 (C), 133.48 (C), 129.83 (C), 127.07 (C), 122.61 (CH), 114.41 (CH), 113.22 (CH), 111.35 (CH), 110.32 (CH), 72.15 (CH₂), 55.90 (3 x CH₃), 55.79 (CH₃), 47.65 (CH), 42.88 (CH), 32.70 (CH₂, CH); MS *m/e* (rel. %): 385 (26), 384 (M⁺, 100), 369 (3), 353 (9), 339 (11), 325 (8), 299 (8), 281 (8), 269 (17), 246 (17), 201 (17), 151 (27), 84 (29), 57 (30); HRMS calcd. for C₂₂H₂₄O₆ 384.1573; found 384.1594.

(-)-Isopicrodimethylretrodendrin 167

Isodimethylretrodendrin **166** (0.022g, 0.056 mmol) was refluxed in sodium

t-butoxide/*t*-butanol solution (10 mL, 0.1 M) for 13 h under N₂. The cloudy solution was acidified (10% HCl) to produce a homogeneous yellow solution which was extracted with CH₂Cl₂, dried (MgSO₄), and the solvent evaporated to give a yellow oil. Chromatography on silica gel (50% ethyl acetate/hexanes) afforded **167** as a yellow solid (18.9 mg, 87%); $[\alpha]_D^{20}$ -17.2° (c 0.376); IR (CH₂Cl₂): 1769, 1514 (s) cm⁻¹; ¹H-NMR (CDCl₃) δ: 6.77 (d, 1H, J = 8.3, H5'), 6.69 (d, J = 1.7, H2'), 6.68 (s, 1H, H5), 6.62 (s, 1H, H8), 6.57 (dd, 1H, J = 8.3, 1.7), 4.44 (m, 2H, H1, H11_β), 3.96 (dd, 1H, J_{11α,3} = 3.4, J_{11α,11β} = 9.1, H11_α), 3.88 (s, 3H), 3.85 (s, 3H), 3.81 (s, 3H), 3.78 (s, 3H), 3.32 (dd, 1H, J_{2,1} = 2.8, J_{2,3} = 9.6, H2), 3.03 (m, 1H, H3), 2.89 (dd, 1H, J_{4β,3} = 6.5, J_{4β,4α} = 15.4, H4_β), 2.51 (dd, 1H, J_{4α,3} = 5.1, J_{4α,4β} = 15.4, H4_α); ¹³C-NMR (CDCl₃) δ: 148.48 (CO), 149.10 (C), 148.13 (C), 148.03 (C), 147.73 (C), 135.35 (C), 129.28 (C), 126.90 (C), 119.68 (CH), 112.63 (CH), 111.70 (2 x CH), 111.14 (CH), 72.87 (CH₂), 55.94 (2 x CH₃), 55.91 (2 x CH₃), 46.62 (CH), 44.35 (CH), 32.78 (CH), 31.47 (CH₂); MS *m/e* (rel. %): 385 (24), 384 (M⁺, 100), 369 (8), 353 (22), 339 (11), 325 (22), 312 (20), 299 (14), 269 (36), 246 (14); HRMS calcd. for C₂₂H₂₄O₆ 384.1573; found 384.1580.

Di-(R-α-methoxycarbonylbenzyl)-1(S)-hydroxy-1(S)-phenyl-1,2,3,4-tetrahydronaphthalene-2(R)-3(S)-dicarboxylate 168

1-Phenyl-benzocyclobuten-1-ol **51** (0.234 g, 1.18 mmol) and fumarate **118** (1 mole equiv. 0.489 g) were refluxed in toluene (5 mL) for 5 h. The solvent was evaporated to give a cream coloured solid which was recrystallized from ethyl acetate/hexanes to give a white powder (0.408 g, 57%); mp 163-165°C; $[\alpha]_D^{20}$ -182° (C 0.247, CHCl₃); IR (CH₂Cl₂) 3448 (OH), 1744 (CO) cm⁻¹; ¹H-NMR (CDCl₃) δ: 7.53 (d, 2H, J = 7.0), 7.47-7.06 (m, 14H), 6.95 (d, 1H, J = 7.6), 6.79 (d, 2H, J = 7.2), 5.93 (s, 1H), 5.73 (s, 1H), 4.10 (s, 1H, OH), 3.91 (d, 1H, J_{2,3} = 11.7, H2), 3.79-3.70 (m, H3), 3.73 (s, 3H), 3.63 (s, 3H), 3.52 (dd, 1H, J_{4e,3} = 4.48, J_{4eq,4ax} = 16.4, H4_{eq}), 3.22 (dd, 1H, J_{4ax,3} = 12.62, J_{4ax,4eq} = 16.4, H4_{ax}); ¹³C-NMR (CDCl₃) δ: 174.14 (CO), 171.30 (CO), 169.64 (CO), 169.24 (CO),

146.72 (C), 140.34 (C), 133.28 (C), 133.10 (C), 132.62 (C), 130.27 (CH), 129.18 (CH), 128.83 (CH), 128.71 (2 x CH), 128.30 (2 x CH), 128.17 (CH), 128.09 (2 x CH), 127.68 (CH), 127.55 (2 x CH), 127.14 (2 x CH), 127.09 (CH), 126.64 (CH), 126.64 (CH), 126.34 (2 x CH), 74.82 (CH), 74.66 (CH), 55.04 (CH), 52.89 (CH₃), 52.60 (CH₃), 39.54 (CH), 32.87 (CH₂); MS *m/e* (rel. %): 293 (3), 249 (8), 232 (9), 231 (4), 206 (19), 205 (100), 204 (15), 203 (19), 202 (16), 195 (11), 190 (4), 150 (19), 149 (37), 127 (7), 121 (20), 107 (45), 105 (19); Analysis calcd. for C₃₆H₃₂O₉: C 71.04%, H 5.30; found C 70.63%, H 5.38%.

Di-(R- α -methoxycarbonylbenzyl)-1(S)-phenyl-1,2,3,4-tetrahydro naphthalene-2(S),3(S)-dicarboxylate 169

Method 1. Cycloadduct **171** (137 mg, 0.225 mmol) was dissolved in CH₂Cl₂ (10 mL). While under a stream of N₂, PBr₃ (50 μ L, 0.143 g, 0.526 mmol, 2.3 mole equiv.) was added resulting in a pinkish coloured solution. This solution was stirred at rt under N₂ for 14.5 h. The solvent was evaporated and the resultant oil placed under high vacuum (0.1 torr, 65°C) for 1 h. The crude bromide was then dissolved in DMSO (10 mL) and NaBH₄ (0.125 g, 3.3 mmol, 15 mole equiv.) added (vigorous fizzing). The mixture was stirred 7 h, diluted with water (10 mL), and extracted with CH₂Cl₂ (4 x 10 mL). The combined organic extracts were then washed with water (20 mL). The organic layer separated, dried (MgSO₄), and the solvent evaporated. The oil was placed under high vacuum (0.1 torr, 65°C) for 3 h. The oil was chromatographed on silica (20% ethyl acetate/hexanes) to give a yellowish oil (23.7 mg, 18%); [α]_D²⁰ +58° (c 0.38, CHCl₃), IR (CH₂Cl₂): 1745 (CO) cm⁻¹, ¹H-NMR (CDCl₃) δ : 7.43-7.35 (m, 6H) 7.25-7.19 (m, 4H), 7.11-7.06 (t, 3H), 7.02-6.86 (m, 7H), 6.03 (s, 1H), 5.66 (s, 1H), 4.72 (d, 1H, J = 5.62, H₁), 3.73 (s, 3H), 3.70 (s, 3H), 3.61-3.50 (m, 2H, H₂, H_{4e}), 3.41 (6 line m, 1H, J_{3,4e} = 5.75, J_{3,4a} = 11.5, J_{3,2} = 11.5, H₃), 3.11 (dd, 1H, J_{4a,3} = 11.5, J_{4a,4e} = 16.5, H_{4a}); ¹³C-NMR (CDCl₃) δ : 174.13 (CO), 171.07 (CO), 169.38 (CO), 168.80 (CO), 141.40 (C), 136.60 (C), 133.68 (C), 133.57 (C), 133.39 (C), 130.22 (CH), 129.37 (2 x CH), 129.18 (CH), 128.70 (2 x CH),

128.66 (CH), 128.47 (CH), 128.27 (2 x CH), 127.91 (2 x CH), 127.85 (2 x CH), 127.18 (2 x CH), 126.90 (CH), 126.86 (CH), 126.68 (CH), 74.66 (CH), 74.02 (CH), 52.23 (CH₃), 52.43 (CH₃), 47.89 (CH), 46.30 (CH), 36.89 (CH), 32.04 (CH₂); MS *m/e* (rel. %): 264 (21), 219 (15), 204 (9), 179 (13), 165 (7), 149 (7), 107 (100), 86 (100), 84 (100).

Method 2. A typical experiment for the reduction of **168** is as follows: Powdered NaBH₄ (0.166 g, 4.38 mmol, 33 mole % H⁻) was added to TFA (2.70 mL, 4.0 g, 35 mmol, 66 mole % H⁺) at -23°C (CCl₄/dry ice bath). After 30 seconds, the cycloadduct **168** (48.4 mg, 0.0795 mmol) in CH₂Cl₂ (1.5 mL) was added to the TFA/NaBH₄ solution (an additional 44 mg of NaBH₄ was added immediately after the addition of the alcohol) and stirred 45 min at -23°C. The solution was diluted with water (5 mL) and then extracted with CH₂Cl₂ (4 x 5 mL), dried (MgSO₄), and evaporated to give a colourless oil. The ¹H-NMR of the crude reaction mixture showed a doublet at 4.72 ppm (*J* = 5.62; H1 of reduction product **169**), double doublet at 4.16 (*J* = 4.53, 6.82; H3 of alkene **172**) and a doublet at 4.35 ppm (*J* = 10; H1 of minor 1,2-*trans* reduction product) in a ratio of 0.58:0.14:0.28. Chromatography of the product on silica (15% ethyl acetate/hexanes) to give a colourless oil (20.5 mg, 35%).

Di-(R- α -methoxycarbonylbenzyl)-4-(R)-hydroxy-1(S)-phenyl-1,2,3,4-tetrahydronaphthalene-2(S)-3(R)-dicarboxylate 171

To a refluxing solution of the fumarate of methyl (R)-mandelate⁹⁹ (2.001 g, 4.85 mmol) and ZnO in dry toluene (20 mL) was added a solution of 1-hydroxy-3-phenyl-1,3-dihydrobenzo[*c*]thiophene-2,2-dioxide⁹⁴ (1.058 g, 4.85 mmol, 1 mole equiv.) in CH₂Cl₂ (20 mL) over a period of 20 min (1 mL aliquots). The solution was allowed to reflux 20 min further. The solution was filtered and the solvent evaporated to give a brown oil. ¹H-NMR analysis of the crude product revealed two doublets at 5.06 ppm (*J*=9.69, H4) and 4.70 ppm (*J*=5.83, H1) indicative of an *exo* cycloadduct.⁹⁴ The product was chromatographed on silica (15-25% ethyl acetate/hexanes) to give an oil

(0.686 g, 23%); IR (CH₂Cl₂): 3490 (br, OH), 1745 (vs, CO), 1236 (s), 1161 (s), 1046 (m) cm⁻¹; [α]_D²⁰ +20° (4.4 g/100 mL); ¹H-NMR (CDCl₃) δ: 7.84 (d, 1H, J = 7.85), 7.47-7.44 (m, 2H), 7.39-7.7.32 (m, 4H), 7.17 (q, 2H), 7.00-6.88 (m, 10H), 6.20 (s, 1H), 5.54 (s, 1H), 5.06 (d, 1H, J_{4,3} = 9.69, H4), 4.70 (d, 1H, J_{1,2} = 5.83), 3.79 (s, 3H), 3.67 (s, 3H), 3.66 (dd, 1H, J_{2,3} = 12.53, J_{2,1} = 5.83), 3.44 (dd, 1H, J_{3,4} = 9.69, J_{3,2} = 12.53); ¹³C-NMR (CDCl₃) δ: 174.10 (CO), 171.52 (CO), 170.20 (CO), 168.58 (CO), 140.94 (C), 136.68 (C), 136.01 (C), 133.05 (C), 132.75 (C), 129.67 (CH), 129.47 (2 x CH), 129.37 (CH), 128.79 (2 x CH), 128.66 (CH), 128.17 (2 x CH), 128.03 (2 x CH), 127.97 (CH), 127.89 (2 x CH), 127.38 (CH), 127.07 (2 x CH), 126.96 (CH), 126.81 (CH), 75.01 (CH), 74.17 (CH), 71.39 (CH), 53.35 (CH₃), 52.46 (CH₃), 46.51 (CH), 46.14 (CH), 46.03 (CH); MS *m/e* (rel. %): 410 (1), 386 (2), 248 (6), 232 (11), 205 (10), 150 (44), 149 (88), 121 (49), 107 (65), 105 (56), 99 (100); Analysis calcd. for C₃₆H₃₂O₉: C 71.0%, H 5.3%; found: C 68.1%, H 4.86%.

Alkene 172

This compound was a by-product from the reduction of **168** and could be easily synthesized in quantitative yield by simple evaporation of **168** from TFA. A sample was recrystallized from ethyl acetate/hexanes; mp 123-127; [α]_D²⁰ -134.8 (c 0.0104 g/mL); IR (CH₂Cl₂): 1749 cm⁻¹; ¹H-NMR (CDCl₃) δ: 7.30-7.17 (m, 15H), 7.09-7.05 (m, 1H), 6.97 (m, 2H), 6.70 (d, 1H, J = 7.68, H8), 5.94 (s, 1H), 5.75 (s, 1H), 4.16 (dd, 1H, J = 4.6, 6.9, H3), 3.47 (dd, 1H, J = 4.6, 16.1, H4a), 3.38 (dd, 1H, J = 6.9, 16.1, H4b), 3.62 (s, 3H), 3.61 (s, 3H); ¹³C-NMR (CDCl₃) δ: 171.84 (CO), 168.89 (CO), 168.82 (CO), 166.92 (CO), 149.55 (C), 138.30 (C), 134.63 (C), 134.37 (C), 133.78 (C), 133.26 (C), 129.62 (CH), 128.91 (CH), 128.88 (CH), 128.69 (CH), 128.56 (3 x CH), 128.29 (3 x CH), 127.92 (2 x CH), 127.83 (CH), 127.46 (3 x CH), 127.29 (2 x CH), 126.84 (CH), 122.79 (C), 74.87 (CH), 74.62 (CH), 52.44 (CH₃), 52.34 (CH₃), 41.31 (CH), 31.31 (CH₂); MS *m/e* (rel. %): 590 (M⁺, 4), 231 (23), 149 (31), 121 (18), 107 (9), 84 (100); HRMS calcd. for C₃₆H₃₀O₈: 590.1940; found 590.1916.

Cycloadduct 174

1-Hydroxy-1-arylbenzocyclobutenol **179** (15.2 mg, 0.048 mmol) and the fumarate of methyl (R)-mandelate **118** (0.048, 0.115 mmol, 2.4 mole equiv.) were refluxed in toluene (5 mL) overnight. The solvent was evaporated at reduced pressure to give a yellow oil which was chromatographed on silica (40% ethyl acetate/hexanes) to give a yellow glassy product (11 mg, 31%); IR (CH₂Cl₂): 3459 (w, OH), 1748 (vs, CO) cm⁻¹; [α]_D²⁰ -126° (c 0.965 g/100 mL); ¹H-NMR (CDCl₃) δ: 7.48-7.44 (m, 2H), 7.41-7.37 (m, 3H), 7.29-7.17 (m, 3H), 7.12 (d, 1H, J = 2.1), 6.99 (dd, 1H, J = 2.1, 8.4), 6.87 (m, 2H), 6.66 (s, 1H, H5), 6.45 (s, 1H, H8), 5.90 (s, 1H), 5.73 (s, 1H), 3.92 (s, 3H), 3.87 (s, 3H), 3.82 (s, 3H), (H2, H3 under methoxyl peaks), 3.73 (s, 3H), 3.63 (s, 3H), 3.61 (s, 3H), 3.44 (dd, 1H, J = 4.6, 16.5, H4eq), 3.17 (dd, 1H, J = 11.7, 16.5, H4a); ¹³C-NMR (CDCl₃) δ: 174.19 (CO), 171.54 (CO), 169.59 (CO), 169.33 (CO), 148.73 (C), 148.48 (C), 147.94 (C), 147.87 (C), 139.23 (C), 133.26 (C), 132.75 (C), 132.39 (C), 129.23 (CH), 128.97 (CH), 128.72 (2 x CH), 128.37 (2 x CH), 127.56 (2 x CH), 127.10 (2 x CH), 125.72 (CH), 118.88 (CH), 112.13 (CH), 110.68 (CH), 110.10 (2 x CH), 76.13 (C), 74.90 (CH), 74.65 (CH), 56.01 (CH₃), 55.91 (CH₃), 55.83 (CH₃), 55.74 (CH₃), 54.91 (CH), 52.83 (CH₃), 52.61 (CH₃), 39.70 (CH), 32.37 (CH₂); MS (rel. %): 710 (6, -H₂O), 516 (31), 394 (100), 368 (16), 351 (54), 325 (34), 324 (31), 107 (69), 91 (64), 77 (46); HRMS calcd. for C₄₀H₄₀O₁₃: 728.2469, 710.2363 (-H₂O); found 728.2501, 710.2369 (-H₂O).

1(S)-(3',4'-Dimethoxyphenyl)-6,7-dimethoxy-1,2,3,4-tetrahydronaphthalene-2(S),3(S)-(methyl (R)-mandelate) dicarboxylate 175

TFA (1.63 mL, 2.41 g, 21.14 mmol, 67 mole %) was cooled to -23°C (dry ice/CCl₄) under N₂. Powdered NaBH₄ (0.1 g, 264 H⁻ equiv. 10.57 mmol, 33 mole %) was immediately added before the TFA had a chance to freeze. After 12 seconds, at which time the effervescence had ceased, the alcohol **174** (35 mg, 0.0480 mmol) in CH₂Cl₂ (1

mL) was added resulting in a dark blue solution. The addition of another 22.6 mg of NaBH₄ removed the blue colour to produce a yellow solution which was stirred for 30 min. The solution was quenched with water (5 mL) and warmed to room temperature over 5 min. The layers were separated and the aqueous phase extracted with CH₂Cl₂ (3 x 5 mL), dried (MgSO₄), and the solvent evaporated. ¹H-NMR analysis of the crude mixture showed two H1 doublets at 4.56 ppm (J = 5.48, 1,2-*cis*, **175**) and 4.22 ppm (J = 9.9, 1,2-*trans*, **183**) in a ratio of 71:29 (**175**:**183**). Only a small amount (≤ 5%) of the alkene could be detected in the spectrum.

175: [α]_D²⁰ +57.4 (0.0054 g/mL); IR (CH₂Cl₂): 1743 (CO), 1519, 1218 (vs) cm⁻¹; ¹H-NMR (CDCl₃) δ: 7.47-7.43 (5 line m, 2H), 7.38-7.36 (m, 3H), 7.22 (tt, 1H), 7.09 (t, 2H), 6.99 (d, 2H), 6.89 (s, 1H), 6.49 (d, 1H, J = 1.96), 6.44 (d, 1H, J = 8.33), 6.39 (s, 1H), 6.32 (dd, 1H, J = 1.96, 8.33), 6.07 (s, 1H), 5.67 (s, 1H), 4.55 (d, 1H, J = 5.46, H1), 3.87 (s, 3H), 3.74 (s, 3H), 3.70 (s, 3H), 3.69 (s, 3H), 3.68 (s, 3H), 3.64 (s, 3H), 3.55 (dd, 1H, J = 4.95, 8.57), 3.48 (t, 1H, J = 6.39), 3.38 (m, 2H), 3.04 (m, 1H); ¹³C-NMR (CDCl₃) δ: 172.24 (CO), 171.17 (CO), 169.49 (CO), 168.9 (CO), 148.11 (C), 148.05 (C), 147.89 (C), 147.77 (C), 133.95 (C), 133.62 (C), 133.37 (C), 129.21 (CH), 128.71 (2 x CH), 128.60 (C), 128.26 (2 x CH), 127.96 (2 x CH), 127.01 (2 x CH), 125.63 (C), 121.77 (CH), 112.81 (CH), 112.21 (CH), 110.40 (2 x CH), 74.61 (CH), 73.90 (CH), 55.83 (3 x CH₃), 55.43 (CH₃), 52.54 (CH₃), 52.43 (CH₃), 48.20 (CH), 45.73 (CH), 37.10 (CH), 31.82 (CH₂); MS *m/e* (rel. %): 712 (91), 563 (11), 397 (68), 370 (20), 369 (21), 351 (54), 325 (71), 149 (100), 121 (88); HRMS calcd. for C₄₀H₄₀O₁₂: 712.2520, found 712.2521.

Minor isomer 183 (characterized by ¹H-NMR only); ¹H-NMR (CDCl₃) δ: 7.45-7.23 (m, 8H), 7.17 (dd, 2H, J = 1.2, 8.3), 6.77 (d, 1H, J = 8.75), 6.67 (m, 3H), 6.25 (s, 1H), 5.84 (s, 1H), 5.73 (s, 1H), 4.23 (d, 1H, J = 9.8, H1), 3.88 (s, 3H), 3.87 (s, 3H), 3.74 (s, 3H), 3.71 (s, 3H), 3.60 (s, 3H), 3.59 (s, 3H), 3.49-3.15 (16 line m, 4H, J_{3,4eq} = 4.62, J_{3,4a} = 10.96)

2-Methyl-4,5,9,10-tetramethoxybenzophenone 176

The benzhydrol **178** (0.541 g, 1.70 mmol) was dissolved in a mixture of ether/CH₂Cl₂ (1:1, 50 mL) and cooled in an ice bath. To the vigorously stirred solution was added CrO₃ (0.5 M CrO₃ in 10% aqueous H₂SO₄; 10 mL, 3 mole equiv.). The solution was stirred 19 h at rt (after 1h the reaction was essentially complete and showed no change after a total of 19 h as indicated by TLC). The solution was separated and the aqueous layer extracted with CH₂Cl₂. The organic fractions were combined and washed with 5% aqueous NaHCO₃ until the wash was colourless. The organic fraction was dried (MgSO₄) and the solvent evaporated to give an oil. The oil was chromatographed on silica (20% ethyl acetate/hexanes) to give a crystalline product (0.5147 g, 96%); mp 121-122°C; IR (CH₂Cl₂): 1653 cm⁻¹; ¹H-NMR (CDCl₃) δ: 7.51 (d, 1H, J = 1.95), 7.29 (dd, 1H, J = 1.95, 8.36), 6.87 (s, 1H), 6.86 (d, 1H, J = 8.36), 3.95 (s, 3H), 3.94 (s, 6H), 3.82 (s, 3H), 2.28 (s, 3H); ¹³C-NMR (CDCl₃) δ: 196.57 (CO), 153.23 (C), 150.24 (C), 149.03 (C), 146.11 (C), 131.15 (C), 130.76 (C), 130.32 (C), 125.60 (CH), 113.72 (CH), 112.26 (CH), 111.48 (CH), 109.86 (CH), 56.10 (CH₃), 56.07 (CH₃), 56.01 (CH₃), 55.93 (CH₃), 19.76 (CH₃); MS *m/e* (rel. %): 316 (M⁺, 32), 315 (7), 301 (8), 285 (43), 223 (12), 150 (11), 149 (100), 129 (24), 112 (10), 104 (10); HRMS calcd. for C₁₈H₂₀O₅: 316.1310; found 316.1309.

2-Methyl-3,4-dimethoxy-3',4'-dimethoxybenzhydrol 178

4-Bromoveratrole (0.569 g, 2.62 mmol) was dissolved in dry THF (15 mL) and placed under nitrogen. The solution was cooled to -78°C and *n*-BuLi (2.5 M, 1 mL, 1.1 mole equiv.) added. The solution was stirred 1 min followed by the addition of 6-methylveratraldehyde **177** (0.430 g, 2.38 mmol) in THF (15 mL). The solution was then warmed to room temperature and stirred 17 h. The reaction was quenched with 15% aqueous NH₄Cl, saturated with NaCl, and extracted with CH₂Cl₂. The combined extracts were dried (Na₂SO₄) and the solvent evaporated to give a brownish oil which crystallized

on standing. The product was chromatographed on silica (20-30% ethyl acetate/hexanes) to give a white solid (0.573 g, 76%); mp 120-122°C; IR (CH₂Cl₂): 3598 (OH), 3513 (br, OH), 1612, 1523 (s), 1419 (s), 1213 (C-O), 1139, 1103, 1028 cm⁻¹; ¹H-NMR (CDCl₃) δ: 7.07 (s, 1H), 6.89 (s, 1H), 6.80 (s, 2H), 6.66 (s, 1H), 5.92 (d, 1H, J = 3 Hz), 3.87 (s, 3H), 3.86 (s, 3H), 3.85 (s, 3H), 3.84 (s, 3H), 2.20 (s, 3H), 2.06 (d, 1H, J = 3 Hz, OH); ¹³C-NMR (CDCl₃) δ: 148.97 (C), 148.41 (C), 147.89 (C), 147.09 (C), 135.79 (C), 133.49 (C), 127.41 (C), 119.28 (CH), 113.72 (CH), 110.93 (CH), 110.26 (CH), 109.85 (CH), 72.77 (CH), 56.06 (CH₃), 55.90 (2 x CH₃), 55.85 (CH₃), 18.77 (CH₃); MS *m/e* (rel. %): 319 (20), 318 (M⁺, 100), 302 (18), 301 (31), 269 (15), 179 (60), 165 (39), 153 (43), 149 (26), 139 (28); HRMS calcd. for C₁₈H₂₂O₅ 318.1468; found 318.1508.

1-Hydroxy-1-(3'4'-dimethoxyphenyl)-4,5-dimethoxybenzocyclobutene 179

To a solution of 4-bromoveratrole (Aldrich, 0.920 g, 2 mole equiv. 4.24 mmol) and THF (15 mL) at -78°C (under N₂) was added *n*-BuLi (2.2 M in hexanes, 1.73 mL, 1.8 mole equiv.). The solution was stirred 1 min followed by the addition of the ketone **182** (0.376 g, 2.11 mmol) in THF (15 mL) over a period of 3.5 minutes. The reaction was stirred an additional 13.5 minutes. The orange solution was quenched with 5% aqueous NH₄Cl (35 mL), saturated (NaCl) and extracted with CH₂Cl₂. The organic layer was dried (MgSO₄) and the solvent evaporated in vacuo. Purification of the orange oil on silica (30-40 ethyl acetate/hexanes) afforded **179** as an orange semi-solid (0.568 g, 85%); IR (CH₂Cl₂): 3589 (OH) cm⁻¹; ¹H-NMR (CDCl₃) δ: (d, 1H, J = 2.04), 6.92 (dd, 1H, J = 2.04, 8.23), 6.84 (s, 1H), 6.80 (d, 1H, J = 8.23), 3.89 (s, 3H), 3.87 (s, 3H), 3.866 (s, 3H), 3.863 (s, 3H), 3.52 (d, 1H, J = 13.4), 3.46 (d, 1H, J = 13.4); ¹³C-NMR (CDCl₃) δ: 151.53 (C), 150.07 (C), 148.85 (C), 148.32 (C), 140.20 (C), 136.58 (C), 133.54 (C), 117.76 (CH), 110.75 (CH), 109.06 (CH), 107.77 (CH), 105.24 (CH), 80.60 (C), 56.28 (CH₃), 56.22 (CH₃), 55.94 (CH₃), 55.88 (CH₃), 49.87 (CH₂); MS *m/e* (rel. %): 316 (M⁺, 55), 301 (21), 285 (100), 269 (24), 254 (15), 241 (13), 226 (11), 179 (25), 165 (57), 139 (30); HRMS

calcd. for $C_{18}H_{20}O_5$: 316.1310; found 316.1311.

1-Hydroxy-4,5-dimethoxybenzocyclobutene **181**¹¹⁷

A solution of vinyl acetate (100 mL) and isoamyl nitrite (3 mole equiv. 8.8 mL, 7.70g, 0.0657 mol) was brought to a reflux over dry 3 Å molecular sieves. To this solution, a solution of 2-amino-4,5-dimethoxybenzoic acid (Aldrich, 4.321 g, 0.0219 mol) in THF (60 mL) was added and refluxed for 17 h. The sample was filtered and the solvent evaporated to give a dark oil. The product was distilled under vacuum (1 mm Hg) to give a yellow oil **180**. The oil was stirred in a 30% aqueous NH_4OH /methanol solution for 17 h. The majority of the methanol was evaporated and the solution then extracted with ethyl acetate, dried ($MgSO_4$) and re-evaporated. Chromatography on silica afforded the benzocyclobutenol (0.822 g, 21% from the anthranilic acid). **181** had spectroscopic properties identical to those previously reported.¹¹⁷

4,5-Dimethoxybenzocyclobutenone **182**

Method 1. 4,5-Dimethoxybenzocyclobutenol **181** (0.086, 0.476 mmol) in dry CH_2Cl_2 (5 mL) was added to a stirred suspension of PCC¹⁰⁸ (2 mole equiv. 0.205 g) in CH_2Cl_2 (5 mL). The solution was stirred 1.3 h at rt. The solution was decanted and the black precipitate washed with diethyl ether. The combined extracts were filtered through silica (1 inch column). The solvent was evaporated leaving a purple solution which crystallized on standing. The product was chromatographed on silica (20% ethyl acetate/hexanes) to afford the desired ketone as a colourless solid (0.0473 g, 55%); 1H -NMR ($CDCl_3$) δ : 7.00 (s, 1H), 6.81 (s, 1H), 3.97 (s, 3H), 3.85 (s, 5H; benzylic CH_2 and OCH_3); identical to that reported by Kametani.¹²⁰ ^{13}C -NMR ($CDCl_3$) δ : 185.67 (CO), 155.93 (C), 151.42 (C), 146.21 (C), 138.71 (C), 105.66 (CH), 102.35 (CH), 56.41 (CH_3), 56.18 (CH_3), 51.06 (CH_2).

Method 2. CrO_3 (0.0614 g, 0.593 mmol) was added to a stirred solution of

CH_2Cl_2 (2 mL) and pyridine (0.0954 g, 1.206 mmol). The sample was fitted with a drying tube and stirred 19 min at rt. A solution of the alcohol (17.8 mg, 0.0988 mmol) in CH_2Cl_2 (2 mL) was added to the wine coloured oxidizing solution and stirred at rt for 15 minutes. The solution was filtered through aluminum oxide (CH_2Cl_2 eluent) and the solvent evaporated (15.5 mg, 88%; larger scale oxidation (0.5 g of **181**) gave a 76% yield of **182**). $^1\text{H-NMR}$ of the crude product indicated that it was >95% pure.

References

1. J.D. Loike. *Trends. Pharm. Soc.* 30 (1984).
2. J.L. Hartwell and A.W. Schrecker. *Fortschr. Chem. Naturst* **15**, 83 (1958).
3. J. King. *New York Philos. Med. J.* **1**, 159 (1844).
4. L.S. King and M. Sullivan. *Science*, **104**, 244 (1946)
5. J.L. Hartwell and M.J. Shear. *J. Cancer. Res.* **7**, 716 (1947).
6. H. Stähelin and A. Von Wartburg. *Prog. Drug Res.* **33**, 169-266 (1989)
7. M. Kuhn, C. Keller-Juslén, and A. Von Wartburg. *Helv. Chim. Acta.* **52**, 944 (1969).
8. C. Keller-Juslén, M. Kuhn, A. Von Wartburg, and H. Stähelin. *J. Med. Chem.* **14**, 936 (1971).
9. K.H. Lee, Y. Imakura, M. Haruna, S.A. Beers, L.S. Thurston, H. Dai, and C. Chen. *J. Nat. Prod.* **52**, 606-613 (1989).
10. Z.Q. Wang, Y.H. Kuo, D. Schnur, J.P. Bowen, S.Y. Liu, F.S. Han, J.Y. Chang, Y.C. Cheng, and K.H. Lee. *J. Med. Chem.* **33**, 2660-2666 (1990).
11. K. Tomioka, Y. Kubota, and K. Koga. *Tetrahedron Lett.* **30**, 2953 (1989).
12. W. Van Uden, B. Homan, H.J. Woerdenbag, N. Pras, and T.M. Malingré. *J. Nat. Prod.* **55**, 102-110 (1992).
13. C.C. Huang, Y. Hou, and J.J. Wang. *Cancer Res.* **23**, 3123 (1973).
14. J.D. Loike and S.B. Horwitz. *Biochemistry*, **15**, 5443 (1976).
15. G.L. Chen, L. Yang, T.C. Rowe, B.D. Halligan, K.M. Tewey, and L.F. Liu. *J. Bio. Chem.* **259**, 13560-13566 (1984).
16. T. Rowe, G. Kupfer, and W. Ross. *Biochem. Pharm.* **34**, 2483-2487 (1985).
17. A. Maxwell and M. Gellert. *Adv. Protein Chem.* **38**, 69-103 (1986).
18. J.C. Wang. *Annu. Rev. Biochem.* **54**, 665 (1985).
19. F. Brewer, J.D. Loike, and S.B. Horwitz. *J. Med. Chem.* **22**, 215-221 (1979).
20. J.D. Loike, C.F. Brewer, H. Sternlicht, W.J. Gensler, and S.B. Horwitz. *Cancer*

- Res.* **38**, 2688 (1978).
21. A.R. Beard, M.G.B. Drew, J. Mann, and L.T.F. Wong. *Tetrahedron*, **43**, 4207-4215 (1987).
 22. J. March, *In Advanced Organic Chemistry. Reactions, Mechanisms, and Structure* (4th edition). John Wiley and Sons, New York. 1992, p 847.
 23. R. Sustmann. *Tetrahedron Lett.* 2721 (1971).
 24. J. Mann and S.E. Piper. *J. Chem. Soc., Chem. Commun.* 430-432 (1982).
 25. J.L. Charlton, M.M. Alauddin, and G.H. Penner. *Can. J. Chem.* **64**, 793 (1986).
 26. P.V. Alston and R.M. Ottenbrite. *J. Org. Chem.* **40**, 1111-1116 (1975).
 27. I. Fleming. *In Frontier Orbitals and Organic Chemical Reactions*. John Wiley and Sons, New York. 1978, p 128.
 28. P.V. Alston, R.M. Ottenbrite, and D.D. Shillady. *J. Org. Chem.* **38**, 4075 (1973).
 29. M. Kakushima. *Can. J. Chem.* **57**, 2564 (1979).
 30. S.D. Kahn, C.F. Pau, L.E. Overman and W.J. Hehre. *J. Am. Chem. Soc.* **108**, 7381-7396 (1986).
 31. P. Guo. MSc. Thesis. University of Manitoba (1992).
 32. J.L. Charlton and M.M. Alauddin. *Tetrahedron*, **43**, 2873-2889 (1987).
 33. C.R. Flynn and J. Michl. *J. Am. Chem. Soc.* **95**, 5802 (1973).
 34. B.J. Arnold, S.M. Mellows, P.G. Sammes, and T.W. Wallace. *J. Chem. Soc. Chem. Comm.* 401 (1974).
 35. T. Durst, E.C. Kozma, and J. Charlton. *J. Org. Chem.* **50**, 4829 (1985).
 36. J. Charlton and T. Durst. *Tetrahedron Lett.* **25**, 2663 (1984).
 37. P.G. Sammes. *Tetrahedron*, **32**, 405 (1976).
 38. C.W. Jefford, G. Bernardinelli, Y. Wang, D.C. Spellmeyer, A. Buda, and K.N. Houk. *J. Am. Chem. Soc.* **114**, 1157-1165 (1992).
 39. J.L. Charlton, K. Koh, and G.L. Plourde. *Tetrahedron Lett.* **30**, 3279 (1989).
 40. J.L. Charlton, G.L. Plourde, K. Koh, and A.S. Secco. *Can. J. Chem.* **67**, 574

- (1989).
41. D.I. Macdonald and T. Durst. *J. Org. Chem.* **53**, 3663-3669 (1988).
 42. M.E. Jung, R.Y. Lam, M.M. Mansuri, and L.M. Speltz. *J. Org. Chem.* **50**, 1087 (1985).
 43. M.E. Jung and G.T. Lowen. *Tetrahedron Lett.* **27**, 5319 (1986).
 44. G.C. Coll, A. Costa, P.M. Deyá, and J.M. Saá. *Tetrahedron Lett.* **32**, 263-266 (1991).
 45. R.B. Woodward and R. Hoffman. *Angew Chem. Int. Ed. Eng.* **8**, 781 (1969).
 46. G.C. Coll, A. Costa, P.M. Deyá, F. Flexas, C. Rotger, and J.M. Saá. *J. Org. Chem.* **57**, 6222-6231 (1992).
 47. P.J. Wagner, M.A. Meador, B. Zhou, and B. Park. *J. Am. Chem. Soc.* **113**, 9630 (1991).
 48. G.A. Kraus and Y. Wu. *J. Org. Chem.* **57**, 2922 (1992).
 49. S.M. Mellows and P.G. Sammes. *J. Chem. Soc. Chem. Comm.* 21 (1971).
 50. B.J. Arnold, P.G. Sammes, and T.W. Wallace. *J. Chem. Soc. Perkin Trans. I.* 409, (1974).
 51. P.K. Das, M.V. Encinas, R.D. Small, and J.C. Scaiano. *J. Am. Chem. Soc.* **101**, 6965 (1979).
 52. M. Azadi-Ardakani and T.W. Wallace. *Tetrahedron*, **44**, 5939 (1988).
 53. K. Uji-ie, K. Kikuchi, and H. Kokubun. *J. Photochem.* **10**, 145 (1979).
 54. M. Pfau, S. Combrisson, J.E. Rowe, and N.D. Heindel. *Tetrahedron*, **34**, 3469 (1978).
 55. M. Pfau, J.E. Rowe, and N.D. Heindel. *Tetrahedron*, **34**, 3469 (1978).
 56. E. Block and R. Stevenson. *J. Chem. Soc. Perkin I.* 308 (1973).
 57. B.J. Arnold, P.G. Sammes, and T.W. Wallace. *J. Chem. Soc. Perkin I.* 415 (1974).
 58. H.M. Walborsky, L. Barash, and T.C. Davis. *Tetrahedron*, **19**, 2333 (1963).
 59. V. Prelog, *Helv. Chim. Acta.* **36**, 308 (1953).

60. I. Alonso, J.C. Carretero, and J.L.G. Ruano. *Tetrahedron*, **32**, 947 (1991).
61. H. Hartmann, A.F.A. Hady, K. Sartor, J. Weetman, and G. Helmchen. *Angew. Chem. Int. Ed. Engl.* **26**, 1143 (1987).
62. A. Avenozo, C.A. Cativiela, J.A. Mayoral, J.M. Peregrina, and D. Sinou. *Tetrahedron Asymmetry*, **1**, 765 (1990).
63. M.P. Bueno, C.A. Cativiela, and J.A. Mayoral. *J. Org. Chem.* **56**, 6551 (1991).
64. B.M. Trost, D. O'Krongly, and J.L. Belletire. *J. Am. Chem. Soc.* **102**, 7595 (1980).
65. Y. Ito, Y. Amino, N. Nakatsuka, and T. Saegusa. *J. Am. Chem. Soc.* **105**, 1586 (1983).
66. J.L. Charlton. *Can. J. Chem.* **64**, 720 (1986).
67. G.H. Posner and D.G. Wettlaufer. *Tetrahedron Lett.* **27**, 667 (1986).
68. J.L. Charlton, G.L. Plourde, and G.H. Penner. *Can. J. Chem.* **67**, 1010 (1989).
69. W. Choy, L.A. Reed, and S. Masamune. *J. Org. Chem.* **48**, 1139 (1983).
70. R. Tripathy, P.J. Carroll, and E.R. Thorton. *J. Am. Chem. Soc.* **112**, 6743 (1990).
71. R. Tripathy, P.J. Carroll, and E.R. Thorton. *J. Am. Chem. Soc.* **113**, 7630 (1991).
72. J.A. Tucker, K.N. Houk and B.M. Trost. *J. Am. Chem. Soc.* **112**, 5465 (1990).
73. M.B. Glinski, J.C. Freed, and T. Durst. *J. Org. Chem.* **52**, 2749 (1987).
74. R.S. Ward. *Synthesis*, **719** (1991).
75. S.P. Forsey, D. Rajapaksa, N.J. Taylor, and R. Rodrigo. *J. Org. Chem.* **54**, 4280 (1989).
76. S. Takano, S. Otaki, and K. Ogasawara. *J. Chem. Soc. Chem. Commun.* 485 (1985).
77. K.G. Das, J. Afzal, and B.G. Bhawal. *Synth. Commun.* **13**, 787 (1983).
78. J. Tanigawa and S. Murahashi. *J. Org. Chem.* **45**, 4538 (1980).
79. V.N. Aiyer and F.C. Chang. *J. Org. Chem.* **40**, 2384 (1975).
80. V.N. Aiyer and F.C. Chang. *J. Org. Chem.* **42**, 246 (1976).
81. A. Gupta and R.J. Rodrigo. *J. Chem. Soc. Chem. Commun.* 959 (1989).

82. S. Takano, N. Sato, S. Otaki, and K. Ogasawara. *Heterocycles*, **25**, 69 (1987).
83. P. Boissin, R. Dhal, and E. Brown. *J. Chem. Res.* **5**, 332 (1991).
84. S. Hanessian and R. Léger. *Synlett*, 402 (1992).
85. K. Tomioka and K. Koga. *Tetrahedron Lett.* **35**, 3315 (1979).
86. A.I. Meyers, G.P. Roth, D. Hoyer, B.A. Barner, and D. Laucher. *J. Am. Chem. Soc.* **110**, 4611 (1988).
87. R.C. Andrews, S.J. Teague, and A.I. Meyers. *J. Am. Chem. Soc.* **110**, 7854 (1988).
88. A. Pelter, R.S. Ward, D.M. Jones, and P. Maddocks. *Tetrahedron Asymmetry*, **3**, 239 (1992).
89. R. Van Speybroeck, H. Guo, J. Van der Eycken, and M. Vandewalle. *Tetrahedron*, **47**, 4675 (1991).
90. T. Morimoto, M. Chiba, and K. Achiwa. *Chem. Pharm. Bull.* **37**, 3161 (1989).
91. T. Morimoto, M. Chiba, and K. Achiwa. *Tetrahedron Lett.* **31**, 261 (1990).
92. W. Choy. *Tetrahedron*, **46**, 2281 (1990).
93. J.L. Charlton and M.M. Alauddin. *J. Org. Chem.* **51**, 3490 (1986).
94. J.L. Charlton, G.L. Plourde, K. Koh, and A.S. Secco. *Can. J. Chem.* **68**, 2022 (1990).
95. J.L. Charlton and K. Koh. *J. Org. Chem.* **57**, 1514 (1992).
96. G.L. Plourde. Ph.D. Thesis. University of Manitoba (1990).
97. L.C. Allen. *Proc. Nat. Acad. Sci.* **72**, 4701 (1975).
98. W.A. Bubb and S. Sternhell. *Aust. J. Chem.* **29**, 1685 (1976).
99. J.L. Charlton and K. Koh. *Synlett*. 333 (1990).
100. PCModel V. 4.0, Serena Software, Bloomington, Indiana (1990). Calculations carried out on a Silicon Graphics IRIS 4D80/GT workstation.
101. W.L. Jorgenson, D. Lim, and J.F. Blake. *J. Am. Chem. Soc.* **115**, 2936 (1993).
102. L. Raimondi, F.K. Brown, J. Gonzalez, and K.N. Houk. *J. Am. Chem. Soc.* **114**, 4796 (1992).

103. SPARTAN V. 2.0. Wavefunction Inc. Irvine, CA, USA. Calculations performed on a Silicon Graphics 4D80/GT workstation.
104. M. Koerner and B. Rickborn. *J. Org. Chem.* **55**, 2662 (1990).
105. Vogel's Textbook of Practical Organic Chemistry. (4th edition). Rev. by B.S. Furiss, A.J. Hannaford, V. Rogers, P.W.G. Smith, and A.R. Tatchell. Longman Group, New York (1978), p. 302.
106. B.J. Arnold, S.M. Mellows, and P.G. Sammes. *J. Chem. Soc. Perkin Trans. I.* 1266 (1973).
107. M.M. Alauddin. Ph.D. Thesis. University of Manitoba (1987).
108. E.J. Corey and J.W. Suggs. *Tetrahedron Lett.* 2647 (1975).
109. G.W. Gribble and C.F. Nutaitis. *Org. Prep. Proc. Int.* **17**, 317 (1985).
110. E. Brown and A. Duagan. *Tetrahedron Lett.* **27**, 3719 (1986).
111. D.C. Ayres, J.A. Harris, P.N. Jenkins, and L. Phillips. *J. Chem. Soc. Perkin Trans. I.* 1343 (1972).
112. Mathematica 2.1 for SPARC. C 1988-92, Wolfram Research Inc. Calculations performed on a Sun-SPARC workstation, University of Manitoba.
113. H. Yamaguchi, M. Arimoto, S. Nakajima, M. Tanoguchi, and Y. Fukada. *Chem. Pharm. Bull.* **34**, 2056 (1986).
114. K. Koh. personal communication.
116. C.F. Nutaitis. *J. Chem. Ed.* **66**, 673 (1989).
115. G.W. Gribble and R.M. Leese. *Synthesis*, 172 (1977).
117. J.L. Charlton, K. Koh, and G.L. Plourde. *Can. J. Chem.* **68**, 2028 (1990).
118. F.A. Carey and R.J. Sundberg. *in* Advances in Organic Chemistry, part B (3rd edition) Plenum Press, New York (1990), p. 599.
119. R. Ratcliffe and R. Rodehorst. *J. Org. Chem.* **35**, 4000 (1970).
120. T. Kametani, Y. Katoh, and K. Fukumoto. *J. Chem. Soc. Perkin I.* 1712 (1974).
121. D.E. Bogucki and J.L. Charlton. Personal communication.

Appendix 1:

^1H -NMR and ^{13}C -NMR Spectra



SAMPLE SPM-4-119 1-H AT 300 MHZ IN CDCL3

SPM4119.001
AU PROG:
TFZG.AU
DATE 12-8-93
SF 300.133
SY 100.0
O1 5500.000
S1 32768
TD 32768
SW 5494.505
HZ/PT .335
PW 8.0
RD 4.000
AQ 2.982
RG 16
NS 32
TE 300
FW 6900
O2 20000.000
DP 63L D0
LB .300
GB .500
CX 38.00
CY 18.50
F1 8.987P
F2 - 5.13P
HZ/CM 75.032
PPM/CM .250
SR 3372.82

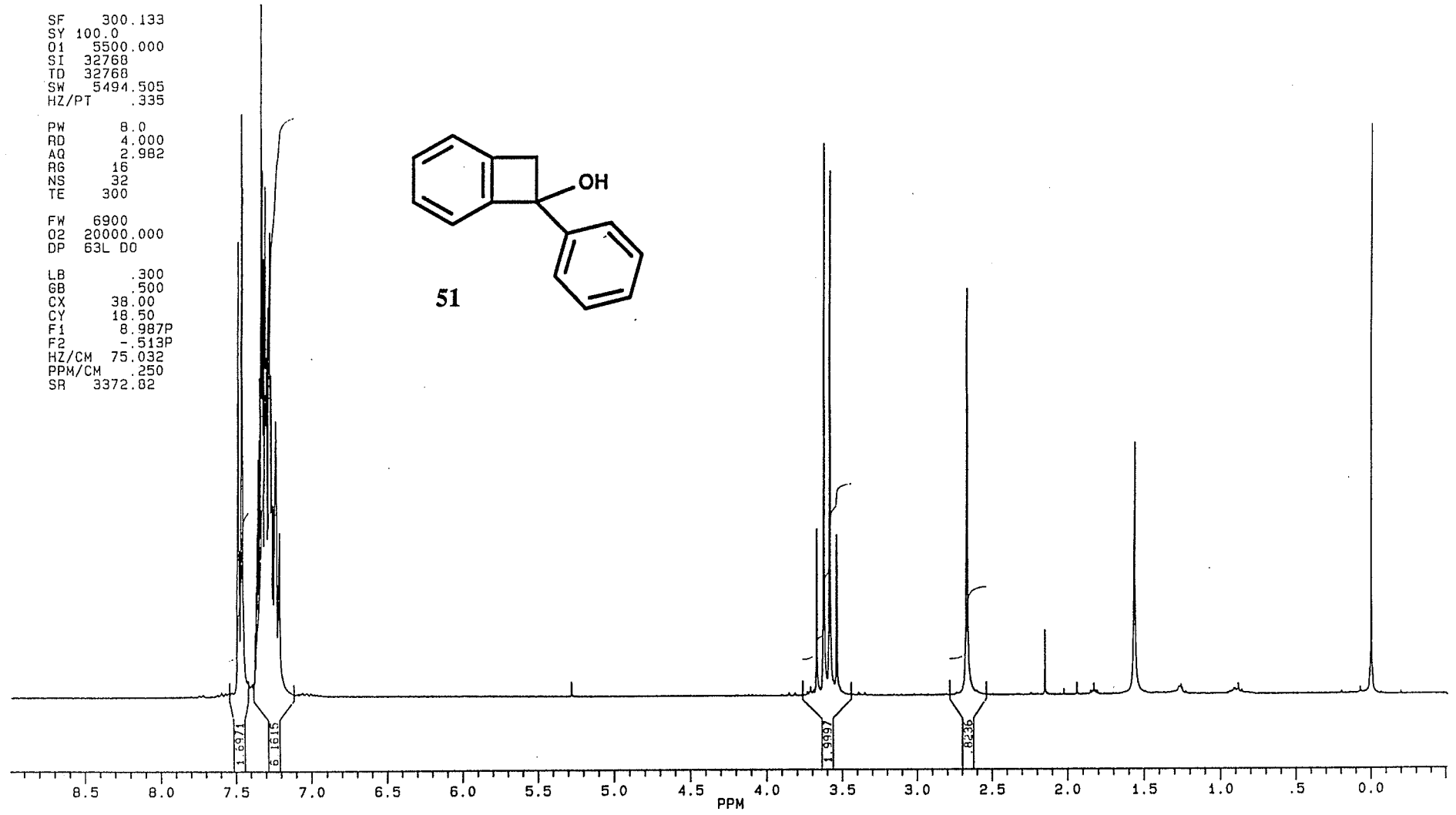
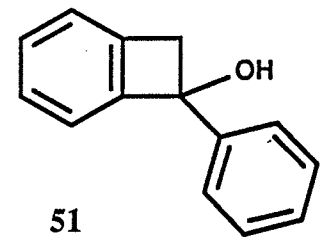
PPM
7.48626
7.48076
7.48226
7.45398
7.39963
7.30011
7.32473
7.31960
7.31666
7.30520
7.30932
7.31614
7.31714
7.30872
7.31721
7.26346
7.23476
7.21117

3.67179
3.67179
3.67179
3.53914

2.67167

1.56411

-0.00034



BRUKER

PPH

SPM4119C.004
AU PROG:
AUTOC13.AU
DATE 12-8-93

SF 75.469
SY 112.0500000
O1 47000.000
SI 32768
TD 32768
SW 17857.143
HZ/PT 1.090

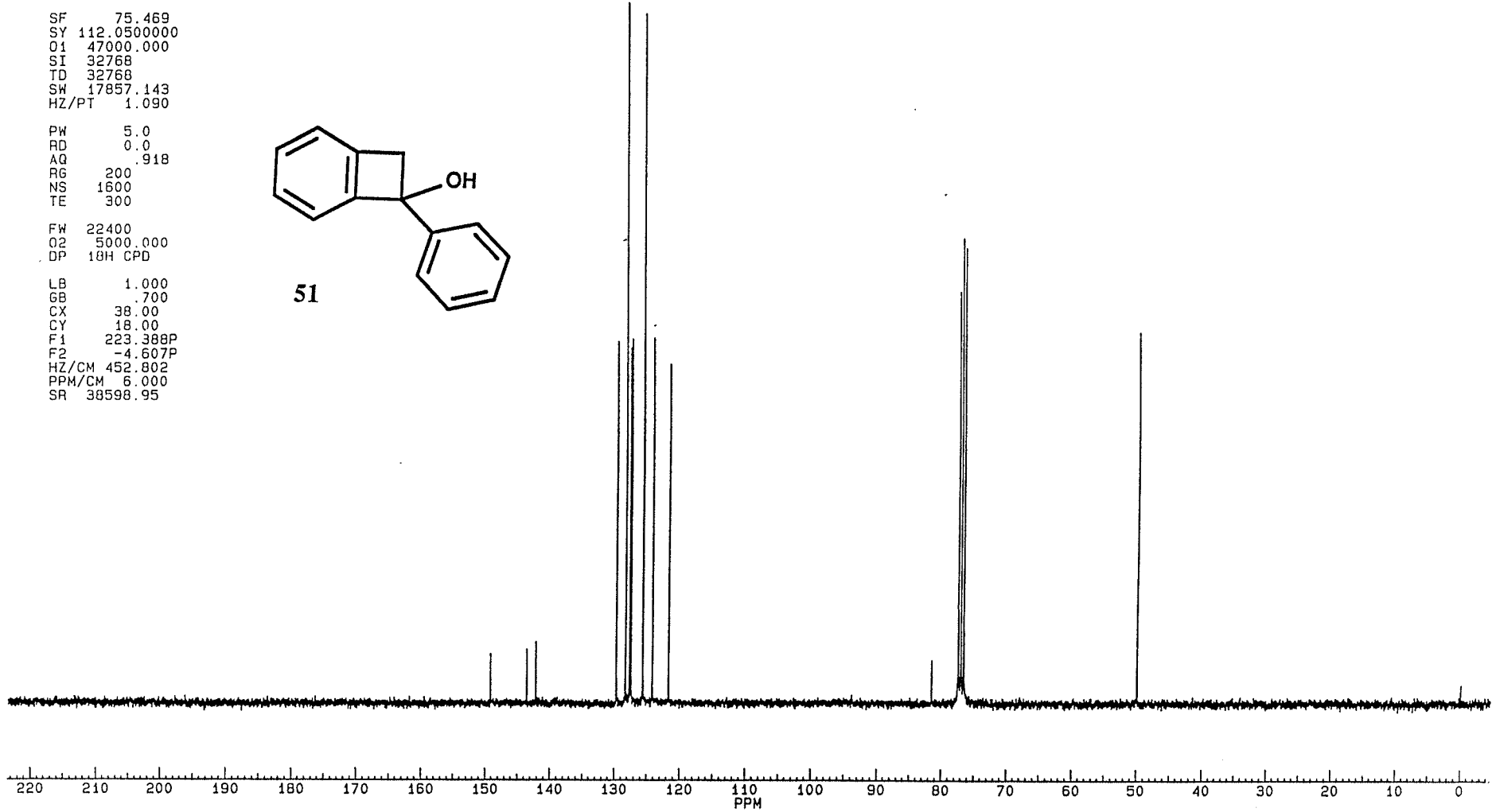
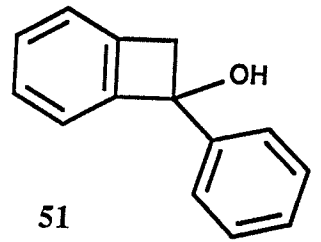
PW 5.0
RD 0.0
AQ .918
RG 200
NS 1600
TE 300

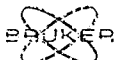
FW 22400
O2 5000.000
DP 10H CPD

LB 1.000
GB 700
CX 38.00
CY 18.00
F1 223.388P
F2 -4.607P
HZ/CM 452.802
PPM/CM 6.000
SR 38598.95

SAMPLE SPM-4-119 13-C AT 75.47 MHZ IN CDCL3

149.071
143.479
142.105
129.646
128.256
127.652
127.406
125.587
124.114
121.629
81.471
77.399
76.876
76.552
49.898





SPM4-4-36
DATE 4-9-92

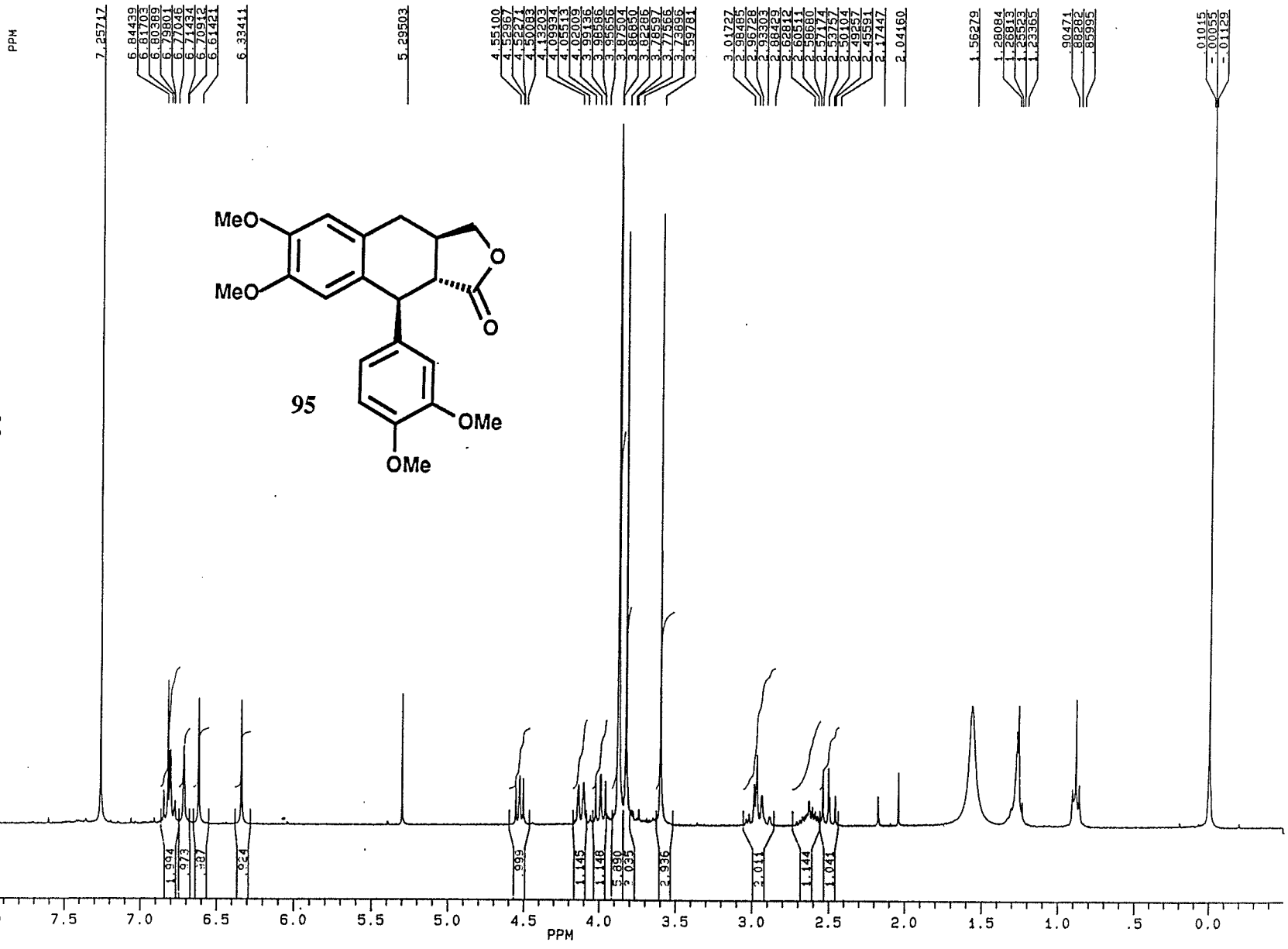
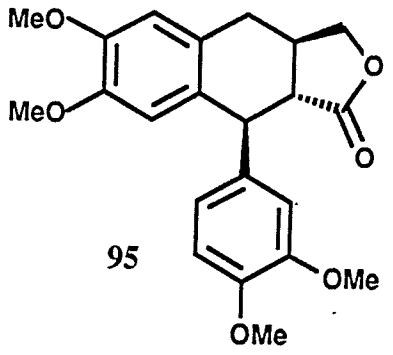
RF 300.135
PZ 100.0
C1 5500.000
SI 22768
TD 22768
SW 5494.505
HZ/PT 225

PW 8.0
PD 4.000
AQ 2.982
RG 100
NS 22
TE 200

FW 6900
L2 20000.000
DP 25L D0

LB 500
GB 500
CX 28.00
CY 15.50
F1 9.000P
F2 1.499P
HZ/CM 75.022
PPM/CM 250
PR 2008.4b

SPM-4-36 IN CDCL3 AT 300 MHZ





PPM

SPM436C.004
AU PROG:
AUTOC13.AU
DATE 6-9-92

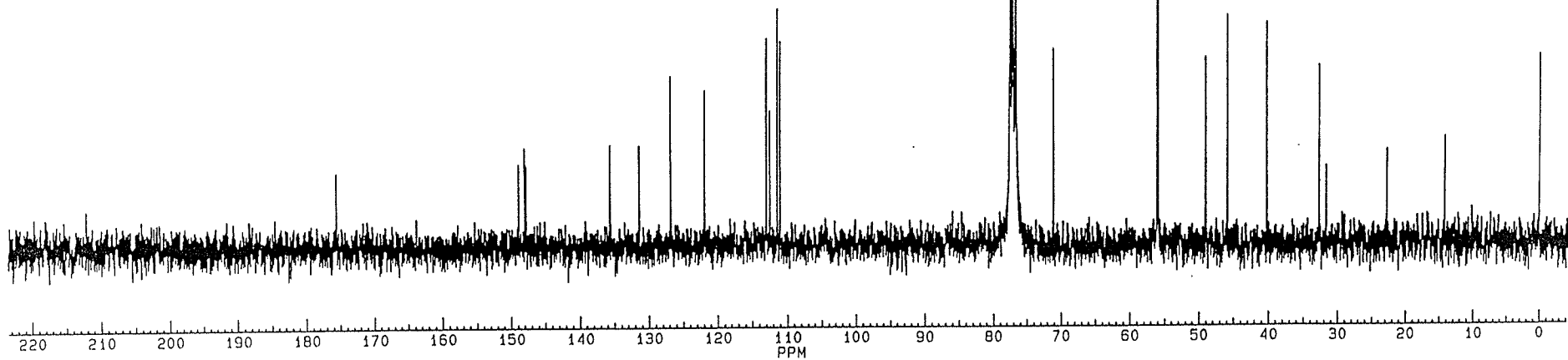
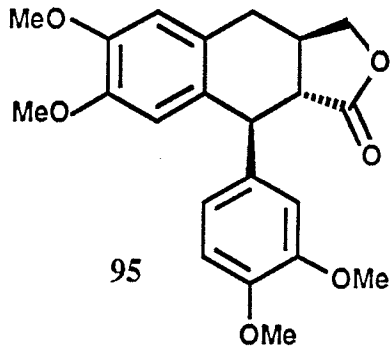
SF 75.469
SY 112.0500000
O1 47000.000
SI 32768
TD 32768
SW 17857.143
HZ/PT 1.090

PW 5.0
RD 0.0
AQ 918
RG 200
NS 4800
TE 300

FW 22400
O2 5000.000
DP 18H CPD

LB 1.000
GB 700
CX 38.00
CY 8.00
F1 223.417P
F2 -4.578P
HZ/CM 452.802
PPM/CM 6.000
SR 38596.77

SAMPLE SPM-4-36 13-C 75.47 MHZ CDCL3



CYANOACRYLATE



PPM

CUH0291.001
DATE 20-8-92

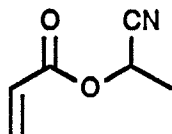
SF 300.133
SY 100.0
Q1 5500.000
SI 32768
TD 32768
SW 5494.505
HZ/PT .335

PW 5.3
RD 4.000
AQ 2.982
RG 1
NS 32
TE 300

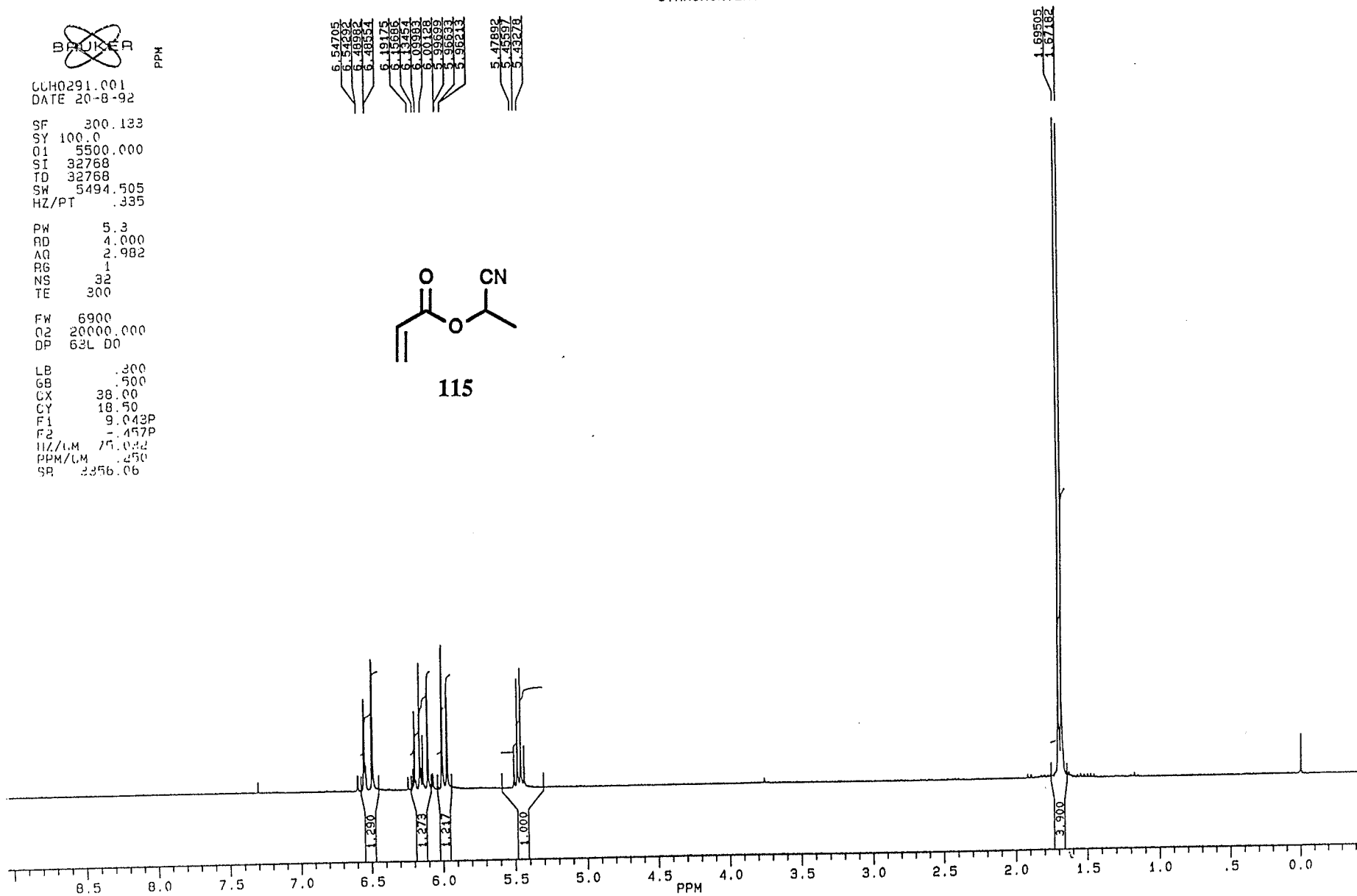
FW 6900
Q2 20000.000
DP 63L D0

LB .300
GB .500
CX 38.00
CY 18.50
F1 9.043P
F2 -.457P
H1/LM 171.032
PPM/LM .250
SR 3356.06

6.54705
6.54294
6.48982
6.48554
6.19175
6.16685
6.14544
6.09983
6.00128
5.96699
5.96933
5.12783
5.12892
5.12892
5.12892



115





SPM456C.004
AU PROG:
AUTOCL3.AU
DATE 24-8-92

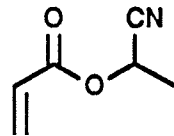
SF 75.469
SY 112.0500000
Q1 47000.000
SI 32768
TD 32768
SW 17857.143
HZ/PT 1.090

PW 5.0
RD 0.0
AQ .918
RG 200
NS 384
TE 300

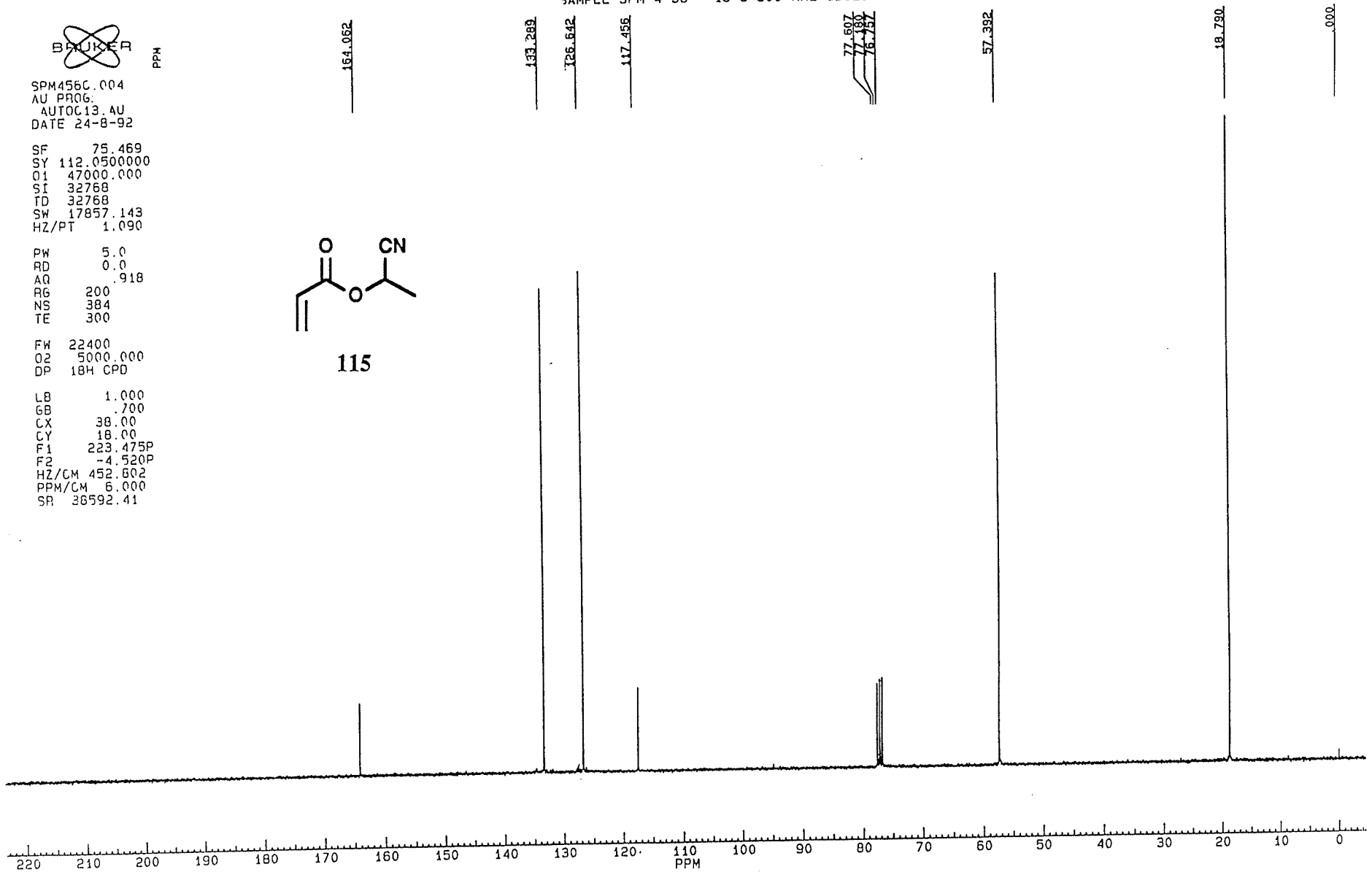
FW 22400
O2 5000.000
DP 18H CPD

LB 1.000
GB .700
CX 38.00
CY 18.00
F1 223.475P
F2 -4.520P
HZ/CM 452.602
PPM/CM 6.000
SR 36592.41

SAMPLE SPM-4-56 13-C 300 MHZ CDCL3



115



SAMPLE SPM-4-77 1-H 300 MHZ CDCL3

BRUKER

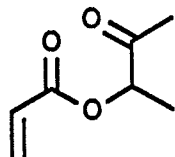
SPM477.001
DATE 8-10-92

SF 300.133
SY 100.0
O1 5500.000
SI 32768
TD 32768
SW 5494.505
HZ/PT .335

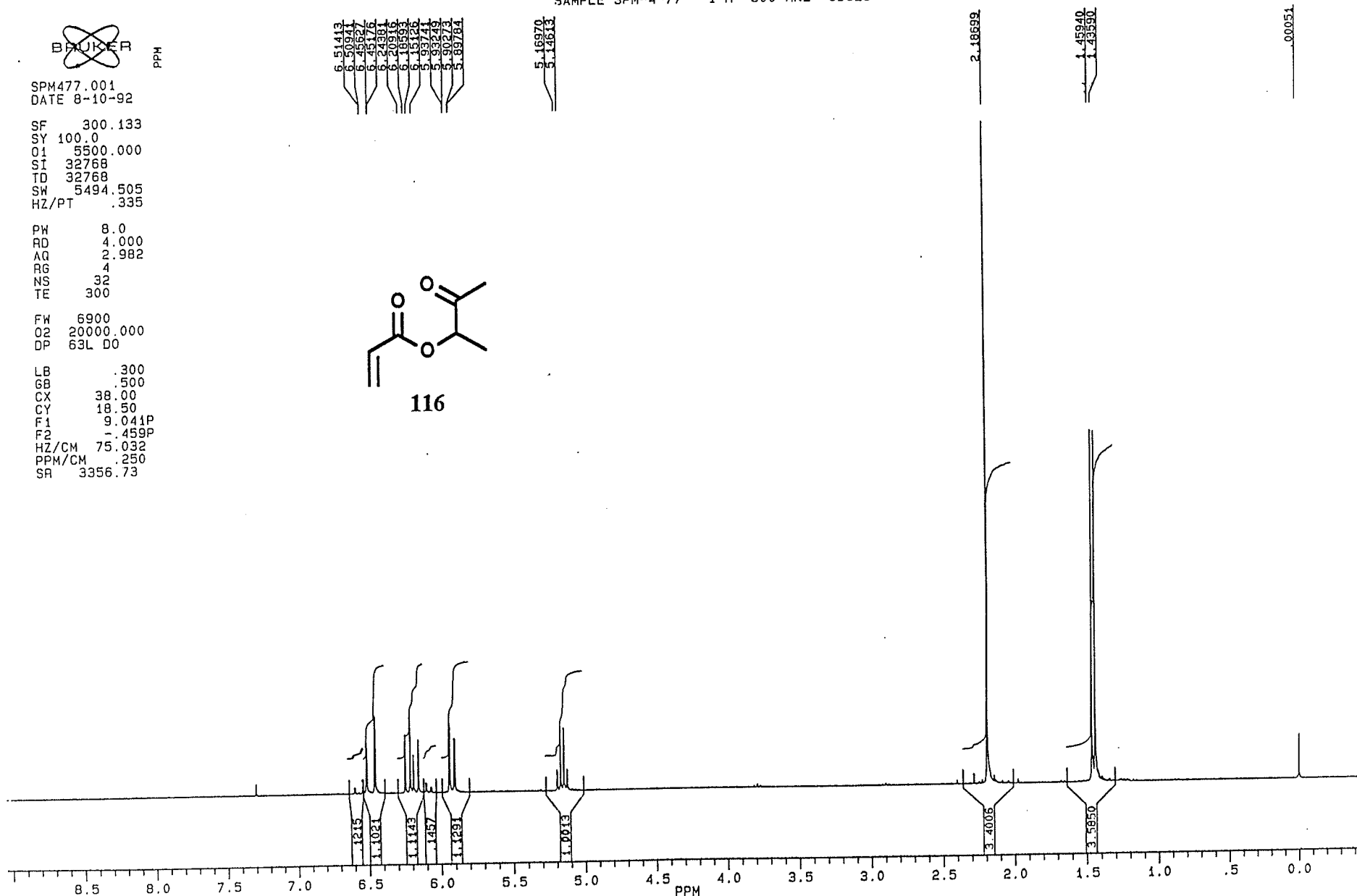
PW 8.0
RD 4.000
AQ 2.982
RG 4
NS 32
TE 300

FW 6900
O2 20000.000
DP 63L D0

LB .300
GB .500
CX 38.00
CY 18.50
F1 9.041P
F2 -.459P
HZ/CM 75.032
PPM/CM .250
SR 3356.73



116



13-C, CDCL3

BUNKER

PPM
205.610

BUTACRYL.004
AU PROG:
AUTOC13 AU
DATE 30-9-92

165.374

131.895

127.668

77.585
77.162
76.736
76.310
75.884
75.458

38.834
37.342

25.581

15.016
13.532

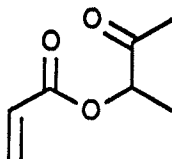
SF 75.469
SY 112.050000
O1 47000.000
SI 32768
TD 32768
SW 17857.143
HZ/PT 1.090

PW 5.0
RD 0.0
AQ .918
RG 200
NS 256
TE 300

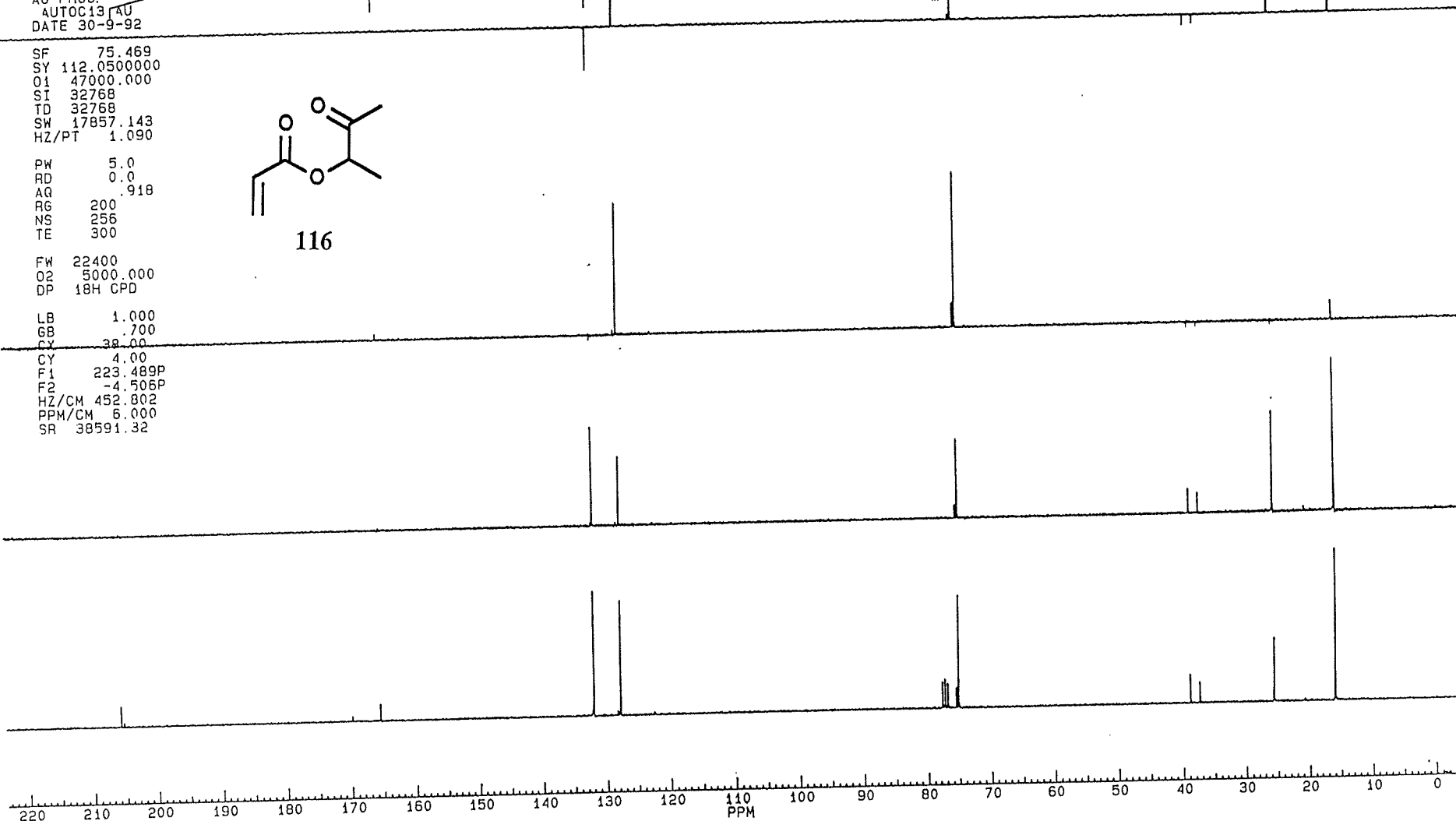
FW 22400
O2 5000.000
DP 18H CPD

LB 1.000
GB .700
CY 38.00

F1 223.489P
F2 -4.505P
HZ/CM 452.802
PPM/CM 6.000
SR 38591.32



116





PPM

SPM2105C.004
AU PROG:
AUTO C13 AU
DATE 16-6-92

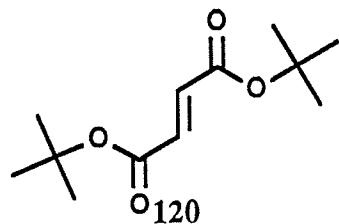
SF 75.469
SY 112.0500000
O1 47000.000
SI 32768
TD 32768
SW 17857.143
HZ/PT 1.090

PW 5.0
PD 0.0
AQ .918
RG 200
NS 1152
TE 300

FW 22400
O2 5000.000
DP 18H CPD

LB 1.000
GB .700
CX 38.00
CY 18.00
F1 223.431P
F2 -4.564P
HZ/CM 452.802
PPM/CM 6.000
SR 38595.68

SAMPLE SPM-2-105 13-C AT 75.47 MHZ IN CDCL3



164.377

134.530

81.638

77.466

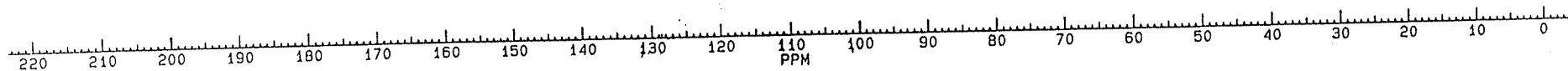
77.000

76.581

27.989

27.744

000



SAMPLE SPM-3-86, 1-H AT 300 MHZ IN CDCL3



SPM386.001
DATE 8-4-92

SF 300.133
SY 100.0
O1 5500.000
SI 32768
ID 32768
SW 5494.505
HZ/PT .335

PW 8.0
RD 4.000
AQ 2.982
RG 8
NS 32
TE 300

FW 6900
O2 20000.000
DP 63L D0

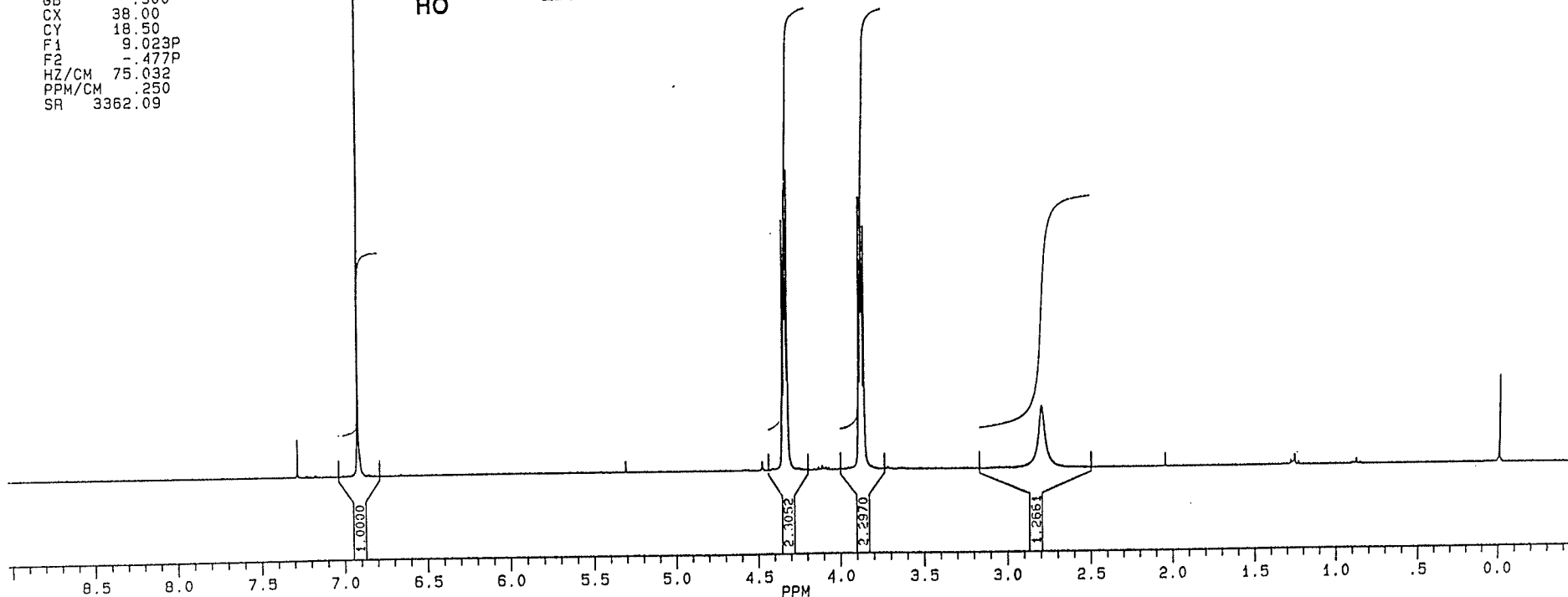
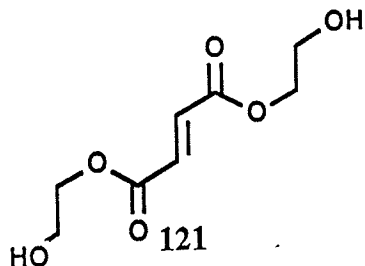
LB .300
GB .500
CX 38.00
CY 18.50
F1 9.023P
F2 -.477P
HZ/CM 75.032
PPM/CM .250
SR 3362.09

6.91543

4.34618
4.33799
4.33094
4.32570
4.31525
3.88497
3.87461
3.86922
3.86513
3.85366

2.79177

-00011



SAMPLE SPM-3-86, 13-C AT 75.47 MHZ IN CDCL3

~~BRUKER~~

PPM

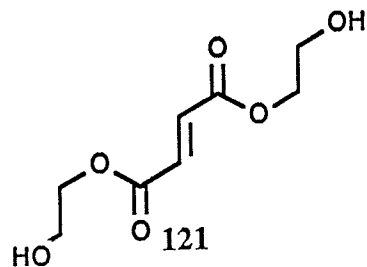
SPM386C.004
AU PROG:
AUTOC13.AU
DATE 9-4-92

SF 75.469
SY 112.0500000
Q1 47000.000
SI 32768
TD 32768
SW 17857.143
HZ/PT 1.090

PW 5.0
RD 0.0
AQ .918
RG 200
NS 512
TE 300

FW 22400
O2 5000.000
DP 18H CPD

LB 1.000
GB 700
CX 38.00
CY 18.00
F1 223.431P
F2 -4.564P
HZ/CM 452.802
PPM/CM 6.000
SR 38595.68



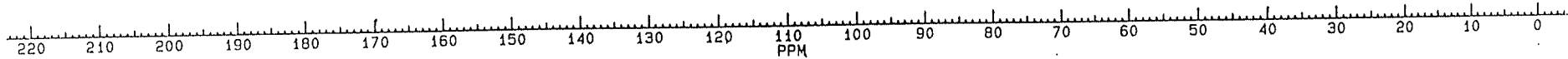
165.056

133.698

77.463
77.000
76.616

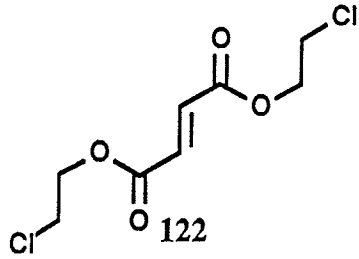
66.865

60.672



PPH

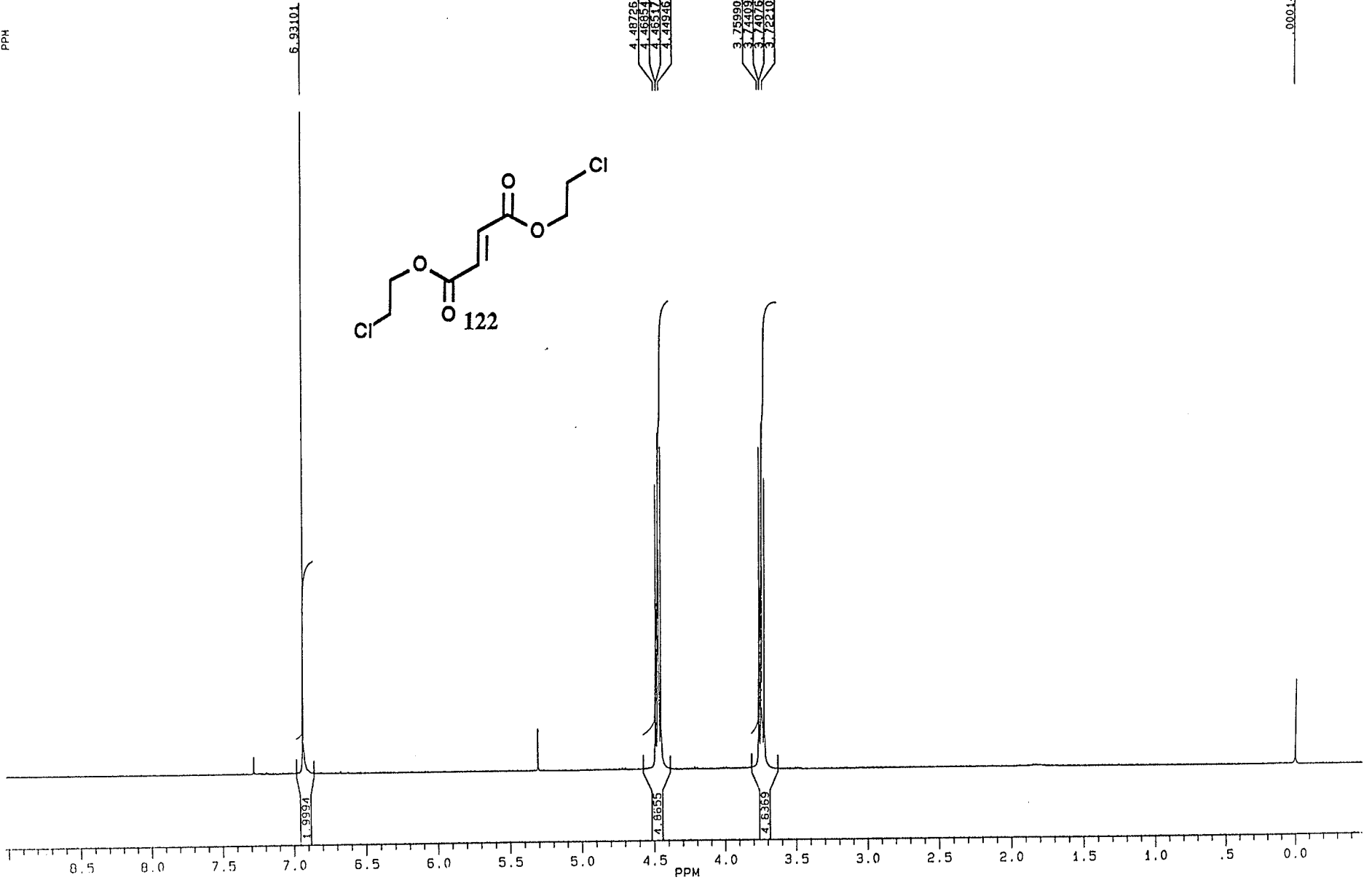
SPM-3-76 IN CDCL



4.48726
4.46657
4.45877
4.44846

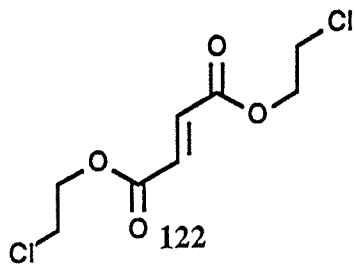
3.75990
3.74007
3.74074
3.72210

0.00014



PPM

SPM-3-76



164.290

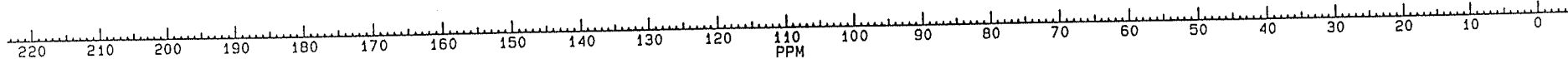
135.295
133.590

111.401

77.511
77.090
76.866

64.873

41.275





CTP12AC.004
DATE 10-7-91

3F 300.133
SY 100.0
Q1 5500.000
SI 32768
TD 32768
SW 5494.505
HZ/PT .335

PH 8.0
PD 4.000
AQ 2.982
PR 100
NS 22
TE 200

FW 5900
DZ 20000.000
DP 52L 00

LB .300
SD .500
CX 25.00
CY 18.50
F1 9.000P
F2 -.049P
HZ/CM 71.475
PPM/CM 238
SR 2267.42

PPM

7.25919

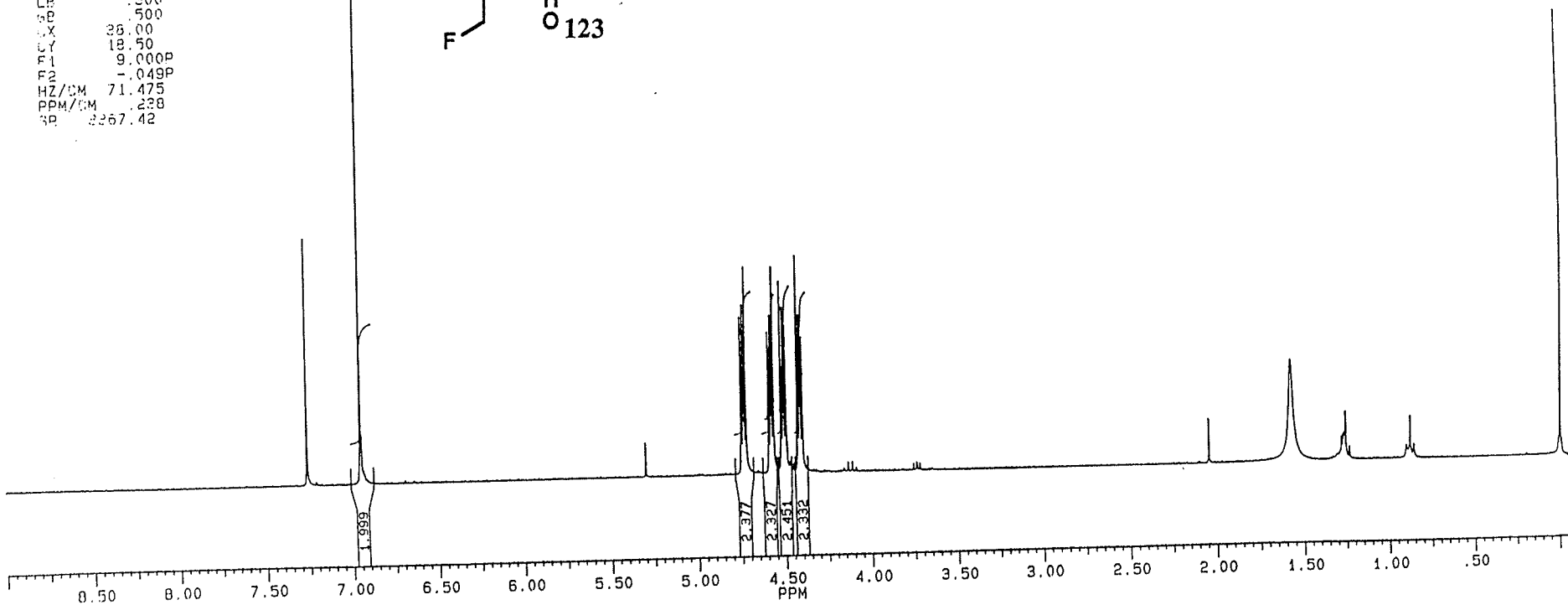
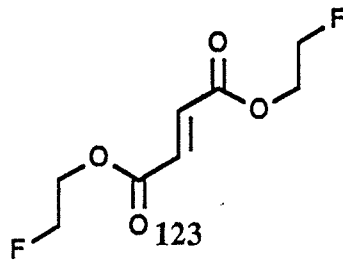
6.94916

SPM-3-77

4.74795
4.73449
4.73003
4.72015
4.59042
4.57118
4.57239
4.56273
4.51912
4.50943
4.49141
4.48331
4.47521
4.41074
4.39732

1.57617

0.113





PPM

SPM377C.001
AU PROG:
POWSTORE.AU
DATE 17-8-93

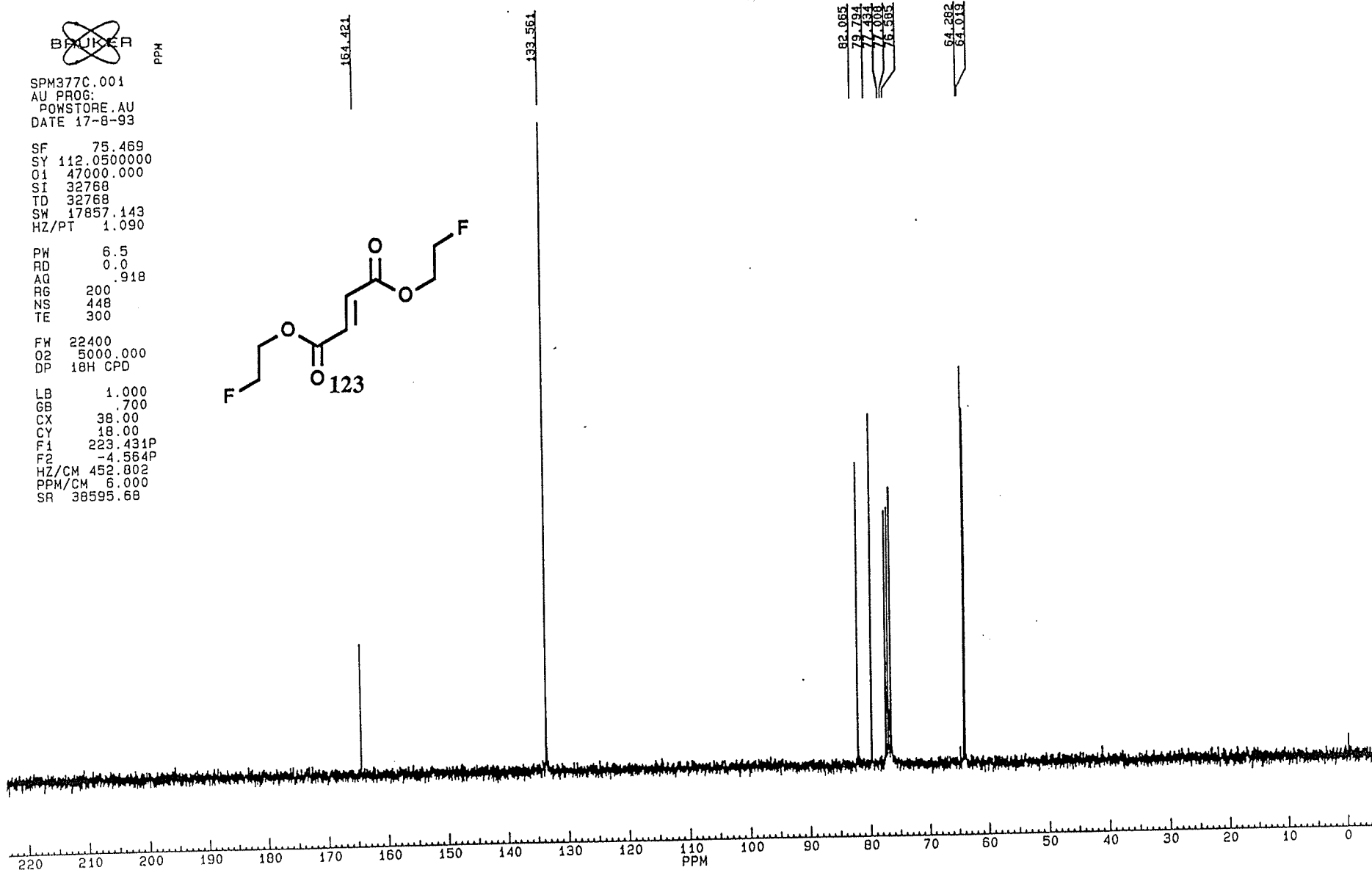
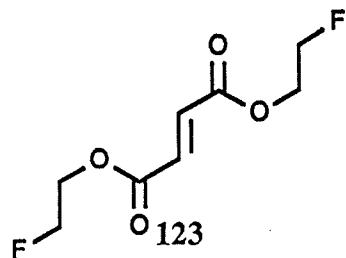
SF 75.469
SY 112.050000
O1 47000.000
SI 32768
TD 32768
SW 17857.143
HZ/PT 1.090

PW 6.5
RD 0.0
AQ .918
RG 200
NS 448
TE 300

FW 22400
O2 5000.000
DP 18H CPD

LB 1.000
GB .700
CX 38.00
CY 18.00
F1 223.431P
F2 -4.564P
HZ/CM 452.802
PPM/CM 6.000
SR 38595.68

SAMPLE SPM-3-77 13-C AT 75.47 MHZ IN CDCL3



SPM-2-18-CHR-16 1-H AT 300 MHZ IN CDCL3

~~BRUKER~~

PPM

SPM21816.001
 AU PRO5
 AUTOM1
 DATE 22-6-89

SF 300.133
 SY 100.0
 Q1 5500.000
 SI 32758
 TD 32758
 SW 5494.505
 HZ/Pf 3.35

PW 3.0
 PD 4.000
 AQ 2.982
 RG 100
 NS 32
 TE 200

FW 5900
 Q2 20000.000
 DP 53L D0

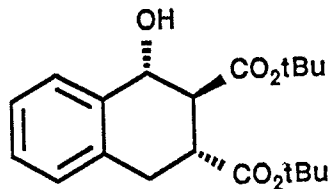
LB .300
 GB .500
 CX 38.00
 CY 19.50
 FI 9.003P
 F2 -4.97P
 HZ/CM 75.032
 PPM/CM .250
 SR 3.253.13

7.55264
 7.25724
 7.22923
 7.22666
 7.20386
 7.19884
 7.08393

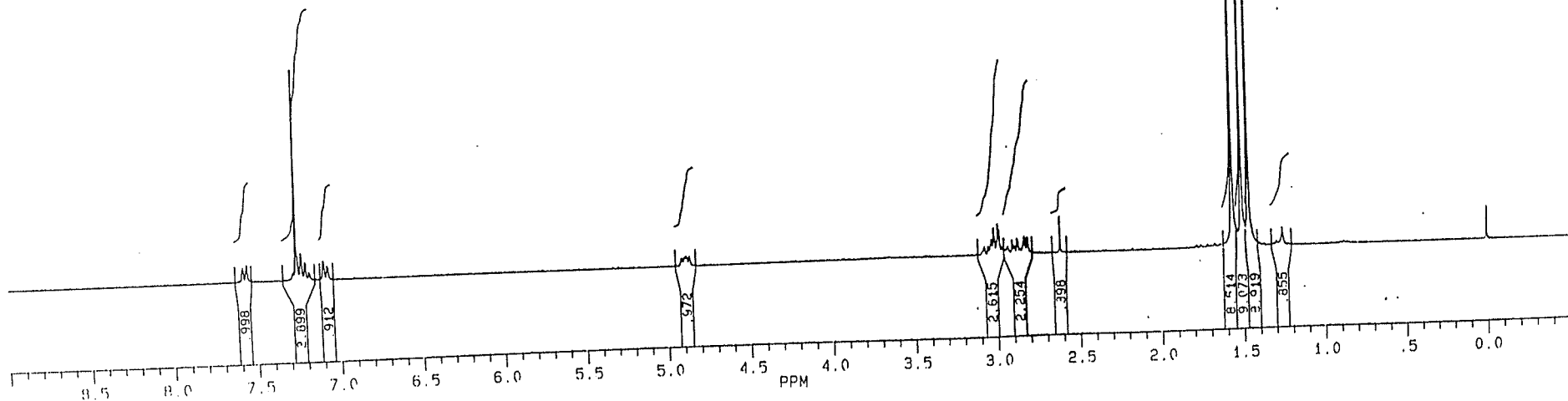
3.01250
 3.00811
 2.99832
 2.97777
 2.86832
 2.61277

1.56055
 1.50202
 1.48042
 1.25519

0.0013



124



BRUKER

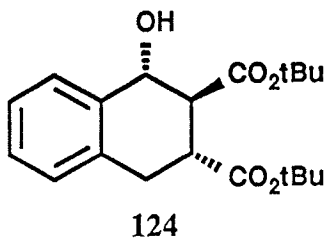
SPM164XC.004
AU PROG:
AUTOC13.AU
DATE 19-12-90

SF 75.469
SY 112.0500000
O1 47000.000
SI 32768
TD 32768
SW 17857.143
HZ/PT 1.090

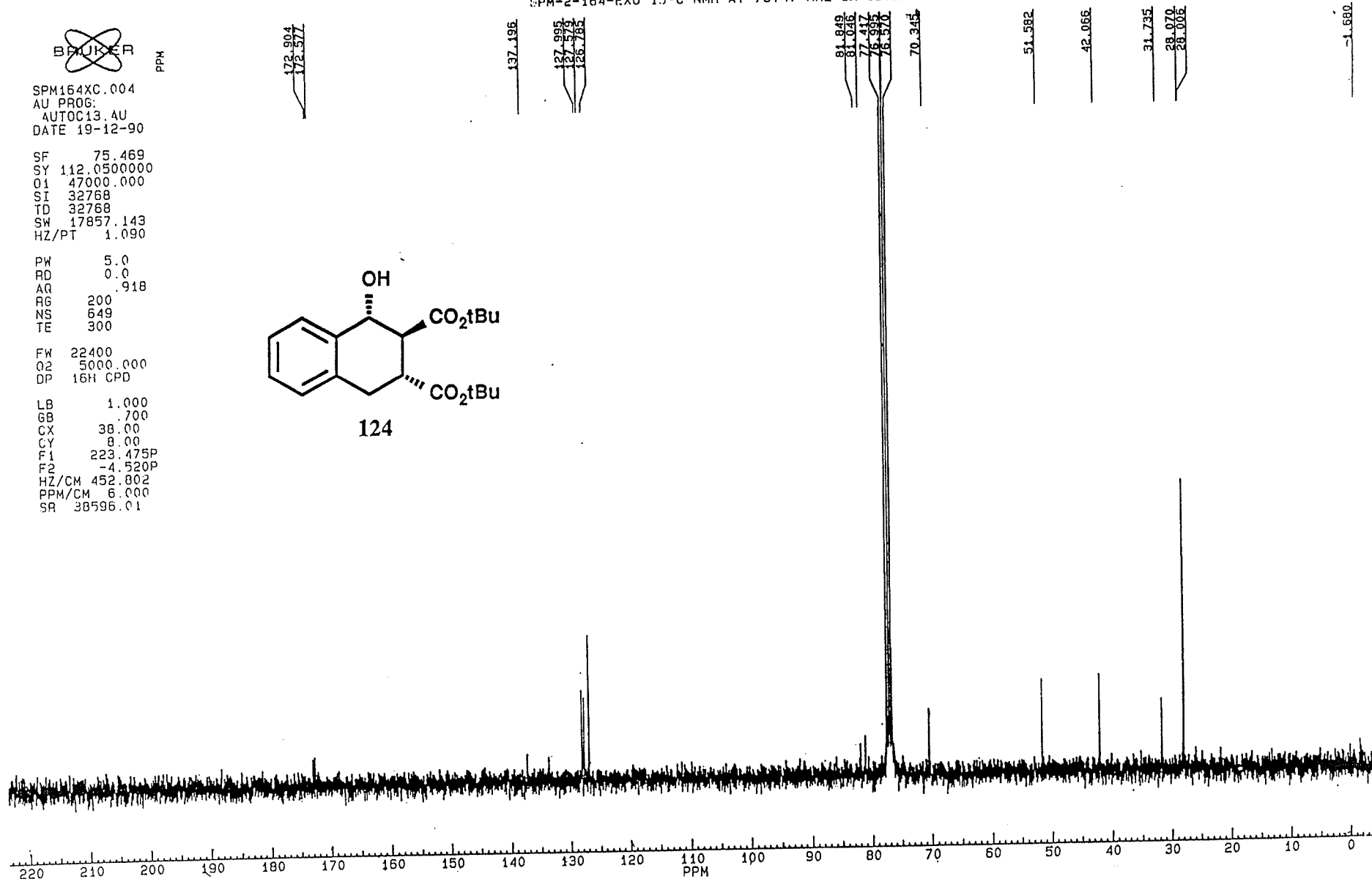
PW 5.0
RD 0.0
AQ .918
RG 200
NS 649
TE 300

FW 22400
Q2 5000.000
DP 16H CPD

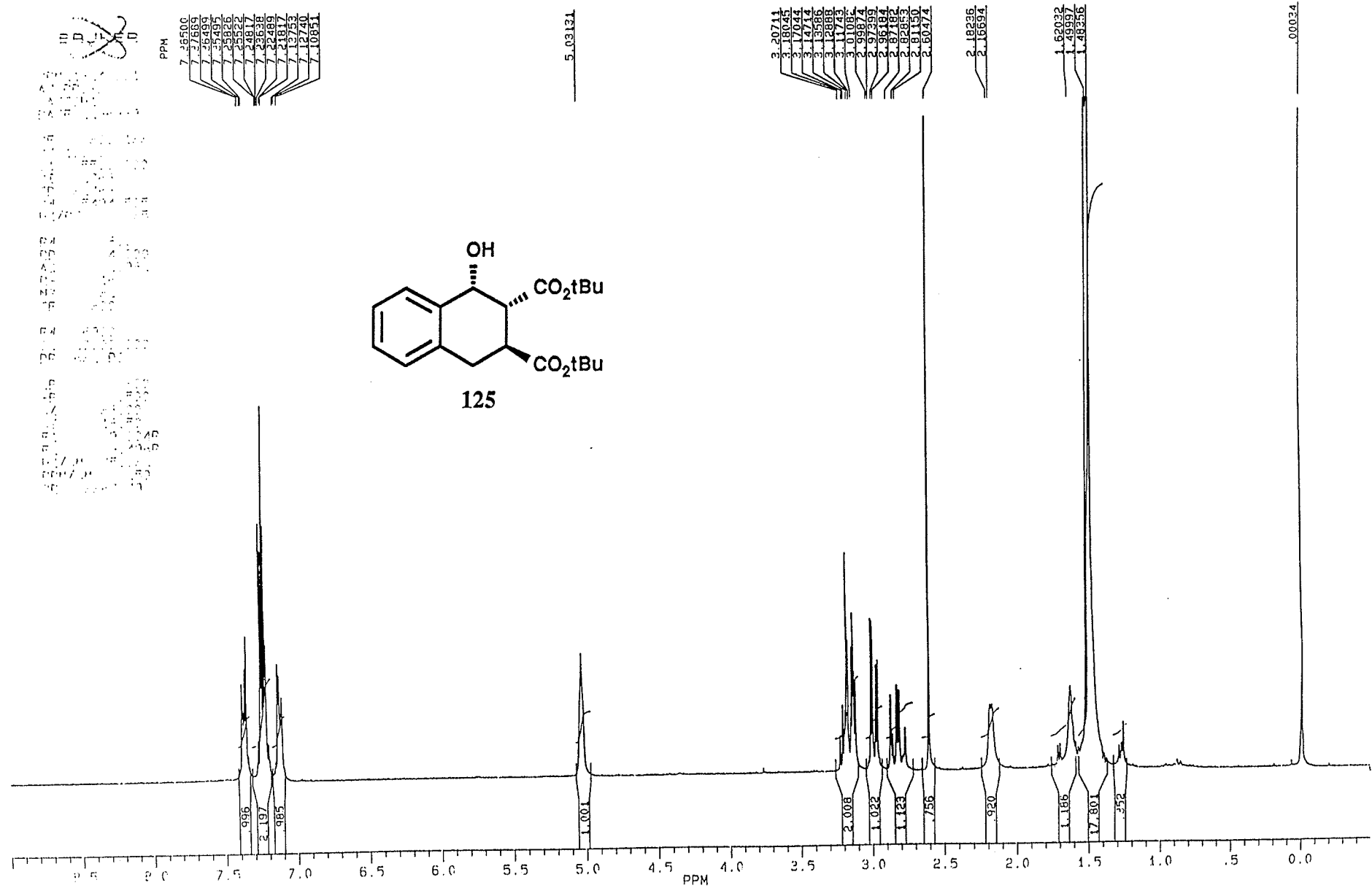
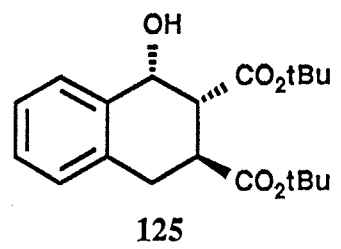
LB 1.000
GB .700
CX 38.00
CY 8.00
F1 223.475P
F2 -4.520P
HZ/CM 452.802
PPM/CM 6.000
SR 38596.01



SPM-2-164-EXO 13-C NMR AT 75.47 MHZ IN CDCL3



SPM-2-18-24 1-H AT 300 MHZ IN CDCL3





SPM2164C.004
AU PROG:
AUTOC13.AU
DATE 19-12-90

SF 75.469
SY 112.050000
O1 47000.000
SI 32768
TD 32768
SW 17857.143
HZ/PT 1.090

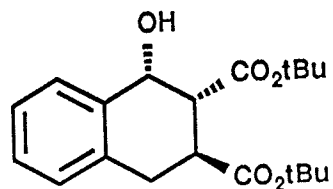
PW 5.0
RD 0.0
AQ .918
RG 200
NS 192
TE 300

FW 22400
O2 5000.000
DP 18H CPD

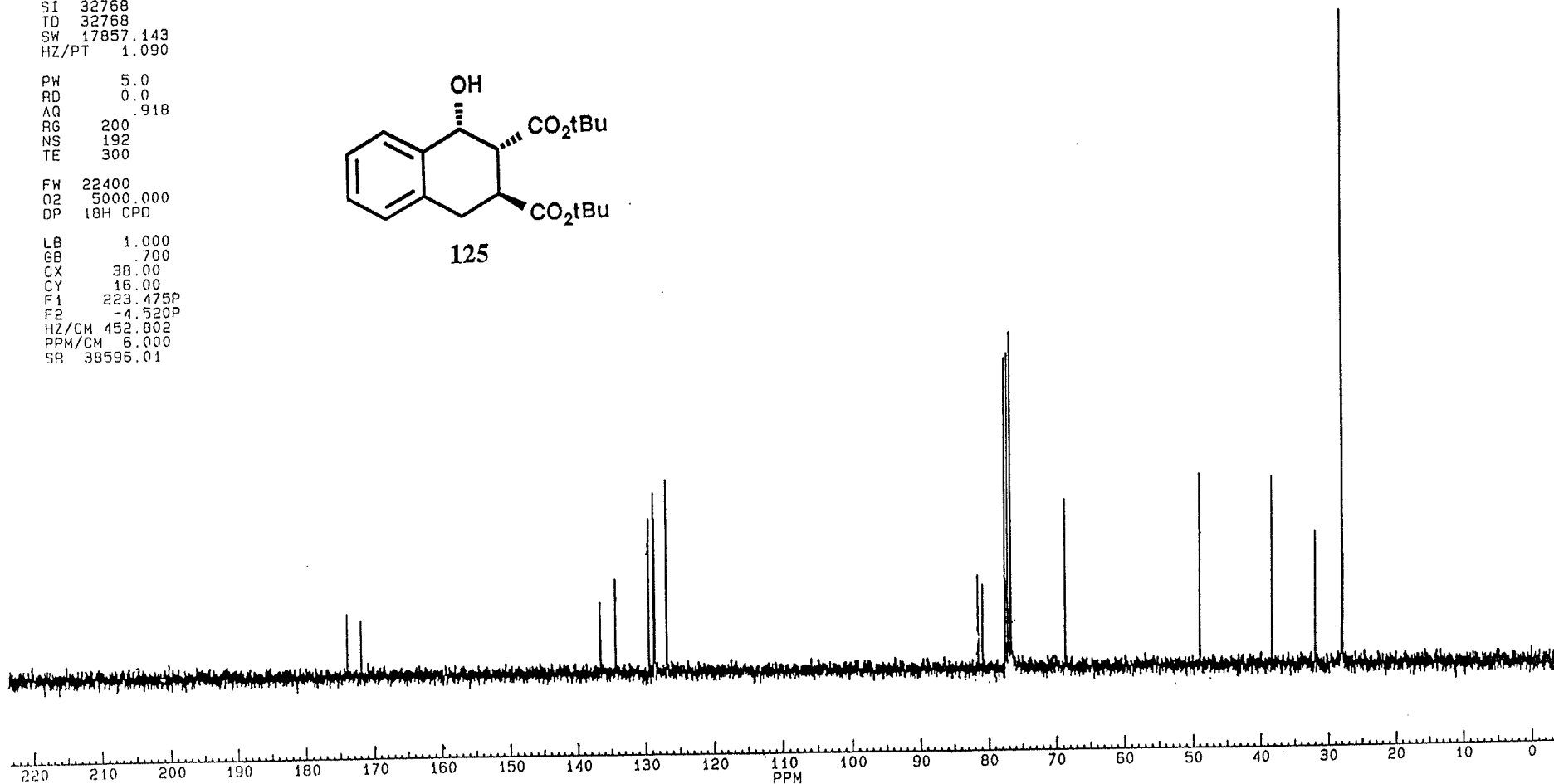
LB 1.000
GB .700
CX 38.00
CY 16.00
F1 223.475P
F2 -4.520P
HZ/CM 452.802
PPM/CM 6.000
SR 38596.01

SPM-2-164-ENDO 13-C NMR AT 75.47 MHZ IN CDCL3

173.834
171.783
136.443
134.189
129.334
128.600
128.467
126.738
81.389
80.680
77.429
77.004
76.581
68.524
48.866
38.295
31.090
27.822
23.732



125



SAMPLE SPM-2-40A, 1-H AT 300 MHZ IN CDCL3

~~BRUKER~~

PPM

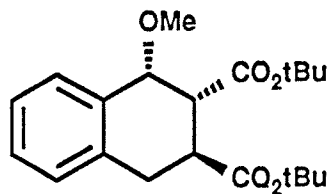
SPM240A.001
DATE 31-3-92

SF 300.133
SY 100.0
Q1 5500.000
SI 32768
TD 32768
SW 5494.505
HZ/PT .335

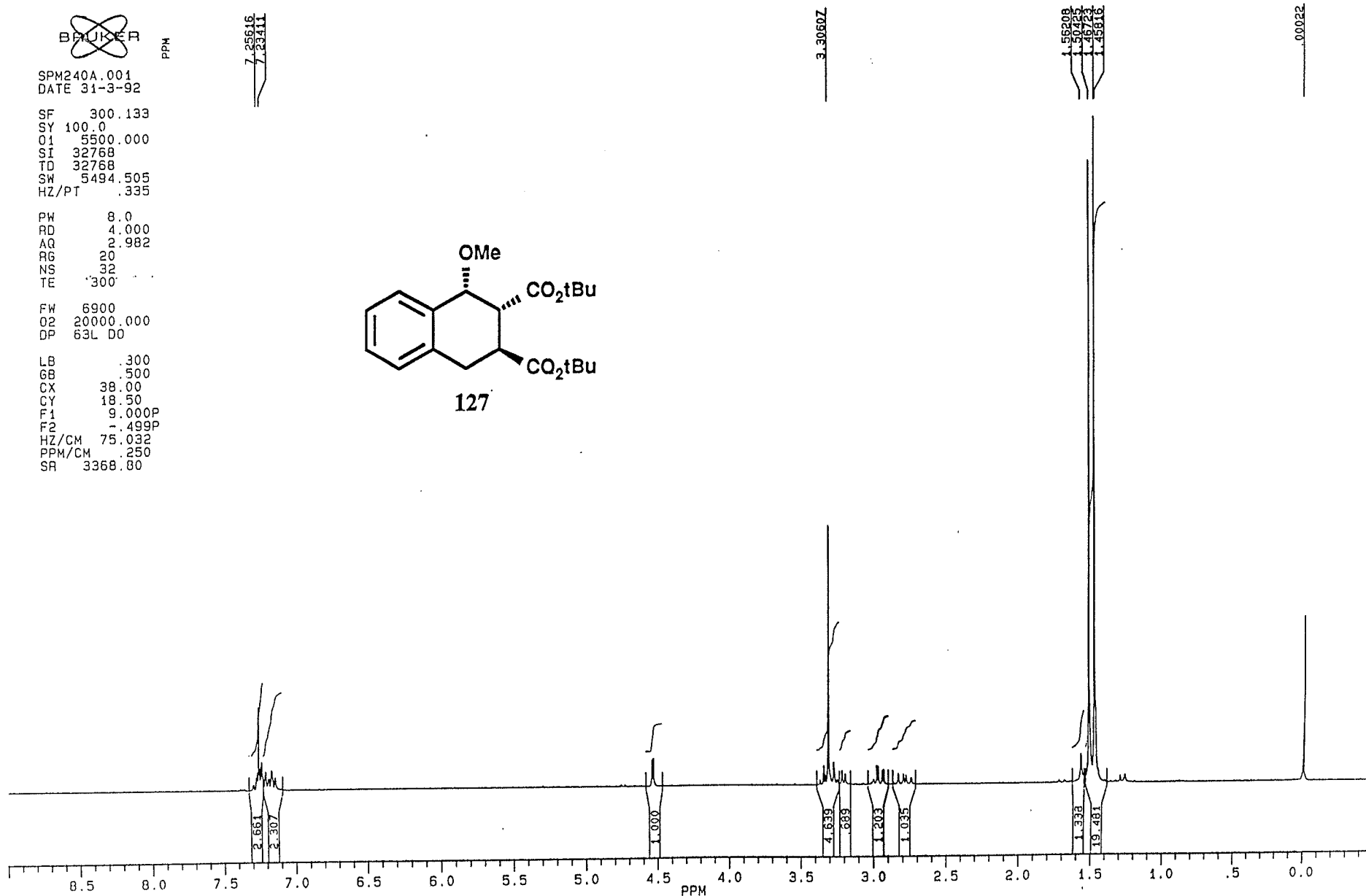
PW 8.0
RD 4.000
AQ 2.982
RG 20
NS 32
TE '300'

FW 6900
O2 20000.000
DP 63L D0

LB .300
GB .500
CX 38.00
CY 18.50
F1 9.000P
F2 .499P
HZ/CM 75.032
PPM/CM .250
SR 3368.80



127



BRUKER

PPM

SPM240AC.004
AU PROG:
AUTOC13.AU
DATE 2-4-92

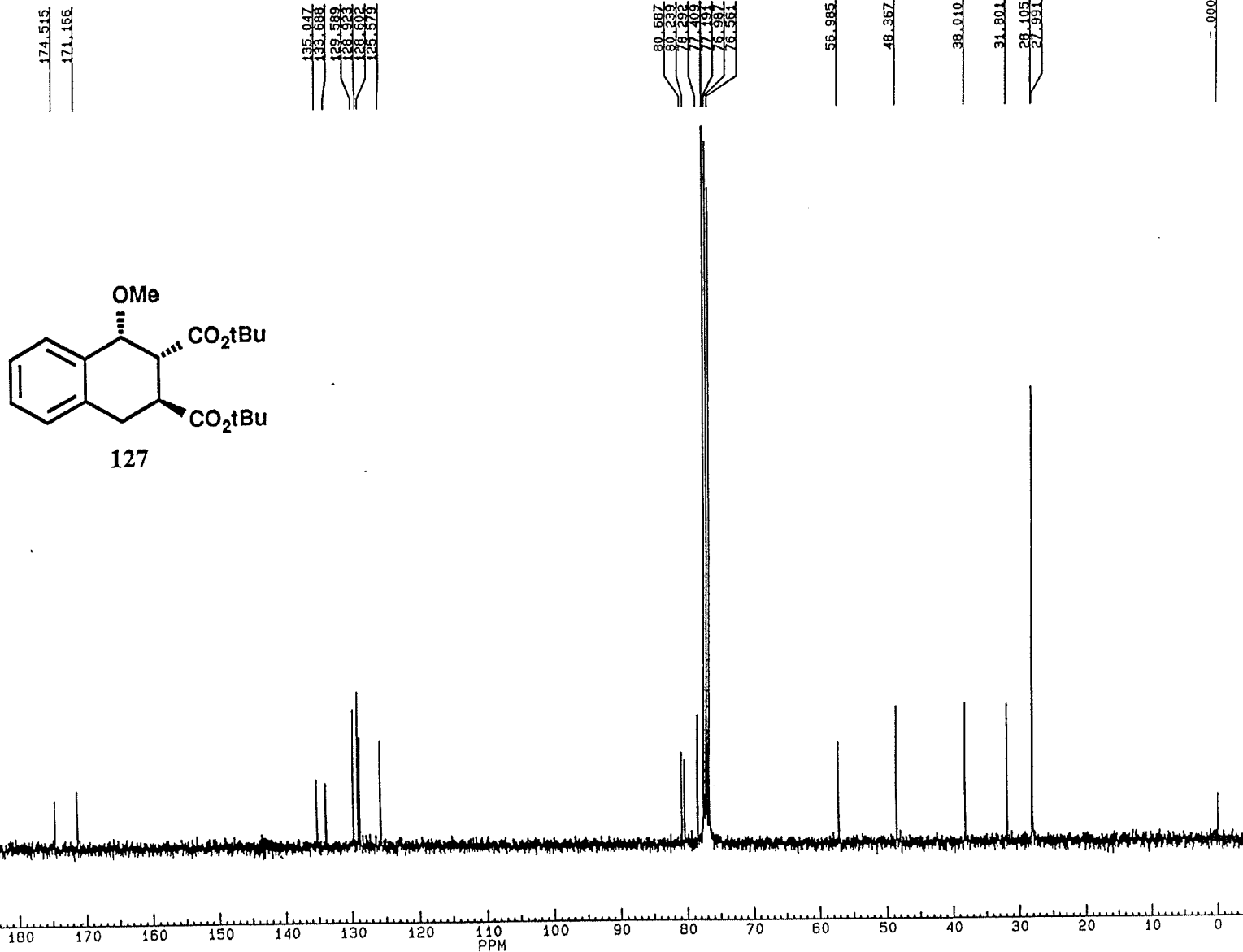
SF 75.469
SY 112.0500000
O1 47000.000
SI 32768
TD 32768
SW 17857.143
HZ/PT 1.090

PW 5.0
RD 0.0
AQ .918
RG 200
NS 1152
TE 300

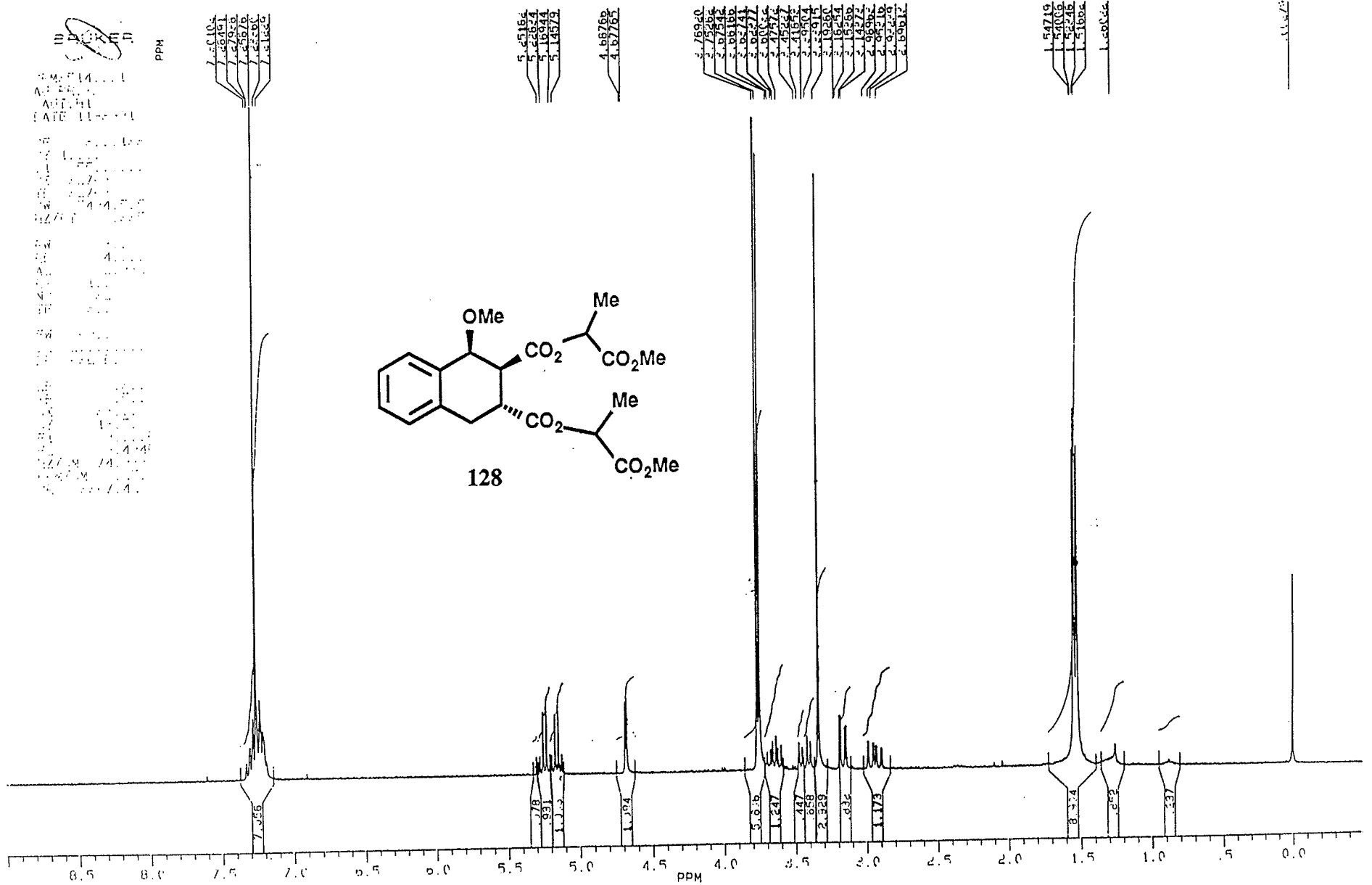
FW 22400
O2 5000.000
DP 18H CPD

LB 1.000
GB .700
CX 38.00
CY 18.00
F1 223.417P
F2 -4.578P
HZ/CM 452.802
PPM/CM 6.000
SR 38596.77

SAMPLE SPM-2-40A, 13-C AT 75.47 MHZ IN CDCL3



SPM-3-51-4 1-H AT 300 MHZ IN CDCL3



SAMPLE SPM-2-26CHR17. 13-C AT 75.47 MHZ IN CDCL3

BRUKER

PPM

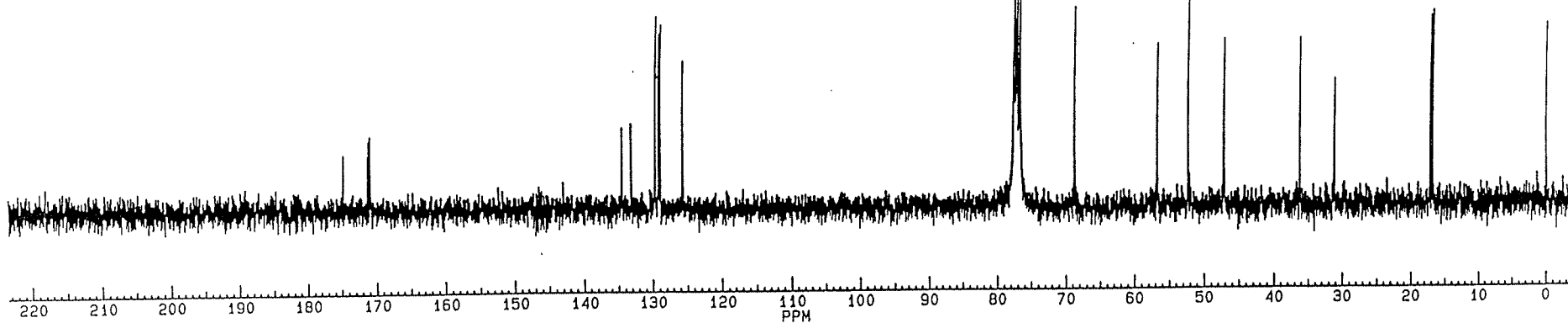
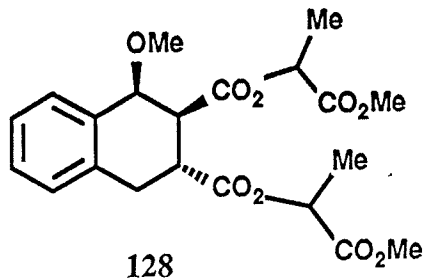
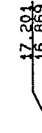
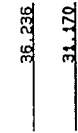
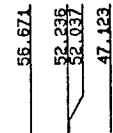
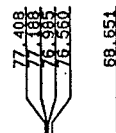
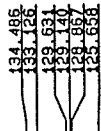
SPCHR17C.004
 AU PROG:
 AUTOC13.AU
 DATE 4-4-92

SF 75.469
 SY 112.0500000
 O1 47000.000
 SI 32768
 TD 32768
 SW 17857.143
 HZ/PT 1.090

PW 5.0
 RD 0.0
 AQ 9.18
 RG 200
 NS 4800
 TE 300

FW 22400
 O2 5000.000
 DP 18H CPD

LB 1.000
 GB .700
 CX 38.00
 LY 8.50
 F1 223.417P
 F2 -4.578P
 HZ/CM 452.802
 PPM/CM 6.000
 SR 38596.77





SPM351.003
DATE 13-5-91

SF 300.133
SY 100.0
C1 5500.000
SI 32768
TD 32768
SW 5494.505
HZ/P1 335

PW 8.0
RD 4.000
AQ 2.982
RG 80
NS 32
TE 300

FW 6900
Q2 20000.000
DP 53L D0

LB .300
GB .500
CX 28.00
LY 18.50
F1 9.005P
F2 1.495P
HZ/CM 75.032
PPM/CM .250
SR 3367.42

7.32672
7.30374
7.29062
7.27392
7.25972
7.23968
7.21810
7.18210
6.90872

5.29844
5.27157
5.24617
5.22482
5.16712
5.14352
5.12000
5.09657

4.66977
4.65876

SPM-3-51-3

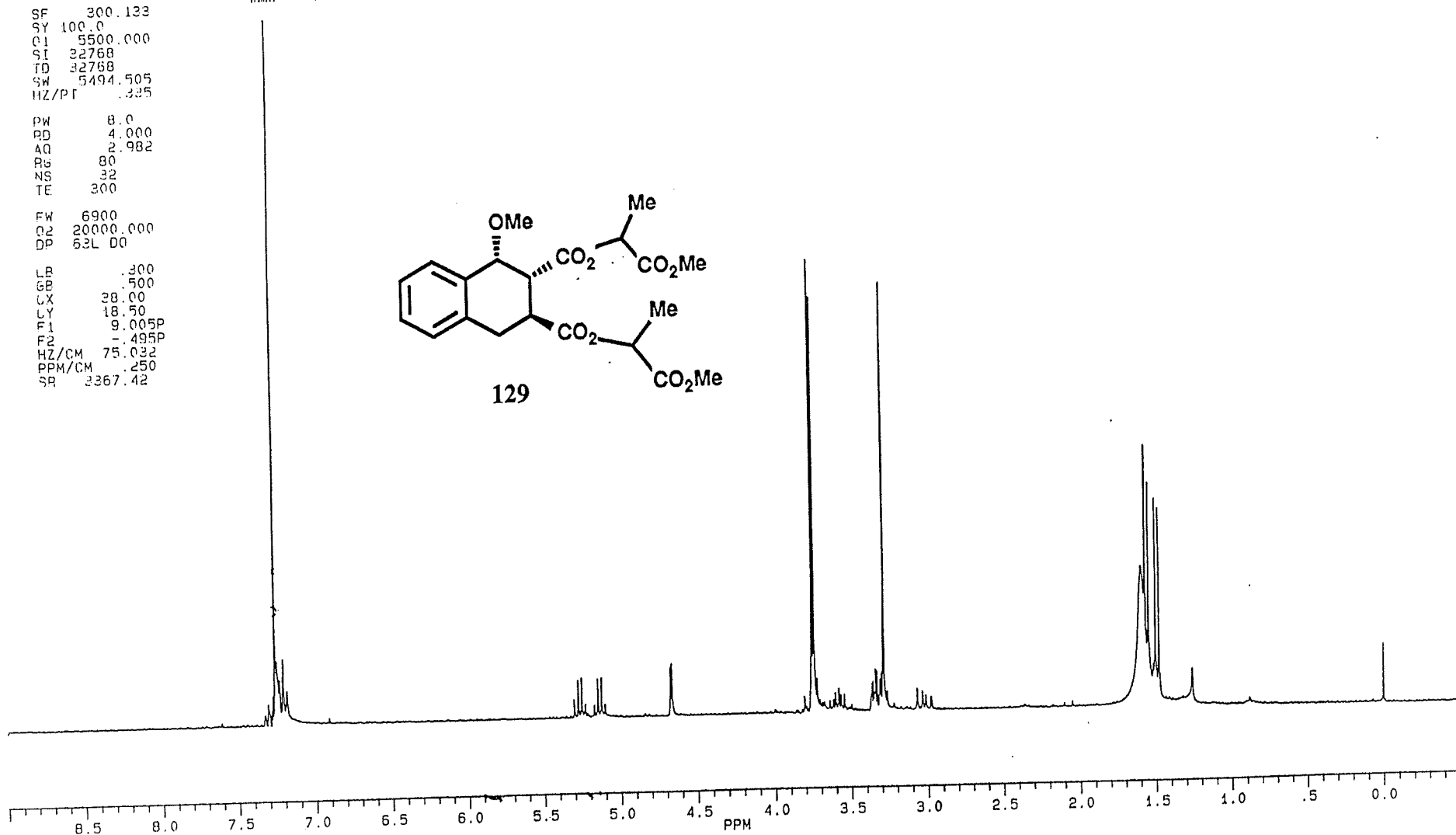
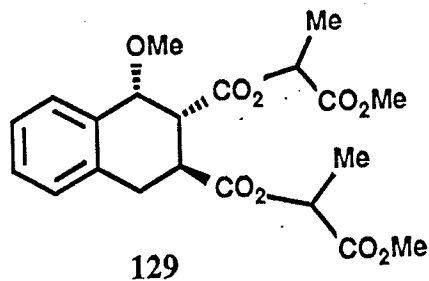
3.80017
3.75103
3.73654
3.71927
3.69961
3.68254
3.67032
3.65783
3.64410
3.63065
3.61848
3.59848
3.59105
3.56777
3.54956
3.54224
3.52310
3.50526
3.48962
3.47484
3.46140
3.44833
3.42802
3.40660
2.97122

2.04486

1.58824
1.56321
1.53975
1.51076
1.49627
1.47277
1.25814

0.88308

0.02700



BRUKER

PPM

SPM226AC.004
AU PROG:
AUTOC13.AU
DATE 19-6-92

SF 75.469
SY 112.0500000
Q1 47000.000
SI 32768
TD 32768
SW 17857.143
HZ/PT 1.090

PW 5.0
RD 0.0
AQ .918
RG 200
NS 2688
TE 300

FW 22400
Q2 5000.000
DP 18H CPD

LB 1.000
GB 700
CX 38.00
CY 18.00
F1 223.417P
F2 -4.578D
HZ/CM 452.802
PPM/CM 6.000
SR 26596.77

SAMPLE SPM-2-26 13-C AT 75.47 MHZ IN CDCL3

173.509
170.969
170.862

134.596
132.914
129.626
129.025
128.890
126.746

77.406
77.182
76.980
76.597
76.521
68.859
68.642

56.731
52.260
52.221

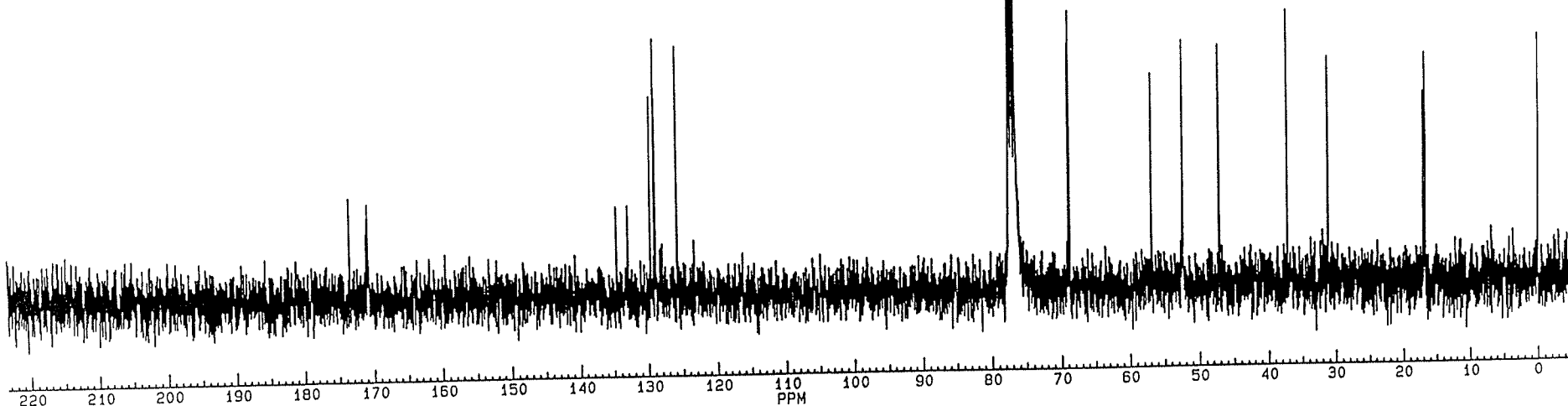
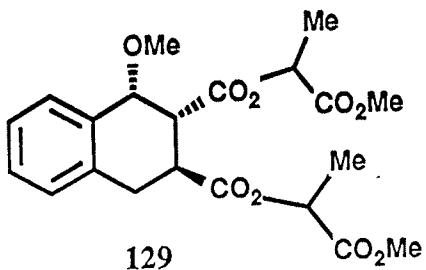
47.038

37.102

31.109

17.050
16.723

000

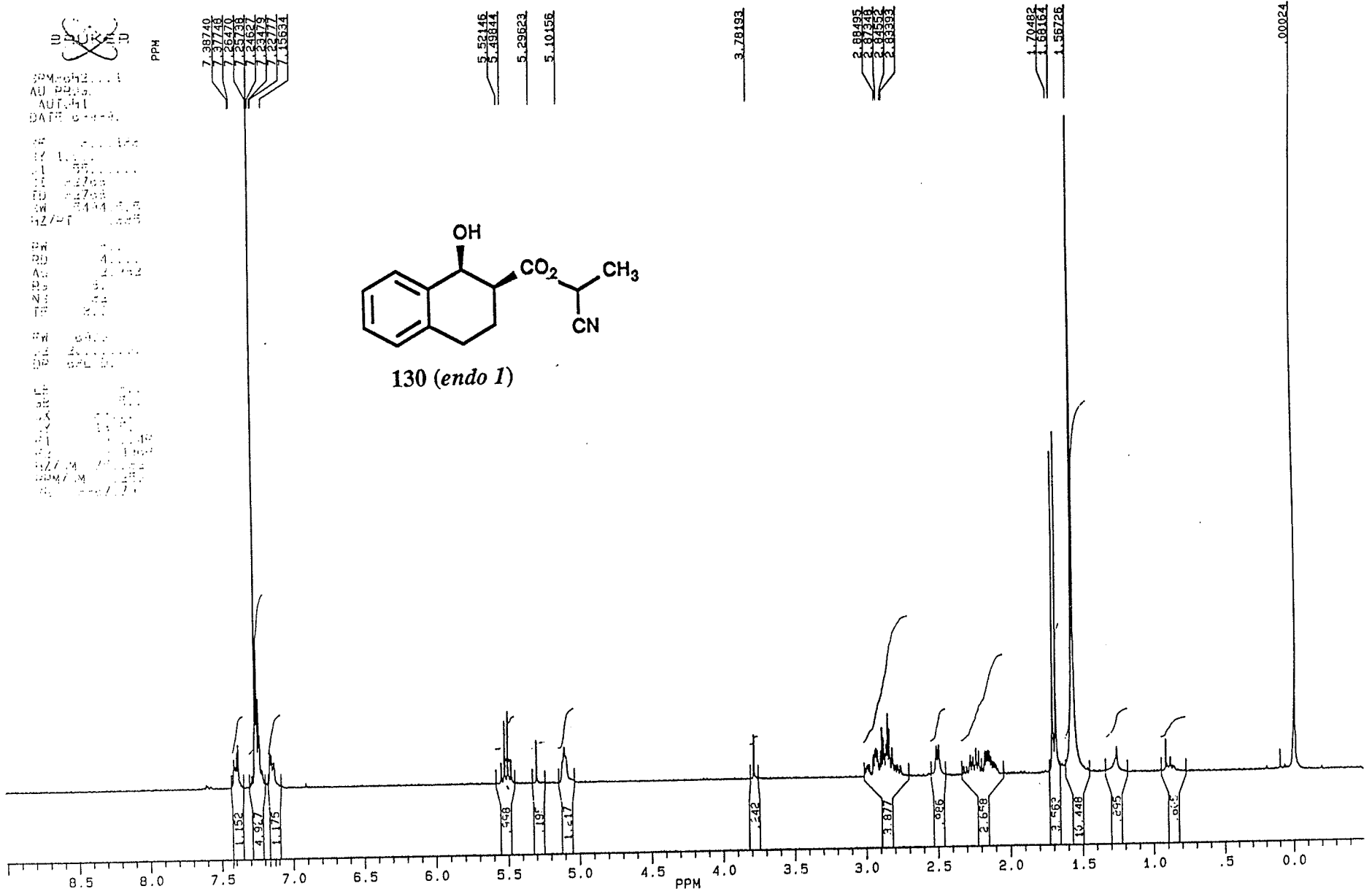
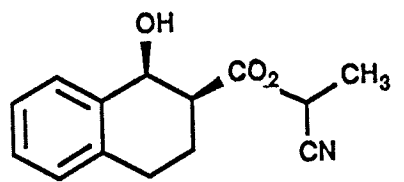


UPLC

SPM-3-6-15-HPLC-2 1-H AT 300 MHZ IN CDCL3
AU P030
AUT 41
DATE 6-4-93

1
F1 1.00
F2 0.10
F3 0.10
F4 0.10
F5 0.10
F6 0.10
F7 0.10
F8 0.10
F9 0.10
F10 0.10
F11 0.10
F12 0.10
F13 0.10
F14 0.10
F15 0.10
F16 0.10
F17 0.10
F18 0.10
F19 0.10
F20 0.10
F21 0.10
F22 0.10
F23 0.10
F24 0.10
F25 0.10
F26 0.10
F27 0.10
F28 0.10
F29 0.10
F30 0.10
F31 0.10
F32 0.10
F33 0.10
F34 0.10
F35 0.10
F36 0.10
F37 0.10
F38 0.10
F39 0.10
F40 0.10
F41 0.10
F42 0.10
F43 0.10
F44 0.10
F45 0.10
F46 0.10
F47 0.10
F48 0.10
F49 0.10
F50 0.10
F51 0.10
F52 0.10
F53 0.10
F54 0.10
F55 0.10
F56 0.10
F57 0.10
F58 0.10
F59 0.10
F60 0.10
F61 0.10
F62 0.10
F63 0.10
F64 0.10
F65 0.10
F66 0.10
F67 0.10
F68 0.10
F69 0.10
F70 0.10
F71 0.10
F72 0.10
F73 0.10
F74 0.10
F75 0.10
F76 0.10
F77 0.10
F78 0.10
F79 0.10
F80 0.10
F81 0.10
F82 0.10
F83 0.10
F84 0.10
F85 0.10
F86 0.10
F87 0.10
F88 0.10
F89 0.10
F90 0.10
F91 0.10
F92 0.10
F93 0.10
F94 0.10
F95 0.10
F96 0.10
F97 0.10
F98 0.10
F99 0.10
F100 0.10

SPM-3-6-15-HPLC-2 1-H AT 300 MHZ IN CDCL3



BRUKER

SPM328H4.001
AU PROG:
AUTOM1
DATE 28-11-90

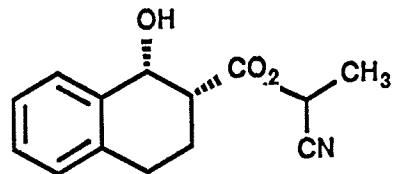
SF 300.133
SY 100.0
O1 5500.000
SI 32768
TD 32768
SW 5494.505
HZ/PT .335

PW 8.0
RD 4.000
AQ 2.982
RG 200
NS 32
TE 300

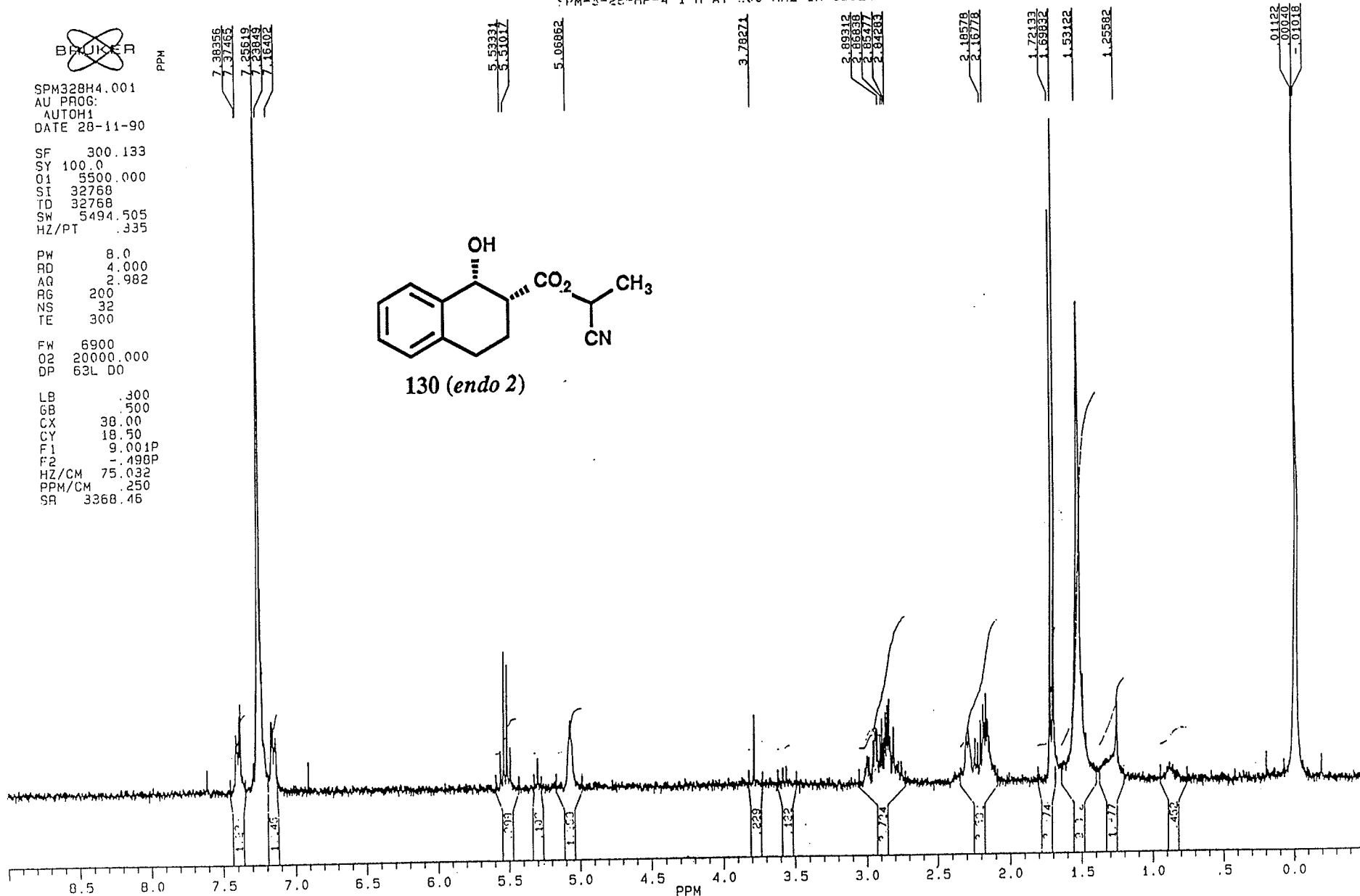
FW 6900
O2 20000.000
DP 63L D0

LB .300
GB .500
CX 38.00
CY 18.50
F1 9.001P
F2 -.498P
HZ/CM 75.032
PPM/CM .250
SR 3368.46

SPM-3-28-HP-4 1-H AT 300 MHZ IN CDCL3



130 (endo 2)



SPM-3-6-27 1-H AT 300 MHZ IN CDCL3



SPM-667.001
A1 6606
AUTOM1
DATE 03-09-99

RF 300.137
P1 100.0
Q1 5500.000
Q2 22765
TE 30.00
PW 4.00
HZ/PT 100.0

FW 8.0
AQ 4.000
RG 2.000
RE 100
NS 32
TE 30.0

FW 6000
AQ 10000.000
RG 2.000

RF 300.137
P1 100.0
Q1 5500.000
Q2 22765
TE 30.00
PW 4.00
HZ/PT 100.0

PPH

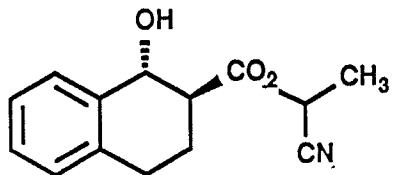
7.25972
7.23435

5.50660
5.48935

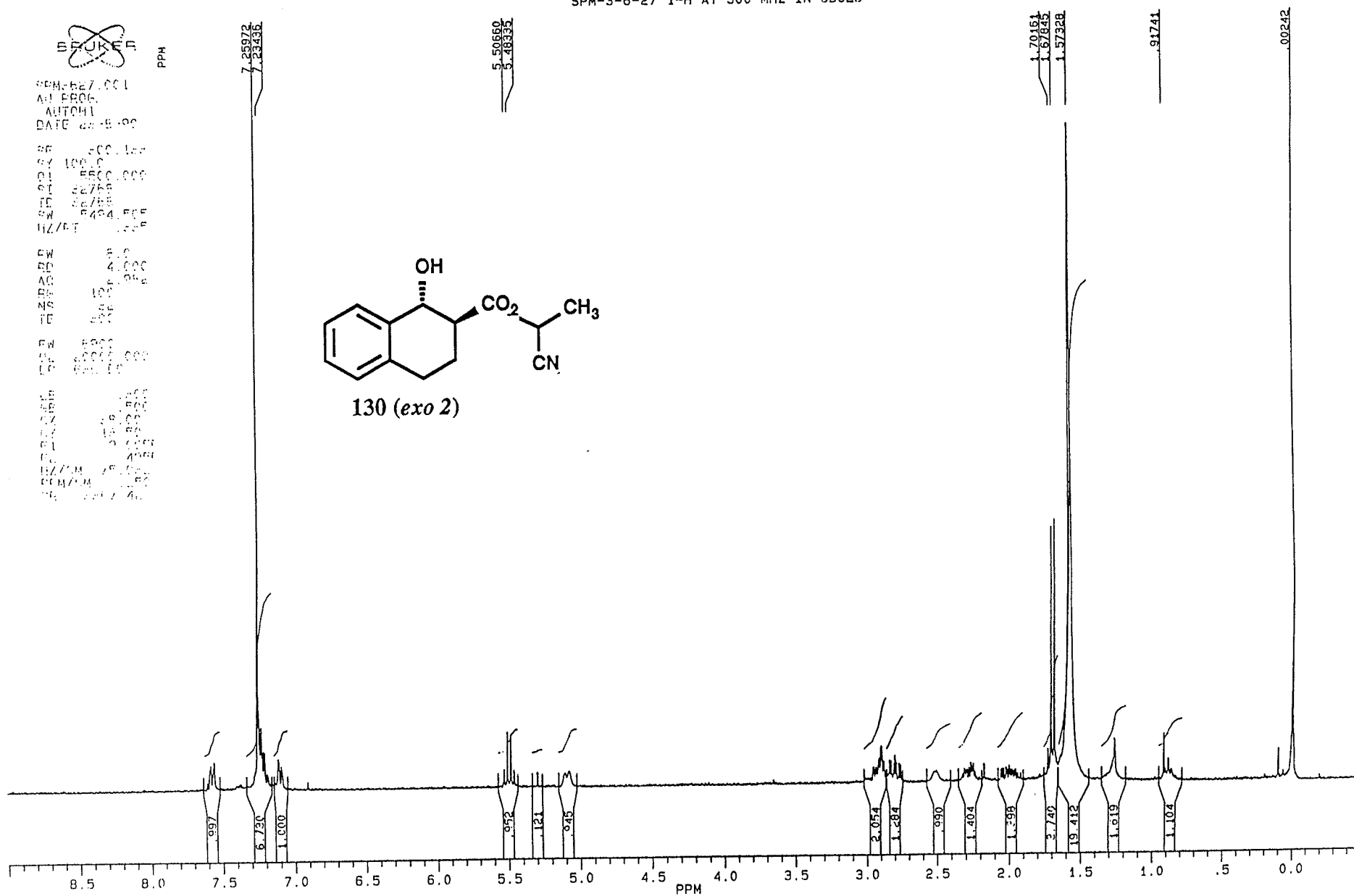
1.70161
1.67842
1.57328

0.91741

0.00242



130 (exo 2)



BRUKER

SPM2155.001
DATE 8-4-92

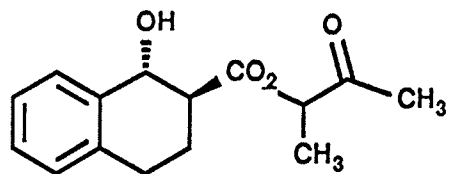
SF 300.133
SY 100.0
Q1 5500.000
SI 32768
TD 32768
SW 5494.505
HZ/PT .335

PW 8.0
RD 4.000
AQ 2.982
RG 20
NS 32
TE 300

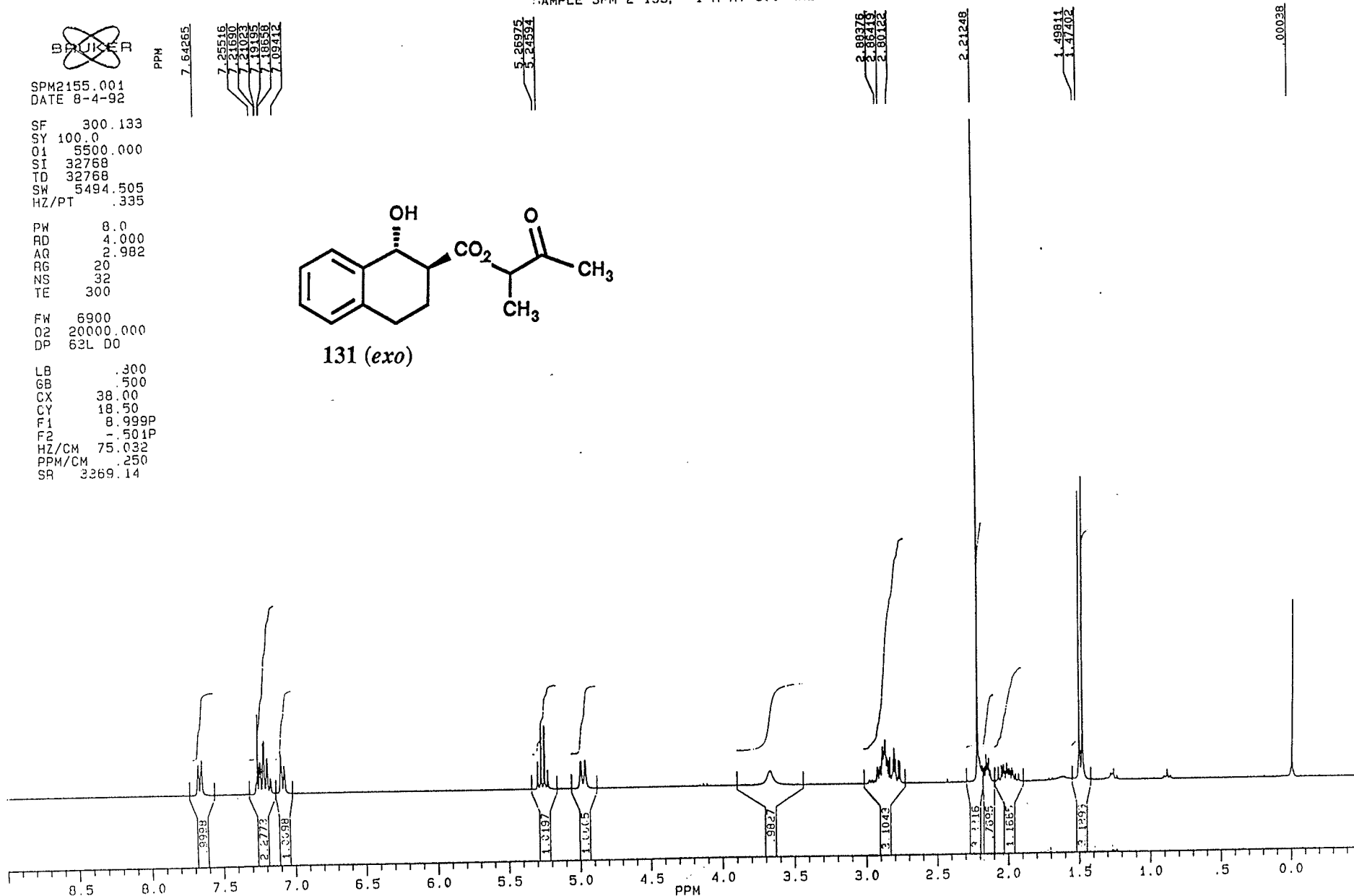
FW 6900
Q2 20000.000
DP 63L D0

LB .300
GB .500
CX 38.00
CY 18.50
F1 8.999P
F2 .501P
HZ/CM 75.032
PPM/CM .250
SR 3269.14

SAMPLE SPM-2-155, 1-H AT 300 MHZ IN CDCL3



131 (exo)





SPM2155C.004
AU PROG:
AUTOC131AU
DATE 9-4-92

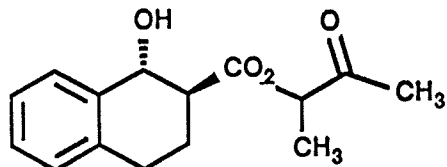
SF 75.469
SY 112.0500000
O1 47000.000
SI 32768
TD 32768
SW 17857.143
HZ/PT 1.090

PW 5.0
RD 0.0
AQ .918
RG 200
NS 4288
TE 300

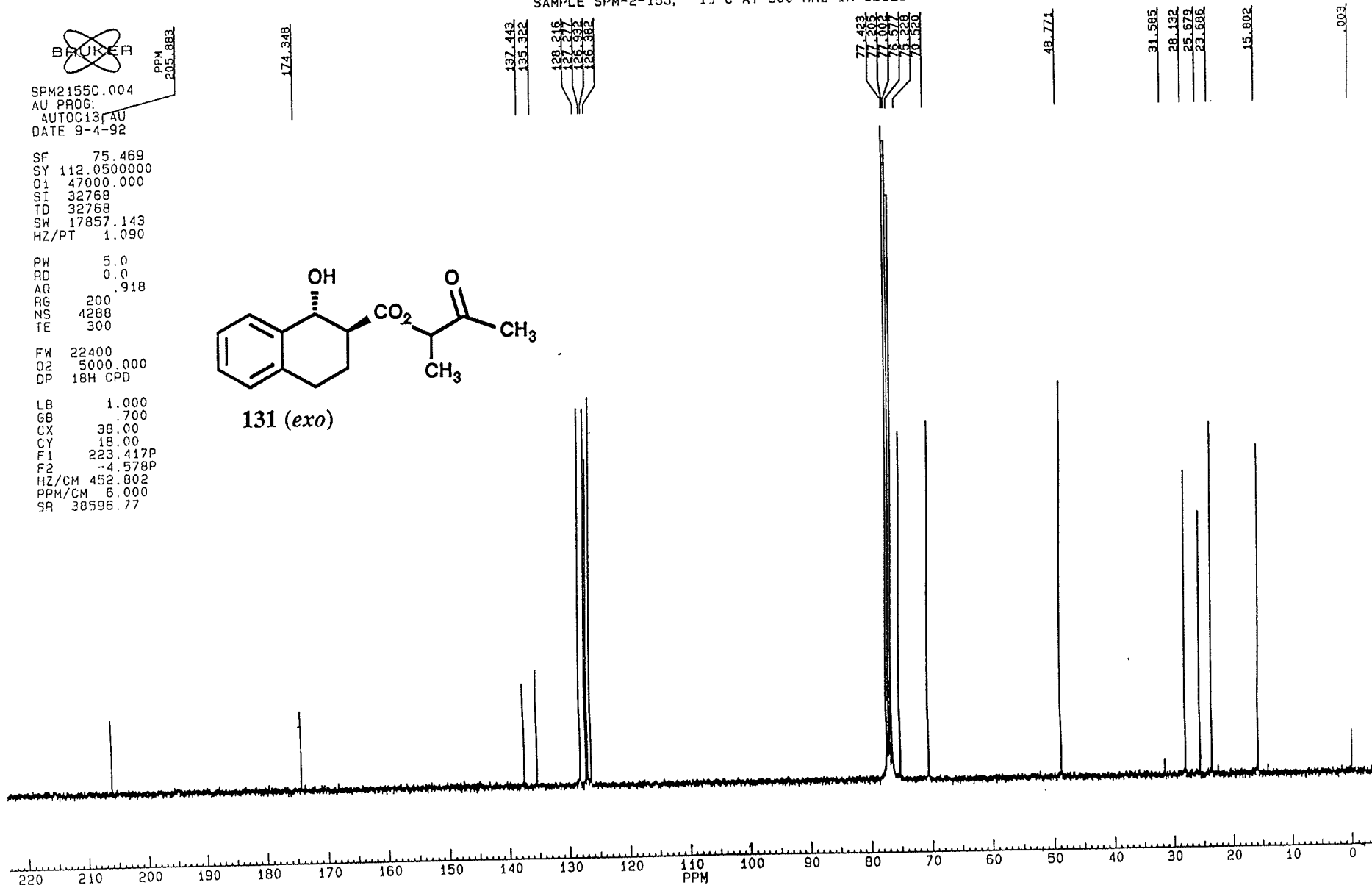
FW 22400
Q2 5000.000
DP 18H CPD

LB 1.000
GB .700
CX 38.00
CY 18.00
F1 223.417P
F2 -4.578P
HZ/CM 452.802
PPM/CM 6.000
SR 38596.77

SAMPLE SPM-2-155, 13-C AT 300 MHZ IN CDCL3



131 (exo)





SPM389L.001
DATE 7-11-91

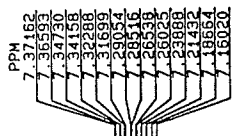
SF 300.133
SY 100.0
Q1 5500.000
SI 32768
TD 32768
SH 5494.505
HZ/PT .335

PW 8.0
RD 4.000
AQ 2.982
RG 20
NS 32
TE 300

FW 6900
Q2 20000.000
DP 62L D0

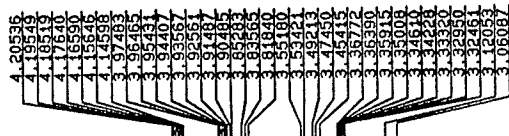
LB .300
GB .500
CX 38.00
CY 18.50
F1 9.005P
F2 1.495P
HZ/CM 75.032
PPM/CM .250
SR 3267.42

SAMPLE SPM-3-89-LAC, 1-H AT 300 MHZ IN CDCL3



5.47390
5.45602

5.28349



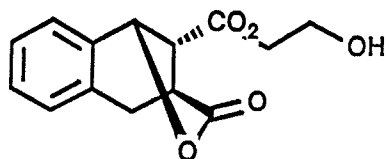
2.04034

1.63225

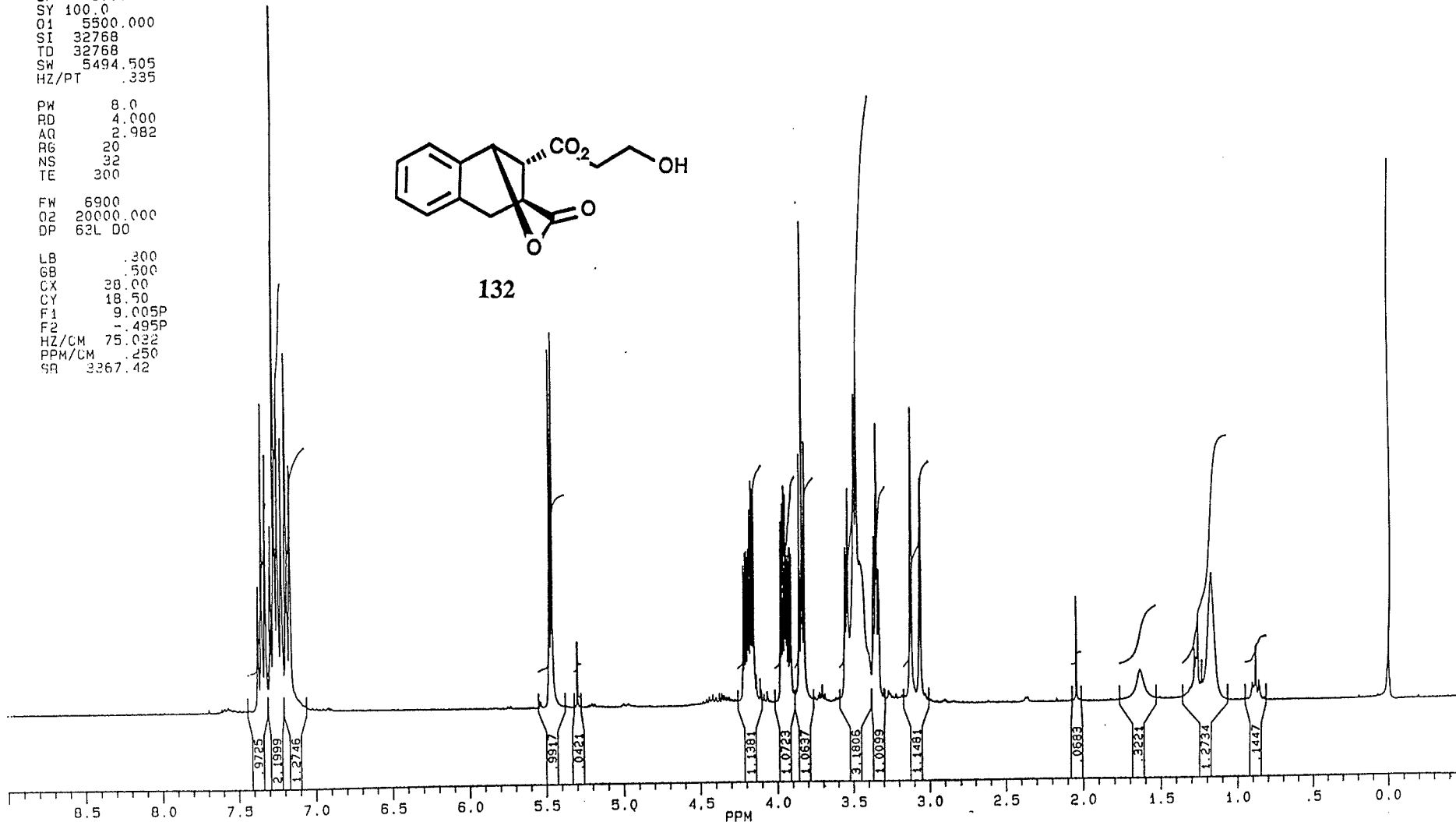
1.28055
1.27602
1.23866
1.17084

.88369

.01133
.00065



132





SPM389LC.004
AU PROG:
AUTOC13.AU
DATE 7-11-91

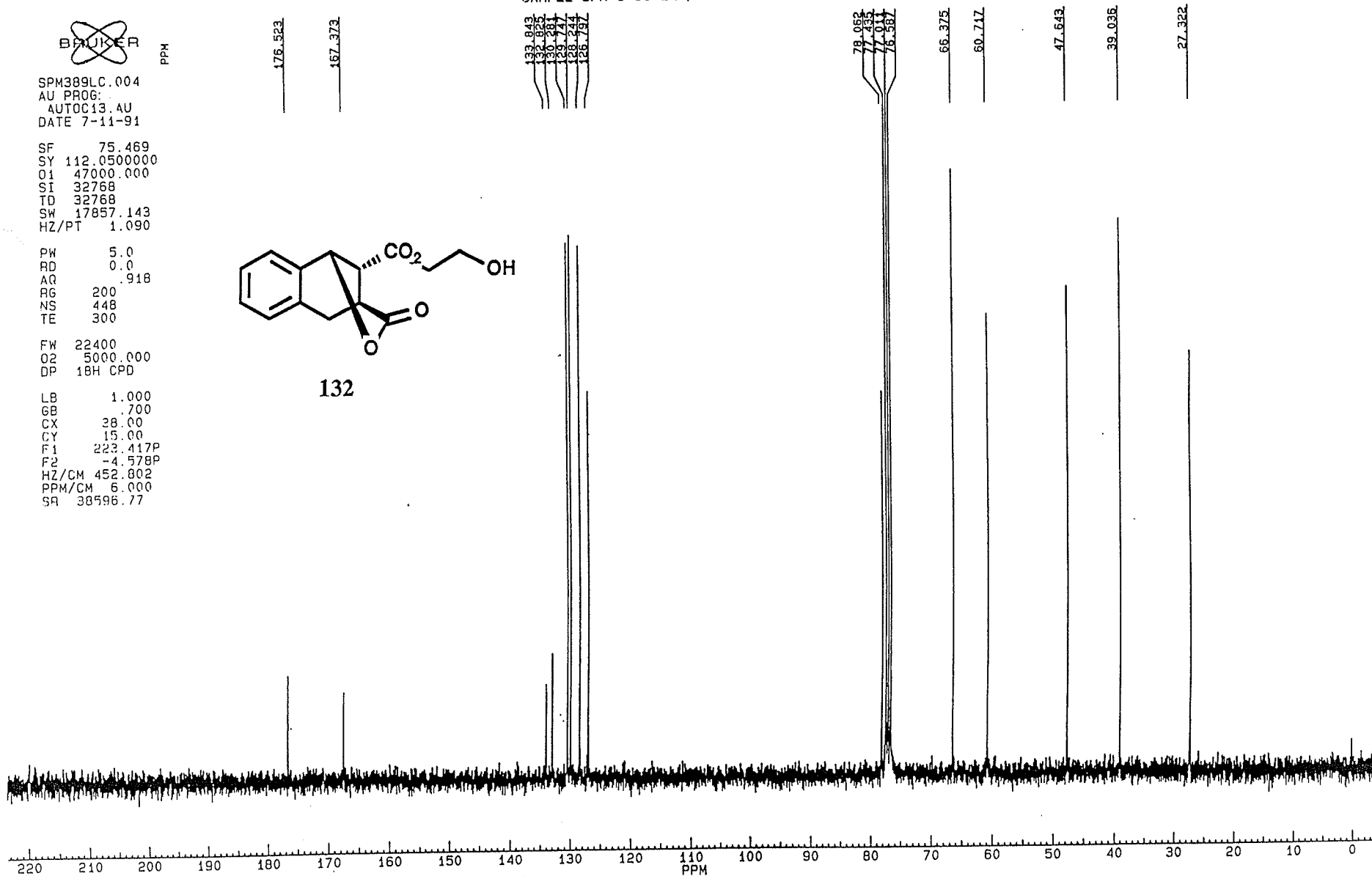
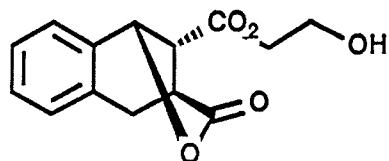
SF 75.469
SY 112.050000
O1 47000.000
SI 32768
TD 32768
SW 17857.143
HZ/PT 1.090

PW 5.0
RD 0.0
AQ .918
RG 200
NS 448
TE 300

FW 22400
O2 5000.000
DP 18H CPD

LB 1.000
GB .700
CX 38.00
CY 15.00
F1 223.417P
F2 -4.578P
HZ/CM 452.802
PPM/CM 6.000
SA 38596.77

SAMPLE SPM-3-89-LAC, 13-C AT 75.47 MHZ IN CDCL3



SPM-2-44-HPLC-3 1-H AT 300 MHZ IN CDCL3

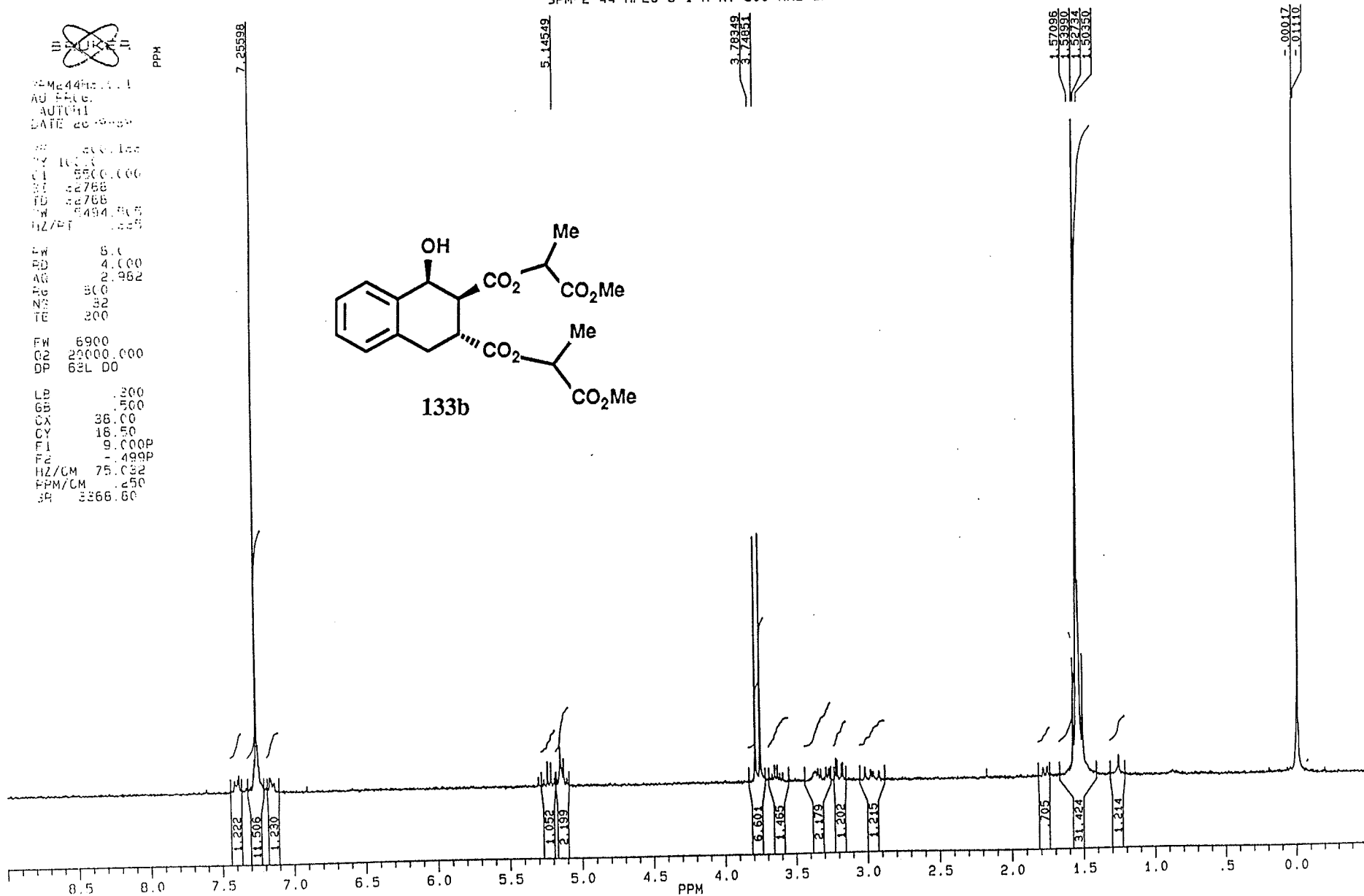
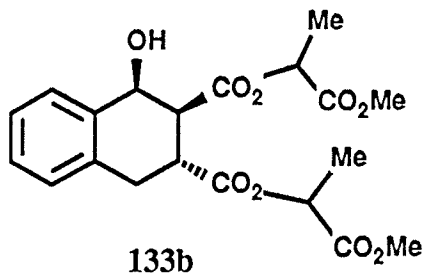


NAME 44HPLC-3
 AU FALG
 AUTUM
 DATE 20-09-88

FW 6900
 RD 4.000
 AG 2.982
 RG 500
 NG 32
 TE 200

FW 6900
 G2 29000.000
 DP 62L D0

LB .200
 GB .500
 CA 36.00
 CY 18.50
 F1 9.000P
 F2 .499P
 HZ/CM 75.022
 FPM/CM .250
 SR 3366.60



SPM-2-44-HPLC-4 1-H AT 300 MHZ IN CDCL3



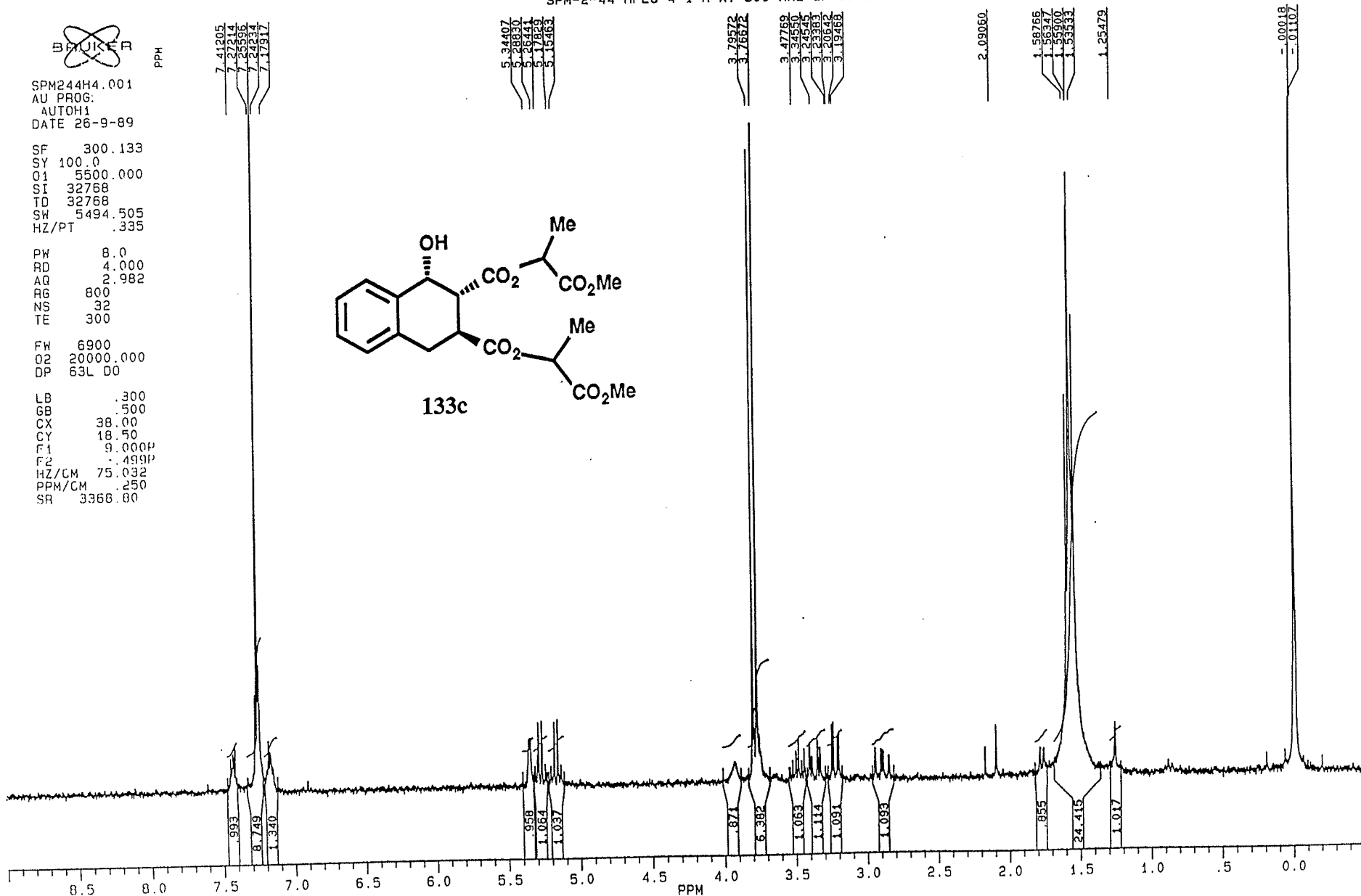
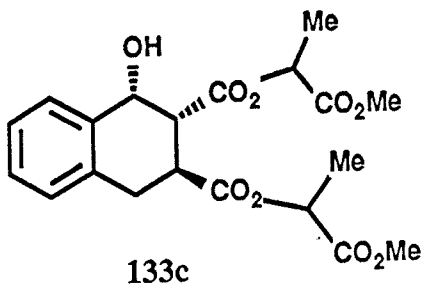
SPM244H4.001
 AU PROG:
 AUTOH1
 DATE 26-9-89

SF 300.133
 SY 100.0
 O1 5500.000
 SI 32768
 TD 32768
 SW 5494.505
 HZ/PT .335

PW 8.0
 RD 4.000
 AQ 2.982
 RG 800
 NS 32
 TE 300

FW 6900
 O2 20000.000
 DP 63L D0

LB .300
 GB .500
 CX 38.00
 CY 18.50
 F1 9.000P
 F2 .499P
 HZ/CM 75.032
 PPM/CM .250
 SR 3366.80



SAMPLE SPM-4-72-exo 1-H 300 MHZ CDCL3

~~BRUNNER~~

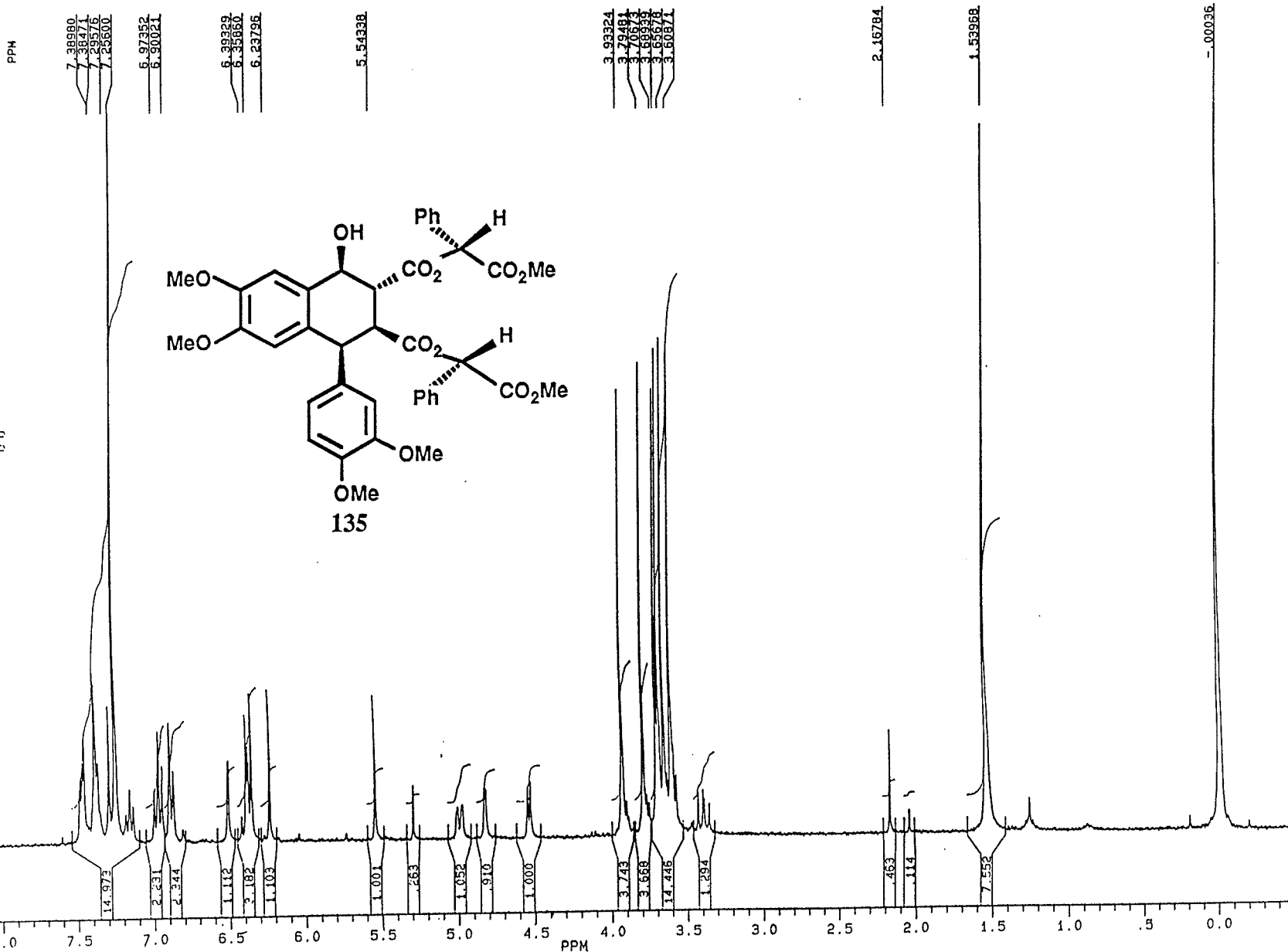
SPM472EX.C01
DATE 5-10-92

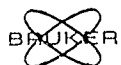
SF 300.133
AQ 100.0
Q1 9580.000
Q2 22768
Q3 22768
Q4 22768
Q5 22768
Q6 22768
Q7 22768
Q8 22768
Q9 22768
Q10 22768
Q11 22768
Q12 22768
Q13 22768
Q14 22768
Q15 22768
Q16 22768
Q17 22768
Q18 22768
Q19 22768
Q20 22768
Q21 22768
Q22 22768
Q23 22768
Q24 22768
Q25 22768
Q26 22768
Q27 22768
Q28 22768
Q29 22768
Q30 22768
Q31 22768
Q32 22768
Q33 22768
Q34 22768
Q35 22768
Q36 22768
Q37 22768
Q38 22768
Q39 22768
Q40 22768
Q41 22768
Q42 22768
Q43 22768
Q44 22768
Q45 22768
Q46 22768
Q47 22768
Q48 22768
Q49 22768
Q50 22768
Q51 22768
Q52 22768
Q53 22768
Q54 22768
Q55 22768
Q56 22768
Q57 22768
Q58 22768
Q59 22768
Q60 22768
Q61 22768
Q62 22768
Q63 22768
Q64 22768
Q65 22768
Q66 22768
Q67 22768
Q68 22768
Q69 22768
Q70 22768
Q71 22768
Q72 22768
Q73 22768
Q74 22768
Q75 22768
Q76 22768
Q77 22768
Q78 22768
Q79 22768
Q80 22768
Q81 22768
Q82 22768
Q83 22768
Q84 22768
Q85 22768
Q86 22768
Q87 22768
Q88 22768
Q89 22768
Q90 22768
Q91 22768
Q92 22768
Q93 22768
Q94 22768
Q95 22768
Q96 22768
Q97 22768
Q98 22768
Q99 22768
Q100 22768

PW 8.0
PD 4.000
AG 2.000
RG 100
NR 20
TE 200

PH 0.00
PE 2.000
PF 0.00

LB 0.00
LX 0.00
LY 0.00
LZ 0.00
L1 0.00
L2 0.00
L3 0.00
L4 0.00
L5 0.00
L6 0.00
L7 0.00
L8 0.00
L9 0.00
L10 0.00
L11 0.00
L12 0.00
L13 0.00
L14 0.00
L15 0.00
L16 0.00
L17 0.00
L18 0.00
L19 0.00
L20 0.00
L21 0.00
L22 0.00
L23 0.00
L24 0.00
L25 0.00
L26 0.00
L27 0.00
L28 0.00
L29 0.00
L30 0.00
L31 0.00
L32 0.00
L33 0.00
L34 0.00
L35 0.00
L36 0.00
L37 0.00
L38 0.00
L39 0.00
L40 0.00
L41 0.00
L42 0.00
L43 0.00
L44 0.00
L45 0.00
L46 0.00
L47 0.00
L48 0.00
L49 0.00
L50 0.00
L51 0.00
L52 0.00
L53 0.00
L54 0.00
L55 0.00
L56 0.00
L57 0.00
L58 0.00
L59 0.00
L60 0.00
L61 0.00
L62 0.00
L63 0.00
L64 0.00
L65 0.00
L66 0.00
L67 0.00
L68 0.00
L69 0.00
L70 0.00
L71 0.00
L72 0.00
L73 0.00
L74 0.00
L75 0.00
L76 0.00
L77 0.00
L78 0.00
L79 0.00
L80 0.00
L81 0.00
L82 0.00
L83 0.00
L84 0.00
L85 0.00
L86 0.00
L87 0.00
L88 0.00
L89 0.00
L90 0.00
L91 0.00
L92 0.00
L93 0.00
L94 0.00
L95 0.00
L96 0.00
L97 0.00
L98 0.00
L99 0.00
L100 0.00





PPM

SM412EXC.004
AU PROG:
AUTO13.AU
DATE 21-4-92

SF 75.469
SY 112.0500000
O1 47000.000
SI 32768
ID 32768
SW 17857.143
HZ/PT 1.090

PW 5.0
RD 0.0
AQ .918
RG 200
NS 384
TE 300

FW 22400
Q2 5000.000
DP 18H CPD

LB 1.000
GB 700
CX 38.00
CY 16.00
F1 223.417P
F2 -4.578P
HZ/CM 452.802
PPM/CM 6.000
SR 38596.77

SAMPLE SPM-4-12EXO, 13-C AT 75.47 MHZ IN CDCL3

174.102
171.632
170.328
168.523

148.782
148.164
148.087
147.811

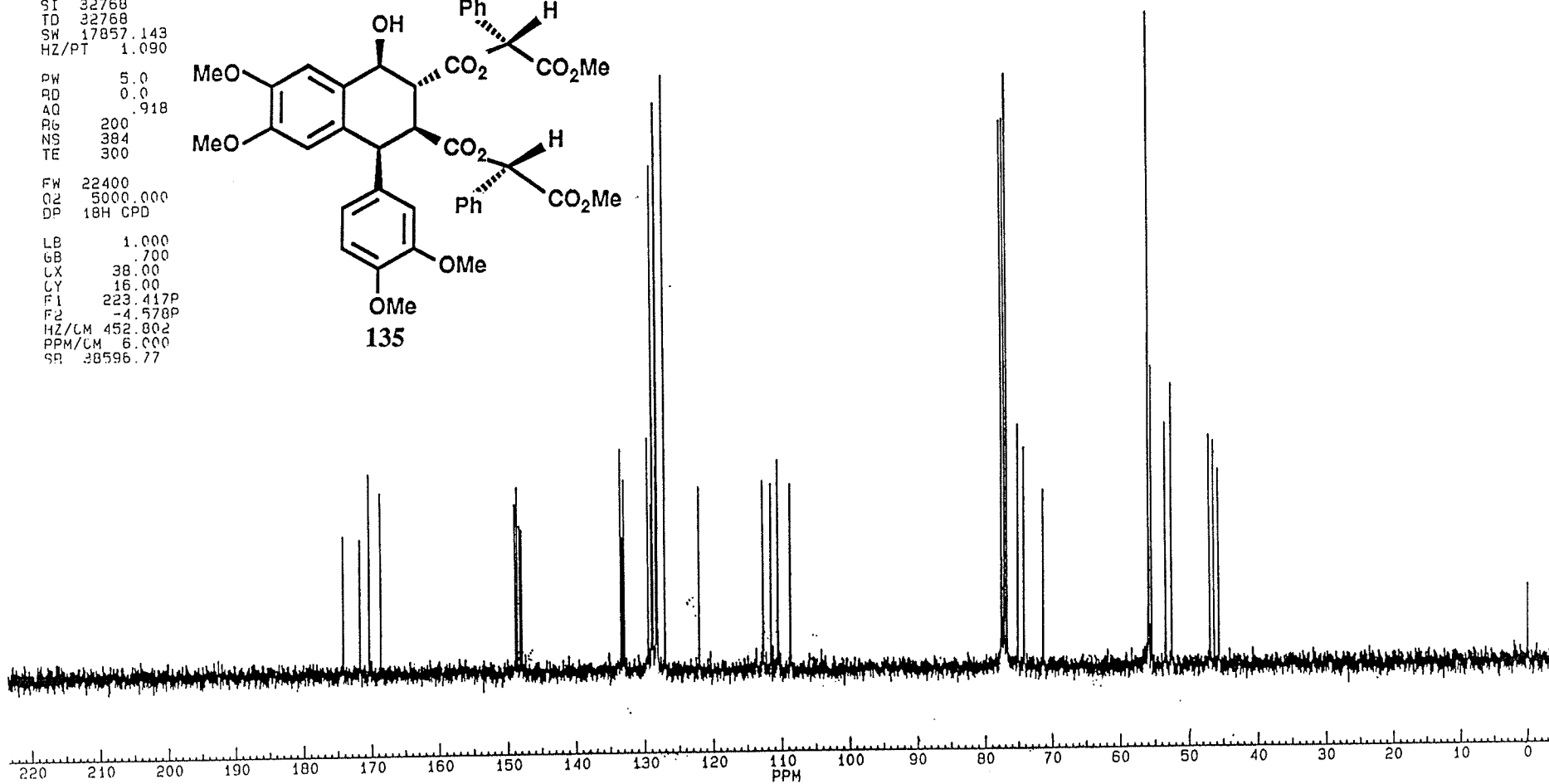
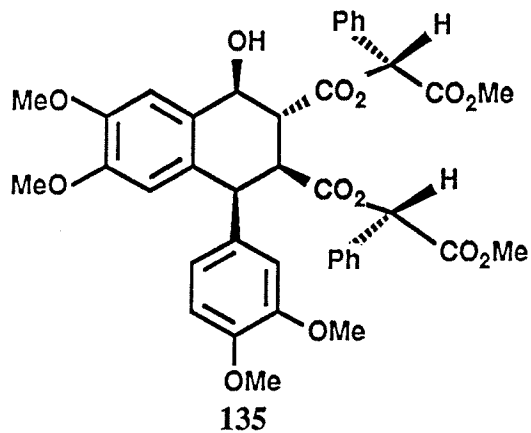
133.328
132.927
132.896
132.865
129.001
128.806
128.678
128.301
128.186
128.029
126.945
121.953

112.605
111.439
110.408
108.633

77.453
77.097
76.847
74.097
74.097
71.203

55.860
55.804
55.394
55.331
52.454
46.907
46.272
45.611

002





PPM

SM412EXC.004
AU PROG:
AUTOC13.AU
DATE 21-4-92

SF 75.469
SY 112.0500000
Q1 47000.000
SI 32768
TD 32768
SW 17857.143
HZ/PT 1.090

PW 5.0
RD 0.0
AQ .918
RG 200
NS 384
TE 300

FW 22400
Q2 5000.000
DP 18H CPD

LB 1.000
GB .700
UX 38.00
CY 16.00
F1 223.417P
F2 -4.578P
HZ/CM 452.802
PPM/CM 6.000
GR 38596.77

SAMPLE SPM-4-12EX0. 13-C AT 75.47 MHZ IN CDCL3

174.102
171.692
170.522
169.522

148.792
148.464
148.087
147.811

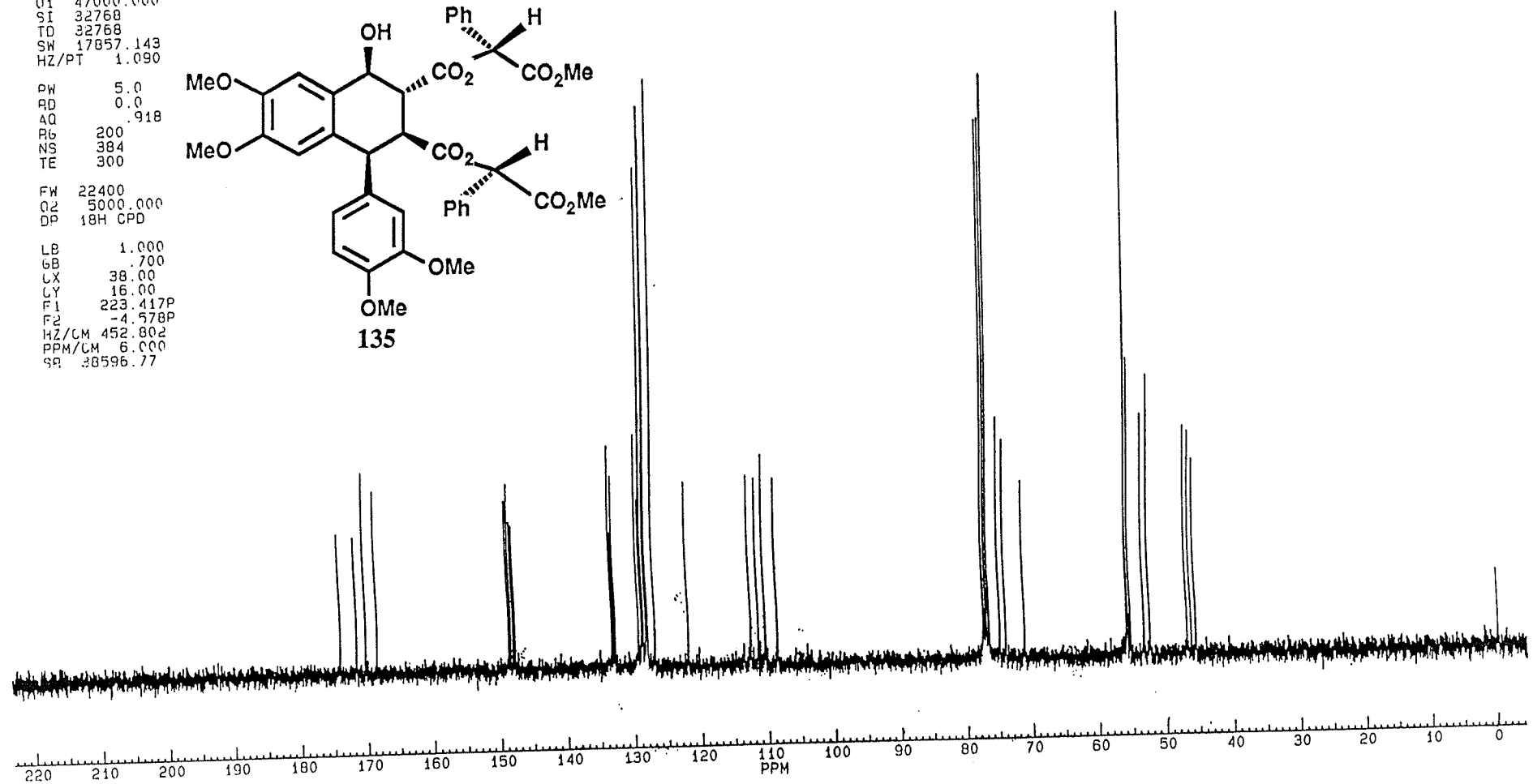
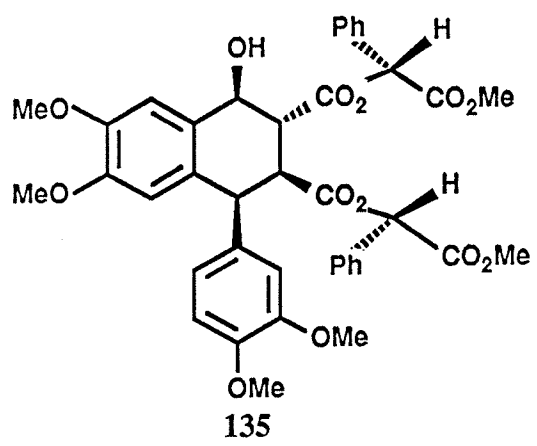
133.328
132.863
132.853
129.393
129.002
128.802
128.874
128.364
128.156
128.072
127.972
127.933

112.605
111.493
110.408
108.633

77.463
77.037
61.615
41.867
41.075
41.205

55.860
55.804
55.384
53.351
52.454

48.907
48.372
48.111



002



SPM335.001
DATE 12-1-93

SF 300.133
SY 100.0
O1 5500.000
SI 32768
TD 32768
SH 5494.505
HZ/PT .335

PW 8.0
RD 4.000
AQ 2.982
RG 16
NS 32
TE 300

FW 6900
O2 20000.000
DP 63L 00

LB .300
GB .500
CX 38.00
CY 18.50
F1 9.004P
F2 -.496P
HZ/CM 75.032
PPM/CM .250
SR 3367.79

SAMPLE SPM-3-35 1-H 300 MHZ CDCL3

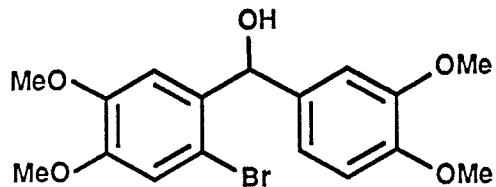
7.25931
7.08337
6.99582
6.98773
6.96149
6.89115
6.86264
6.85337
6.79782

6.08038

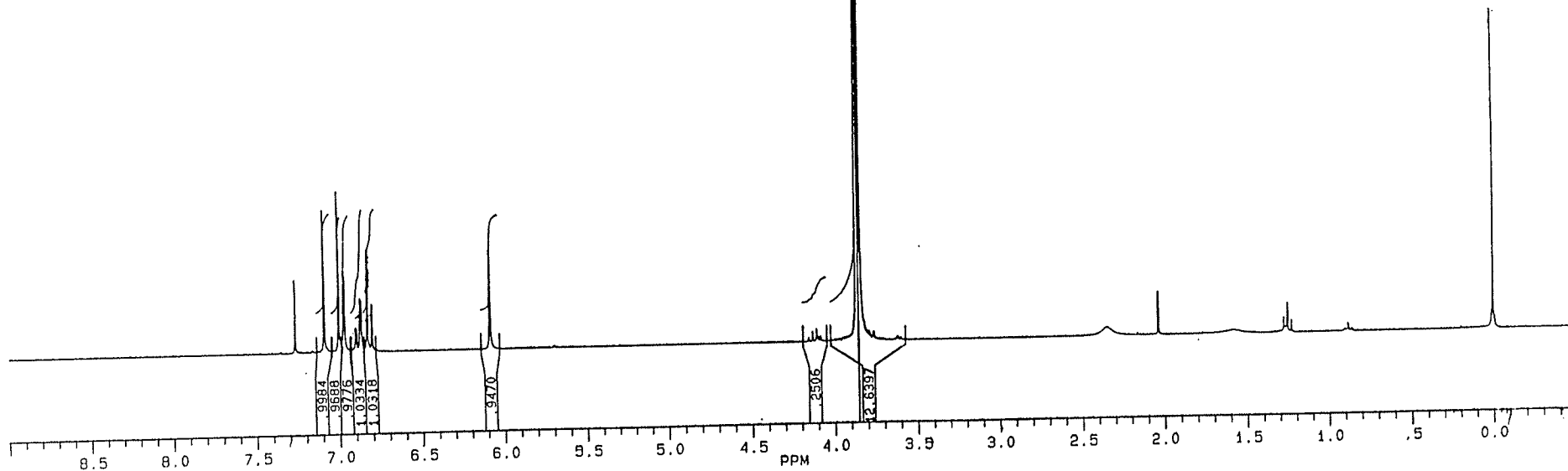
3.85927
3.85271
3.84615
3.83959
3.83303

2.03752

0.00000



142



BAIJKER

SPM335C.004
AU PROG:
AUTO13.AU
DATE 12-1-93

SF 75.469
SY 112.0500000
Q1 47000.000
SI 32768
TD 32768
SW 17857.143
HZ/PT 1.090

PW 5.0
RD 0.0
AQ .918
RG 200
NS 768
TE 300

FW 22400
O2 5000.000
DP 18H CPD

LB 1.000
GB .700
CX 38.00
CY 18.00
F1 223.417P
F2 -4.578P
HZ/CM 452.802
PPM/CM 6.000
SR 38596.77

SAMPLE SPM-3-35 13-C 75.47 MHZ CDCL3

148.905
148.478

135.086
134.754

118.989

115.334

112.575

110.942

110.782

110.034

77.435

77.000

76.565

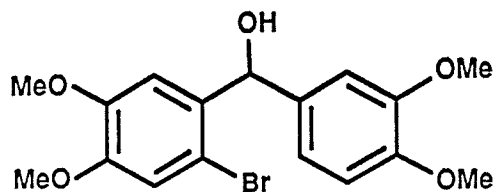
76.130

56.180

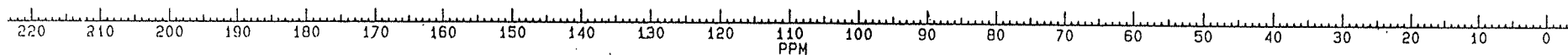
55.745

55.310

002



142





RASTMS.001
DATE 26-7-93

SF 300.133
SY 100.0
O1 5500.000
SI 32768
TD 32768
SW 5494.505
HZ/PT .335

PW 8.0
RD 4.000
AQ 2.982
RG 8
NS 16
TE 300

FW 6900
O2 20000.000
DP 63L D0

LB -.100
GB .500
CX 38.00
CY 18.50
F1 9.033P
F2 -.467P
HZ/CM 75.032
PPM/CM .250
SR 3359.07

7.54899
7.54327
7.38947
7.38139
7.37071
7.36761
7.37883
6.88378
6.87038
6.84285

5.29529

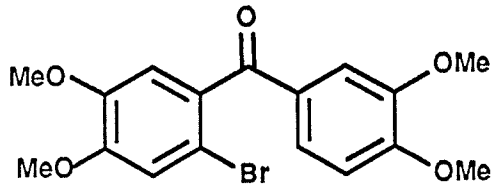
SPM-4-29

4.08305
3.95731
3.94987
3.94417
3.93783
3.88250
3.87562
3.87028
3.85430
3.70077

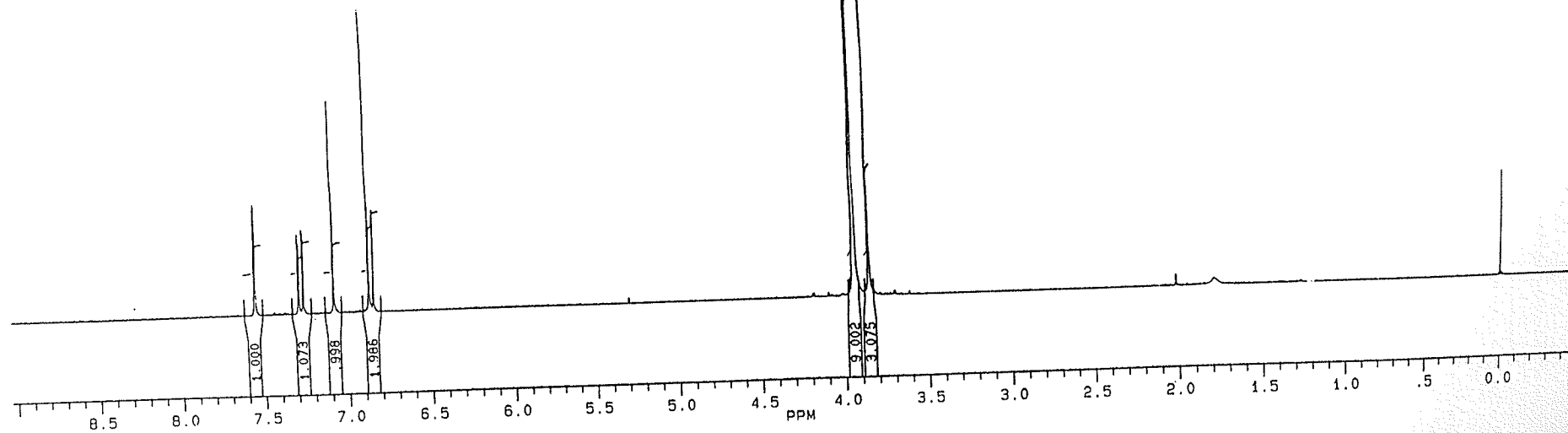
2.00992

1.78241

0.00013



143



BRUKER

PPM
194.282

SPM347C.004
AU. PROG:
AUTOC13. AU
DATE 28-7-93

SF 75.469
SY 112.0500000
O1 47000.000
SI 32768
TD 32768
SW 17857.143
HZ/PT 1.090

PW 5.0
RD 0.0
AQ .918
RG 200
NS 128
TE 300

FW 22400
O2 5000.000
DP 18H CPD

LB 1.000
GB .700
CX 38.00
CY 12.00
F1 223.475P
F2 -4.520P
HZ/CM 452.802
PPM/CM 6.000
SR 38592.41

13-C, CDCL3

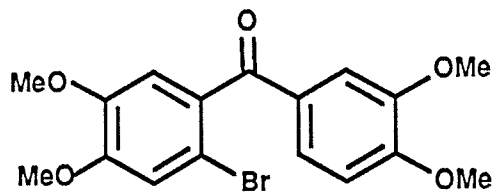
153.850
150.802
149.245
148.188

132.778
129.528
126.281

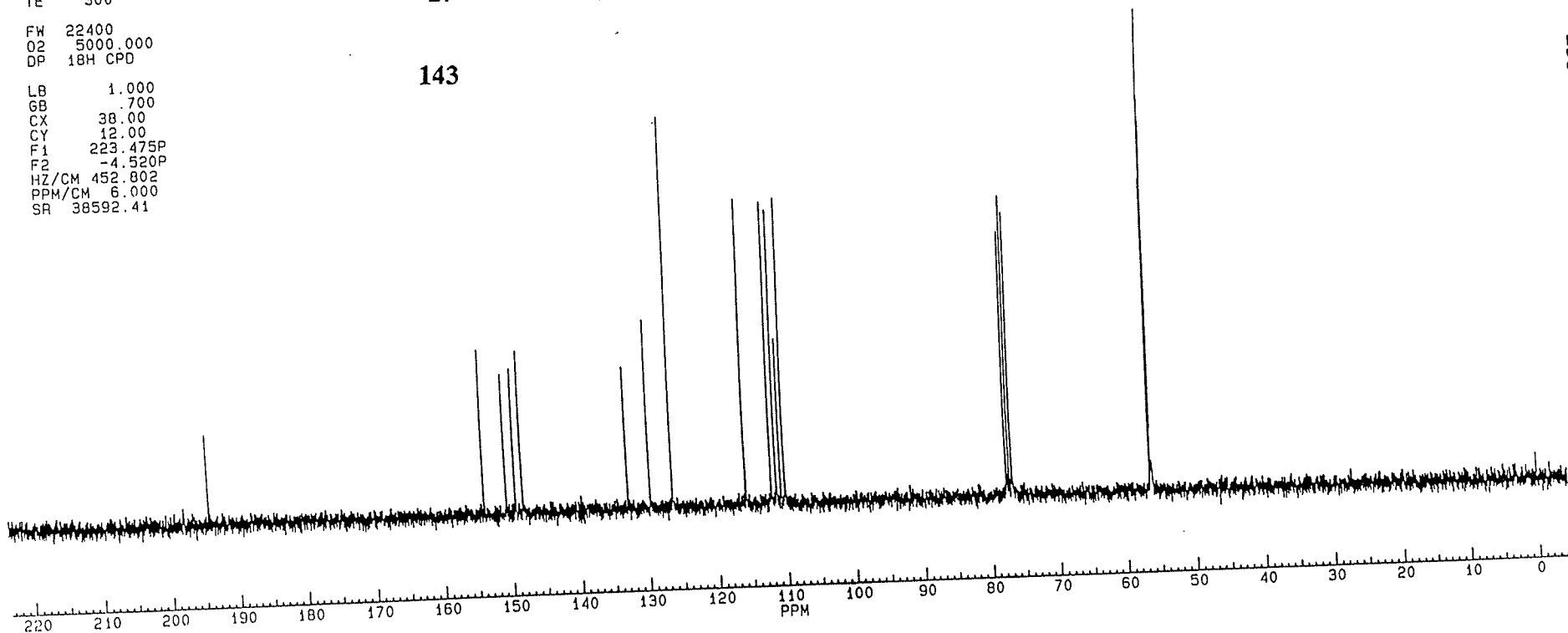
115.747
112.018
111.288
110.539
109.995

77.543
77.120
76.698

56.364
56.223
56.148
56.082



143



B
K
L
I
K
E
R

SPM355.001
AU PROG:
TFZG.AU
DATE 3-6-93

SF 300.133
SY 100.0
C1 5500.000
SI 32768
TD 32768
SW 5494.505
HZ/PT .335

PW 8.0
RD 4.000
AQ 2.982
RG 40
NS 32
TE 300

FW 6900
O2 20000.000
DP 63L D0

LB 300
GB 500
CX 38.00
CY 18.50
F1 9.005P
F2 - .495P
HZ/CM 75.032
PPM/CM .250
SR .3367.46

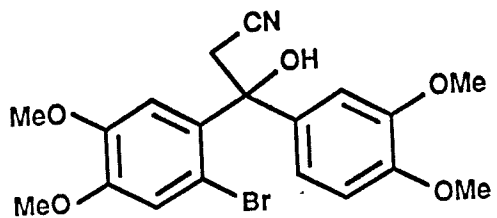
SAMPLE SPM-3-55 1-H AT 300 MHZ IN CDCL3

7.45183
7.25917
7.01820
6.85576
6.80050

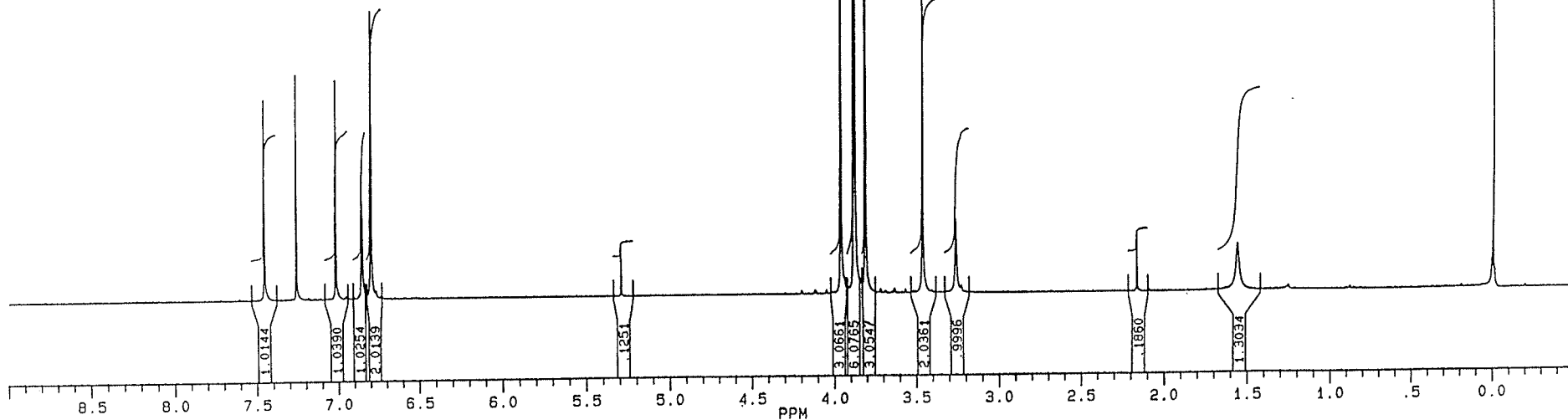
5.29530
3.95223
3.88290
3.87591
3.87216
3.46359
3.26288

2.16581
1.56011

.00021



144



BRUKER

PPM

SPM355C.004
AU PROG:
AUTOC13.AU
DATE 5-6-93

SF 75.469
SY 112.050000
O1 47000.000
SI 32768
TD 32768
SW 17857.143
HZ/PT 1.090

PW 5.0
RD 0.0
AQ .918
RG 200
NS 3840
TE 300

FW 22400
O2 5000.000
DP 18H CPD

LB 1.000
GB .700
CX 38.00
CY 18.00
F1 223.417P
F2 -4.578P
HZ/CM 452.802
PPM/CM 6.000
SR 38596.77

SAMPLE SPM-3-55 13-C AT 75.47 MHZ IN CDCL3

149.177
149.047
148.002

135.811
133.777

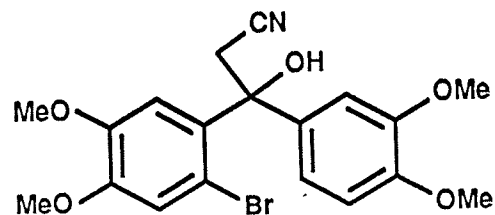
118.716
117.736
117.082
111.813
110.719
109.673

77.417
77.198
76.892
76.716
76.570

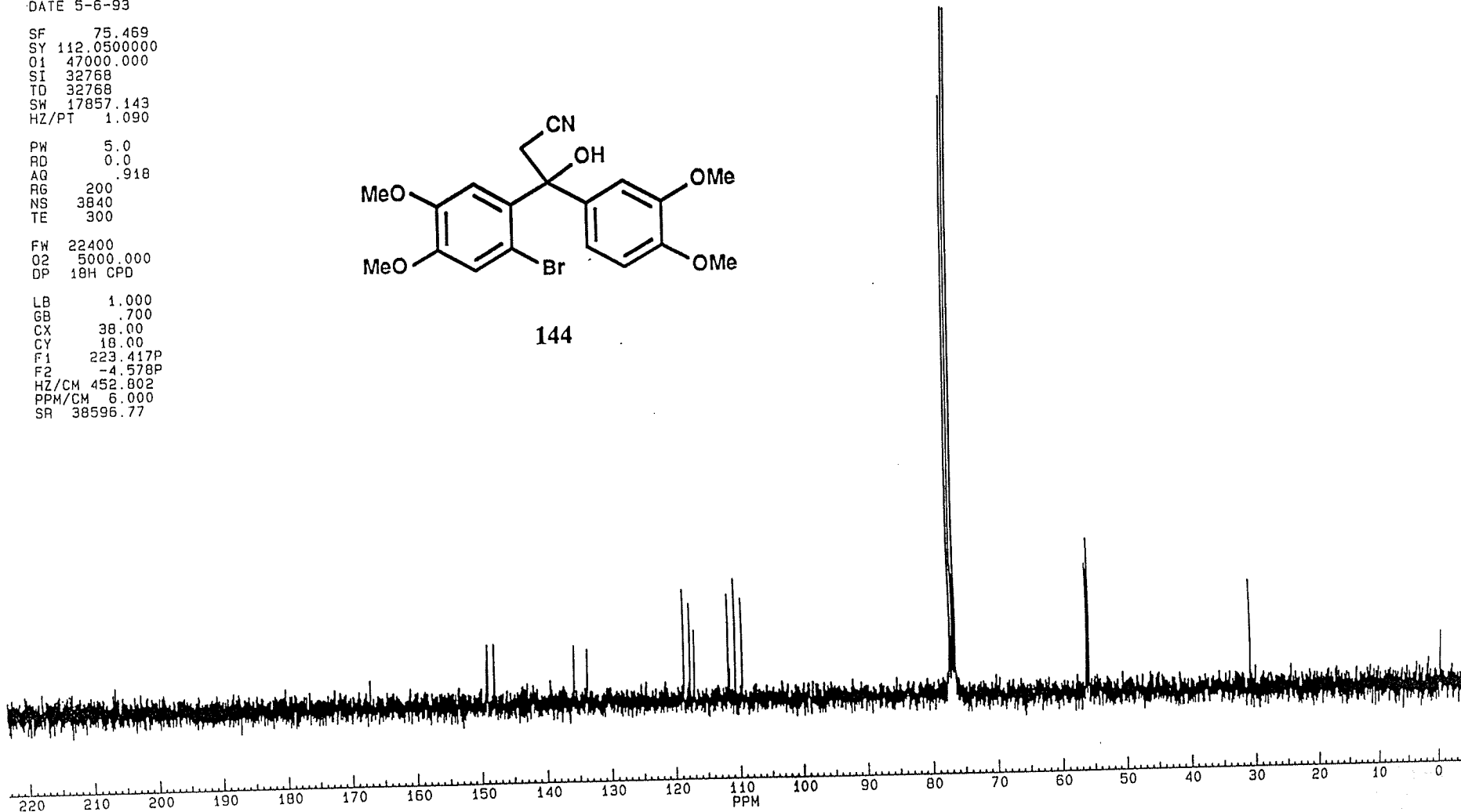
55.284
55.243
55.192
55.177

150.951

000



144





PPM

SPM-3-48 1-H AT 300 MHZ IN CDCL3

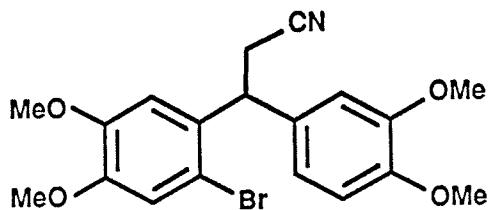
SPM348.001
AU PROG:
AUTOH1
DATE 12-2-91

SF 300.133
SY 100.0
O1 5500.000
SI 32768
TD 32768
SW 5494.505
HZ/PT .335

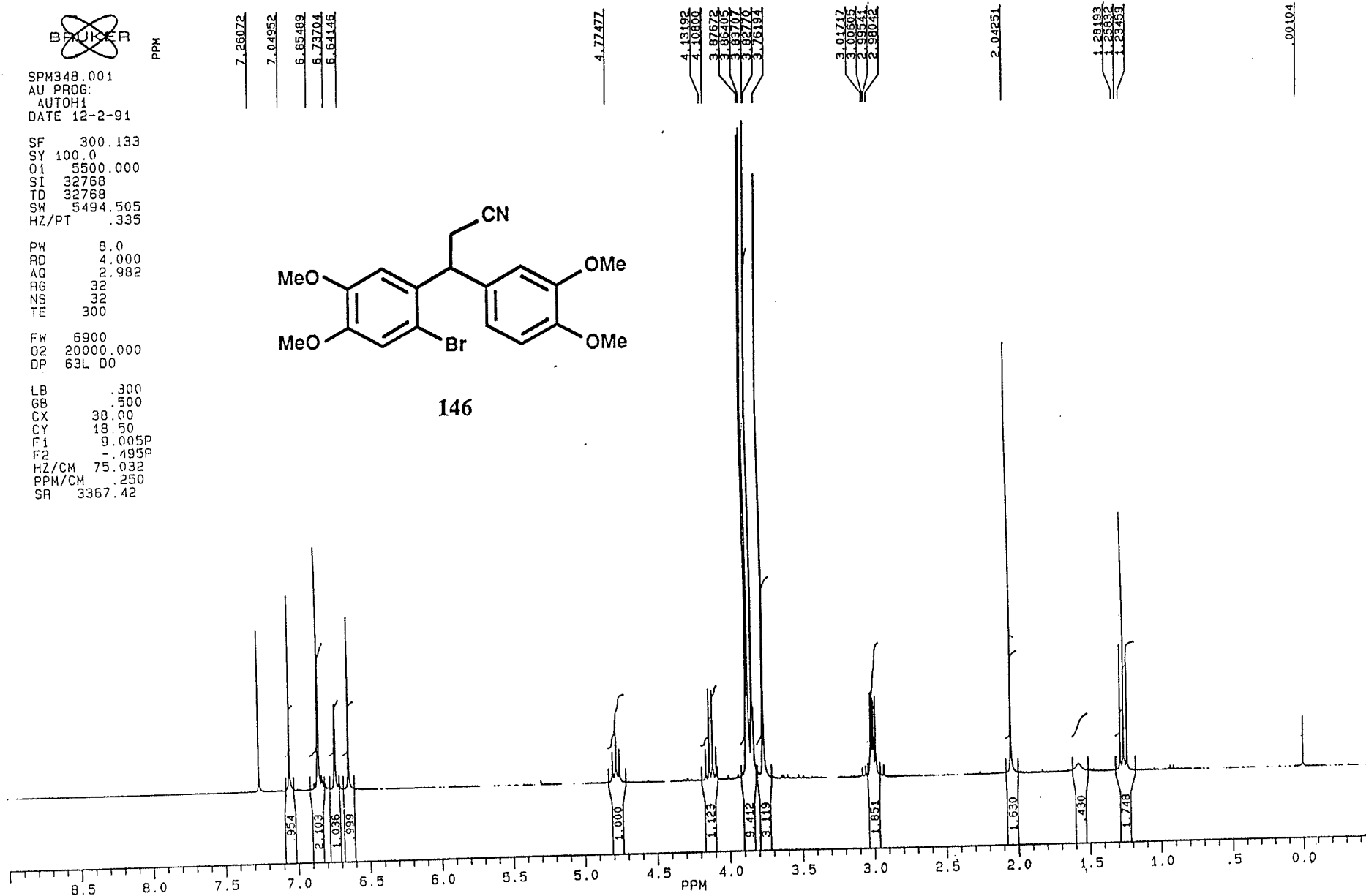
PW 8.0
RD 4.000
AQ 2.982
RG 32
NS 32
TE 300

FW 6900
O2 20000.000
DP 63L D0

LB .300
GB .500
CX 38.00
CY 18.50
F1 9.005P
F2 -.495P
HZ/CM 75.032
PPM/CM .250
SR 3367.42



146



BRUKER

PPM

SPM359.004
AU PROG:
AUTOC13.AU
DATE 2-6-93

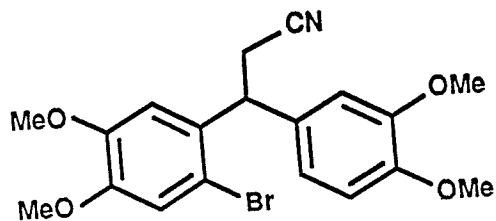
SF 75.469
SY 112.0500000
O1 47000.000
SI 32768
TD 32768
SW 17857.143
HZ/PT 1.090

PW 5.0
RD 0.0
AQ .918
RG 200
NS 2560
TE 300

FW 22400
O2 5000.000
DP 18H CPD

LB 1.000
GB .700
CX 38.00
CY 18.00
F1 223.402P
F2 -4.593P
HZ/CM 452.802
PPM/CM 6.000
SR 38597.86

SAMPLE SPM-3-59 13-C AT 75.47 MHZ IN CDCL3



146

149.167
148.923
148.902
148.331

132.531
132.391

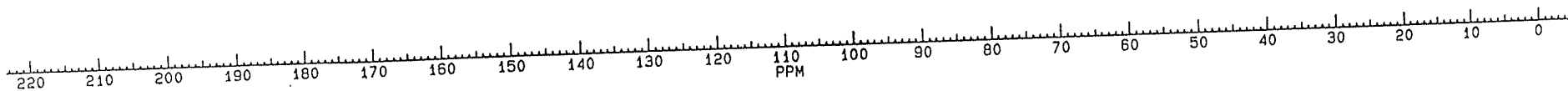
119.177
118.154
115.811
114.365
111.478
111.200

77.465
77.042
76.616

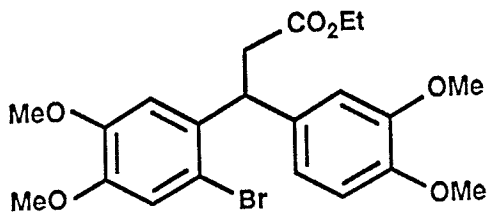
56.154
55.948
55.864

44.857

23.237



PPM



147

SPM-3-56

7.00561
6.77508
6.69016

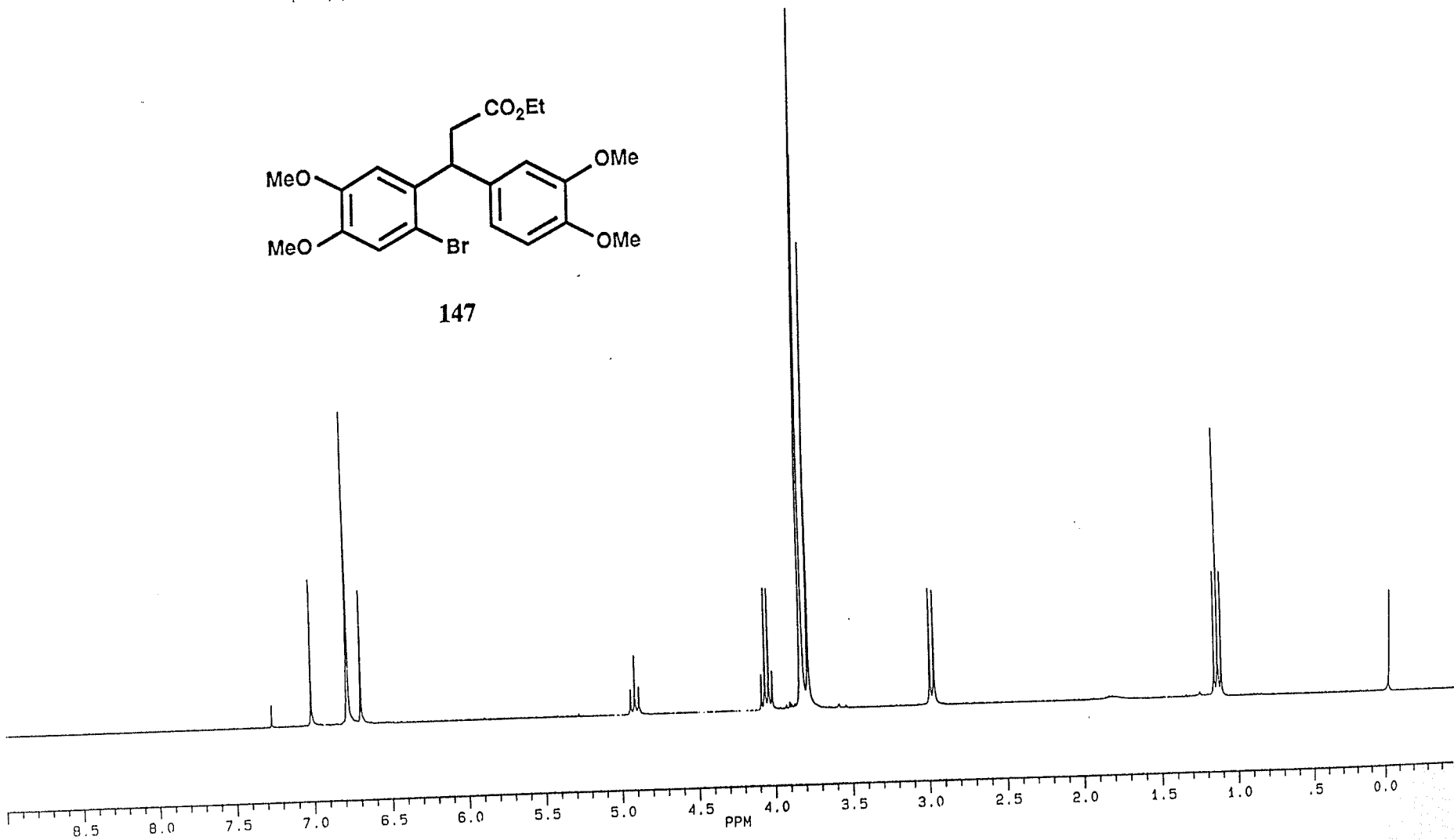
4.93123
4.90418
4.87728

4.07880
4.05508
4.03141
4.00767
3.82444
3.81974
3.77336

2.98594
2.95896

1.15023
1.12553
1.10287

-0.1334



BRUKER

PPH

SPM356C.TMP
AU PROG:
AUTOCL3.AU
DATE 28-7-93

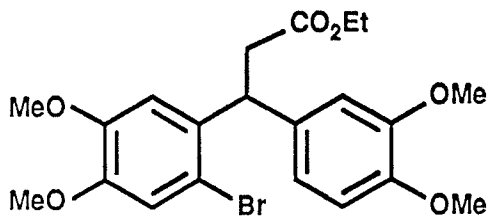
SF 75.469
SY 112.050000
O1 47000.000
SI 32768
TD 32768
SW 17857.143
HZ/PT 1.090

PW 5.0
RD 0.0
AQ .918
RG 200
NS 320
TE 300

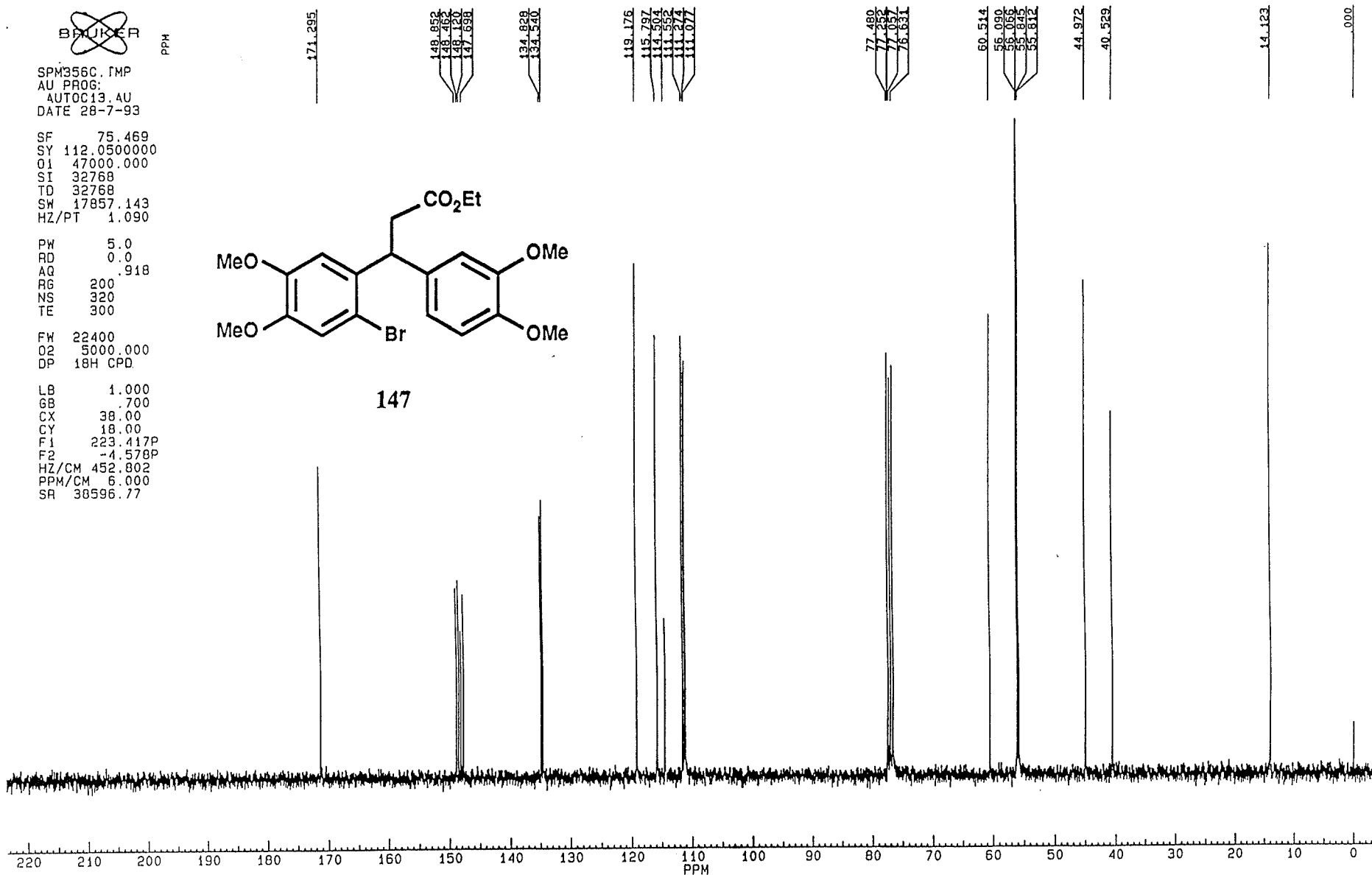
FW 22400
O2 5000.000
DP 18H CPD

LB 1.000
GB .700
CX 38.00
CY 18.00
F1 223.417P
F2 -4.578P
HZ/CM 452.802
PPM/CM 6.000
SR 38596.77

SPM-3-56 IN CDCL3 AT 75.47 MHZ



147



SPM-2-112 1-H AT 300 MHZ IN CDCL3



SPM2112.001
AU PROG:
AUTOH1
DATE 4-4-90

SF 300.133
SY 100.0
O1 5500.000
SI 32768
TD 32768
SW 5494.505
HZ/PT .335

PW 8.0
RD 4.000
AQ 2.982
RG 40
NS 32
TE 300

FW 6900
O2 20000.000
DP 63L D0

LB .300
GB .500
CX 38.00
CY 18.50
F1 9.005P
F2 -.495P
HZ/CM 75.032
PPM/CM 250
SR 3367.42

PPM

7.26072
7.13618
6.99555
6.99281
6.84696
6.77167

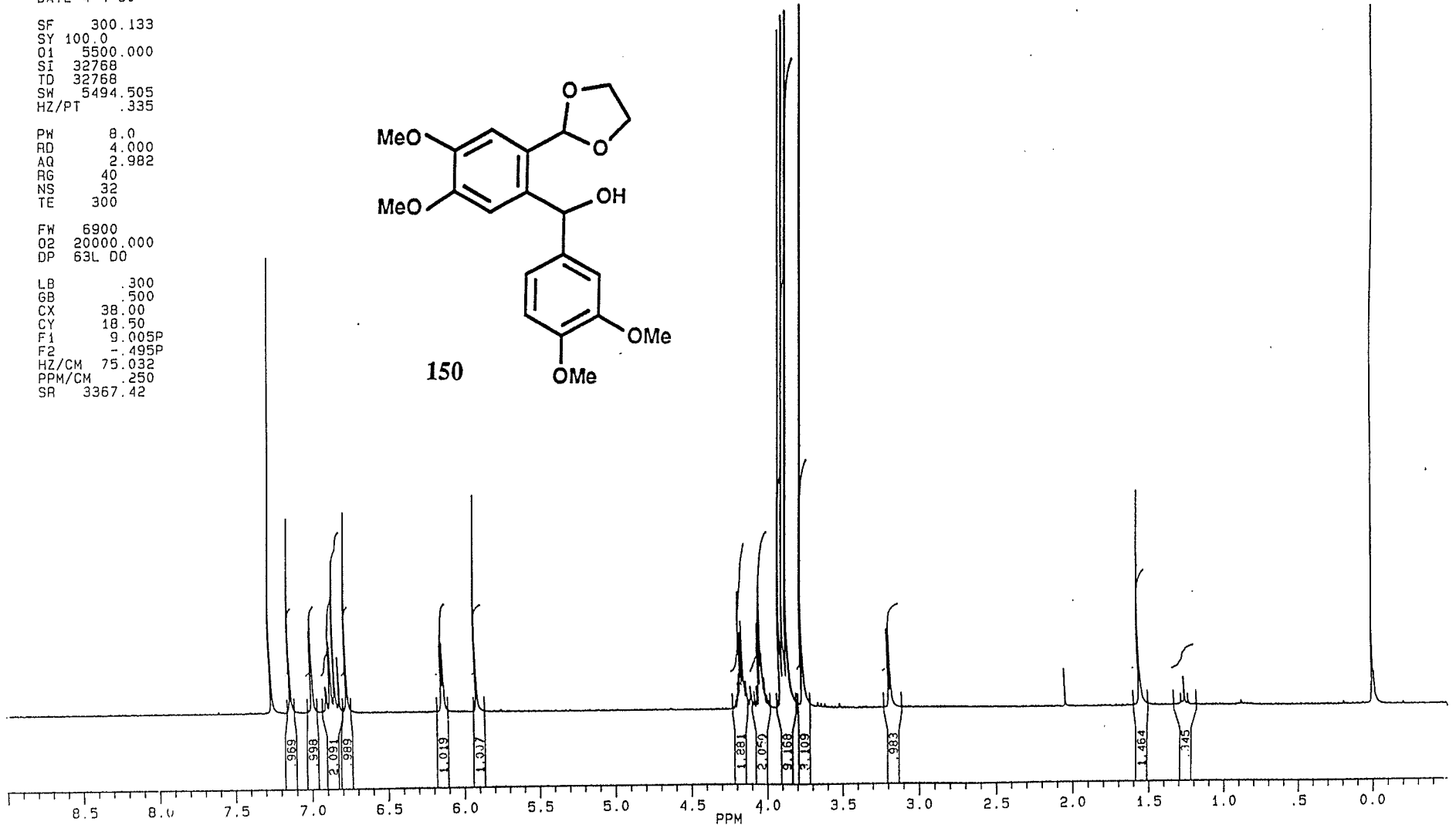
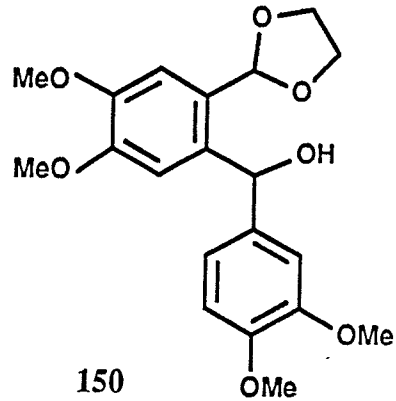
5.91891

4.17242
4.15083
4.04685
4.03214
3.90669
3.89246
3.85680
3.76018

3.17768

1.55392

.00334



SAMPLE SPM-3-45 1-H AT 300 MHZ IN CDCL3

BRUKER

SPM345.001
AU PROG:
TFZG.AU
DATE 2-6-93

SF 300.133
SY 100.0
O1 5500.000
SI 32768
TD 32768
SW 5494.505
HZ/PT .335

PW 8.0
RD 4.000
AQ 2.982
RG 20
NS 32
TE 300

FW 6900
O2 20000.000
DP 63L D0

LB .300
GB .500
CX 38.00
CY 18.50
F1 9.009P
F2 -.491P
HZ/CM 75.032
PPM/CM .250
SR 3366.12

PPM

7.34320
7.26369

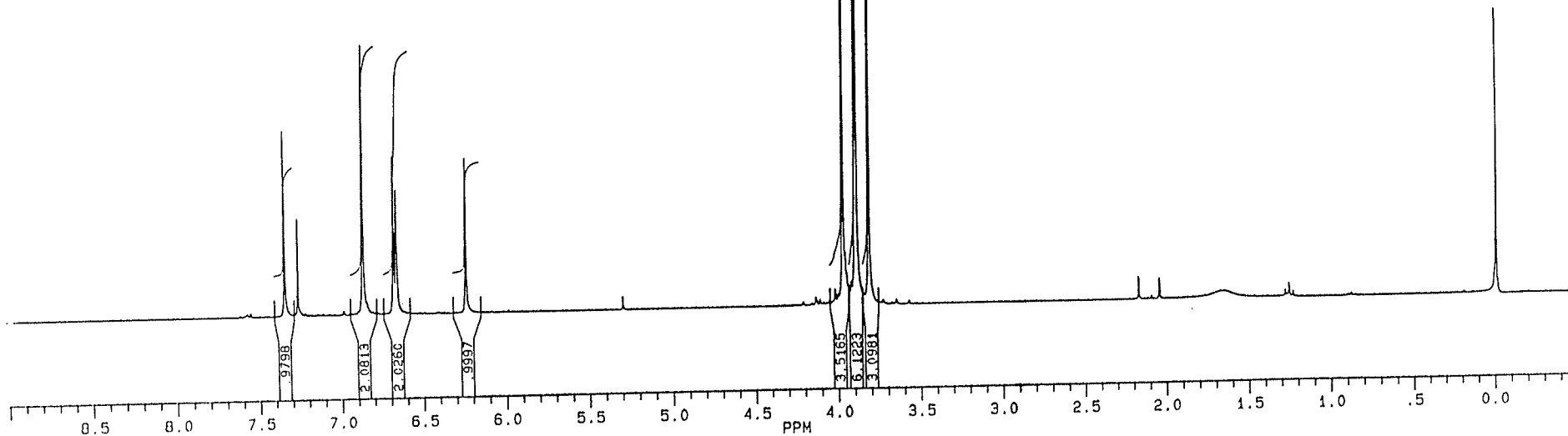
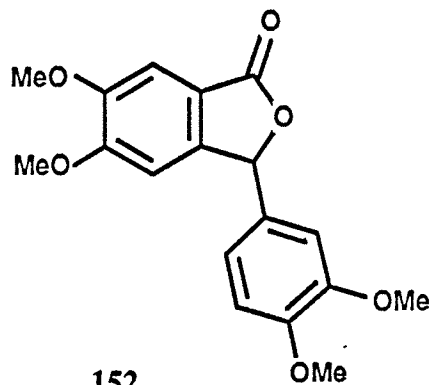
6.66939
6.66524

6.69044
6.66161

6.23868

3.96720
3.89170
3.88734
3.81115

-0.00047





SPM345C.004
AU PROG:
AUTOC13.AU
DATE 3-6-93

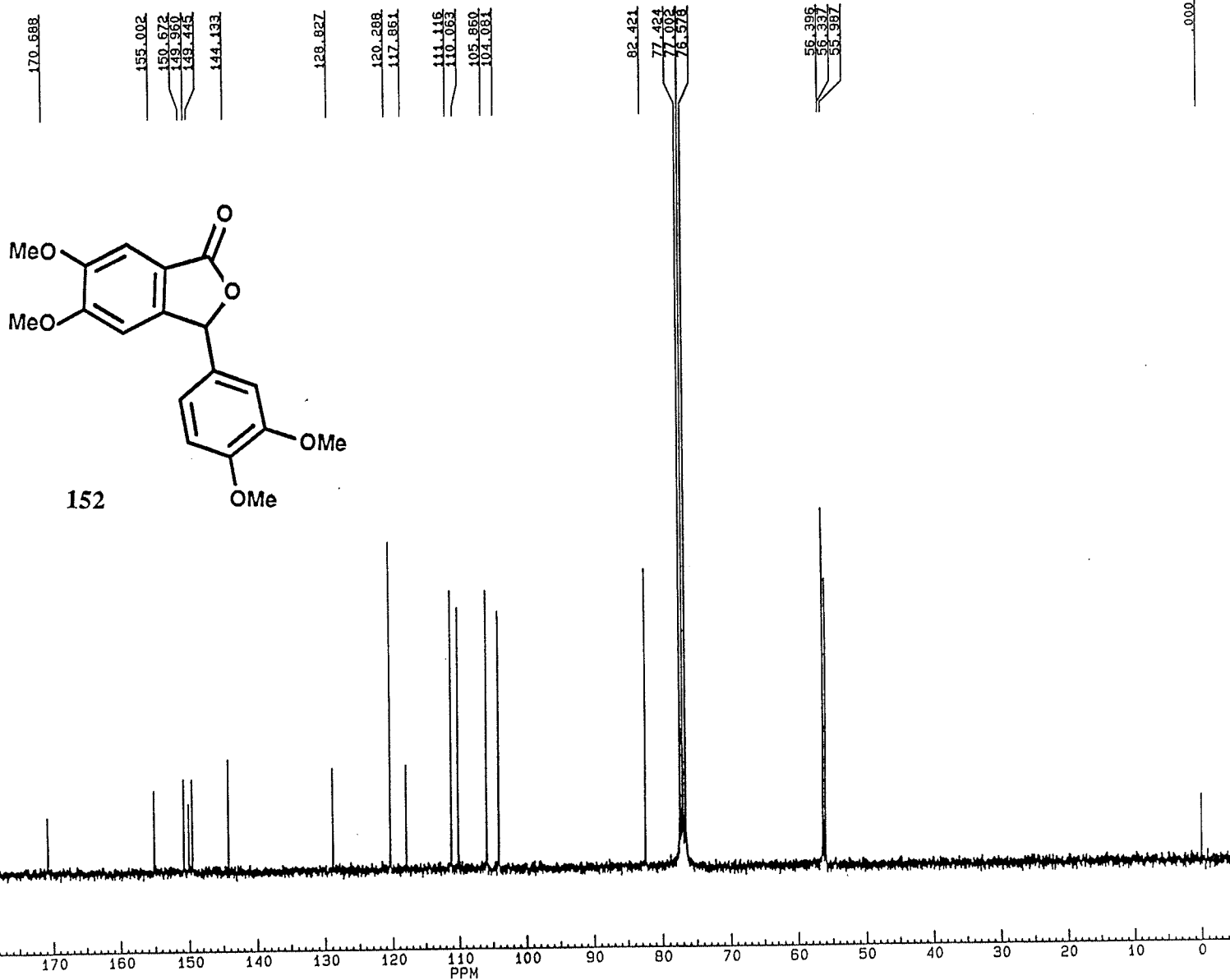
SF 75.469
SY 112.050000
O1 47000.000
SI 32768
TD 32768
SW 17857.143
HZ/PT 1.090

PW 5.0
RD 0.0
AQ .918
RG 200
NS 3200
TE 300

FW 22400
O2 5000.000
DP 18H CPD

LB 1.000
GB .700
CX 38.00
CY 8.00
F1 223.417P
F2 -4.578P
HZ/CM 452.802
PPM/CM 6.000
SR 38596.77

SAMPLE SPM-3-45 13-C AT 75.47 MHZ IN CDCL3



SAMPLE SPM-3-52 1-H AT 300 MHZ IN CDCL3



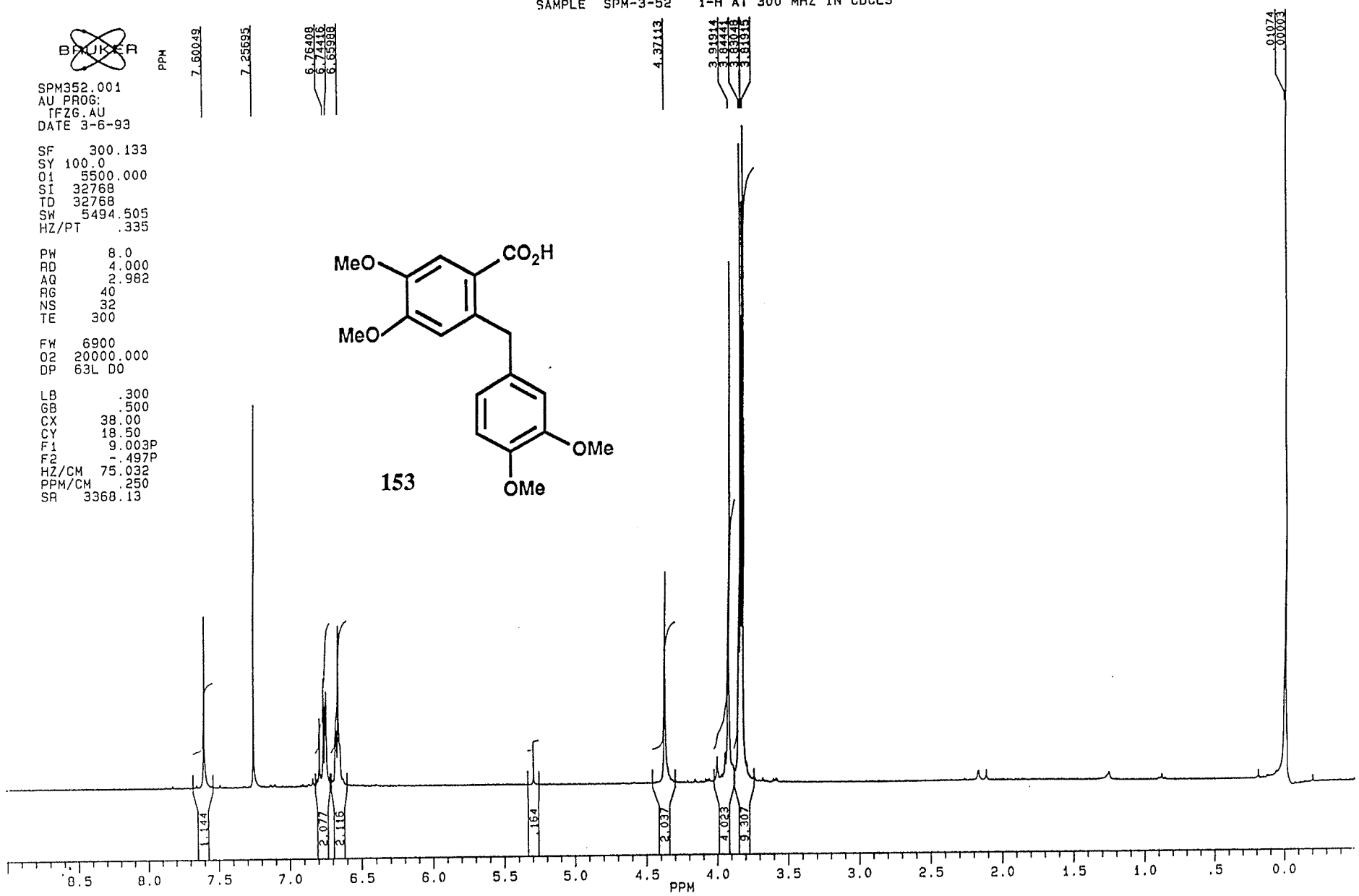
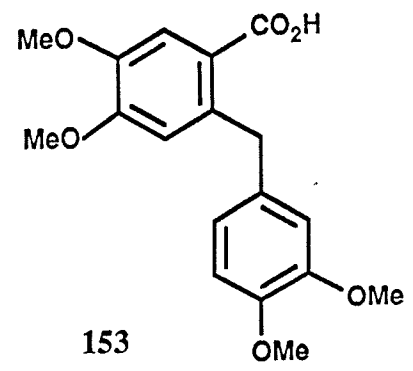
SPM352.001
AU PROG:
TFZG.AU
DATE 3-6-93

SF 300.133
SY 100.0
O1 5500.000
SI 32768
TD 32768
SW 5494.505
HZ/PT .335

PW 8.0
RD 4.000
AQ 2.982
RG 40
NS 32
TE 300

FW 6900
O2 20000.000
DP 63L D0

LB .300
GB .500
CX 38.00
CY 18.50
F1 9.003P
F2 -.497P
HZ/CM 75.032
PPM/CM .250
SR 3368.13



BRUKER

SPM352C.004
AU PROG:
AUTOC13.AU
DATE 4-6-93

SF 75.469
SY 112.0500000
O1 47000.000
SI 32768
TD 32768
SW 17857.143
HZ/PT 1.090

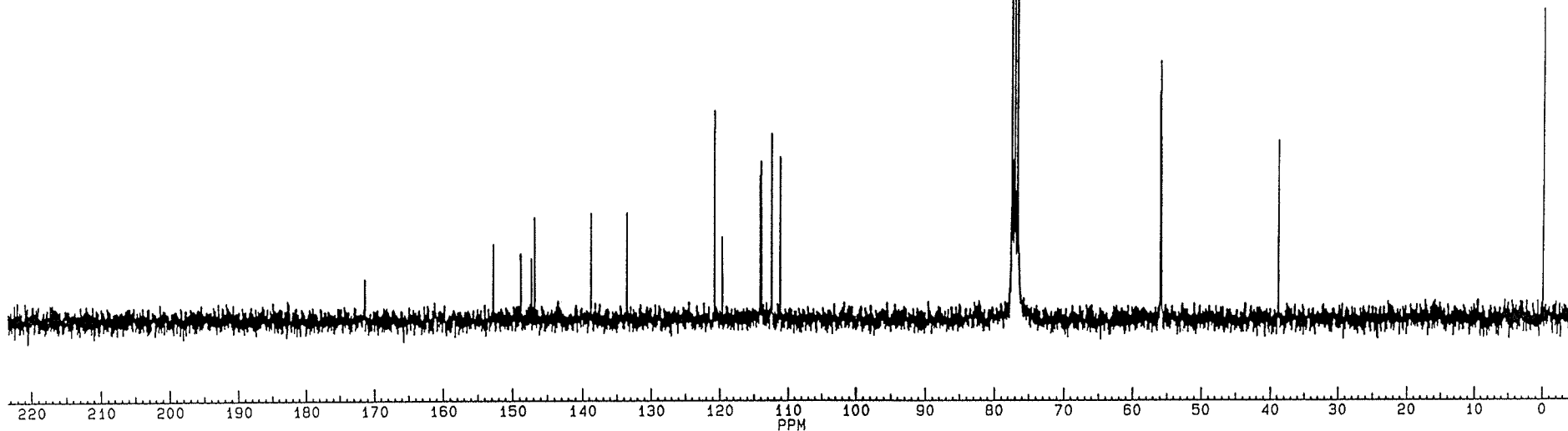
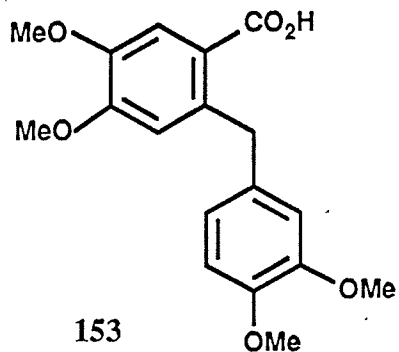
PW 5.0
RD 0.0
AQ .918
RG 200
NS 4160
TE 300

FW 22400
O2 5000.000
DP 18H CPD

LB 1.000
GB .700
CX 38.00
CY 5.00
F1 223.417P
F2 -4.578P
HZ/CM 452.802
PPM/CM 6.000
SR 38596.77

SAMPLE SPM-3-52 13-C AT 75.47 MHZ IN CDCL3

171.333
152.706
148.796
147.278
146.803
138.744
133.518
120.737
119.623
114.107
113.267
112.205
111.143
77.410
77.193
76.989
76.565
55.033
55.904
55.873
55.800
38.965
000



~~BRUKER~~

PPH

SAMPLE SPM-3-120.13-C AT 75.47 MHZ IN CDCL3

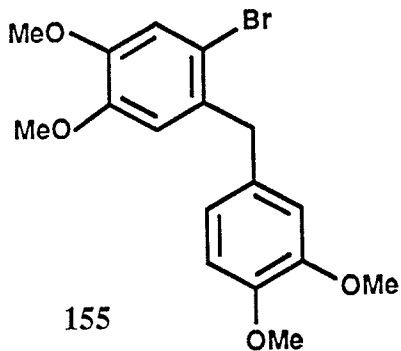
SPM3120C.004
AU PROG:
AUTOC13.AU
DATE 19-11-91

SF 75.469
SY 112.0500000
O1 47000.000
SI 32768
TD 32768
SW 17857.143
HZ/PT 1.090

PW 5.0
RD 0.0
AQ .918
RG 200
NS 512
TE 300

FW 22400
O2 5000.000
DP 18H CPD

LB 1.000
GB .700
CX 38.00
CY 16.00
F1 223.402P
F2 -4.593P
HZ/CM 452.802
PPM/CM 6.000
SR 38597.86



148.907
148.419
148.045
147.456

132.475
132.401

120.848

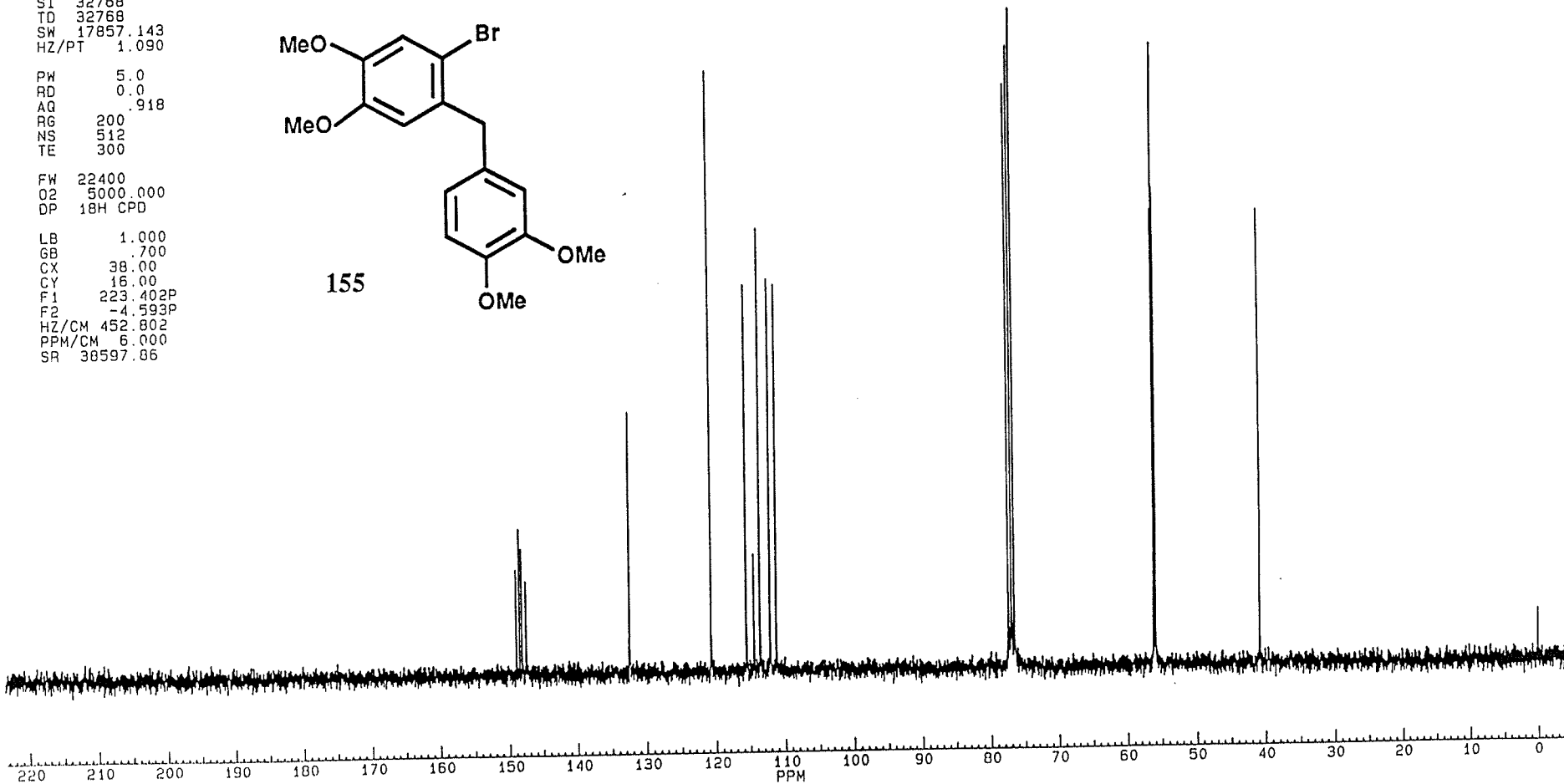
115.514
114.417
113.531
112.107
111.196

77.433
77.007
76.384

56.153
55.992
55.872
55.822

40.830

-.005



BRUNNEN

PPM

SPME1520.004
 AU PROC.
 AUTOCAL AU
 DATE 27-2-92

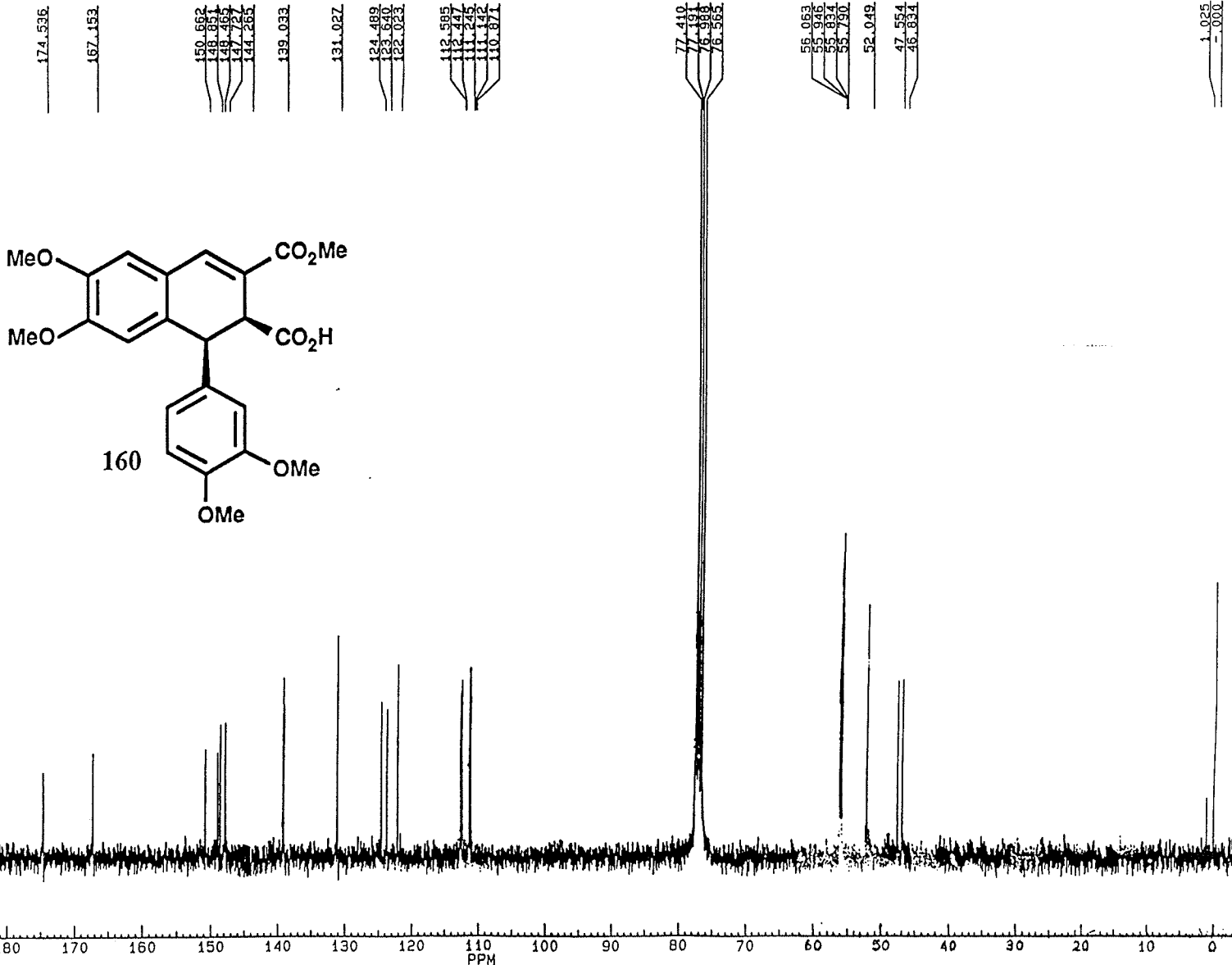
SF 75.489
 SY 112.0500000
 Q1 47000.000
 SI 32768
 ID 32768
 SW 17857.143
 HZ/PT 1.090

PW 5.0
 RD 0.0
 AQ 1.918
 PR 200
 NS 3200
 TE 300

FW 22400
 QZ 5000.000
 DP 15H 0X

LB 1.000
 GB 1.700
 SX 36.00
 SY 3.00
 FI 223.417P
 FE -4.578P
 HZ/LM 452.802
 PPM/LM 6.000
 SP 28596 77

SAMPLE SPM-3-152, 13-C AT 75.47 MHZ IN CDCL3





SPM487A.001
DATE 9-11-92

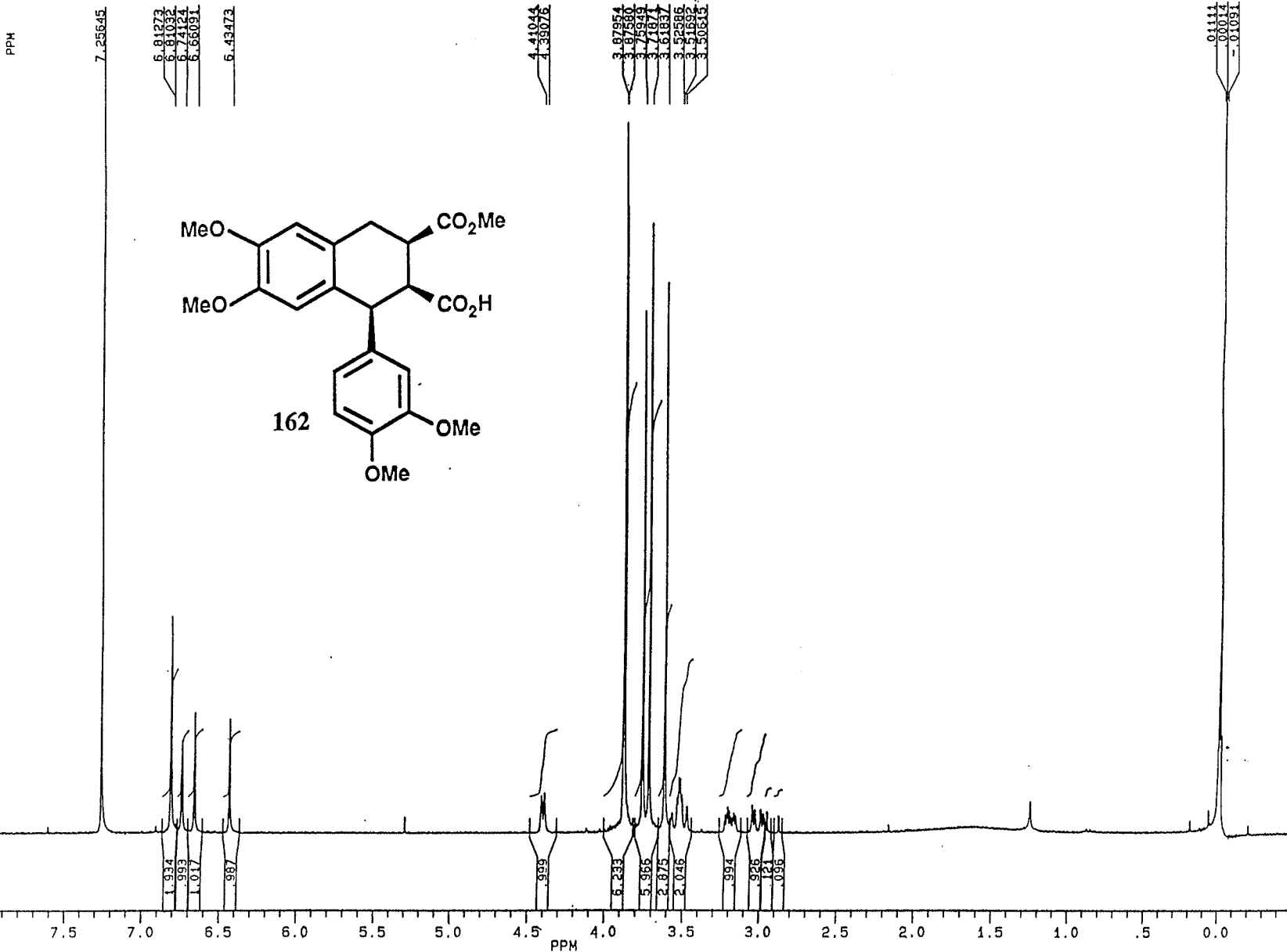
SF 300.133
SY 100.0
Q1 5500.000
SI 32768
TD 32768
SH 5494.505
HZ/PT .335

PW 8.0
RD 4.000
AQ 2.982
RG 80
NS 32
TE 300

FW 6900
O2 20000.000
DP 63L D0

LB .300
GB .500
CX 38.00
CY 18.50
F1 9.001P
F2 1.498P
HZ/CM 75.032
PPM/CM .250
SR 3368.46

SAMPLE SPM-4-87A 1-H 300 MHZ CDCL3



BRUKER

PPM

SPM467AC.004
AU PROS:
AUTOL3.AU
DATE 10-11-92

SF 75.469
SY 112.0500000
Q1 47000.000
QI 22768
QD 22768
QW 17857.143
HZ/PT 1.090

PW 5.0
PD 0.0
AQ 0.918
RE 200
NE 2200
FE 200

FW 22400
QZ 5000.000
DE 154.500

LE 1.000
SE 0.700
EX 25.00
CY 5.00
FL 222.417P
FE -4.576P
HZ/M 452.802
FEM/M 5.000
RE 22590.77

SAMPLE SPM-4-87A 13-C 75.47 MHZ CDCL3

175.694
173.249

148.608
148.085
147.607
147.124

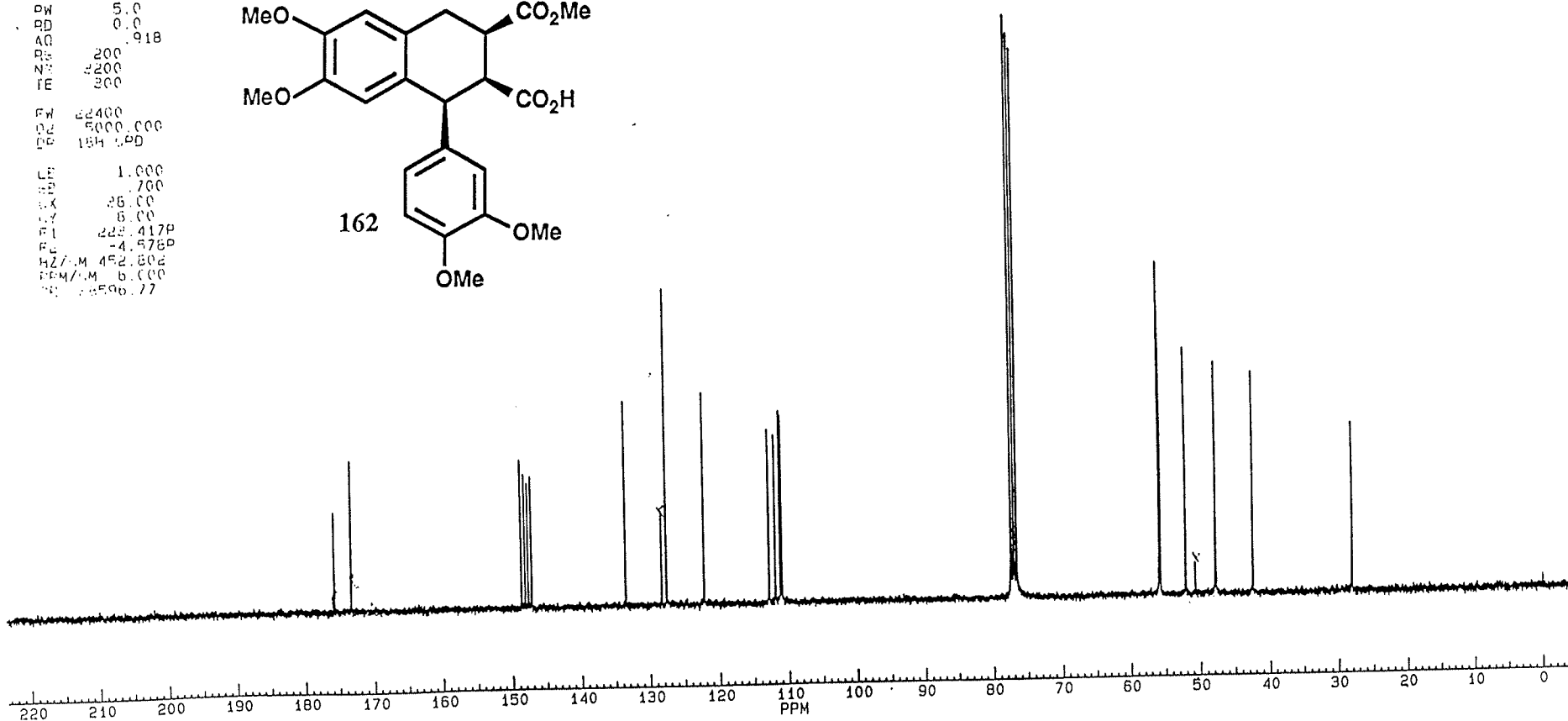
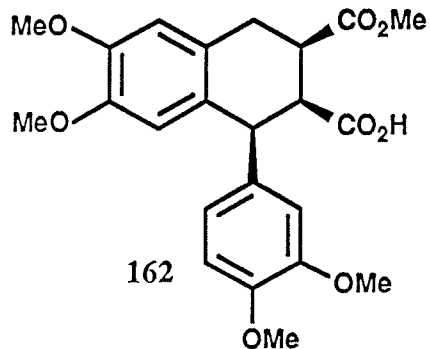
133.458
129.378
127.576
122.180

113.788
111.976
110.924

77.437
77.219
77.002
76.589

55.915
55.846
55.787
55.742
52.119
50.749
47.899
47.833
42.501

28.149





SPM436A.001
DATE 88-7-98

RF 400.138
CY 100.0
P1 9.99
PC 22758
PD 26788
PW 5494.506
HZ/PT 100.0

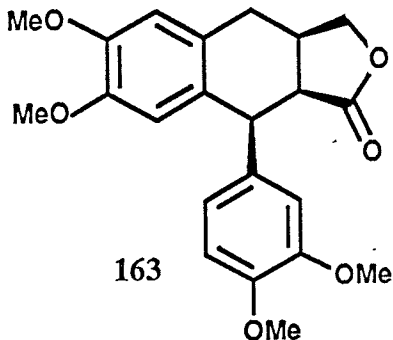
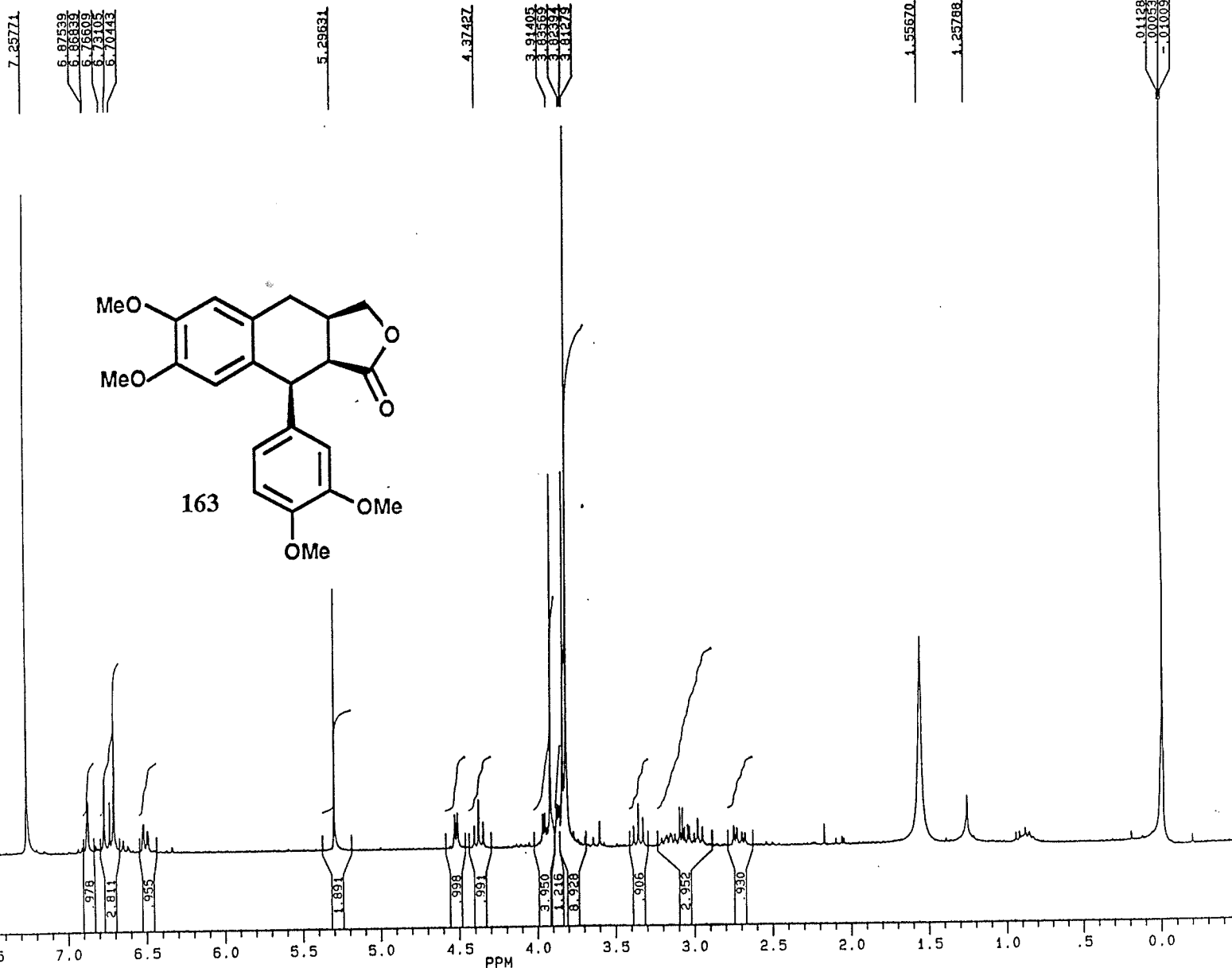
PW 8.1
PD 4.100
AQ 2.988
RF 8.1
NR 2.1
TE 2.1

PW 69.1
PC 200.000
DC 69.1 D1

CB 1.000
CD 1.000
EX 1.000
FL 1.000
FR 1.000
HZ/M 75.000
PDM/M 1.000
PR 1.000

SAMPLE SPM-4-36A 1-H AT 300 MHZ IN CDCL3

PPM





SPM47C.004
AU PROG.
AUTOL13.AU
DATE 27-2-92

SF 75.469
SY 112.0500000
Q1 47000.000
SI 32768
FD 32768
SW 17857.143
HZ/PT 1.090

PW 5.0
RD 0.0
AQ .918
RG 200
NS 4416
TE 300

FW 22400
Q2 5000.000
DP 18H CPD

LB 2.000
GB .700
CX 38.00
CY 8.00
F1 223.417P
F2 -4.578P
HZ/CM 452.802
PPM/CM 6.000
SR 35596.77

SAMPLE SPM-4-7, 13-C AT 75.47 MHZ IN CDCL3

178.043

148.765
148.173
148.011

131.003
130.642
127.741

120.783

112.637
111.771
111.533
110.900

77.406
77.189
76.983
76.559
74.231

66.117

56.057
55.862
55.804
55.702
53.394

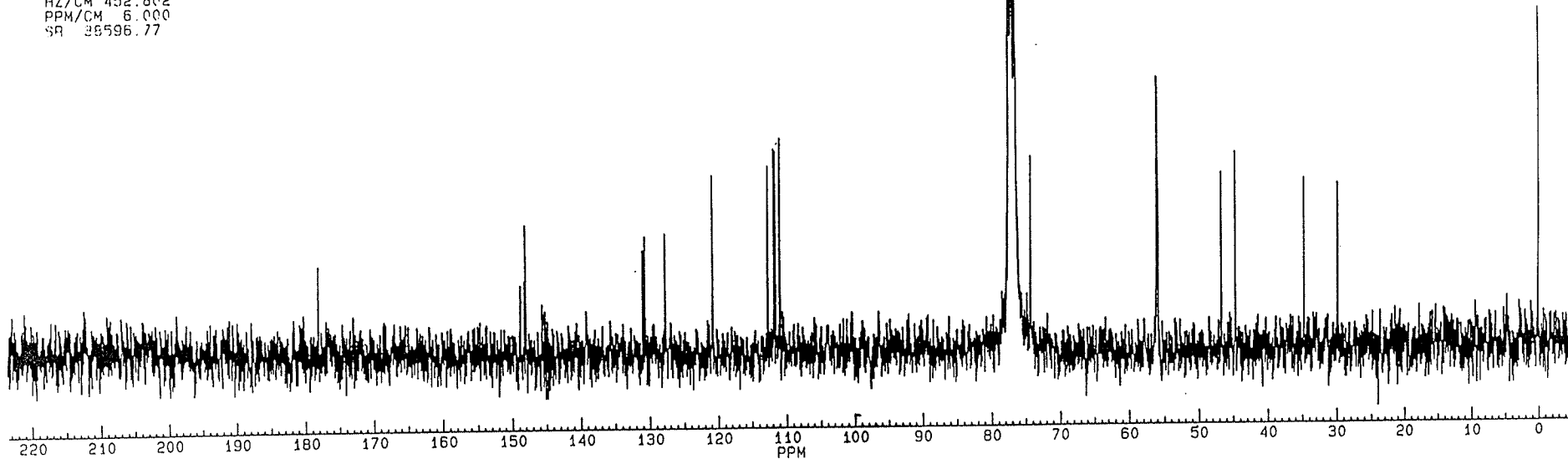
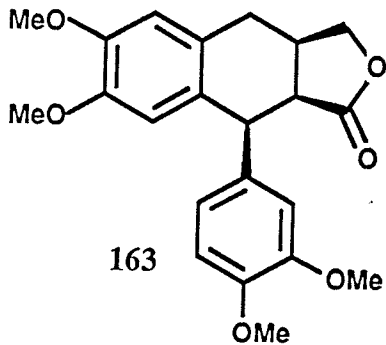
46.651
44.937

34.713

29.856

23.590

.003





SPM431.CC1
DATE 3-7-92

SF 300.123
SY 100.0
Q1 5500.000
SI 22768
ID 22768
SH 5494.505
HZ/PT 225

PW 3.0
PD 4.000
AQ 0.082
RG 20
NS 22
TE 200

FW 6900
S2 20000.000
DP 62L DP

LP 500
GB 500
CX 500
CY 180.00
F1 1.00FB
F2 1.49FB
HZ/CM 78.000
PPM/CM 250
PR 227.42

SPM-4-31

PPM

7.25977

6.81836
6.73520
6.69200
6.61679
6.51081
6.46520
6.41371
6.39762

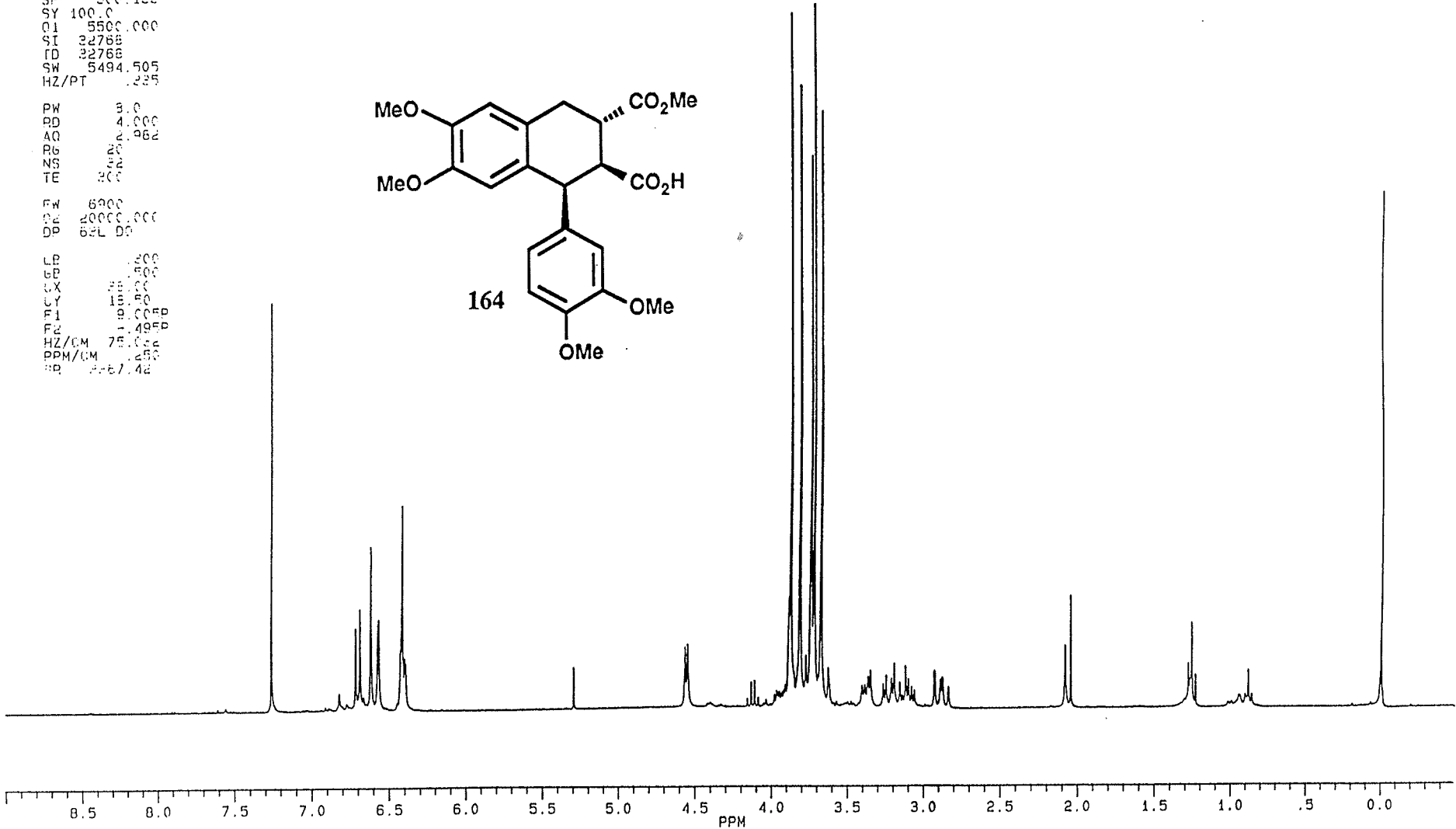
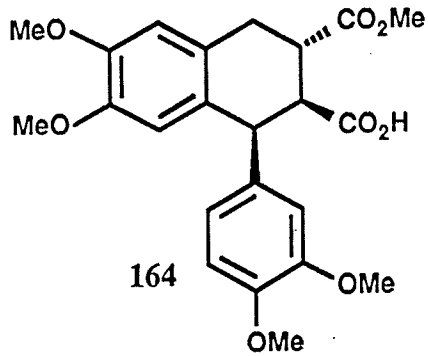
5.29504

4.56332
4.34533
4.31112
4.28662
4.26322
4.24066
4.21726
4.19420
4.17150
4.14850
4.12579
4.10339
4.08083
4.05891
4.03692
4.01492
3.99292
3.97093
3.94893
3.92694
3.90494
3.88294
3.86094
3.83894
3.81694
3.79494
3.77294
3.75094
3.72894
3.70694
3.68494
3.66294
3.64094
3.61894
3.59694
3.57494
3.55294
3.53094
3.50894
3.48694
3.46494
3.44294
3.42094
3.39894
3.37694
3.35494
3.33294
3.31094
3.28894
3.26694
3.24494
3.22294
3.20094
3.17894
3.15694
3.13494
3.11294
3.09094
3.06894
3.04694
3.02494
3.00294
2.98094
2.95894
2.93694
2.91494
2.89294
2.87094
2.84894
2.82694
2.80494
2.78294
2.76094
2.73894
2.71694
2.69494
2.67294
2.65094
2.62894
2.60694
2.58494
2.56294
2.54094
2.51894
2.49694
2.47494
2.45294
2.43094
2.40894
2.38694
2.36494
2.34294
2.32094
2.29894
2.27694
2.25494
2.23294
2.21094
2.18894
2.16694
2.14494
2.12294
2.10094
2.07894
2.05694
2.03494
2.01294
1.99094
1.96894
1.94694
1.92494
1.90294
1.88094
1.85894
1.83694
1.81494
1.79294
1.77094
1.74894
1.72694
1.70494
1.68294
1.66094
1.63894
1.61694
1.59494
1.57294
1.55094
1.52894
1.50694
1.48494
1.46294
1.44094
1.41894
1.39694
1.37494
1.35294
1.33094
1.30894
1.28694
1.26494
1.24294
1.22094
1.19894
1.17694
1.15494
1.13294
1.11094
1.08894
1.06694
1.04494
1.02294
1.00094
0.97894
0.95694
0.93494
0.91294
0.89094
0.86894
0.84694
0.82494
0.80294
0.78094
0.75894
0.73694
0.71494
0.69294
0.67094
0.64894
0.62694
0.60494
0.58294
0.56094
0.53894
0.51694
0.49494
0.47294
0.45094
0.42894
0.40694
0.38494
0.36294
0.34094
0.31894
0.29694
0.27494
0.25294
0.23094
0.20894
0.18694
0.16494
0.14294
0.12094
0.09894
0.07694
0.05494
0.03294
0.01094

1.28164
1.25792
1.23393

.86373

0.1125
0.0043
-0.1053





PPM

SPM-4-54 IN CDCL3 AT 75.47 MHZ

SPM454C.004
AU PROG:
AUTOC13.AU
DATE 21-11-92

SF 75.469
SY 112.0500000
O1 47000.000
SI 32768
TD 32768
SH 17857.143
HZ/PT 1.090

PW 5.0
RD 0.0
AQ .918
RG 200
NS 1600
TE 300

FW 22400
O2 5000.000
DP 18H CPD

LB 1.000
GB .700
CX 38.00
CY 18.00
F1 223.417P
F2 -4.578P
HZ/CM 452.802
PPM/CM 6.000
SR 38596.77

178.082
175.457

148.435
148.102
147.971

133.920

128.680

125.572

121.674

112.646
112.339
111.172
110.992
110.358

77.427
77.208
77.004
76.583

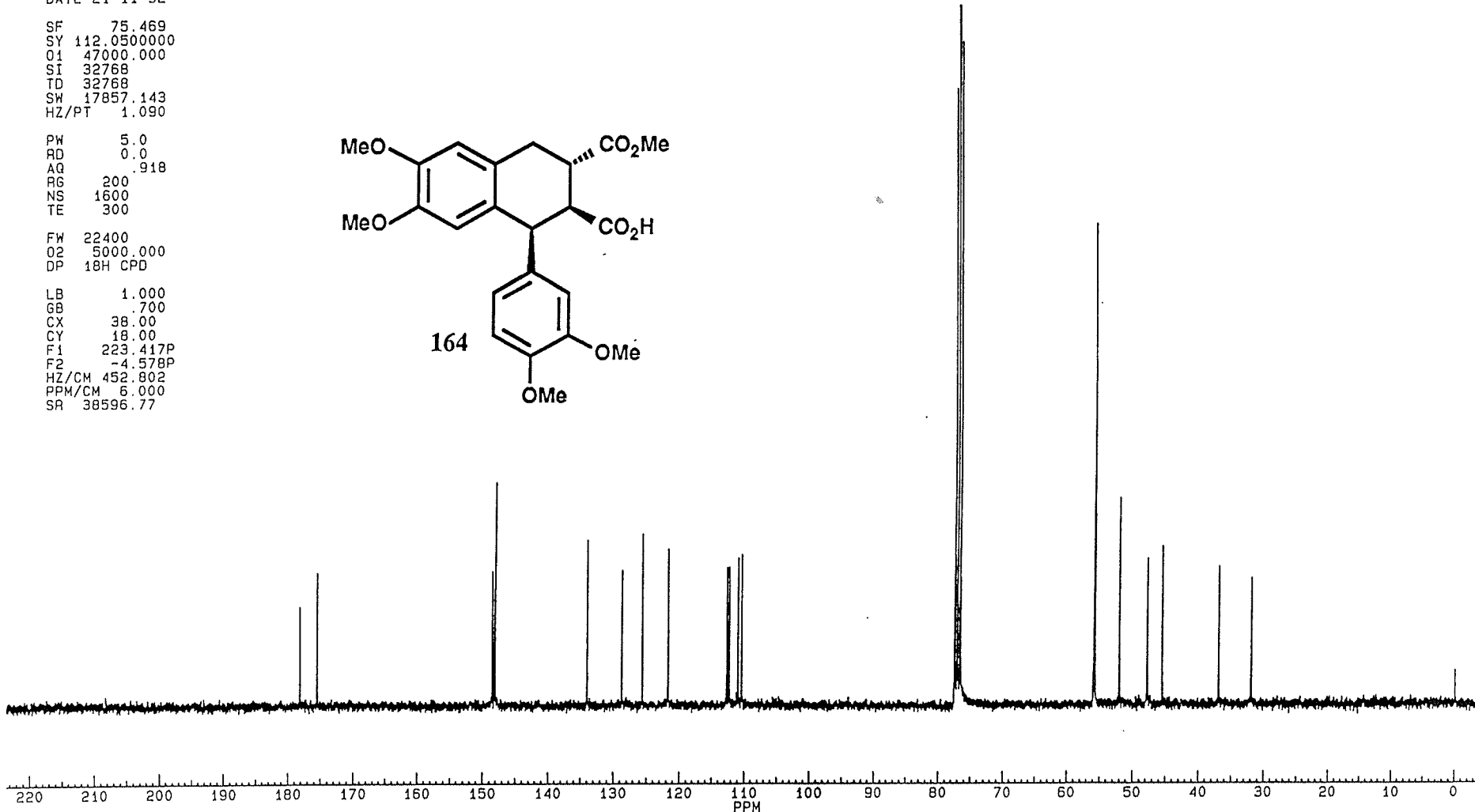
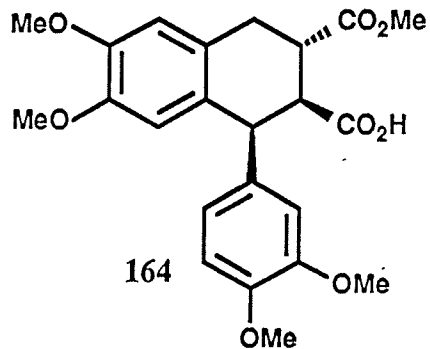
55.935
55.848
55.764
55.687
55.610

47.785
45.508

36.934

31.989

-.001





SPMISORE.001
DATE 20-9-92

SF 300.133
SY 100.0
Q1 5500.000
SI 32768
TD 32768
SW 5494.505
HZ/PT .335

PW 8.0
RD 4.000
AQ 2.982
RG 20
NS 32
TE 300

FW 6900
Q2 20000.000
DP 63L D0

LB .300
GB .500
CX 38.00
CY 18.50
F1 9.005P
F2 -.495P
HZ/CM 75.032
PPM/CM .250
SR 3367.42

PPH

7.35604
7.26011

6.71237
6.69237
6.67237
6.65237
6.63237
6.61237
6.59237
6.57237
6.55237
6.53237
6.51237
6.49237
6.47235
6.45235
6.43235
6.41010

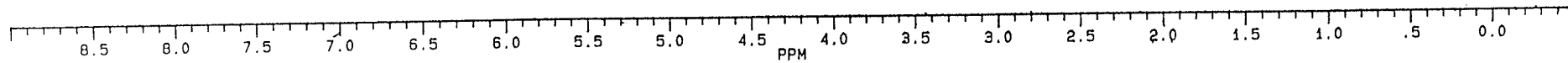
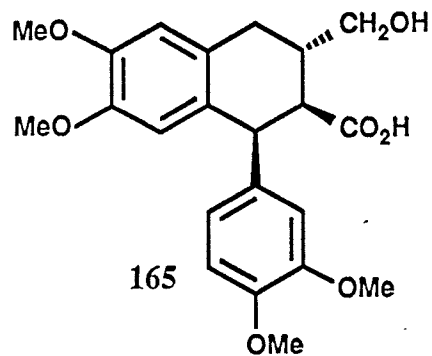
4.47504
4.45689

3.69630
3.67360
3.65100
3.62840
3.60580
3.58320
3.56060
3.53800
3.51540

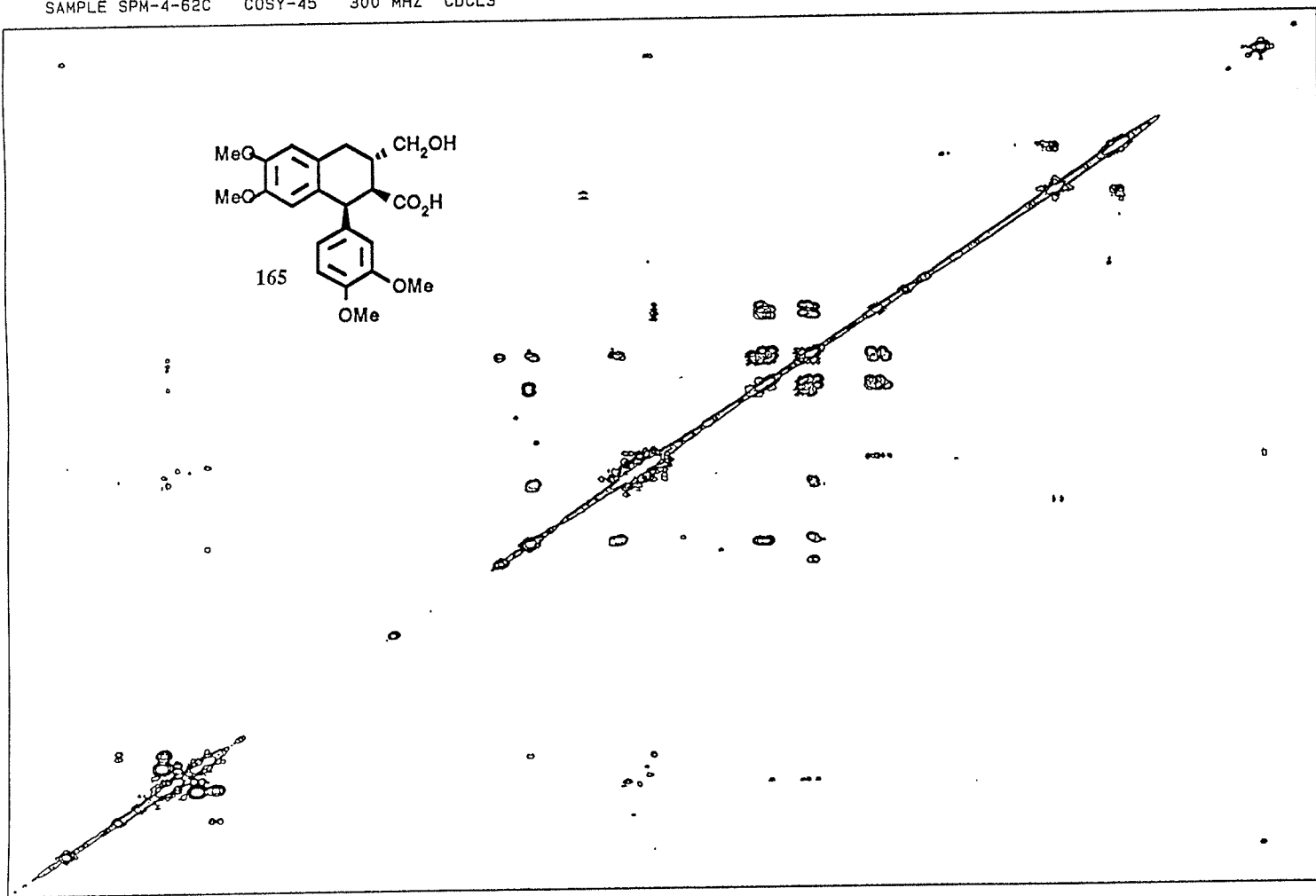
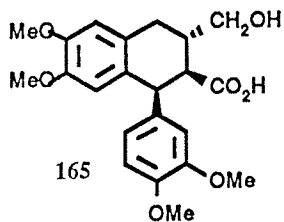
3.07590
3.05330
3.03070
3.00810
2.98550
2.96290
2.94030
2.91770
2.89510
2.87250
2.85000
2.82740
2.80480
2.78220
2.75960
2.73700

2.35699
2.33700

0.1179
0.0113
-0.0986



SAMPLE SPM-4-62C COSY-45 300 MHZ CDCL3



SPM COSY.SMX
 AU PROG:
 COSY.AU
 DATE 15-9-92

SI2 1024
 SI1 512
 SW2 2392.344
 SW1 1196.172
 NDO 1

WDW2 S
 WDW1 S
 SSB2 0
 SSB1 0
 MC2 M
 PLIM ROW:
 F1 7.6130
 F2 -1.3420
 AND COLUMN:
 F1 7.6130
 F2 -1.3420
 D1 5.000000
 P1 11.00
 D0 .000000
 P2 5.50
 RD 0.0
 PW 0.0
 DE 262.60
 NS 16
 DS 2
 NE 2
 IN .0004180

7.5 7.0 6.5 6.0 5.5 5.0 4.5 4.0 3.5 3.0 2.5 2.0 1.5 1.0 .5 0.0
 PPM

0.0
 .5
 1.0
 1.5
 2.0
 2.5
 3.0
 3.5
 4.0
 4.5
 5.0
 5.5
 6.0
 6.5
 7.0
 7.5
 PPM

BRUKER

PPM

SPM462CC.004
AU PROG:
AUTOC13.AU
DATE 8-9-92

SF 75.469
SY 112.0500000
O1 47000.000
SI 32768
TD 32768
SW 17857.143
HZ/PT 1.090

PW 5.0
RD 0.0
AQ .918
RG 200
NS 1088
TE 300

FW 22400
Q2 5000.000
DP 18H CPD

LB 1.000
GB .700
CX 38.00
CY 18.00
F1 223.417P
F2 -4.578P
HZ/CM 452.802
PPM/CM 6.000
SR 38596.77

SAMPLE SPM-4-62C 13-C 75.47 MHZ COCL3

178.148

148.152
147.909
147.784
147.573

134.657

129.096
127.304

121.817

113.222
113.021
112.066
111.367
110.762

77.437
77.218
77.015
76.589

65.336

55.857
55.820
55.803
55.704

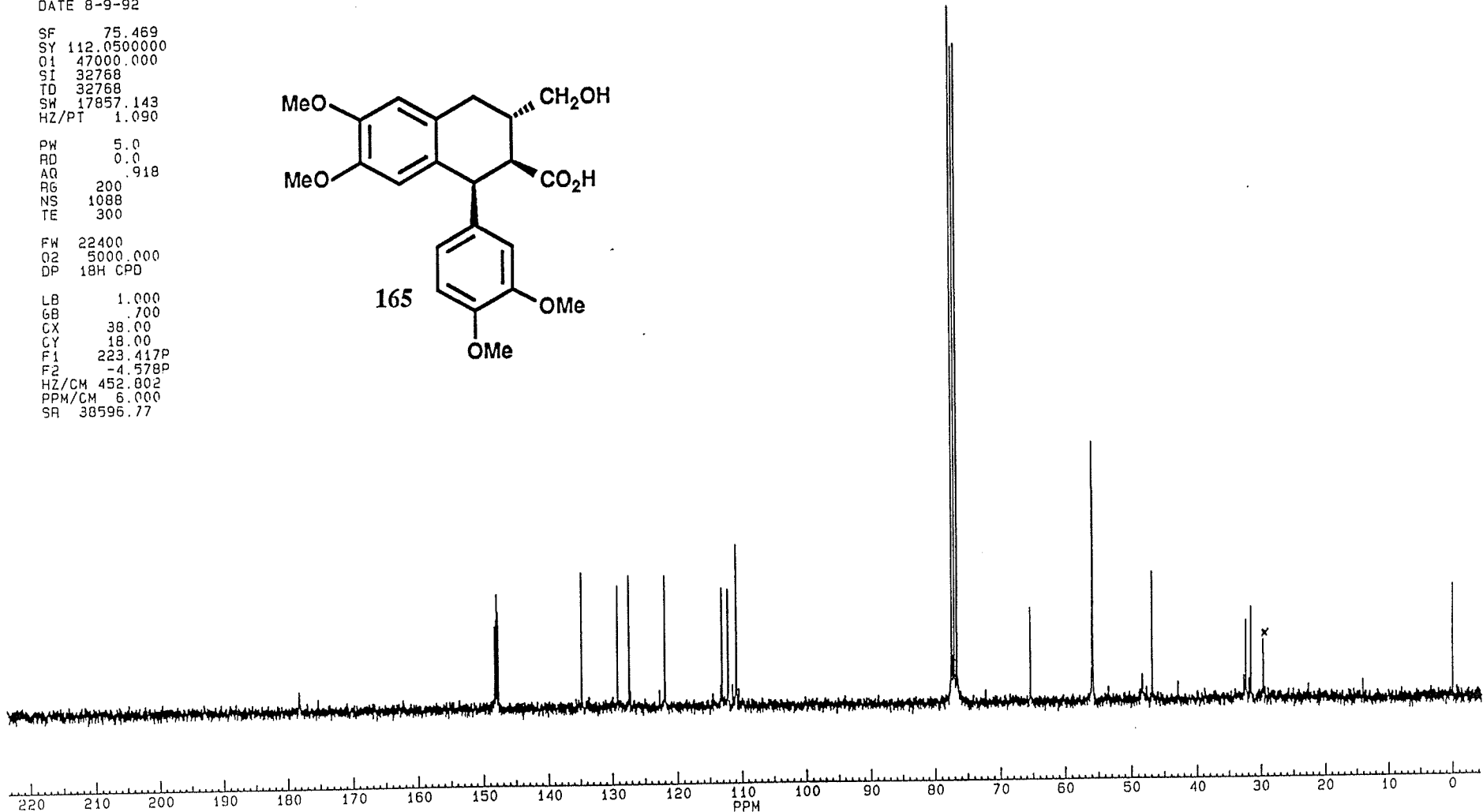
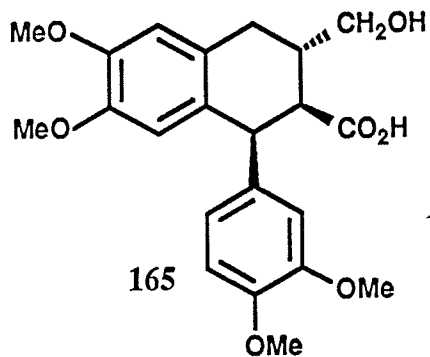
48.320
46.792

42.868

32.692
32.380
31.919
31.596
29.692

14.110

.000



~~BRUKER~~

SPM444A.001
DATE 11-1-93

SF 300.133
SY 100.0
O1 5500.000
SI 32768
TD 32768
SW 5494.505
HZ/PT .335

PW 8.0
RD 4.000
AQ 2.982
RG 32
NS 32
TE 300

FW 6900
O2 20000.000
DP 63L D0

LB .300
GB .500
CX 38.00
CY 22.00
F1 9.004P
F2 -.496P
HZ/CM 75.032
PPM/CM .250
SR 3367.79

SAMPLE SPM-4-44A 1-H 300 MHZ CDCL3

PPH

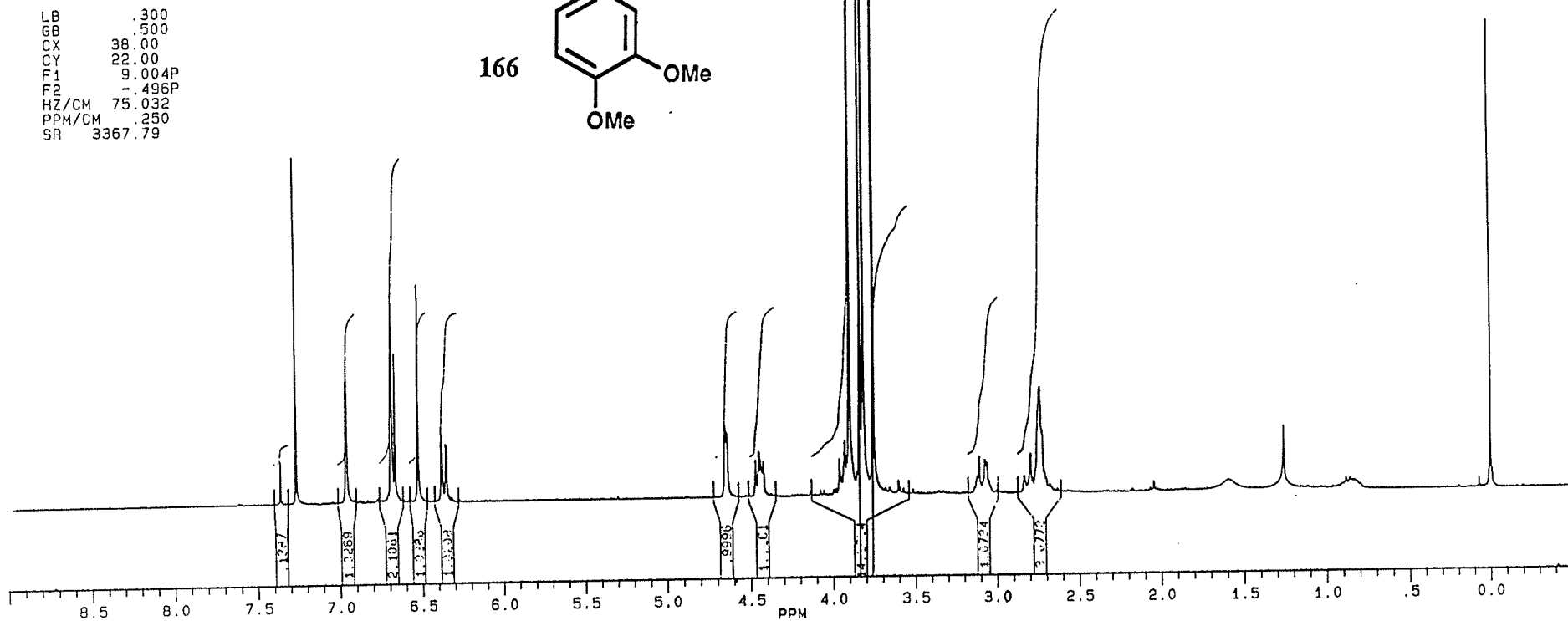
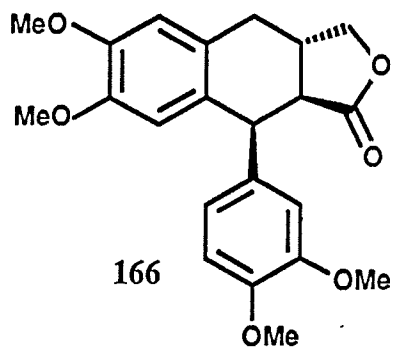
7.35537
7.25941
6.95786
6.95119
6.68693
6.68023
6.65948
6.51959
6.37705
6.37032
6.34948
6.34280

4.64825
4.63701
4.46659
4.44557
4.43775
4.41746
3.95735
3.92457
3.91399
3.89666
3.83447
3.81439
3.75989

3.40602
3.07132
2.79350
2.74009
2.72614

1.25558

.00013



BRUKER

PPM

SPM473C.004
AU PROG:
AUTO13.AU
DATE 1-11-92

SF 75.469
SY 112.0500000
Q1 47000.000
SI 32768
TD 32768
SW 17857.143
HZ/PT 1.090

PW 5.0
RD 0.0
AQ .918
RG 200
NS 1280
TE 300

FW 22400
Q2 5000.000
DP 16H CPD

LB 1.000
GB .700
CX 38.00
CY 6.00
F1 223.417P
F2 -4.578P
HZ/CM 452.802
PPM/CM 6.000
SR 38596.77

SAMPLE SPM-4-73 13-C 75.47 MHZ Q1 L3

175.097

148.234
148.032
147.872

133.475
129.892
127.074
122.612

114.407
113.222
111.351
110.322

77.408
77.000
76.592
72.131

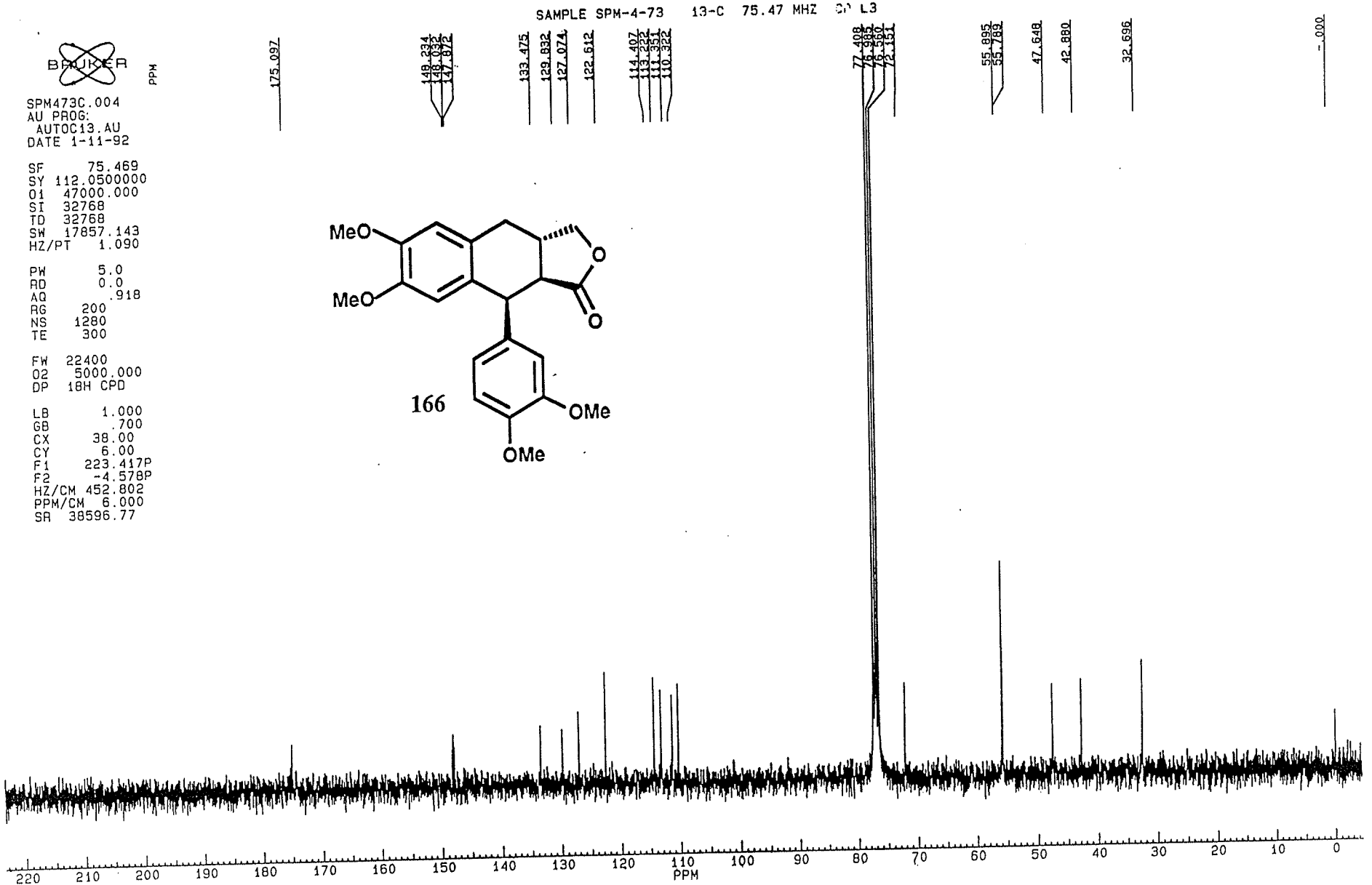
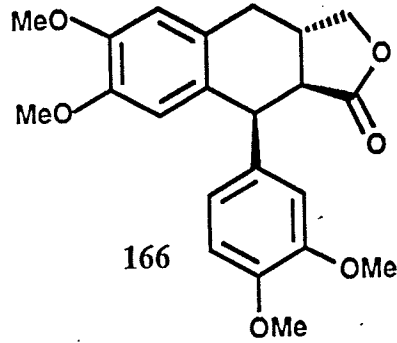
55.895
55.783

47.648

42.880

32.696

-.000



Bruker

SPM492.C01
DATE 10-11-92

RF 300.132
RY 100.0
Q1 5500.000
Q2 32768
Q3 32768
Q4 5494.505
HZ/PT 335

PW 8.0
PD 4.000
AQ 2.982
RG 40
NR 32
TE 300

FW 6500
FL 50000.000
DP 327.00

LP 200
LX 500
LY 88.00
LZ 18.50
P1 9.0010
P2 1.4980
R1/M 75.032
R2/M 1.250
R3 1.08.40

SAMPLE SPM-4-92 1-H 300 MHZ CDCL3

7.25849

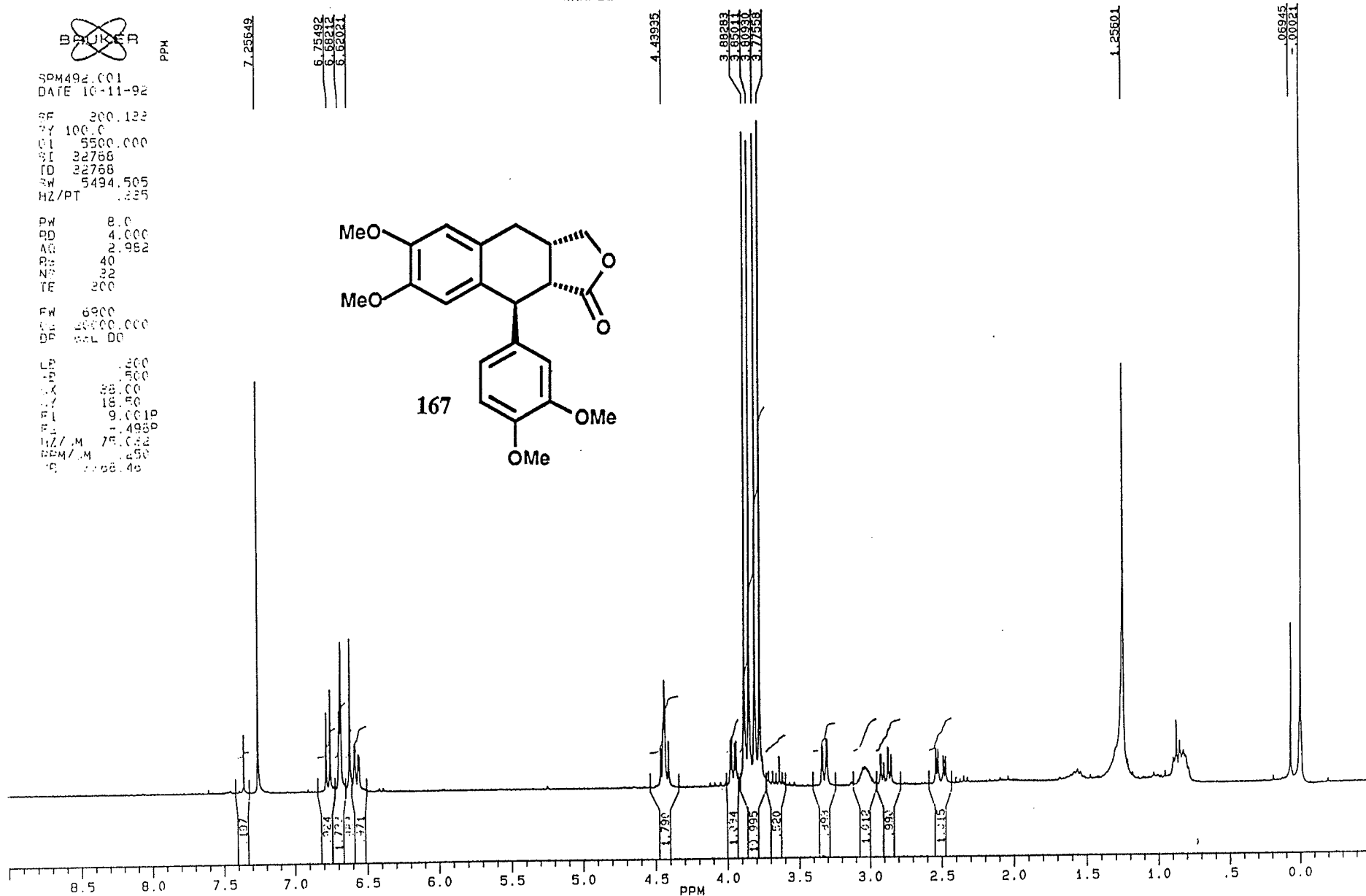
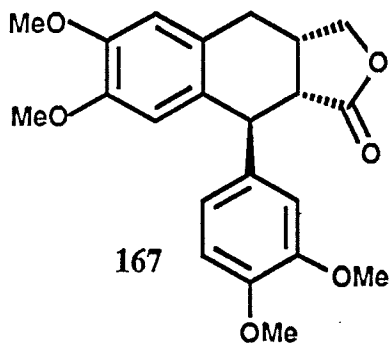
6.75492
6.68212
6.62021

4.43935

3.89293
3.85011
3.80729
3.76447
3.72165

1.09527

0.06945
0.00000





SPM4101C.004
 AU PROG:
 AUTO C13.4U
 DATE 18-1-93

SF 75.469
 SY 112.0500000
 O1 47000.000
 SI 32768
 TD 32768
 SW 17857.143
 HZ/PT 1.090

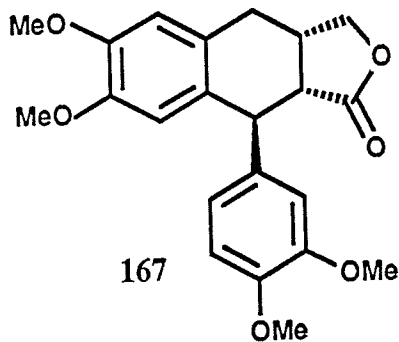
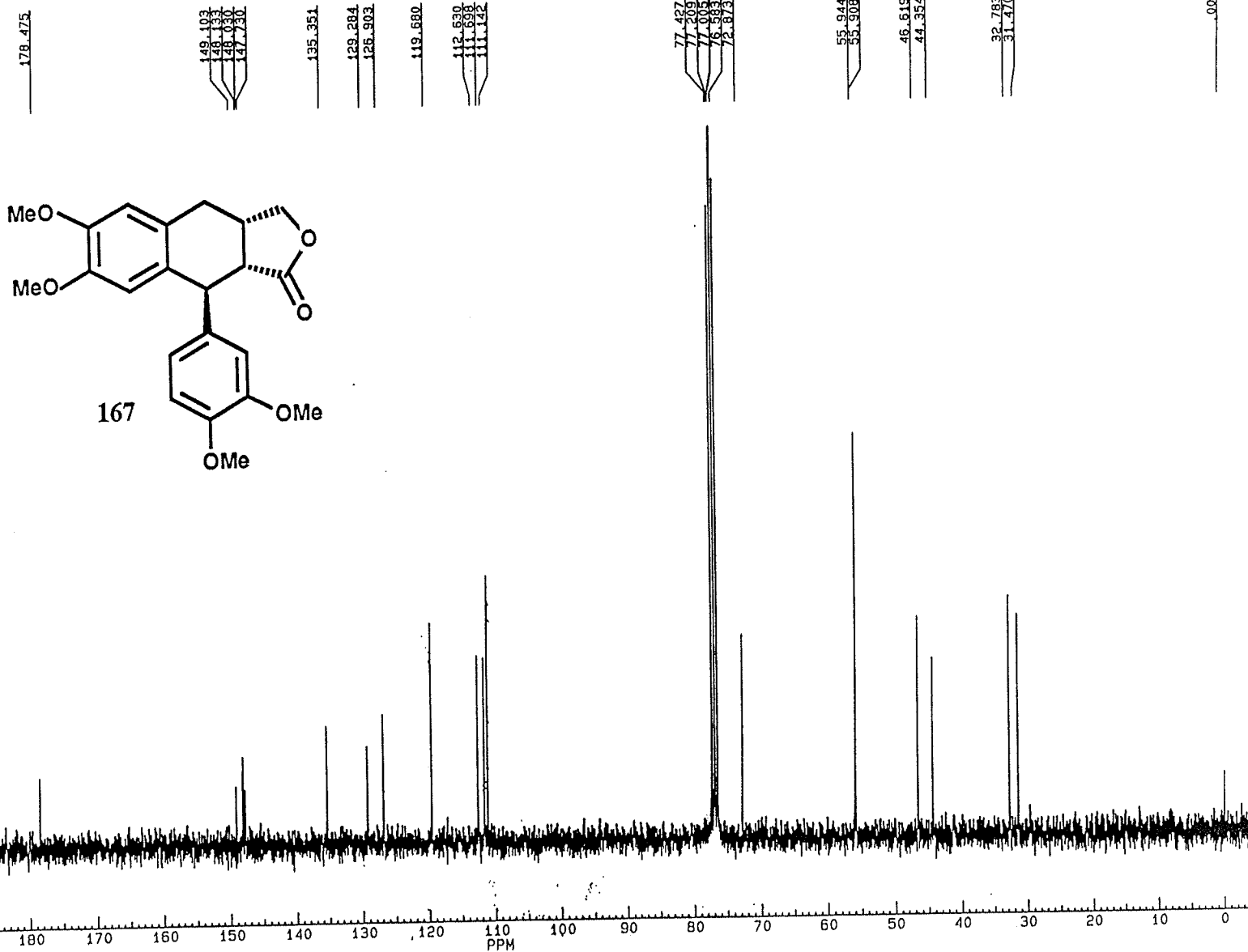
PW 5.0
 RD 0.0
 AQ .918
 RG 200
 NS 448
 TE 300

FW 22400
 O2 5000.000
 DP 18H CPD

LB 1.000
 GB .700
 CX 38.00
 CY 6.00
 F1 223.417P
 F2 -4.578P
 HZ/CM 452.802
 PPM/CM 6.000
 SR 38596.77

PPM

SAMPLE SPM-4-101 13-C 75.47 MHZ CDCL3



BRUKER

SPM4120.001
AU PROG:
TFZG.AU
DATE 12-8-93

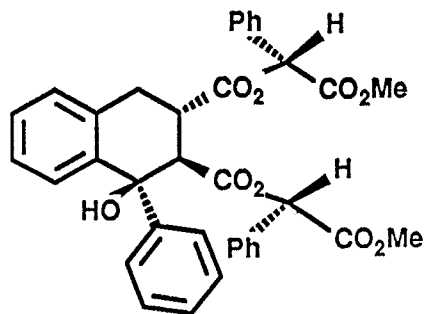
SF 300.133
SY 100.0
O1 5500.000
SI 32768
TD 32768
SW 5494.505
HZ/PT .335

PW 8.0
RD 4.000
AQ 2.982
RG 20
NS 32
TE 300

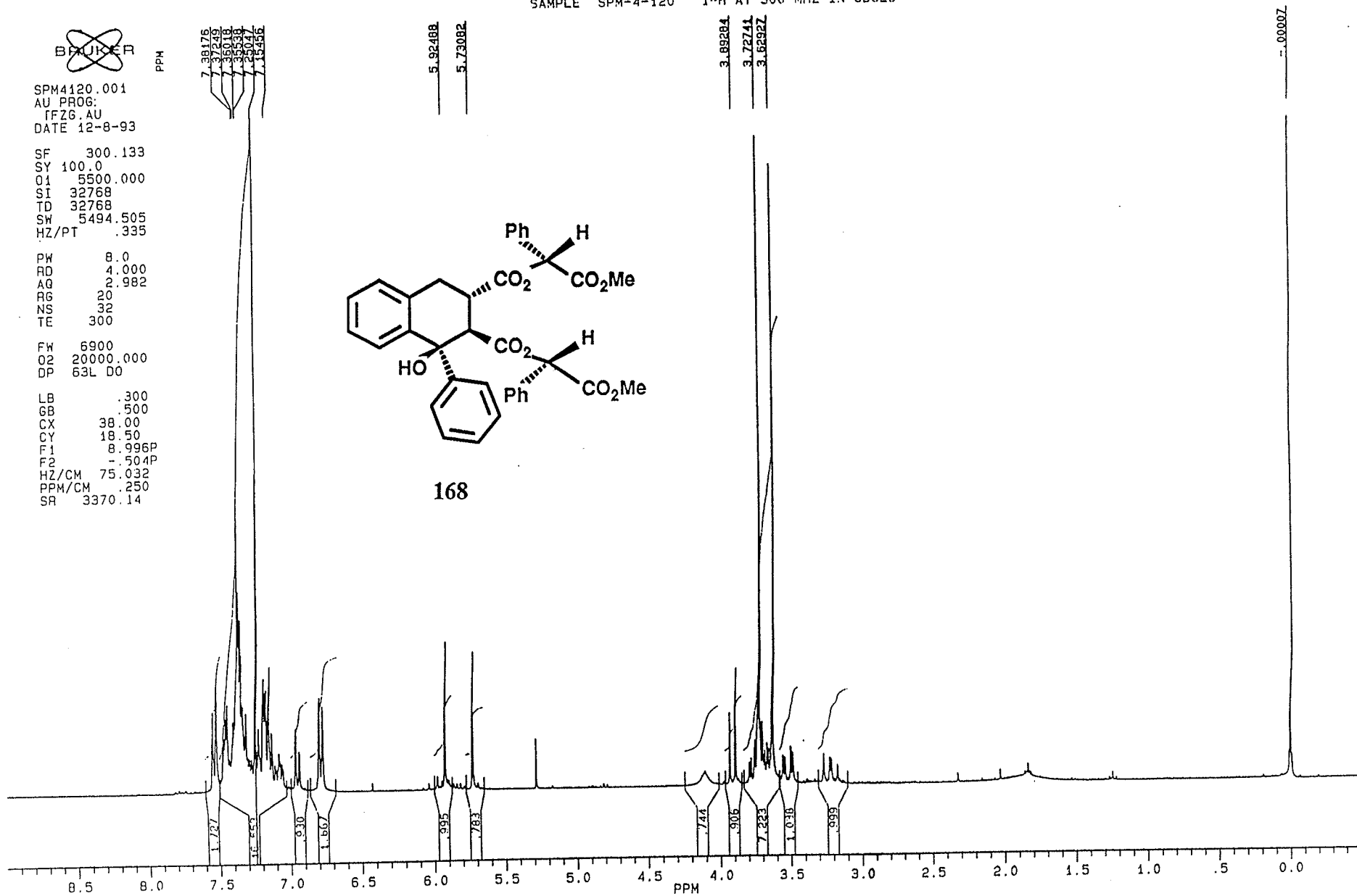
FW 6900
O2 20000.000
DP 63L D0

LB .300
GB .500
CX 38.00
CY 18.50
F1 8.996P
F2 .504P
HZ/CM 75.032
PPM/CM .250
SR 3370.14

SAMPLE SPM-4-120 1-H AT 300 MHZ IN CDCL3



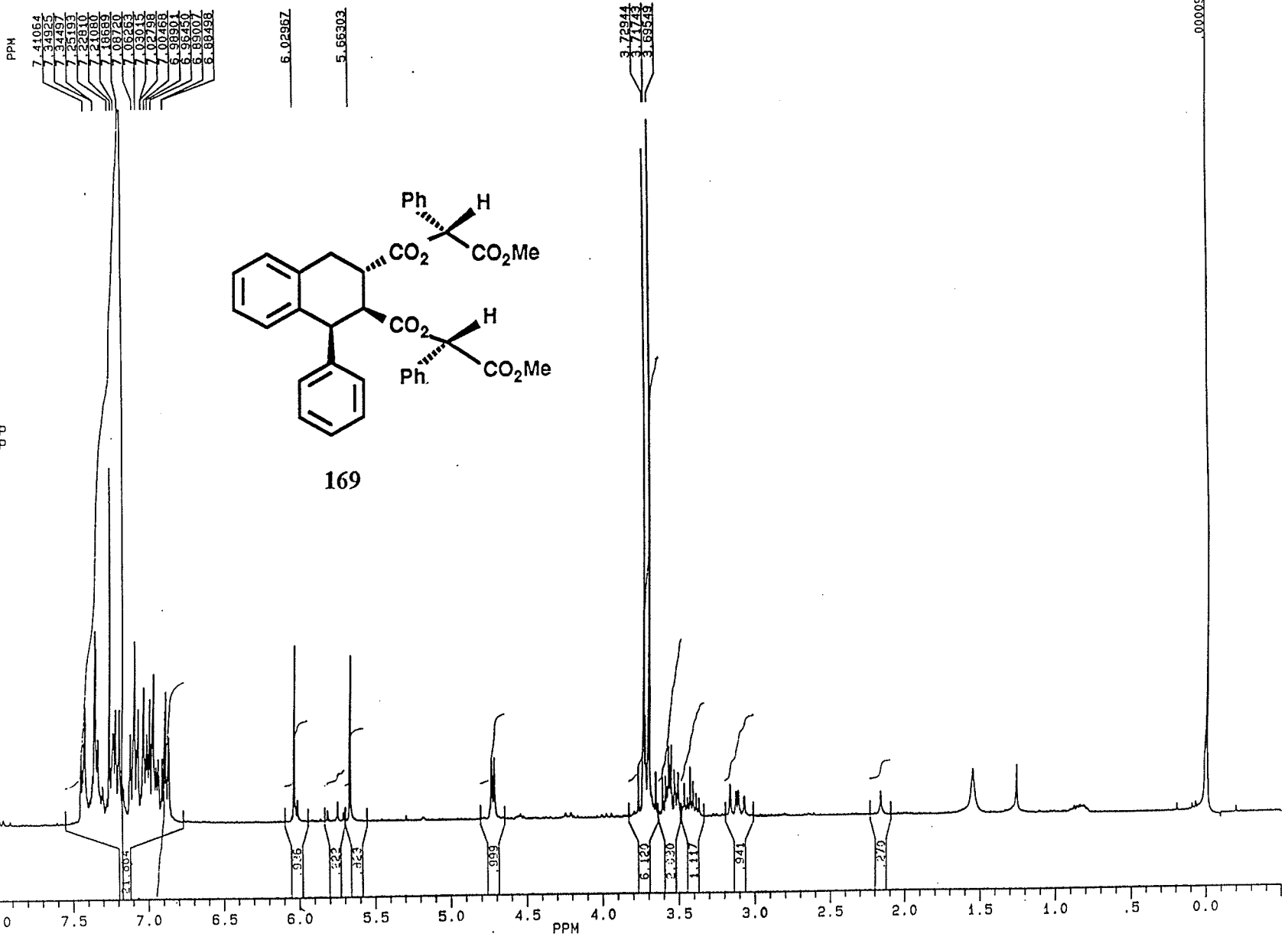
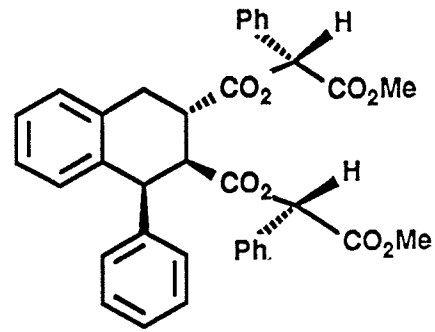
168





SPM489A.001
DATE 12-2-93
SF 300.133
SY 100.0
O1 5500.000
SI 32768
TD 32768
SW 5494.505
HZ/PT .335
PW 8.0
RD 4.000
AQ 2.982
RG 32
NS 32
TE 300
FW 6900
O2 20000.000
DP 63L 00
LB .300
GB .500
CX 38.00
CY 18.50
F1 8.997P
F2 -.503P
HZ/CM 75.032
PPM/CM .250
SR 3369.81

SAMPLE SPM-4-89-A 1-H 300 MHZ CDCL3





PPM

SPM485AC.004
AU PRO6
AUTOC13.AU
DATE 27-10-92

SF 75.469
SY 112.0500000
Q1 47000.000
SC 22766
SD 22766
SW 17857.142
HZ/PT 1.090

PW 5.0
RD 0.0
AQ 0.918
RG 200
NS 4600
TE 300

FW 22400
Q2 5000.000
DP 184.000

LB 1.000
GB 0.700
CX 56.00
CY 5.00
F1 228.417P
F2 -4.676P
HZ/LM 452.602
PPM/LM 5.100
SR 38596.77

SAMPLE SPM-4-85A 13-C 75.47 MHZ CDCL3

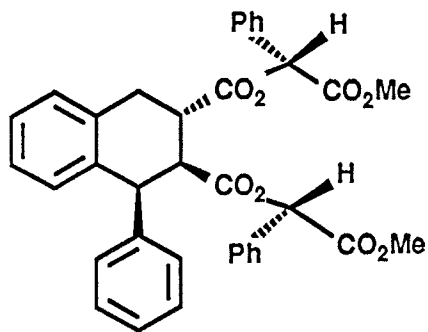
174.128
171.955
169.375
168.796

141.401
136.598
133.678
133.574
133.391
130.741
130.543
128.763
128.680
128.681
128.470
128.273
127.912
127.854
127.796
127.176
127.076
126.901
126.899
126.677

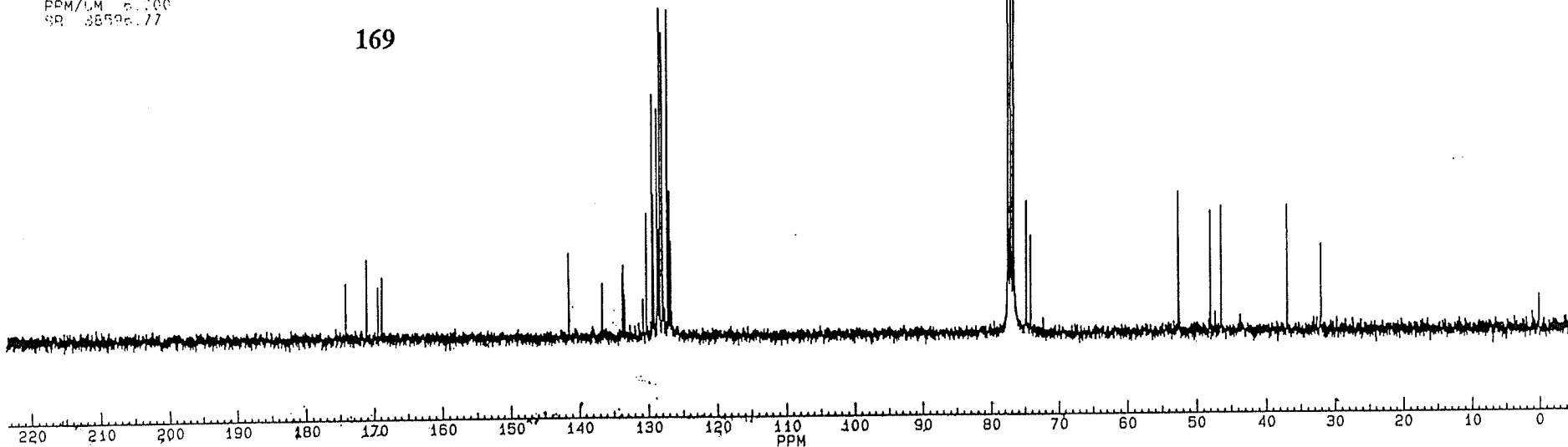
77.410
77.193
76.986
76.566
74.661
74.022

52.526
52.433
47.888
46.301

36.885
32.044



169



PPH
 7.85308
 7.82692
 7.46603
 7.45947
 7.44987
 7.44900
 7.43375
 7.40841
 7.38383
 7.37432
 7.36934
 7.35344
 7.33991
 7.32089
 7.30853
 7.29870
 7.29443
 7.24862
 7.23193
 7.19183
 6.99093
 6.99457
 6.86820
 6.85067
 6.84382
 6.81790
 6.89480
 6.87470
 6.20286

5.53540

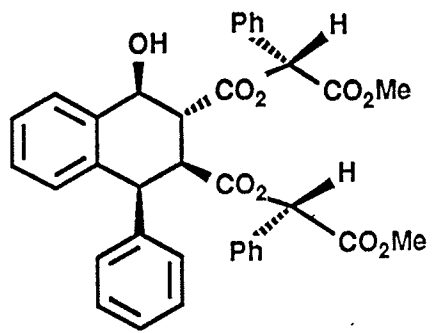
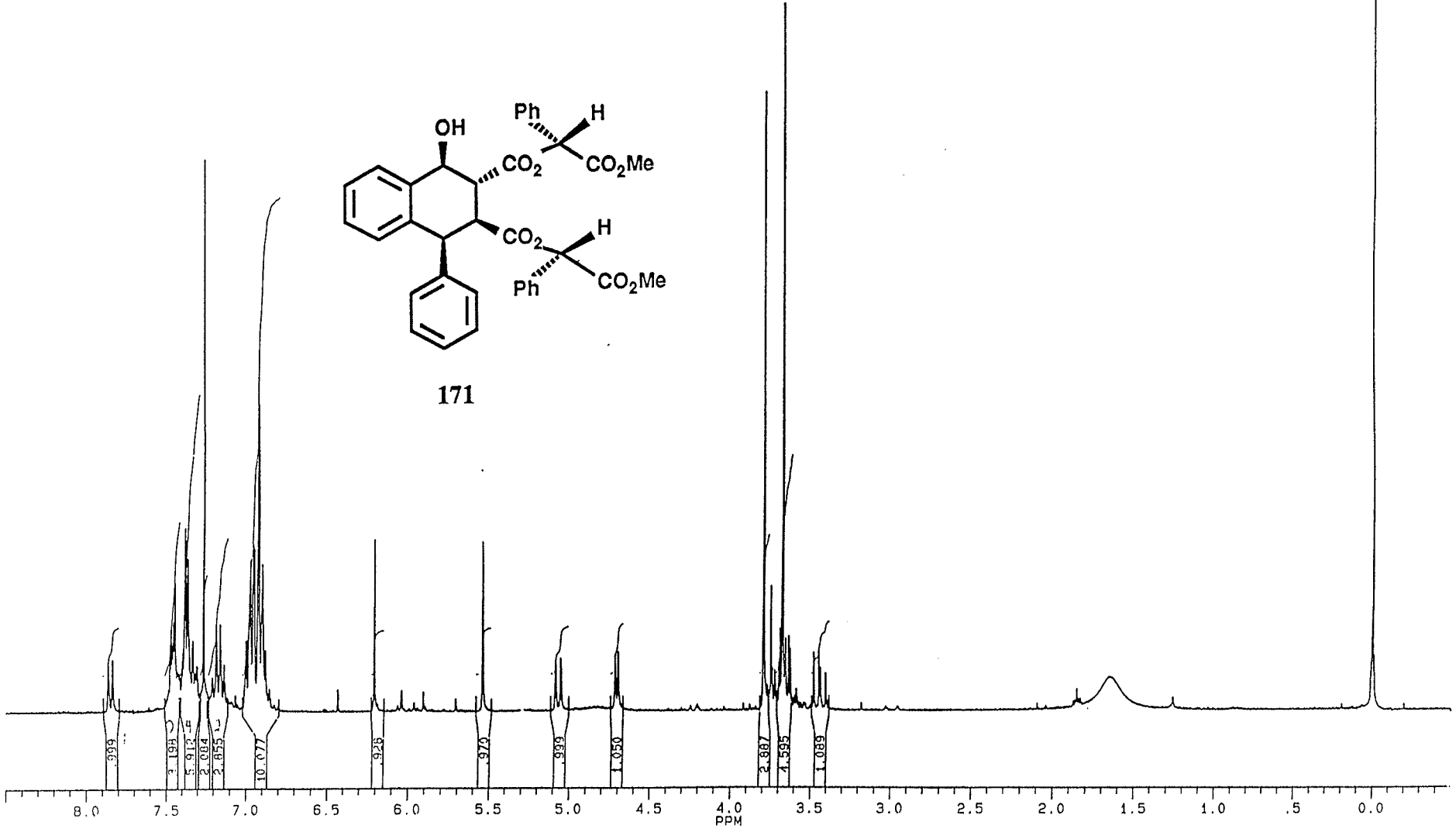
5.08094
 5.04865

4.71231
 4.69287

SPM-4-64 IN CDCL3

3.78943
 3.74430
 3.73671
 3.71887
 3.69350
 3.68605
 3.67189
 3.65439
 3.64291
 3.63471
 3.44245
 3.43237
 3.40080

0.1066
 -0.0010
 -0.0112



171



PPH

SPM464C.004
AU PROG:
AUTOC13.AU
DATE 29-7-93

SF 75.469
SY 112.0500000
O1 47000.000
SI 32768
TD 32768
SW 17857.143
HZ/PT 1.090

PW 5.0
RD 0.0
AQ .918
RG 200
NS 1600
TE 300

FW 22400
O2 5000.000
DP 18H CPD

LB 1.000
GB .700
CX 38.00
CY 8.00
F1 223.417P
F2 -4.578P
HZ/CM 452.802
PPM/CM 6.000
SR 38596.77

SAMPLE SPM-4-64 13-C AT 75.47 MHZ IN CDCL3

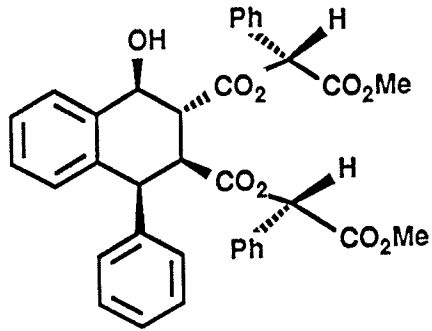
174.096
171.517
170.198

40.944
36.690
36.374
36.171
33.973
33.376
28.789
28.664
28.172
28.026
27.884
27.373
27.073
26.952
26.806

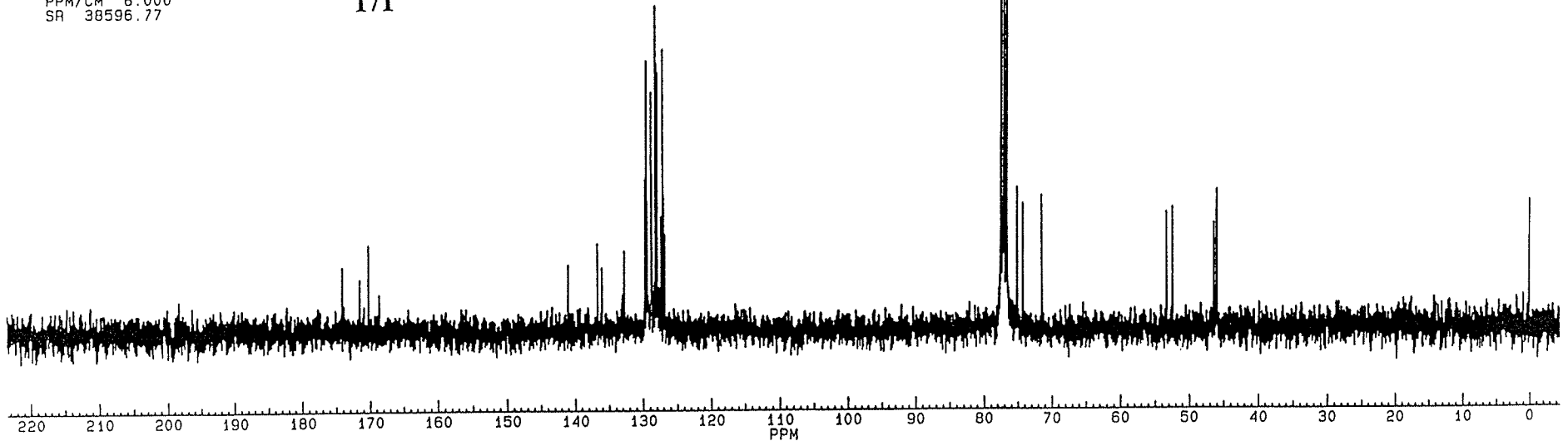
77.410
77.191
76.969
76.556
75.012
74.171
71.367

53.347
52.453
46.509
46.145
46.027

001



171



SAMPLE SPM-4-27 1-H AT 300 MHZ IN CDCL3

BRUKER

SPM427.001
DATE 15-6-92

SF 300.133
SY 100.0
O1 5500.000
SI 32768
TD 32768
SW 5494.505
HZ/PT .335

PW 8.0
RD 4.000
AQ 2.982
RG 8
NS 32
TE 300

FW 6900
Q2 20000.000
DP 62L D0

LB .300
GB .500
CX 38.00
CY 18.50
F1 8.980P
F2 -5.12P
HZ/CM 75.032
PPM/CM .250
SR 3372.49

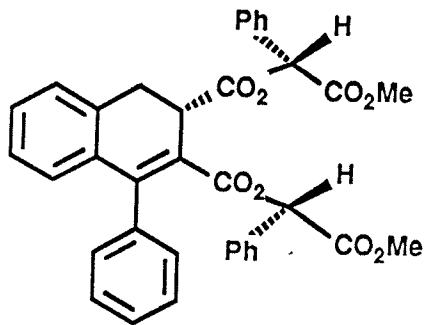
PPM

7.30537
7.30126
7.29176
7.28266
7.27317
7.19699
7.17139

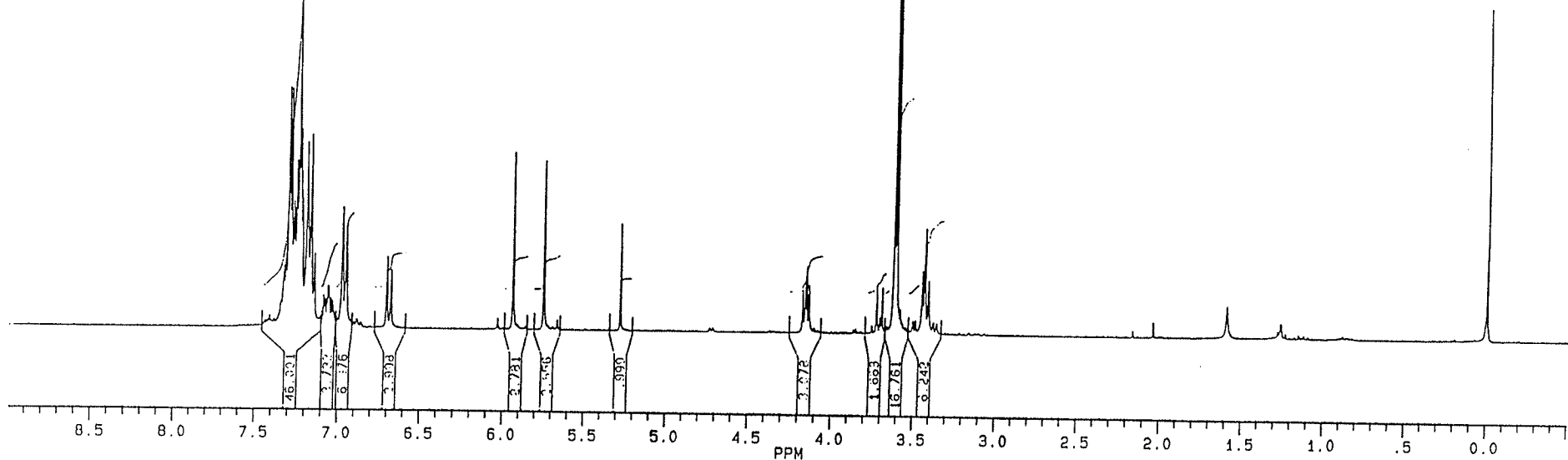
5.93742
5.74756

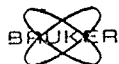
3.52424
3.52129
3.51834

0.00000



172





SPM427C.004
 AU PROG:
 AUTOC13.AU
 DATE 15-6-92

SF 75.469
 SY 112.0500000
 O1 47000.000
 SI 32768
 ID 32768
 SW 17857.143
 HZ/PT 1.090

PW 5.0
 RD 0.0
 AQ .918
 RG 200
 NS 640
 TE 300

FW 22400
 Q2 5000.000
 DP 18H CPD

LB 1.000
 GB .700
 CX 38.00
 CY 18.00
 F1 223.388P
 F2 -4.607P
 HZ/CM 452.802
 PPM/CM 6.000
 SR 26598.95

SAMPLE SPM-4-27 13-C AT 75.47 MHZ IN CDCL3

171.843
 168.885
 168.818
 168.322

149.553
 138.399
 134.626
 131.374
 129.777
 129.438
 129.090
 128.992
 128.668
 128.285
 127.816
 127.464
 127.290
 126.844
 122.789

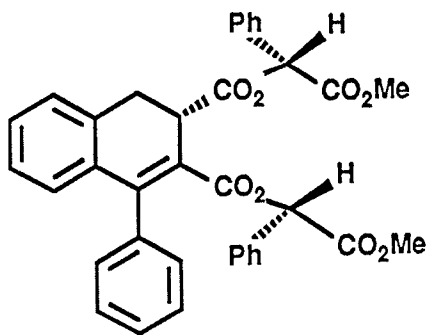
77.417
 76.896
 76.840
 74.612
 74.612

52.443
 52.344

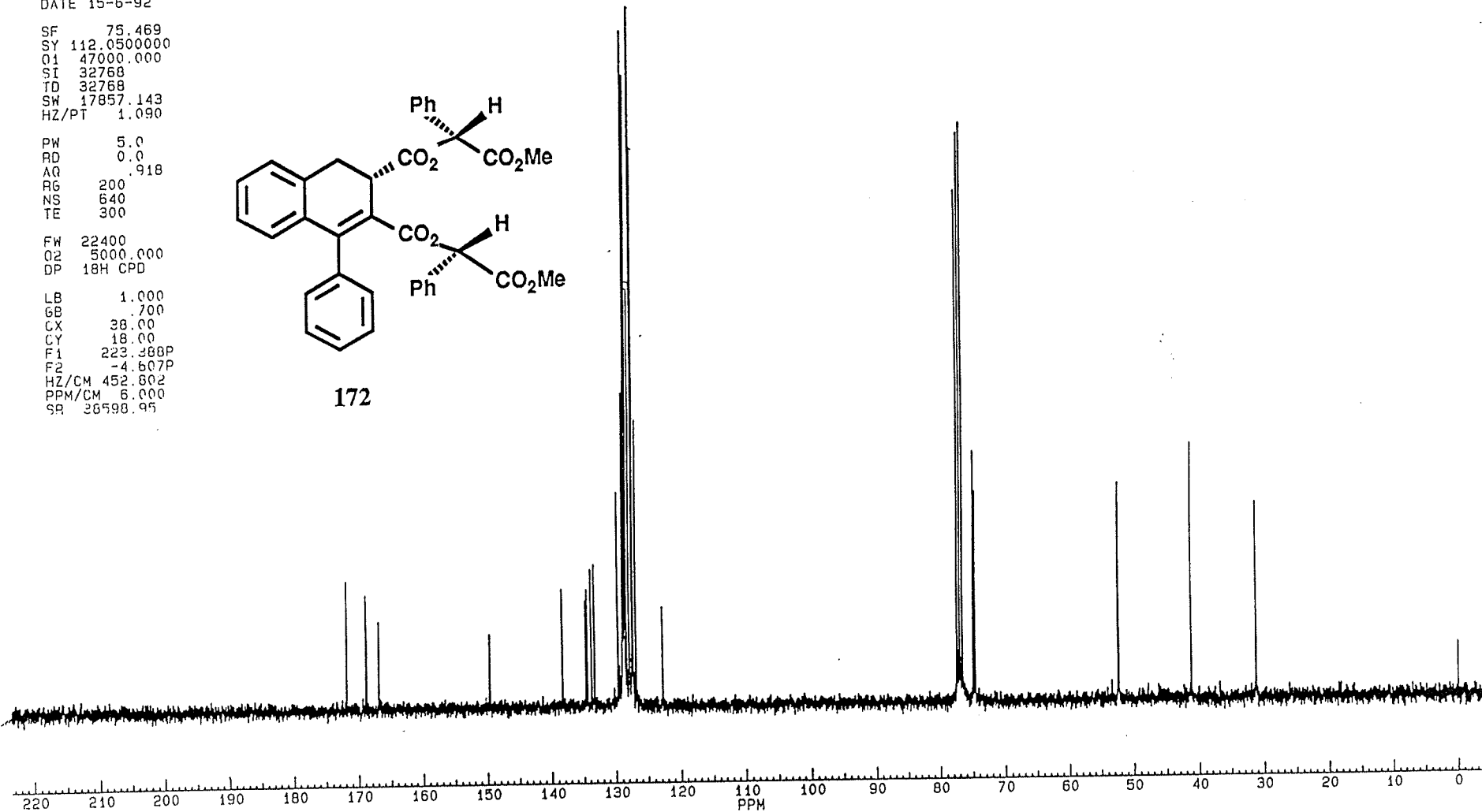
41.305

31.312

- .001



172





SPM4112B.001
AU PROG:
TFZG.AU
DATE 16-4-93

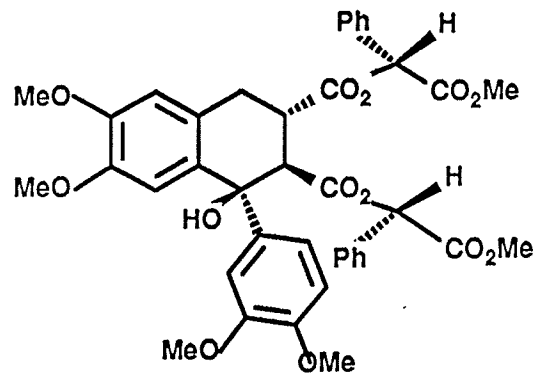
SF 300.133
SY 100.0
O1 5500.000
SI 32768
TD 32768
SH 5494.505
HZ/PT .335

PW 8.0
RD 4.000
AQ 2.982
RG 100
NS 64
TE 300

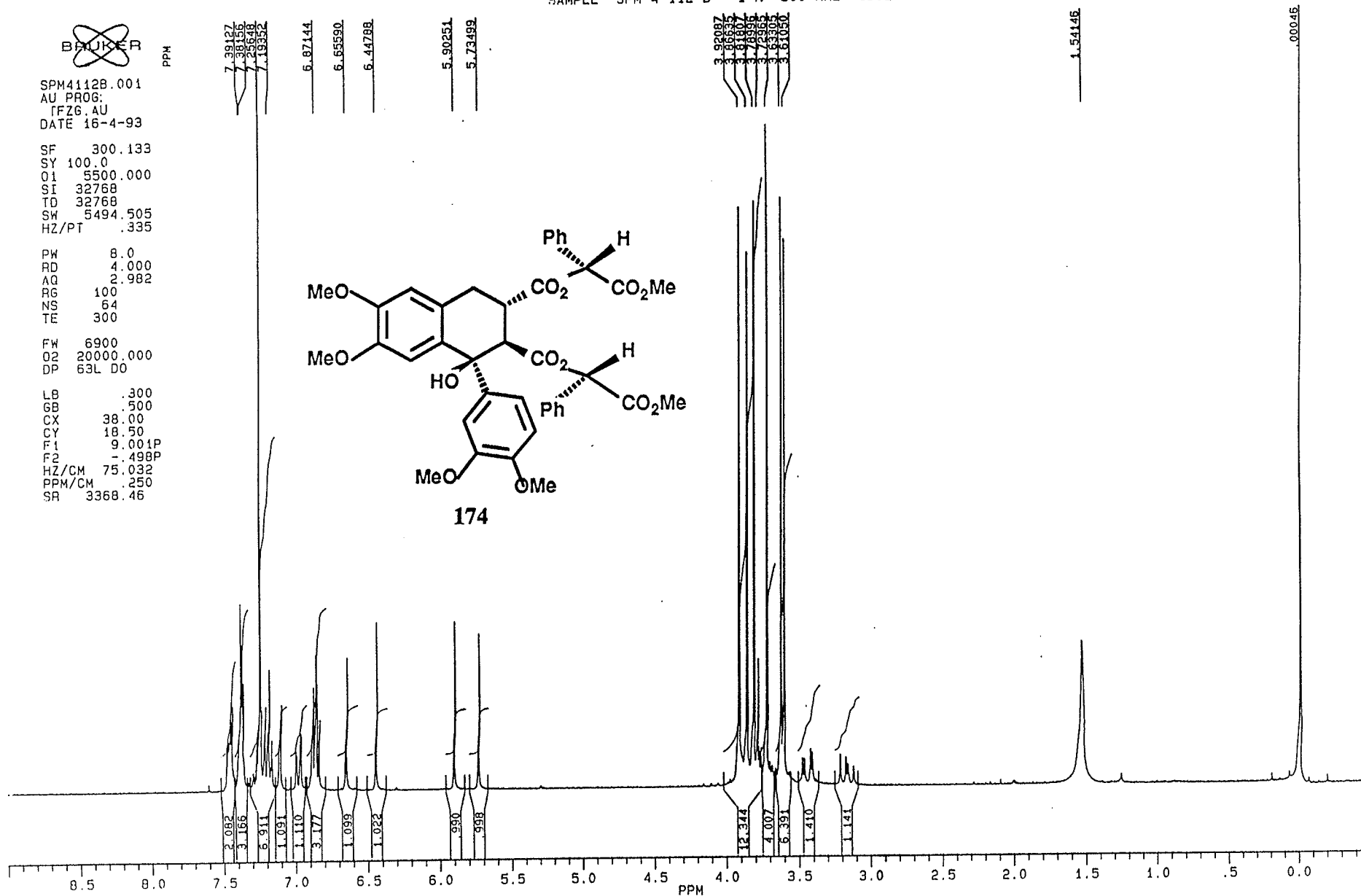
FW 6900
O2 20000.000
DP 63L D0

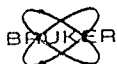
LB .300
GB .500
CX 38.00
CY 18.50
F1 9.001P
F2 - .498P
HZ/CM 75.032
PPM/CM .250
SR 3368.46

SAMPLE SPM-4-112-B 1-H 300 MHZ CDCL3



174





SPM112BC.004
AU PROG:
AUTO13.AU
DATE 20-4-93

SF 75.469
SY 112.0500000
O1 47000.000
SI 32768
TD 32768
SW 17857.143
HZ/PT 1.090

PW 5.0
RD 0.0
AQ .918
RG 200
NS 6272
TE 300

FW 22400
O2 5000.000
DP 18H CPD

LB 1.000
GB .700
CX 38.00
CY 6.00
F1 223.417P
F2 -4.578P
HZ/CM 452.802
PPM/CM 6.000
SR 38596.77

SAMPLE SPM-4-112-B 13-C 75.47 MHZ CDCL3

174.185
171.541
169.890
169.334

148.726
148.477
147.941
147.873

139.231
138.250
137.750
132.389
129.226
128.958
128.722
128.371
127.564
127.107
125.777
118.884

112.124
110.684
110.036

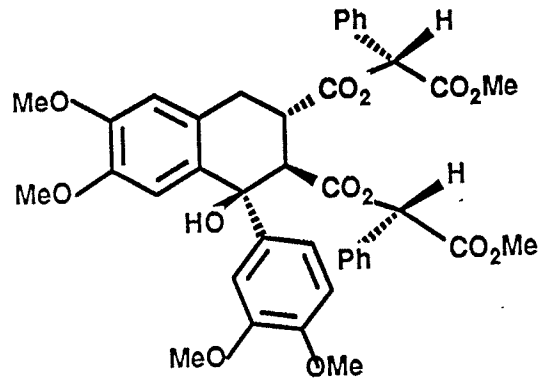
77.407
77.189
76.983
76.553
76.134
74.898
74.652

35.005
35.000
32.747
32.602
32.530
32.430
32.614

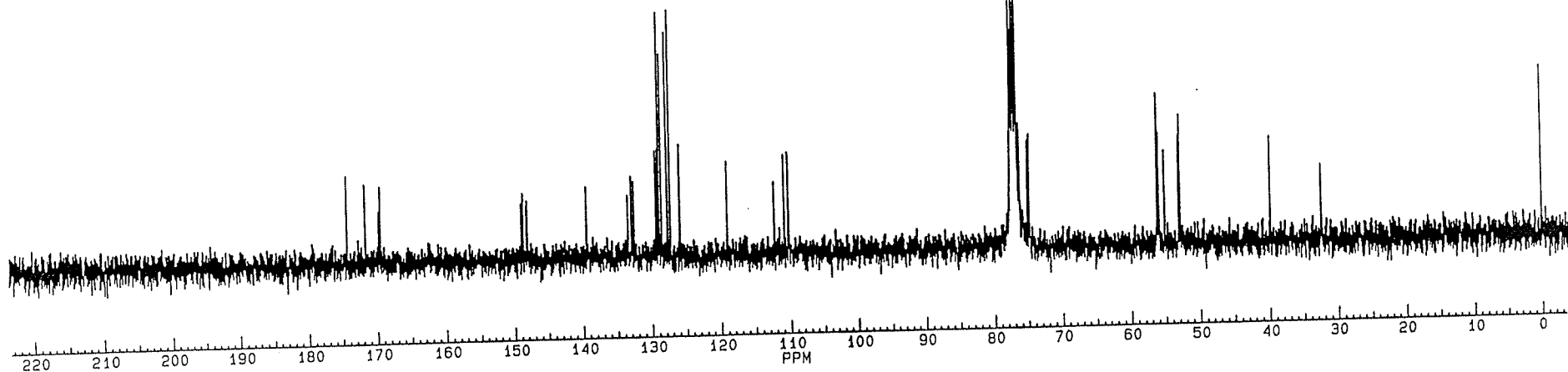
39.701

32.367

100



174



PPM

7.46623
7.45992
7.45004
7.44365
7.43441
7.38050
7.37394
7.35487
7.35062
7.34063
7.32017
7.25618
7.23804
7.22036
7.21363
7.20705
7.19339
7.18917
7.18477
7.10956
7.08332
7.05484
7.05870
7.00781
6.97392
6.66746
6.48845
6.48203
6.44807
6.42031
6.38847
6.33692
6.33026
6.30933
6.30277
6.08472
5.66600

4.56248
4.54428

SPM-4-11482 IN CDCL3

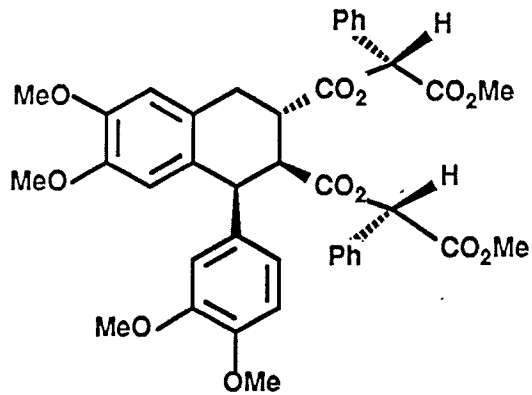
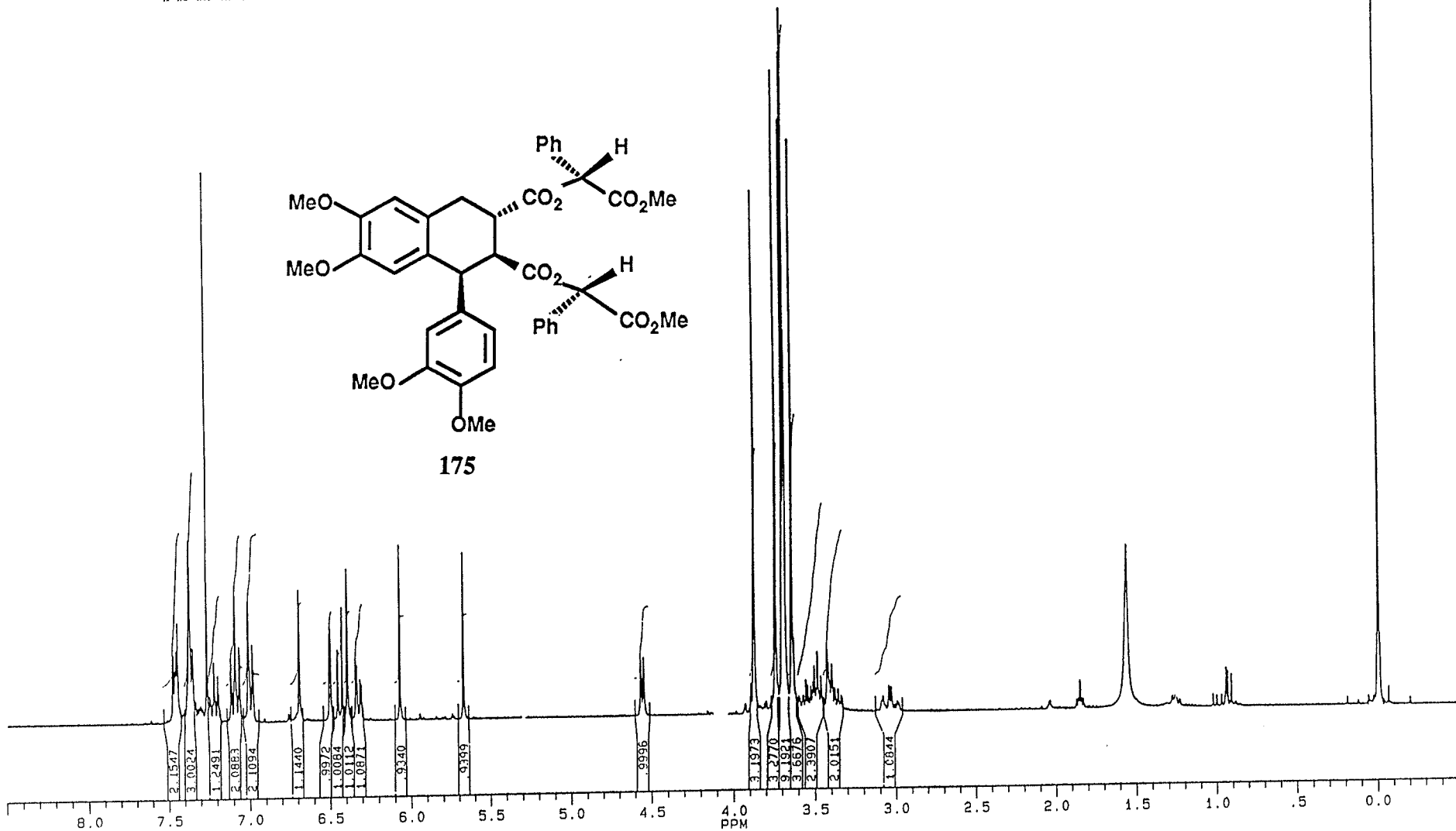
3.88963
3.86886
3.76440
3.73667
3.69500
3.68616
3.67833
3.65676
3.62689
3.59390
3.55711
3.54004
3.52264
3.50681
3.48712
3.46442
3.42226
3.39476
3.37570
3.35495
3.04227
3.02626

1.85003

1.56405

94278
93302
91070

0.1023
-0.0023
-0.1163
-0.02463



175



SPM4114C.004
AU PROG:
AUTOC13.AU
DATE 4-8-93

SF 75.469
SY 112.0500000
O1 47000.000
SI 32768
TD 32768
SW 17857.143
HZ/PT 1.090

PW 5.0
RD 0.0
AQ .918
RG 200
NS 2240
TE 300

FW 22400
O2 5000.000
DP 18H CPD

LB 1.000
GB .700
CX 38.00
CY 8.00
F1 223.417P
F2 -4.578P
HZ/CM 452.802
PPM/CM 6.000
SR 38596.77

PPM

174.242
171.166
169.490

148.113
148.049
147.886
147.769

SAMPLE SPM-4-114-B2 13-C AT 75.47 MHZ IN CDCL3

133.949
133.616
133.375
129.212
128.706
128.604
128.359
127.957
127.012
125.627
121.774

112.811
112.201
110.301

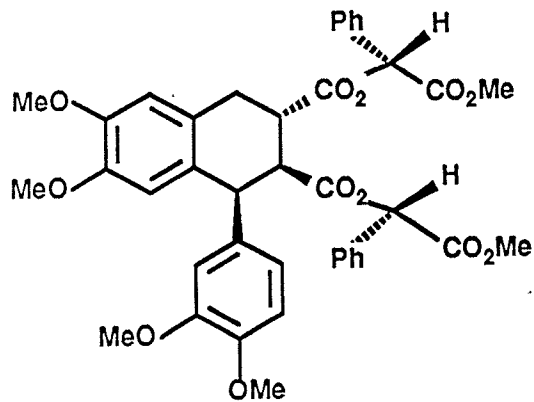
77.407
76.996
76.585
74.900
74.300

55.930
55.363
52.743
52.532
48.201
45.728

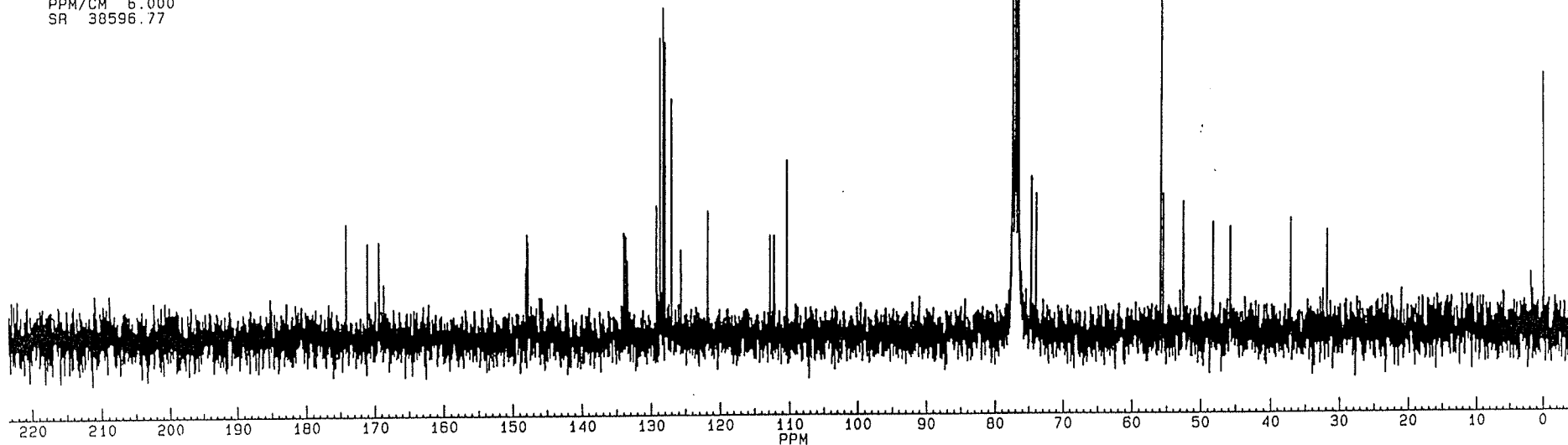
37.104

31.816

.001



175



SAMPLE SPM-4-29 1-H AT 300 MHZ IN CDCL3

~~BRUKER~~

SPM429.001
DATE 6-7-92

SF 300.133
SY 100.0
O1 5500.000
SI 32768
TD 32768
SH 5494.505
HZ/PT .335

PW 8.0
RD 4.000
AQ 2.982
RG 80
NS 32
TE 300

FW 6900
O2 20000.000
DP 62L D0

LB .300
GB .500
CX 38.00
CY 18.50
F1 9.003P
F2 - .497P
HZ/CM 75.032
PPM/CM .250
SR 3368.13

PPM

7.51740
7.51030

7.25751

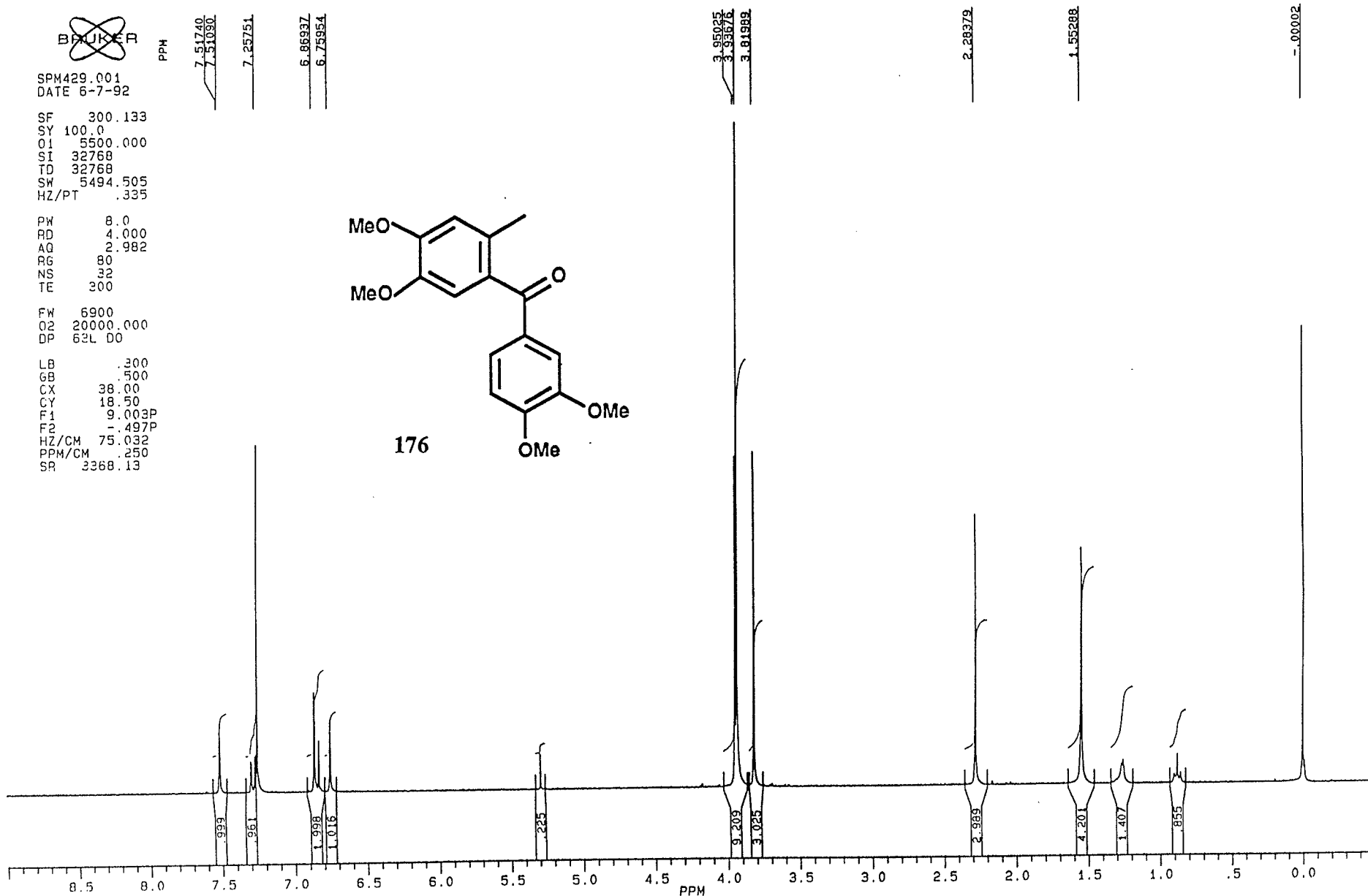
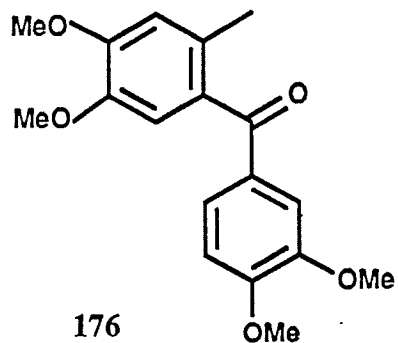
6.86937
6.75954

3.95025
3.93676
3.81989

2.28379

1.55288

-.00002





SPM429C.004
 AU PROG:
 AUTOC13.AU
 DATE 6-8-93

SF 75.469
 SY 112.0500000
 O1 47000.000
 SI 32768
 TD 32768
 SW 17857.143
 HZ/PT 1.090

PW 5.0
 RD 0.0
 AQ .918
 RG 200
 NS 448
 TE 300

FW 22400
 O2 5000.000
 DP 18H CPD

LB 1.000
 GB .700
 CX 38.00
 CY 18.50
 F1 219.965P
 F2 -5.026P
 HZ/CM 446.836
 PPM/CM 5.921
 SR 38595.68

SAMPLE SPM-4-29 13-C AT 75.47 MHZ IN CDCL3

153.229
 150.237
 149.827
 146.110

131.419
 130.712
 130.321
 125.600

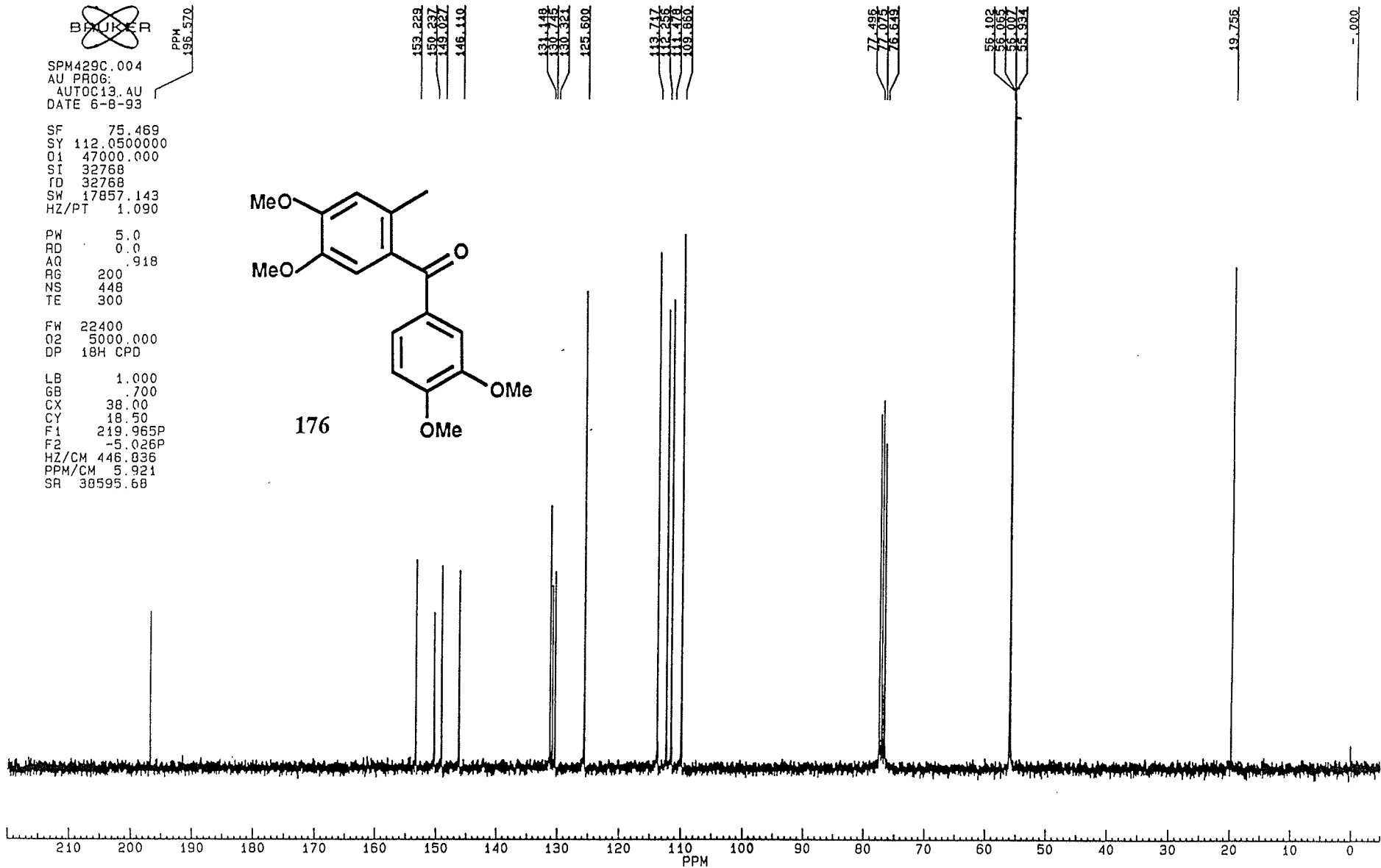
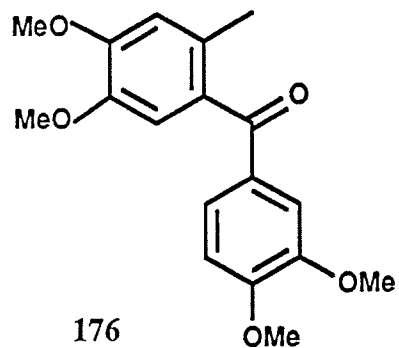
113.717
 112.256
 111.478
 109.860

77.496
 77.073
 76.849

56.102
 56.065
 56.007
 55.934

19.756

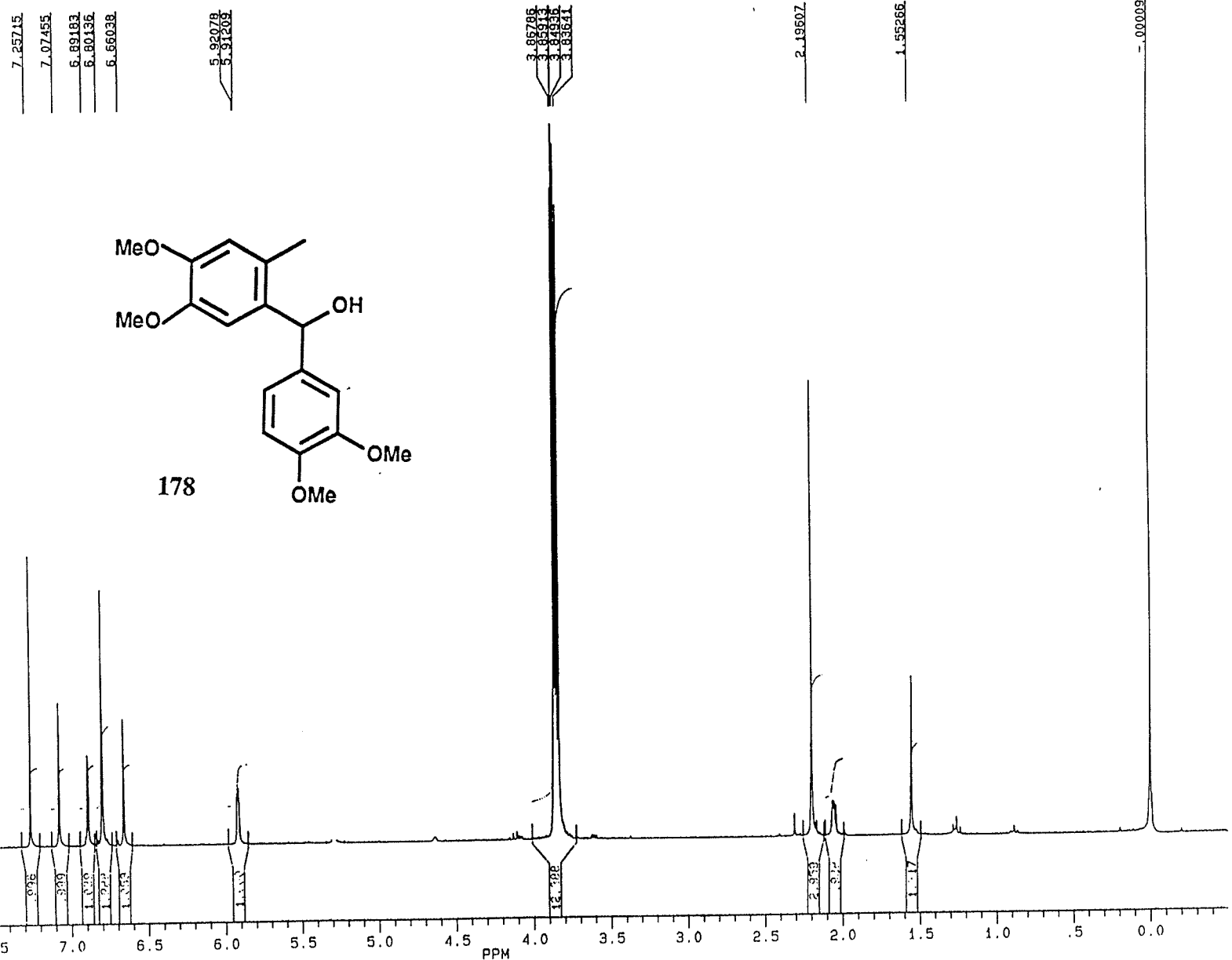
-.000



SAMPLE SPM-4-28 1-H AT 300 MHZ IN CDCL3

BAIJER

PPM
SPM428.001
DATE 25-6-92
SF 300.133
SY 100.0
Q1 5500.000
SI 32768
TD 32768
SW 5494.505
HZ/PT .335
PW 8.0
RD 4.000
AQ 2.982
RG 32
NS 32
TE 300
FW 6900
Q2 20000.000
DP 63L 00
LB .300
GB .500
CX 38.00
CY 18.50
F1 9.001P
F2 - .496P
HZ/CM 75.032
PPM/CM .250
SR 3368.46



178

277

BRUKER

PPH

SPM428C.004
AU PROG:
AUTOC13.AU
DATE 29-6-92

SF 75.469
SY 112.0500000
O1 47000.000
SI 32768
TD 32768
SW 17857.143
HZ/PT 1.090

PW 5.0
RD 0.0
AQ .918
RG 200
NS 832
TE 300

FW 22400
O2 5000.000
DP 18H CPD

LB 1.000
GB .700
CX 38.00
CY 4.00
F1 223.417P
F2 -4.578P
HZ/CM 452.802
PPM/CM 6.000
SR 38596.77

SPM-4-28C AT 75.47 MHZ IN CDCL3

148.970
148.407
147.885
147.093

135.793
133.487

127.408

119.280

113.720

110.928

109.332

109.356

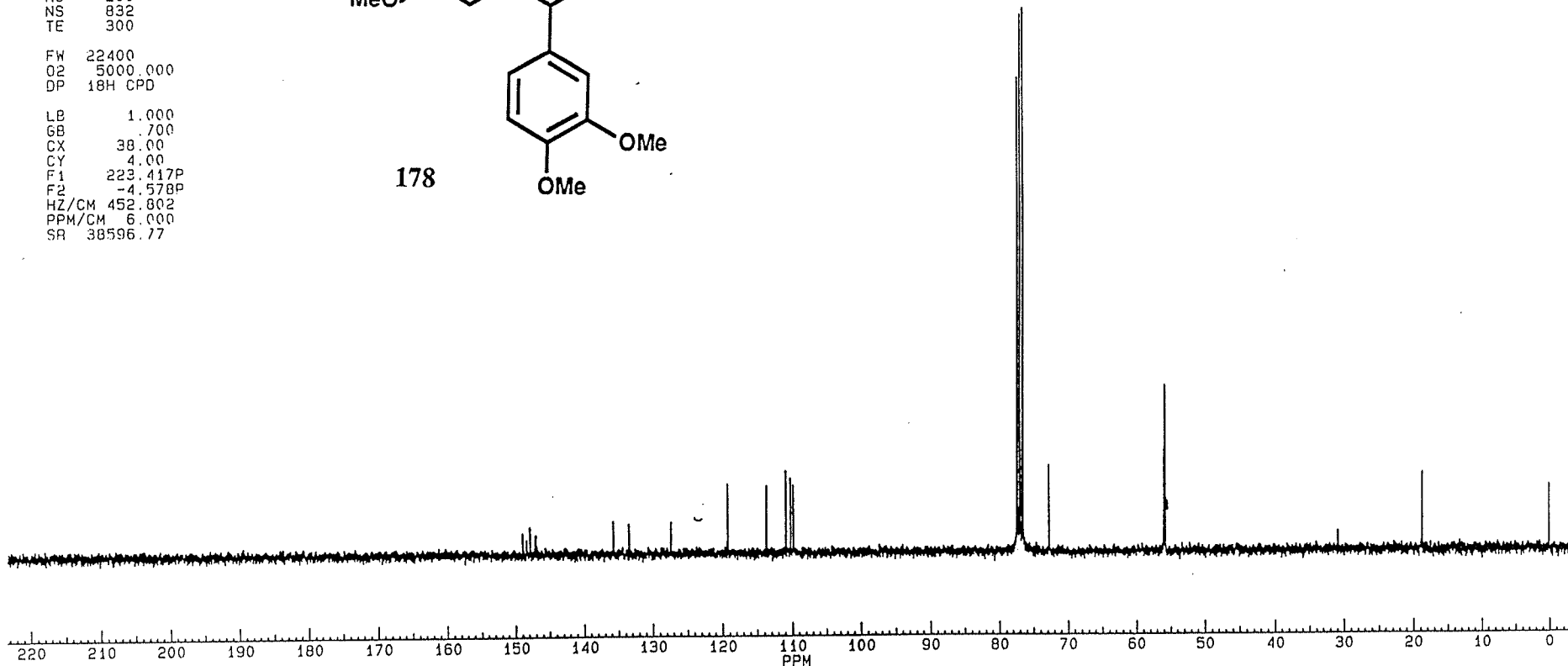
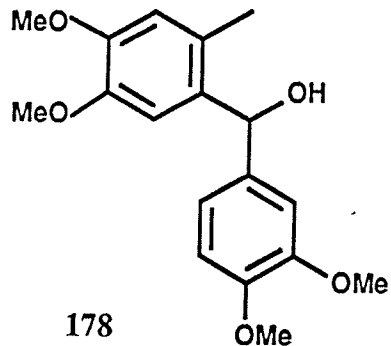
77.417
77.136
76.989
76.570
72.773

56.064
55.903
55.847

30.907

18.775

.001





SPM3110.001
DATE 19-9-91

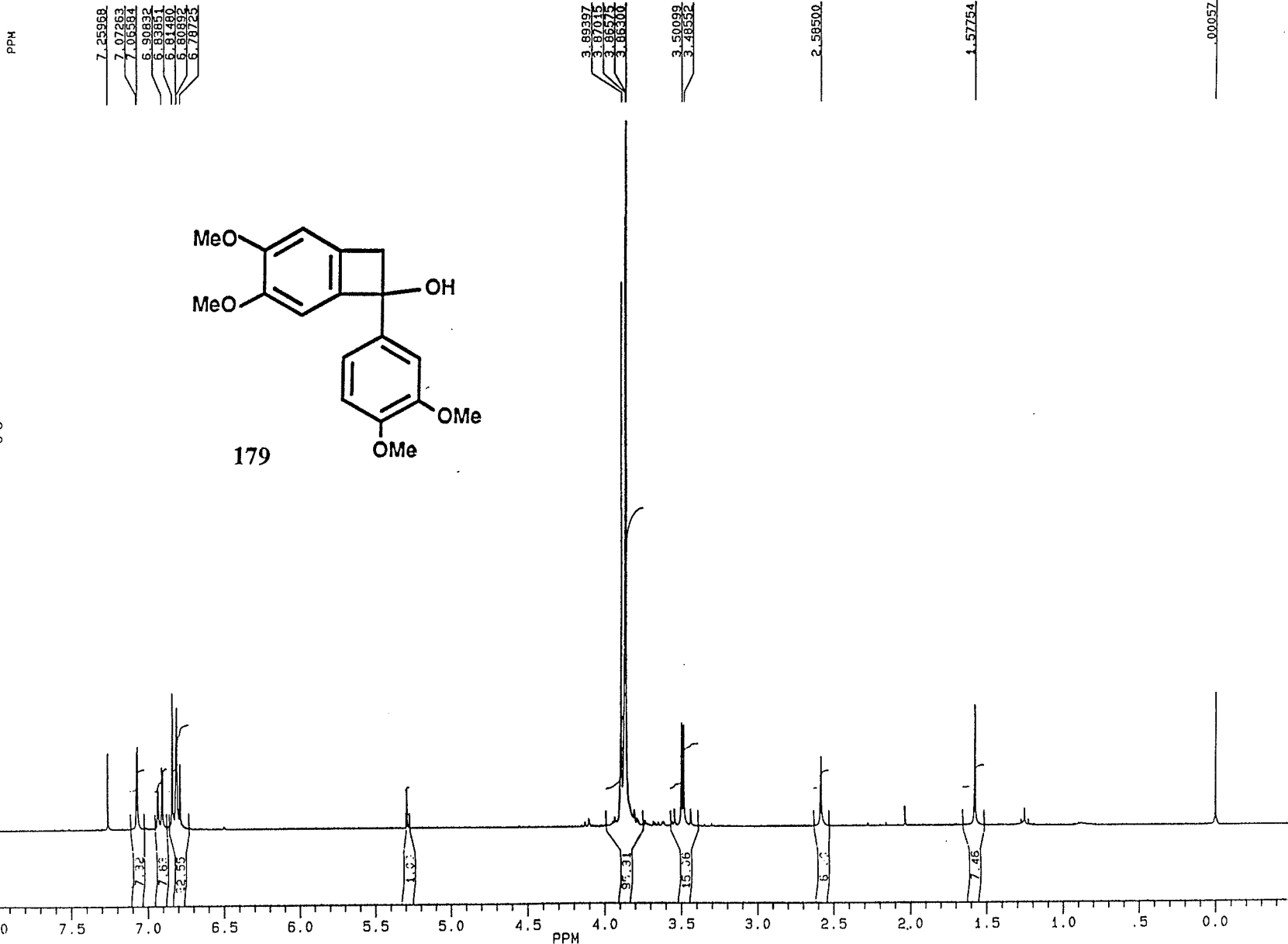
SF 300.132
SY 100.0
O1 5500.000
SI 32768
FD 32768
SW 5494.505
HZ/PT .335

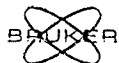
PW 8.0
RD 4.000
AQ 2.982
RG 20
NS 32
TE 300

FW 6900
O2 20000.000
DP 63L D0

LB .200
GB .500
CX 38.00
CY 18.50
F1 9.005P
F2 -.495P
HZ/LM 75.032
PPM/LM .250
GR 3267.46

SAMPLE SPM-3-110, 1-H AT 300 MHZ IN CDCL3





SPM41160.004
 AU PROb
 AUTOC12.AU
 DATE 8-7-92

RF 75.469
 SY 112.050000
 Q1 47000.000
 QI 24768
 ID 24768
 RW 17857.142
 HZ/PT 1.090

PW 5.0
 PD 0.6
 AC 916
 Re 200
 NS 2560
 TE 200

FW 22400
 G2 5000.000
 DP 184.000

LP 1.000
 EP 1.700
 EX 28.00
 CY 18.00
 F1 223.4170
 F2 -4.5760
 HZ/LM 452.802
 RPM/LM 0.000
 RP 26596.77

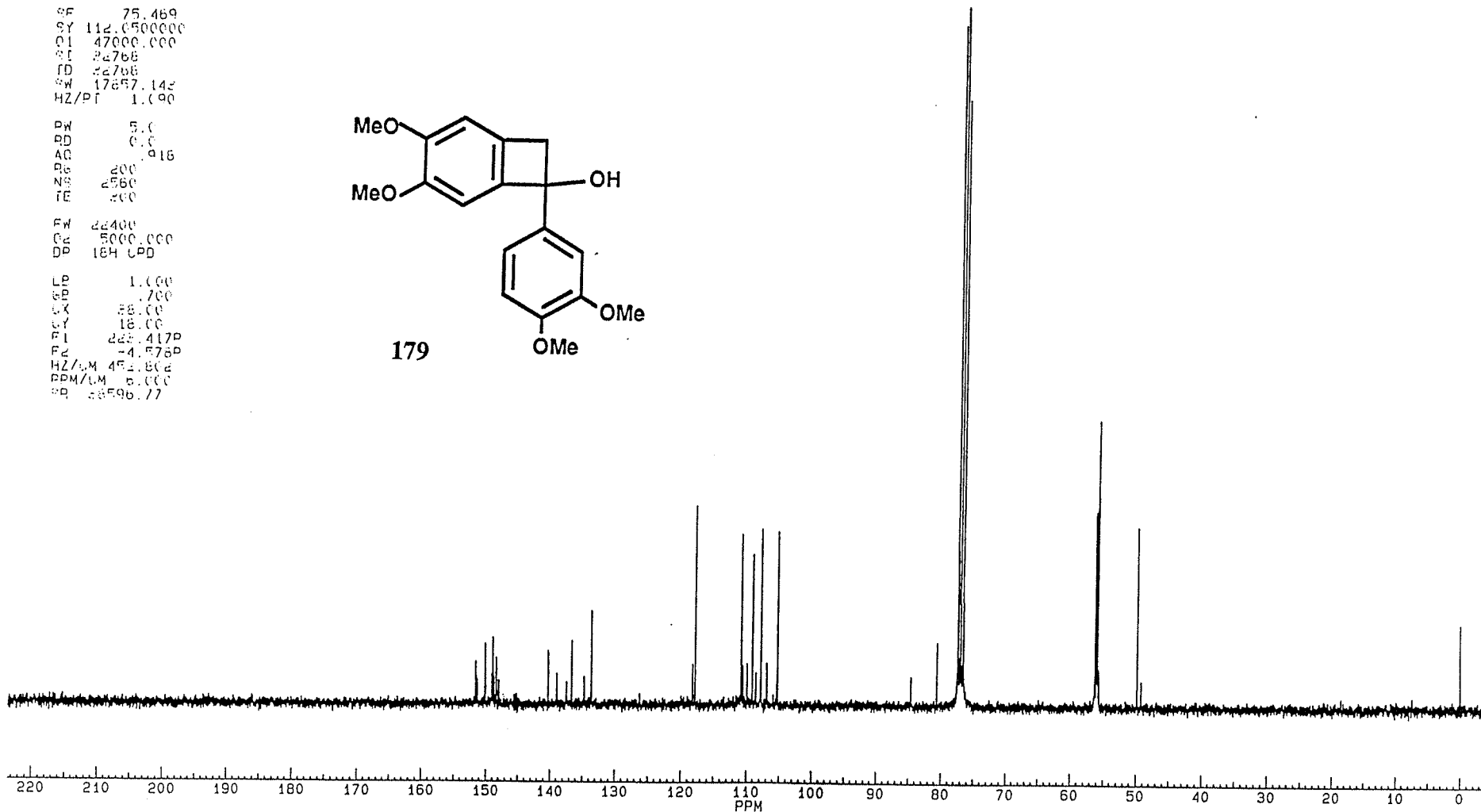
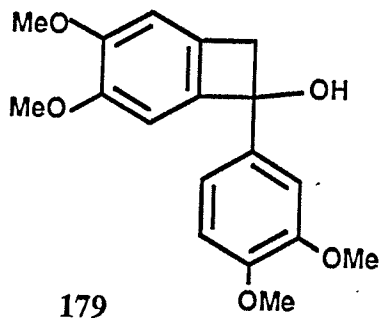
SAMPLE SPM-4-116 13-C AT 75.47 MHZ IN CDCL3

151.530
150.283
150.065
149.070
148.853
148.680
148.319
147.362
139.397
137.230
134.622
133.511

119.179
117.751
110.754
109.822
109.054
108.501
107.768
106.851
105.238

84.557
80.503
77.424
77.205
77.003
76.375

55.283
56.221
56.035
55.935
55.884
55.669
49.869
49.239



1000

BRUKER

SPM4114A.001
AU PR06:
TFZG.AU
DATE 28-5-92

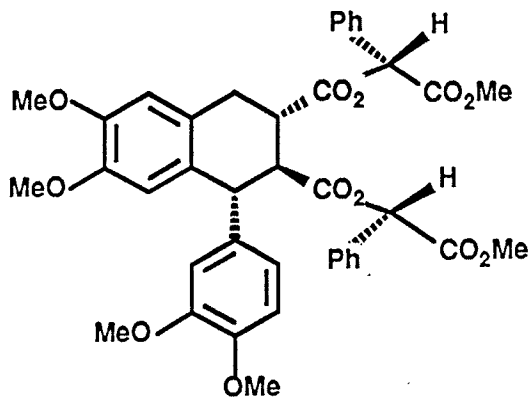
SF 300.123
SY 100.0
OI 5500.000
SI 32768
TD 32768
SW 5494.505
HZ/PT 225

PW 8.0
RD 4.000
AQ 2.982
RG 60
NS 64
TE 200

FW 6900
OZ 20000.000
DP 62L D0

LB .300
GB .500
CX 28.00
CY 18.50
F1 9.000P
F2 .499P
HZ/LM 75.032
PPM/LM .250
SQ 2269.14

SAMPLE SPM-4-114-A 1-H AT 300 MHZ IN CDCL3



183

